Utilising proteomics-derived data to identify novel biomarker signatures in Multiple Myeloma

Maynooth University
National University of Ireland Maynooth

A thesis submitted to Maynooth University for the degree of Doctor of Philosophy by

Katie Dunphy, B. Sc.

January 2024

Supervisor:

Dr. Paul Dowling
Department of Biology
Maynooth University
Co. Kildare
Ireland

Co-Supervisor:

Prof. Peter O'Gorman
Department of Haematology
Mater Misericordiae University Hospital
Dublin 7
Ireland

Head of Department:

Prof. Paul Moynagh
Department of Biology
Maynooth University
Co. Kildare
Ireland

Table of Contents

List of Figures viii

List of Tables xiii

Declaration xvii

Research Dissemination & Achievements xviii

Abbreviations xxi

Acknowledgements xxiv

Abstract xxvi

Chapter 1 Introduction 1

1.1 Multiple Myeloma 2
1.1.1 Introduction to multiple myeloma 2
1.1.2 Incidence and epidemiology 2
1.2 Risk stratification of multiple myeloma 4
1.3 Genetic factors associated with multiple myeloma 6
1.4 Treatment of multiple myeloma 8
1.4.1 Current treatment options 9
1.4.2 Proteasome inhibitors 11
1.4.3 Immunomodulatory drugs 11
1.4.4 Immunotherapy 12
1.5 The bone marrow microenvironment in multiple myeloma 14
1.5.1 The bone marrow microenvironment and B cell development 14
1.5.2 Cellular and soluble interactions in multiple myeloma 15
1.6 Drug resistance in multiple myeloma 17
1.6.1 General mechanisms of resistance 18
1.6.2 Resistance to proteasome inhibitors 19
1.6.3 Resistance to immunomodulatory drugs 20
1.6.4 Resistance to monoclonal antibodies 21
1.6.5 Ex vivo screening methods for assessing drug resistance 21
1.7 Extramedullary multiple myeloma 22
1.7.1 Incidence 23
1.7.2 Diagnosis, prognosis, and treatment of EMM 24
1.8 Precision medicine using proteomic techniques 26
1.8.1 Biomarkers 27
1.8.2 Proteomics 30
1.8.3 Mass spectrometry 30
1.8.3.1 Label-free quantitation 31
1.8.3.2 Label-based quantitation 32
1.8.4 Affinity-based proteomics 32
1.8.5 Post translational modifications 33
1.8.6 Bioinformatics 34
1.9 Aims of the project 35

Chapter 2 Materials and Methods 38

2.1 General chemicals and reagents 39
2.2 Patient samples 44
2.3 Bone marrow mononuclear cell isolation and cell lysis 45
2.4 Protein quantitation using the Pierce™ 660nm protein assay 46
2.5 Protein quantitation using the Qubit™ protein assay 46
2.6 Immunodepletion of blood plasma 47
2.7 Filter-Aided Sample Preparation (FASP) 47
2.8 Tandem Mass Tag (TMT) labelling 48
2.9 C18 sample clean-up 48
2.10 Immobilized Metal Affinity Chromatography (IMAC) phosphopeptide enrichment 49
2.11 Mass spectrometry analysis 50
2.11.1 Label-free mass spectrometry using Q-Exactive 50
2.11.2 Label-free mass spectrometry using Orbitrap Fusion Tribrid 51
2.11.3 Label-based mass spectrometry using Orbitrap Fusion Tribrid 51
2.11.4 Quantitative proteomic profiling using MaxQuant and Perseus 52
2.11.5 Quantitative proteomic profiling using Proteome Discoverer 2.5 53
2.11.6 Quantitative proteomic profiling using Progenesis QI software 53
2.11.7 Bioinformatics analysis and *in silico* data analyses 54
2.12 *In silico* analysis of the MMRF CoMMpass dataset 55
2.13 Targeted metabolomics 55
2.13.1 Sample preparation and analysis 55
2.13.2 Data processing and metabolite quantification 56
2.13.3 Statistical analysis of metabolomics data 56
2.14 Enzyme-linked immunosorbent assays 56
2.14.1 Quantitation of mono- and oligo-nucleosomes in plasma 57
2.14.2 Quantitation of nucleosomal citrullinated histone H3 in plasma 58
2.14.3 Statistical analysis of immunoassay results 58
2.15 Immunoblotting 59
2.16 Measurement of plasma cytokine levels using proximity extension assay 60

Chapter 3 Phosphoproteomic profiling of multiple myeloma based on *ex vivo* drug sensitivity resistance testing identifies distinct phosphorylation signatures associated with drug response 61

3.1 Introduction 62
3.2 Experimental design and methods 64
3.2.1 Patient samples and clinical information 64
3.2.2 Label-based mass spectrometry analysis of primary CD138+ myeloma cells 67
3.2.3 Data analysis and bioinformatic analysis of mass spectrometry results 68
3.2.4 Western blotting verification 69
3.3 Results 70
3.3.1 Stratification of plasma samples based on *ex vivo* drug sensitivity resistance testing 70
3.3.2 Quantitative phosphoproteomics of CD138+ myeloma cell lysates 70

3.3.2.1 Analysis of the proteome of CD138+ myeloma cell lysates stratified into four chemosensitivity groups 71
3.3.2.2 Analysis of the phosphoproteome of CD138+ myeloma cell lysates stratified into four chemosensitivity groups 77
3.3.3 Evaluation of MM patient response to individual drugs based on *ex vivo* drug sensitivity scores 83
3.3.3.1 Phosphoproteomic analysis of CD138+ myeloma cells based on sensitivity/resistance to proteasome inhibitors 84
3.3.3.2 Phosphoproteomic analysis of CD138+ myeloma cells based on sensitivity/resistance to immunomodulatory drugs 89
3.3.3.3 Phosphoproteomic analysis of CD138+ myeloma cells based on sensitivity/resistance to a HSP90 inhibitor 92
3.3.3.4 Phosphoproteomic analysis of CD138+ myeloma cells based on sensitivity/resistance to a PYK2 and FAK inhibitor 97
3.3.3.5 Phosphoproteomic analysis of CD138+ myeloma cells based on sensitivity/resistance to a CDK9 inhibitor 101
3.3.3.6 Western blotting verification of mass spectrometry results 105
3.4 Discussion 107
3.5 Conclusion 115

Chapter 4 Using untargeted and targeted plasma proteomics to identify plasma biomarkers of therapeutic response based on *ex vivo* drug sensitivity resistance testing 116

4.1 Introduction 117
4.2 Experimental design and methods 119
4.2.1 Patient samples 119
4.2.2 Label-free mass spectrometry analysis of MM plasma 125
4.2.3 Data analysis of mass spectrometry results 126
4.2.4 Targeted proteomic analysis using the Olink Target 48 panel 126
4.3 Results 127
4.3.1 Stratification of plasma samples based on *ex vivo* drug sensitivity resistance testing 127
4.3.2 Plasma proteomic analysis using label-free LC-MS/MS 129
4.3.2.1 Statistical analysis reveals a change in the plasma proteome between the four chemosensitivity groups 129
4.3.2.2 Plasma samples can be stratified based on drug sensitivity scores related to individual drugs 131
4.3.2.3 Proteomic analysis of plasma based on sensitivity/resistance to bortezomib 133
4.3.2.4 Proteomic analysis of plasma based on sensitivity/resistance to lenalidomide 134
4.3.2.5 Proteomic analysis of plasma based on sensitivity/resistance to dinaciclib 135
4.3.2.6 Proteomic analysis of plasma based on sensitivity/resistance to PF-04691502 136
4.3.2.7 Proteomic analysis of plasma based on sensitivity/resistance to quisinostat 137
4.3.2.8 Proteomic analysis of plasma based on sensitivity/resistance to venetoclax 138

4.3.2.9 Proteomic analysis of plasma based on sensitivity/resistance to navitoclax 139
4.3.3 Plasma proteomic analysis using targeted proximity extension assay technology 140
4.3.3.1 Targeted analysis of cytokine concentrations across four chemosensitivity groups 141
4.3.3.2 Evaluation of cytokine concentrations in MM plasma stratified based on drug sensitivity/resistance to individual drugs 142
4.3.3.3 Increased plasma levels of interleukin-15 correlate with sensitivity to MEK inhibitors 145
4.4 Discussion 146
4.5 Conclusion 155

Chapter 5 Proteomic profiling of bone marrow mononuclear cells in extramedullary multiple myeloma 157

5.1 Introduction 158
5.2 Experimental design and methods 162
5.2.1 Patient samples and clinical information 162
5.2.2 Label-free mass spectrometry analysis of BMNCs using Thermo Orbitrap Fusion Tribrid mass spectrometer 163
5.2.3 Data analysis and bioinformatic analysis of mass spectrometry results 164
5.2.4 Gene expression analysis using the MMRF CoMMpass dataset 165
5.2.5 Evaluation of neutrophil extracellular traps in EMM plasma 165
5.3 Results 165
5.3.1 Comparison of clinical information from MM patients with and without extramedullary spread 165
5.3.2 Identification of differentially abundant proteins in the bone marrow of MM patients with and without extramedullary spread 166
5.3.3 Evaluating the association of significantly increased proteins in EMM BMNCs with MM prognosis using MMRF CoMMpass study data 170
5.3.4 Bioinformatics of differential proteins in EMM bone marrow mononuclear cells versus MM bone marrow mononuclear cells 173
5.3.5 Evaluating the heparanase/CD138 axis in EMM patients 181
5.3.6 Evaluation of “neutrophil extracellular trap formation” in EMM plasma 182
5.4 Discussion 184
5.5 Conclusion 192

Chapter 6 Proteomic profiling of blood plasma from multiple myeloma patients with and without extramedullary spread 194

6.1 Introduction 195
6.2 Experimental design and methods 197
6.2.1 Patient samples and clinical information 198
6.2.2 Label-free mass spectrometry analysis of EMM and MM plasma samples using a Q-Exactive mass spectrometer 198
6.2.3 Data analysis of mass spectrometry results 199
6.2.4 Verification of results using enzyme-linked immunosorbent assays (ELISAs) 199
6.2.5 Statistical analysis of ELISA results 199

6.2.6 Targeted proteomic analysis using Olink Target 48 panel 200
6.3 Results 200
6.3.1 Identification of significantly differentially abundant proteins in the plasma of EMM and MM patients 200
6.3.2 ELISA verification analysis of differentially abundant plasma proteins in EMM plasma 203
6.3.3 ELISA analysis of serial EMM plasma samples 206
6.3.4 Evaluation of VCAM1, HGFA, PEDF, and ELA2 plasma concentrations in an independent MM patient cohort 207
6.3.5 Association of VCAM1, HGFA, PEDF and ELA2 plasma concentrations with clinical parameters 208
6.3.6 Association of VCAM1, HGFA, PEDF, and ELA2 plasma concentrations with drug response 211
6.3.7 Targeted proteomic analysis of EMM plasma using the PEA-based Olink Target 48 Cytokine panel 215
6.4 Discussion 216
6.5 Conclusion 225

Chapter 7 Targeted metabolomic analysis of blood plasma from multiple myeloma patients with and without extramedullary spread 226

7.1 Introduction 227
7.2 Experimental design and methods 229
7.2.1 Patient samples 229
7.2.2 Targeted metabolomics analysis of MM and EMM patient plasma 230
7.3 Results 231
7.3.1 Data collection and cleaning 231
7.3.2 Comparison of metabolomic profiles identifies a trend towards increased lipid levels in EMM compared to MM plasma 232
7.3.3 Evaluation of biologically relevant metabolite ratios in EMM and MM plasma 232
7.3.4 Orthogonal projection to latent structure discriminant analysis (OPLS-DA) and identification of metabolites contributing to MM and EMM group distinction 236
7.3.5 Identification of differentially abundant metabolites in MM and EMM plasma 238
7.3.6 Evaluation of differentially abundant metabolites/metabolite ratios as plasma-based markers of extramedullary myeloma 242
7.3.7 Integration of plasma metabolomics and proteomics using correlation analysis 246
7.4 Discussion 248
7.5 Conclusion 252

Chapter 8 General Discussion 254

8.1 Discussion 255
8.2 Future work 268
8.3 Conclusion 271

Chapter 9 Bibliography 272

Chapter 10 Appendix 364

List of Figures

Chapter 1

Figure 1.1: Developments in the risk stratification of multiple myeloma patients 6
Figure 1.2: Guidance for the treatment of multiple myeloma 10
Figure 1.3: Mechanisms of drug resistance in multiple myeloma 18
Figure 1.4: Extramedullary multiple myeloma 23
Figure 1.5: Proteomic techniques contributing to precision medicine 27
Figure 1.6: The process of biomarker discovery in biofluids and their clinical applications 29
Figure 1.7: Different post translational modifications (PTMs) and their roles in the mammalian cell 34

Chapter 3

Figure 3.1: Cytogenetic data associated with the patient cohort 67
Figure 3.2: Visualization of phosphorylated peptides and sites distribution 71
Figure 3.3: Principal component analysis (PCA) of reporter ion intensity values from proteins identified in the four chemosensitivity groups 72
Figure 3.4: Hierarchical clustering analysis of statistically significant differentially abundant (SSDA) proteins 74
Figure 3.5: Gene ontology enrichment analysis of proteins found to be statistically significantly increased in Group 4 75
Figure 3.6: Gene ontology enrichment analysis of proteins found to be statistically significantly increased in Group 1 76
Figure 3.7: Principal component analysis (PCA) of reporter ion intensity values from phosphopeptides identified in the four chemosensitivity groups 77
Figure 3.8: Hierarchical clustering analysis of statistically significant differentially abundant (SSDA) phosphorylation sites 79
Figure 3.9: Gene ontology enrichment analysis of phosphoproteins found to be statistically significantly increased in Group 4 80
Figure 3.10: Gene ontology enrichment analysis of phosphoproteins found to be statistically significantly increased in Group 1 81
Figure 3.11: Bioinformatic analysis of phosphorylation motifs and upstream kinases 82

Figure 3.12: Sample stratification into “Most Resistant” and “Most Sensitive” groups for each of the five individual therapeutics analysed 83
Figure 3.13: Comparison of drug sensitivity scores in “most sensitive” and “most resistant” groups associated with each individual drug 84
Figure 3.14: Volcano plots of CD138+ myeloma cells considered ‘Most Sensitive’ and ‘Most Resistant’ to bortezomib 86
Figure 3.15: Bioinformatic analysis of phosphorylation sites associated with bortezomib sensitivity and resistance 87
Figure 3.16: Volcano plots of CD138+ myeloma cells considered ‘Most Sensitive’ and ‘Most Resistant’ to lenalidomide 90
Figure 3.17: Bioinformatic analysis of phosphorylation sites associated with lenalidomide sensitivity and resistance 91
Figure 3.18: Volcano plots of CD138+ myeloma cells considered ‘Most Sensitive’ and ‘Most Resistant’ to luminespib 94
Figure 3.19: Bioinformatic analysis of phosphorylation sites associated with luminespib sensitivity and resistance 95
Figure 3.20: Volcano plots of CD138+ myeloma cells considered ‘Most Sensitive’ and ‘Most Resistant’ to PF 431396 98
Figure 3.21: Bioinformatic analysis of phosphorylation sites associated with PF 431396 sensitivity and resistance 99
Figure 3.22: Volcano plots of CD138+ myeloma cells considered ‘Most Sensitive’ and ‘Most Resistant’ to alvocidib 102
Figure 3.23: Bioinformatic analysis of phosphorylation sites associated with alvocidib sensitivity and resistance 103
Figure 3.24: Comparative western blot analysis of α-actinin abundance in Group 4 and Group 1 myeloma cell lysates 106
Figure 3.25: Comparative western blot analysis of FLNA S2152 abundance in Group 4 and Group 1 myeloma cell lysates 106
Figure 3.26: Comparative western blot analysis of PRKACA abundance in Group 4 and Group 1 myeloma cell lysates 107

Chapter 4

Figure 4.1: Cytogenetic data from sampling date of patient cohort 125

Figure 4.2: Clinical information on the overall survival of the four chemosensitivity groups 128
Figure 4.3: Sample stratification into “Most Resistant” and “Most Sensitive” groups for each of the seven individual therapeutics analysed 132
Figure 4.4: Comparison of drug sensitivity scores in “most sensitive” and “most resistant” groups associated with each individual drug 133
Figure 4.5: Label-free quantitative proteomic analysis of plasma samples “most sensitive” and “most resistant” to the proteasome inhibitor, bortezomib 134
Figure 4.6: Label-free quantitative proteomic analysis of plasma samples “most sensitive” and “most resistant” to the immunomodulatory drug, lenalidomide 135
Figure 4.7: Label-free quantitative proteomic analysis of plasma samples “most sensitive” and “most resistant” to the cyclin dependent kinase (CDK) inhibitor, dinaciclib 136
Figure 4.8: Label-free quantitative proteomic analysis of plasma samples “most sensitive” and “most resistant” to the PI3K and mTOR inhibitor, PF-04691502 137
Figure 4.9: Label-free quantitative proteomic analysis of plasma samples “most sensitive” and “most resistant” to the pan-HDAC inhibitor, quisinostat 138
Figure 4.10: Label-free quantitative proteomic analysis of plasma samples “most sensitive” and “most resistant” to the BCL2 inhibitor, venetoclax 139
Figure 4.11: Label-free quantitative proteomic analysis of plasma samples “most sensitive” and “most resistant” to the BCL-2 and BCL-xL inhibitor, navitoclax 140
Figure 4.12: Plasma concentrations of differentially abundant cytokines across chemosensitivity groups 142
Figure 4.13: Plasma concentrations of cytokines identified as differentially abundant between groups considered ‘most sensitive’ and ‘most resistant’ to lenalidomide 143
Figure 4.14: Plasma concentrations of cytokines identified as differentially abundant between groups considered ‘most sensitive’ and ‘most resistant’ to dinaciclib 144
Figure 4.15: Plasma concentrations of cytokines identified as differentially abundant between groups considered ‘most sensitive’ and ‘most resistant’ to PF-04691502 144
Figure 4.16: Plasma concentrations of cytokines identified as differentially abundant based on *ex vivo* drug response to venetoclax and navitoclax 145

Chapter 5

Figure 5.1: Overview of neutrophil extracellular trap (NET) formation 161
Figure 5.2: Clinical information of the patient cohort 166
Figure 5.3: Proteomic profile of BMNCs from EMM patients and medullary MM patients 167
Figure 5.4: Kaplan–Meier curves illustrating genes whose expression (high/low) is significantly associated with survival in MM using the MMRF CoMMpass RNASeq dataset 171
Figure 5.5: Survival graphs illustrating the difference in OS between patients with high expression and low expression of the seven proteins identified as potential prognostic biomarkers in the CoMMpass dataset 172
Figure 5.6: Enrichment map of proteins increased (red) and decreased (blue) in abundance in EMM highlights the functional clusters associated with EMM 174
Figure 5.7: Bubble maps for GOMF analyses of differentially abundant proteins 175
Figure 5.8: Bubble maps for GOCC analyses of differentially abundant proteins 176
Figure 5.9: KEGG map highlighting proteins associated with leukocyte transendothelial migration 179
Figure 5.10: KEGG map highlighting proteins associated with the RAP1 signalling pathway 180
Figure 5.11: KEGG map highlighting proteins associated with the focal adhesion pathway 180
Figure 5.12: KEGG map highlighting proteins associated with neutrophil extracellular trap formation 181
Figure 5.13: Alterations in heparanase, CD138, and circulating CD138 levels in bone marrow and plasma of EMM and MM patients 182
Figure 5.14: Plasma concentrations of neutrophil elastase (ELA2), myeloperoxidase (MPO), and calprotectin in MM patient plasma compared to EMM patient plasma 183
Figure 5.15: Plasma levels of citrullinated histone H3 and nucleosomes in MM patient plasma compared to EMM patient plasma 184

Chapter 6

Figure 6.1: Appearance of intra- and extra-medullary lesions in multiple myeloma by ^{18}F-FDG PET/CT 196

Figure 6.2: Differential abundance analysis of quantitative proteomics data from EMM and MM plasma 201
Figure 6.3: STRING analysis with functional enrichment of significantly differentially abundant proteins in EMM versus MM plasma 203
Figure 6.4: Plasma levels of statistically significantly differentially abundant proteins measured by ELISA 204
Figure 6.5: Receiver operating characteristic (ROC) curve analysis of four potential EMM biomarkers 205
Figure 6.6: Logistic regression analysis evaluating four-biomarker panel performance 206
Figure 6.7: Bar charts illustrating ELISA analysis of four serial EMM samples 207
Figure 6.8: Survival analysis of MM patient samples to identify the prognostic potential of circulating plasma proteins 209
Figure 6.9: Association of VCAM1, HGFA, PEDF, and ELA2 plasma concentrations with high-risk cytogenetic abnormalities (HRCAs) 210
Figure 6.10: Plasma concentrations of VCAM1, HGFA, PEDF, and ELA2 in MM patients stratified based on *ex vivo* drug sensitivity resistance testing (DSRT) 212
Figure 6.11: Association of plasma concentrations of VCAM1 and PEDF with drug response 214
Figure 6.12: Correlation of VCAM1 plasma concentrations with BCL2 inhibitor sensitivity 215
Figure 6.13: Plasma concentrations of statistically significantly differentially abundant cytokines as determined by proximity extension targeted proteomics assay 216

Chapter 7

Figure 7.1: Metabolite coverage across chemical classes 231
Figure 7.2: Metabolite-metabolite correlation analysis 232
Figure 7.3: Comparison of plasma levels of various metabolite classes in EMM and MM patients 234
Figure 7.4: Metabolomics pattern recognition using multivariate approaches 238
Figure 7.5: Identification of differentially abundant metabolites 240
Figure 7.6: Plasma concentration [µM] of metabolites with AUC values > 0.8 plotted as boxplots 245

Figure 7.7: Multivariate receiver operating characteristic (ROC) curves indicating the discriminatory power of plasma metabolite combinations 246
Figure 7.8: Spearman's correlation matrix between differential metabolites and proteins in EMM plasma 247

Chapter 8

Figure 8.1: Cross-comparison of phosphoproteomics data across different drug sensitivities 258
Figure 8.2: Framework for the clinical application of *ex vivo* drug screening in combination with molecular profiling 262
Figure 8.3: Summary of the proteomic alterations identified in this thesis when comparing extramedullary multiple myeloma and multiple myeloma without extramedullary spread 266

List of Tables

Chapter 1

Table 1.1: Criteria for the diagnosis of MGUS, sMM, high-risk sMM, and MM 4
Table 1.2: Approximate frequency of cytogenetic abnormalities in MM 8

Chapter 2

Table 2.1: List of chemicals, reagents and consumables used throughout this project 39
Table 2.2: Composition of buffer/solutions used throughout this project 40
Table 2.3: List of antibodies and enzymes used throughout this project 42
Table 2.4: Commercial kits used throughout this project 43
Table 2.5: Technical and analytical equipment used throughout this project 44
Table 2.6: Patient cohorts evaluated in each chapter of this thesis 45

Chapter 3

Table 3.1: Clinical characteristics of patient cohort 65
Table 3.2: Details of treatment course of each patient within the cohort 66
Table 3.3: Sample groupings based on drug sensitivity/resistance 70
Table 3.4: Top 10 phosphorylation sites with significantly increased abundance in MM samples considered most resistant to bortezomib 88
Table 3.5: Top 10 phosphorylation sites with significantly increased abundance in MM samples considered most sensitive to bortezomib 88
Table 3.6: Top 10 phosphorylation sites with significantly increased abundance in MM samples considered most resistant to lenalidomide 92
Table 3.7: Phosphorylation sites with significantly increased abundance in MM samples considered most sensitive to lenalidomide 92
Table 3.8: Top 10 phosphorylation sites with significantly increased abundance in MM samples considered most resistant to luminespib 96
Table 3.9: Top 10 phosphorylation sites with significantly increased abundance in MM samples considered most sensitive to luminespib 96
Table 3.10: Top 10 phosphorylation sites with significantly increased abundance in MM samples considered most resistant to PF 431396 100

Table 3.11: Top 10 phosphorylation sites with significantly increased abundance in MM samples considered most sensitive to PF 431396 100
Table 3.12: Top 10 phosphorylation sites with significantly increased abundance in MM samples considered most resistant to alvocidib 104
Table 3.13: Top 10 phosphorylation sites with significantly increased abundance in MM samples considered most resistant to alvocidib 104

Chapter 4

Table 4.1: Clinical characteristics of patient cohort 120
Table 4.2: Details of treatment course of each patient within the cohort 121
Table 4.3: Sample groupings based on *ex vivo* drug sensitivity/resistance 128
Table 4.4: Proteins of differential abundance between the four chemosensitivity groups 129
Table 4.5: Proteins of differential abundance between sensitive (Group 1&2) and resistant (Group 3&4) groups 131
Table 4.6: List of significantly differentially abundant cytokines across the four MM chemosensitivity groups 141
Table 4.7: Spearman rank correlation analysis between individual drug sensitivity scores and plasma concentrations of IL-15 146

Chapter 5

Table 5.1: Clinical and demographic characteristics of patient cohort 163
Table 5.2: List of 25 proteins most significantly increased in abundance in EMM BMNCs compared to MM BMNCs 168
Table 5.3: List of 25 proteins most significantly decreased in abundance in EMM BMNCs compared to MM BMNCs 169
Table 5.4: KEGG enrichment analysis of proteins significantly increased in abundance in EMM BMNCs 178
Table 5.5: KEGG enrichment analysis of proteins significantly decreased in abundance in EMM BMNCs 179

Chapter 6

Table 6.1: List of statistically significantly differentially abundant proteins in the plasma of EMM patients compared to MM patients without extramedullary spread 202
Table 6.2: Statistical comparison of VCAM1, HGFA, and PEDF plasma concentrations in second MM patient cohort and EMM patient cohort 208
Table 6.3: Summary of significant correlations between individual drug sensitivity scores and plasma concentrations of VCAM1, HGFA, PEDF, and ELA2 213

Chapter 7

Table 7.1: Statistical analysis of metabolite ratios in MM and EMM plasma 235
Table 7.2: Metabolites of differential abundance in the plasma of MM and EMM patients 241
Table 7.3: Receiver operating characteristic curve analysis of differentially abundant metabolites in MM and EMM plasma 244

Chapter 8

Table 8.1: Potential targets/markers and associated therapeutics for the treatment of EMM patients based on the current literature 267

Declaration

This thesis has not previously been submitted in whole or part to this, or any other University, for any other degree. This thesis is sole work of the author, except where stated otherwise.

Signed _____

Katie Dunphy, BSc.

Date _____

Research dissemination and achievements

Publications

Review Articles

Dunphy, K.; Dowling, P.; Bazou, D.; O'Gorman, P. Current Methods of Post-Translational Modification Analysis and Their Applications in Blood Cancers. Cancers 2021, 13, 1930. https://doi.org/10.3390/cancers13081930

Dunphy, K.; O'Mahoney, K.; Dowling, P.; O'Gorman, P.; Bazou, D. Clinical Proteomics of Biofluids in Haematological Malignancies. Int. J. Mol. Sci. 2021, 22, 8021. https://doi.org/10.3390/ijms22158021

Book Chapters

Dunphy, K.; Dowling, P. DIGE-Based Biomarker Discovery in Blood Cancers. Methods in Molecular Biology. 2023, vol 2596,105-112. Springer US, New York, NY. https://doi.org/10.1007/978-1-0716-2831-7_8.

Dunphy, K.; Bazou, D.; Dowling, P. Analysis of Cancer Cell Line Secretomes: A Complementary Source of Disease-Specific Protein Biomarkers. Cancer Cell Culture: Methods and Protocols. Methods in Molecular Biology, 2023, vol 2645., 277-287. Springer US, New York, NY. https://doi.org/10.1007/978-1-0716-3056-3_18

Research Articles

Dunphy, K.; Bazou, D.; Henry, M.; Meleady, P.; Miettinen, JJ.; Heckman, CA.; Dowling, P.; O'Gorman, P. Proteomic and Metabolomic Analysis of Bone Marrow and Plasma from Patients with Extramedullary Multiple Myeloma Identifies Distinct Protein and Metabolite Signatures. Cancers 2023, 15, 3764. https://doi.org/10.3390/cancers15153764

Dowling, P.; Tierney, C.; **Dunphy, K**.; Miettinen, JJ.; Heckman, CA.; Bazou, D.; O'Gorman, P. Identification of Protein Biomarker Signatures for Acute Myeloid

Leukemia (AML) Using Both Nontargeted and Targeted Approaches. Proteomes. 2021 30;9(4):42. https://doi.org/10.3390%2Fproteomes9040042

Presentations

Poster presentations

Characterisation of the tumour proteome in primary extramedullary multiple myeloma identifies key proteins associated with transendothelial migration. **Katie Dunphy**, Despina Bazou, Michael Henry, Paula Meleady, Paul Dowling, and Peter O'Gorman. American Society of Haematology (ASH) Annual Meeting 2021 – Virtually.

Phosphoproteomic analysis of primary myeloma patient samples identifies distinct phosphorylation signatures correlating with chemo-sensitivity profiles in an *ex vivo* drug sensitivity testing platform. **Katie Dunphy**, Paul Dowling, Juho Miettinen, Caroline Heckman, Paula Meleady, Michael Henry, Despina Bazou and Peter O'Gorman. American Society of Haematology (ASH) Annual Meeting 2021 – Virtually.

Proteomic and Phosphoproteomic Analysis of Primary Myeloma Plasma Cells Identifies Distinct Phosphorylation Events Associated with Resistance to Proteasome Inhibitors using an Ex Vivo Drug Sensitivity Testing Platform. **Katie Dunphy**, Paul Dowling, Juho J. Miettinen, Caroline A. Heckman, Despina Bazou, Paula Meleady, Michael Henry, and Peter O'Gorman. European Proteomics Association (EuPA) Annual Congress 2022 – Leipzig, Germany.

Targeted Metabolomics Approach Identifies Alterations in the Plasma Metabolome of Multiple Myeloma Patients with and without Extramedullary Spread. **Katie Dunphy**, Despina Bazou, Paul Dowling and Peter O'Gorman. American Society of Haematology (ASH) Annual Meeting 2022 – Louisiana, USA.

Proteomic Characterisation of the Plasma Proteome in Extramedullary Multiple Myeloma Identifies Potential Prognostic Biomarkers. **Katie Dunphy**, Despina Bazou, Paul Dowling and Peter O'Gorman. American Society of Haematology (ASH) Annual Meeting 2022 – Louisiana, USA.

Combining *ex vivo* drug sensitivity testing with phosphoproteomics to detect novel markers of therapeutic response in multiple myeloma. **Katie Dunphy**, Paul Dowling, Juho J. Miettinen, Caroline A. Heckman, Despina Bazou, Paula Meleady, Michael Henry, and Peter O'Gorman. Irish Mass Spectrometry Society Annual Meeting 2023 – Dublin, Ireland. Biology Research Day 2023 – Maynooth University, Ireland.

Oral Presentations

Proteomic analysis of matched extramedullary multiple myeloma bone marrow mononuclear cells and blood plasma patient samples. **Katie Dunphy**, Despina Bazou, Michael Henry, Paula Meleady, Paul Dowling, and Peter O'Gorman. Biology Research Day 2022 – Maynooth University, Ireland.

Understanding extramedullary multiple myeloma using quantitative proteomics. **Katie Dunphy**, Despina Bazou, Michael Henry, Paula Meleady, Paul Dowling and Peter O'Gorman. Functional Precision Medicine for Blood Cancer Workshop & Symposium 2022 – Helsinki, Finland.

Awards

Runner-up oral presentation prize. Biology Research Day 2022, Maynooth University.

1st prize for best poster presentation. Biology Research Day 2023, Maynooth University.

1st prize for best poster presentation. Irish Mass Spectrometry Society Annual Meeting 2023 – Dublin, Ireland.

BSPR Travel Bursary. Awarded by the British Society of Proteomics Research to present at the European Proteomics Association (EuPA) Annual Congress 2022 in Leipzig, Germany.

EuPA Travel Grant. Awarded by the European Proteomics Association (EuPA) to present at the European Proteomics Association (EuPA) Annual Congress 2022 in Leipzig, Germany.

Irish Cancer Society Translational Cancer Research Networking Award. Awarded by the Irish Cancer Society to attend the American Society of Haematology (ASH) Annual Meeting in New Orleans, Louisiana.

Abbreviations

^{18}F-FDG PET/CT	Flourine-18 fluorodeoxyglucose positron emission tomography/computed tomography
ABC	Ammonium bicarbonate
ACN	Acetonitrile
ACTN1	α-actinin
AML	Acute myeloid leukemia
ANOVA	Analysis of variance
APRIL	A proliferation-inducing ligand
ASCT	Autologous stem cell transplantation
AUC	Area under the curve
B2M	Beta-2-microglobulin
BAFF	B cell activating factor
BME	Bone marrow microenvironment
BMECs	Bone marrow endothelial cells
BMNCs	Bone marrow mononuclear cells
BSA	Bovine serum albumin
CAM-DR	Cell adhesion-mediated drug resistance
CAR-T	Chimeric antigen receptor T cell
CCND1	Cyclin D1
CCND3	Cyclin D3
CD38	Cluster of differentiation 38
CDK	Cyclin dependent kinase
CID	Collision induced dissociation
CK2	Casein kinase 2
CoMMpass	Clinical outcomes in MM to personal assessment of genetic profile
CRAB	Hypercalcemia, renal dysfunction, anemia, lytic bone lesions
CRBN	Cereblon
CT	Computed tomography
Da	Dalton
dH_2O	Deionized water
DTT	Dithiothreitol
DSRT	Drug sensitivity resistance testing
DSS	Drug sensitivity score
EDTA	Etheylenediaminetetraacetic acid
ELA2	Neutrophil elastase
EMD	Extramedullary disease
EMM	Extramedullary multiple myeloma
EMT	Epithelial mesenchymal transition
FA	Focal adhesion
FAK	Focal adhesion kinase
FASP	Filter aided sample preparation
FDA	Food and drug administration
FDR	False discovery rate
FGFR3	Fibroblast growth factor receptor 3
FHRB	Finnish Hematology Registry and Clinical Biobank

FIMM	Institute for Molecular Medicine Finland
FISH	Fluorescent *in situ* hybridization
FLT3	FMS-like tyrosine kinase
FLT3LG	FMS-like tyrosine kinase ligand
FN	Fibronectin
GO	Gene ontology
GOBP	Gene ontology biological process
GOMF	Gene ontology molecular function
GOCC	Gene ontology cellular component
GSN	Gelsolin
HCD	Higher energy collisional dissociation
HCl	Hydrochloric acid
HDT	High dose chemotherapy
HEPES	4-(2-hydroxyethyl)-1-piperazineethanesulfonic acid
HGFA	Hepatocyte growth factor activator
HIF1α	Hypoxia-inducible factor 1 alpha
HRP	Horseradish peroxidase
HSC	Hematopoietic stem cell
HSP	Heat shock protein
IAA	Iodoacetamide
IGH	Immunoglobulin heavy chain
IKK	I kappa B kinase
IL	Interleukin
IMAC	Immobilised metal ion affinity chromatography
IMiD	Immunomodulatory drug
IMWG	International Myeloma Working Group
IPP	ILK-PINCH-Parvin
ISS	International Staging System
KEGG	Kyoto Encyclopedia of Genes and Genomes
kHz	Kilohertz
KSEA	Kinase substrate enrichment analysis
LC	Liquid chromatography
LC-MS/MS	Liquid chromatography tandem mass spectrometry
LDH	Lactate dehydrogenase
LFQ	Label-free quantitation
LOD	Limit of detection
mAb	Monoclonal antibody
MAF	Transcription factor Maf
MAPK	Mitogen activated protein kinase
MDE	Myeloma-defining events
MDR	Multi-drug resistant
MGUS	Monoclonal gammopathy of undetermined significance
MM	Multiple myeloma
MMP9	Matrix metalloproteinase 9
MMRF	Multiple myeloma research foundation
MMSET	Multiple myeloma SET domain-containing protein
MPO	Myeloperoxidase
MRI	Magnetic resonance imaging
mTOR	Mammalian target of rapamycin

NaOH	Sodium hydroxide
NCAM	Neural cell adhesion molecule
NDMM	Newly diagnosed multiple myeloma
NET	Neutrophil extracellular trap
NFκB	Nuclear factor – kappa beta
NGS	Next generation sequencing
NK	Natural killer
OD	Optical density
OPLS-DA	Orthogonal projection to latent structure discriminant analysis
OS	Overall survival
PBS	Phosphate buffer saline
PCA	Principal component analysis
PECAM1	Platelet/endothelial cell adhesion molecule 1
PEDF	Pigment epithelium derived factor
PET	Positron emission tomography
PFS	Progression-free survival
PI	Proteasome inhibitor
PI3K	Phosphoinositide 3-kinase
PKA	Protein kinase
PRKCB	Protein kinase C beta
PTM	Post translational modification
PYK2	Proline-rich tyrosine kinase 2
QC	Quality control
qPCR	Quantitative polymerase chain reaction
RISS	Revised International Staging System
ROC	Receiver operating characteristic
ROS	Reactive oxygen species
RRMM	Relapsed refractory multiple myeloma
SDS	Sodium dodecyl sulfate
Ser	Serine
SFKs	Src family kinases
sMM	Smouldering multiple myeloma
SSDA	Statistically significant differentially abundant
STRING	Search tool for the retrieval of interacting genes
TCA	Tricarboxylic acid cycle
TEAB	Triethylammonium bicarbonate
TFA	Trifluoroacetic acid
Thr	Threonine
TMT	Tandem mass tags
Tyr	Tyrosine
UA	Urea
V	Volts
VCAM1	Vascular cell adhesion molecule 1
VEGF	Vascular endothelial growth factor
VIP	Variable importance in the projection
VLA-4	Very late antigen 4
VRd	Bortezomib, lenalidomide, and dexamethasone

Acknowledgements

First and foremost, I would like to thank my supervisor, Dr. Paul Dowling. Your constant support and guidance has helped make my PhD journey that bit easier over the last four years. If it wasn't for your and Ciara's encouragement during my final year undergraduate project, I never would have believed I was capable of pursuing a PhD, let alone completing one. I'm sure neither of you remember these conversations but they were key to building my confidence as a researcher and I will always be grateful for that. Thank you for teaching me everything I know about proteomics, for always being available to listen to my never-ending questions, and for your ability to help me refocus when I would wander down protein rabbit holes. It has been a pleasure to have you as my mentor and I will miss our proteomics chats and analysis of Kilkenny hurling!

Thank you to Prof. Peter O'Gorman, I will always be grateful for your insight into the clinical needs of patients and focusing my attention on the clinical applications of my research. It is easy to get lost in the science in the lab and I am massively appreciative of your input as my co-supervisor. A huge thank you to Dr. Despina Bazou, you have always been a friendly face on my visits to the Mater and your contributions and advice have been invaluable throughout so many parts of this project. I would also like to acknowledge our collaborators at the Institute of Molecular Medicine, Finland, especially Dr. Juho Miettinen for your help with the *ex vivo* drug sensitivity resistant testing aspect of my project.

Thank you to Dr. Rebecca Owens, Dr. Marion Butler, and Prof. Kevin Kavanagh for taking the time to attend my annual review assessments. I am hugely grateful for the feedback you have given me throughout my PhD. Thank you to Michelle, Aine and all the administration and technical staff in the Biology Department for the help over the years. Thank you to all the other labs in the Biology Department for allowing me to use equipment, lending chemicals or just for the coffee and lunch breaks! The chats during lunch (especially after the social distancing era) have always been a great escape from work over the years! Thank you to Stephen for being a great lab mate and for your help throughout the years, especially showing me around the lab at the start of my PhD.

To the gals (the OG's), thank you for all the support over the years and for always being there no matter what, even after 15 years of friendship! Thank you for all the laughs, tea dates, and nights out - Isn't it so nice we're all still friends!? A special thank you to Emily for all the sea swims and post-swim almond croissants, they have provided a much-needed mental break over the past two years. I am so grateful for each one of you (Bring on Vegas!). To (Boyfriend) Paul, it's hard to describe how thankful I am for all your support over the last few years. Thank you for tolerating leaving Cork to visit me, providing a constant supply of sweets, listening to all my concerns and stresses (even when you weren't sure what I was talking about) and providing encouragement at times when problems felt insurmountable.

To my family – Mam, Dad, Mark, JJ, (Brother) Paul, and Susan – I don't say this enough, but you have been such a good support for me throughout my life. Mam and Dad, you are two of hardest working people I know, and you have instilled this value in me which I am so thankful for. Dad, thank you for always making sure my car is drivable in return for a bottle of red wine every once in a while! Mam, you're so selfless in everything you do for our family, and I'll never be able to thank you for everything. All the chats, the many dinners you've cooked, the spa trips, and everything in between has meant so much. I can't describe how grateful I am for everything you both have done for me over the years. Thank you to Susan who despite living on the other side of the world, has been hugely supportive throughout the last 4 years from my decision to apply for the PhD to this point. You have been such a great role model (most of the time, lol) and I can't wait to plan more trips together now that I'll have a 'real job'! A special mention to my niece, Eva, you've brought such fun to all our lives and I'm so excited to watch you grow up. I can't finish my acknowledgements without thanking Koby (the dog) for tolerating my incessant cuddles and for all the entertainment he's brought since joining the family!

Finally, I would like to thank each and every one of the patients who participated in this research and all multiple myeloma research. I hope that our efforts will continue to contribute to better patient care and outcomes.

Abstract

Multiple myeloma (MM) is characterized by the clonal expansion of plasma cells in the bone marrow that results in end-organ damage, including hypercalcemia, renal dysfunction, infection, anemia, and bone disease. Despite the introduction of novel therapeutics, MM remains an incurable disease mainly due to repeated relapses and resistance to current chemotherapies. The development of extramedullary multiple myeloma (EMM), an aggressive form of MM associated with the colonisation of soft tissues or organs by myeloma cells, is associated with a poor prognosis. There remains a critical unmet need for effective treatments for patients with refractory disease and aggressive extramedullary disease. Given the potential of predictive biomarker panels to optimise treatment regimens, a phosphoproteomic analysis based on *ex vivo* drug responses to a selection of drug classes was performed. Results showed an increased abundance of proteins and phosphoproteins associated with cell adhesion and a decreased abundance of proteins and phosphoproteins associated with protein translation in multi-drug resistant myeloma cells based on *ex vivo* drug response. Furthermore, a proteomic analysis of MM patient plasma stratified based on *ex vivo* drug responses identified circulating proteins, including interleukin-15, as potential predictive biomarkers of drug response. Using label-free mass spectrometry, distinct alterations in the proteomic profile of bone marrow mononuclear cells from EMM patients compared to MM patients were identified. Bioinformatic analysis revealed an increased abundance of proteins linked to a poor prognosis in MM, and potential cellular mechanisms, including leukocyte transendothelial migration, associated with EMM. Proteomic and metabolomic evaluation of plasma samples from MM patients with and without extramedullary spread confirmed a distinct phenotypic change in EMM patients. Three proteins, namely, vascular cell adhesion molecule 1, hepatocyte growth factor activator, and pigment epithelium derived factor, were verified as promising biomarkers of EMM. Overall, this thesis provides novel insights into aggressive phenotypes of MM and identifies promising biomarkers for future validation studies.

Chapter 1

Introduction

1.1 Multiple Myeloma

1.1.1 Introduction to Multiple Myeloma

Cancer is one of the leading causes of death worldwide. In Ireland, approximately 30% of deaths each year are caused by cancer (Cancer in Ireland 1995-2021:Annual statistical report of the National Cancer Registry 2023). The malignant transformation of cells occurs through a multi-stage process whereby genetic abnormalities promote the constitutive proliferation and survival of cancerous cells. Cancer can occur anywhere throughout the body and is typically classified based on the cell of origin or location of the tumour. Hematological malignancies refer to cancers that originate in the blood or bone marrow, and include leukemia, lymphoma, and multiple myeloma (Rahman and Mansour 2019).

Plasma cells are terminally differentiated B lymphocytes that play a central role in the healthy functioning of the immune system through the production of antibodies (D'Souza and Bhattacharya 2019). Multiple myeloma (MM) is a malignancy of plasma cells characterized by their uncontrolled proliferation within the bone marrow. Myeloma cells produce a high level of abnormal monoclonal (M) protein that can be detected in the blood or urine to aid diagnosis (Hideshima *et al.* 2007). MM is a complex, heterogenous malignancy initiated by various complex cytogenetic abnormalities and supported by signals within the bone marrow niche (Giannakoulas *et al.* 2021). The overall survival of myeloma patients has significantly improved in recent years in concordance with the introduction of novel therapeutics. Despite this, MM remains an incurable cancer mainly due to the development of drug resistance and repeated relapses.

1.1.2 Incidence and epidemiology

Although MM is considered a rare disease as it makes up only 1% of all cancers, it is the second most common type of blood cancer behind non-Hodgkins lymphoma (Siegel *et al.* 2019). Globally, the incidence of MM was over 160,000 and mortality was over 105,000 in 2020 (Ludwig *et al.* 2020; Huang, Chan, *et al.* 2022). In Ireland, over 350 people are diagnosed each year (Cancer in Ireland 1995-2021:Annual statistical report of the National Cancer Registry 2023). Following the introduction

of novel treatments including proteasome inhibitors and immunomodulatory drugs in recent years, the five year survival rate of MM patients has significantly improved, from 24.6% in 1976 to 53.7% in 2016 (Howlader *et al.* 2019). MM most often occurs in people over the age of 65 and is very rarely diagnosed in individuals under 30 (Kazandjian 2016). Males, as well as people of African descent, are more likely to be diagnosed with MM (Landgren and Weiss 2009). A family history of hematologic malignancies can increase the risk of an MM diagnosis (VanValkenburg *et al.* 2016). Additional risk factors include pesticide exposure, obesity, and chronic inflammation (van de Donk *et al.* 2021).

Almost all cases of MM are preceded by premalignant plasma cell disorders, progressing from monoclonal gammopathy of undetermined significance (MGUS) to smouldering multiple myeloma (sMM) and finally to active multiple myeloma. In certain cases, active MM can progress to extramedullary multiple myeloma; an aggressive subtype of myeloma associated with a poor prognosis (Pinto *et al.* 2020). MGUS, sMM, and MM have specific diagnostic criteria defined by the International Myeloma Working Group (IMWG), as outlined in **Table 1.1** (Rajkumar 2020). A diagnosis of active MM requires >10% malignant plasma cells in the bone marrow upon bone marrow biopsy and the presence of one or more myeloma-defining events (MDEs). MDE include evidence of end organ damage, which is often defined by the acronym, CRAB. CRAB features are common clinical manifestations of multiple myeloma which specifically refer to hypercalcemia, renal dysfunction, anemia, and lytic bone lesions. Hypercalcemia occurs mainly due to bone destruction, while excess abnormal M protein can accumulate in and damage the kidneys. The proliferation of myeloma cells in the bone marrow affects normal hematopoiesis, often resulting in a lack of red blood cells. Lytic bone lesions occur as myeloma cells stimulate the activation of bone-destroying osteoclasts and the inhibition of bone-forming osteoblasts, resulting in bone disease (Padala *et al.* 2021). The three other MDEs are malignant plasma cells >60% in the bone marrow, involved: uninvolved serum free light chain ratio >100 and >1 focal lesion detected by magnetic resonance imaging (MRI) (Rajkumar 2018, 2020).

Previous approaches to the management of MGUS and sMM mainly involved continued observation to detect signs of end organ damage. However, recent phase 3

clinical trials demonstrating delayed progression to active MM have led hematology experts to recommend the treatment of patients with high-risk sMM, as described in **Table 1.1**, with lenalidomide or a lenalidomide and dexamethasone drug combination (Mateos *et al.* 2016; Lonial, Jacobus, *et al.* 2020; Lonial *et al.* 2022; Rajkumar 2022). In the case of MGUS or low-risk sMM, continued observation of indicators of disease progression, such as elevated monoclonal protein, are recommended (Rajkumar 2022).

Table 1.1: Criteria for the diagnosis of MGUS, sMM, high-risk sMM, and MM. *Adapted from (Rajkumar 2022).

Monoclonal Gammopathy of Undetermined Significance	Smouldering Multiple Myeloma	High-Risk Smouldering Multiple Myeloma	Multiple Myeloma
• Serum monoclonal protein <3g/dL • Clonal bone marrow plasma cells <10% • No end-organ damage	• Serum monoclonal protein ≥ 3g/dL **OR** Urinary monoclonal protein ≥ 500mg per 24hr **OR** Clonal bone marrow plasma cells between 10-60% • No end-organ damage	Presence of 2 or 3 of the following: • Serum monoclonal protein ≥ 3g/dL • Involved: uninvolved serum free light chain ratio > 20 • Clonal bone marrow plasma cells >20%	• Clonal bone marrow plasma cells ≥10% OR Presence of bony or extramedullary plasmacytoma The presence of one or more myeloma defining events: • Hypercalcemia • Renal dysfunction • Anemia • Bone lesions • Clonal bone marrow plasma cells ≥60% • Involved: uninvolved serum free light chain (FLC) ratio ≥ 100 • >1 focal lesion larger than 5mm on magnetic resonance imaging (MRI)

1.2 Risk stratification of MM

Once a diagnosis of MM is confirmed, patients undergo risk stratification to determine prognosis and aid therapeutic decision-making. A combination of laboratory tests, imaging tests, and genetic tests are used to evaluate the disease characteristics of individual patients. Laboratory tests measuring serum albumin

levels, beta-2-microglobulin (B2M) levels, and serum lactate dehydrogenase (LDH) levels contribute to risk stratification. Imaging technologies such as positron emission tomography/computed tomography (PET/CT) are used to detect bone lesions and/or extramedullary plasmacytomas. Genetic tests, including karyotyping and fluorescent in situ hybridization (FISH), are used to detect hyperdiploidy, immunoglobulin translocations, and deletions or gains of distinct chromosomal regions (Hagen *et al.* 2022). The use of the high-throughput genomic technology, next generation sequencing (NGS), is becoming more common in clinical settings with the hope of advancing precision medicine in multiple myeloma (Castaneda and Baz 2019; Bolli *et al.* 2020).

Prognostic evaluation of MM was traditionally performed using the Durie-Salmon staging system (Durie and Salmon 1975). This system was replaced by the International Staging System (ISS), which has since been replaced by the Revised ISS (RISS) (Greipp *et al.* 2005; Palumbo *et al.* 2015) (**Figure 1.1**). The Durie-Salmon staging system stratified patients into three stages based on laboratory tests for hemoglobin, calcium, immunoglobulins, monoclonal protein and the presence or number of bone lesions. Subsequently, the ISS incorporated serum levels of β2-microglobulin and albumin. In 2015, a revision of the ISS included the high-risk cytogenetic abnormalities, t(4;14), t(14;16), and del(17p), and elevated serum lactate dehydrogenase (LDH) as factors associated with stage III MM. In an effort to further risk stratify the highly heterogenous intermediate stage, a second revision of the ISS (R2ISS) recently described by the European Myeloma Network considers, in addition to the factors included in the RISS, the newly identified poor prognostic indicators, gain of chromosome 1q and more than one high-risk cytogenetic abnormality present (D'Agostino *et al.* 2022). Elevated serum B2M and LDH levels, reduced albumin levels, and the presence of the high-risk cytogenetics t(4;14), t(14;16), or del(17p), are associated with high-risk multiple myeloma (Rajkumar 2022). Furthermore, extramedullary multiple myeloma presents as an independent poor prognostic factor (Stork *et al.* 2022).

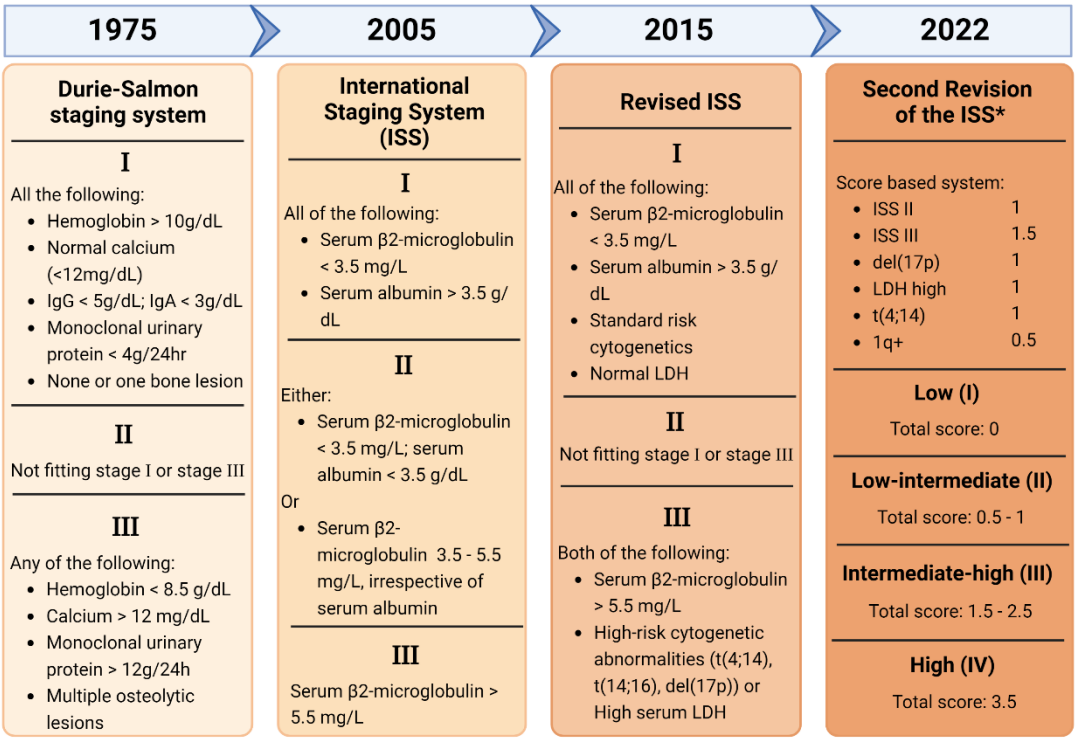

Figure 1.1: Developments in the risk stratification of multiple myeloma patients. Several different staging systems have been introduced for the risk stratification of MM patients over the last 50 years. *This risk stratification approach has not yet been globally implemented.

1.3 Genetic factors associated with multiple myeloma

The genetics of MM is inherently complex with no single genetic alteration underlying the initiation and progression of this malignancy. Instead, a multitude of genetic abnormalities including chromosomal translocations, aneuploidy, structural variants, and single nucleotide variants contribute to MM pathogenesis (Morgan *et al.* 2012). Primary genetic events including chromosomal translocations, which often involve the immunoglobulin heavy chain (IGH) gene locus, and aneuploidy, contribute to the evolution of MGUS and sMM to active myeloma. Interestingly, hyperdiploidy rarely co-occurs with IGH translocations, and MM is sometimes categorized into hyperdiploid and non-hyperdiploid MM (Chng *et al.* 2007). Secondary genetic events including copy-number abnormalities and gene mutations contribute to MM progression and the development of drug resistance (Castaneda and Baz 2019). **Table 1.2** shows the approximate frequencies of various cytogenetic abnormalities in MM.

Translocations involving IGH have been reported to occur in up to 50% of MM patients. These translocations juxtapose various oncogenes, depending on the involved loci, with the transcriptionally active enhancers of the IGH gene, resulting in oncogene overexpression. The five most common IGH translocations are t(11;14), t(4;14), t(6;14), t(14;16), and t(14;20), which affect the oncogenes, cyclin D1 (CCND1), fibroblast growth factor receptor 3/ multiple myeloma SET domain-containing protein (FGFR3/MMSET), cyclin D3 (CCND3), transcription factor Maf (MAF), and transcription factor MafB (MAFB), respectively (Kim *et al.* 2014). T(4;14), t(14;16), and t(14;20) are high-risk translocations associated with a poor prognosis, whereas t(11;14) and t(6;14) are considered standard-risk translocations (Abdallah *et al.* 2020).

Hyperdiploid genetic events typically involve trisomies of the odd-numbered chromosomes 3, 5, 7, 9, 11, 15, 19 and 21, and indicate a favourable outcome in MM. Despite one study suggesting a possible abrogation of the poor prognostic implications of t(4;14) in the presence of trisomies 3 and 5, this was contradicted by a subsequent study reporting that the co-existence of hyperdiploidy does not abrogate the poor prognostic value of high-risk cytogenetic abnormalities (Chretien *et al.* 2015; Pawlyn *et al.* 2015). Regarding non-hyperdiploid genetic events, a hypodiploid karyotype (<44 chromosomes) is associated with an adverse prognosis and the presence of more aggressive abnormalities such as deletions of 1p and 17p (Qazilbash *et al.* 2007).

IGH translocations and hyperdiploidy are early-stage oncogenic events commonly detected in MGUS and sMM prior to progression to active MM (Lionetti *et al.* 2021; Oben *et al.* 2021). In contrast, secondary oncogenic events often occur later in the course of the disease and contribute to MM progression. More complex structural variants including *MYC* translocations, gain of chromosome 1q (+1q), and deletions of chromosomes 1p, 11q, 12p, 13q, 14q, 16q, and 17p, have been identified as secondary genetic events in MM (Castaneda and Baz 2019). Gain of function mutations in oncogenes including NRAS, KRAS, and CCND1, loss of function mutations in tumour suppressor genes such as p53 and retinoblastoma 1 (RB1), and various mutations in genes associated with the nuclear factor kappa beta (NFκB) pathway promote MM progression (Chesi and Bergsagel 2013).

Table 1.2: Approximate frequency of cytogenetic abnormalities in MM.

Cytogenetic Abnormality	Frequency in MM	Reference
Primary cytogenetic abnormalities		
IGH Translocations		
t(11;14)	15-20%	(Manier *et al.* 2017; Corre, Munshi, *et al.* 2021)
t(4;14)	~15%	(Manier *et al.* 2017; Cardona-Benavides *et al.* 2021; Corre, Munshi, *et al.* 2021)
t(14;16)	2-5%	(Goldman-Mazur *et al.* 2021; Rajkumar 2022)
t(6;14)	1-2%	(Manier *et al.* 2017)
t(14;20)	~1%	(Manier *et al.* 2017; Cardona-Benavides *et al.* 2021)
Hyperdiploidy	50-60%	(Clarke *et al.* 2024)
Hypodiploidy	13-20%	(Jurczyszyn *et al.* 2021)
Secondary cytogenetic abnormalities		
1q gain	35-40%	(Manier *et al.* 2017; Hanamura 2021)
1p deletion	~30%	(van Nieuwenhuijzen *et al.* 2018; Hanamura 2022)
17p deletion	5-10%	(Hanamura 2022)
MYC translocations	15-40%	(Clarke *et al.* 2024)

1.4 Treatment of Multiple Myeloma

A breakthrough in the treatment of MM occurred in the 1960s with studies reporting a significant improvement in MM patients treated with the alkylating agent, melphalan, and corticosteroid, prednisone (Mass 1962; Hoogstraten *et al.* 1967). The combination regimen of melphalan and prednisone (MP) became the standard treatment for MM for decades until autologous stem cell transplantation (ASCT) was introduced in the 1980s (Barlogie *et al.* 1987; Kyle and Rajkumar 2008). ASCT in combination with high dose chemotherapy (HDT) significantly improved response rates of MM patients and remains the mainstay treatment for transplant-eligible patients today. ASCT involves collecting and storing the patient's own stem cells prior to HDT. Following treatment with HDT, the stem cells are administered to the patient to aid immune reconstitution (Minnie and Hill 2021). As MM is characterised by clonal heterogeneity and drug resistance, drug combinations that include therapeutics with distinct mechanisms of action have been widely adopted as the standard of care (Brioli *et al.* 2014). In the past two decades, the approval of novel therapeutics including proteasome inhibitors, immunomodulatory drugs, histone

deacetylase inhibitors (HDACi), monoclonal antibodies, chimeric antigen receptor T-cell (CAR-T) therapy, and bispecific antibodies have been central to the improved survival outcome of MM patients.

1.4.1 Current treatment options

Following an MM diagnosis, the treatment regimen is decided based on ASCT eligibility and risk stratification, as outlined in **Figure 1.2**. Historic clinical trials evaluating the efficacy of ASCT excluded patients over the age of 65, however, recent data has shown that patients over 65 can benefit from ASCT, with frailty and the presence of comorbidities being better predictors of ASCT efficacy (Child *et al.* 2003; Sharma *et al.* 2014; Parrondo *et al.* 2020). Prior to ASCT, 3-4 cycles of induction therapy is recommended, which often consists of the triplet combination of bortezomib, lenalidomide, and dexamethasone (VRd) for standard-risk MM, with the potential addition of daratumumab to the regimen in high-risk MM (Rajkumar 2022). As outlined in **Figure 1.2**, longer cycles of VRd or daratumumab, lenalidomide, and dexamethasone are recommended for the initial treatment of transplant-ineligible patients. Treatment-related toxicities also dictate therapeutic decision-making, especially in older adults who are often more susceptible to treatment-related toxicities (Mehta *et al.* 2010). For example, bortezomib-based regimens may need to be altered during the course of treatment due to the emergence of treatment-related peripheral neuropathy (Argyriou *et al.* 2008). The major treatment-related toxicity of concern in the era of immune cell activating bispecific antibodies and CAR-T cell therapies is cytokine release syndrome, a potentially life-threatening toxicity that occurs due to the rapid immune cell activation and the release of large amounts of pro-inflammatory cytokines (Hu, Li, *et al.* 2022; Moreau *et al.* 2022).

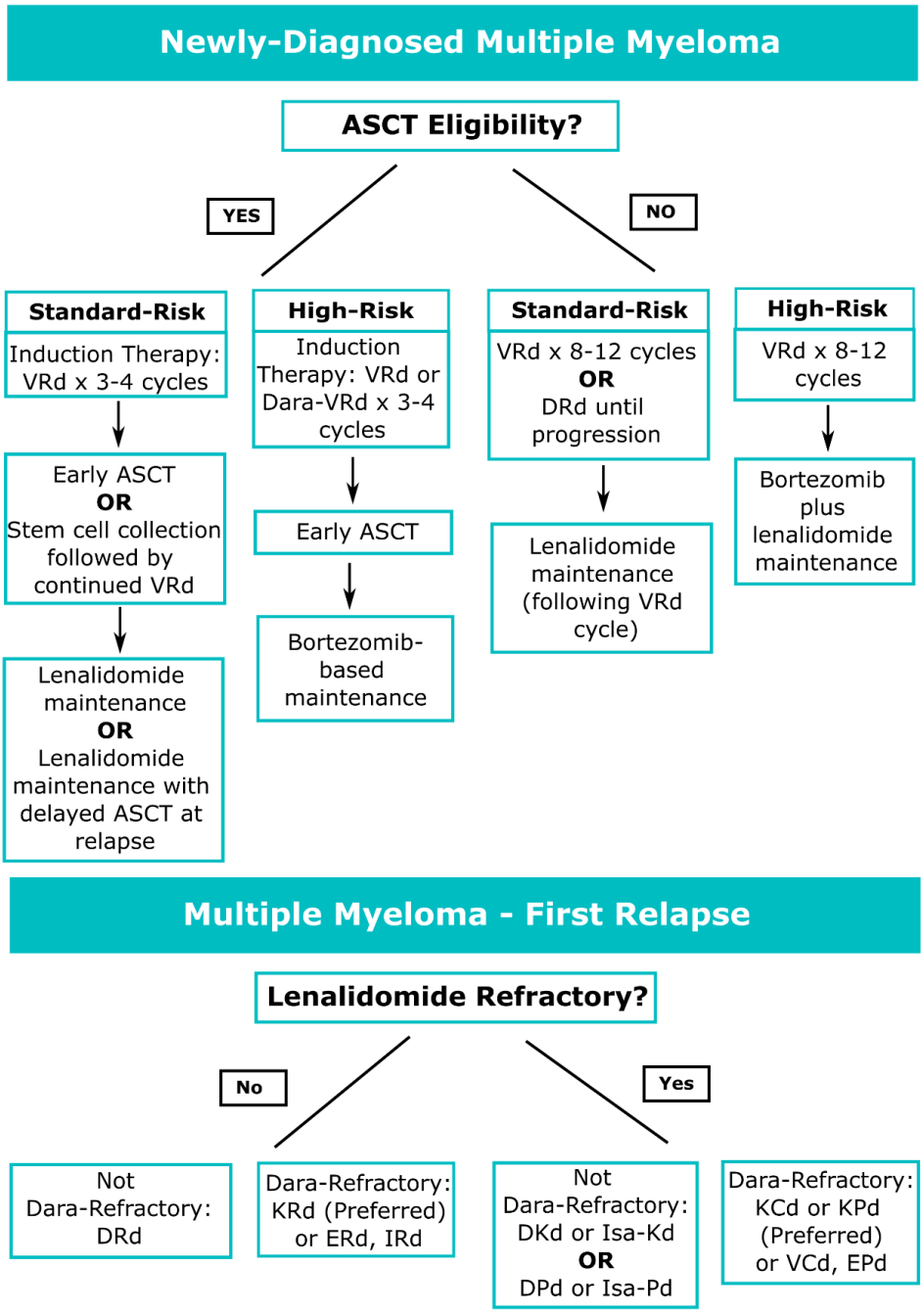

Figure 1.2: Guidance for the treatment of multiple myeloma. Treatment approaches for transplant eligible and transplant ineligible newly diagnosed multiple myeloma and multiple myeloma patients at first relapse as outlined in the 2022 Multiple Myeloma update. ASCT, autologous stem cell transplantation; VRd, bortezomib, lenalidomide, dexamethasone; Dara, daratumumab; DRd, daratumumab, lenalidomide, dexamethasone; KRd, carfilzomib, lenalidomide, dexamethasone; ERd, elotuzumab, lenalidomide, dexamethasone; IRd, ixazomib, lenalidomide, dexamethasone; DKd, daratumumab, carfilzomib, dexamethasone; Isa-Kd, isatuximab, carfilzomib, dexamethasone; DPd, daratumumab, pomalidomide, dexamethasone; Isa-Pd, isatuximab, pomalidomide, dexamethasone; KCd, carfilzomib, cyclophosphamide, dexamethasone; KPd, carfilzomib, pomalidomide, dexamethasone; VCd, bortezomib, cyclophosphamide, dexamethasone; EPd, elotuzumab, pomalidomide, dexamethasone. *Adapted from (Rajkumar 2022).

*Figure adapted from (Rajkumar 2022)

1.4.2 Proteasome inhibitors

Myeloma cells produce large amounts of M protein, making them susceptible to drugs targeting protein degradation pathways (Manasanch *et al.* 2014). The first-in-class proteasome inhibitor, bortezomib, was approved for the treatment of MM in 2003 and has since become the backbone of various clinically used combination regimens (Richardson *et al.* 2003). The second and third generation proteasome inhibitors (PIs), carfilzomib and ixazomib, respectively, have since been approved as MM treatments. PIs target the 26S proteasome, inhibiting protein degradation and exerting their anti-myeloma activity by triggering the terminal unfolded protein response, blocking the degradation of tumour suppressing proteins such as p53, and inhibiting the NFκB pathway (Berenson *et al.* 2001; Obeng *et al.* 2006; Halasi *et al.* 2014). The multiprotein 26S proteasome is made up of two components: the 20S proteolytic core which consists of two outer α-subunit rings and two inner β-subunit rings, and 19S regulatory complexes which cap one or both ends of the 20S core (Bard *et al.* 2018). Proteolytic cleavage occurs in the 20S core and is mediated by the chymotrypsin-like activity, trypsin-like activity, and caspase-like activity of the β5, β2 , and β1 subunits, respectively. Initial studies reported the β5 subunit as the rate-limiting protease of proteolysis; hence, bortezomib, carfilzomib, and ixazomib primarily target the β5 subunit of the proteasome (Arendt and Hochstrasser 1997; Heinemeyer *et al.* 1997). However, recent studies have found that at high concentrations, these PIs also co-inhibit β1 and/or β2 subunits, and co-inhibition of β5 and β2 by carfilzomib exhibits the highest cytotoxicity, even in PI-resistant MM (Kraus *et al.* 2015; Besse *et al.* 2019). PIs remain a crucial component of therapeutic regimens for MM patients.

1.4.3 Immunomodulatory drugs

The finding that MM is associated with increased bone marrow angiogenesis led to the evaluation of the anti-angiogenic agent, thalidomide, in relapsed refractory MM in 1999 (Singhal *et al.* 1999; Vacca *et al.* 1999). Thalidomide, along with the more recently developed lenalidomide and pomalidomide, are considered immunomodulatory drugs (IMiD), due to their augmentation of the immune system response. In MM, IMiDs, have been found to modulate immune cells via co-stimulating T-cells, augmenting NK cell cytotoxicity, suppressing T regulatory cells,

and inhibiting the production of pro-inflammatory cytokines including tumour necrosis factor – alpha (TNF-α) (Muller *et al.* 1996; Davies *et al.* 2001; LeBlanc *et al.* 2004; Galustian *et al.* 2009). A landmark article published in 2010, identified Cereblon (CRBN), the substrate recognition component of the DCX (DDB1-CUL4-X-box) E3 protein ligase complex, as a primary target of IMiDs (Ito *et al.* 2010). The expression of CRBN was subsequently found to be required for the anti-myeloma activity of IMiDs (Zhu, Braggio, *et al.* 2011). IMiDs bind to CRBN and modulate its substrate specificity, resulting in the degradation of the transcription factors Ikaros (IKZF1) and Aiolos (IKZF3), that have been widely reported to be essential for myeloma cell survival (Krönke *et al.* 2014). Maintenance therapy has become a crucial aspect of MM treatment in the last decade. Less intensive maintenance therapies after frontline treatment increase the depth of response and progression-free survival (PFS) (Alonso *et al.* 2020). The second generation IMiD, lenalidomide is currently the standard of care for maintenance therapy, as evaluated by various phase 3 clinical trials (Holstein *et al.* 2017; McCarthy *et al.* 2017).

1.4.4 Immunotherapy

In the last decade, the treatment of MM has moved into the new era of immunotherapy. Since the approval of rituximab for the treatment of relapsed/refractory non-Hodgkins B cell lymphoma, over 20 unconjugated monoclonal antibodies (mAbs) have received FDA approval as targeted cancer therapies (Zahavi and Weiner 2020). The introduction of mAbs as anticancer agents revolutionized cancer treatment through their ability to target tumour-specific or overexpressed antigens on the surface of cancer cells. MAbs exert their anti-cancer effects by direct blockage of ligand-receptor binding and/or indirect activation of the immune system via antibody-dependent cellular cytotoxicity (ADCC) and complement-dependent cytotoxicity (CDC) (Lyu *et al.* 2022). Several overexpressed MM-specific surface proteins have emerged as promising mAb-directed targets. The anti- cluster of differentiation 38 (CD38) monoclonal antibodies, daratumumab and isatuximab, and the anti- signaling lymphocytic activation molecule family member 7 (SLAMF7) monoclonal antibody, elotuzumab, have been approved for the treatment of MM (Gormley *et al.* 2017; Moreau *et al.* 2019; Ishida *et al.* 2022). CD38 is a cell surface protein highly expressed on myeloma cells that acts as an

adhesion molecule and ectoenzyme (Costa *et al.* 2019). SLAMF7 is a homotypic surface receptor that is highly expressed on plasma cells and expressed on other immune cells including NK cells (Wang, Sanchez, *et al.* 2016). SLAMF7 receptor engagement can have activating or inhibitory effects depending on the presence or absence of the adaptor protein Ewing's sarcoma-associated transcript-2 (EAT-2), respectively (Cruz-Munoz *et al.* 2009). As NK cells express high amounts of EAT-2, elotuzumab triggers SLAMF7 on NK cells, leading to NK cell activation and enhanced NK cytotoxicity (Collins *et al.* 2013). Elotuzumab also possesses anti-myeloma activity via ADCC and disrupting myeloma cell interactions with bone marrow stromal cells (Tai *et al.* 2008).

Developing on the success of the unconjugated mAbs described above, antibody-drug conjugates and bispecific antibodies have recently shown impressive efficacy in clinical trials in RRMM (Lonial, Lee, *et al.* 2020; Moreau *et al.* 2022). Antibody-drug conjugates (ADCs) are composed of a monoclonal antibody with specificity for a target antigen attached to a cytotoxic drug via a chemical linker. The mechanism of action of ADCs depends on their endocytosis by the cancer cell and subsequent lysosomal degradation to release the cytotoxic agent and cause cell death (Hartley-Brown and Richardson 2022). Various surface antigens including CD38, that are highly expressed on myeloma cells have been evaluated as targets for ADCs. The first ADC to receive FDA approval for the treatment of MM was belantamab mafodotin (Bela), which targets B cell maturation antigen (BCMA). BCMA is a member of the TNF superfamily that is expressed in normal B-lymphocytes and myeloma cells. Due to its almost exclusive presence on the surface of plasma cells, BCMA has become a key target for MM treatment (Mikhael 2020). Phase I and phase II clinical trials evaluating Bela in RRMM patients demonstrated promising overall response rates above 30% in a heavily pretreated patient population, many of whom were triple- or penta-refractory to several drug classes including anti-CD38 monoclonal antibodies (Trudel *et al.* 2018; Lonial, Lee, *et al.* 2020). The DREAMM-9 trial is evaluating Bela in combination with bortezomib, lenalidomide, and dexamethasone for the treatment of ASCT-ineligible newly diagnosed MM is ongoing (Usmani *et al.* 2021). Sixteen clinical trials evaluating ADCs in MM are currently active or recruiting participants.

Researchers developed on monoclonal antibodies to create bispecific molecules capable of targeting two unique epitopes on target antigens (Ma *et al.* 2021). Bispecific molecules include bispecific antibodies and bispecific T cell engagers (BiTEs) which differ only based on the BiTEs lack of an Fc domain. The majority of bispecifics developed for the treatment of MM bind to the tumour-specific antigens, BCMA or CD38, and the T cell co-receptor CD3 to directly stimulate T cell activation and subsequent myeloma cell death (Cho *et al.* 2022). The first bispecific antibody for the treatment of MM, teclistamab, was approved in early 2022 based on results from the phase 1/2 MajesTEC-1 trial (Moreau *et al.* 2022). Teclistamab simultaneously targets BCMA on myeloma cells and CD3 on T cells to induce MM cell death. Various bispecific antibodies are currently in clinical trials for the treatment of myeloma (Granger *et al.* 2023).

The introduction of chimeric antigen receptor T (CAR-T) cells was a major breakthrough in the treatment of hematological malignancies. CAR-T cell therapy involves the genetic engineering of the T cell receptor to redirect specificity for a target tumour antigen (Huang, Huang, *et al.* 2022). Two CAR-T cell therapies, idecabtagene vicleucel and ciltacabtagene autoleucel, targeting BCMA have been approved for the treatment of RRMM (Munshi *et al.* 2021; Martin *et al.* 2023). The remarkable efficacy demonstrated by immunotherapeutics in the treatment of MM suggests a central role for this class of biologics in future MM therapeutic regimens.

1.5 The bone marrow microenvironment in MM

1.5.1 The bone marrow microenvironment and B cell development

The bone marrow microenvironment (BME) is a complex cellular system comprising of hematopoietic and non-hematopoietic cells along with soluble factors and matrix proteins that interact to sustain hematopoiesis (Sánchez-Lanzas *et al.* 2022). The highly vascularized and innervated architecture of the bone marrow supports the production of hematopoietic cells. The complexity of the BME is heightened by the presence of multiple specialized niches which coordinate to regulate hematopoietic stem cell (HSC) maintenance, self-renewal, differentiation into myeloid and lymphoid lineages, and proliferation (Ayhan *et al.* 2021). The composition of these

niches remains poorly understood although the BM can largely be classified into the endosteal and vascular niches (Ashok *et al.* 2022).

B lymphocytes originate in the bone marrow, developing from HSCs in a multistep maturation process. Early B cell development in the bone marrow results in the generation of IgM-expressing immature B cells which migrate from the bone marrow to secondary lymphoid organs for maturation where they become mature B cells (Tsai *et al.* 2019). Upon activation, mature B cells enter a highly specialized, transient structure known as the germinal centre. Within the germinal centre, B cells undergo class switching, somatic hypermutation, and clonal expansion facilitating the differentiation of B cells with receptors of high affinity for the activating antigen into memory B cells or terminally differentiated plasma cells. Antibody-secreting plasma cells return to the bone marrow where they become long-lived plasma cells persisting within specialized regions of the bone marrow for extended periods of time (Roth *et al.* 2014). The sustained survival of plasma cells is considered dependent on cellular interactions and soluble factors within the BME (Cassese *et al.* 2003). This observation affirms the central role of the bone marrow niche in MM development and myeloma cell survival.

1.5.2 Cellular and soluble interactions in MM

The impact of the tumour microenvironment in cancer progression has long been established and reviewed (Anderson and Simon 2020; Baghban *et al.* 2020). In MM, the composition of the BME is altered to create a pro-tumorigenic milieu in which cell-to-cell interactions and secreted cytokines and growth factors promote MM cell proliferation and survival (García-Ortiz *et al.* 2021). The interaction between myeloma cells and cells of the BME including mesenchymal stromal cells, bone marrow stromal cells (BMSCs), osteoclasts, osteoblasts, adipocytes, myeloid cells, and lymphoid cells activates/suppresses various signalling pathways regulating the immune response, angiogenesis, and cell adhesion (Hou *et al.* 2019).

Within the BME, myeloma cells adhere to bone marrow stromal cells (BMSCs) stimulating pro-tumorigenic signalling pathways which directly or indirectly promote myeloma progression (Xu *et al.* 2018). The cell-to-cell interaction between myeloma cells and BMSCs is mediated via the expression of adhesion molecules

including vascular cell adhesion molecule 1 (VCAM1) and intercellular adhesion molecule 1 (ICAM1) on BMSCs and integrins such as integrin alpha 4 (ITGA4) and integrin beta 1 (ITGA1) on myeloma cells (Uchiyama *et al.* 1992, 1993). Physical cell contact between BMSCs and myeloma cells has been widely reported to contribute to the development of cell-adhesion mediated drug resistance (CAM-DR) (Nefedova *et al.* 2003). In addition, this cellular interaction activates signalling pathways which stimulate the secretion of soluble factors into the tumour microenvironment which provide growth and survival signals to MM cells (Huang *et al.* 2021).

Bone formation is tightly regulated by a balancing crosstalk between bone-resorbing osteoclasts and bone-forming osteoblasts (Roodman 2009). In MM, this crosstalk is dysregulated leading to lytic bone lesions which increase disease burden and morbidity. Cellular interactions between myeloma cells and osteoclasts simultaneously stimulate osteoclast activation while promoting myeloma cell growth and survival (Garrett *et al.* 1987; Abe *et al.* 2004; Lee *et al.* 2004). A key pathway implicated in MM-associated bone disease is the receptor activator of NFκB (RANK)/ receptor activator of NFκB ligand (RANKL)/ osteoprotegerin (OPG) system. RANK binding to RANKL promotes osteoclastogenesis whereas OPG acts as an antagonist for RANKL, preventing binding to RANK (Sezer *et al.* 2003). Cell-to-cell contact between myeloma cells and bone marrow stromal cells stimulates BMSCs expression of RANKL while simultaneously inhibiting OPG secretion (Giuliani *et al.* 2001; Pearse *et al.* 2001). In addition, syndecan 1 (CD138), which is highly expressed on myeloma cells, can bind OPG leading to its internalization and lysosomal degradation (Standal *et al.* 2002). This activation of osteoclasts creates a positive feedback loop, whereby increased osteoclast activation subsequently promotes myeloma cell proliferation, immunosuppression, and angiogenesis (Hecht *et al.* 2008; Tai *et al.* 2018).

Two of the most important soluble mediators contributing to MM survival and proliferation in the bone marrow are B-cell-activating factor (BAFF) and A proliferation-inducing ligand (APRIL). BAFF and APRIL are members of the tumour necrosis factor (TNF) superfamily, that are predominantly expressed by osteoclasts within the BME (Abe *et al.* 2006). The binding of these factors to

abundantly expressed receptors on MM cells such as BCMA, a common target of current immunotherapeutics, triggers the activation of nuclear factor- kappaB (NF-κB), protein kinase B (AKT), and mitogen activated protein kinase (MAPK) pathways to promote MM growth and survival (Moreaux *et al.* 2004). Interleukin-6 (IL6) is a cytokine with a well-established role as a proliferative and survival factor in MM. IL6 is mainly secreted by cells within the BME, notably BMSCs, but is also produced by MM cells in some cases (Kawano *et al.* 1988; Klein *et al.* 1989). Other soluble factors within the BME with roles in MM pathogenesis include stromal cell-derived factor-1 (SDF-1), tumor necrosis factor alpha (TNF-α), interleukin-17 (IL-17), vascular endothelial growth factor (VEGF) insulin-like growth factor-1 (IGF-1).

1.6 Drug resistance in Multiple Myeloma

The FDA approval of over ten new myeloma treatments since 2010 has seen improvements in progression free survival (PFS) and overall survival for MM patients. However, multiple myeloma remains an incurable malignancy mainly due to repeated relapses as patients develop resistance to current therapeutics. Intrinsic and extrinsic mechanisms play a role in the drug resistance of MM cells (**Figure 1.3**) (Solimando *et al.* 2022). Furthermore, the inherent intratumoral heterogeneity associated with MM contributes to the selection of resistant subclones which subsequently become the dominant myeloma clone in a process known as clonal evolution (Salomon-Perzyński *et al.* 2021).

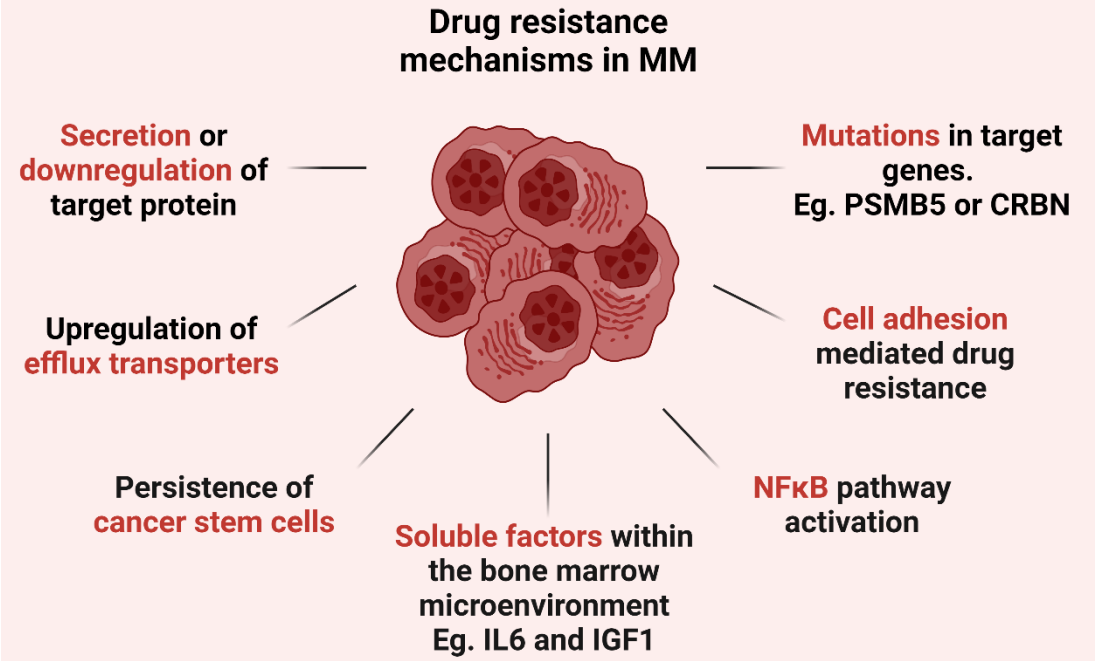

Figure 1.3: Mechanisms of drug resistance in multiple myeloma. Intrinsic mechanisms include mutations of target genes, upregulation of efflux transporters, secretion of target proteins, and NFκB pathway activation. Extrinsic mechanisms include cell adhesion mediated drug resistance and soluble factors within the bone marrow microenvironment. The persistence of myeloma stem cells which are intrinsically resistant to many chemotherapeutics can also lead to drug resistance. PSMB5, proteasome 20S subunit beta 5; CRBN, cereblon; IL6, interleukin 6; IGF, insulin growth factor 1.

1.6.1 General mechanisms of drug resistance

The overexpression of drug efflux pumps, which remove chemotherapeutic drugs from cancer cells, is a common multidrug resistance mechanism (Gottesman and Pastan 2015). This abnormal transport of drugs occurs due to the overexpression of ATP-binding cassette (ABC) transporters, such as P-glycoprotein (P-gp), ATP-binding cassette sub-family G member 2 (ABCG2) and major vault protein (MVP) (Grogan *et al.* 1993; Rimsza *et al.* 1999; Turner *et al.* 2006). Drugs targeting drug efflux pumps have been developed and have demonstrated some promise in re-sensitizing drug-resistant myeloma cells, however none have been approved for the treatment of MM (Muz *et al.* 2017; Besse *et al.* 2018). Moreover, a study evaluating the efficacy of combining proteasome inhibitors and P-gp inhibitors in PI-resistant MM cell lines indicated no increase in the efficacy of bortezomib and carfilzomib (Mynott and Wallington-Beddoe 2021). Thus, other mechanism of resistance may contribute more to PI resistance in MM.

1.6.2 Resistance to proteasome inhibitors

Genetic mutations in drug target genes or signalling pathways constitutes intrinsic mechanisms of resistance to MM therapeutics. Mutations in the PSMB5 gene which encodes the proteolytically active β5 proteasome subunit and is the main target of the proteasome inhibitors, bortezomib and carfilzomib, have been identified in bortezomib-resistant cell lines (Oerlemans *et al.* 2008). In addition, a recent study validated the presence of four somatic mutations associated with bortezomib resistance in the PSMB5 gene of an MM patient undergoing prolonged bortezomib treatment, while also highlighting the process of clonal evolution in MM by identifying an increased incidence of PSMB5 mutations in a relapsed MM patient who had received prolonged bortezomib treatment (Barrio *et al.* 2019).

Another intrinsic mechanism of PI resistance is compensatory via the activation of the aggresomal protein pathway, which provides an alternative mechanism to the proteasome for the clearance of proteins (Kumar and Rajkumar 2008). The histone deacetylase (HDAC), HDAC6, facilitates aggresomal degradation by recruiting ubiquitinated proteins and transporting them to aggresomes where they are subsequently subjected to lysosomal degradation (Kawaguchi *et al.* 2003). The combination of panobinostat, a pan-HDAC inhibitor, with bortezomib and dexamethasone as a treatment for MM received FDA approval based on the PANORAMA-1 trial (San-Miguel *et al.* 2016). Combining panobinostat and bortezomib blocks proteasomal degradation and the activation of the aggresome/autophagy pathway by inhibiting the HDAC6-mediated transportation of ubiquitinated proteins to aggresomes, resulting in a synergistic effect and improved efficacy (Hideshima *et al.* 2016; Vogl *et al.* 2017). Heat shock proteins (HSPs) act as molecular chaperones that facilitate protein folding and maintain cellular protein homeostasis (Hu, Yang, *et al.* 2022). The upregulation of HSPs has been reported to contribute to bortezomib resistance by increasing the tumour cells' ability to deal with misfolded proteins. Several HSPs including glucose-regulated protein 78 (GRP78), heat shock protein 90 (HSP90), and heat shock protein 27 (HSP27), have been implicated in bortezomib resistance in MM (Mitsiades *et al.* 2002; Chauhan *et al.* 2003; Malek *et al.* 2014).

The bone marrow microenvironment can promote drug resistance via CAM-DR and the secretion of soluble factors that contribute to drug resistance (Meads *et al.* 2009). BMSC binding to MM cells stimulates the production and secretion of IL6 from BMSCs which subsequently promotes bortezomib resistance through STAT3 pathway activation (Chauhan *et al.* 1996; Chong *et al.* 2019). BMSCs have also been reported to increase NF-κB activity in MM cells which induces PI-resistance through the activation of pro-survival signalling (Markovina *et al.* 2008a). Interestingly, exosomes derived from BMSCs have also been found to promote survival and induce drug resistance (Wang, Hendrix, *et al.* 2014).

1.6.3 Resistance to immunomodulatory drugs

As described above, immunomodulatory drugs have immune-modulating functions in addition to the ability to alter the substrate specificity of CRBN. As CRBN is required for IMiD activity against MM cells, decreased expression of CRBN in cell lines has been associated with reduced response to IMiDs (Zhu, Braggio, *et al.* 2011; Huang *et al.* 2014). CRBN mutations have also been implicated as mechanisms of IMiD resistance. Recent comprehensive genomic analyses have identified various genetic abnormalities within the CRBN gene in MM patients refractory to IMiDs (Kortüm *et al.* 2016; Gooding *et al.* 2021). Another mechanism of IMiD resistance involves the interaction of the substrate binding competitors, RUNX1 and RUNX3, with CRBN which blocks the CRBN-IKZF1/3 interaction and subsequent degradation of IKZF1 and IKZF3 (Zhou *et al.* 2019).

Resistance to IMiDs can also develop independently of abnormalities associated with CRBN. Similarly to PI-resistance, increased IL6 expression and STAT3 pathway activation contribute to IMiD resistance (Zhu *et al.* 2019). A recent proteomic analysis discovered a link between cyclin dependent kinase 6 (CDK6) upregulation and IMiD resistance, providing a rationale for the inhibition of CDK6 in IMiD resistance MM (Ng *et al.* 2022). The immune cell activating mechanism of IMiDs can also be obstructed due to immune cell exhaustion within the BME (Neri *et al.* 2018; Lucas *et al.* 2020).

1.6.4 Resistance to monoclonal antibodies

The introduction of monoclonal antibodies as MM therapeutics has resulted in improved clinical outcomes – however, resistance remains an issue. As mAbs target cell surface receptors, a common mechanism of resistance is the reduction of cell surface levels of the target protein by intrinsic downregulation of the target gene, target endocytosis, or releasing extracellular vesicles expressing the target (Saltarella *et al.* 2020). Low expression of the target of daratumumab and isatuximab, CD38, is associated with a poor clinical response (Nijhof *et al.* 2016). However, a significant reduction in CD38 expression has been observed upon exposure to daratumumab, indicating the involvement of other mechanisms in daratumumab resistance (Krejcik *et al.* 2017). The expression of CD38 on other immune cells, including NK cells, can lead to off-target effects whereby NK cells are depleted within the BME which may impact NK-mediated antibody-dependent cell-mediated cytotoxicity (ADCC), although this has not been proven (Casneuf *et al.* 2017). Indeed, the phenotype of NK cells seems to have more of an impact on the development of daratumumab resistance as a recent study reported a higher proportion of NK cells with an exhausted/activated phenotype (TIM-3^+, HLA-DR^+ NK cells) in MM patients not responding to daratumumab (Verkleij *et al.* 2023). Similar drug resistance mechanisms have been reported for other targeted immunotherapies (Li, Zhang, Cao, *et al.* 2023).

1.6.5 *Ex vivo* screening methods for assessing drug resistance

With drug resistance representing a serious unmet need in MM, functional precision medicine has garnered increasing attention as a method to evaluate drug resistance and guide clinical decision making in a personalized manner. Functional precision medicine in oncology often refers to the use of an *ex vivo* drug screening approach to evaluate the therapeutic efficacy of numerous drugs on primary tumour cells (Letai 2022). This technique is often combined with molecular analyses in an effort to identify molecular phenotypes linked to drug response. Various *ex vivo* drug screening methods have been developed in recent years.

Ex vivo drug testing has commonly been performed using bulk viability-based assays which quickly generate large amounts of data in a robust and efficient manner.

However, bulk viability-based assays are limited in their inability to identify small resistant sub-clones and their endpoint measurement whereby responding or non-responding cells may be missed due to timings (Cetin *et al.* 2017; Kimmerling *et al.* 2018; Rosenquist *et al.* 2023). Therefore, more advanced technologies including single-cell analysis have been developed to evaluate therapeutic susceptibility in blood cancers. For example, Spinner and colleagues developed an high-throughput flow cytometry-based *ex vivo* drug sensitivity screening platform that facilitates the assessment of both cytotoxicity and cell differentiation (Spinner *et al.* 2020). Further research using this platform found that *ex vivo* drug sensitivity correlates with the clinical response of paediatric AML patients who received conventional chemotherapy (Strachan *et al.* 2022). A recent study reported a single-cell image-based *ex vivo* drug testing approach, termed pharmacoscopy, as a clinically relevant strategy to improve treatment decision-making in MM (Kropivsek *et al.* 2023). This technique represents a fast, high-throughput, automatable approach to evaluate drug response by combining single-cell, spatial and morphologic resolution (Heinemann *et al.* 2022).

The area of precision medicine in haematological malignancies is rapidly evolving. Functional precision medicine approaches are currently being evaluated in the clinical setting and developments in downstream omics technologies has improved our ability to analyse the molecular phenotype of treatment refractory patients (Rosenquist *et al.* 2023).

1.7 Extramedullary Multiple Myeloma

Extramedullary multiple myeloma (EMM) is a less frequent, but aggressive subtype of MM, driven by the ability of a sub-clone to grow independently of the BM microenvironment, and is often characterised by increased clonal proliferation, evasion of cell death, and resistance to treatment, leading to a poor prognosis (Bhutani *et al.* 2020) (**Figure 1.4**). There has been some confusion surrounding the nomenclature of extramedullary multiple myeloma or extramedullary disease (EMD), with some studies including paraskeletal lesions, which arise from the expansion of tumour masses from the bone into the soft tissue of the parasketetal area, within the definition of EMD (Wu *et al.* 2009; Gagelmann *et al.* 2018; Jagosky and Usmani 2020). Other studies have defined EMM as solely the presence of distal

organ or soft-tissue lesions resulting from the hematogenous spread of myeloma cells from the bone marrow (Short *et al.* 2011; Bladé *et al.* 2022a). However, the general consensus, with the support of a recent expert review, defines two types of EMD: paraskeletal involvement derived from bone lesions and EMM of soft tissues derived from hematogenous spread (Rosiñol *et al.* 2021). Despite the presence of malignant plasma cells outside the bone marrow, solitary plasmacytomas and plasma cell leukemia are considered distinct entities and are not considered EMM (Bhutani *et al.* 2020).

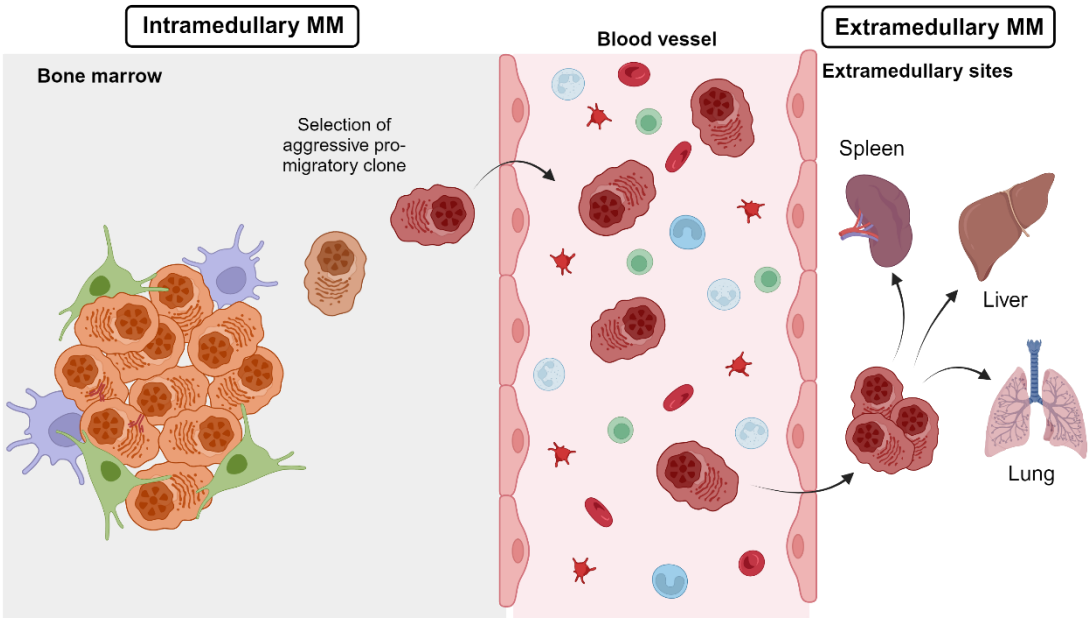

Figure 1.4: Extramedullary multiple myeloma. Schematic illustrating the development of extramedullary multiple myeloma via the migration of myeloma cells into the circulatory system followed by extravasation into soft tissue or organs where myeloma cells proliferate and develop into extramedullary lesions.

1.7.1 Incidence

The true incidence of EMM which arises from hematogenous spread (known as EMM from here on) is difficult to ascertain as studies often use varying definitions of EMM and varying diagnostic methods (Short *et al.* 2011). The incidence of EMM was reported to increase in the era of novel agents, leading to speculation that combined PI and IMiD-based therapeutic regimens inadvertently select for aggressive MM clones with a higher capacity for extramedullary spread (Varettoni *et al.* 2010). However, a comprehensive study by Varga et al., revealed no evidence of increased risk of EMM following front-line treatment with lenalidomide and bortezomib combinations (Varga *et al.* 2015). The increased incidence is likely due

to improvements in the sensitivity of imaging technologies as well as the longer survival rates of MM patients (Bansal *et al.* 2021). EMM can be detected at diagnosis (primary EMM) or at relapse (secondary EMM), with a higher incidence of secondary EMM compared to primary EMM (Bladé *et al.* 2022a). In a review of over 1000 patients with NDMM in 2003, only 4 patients (0.4%) presented with extramedullary lesions whereas a 2011 study of 174 patients, found 3 patients (1.7%) presented with EMD at diagnosis whereas 13 patients (7.5%) developed EMD during the course of treatment (Kyle *et al.* 2003; Short *et al.* 2011). The incidence of EMM at diagnosis ranges from 0.4% to 4.8%, while the incidence in RRMM ranges from 3.4% to 14% (Kyle *et al.* 2003; Pour *et al.* 2014; Deng, Xu, *et al.* 2015).

1.7.2 Diagnosis, prognosis, and treatment of EMM

Whole body magnetic resonance imaging (MRI) and positron emission tomography/computed tomography (PET/CT) have been recommended as imaging technologies capable of detecting extramedullary lesions (Mesguich *et al.* 2022). A recent consensus statement from the IMWG recommends the use of flourine-18 fluorodeoxyglucose PET/CT (^{18}F-FDG PET/CT) during the diagnostic work-up of MM patients with suspected extramedullary or solitary plasmacytomas (Cavo *et al.* 2017). One of the main advantages of ^{18}F-FDG PET/CT is the ability to discriminate metabolically active extramedullary sites from metabolically inactive lesions. Following the detection of an extramedullary plasmacytoma, an EMM diagnosis is confirmed by biopsy (Touzeau and Moreau 2016).

The presence of extramedullary lesions is an independent poor prognostic factor associated with significantly shorter PFS and OS (Usmani *et al.* 2012; Kraeber-Bodéré *et al.* 2022). Several studies have reported a worse prognosis in patients with soft tissue EMM when compared to MM patients with paraskeletal involvement (Zhou *et al.* 2020; Jiménez-Segura *et al.* 2022). Varying PFS and OS rates have been reported for EMM over the years (Bladé *et al.* 2022a). A comprehensive, retrospective study by the European Society for Blood and Marrow Transplantation (EBMT) found 139 of the 3744 NDMM patients identified presented with EMM. The 3-year PFS and OS for EMM patients was significantly worse at 39.9% and 58%, respectively, compared to 50% and 77.7%, respectively, for patients with

paraskeletal involvement, and 47.9% and 80.1%, respectively, for MM patients without extramedullary involvement. Gagelmann et al. also reported that EMM patients with multiple sites of extramedullary involvement showed a significantly reduced 3-year PFS when compared to those with single site involvement (Gagelmann *et al.* 2018). In RRMM, a multicenter retrospective study evaluating the outcome of MM patients with extramedullary and paraskeletal involvement found that patients diagnosed with EMM at relapse had the worst prognosis with a PFS of 13.6 months and OS of 11.4 months. Patients presenting with EMD at diagnosis have an improved PFS and OS of 38.9 and 46.5 months, respectively, compared to EMD diagnosed at relapse (Beksac *et al.* 2020).

Several reviews and recommendations focusing on how best to treat patients with extramedullary lesions agree that an aggressive treatment approach is required (Touzeau and Moreau 2016; Li, Ji, *et al.* 2022; Li, Sun, *et al.* 2022). As of the time of writing, no prospective clinical trials focusing specifically on EMM patients have been published. Therefore, there are currently no specific, targeted therapeutic regimens for the treatment of EMM. Current literature points to poor responses to current MM therapeutics, and the lack of prospective studies specific to EMM patients hampers a clinician's ability to make strong treatment recommendations. In addition, despite the success of immunotherapies for the treatment of MM, preliminary studies indicate that the long-term efficacy of these treatments is significantly worse in patients with EMM compared to MM patients without extramedullary spread (Jelinek *et al.* 2022; Li, Liu, *et al.* 2022a). It is clear that novel therapeutic strategies are required to improve the outcome of EMM patients.

Despite the poor prognosis associated with EMM, a literature review of EMD in MM patients revealed a lack of articles focused on the molecular pathogenesis of extramedullary transition. Due to the rarity of EMM and the heterogeneous locations of extramedullary lesions, case studies are often published (Xie *et al.* 2015; Markovic *et al.* 2019; Tyczyńska *et al.* 2023). Therefore, little is known about the molecular mechanisms that underly the development of EMM. Section 5.1 provides further information on current literature related to the molecular mechanisms associated with EMM.

1.8 Precision medicine using proteomics techniques

Developing precision medicine approaches has become an objective of many scientists and clinicians who strive for a more personalized approach to the treatment of cancer. Precision medicine uses molecular information from genomics, proteomics, transcriptomics, in addition to lifestyle and environmental information from an individual to improve health outcomes by preventing, diagnosing, and treating disease (Lancet 2021). In recent years, there have been major technological improvements in the proteomics field with the availability of various competent technologies and more robust workflows which are consistently bringing us closer to bridging the gap between laboratory-based research and clinical applications (**Figure 1.5**). Over 20 drugs are FDA approved for the treatment of multiple myeloma; and with the high likelihood of patients becoming resistant to various drugs, it is crucial patients receive an appropriate treatment course that provides the best chance of a long-term response. Unfortunately, MM is still treated empirically with conventional myeloma therapies, and despite various cytogenetic variants of MM being identified, no targeted therapies are currently approved for the treatment of these subgroups. The biggest challenge facing the implementation of precision medicine approaches in MM is the inherent heterogeneity within the tumour microenvironment which often cultivates various sub-clones with distinct molecular characteristics that may become dominant over the course of the disease (Pan and Richter 2022).

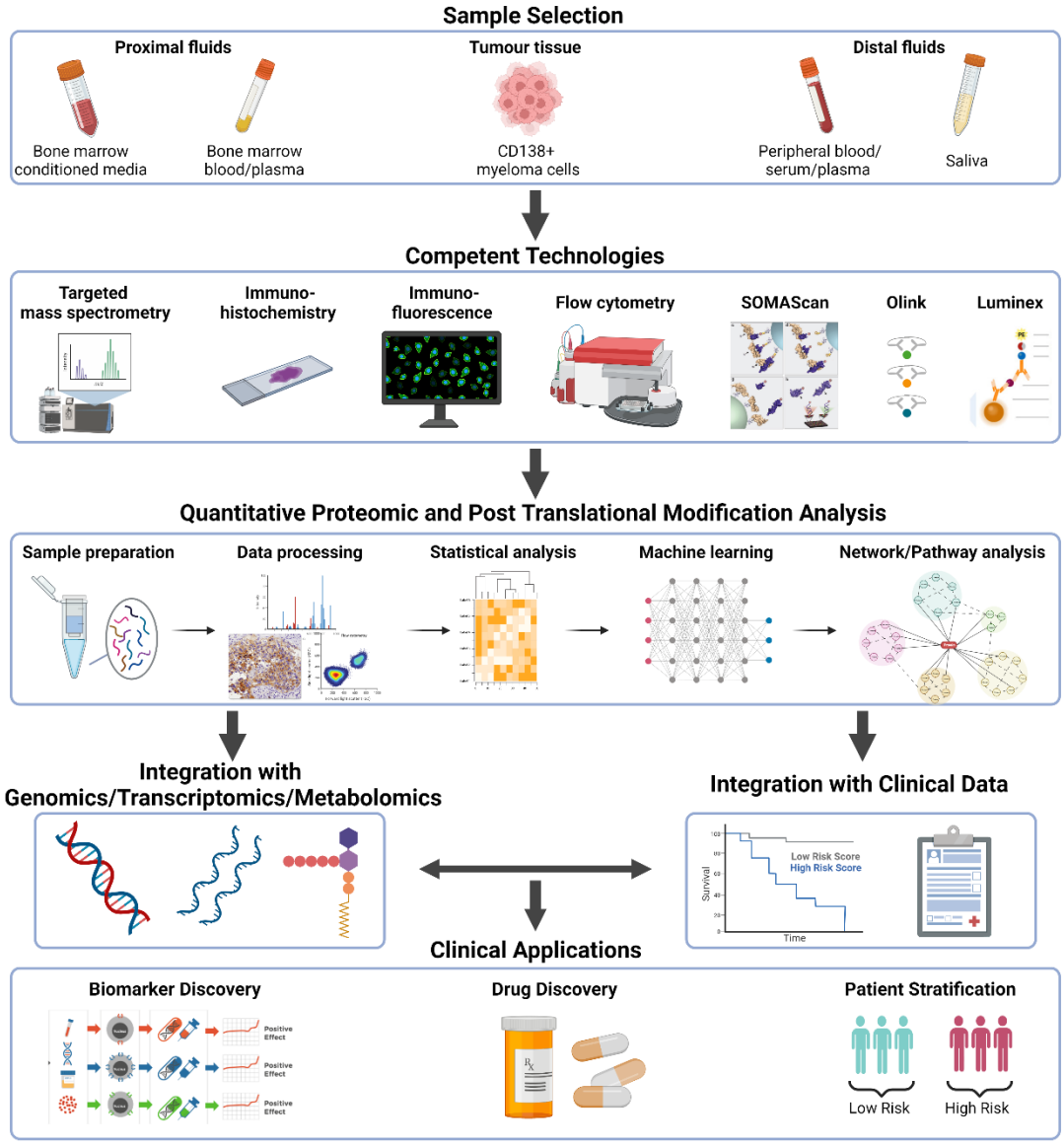

Figure 1.5: Proteomic techniques contributing to precision medicine. This figure highlights the process for applying proteomic-based precision medicine approaches in a clinical setting. Proteins can be detected and quantified in various biological samples by competent proteomic technologies. The data generated from these studies can be analysed and integrated with clinical data and other "omic" technologies to contribute to clinical applications.

*Figure was adapted from (Correa Rojo *et al.* 2021).

1.8.1 Biomarkers

Biomarkers are measurable indicators that can identify a specific physiological or pathological process. In the era of precision medicine, biomarkers are required to help tailor treatment regimens and improve clinical outcomes for individual patients. Protein biomarkers can serve as diagnostic indicators, prognostic indicators, markers for monitoring disease progression, and as predictive markers to predict patients'

response to treatment (Ou *et al.* 2021). Evaluating protein biomarkers in patient samples has the potential to improve health outcomes by contributing to an earlier diagnosis, an accurate prognosis, a disease monitoring regimen, and the selection of therapeutic regimens that individual patients are most likely to respond to. Valuable protein biomarkers can be identified in tissues and biofluids, although biofluids such as plasma, serum, saliva, and urine, are often preferred due to the ease of longitudinal sampling, low cost, and minimally invasive nature of sample collection in comparison to tissue biopsies (Marrugo-Ramírez *et al.* 2018). Notably, MM patients must undergo a highly invasive and painful bone marrow biopsy procedure to obtain tumour tissue, thus highlighting the need for biofluid-based biomarkers in MM. The discovery of novel proteomic biomarkers in biofluids can be challenging due to highly dynamic protein concentration ranges, particularly in serum and plasma, which can hinder the detection of low abundant proteins. Therefore, depending on the biofluid being analysed, the proteomic target, and the analytical technique being used, additional sample preparation steps may be required to improve the likelihood of detecting clinically relevant biomarkers (**Figure 1.6**) (Dunphy, O'Mahoney, *et al.* 2021).

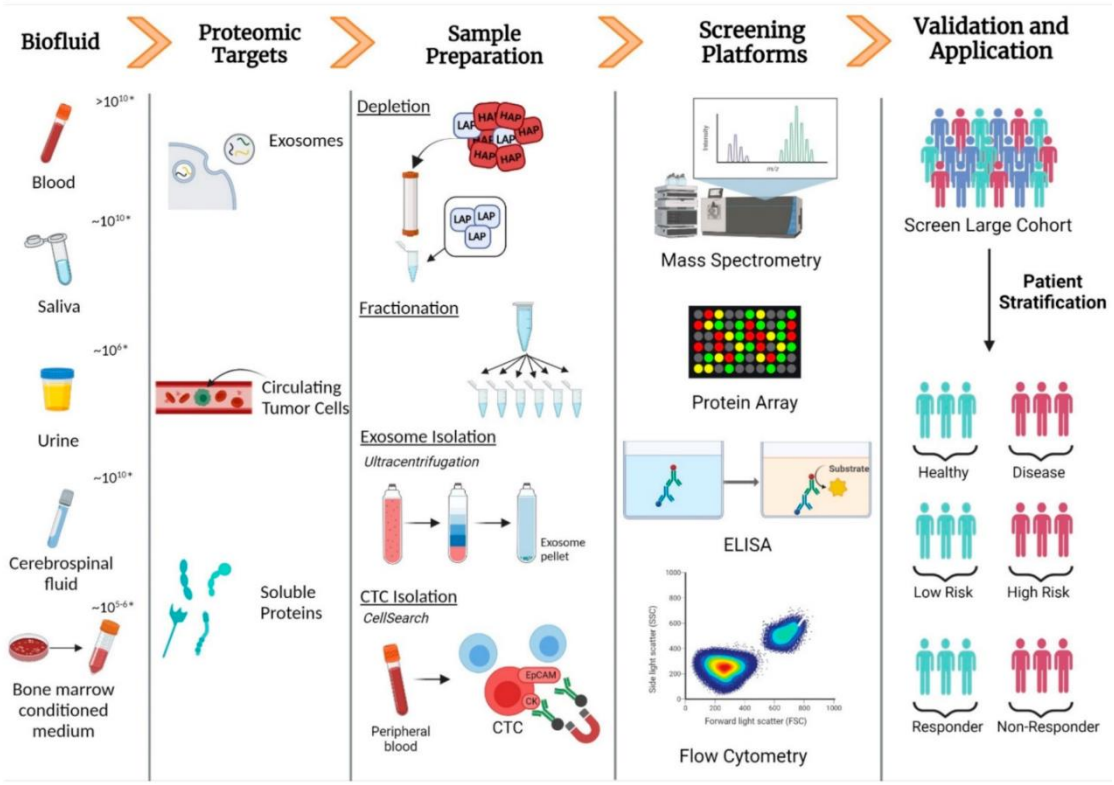

Figure 1.6: The process of biomarker discovery in biofluids and their clinical applications. Biomarker discovery involves selecting an appropriate biofluid, adapting sample preparation to optimise the detection of protein targets, choosing an appropriate screening platform and validation of the results in an independent cohort of samples. HAP, high-abundance protein; LAP, low-abundance protein; CTC, circulating tumour cell; ELISA, enzyme-linked immunosorbent assay; EpCAM, epithelial cell adhesion molecule; CK, cytokeratin. * Dynamic range of corresponding biofluid. Created using BioRender.

*Image taken from (Dunphy, O'Mahoney, *et al.* 2021)

An ideal biomarker is disease-specific, has high specificity and sensitivity in all patients, is indicative of the severity of the disease, easily distinguishable from disease-free patients and demonstrates reversibility during treatment of the disease (Wong 2011). Despite progress in the field of biomarker discovery, no such ideal biomarkers exist, and few protein biomarkers have made it into the clinic. This stems from difficulties translating biomarkers from the "benchtop" to clinical use due to low reproducibility, a lack of method standardisation, and the need for clinical-grade technologies to be used for biomarker detection in the clinic (Kearney *et al.* 2018). Recent studies have focused more on sequential validation in large cohorts of samples and the use of biomarker panels, incorporating multiple markers to improve the accuracy of a clinical test. Furthermore, technological improvements have led to more robust proteomic platforms for biomarker discovery which will undoubtedly

lead to the clinical application of proteomic biomarkers to improve the diagnostic, prognostic, and predictive power in clinical settings (Dunphy, O'Mahoney, *et al.* 2021).

1.8.2 Proteomics

Proteins are the functional products of gene expression and are required for basically all cellular activities. Proteomics involves the characterization and mapping of proteins, a complex task due to the dynamic nature of the proteome. There are various proteomic applications which aim to decipher the complex proteome including structural and spatial proteomics, analysing protein-protein interactions, and evaluating post translational modifications (PTMs). Each of these applications can provide valuable information to aid scientists elucidate disease-related mechanisms, discover novel diagnostic/prognostic biomarkers, and identify therapeutic targets (Kwon *et al.* 2021). Improvements in the analytical sensitivity of proteomics technologies in recent years has seen significant breakthroughs in identifying protein biomarkers and therapeutic targets in various diseases. The field of proteomics is constantly developing, and as single cell RNA sequencing has taken centre stage in the last decade, the emerging field of single cell proteomics has made considerable technological advancements in recent years and holds promise to unravel the heterogeneity of complex cellular samples (Bennett *et al.* 2023).

1.8.3 Mass spectrometry

One of the most powerful analytical techniques applied in proteomic studies is mass spectrometry (MS), which facilitates large-scale quantitative profiling of proteins. Untargeted proteomics, or discovery proteomics, is often performed using liquid chromatography – tandem mass spectrometry (LC-MS/MS) to quantify thousands of proteins in a single sample. The "bottom-up" proteomics approach is often applied for LC-MS/MS whereby proteins in a biological sample are cleaved by a protease prior to MS (Doll *et al.* 2019). Sample preparation requires the isolation, denaturation, reduction, and alkylation of proteins followed by protein digestion using the appropriate enzyme, often trypsin. Depending on the type of samples being analysed, additional sample preparation techniques, such as immunodepletion of plasma or serum, or peptide fractionation of complex samples, may be required to

increase the likelihood of identifying proteins of low abundance. The digested samples are then injected into the LC-MS/MS system for analysis. As the peptides enter the LC, they will bind to the non-polar stationary phase proportionally to their hydrophobicity, resulting in hydrophilic peptides eluting from the column before hydrophobic peptides. This improves accuracy by separating peptides before they enter the mass spectrometer. LC eluent is transferred to the ion source of the mass spectrometer where peptides are ionized via ionization technologies such as matrix-assisted laser desorption/ionization (MALDI) or electro-spray ionization (ESI). Following ionization, peptide precursor ions are fragmented using one of several fragmentation techniques, most commonly collision-induced dissociation (CID) or high-energy collision dissociation (HCD). The resulting product ions are characterized based on their mass-to-charge (m/z) ratios and relative abundance to produce MS/MS spectra which are matched to theoretical MS/MS spectra available on databases for peptide identification (Sinha and Mann 2020).

1.8.3.1 Label-free quantitation

Quantitative proteomics is particularly useful for precision medicine as it facilitates the comparison of protein levels in different patient cohorts, thus aiding in the detection of novel biomarkers and therapeutic targets. Quantitative data can be obtained during MS analyses using label-free or label-based techniques. These techniques have strengths and limitations, each of which may be more suitable for certain analyses or laboratories. Label-free quantitation (LFQ) refers to the use of peak intensity analysis or spectral counting for quantitation. For peak intensity analysis, the intensities of the chromatographic peptide peaks are extracted (extracted-ion chromatogram) based on the peptide precursor *m/z* ratio and compared between LC-MS/MS datasets (Ball *et al.* 2023). Spectral counting enables protein quantitation by counting the number of MS/MS spectra derived from peptides from the same protein in each LC-MS/MS dataset (Drabovich *et al.* 2013). Both label-free quantitation approaches are reliant on efficient sample preparation and reproducible liquid chromatography and mass spectrometry parameters between LC-MS/MS runs. However, LFQ is often chosen due to the relative simplicity of sample preparation, lower costs, and a higher proteome coverage (Li *et al.* 2012; Megger *et al.* 2014; Anand *et al.* 2017).

1.8.3.2 Label-based quantitation

During label-based quantitation, proteins or peptides are enzymatically or chemically labelled using differential mass tags, such as tandem mass tag (TMT) or isobaric tag for relative and absolute quantification (iTRAQ), which facilitates multiplexing of samples (Dunphy, Dowling, *et al.* 2021). The metabolic labelling technique, stable isotope labelling of amino acids in cell culture (SILAC), involves the *in vitro* labelling of peptides by growing cells in cultures with an isotopically defined medium, which can be differentiated during MS analysis. Heavy isotopic versions of naturally occurring elements, such as ^{15}N and ^{13}C, are used followed by mixing the samples and MS analysis. A drawback of SILAC is the need for metabolically active sample sources which can limit the use of this technique in clinical proteomics (Ong and Mann 2006). The isobaric labelling technologies, TMT and iTRAQ, overcome this limitation by labelling target compounds using chemical tags with identical masses. During LC-MS/MS analysis, peptide fragmentation reveals reporter ions of variable molecular weights each corresponding to a specific sample (Anand *et al.* 2017). Label-based quantitation overcomes the issue of missing values associated with LFQ, however, labelling samples often requires more complex sample preparation protocols, is more costly than LFQ, and is limited by the number of samples that can be multiplexed in a single experiment (Bantscheff *et al.* 2012).

1.8.4 Affinity-based proteomics

The field of affinity-based proteomics has seen significant improvements with the emergence of new technologies including the proximity extension assay (PEA)-based Olink platform and aptamer-based SomaScan assays (Smith and Gerszten 2017). The Olink platform uses antibody pairs conjugated to unique DNA oligonucleotides which hybridize to the matched antibody when in close proximity. This results in the generation of a unique DNA receptor sequence which can be quantified by quantitative polymerase chain reaction (qPCR) or NGS (Petrera *et al.* 2021). The recent introduction of the Olink Explore HT platform facilitates the measurement of over 5,000 proteins in a few microliters of sample. In contrast, the SomaLogic technology can measure up to 7,000 proteins by using modified single-stranded nucleotide aptamers known as SOMAmers, which bind specifically to target proteins present in a biological sample. The antibody-based Luminex platform

has also demonstrated considerable improvements with the capacity to detect up to 500 proteins in a single experiment (Shami-Shah *et al.* 2023). Affinity proteomic platforms are particularly powerful for the analysis of the complex serum/plasma proteome, which has a large dynamic range that hinders the ability of LC-MS/MS to detect low abundant proteins (Palstrøm *et al.* 2022). Plasma samples are often immunodepleted to remove high abundant proteins prior to MS analysis to improve proteome coverage (Woo and Zhang 2023).

1.8.5 Post translational modifications

Post translational modification (PTM) refers to the biochemical modification of proteins following protein synthesis, or post-translationally. PTMs are found throughout the cell and play roles in the regulation of almost all biological processes including the cell cycle, degradation, apoptosis, cell signalling, and transcription. Over 200 PTMs have been reported in eukaryotes with the most studied being phosphorylation, glycosylation, ubiquitination, sumoylation, acetylation and methylation (Yakubu *et al.* 2019). Different PTMs can stimulate different protein responses such as the activation or inhibition of enzymatic activity, interactions with other proteins, or a change in localisation (**Figure 1.7**). Aberrant post translational modification of proteins, without a change in protein abundance, can alter the normal functioning of signalling pathways and have been implicated in pathogenesis of a variety of diseases (Dunphy, Dowling, *et al.* 2021).

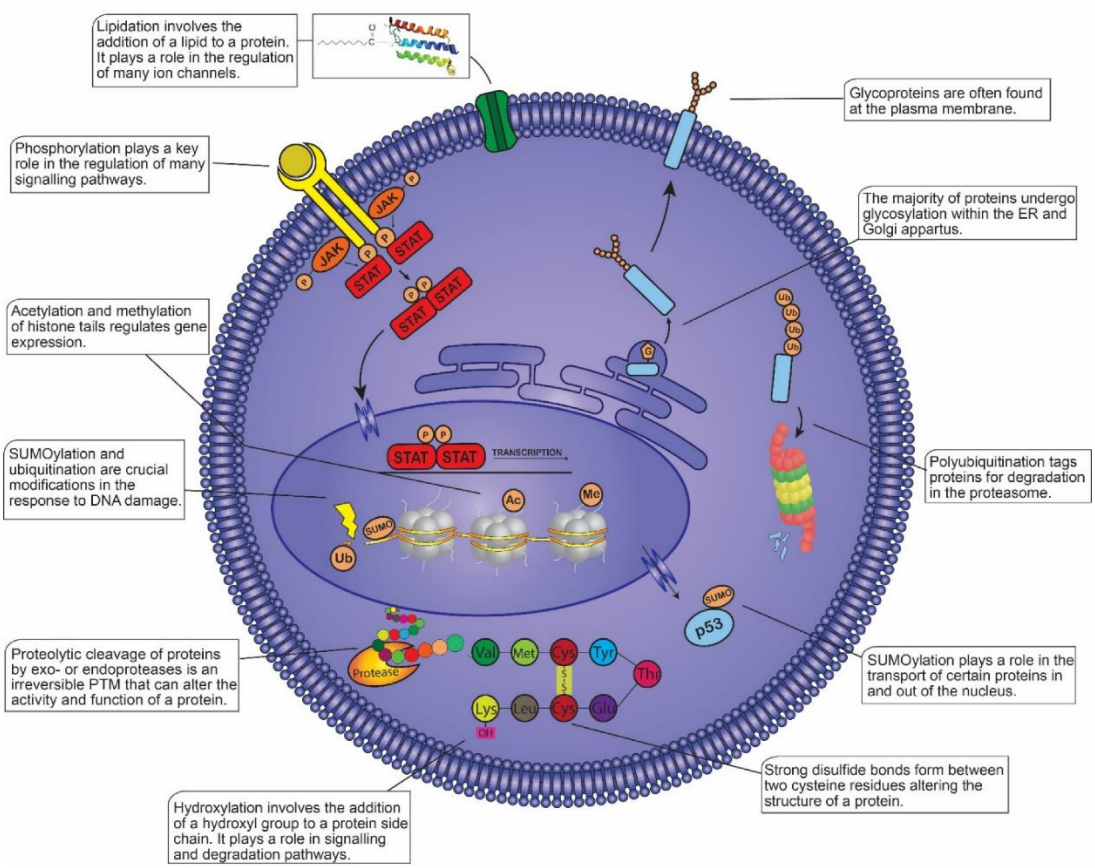

Figure 1.7: Different post translational modifications (PTMs) and their roles in the mammalian cell. PTMs are essential to maintain cellular physiology. They play a role in almost all cellular processes.

*Image from (Dunphy, Dowling, *et al.* 2021).

1.8.6 Bioinformatics

Mass spectrometry studies generate large amounts of proteomic data, with quantitative information on thousands of proteins. These large datasets require rigorous analysis using various automated programs to convert the mass spectrometer raw data into biologically meaningful results (Lavallée-Adam *et al.* 2015). Various sophisticated software such as the Mascot and Sequest search engines, are used to annotate mass spectra with peptides using protein sequence databases and spectral libraries (Brosch *et al.* 2009). Computational proteomics platforms such as Proteome Discoverer and MaxQuant simplify data analysis of mass spectrometry data by streamlining peptide identification, peptide quantitation and the assignment of peptides to their parent proteins (Palomba *et al.* 2021). Software such as Perseus also simplify the interpretation of proteomics data and

statistical analysis to identify proteins of differential abundance between groups (Tyanova and Cox 2018). Downstream data analysis of statistically significant differentially abundant (SSDA) proteins can include functional annotation and enrichment tools such as the Database for Annotation, Visualization and Integrated Discovery (DAVID) and G:profiler. Evaluating the protein-protein interactions between proteins identified in an MS experiment using specific tools such as the Search Tool for the Retrieval of INteracting Genes/Proteins (STRING), can aid the interpretation of proteomics data (Sinitcyn *et al.* 2018).

1.9 Aims of the project

Despite decades of research and the approval of numerous therapeutics, multiple myeloma remains an incurable malignancy. MM patients face a high symptom burden with end organ damage resulting in physical pain, prolonged treatment affecting mental wellbeing, and mortality (Ramsenthaler *et al.* 2016). A significant amount of research has focused on improving our understanding of myeloma pathogenesis and identifying mechanisms of drug resistance and novel biomarkers.

Proteins represent the functional unit of the cell and are the target of almost all FDA-approved targeted therapies. Many diagnostic tools, clinical tests and some therapeutics are protein-based, signifying the importance of proteomics data in identifying novel biomarkers and therapeutic targets. Major technological improvements in the proteomics field have led to more robust workflows which are continuously bring us closer to establishing clinical applications. Mass spectrometry represents a powerful analytical tool that facilitates large-scale, quantitative profiling of proteins. This allows the comparison of proteomic profiles from distinct populations to identify alterations in protein signatures. This research project aimed to use mass spectrometry-based discovery proteomics to identify aberrant protein signatures in primary multiple myeloma samples.

Chapter 3

Drug resistance remains one of the most significant barriers to the effective treatment and survival of MM patients. To determine proteomic and phosphoproteomic changes in drug sensitive and drug resistance MM, we combined *ex vivo* drug

sensitivity resistance testing (DSRT) and mass spectrometry. 20 primary MM patient CD138+ samples were tested using a panel of approximately 141 FDA-approved and investigational drugs. A label-based phosphoproteomic analysis was performed to evaluate the proteomic and phosphoproteomic alterations between those considered most and least sensitive to a variety of selected drug classes.

Chapter 4

Invasive and painful bone marrow biopsies remain the gold standard for diagnostic and prognostic applications in MM. Therefore, there is an urgent need for minimally invasive protein biomarkers of MM to predict and monitor therapeutic response. Blood-based biomarkers can easily be implemented in a clinical setting for monitoring prior to and during treatment with minimal discomfort for patients. Thus, blood plasma was obtained from patients with corresponding *ex vivo* DSRT data for proteomic analysis to identify plasma-derived markers of drug resistance/sensitivity.

Chapter 5

Extramedullary multiple myeloma is associated with a poor prognosis yet limited molecular studies have been published in the literature. At the time of writing, only one proteomics-focused study has been performed, with no mass spectrometry analyses identified in the literature. To address this research gap, a mass spectrometry-based proteomics analysis was conducted to compare the proteomic profiles within the bone marrow niche of MM patients with and without extramedullary spread.

Chapters 6 and 7

Blood-based markers of EMM may help clinicians detect extramedullary spread or aggressive disease at an earlier stage. Incorporating testing for blood-based EMM markers during routine visits could lead clinicians to perform appropriate imaging tests, such as an MRI or ^{18}F-FDG PET/CT, to detect extramedullary lesions at an earlier stage. To identify novel markers of EMM, a quantitative mass spectrometry analysis was performed on plasma samples from MM patients with and without extramedullary spread. In addition, a targeted metabolomics analysis of these plasma samples was performed to identify soluble metabolite biomarkers of EMM.

In summary, the overall aim of this thesis was to use quantitative mass spectrometry to provide in-depth proteomic profiling of MM patients stratified based on drug response and the presence of extramedullary lesions. Identifying protein signatures associated with drug resistance/sensitivity can improve our understanding of molecular mechanisms and signalling pathways that govern individual drug responses. Identifying protein signatures associated with EMM can help researchers decipher the molecular mechanisms that facilitate the escape of myeloma cells from the bone marrow and subsequent survival and proliferation of myeloma cells at extramedullary sites. Antibody-based validation methods were used to confirm changes in protein abundance and identify potential biomarkers for future validation in a larger cohort of patients, with the ultimate goal being the implementation of testing for these biomarkers in a clinical setting.

Chapter 2

Materials and Methods

2.1 General chemicals and reagents

Deionized H_2O (dH_2O) was obtained following purification of distilled water using a Millipore Milli-Q apparatus. A list of general chemicals and reagents, buffer solutions, antibodies, commercial kits, and equipment used throughout the project are provided in the tables below, respectively (**Table 2.1**, **Table 2.2**, **Table 2.3**, **Table 2.4**, **Table 2.5**).

Table 2.1: List of chemicals, reagents and consumables used throughout this project.

Name of Chemical/Reagent	Company	Identifier
Ammonium Bicarbonate	Sigma	Cat# A6141
Anhydrous acetonitrile	Sigma	Cat# 271004
Bovine serum albumin (BSA)	Sigma	Cat# A3156
Dithiothreitol (DTT)	Sigma	Cat# D9163
Dried skimmed milk	Marvel	N/A
Ethylenediaminetetraacetic acid (EDTA)	Sigma	Cat# ED
Glycine	Sigma	Cat# G7126
HEPES	Sigma	Cat# H3375
Hydrochloric acid (HCl)	Sigma	Cat# 258148
Iodoacetamide (IAA)	Sigma	Cat# I1149
Ionic detergent compatibility reagent	Thermo Fisher Scientific Inc.	Cat# 22663
Laemmli buffer	Sigma	Cat# S3401
LC-MS grade water	Thermo Fisher Scientific Inc.	Cat# 51140
Methanol	Fisher Scientific	Cat# 10675112
MOPS	Sigma	Cat# M1254
Normal goat serum	R&D Systems	Cat# DY005
Pierce™ ECL Western Blotting Substrate	Thermo Fisher Scientific	Cat# 32106
Protease inhibitors	Cell Signaling Technology	Cat# 5871
Sodium Dodecyl Sulfate (SDS)	Sigma	Cat# L3771
Sodium hydroxide (NaOH)	Sigma	Cat# S8045
Triethylammonium bicarbonate (TEAB)	Thermo Fisher Scientific Inc.	Cat# 90114
Trifluoroacetic Acid	Sigma	Cat# T6508
Trizma® Base	Sigma	Cat# T6066

Name of Chemical/Reagent	Company	Identifier
Tween® 20	Sigma	Cat# P1379
Urea	Sigma	Cat# U0631
Consumables		
Corning™ Costar™ 96-well, cell culture-treated, flat-bottom microplate	Fisher Scientific	Cat# 3595
Eppendorf® DNA LoBind tubes, 1.5ml	Sigma	Cat# EP0030108051
Eppendorf® DNA LoBind tubes, 2ml	Sigma	Cat# EP0030108078
Qubit™ assay tubes	Invitrogen	Cat# Q32856
Vivacon 500, 30,000 MWCO Hydrosart	Sartorius	Cat# VN01H22
NuPAGE™ 10%, Bis-Tris, 1.0–1.5 mm, Mini Protein Gels (10-well or 12-well)	Invitrogen	Cat# NP0301BOX Cat# NP0302BOX
PageRuler™ Plus Prestained Protein Ladder, 10 to 250 kDa	Thermo Fisher Scientific Inc.	Cat# 26619

Table 2.2: Composition of buffer/solutions used throughout this project.

Experiment	Buffer/Solution	Composition
Filter aided sample preparation for mass spectrometry	0.1M Tris/HCl, pH 8.5	In dH_2O
	8M UA	In 0.1M Tris/HCl, pH 8.5
	50mM IAA	In 8M UA
	50mM ABC	In dH_2O
	50mM HEPES, pH 8.5	In dH2O, pH adjusted using NaOH.
	LC/MS sample buffer	20% ACN, 2% TFA in dH_2O
Tandem mass tag (TMT) labelling	100mM TEAB	From 1M TEAB stock solution diluted in LC/MS grade H2O
	5% hydroxylamine	In 100mM TEAB
C18 sample clean-up	Activation solution	50% ACN, 50% LC/MS grade H_2O
	Equilibration solution/ Wash solution	2.5% ACN, 0.25% TFA made up in LC/MS grade H_2O
	Elution buffer	80% ACN in LC/MS grade H_2O
Phosphopeptide enrichment (IMAC)	Binding/ wash buffer	0.1% TFA, 80% ACN
	Elution buffer	5% ammonium hydroxide (NH4OH) in water
Western blotting	Laemmli buffer	4% SDS, 20% glycerol, 10% 2-mercaptoethanol, 0.004% bromphenol blue, 0.125 M Tris HCl, pH approx. 6.8
	1x Running buffer	12.12g Tris, 20.92g MOPS, 2g SDS, 0.3g EDTA made up to 2L with dH_2O
	1x Transfer buffer	25mM Tris, 192 mM Glycine, 20% Methanol in dH_2O
	Blocking buffer	4% non-fat dry milk, 0.05% Tween, made up in PBS

Table 2.3: List of antibodies and enzymes used throughout this project.

Name of Antibody/Enzyme	Company	Identifier
α-Actinin (D6F6) XP® Rabbit mAb	Cell Signalling Technology	Cat# 6487
Anti-mouse IgG, HRP-linked Antibody	Cell Signalling Technology	Cat# 7076
Anti-phospho Bad (Ser99) Antibody	Sigma	Cat# AB10424
Anti-rabbit IgG, HRP-linked Antibody	Cell Signalling Technology	Cat# 7074
Phospho-Filamin A (Ser2152) Polyclonal Antibody	Invitrogen	Cat# PA5-40239
Phospho-SRC (Ser17) Polyclonal Antibody	Invitrogen	Cat# PA5-105147
ProteaseMax™ Surfactant, lyophilized	Promega	Cat# V207A
Sequencing Grade Modified Trypsin	Promega	Cat# V5111
Trypsin Gold, Mass Spectrometry Grade	Promega	Cat# V5280

Table 2.4: Commercial kits used throughout this project.

Name of Kit	Company	Identifier
Pierce™ 660nm Protein Assay Kit	Thermo Fisher Scientific	Cat# 22662
Pierce™ Bovine Serum Albumin Standard Pre-Diluted Set	Thermo Fisher Scientific	Cat# 23208
High-Select™ Fe-NTA Phosphopeptide Enrichment Kit	Thermo Fisher Scientific	Cat# A32992
TMT10plex Isobaric Label Reagent Set	Thermo Fisher Scientific	Cat# 90111
Cell Death Detection ELISA^{PLUS}	Roche Diagnostics	SKU #11774425001
Proteome Purify 12 Human Serum Protein Immunodepletion Resin	R&D Systems	Cat# IDR012
DuoSet ELISA Ancillary Reagent Kit 2	R&D Systems	Cat# DY008B
DuoSet ELISA Ancillary Reagent Kit 3	R&D Systems	Cat# DY009B
Human VCAM-1/CD106 DuoSet ELISA	R&D Systems	Cat# DY809
Human Aminopeptidase N/CD13 DuoSet ELISA	R&D Systems	Cat# DY3815
Human Butyrylcholinesterase/BCHE DuoSet ELISA	R&D Systems	Cat# DY6137
Human HGF Activator DuoSet ELISA	R&D Systems	Cat# DY1514
Human alpha 2-Macroglobulin DuoSet ELISA	R&D Systems	Cat# DY1938
Human Serpin F1/PEDF DuoSet ELISA	R&D Systems	Cat# DY1177
Human Syndecan-1 DuoSet ELISA	R&D Systems	Cat# DY2780
Human S100A8/S100A9 Heterodimer DuoSet ELISA	R&D Systems	Cat# DY8226
Human Neutrophil Elastase/ELA2 DuoSet ELISA	R&D Systems	Cat# DY9167
Qubit™ Protein Assay Kit	Invitrogen	Cat# Q33211

Table 2.5: Technical and analytical equipment used throughout this project.

Equipment	Name of Device	Company
Centrifuge	Eppendorf 5417 R centrifuge	Eppendorf
Liquid Chromatography	Ultimate 3000 NanoLC system	Dionex Corporation, USA
Mass Spectrometers	Q-Exactive	Thermo Fisher Scientific
	Orbitrap Fusion Tribrid Mass Spectrometer	Thermo Fisher Scientific
Chemiluminescent Detector	G:BOX Chemi XRQ	Syngene
Other	Thermomixer Comfort	Eppendorf
	Genevac™ miVac Centrifugal Concentrator	Genevac (11574604)
	Sonoplus HD 2200	Bandelin
	Electrophoresis System	Invitrogen
	Eppendorf Biophotometer	Eppendorf
	Qubit® fluorometer version 2.0	Thermo Fisher Scientific

2.2 Patient samples

Different patient cohorts were analysed for specific sections of this thesis. Ethical approval was granted by the Mater Misericordiae University Hospital Research ethics committee (1/378/1158). For the phosphoproteomic analysis (Chapter 3), 20 bone marrow aspirates were collected from 7 diagnostic and 13 relapsed MM patients. Ethical approval was obtained from the participating hospitals in compliance with the Declaration of Helsinki. These samples were obtained from collaborators at the Institute for Molecular Medicine Finland (FIMM), University of Helsinki, Finland.

For our proteomic analysis of plasma samples stratified based on *ex vivo* drug response (Chapter 4), 44 etheylenediaminetetraacetic acid (EDTA) plasma samples were obtained from the Finnish Hematology Registry and Clinical Biobank (FHRB) with full ethical approval.

For our EMM study (Chapter 5), bone marrow mononuclear cells (BMNCs) and EDTA treated plasma from 17 patients were obtained from the FHRB. The FHRB is authorized and approved by the Finnish National Supervisory Authority for Welfare and Health (Valvira) and Finnish National Medical Ethics Committee, respectively. 4 additional serial EDTA plasma samples were obtained from the FHRB. **Table 2.6** details which patient cohorts were used in each chapter. Patient details are provided in the experimental design and methods section of subsequent chapters.

Table 2.6: Patient cohorts evaluated in each chapter of this thesis.

Chapter	Samples evaluated
3. Phosphoproteomic profiling of multiple myeloma based on ex vivo drug sensitivity resistance testing identifies distinct phosphorylation signatures associated with drug response	20 MM bone marrow aspirate samples with associated *ex vivo* drug response data
4. Using untargeted and targeted plasma proteomics to identify plasma biomarkers of therapeutic response based on ex vivo drug sensitivity resistance testing	44 MM EDTA plasma samples with associated ex vivo drug response data
5. Proteomic profiling of bone marrow mononuclear cells in extramedullary multiple myeloma	• 17 bone marrow mononuclear cell samples from MM and EMM patients • 17 EDTA plasma samples from MM and EMM patients
6. Proteomic profiling of blood plasma from multiple myeloma patients with and without extramedullary spread	• 17 EDTA plasma samples from MM and EMM patients • 44 samples of EDTA plasma with associated ex vivo drug response data
7. Targeted metabolomic analysis of blood plasma from multiple myeloma patients with and without extramedullary spread	17 EDTA plasma samples from MM and EMM patients

2.3 Bone marrow mononuclear cell isolation and cell lysis

BMNCs cryopreserved in 10% DMSO/90% serum were shipped on dry ice and stored at -80°C for 5 days. The BMNCs were thawed quickly in a 37°C water bath. Approximately 2,000,000 BMNCs were removed and washed twice with 1X phosphate-buffered saline (PBS). Cells were pelleted by centrifuging at 400 x g for 5 minutes. The supernatant was removed, and cell pellets were solubilized in 200µl of lysis buffer (4% SDS, 100mM Tris/HCl pH 7.6, 0.1M DTT, protease inhibitors). The samples were incubated at 95°C for 3 minutes, then incubated on ice for 30-60

minutes. Heating is performed to promote denaturation, reduction, and subsequent inactivation of the proteases. Samples must also be cooled prior to sonication due to the excess amount of heat created during this process. Sonication was used to disrupt the cellular membrane and shear DNA to reduce DNA interference during downstream processing. Sonication was performed using a sonication probe (Bandelin Sonopuls, Bandelin electronic, Berlin), on low power (20kHz). Samples were sonicated for 10 seconds then placed on ice for 45-60 seconds. This process was repeated three times. Samples were kept on ice for 5 minutes followed by centrifugation at 10,000 x g for 20 minutes at 4°C. The supernatant was collected in a new tube and stored at -80°C.

2.4 Protein quantitation using Pierce™ 660nm protein assay

The Pierce™ 660nm protein assay was used for protein quantitation. As samples contained greater than 0.0125% SDS, 1g of ionic detergent compatibility reagent (IDCR) was first added to 20ml of Pierce™ 660nm protein assay reagent and mixed thoroughly. A standard curve ranging from 125µg-2000µg was produced using pre-diluted bovine serum albumin (BSA) standards. 10µl of sample, pre-diluted standards and an appropriate blank were added in triplicate to separate microplate wells of a 96 well plate. 150µl of the IDCR-Pierce™ 660nm protein assay reagent mixture was added to each well. The plate was covered and mixed using the Thermomixer comfort (Eppendorf) for 1 minute at 300rpm. The plate was incubated at room temperature for 5 minutes. Absorbance readings at λ=660nm were recorded. An online ELISA Analysis tool (https://www.myassays.com/) was used to create a four-parameter logistic regression standard curve, which was subsequently used to determine the protein concentration of the unknown samples.

2.5 Protein quantitation using the Qubit™ protein assay

The Qubit™ protein assay was also used for protein quantitation. All reagents were brought to room temperature before starting the protocol. The Qubit® working buffer was prepared away from direct light via a 1:200 dilution of the Qubit® protein assay reagent in Qubit® protein assay buffer followed by thorough mixing. 10µl of each standard (Qubit® Protein Standard #1, #2, and #3) was added to 190µl of the Qubit® working buffer. Samples were diluted as required. Between 1-20µl of

sample was added to 180-199µl of Qubit® working buffer to make a total volume of 200µl. The resulting solutions were thoroughly mixed and incubated in the dark at room temperature for 15 minutes. Protein concentration was measured using the Qubit® fluorometer version 2.0 and results were multiplied by the appropriate dilution factor, if applicable.

2.6 Immunodepletion of blood plasma

EDTA plasma obtained from the FHRB was shipped on dry ice, aliquoted and stored at -80°C. Twelve highly abundant plasma proteins (alpha 1-acid glycoprotein, alpha 1-antitrypsin, alpha 2-macroglobulin, albumin, apolipoprotein A-I, apolipoprotein A-II, fibrinogen, haptoglobin, IgA, IgG, IgM, and transferrin) were depleted using the Proteome Purify 12 Human Serum Protein Immunodepletion Resin (R&D Systems). Briefly, 10µl of plasma was mixed with 1ml of immunodepletion resin for 60 minutes using a rotary shaker. The mixture was transferred to Spin-X filter units and centrifuged at 1500 x g for 2 minutes. The protein concentration of the resulting eluate was determined using the Pierce™ 660nm protein assay or the Qubit™ protein assay.

2.7 Filter-Aided Sample Preparation (FASP)

Buffer exchange and proteolytic digestion for each mass spectrometry experiment was performed using the FASP technique (Wiśniewski *et al.* 2009). Samples were subject to a series of centrifugal steps using 8M Urea (UA) and 50mM IAA to facilitate detergent removal, buffer exchange and protein alkylation. Initially, a specific concentration of protein from each sample (specified in each experimental chapter) was mixed with 200µl or 400µl of 8M UA in the spin filter unit and centrifuged at 14,000 x g for 30 minutes. 200µl of UA was added and centrifuged at 14,000 x g for 15 minutes. Flow-through was discarded. 100µl of 50mM IAA was added to each filter unit, mixed at 600rpm for 1 minute in a thermomixer and incubated at room temperature for 20 minutes. Samples were incubated in the dark as IAA is a light-sensitive compound. Samples were centrifuged at 14,000 x g for 10 minutes followed by two subsequent centrifugation steps with 100µl of 8M UA. 100µl of the digestion buffer (50mM HEPES, pH 8.5 or 50mM ABC) was added to all filter units and centrifuged at 14,000 x g for 10 minutes. This step was repeated

twice. Trypsin digestion was carried out using either Sequencing Grade Modified Trypsin (V5111, Promega) or Trypsin Gold, Mass Spectrometry Grade (V5280, Promega) with ProteaseMax™ Surfactant (V207A, Promega). For trypsin digestion, an enzyme-to-protein ratio specific to each mass spectrometry analysis, was determined and made up in digestion buffer. The samples were mixed at 600rpm in a thermo-mixer for 1 minute followed by overnight incubation in a wet chamber at 37ºC. The filter units were transferred to new collection tubes and centrifuged. 40µl of digestion buffer was added to all samples, followed by centrifugation at 14,000 x g for 10 minutes. The resulting eluate contained the tryptic peptides. Specific protein concentrations, enzyme-to-protein ratios and digestion buffers used are outlined within the experimental design and methods section of each experimental chapter.

2.8 Tandem Mass Tag (TMT) Labelling

Peptide eluates from the FASP protocol were subject to isobaric labelling using two TMT10plex Isobaric Label Reagent Sets (Thermo Fisher Scientific Inc.). The two sets of TMT label reagents were brought to room temperature. 41µl of anhydrous acetonitrile was added to each 0.8mg TMT Label Reagent tube. The tubes were occasionally vortexed over 5 minutes to allow the reagents to dissolve. To prevent under- or over-labelling of peptides, a TMT label reagent to protein ratio of ~8:1 was used. 10µl of the appropriate TMT Label Reagent was added to each protein digest. The isobaric tag corresponding to each sample was recorded. The reaction was incubated at room temperature for 1hr with occasional vortexing. 2µl of 5% hydroxylamine was added to each sample and incubated for 15 minutes to quench the reaction. 90µl from each sample was combined resulting in two sample preparations each containing 10 labelled samples. Both pooled samples were partially dried, and the remaining sample in each was acidified at a 1:7 ratio (1-part acidic sample buffer, 7 parts sample) using 2% TFA, 20% ACN. The sample preparations were stored at -20°C.

2.9 C18 Sample Clean-Up

Pierce C18 Spin Columns (Thermo Fisher Scientific Inc.) were used to remove interfering contaminants from each sample preparation. To equilibrate the desalting resin, the spin columns were placed in a receiver tube and 200µl of Activation Buffer

(50% ACN) was added and centrifuged at 1500 x g for 1 minute. The flowthrough was discarded, and this step was repeated once. 200µl of Equilibration Solution (0.25% TFA in 2.5% ACN) was added to the column and centrifuged at 1500 x g for 1 minute. The flowthrough was discarded, and this step was repeated once. The labelled sample preparations were added to the equilibrated C18 spin columns. The columns were added to fresh receiver tubes and centrifuged at 1500 x g for 1 minute. The flowthrough was recovered, and this step was repeated once. 200µl of Wash Solution (0.25% TFA in 2.5% ACN) was added to each column and centrifuged at 1500 x g for 1 minute. The flowthrough was discarded, and this step was repeated once. The columns were placed in a fresh tube, 20µl of Elution Buffer (80% ACN) was added and centrifuged at 1500 x g for 1 minute. This step was repeated once. The sample was dried in a speed vacuum concentrator and stored at -80°C.

2.10 Immobilized Metal Affinity Chromatography (IMAC) Phosphopeptide Enrichment

Phosphopeptides were enriched using the High-Select™ Fe-NTA Phosphopeptide Enrichment Kit (Thermo Fisher Scientific Inc.). The dried-out labelled peptide samples were resuspended in 200µl of Binding/Wash Buffer. To equilibrate the columns, they were placed in a 2ml microcentrifuge collection tube and centrifuged at 1000 x g for 30 seconds to remove storage buffer. 200µl of Binding/Wash Buffer was added to the columns and centrifuged at 1000 x g for 30 seconds. The flow-through was discarded and this step was repeated once. A white Luer plug was used to cap the bottom of the columns and they were placed in empty microcentrifuge tubes. 200µl of each suspended peptide sample was added to each equilibrated column. The screw caps were closed, and the resin was mixed with the sample by carefully tapping the bottom plug until the resin was in suspension (15-20 seconds). The samples were incubated for 30 minutes with gentle mixing every 10 minutes. The columns were placed in a microcentrifuge tube, centrifuged at 1000 x g for 30 seconds and the flow-through was recovered. The columns were washed by adding 200µl of Binding/Wash Buffer followed by centrifugation at 1000 x g for 30 seconds. This step was repeated for a total of 3 washes and the flow-through recovered. The columns were washed by adding 200µl of LC-MS/MS grade water, centrifuging at 1000 x g for 30 seconds and discarding the flow-through. To elute the

phosphopeptides, 100µl of Elution Buffer was added to the column and centrifuged at 1000 x g for 30 seconds. This step was repeated once. The eluate (phosphorylated fraction) was dried immediately in a speed vacuum, resuspended in 0.25% TFA, 2.5% ACN, and stored at -20°C. The unphosphorylated fraction (flow-through) was acidified at a 1:8 ratio of acidification buffer (2% TFA, 20% ACN) to sample and stored at -20°C.

2.11 Mass Spectrometry Analysis

Mass spectrometry analyses were performed using two mass spectrometers; the Q-Exactive mass spectrometer (Thermo Fisher Scientific) located in the Proteomics Suite at Maynooth University and the Orbitrap Fusion Tribrid mass spectrometer (Thermo Fisher Scientific) located in the proteomics facility of the National Institute of Cellular Biotechnology, Dublin City University. The analysis of EMM plasma samples (Chapter 3) was conducted using the Q-Exactive at Maynooth University. All other proteomic and phosphoproteomic analyses were conducted using the Orbitrap Fusion Tribrid.

2.11.1 Label-free mass spectrometry analysis using Q-Exactive

Proteomic analysis was performed using the Ultimate 3000 NanoLC system (Dionex Corporation, Sunnyvale, CA, USA) coupled with a Q-Exactive mass spectrometer (Thermo Fisher Scientific). The maximum loading volume is 14µl. Samples were loaded onto a C18 trap column (C18 PepMap, 300 µm id × 5 mm, 5 µm particle size, 100 Å pore size; Thermo Fisher Scientific) and resolved on an analytical Biobasic C18 Picofrit column (C18 PepMap, 75 µm id × 500 mm, 2 µm particle size, 100 Å pore size; Dionex). Peptides generated were eluted over a 120-minute binary gradient as follows: solvent A [2% (v/v) ACN and 0.1% (v/v) formic acid in LC-MS grade water] and 0-90% solvent B [80% (v/v) ACN and 0.1% (v/v) formic acid in LC-MS grade water]. The column flow rate was set to 0.3µl/min. A data dependent acquisition strategy was used, and the mass spectrometer was externally calibrated. Full-scan spectra were collected in positive mode at a fixed resolution of 140,000 and a mass range of 300-1700 m/z. Fragmentation spectra were acquired by collision-induced dissociation (CID) of the fifteen most intense ions per scan, at a resolution of 17,500. A dynamic exclusion window was applied within 30s.

Precursor ions were isolated based on an isolation window of 2 m/z and one micro-scan were used to collect suitable tandem mass spectra.

2.11.2 Label-free mass spectrometry analysis using Orbitrap Fusion Tribrid

Mass spectrometry analysis was performed using the Thermo UltiMate RSLC3000 nano system directly coupled in-line with the Thermo Orbitrap Fusion Tribrid™ mass spectrometer. The maximum loading volume is 6.4µl. Samples were loaded onto the trapping column (PepMap100, C18, 300 µm × 5 mm, 5 µm particle size, 100 Å pore size; Thermo Fisher Scientific) for 3 minutes at a flow rate of 25 µL/min with 2% (v/v) ACN, 0.1% (v/v) TFA. Peptides were resolved on an analytical column (Acclaim PepMap 100, 75 µm × 50 cm, 3 µm bead diameter column; Thermo Fisher Scientific) using the following binary gradient; solvent A (0.1% (v/v) formic acid in LC-MS grade water) and solvent B (80% (v/v) ACN, 0.08% (v/v) formic acid in LC-MS grade water) using 2–32% B for 75 minutes, 32–90% B in 5 minutes and holding at 90% for 5 minutes at a flow rate of 300 nL/min. A data dependent acquisition strategy with MS1 full scans in the 380–1500 m/z range was performed with a resolution of 120,000 at 200 m/z, targeted automatic gain control (AGC) set to accumulate 4 × 105 ions, and a maximum injection time of 50ms. A top-speed approach with a cycle time of 3s was used for tandem MS analysis, with selected precursor ions isolated with an isolation width of 1.6 Da. The intensity threshold for fragmentation was set to 5000 and included peptides with charge states of 2+ to 7+. A higher energy collision dissociation (HCD) approach was applied with a normalized collision energy of 28% and tandem MS spectra were acquired in the linear ion trap with a fixed first m/z of 110, and a dynamic exclusion of 50 s was applied. AGC was set to 2 × 104 with a maximum injection time set at 35ms.

2.11.3 Label-based mass spectrometry analysis using Orbitrap Fusion Tribrid

Mass spectrometry analysis was performed using the Thermo UltiMate RSLC3000 nano system directly coupled in-line with the Thermo Orbitrap Fusion Tribrid™ mass spectrometer. For both the phospho-enriched and non-enriched samples, volumes equivalent to 1µg of digested peptides were loaded onto the trapping column (PepMap100, C18, 300 µm × 5 mm; Thermo Fisher Scientific) for 3 minutes at a flow rate of 25 µL/min with 2% (v/v) ACN, 0.1% (v/v) TFA. Peptides were

resolved on an analytical column (Easy-Spray C18 75 μm × 250 mm, 2 μm bead diameter column) using the following gradient: 98% solvent A (0.1% (v/v) formic acid in LC-MS grade water) to 35% solvent B (80% (v/v) ACN, 0.08% (v/v) formic acid in LC-MS grade water) over 120 min at a flow rate of 300 nL/min. The mass spectrometer was operated in data dependent acquisition (DDA) mode with multi-notch synchronous precursor selection MS3 scanning for TMT tags. The scan sequence for the Orbitrap Fusion Tribrid began with the acquisition of MS1 spectra over 400 – 1,400 m/z in the Orbitrap at a resolution of 120,000 at 200 m/z. Automatic gain control (AGC) was set to accumulate 4 x 10^5 ions with a maximum injection time of 100ms and 50ms for the unenriched and phospho-enriched samples, respectively. MS2 analysis was performed in the ion trap using a top-speed approach with 3 second cycles. For the unenriched samples, an intensity threshold of 5,000 was used and charge states 2+ to 7+ were included. For the phosphor-enriched samples, an intensity threshold of 10,000 was used and charge states 2+ to 6+ were included. Collision induced dissociation (CID) fragmentation was applied and normalised collision energy was optimised at 35%. A dynamic exclusion of 50s was applied with a mass tolerance of 10 ppm and the AGC target was set at 10^4. For MS3 analysis (synchronous precursor selection), precursors within the mass range 400-1200 m/z were selected, an isolation window of 2 m/z was used, and isobaric tag loss exclusion set for TMT. Selected precursors were fragmented by higher energy collisional dissociation (HCD) (65% collisional energy) and detected using the Orbitrap over 100-500 m/z at a resolution of 60,000 at 200 m/z. The AGC target was set to 10^5 and the maximum injection time set at 105ms.

2.11.4 Quantitative analysis of mass spectrometric data using MaxQuant and Perseus

Quantitative analysis of raw mass spectrometry files from Chapter 3 was performed in MaxQuant (version 1.6.1.0), which has an in-built Andromeda search engine that was used to search the detected features against the UniProtKB-SwissProt Homo Sapiens reference database. The following search parameters were used: i) PTM set to true, ii) first search peptide tolerance of 20 ppm, ii) main search peptide tolerance of 4.5 ppm, iii) cysteine carbamidomethylation set as a fixed modification, iv) methionine oxidation and phospho STY set as variable modifications, v) a maximum

of two missed cleavage sites and vi) a minimum peptide length of seven amino acids. Match between runs was selected. A target-decoy-based false discovery rate (FDR) approach set to 1% for both peptides and proteins was used (Grassl *et al.* 2016). The "Phospho.(STY)Sites.txt" file produced by MaxQuant was further analysed using Perseus (version 1.6.14.0). Phosphopeptides that matched to the reverse database, or a contaminants database were removed. Phosphopeptides were stringently filtered based on localization probability > 0.95. To eliminate peptides that were identified in one plex and not the other, phosphopeptides with values above the minimum reporter intensity value in eleven samples were included in the analysis. To normalize data for sample loading and batch effects, the internal reference scaling method was used (Plubell *et al.* 2017). Following normalization, the data was re-imported into Perseus (version 1.6.14.0) for statistical analysis. Reporter ion intensities were log2 transformed. Analysis of variance (ANOVA) and two sample t-tests were performed to identify statistically significant differentially abundant proteins and phosphorylation sites.

2.11.5 Quantitative analysis of mass spectrometric data using Proteome Discoverer 2.5

Raw files were searched using Proteome Discoverer 2.5 (Thermo Fisher Scientific). Protein identification and label-free quantitation (LFQ) was performed. Precursor and fragment ion mass tolerances were set to 10ppm and 0.6 Da, respectively. The enzyme was set as Trypsin with a maximum of 2 cleavages permitted. For SEQUEST searches, the UniProtKB-SwissProt Homo Sapiens reference database was used. Carbamidomethylation was set as a fixed modification while methionine oxidation was set as a dynamic modification. Default settings were used for the remaining parameters. Only high confidence proteins were retained for subsequent statistical analysis. The resulting dataset was imported into Perseus (version 1.6.14.0) for statistical analysis.

2.11.6 Quantitative analysis of mass spectrometric data using Progenesis QI for Proteomics Software

Progenesis QI for Proteomics was used to analyse raw label-free data generated from the Orbitrap Fusion Tribrid mass spectrometer. After importation of raw files, data

alignment was performed based on the LC retention time of each sample, with the use of a reference run selected based on the sample run which yielded the most peptide ions. Retention times were aligned based on this reference run and peak intensity normalisation performed. The resulting data was filtered based on peptide features with ANOVA p-value < 0.05 between experimental groups, mass peaks with charge states from +1 to +5, and greater than one isotope per peptide. Following filtering, the data was exported (mgf file) to Proteome Discoverer 2.2 where protein identification was performed using Mascot and Sequest HT search engine algorithms and Percolator. To ensure confident protein identification, a number of criteria were applied: (i) peptide mass tolerance set to 10 ppm, (ii) MS/MS mass tolerance set to 0.02 Da, (iii) an allowance of up to two missed cleavages, (iv) carbamidomethylation set as a fixed modification and (v) methionine oxidation set as a variable modification (Murphy et al., 2017b). Only high confidence peptides and those with XCorr scores greater than 1.5 were re-imported back into the Progenesis QI for Proteomics platform. Differentially abundant proteins were identified based on an ANOVA p-value ≤0.05 between experimental groups, and proteins with ≥2 peptides matched.

2.11.7 Bioinformatics analysis and *in silico* data analyses

Several freely available bioinformatic softwares were used throughout this project to interrogate proteomics data and derive biological meaning from large datasets. To evaluate protein-protein interactions between differentially abundant proteins, the Search Tool for the Retrieval of INteracting Genes/Proteins (STRING) database (version 11.5) (http://string-db.org/) which incorporates direct physical interactions as well as functional associations, was used. Unless otherwise stated, the minimum required interaction score was set to high confidence (>0.7). Protein networks were constructed online using STRING and exported to Cytoscape (version 3.10.0) for visualization.

Kyoto Encyclopedia of Genes and Genomes (KEGG) pathway enrichment and gene ontology (GO) enrichment analysis was performed by submitting Uniprot accession IDs to the G:profiler online bioinformatics tool (https://biit.cs.ut.ee/gprofiler/gost) (Raudvere *et al.* 2019). Electronic GO annotations were excluded, and the term size was set to between 5 and 2000. Cytoscape (version 3.10.0) was used to visualize

protein networks and functional networks. KEGG pathways of significant interest were examined further using the "KEGG Mapper" section of the KEGG database (https://www.genome.jp/kegg/mapper/). Uniprot accession IDs were converted to KEGG identifiers using the "Convert ID" tool within the KEGG database. The KEGG identifiers were subsequently inputted into the "Color Pathway" tool to highlight the proteins found in our dataset within KEGG pathways.

2.12 *In silico* analysis of the MMRF CoMMpass dataset

The Multiple Myeloma Research Foundation (MMRF) Relating Clinical Outcomes in MM to Personal Assessment of Genetic Profile (CoMMpass) dataset was used to obtain clinical information and RNA-seq data from primary MM patient samples (Settino *et al.* 2020). Gene expression profiles and survival data of patients with MM (n = 784) were obtained and analysed using UCSC Xena (Goldman *et al.* 2020) (https://xena.ucsc.edu/)(accessed on 17/11/2022). Raw count values and clinical data were downloaded from the Xena website and normalised using the R package "deseq2". Survival analysis was performed using the "survival" and "RegParallel" packages and survival curves were illustrated using the Kaplan Meier method.

2.13 Targeted metabolomics

2.13.1 Sample Preparation and Analysis

Targeted metabolomics analysis of plasma was performed at the UCD Conway Metabolomic Facility using a SCIEX QTRAP 6500+ LC/MS instrument. Plasma samples were prepared based on the MxP® Quant 500 assay manual (Biocrates Life Sciences, Innsbruck, Austria) for a targeted metabolomic analysis according to the manufacturer's instructions. 10µL of plasma was loaded on a 96 well plate and the samples were dried and derivatized by adding 50µL of 5% phenyl isothiocyanate derivatization solution in ethanol/water/pyridine (volume ratio 1/1/1). The plate was then dried under nitrogen. After derivatization, 300µL of ammonium acetate in methanol (5 mM) was added into each well and the plate was left to shake for 30 mins. In the next step, the plate was centrifuged at 500g for 2 mins, and the elute was diluted for two analysis methods. 150µL of elute was mixed with 150µL of high-performance liquid chromatography (HPLC)-grade water for liquid chromatography

tandem mass spectrometry (LC-MS/MS) analysis. Additionally, 10µL of eluate was diluted with 490µL of methanol running solvent for flow injection analysis tandem mass spectrometry (FIA-MS/MS) analysis. For both LC-MS/MS and FIA-MS/MS method, the multiple reaction monitoring (MRM) scan type, which was optimized by Biocrates Life Sciences were applied to identify and quantify/semi-quantify the metabolites.

2.13.2 Data processing and metabolite quantification

MetIDQ software provided by Biocrates Life Sciences was applied to process data. Amino acids and part of amino acid related metabolites and biogenic amines were quantified using isotopically labelled internal standards and seven-point calibration curves. All other metabolites were semi-quantified by using internal standards. Data quality was assessed by investigating the accuracy and reproducibility of QC sample, provided with Quant 500 assay. The metabolite concentrations in micromoles were exported, and any metabolites above the limit of detection (LOD) in > 75% of samples were included for further statistical analyses.

2.13.3 Statistical analysis of metabolomics data

Data was imported into MetaboAnalyst 5.0 for statistical analysis. Feature filtering was performed based on relative standard deviation (RSD) and the resulting data was log-transformed. Metabolites of interest were identified using a student's t-test based on p-value < 0.05 between experimental groups. Supervised statistical approaches including orthogonal projection to latent structure (OPLS) modelling were used to further interrogate the data.

2.14 Enzyme-linked immunosorbent assays

ELISAs were used to verify changes in the abundance of soluble markers identified in our mass spectrometry analysis. The DuoSet ELISA Ancillary Reagent Kit 2 (R&D Systems) containing supplemental reagents was used for all ELISAs performed. ELISAs were performed as per the manufacturers protocol. Prior to each experimental ELISA, an optimisation ELISA was performed to determine the optimal sample dilution. Firstly, all reagents were equilibrated to room temperature. Microtiter wells were coated with 100µl of the appropriate capture antibody, sealed,

and incubated overnight at room temperature. Wells were aspirated and washed three times with wash buffer (0.05% Tween® 20 in PBS, pH 7.2-7.4). To reduce non-specific binding, plates were blocked for a minimum of one hour by adding 300µl of reagent diluent (1% BSA in PBS) to each well. Plates were again washed three times. 100µl of samples or standards, at the appropriate dilution, were added and the plate was sealed and incubated at room temperature for two hours. Following binding of the protein of interest to the capture antibody, the plates were washed three times. 100µl of biotinylated detection antibody was added to each well and the plate was incubated for two hours. The plates were again washed three times, followed by the addition of 100µl of streptavidin conjugated to horseradish peroxidase (HRP). To produce a colorimetric signal, 100µl of substrate solution was added and the plates were incubated for approximately 20 minutes in the dark. Following colour development, 50µl of stop solution (2N H_2SO_4) was added to stop the reaction. Finally, absorbance values were determined by reading the plates on a microplate reader set at 450nm. The online software MyAssays (myassays.com) was used to generate a four-parameter logistic (4-PL) curve to calculate the concentrations of each protein analysed.

2.14.1 Quantitation of mono- and oligonucleosomes in plasma

A commercially available ELISA-based assay was used to quantify the levels of mono- and oligonucleosomes in patient plasma. The Cell Death Detection ELISA^{PLUS} kit (#11 774 425 001) was purchased from Roche Diagnostics. The ELISA was performed as per the manufacturer's guidelines, with slight deviations. 20µl of plasma and incubation buffer was added to each well of the streptavidin-coated microplate at a 1:1 ratio. 80µl of the immunoreagent, made up of 1:20 volume of anti-DNA-POD, 1:20 volume of anti-histone-biotin, and 18:20 volume of incubation buffer, was added to each well. The microplate was sealed and incubated on a thermomixer set to 300rpm for 2 hours at room temperature. The plate was washed three times with incubation buffer followed by the addition of 100µl of ABTS (2,2'-Azinobis [3-ethylbenzothiazoline-6-sulfonic acid]-diammonium salt) substrate solution into each well. The microplate was incubated on a thermomixer set to 300rpm until colour development occurred (20-30 minutes). 100µl of the ABTS Stop Solution was added to each well and the absorbance was measured at 405nm.

The blank value (100µl ABTS Stop Solution only) was subtracted from the final absorbance values for each well.

2.14.2 Quantitation of nucleosomal citrullinated histone H3 in plasma

An ELISA-based assay previously described by Thalin et al., was used to quantify the neutrophil extracellular trap marker, nucleosomal citrullinated histone H3 (H3Cit), in patient plasma (Thålin *et al.* 2020). Reagents were equilibrated to room temperature. A high-bind clear polystyrene microplate (R&D Systems, #DY990) was coated with anti-histone H3 (citrulline R8) antibody (Abcam, #ab232939) at a concentration of 5µg/ml. Primary antibody was diluted accordingly in sterile PBS (R&D Systems, #DY006). The microplate was incubated overnight at 4ºC. The plate was washed three times with wash buffer (R&D Systems, #WA126). The plate was blocked with 300µl of reagent diluent (1% BSA in PBS) (R&D Systems, #DY995) for 1.5 hrs at room temperature. The plate was washed three times. 20µl of plasma and incubation buffer (Cell Death Detection ELISA^{PLUS} kit, #11 774 425 001) at a 1:1 ratio was added to each well with 80µl of the detection antibody anti-DNA-POD (Cell Death Detection ELISA^{PLUS} kit, #11 774 425 001) at a 1:20 dilution. The plate was incubated at room temperature for 2 hrs with shaking (300rpm) using a thermomixer. The plate was washed three times and 100µl of 3,3′,5,5′-Tetramethylbenzidine (TMB) substrate solution (R&D Systems, #DY999B) was added to each well. The plate was incubated out of direct light until a dark blue colour developed (approximately 10 min). The reaction was stopped by adding 50µl of stop solution (R&D Systems, # DY994) to each well and the optical density (OD) was determined by reading the plates on a microplate reader set at 450nm.

2.14.3 Statistical analysis of immunoassay results

Statistical analysis of immunoassay results was performed using Graphpad Prism (8.0.2.263) and MedCalc (version 20.118). Normality was determined using the D'Agostino and Pearson test unless otherwise stated. Based on the results of normality testing, a student's t-test or a Mann Whitney rank test was performed to determine statistical significance based on a $p\text{-value}<0.05$. Graphs illustrating these results were created using GraphPad Prism. Receiver-operating characteristic (ROC) curve analysis was performed using MedCalc to evaluate the discriminatory ability

of potential biomarkers. ROC plots were created in MedCalc by plotting all sensitivity values (true positive fraction) on the y-axis against their equivalent (100-specificity) values (false positive fraction) for all available thresholds on the x-axis. Optimal cut-off points were determined using Youden's index. The area under the curve (AUC) was calculated to summarise the accuracy of the classification. Logistic regression analysis was performed in MedCalc using the Enter method. Throughout this thesis, we consider AUC values ranging from 0.5 to 0.7 as poor, 0.7–0.8 as average, 0.8–0.9 as good and > 0.9 as excellent.

2.15 Immunoblotting

Immunoblotting analysis was performed to verify selected proteins and phosphorylation sites identified by LC-MS/MS analysis. Immunoblotting was performed as described previously, with slight alterations. Unless otherwise stated, 5µg of protein was loaded per lane. Cell lysates were incubated with Laemmli buffer at a 1:1 ratio and heated at 95ºC for 3 minutes. Invitrogen Bolt 4–12% Bis-Tris gels were used for protein separation. 5µl of molecular weight markers were loaded into the first lane followed by 5µg of protein per lane. The gel rig was filled with SDS running buffer and electrophoresis was performed at 180V. Electrophoresis was terminated once the bromophenol blue tracking dye reached the end of the gel. Gels were carefully removed from the gel cassette and placed in transfer buffer for subsequent transfer onto nitrocellulose membranes. Protein transfer was performed based on the method described by Towbin and colleagues (Towbin *et al.* 1979). Proteins were transferred onto nitrocellulose membranes in a Trans-Blot cell from Bio-Rad laboratories by wet transfer at 100 V for 60 min at 4°C. Transfer efficiency was assessed using Ponceau reversible stain (0.1% Ponceau, 5% acetic acid). To prevent non-specific binding, membranes were blocked for 1 hr at room temperature using a milk protein blocking buffer (4% w/v fat-free milk powder, 0.05% Tween 20 made up in PBS), followed by incubation with appropriately diluted primary antibodies overnight at 4°C with gentle agitation. On the second day, the membranes were washed in blocking buffer for 10 min, and then incubated with appropriately diluted HRP-conjugated secondary antibodies for 1 hr at room temperature with gentle agitation. Membranes were twice washed with blocking buffer for 10 min each and twice washed with PBS for 10 min each. The membrane was incubated

with enhanced chemiluminescence (ECL) western blotting substrate for ~5 min for visualisation of the target protein bands. Densitometric scanning and statistical analysis of immunoblots was performed using a HP PSC-2355 scanner and ImageJ software (NIH, Bethesda, MD, USA) along with Graphpad Prism software (version 8.0.2.263) (San Diego, CA, USA). Normality was determined using the D'Agostino and Pearson test, and student t-test or Mann Whitney rank test was performed whereby a p value ≤ 0.05 was deemed to be statistically significant.

2.16 Measurement of plasma cytokine levels using Proximity Extension Assay (PEA)

A targeted proteomic analysis was performed on 40 plasma samples. 9 EMM plasma samples and 31 MM plasma samples with corresponding *ex vivo* drug response data were analysed using Olink proteomics' (Olink, Uppsala, Sweden) PEA technology. The Olink® Target 48 Cytokine panel was used to quantify the levels of 45 cytokines in plasma (**Supp. File 2.1**). The Olink technology is based on the proximity extension assay (PEA), which uses antibody pairs, labelled with DNA oligonucleotides. The antibody pairs bind to their respective proteins in the samples which brings the DNA oligonucleotides into proximity, resulting in hybridization and extension catalysed by DNA polymerase. The resulting DNA barcode is amplified by polymerase chain reaction (PCR) and quantified by microfluidic quantitative (qPCR). Further details on the assay protocol and validation data are available on the manufacturer's website (https://olink.com/products-services/target/). Samples were sent to Randox Laboratories (Antrim, UK) on dry ice for analysis. Samples were randomly plated in a 96-well plate. Three internal quality controls, namely the incubation control, extension control and detection control were added to each sample. After the run, quality control checks were performed, and quantitative results were obtained for 33 plasma samples. Protein concentrations were expressed in pg/ml. The non-parametric Mann Whitney and Kruskal-Wallis tests were used to determine statistically significant ($p < 0.05$) differences in cytokine plasma levels as the data did not follow a normal distribution.

Chapter 3

Phosphoproteomic profiling of multiple myeloma based on *ex vivo* drug sensitivity resistance testing identifies distinct phosphorylation signatures associated with drug response

3.1 Introduction

Protein phosphorylation is one of the most extensively studied post translational modifications due to the key role it plays in almost all cellular processes, particularly in signal transmission. Phosphorylation occurs when a phosphoryl group is added to an amino acid residue, resulting in the formation of a phosphodiester bond (Ardito *et al.* 2017). The majority of phosphorylation events occur on serine residues (~90%), followed by threonine residues (~9%), and a small percentage on tyrosine residues (<1%). Phosphorylation has also been reported to occur on histidine, arginine, lysine, and cysteine residues, although these are less studied (Adam and Hunter 2018). The process of amino acid phosphorylation is reversible whereby protein kinases catalyse and protein phosphatases reverse phosphorylation. Alterations in the function or abundance of kinases and phosphatases can alter the extent of protein phosphorylation, which can impact protein functionality through changes in protein localisation, signal transduction or other biological processes.

Signalling pathways often rely on phosphorylation cascades catalysed by various kinases for signal transduction. These signalling pathways are often implicated in the initiation and development of disease. Therefore, unsurprisingly, abnormal phospho-signalling contributes to the onset and progression of cancer. Numerous signal transduction pathways including the phosphoinositide 3-kinase (PI3K)/AKT/mammalian target of rapamycin (mTOR) signalling pathway and the Ras/MAPK signalling pathway, are known to be aberrantly activated in various cancers. The activation of these cascades promotes tumour growth and survival (Yip and Papa 2021). Other signalling pathways such as the VEGF pathway which stimulates angiogenesis, play key roles in tumour progression. Due to the central role of kinases in signalling pathways, they are often the targets of FDA-approved and investigational therapeutics. For example, receptor tyrosine kinases are key signal transduction mediators that when activated by binding of their cognate ligand, stimulate downstream signalling. Receptor tyrosine kinases with well-known roles in cancer initiation and progression include FMS-like tyrosine kinase 3 (FLT3) and VEGF receptor. Tyrosine kinase inhibitors represent a large class of targeted therapeutics used in the treatment of solid and liquid cancers including breast cancer and chronic myeloid leukemia (Natoli *et al.* 2010).

The study of protein phosphorylation, termed phosphoproteomics, can help reveal key phosphoproteins and phosphorylation sites in signalling pathways. Mass spectrometry remains the most powerful analytical technique applied in phosphoproteomic studies, facilitating large-scale, high resolution, quantitative profiling of phosphorylated proteins. Despite being the most comprehensively studied post translation modification, MS-based analysis of phosphorylation events remains challenging mainly due to substoichiometric phosphorylation, referring to the inherent underrepresentation of phosphopeptides when compared to their unmodified peptide counterpart in complex peptide mixtures (Steen *et al.* 2006). This substoichiometry can hamper phosphopeptide identification, however, the use of phosphopeptide enrichment methods and highly sensitive, high-resolution mass spectrometers have improved the robustness of phosphoproteomics studies leading to the identification of greater numbers of phosphopeptides. The electrophoresis and antibody-based method, Western blotting, is commonly used for targeted analyses of phosphorylation sites, whereby the separated proteins are exposed to phosphorylation site specific antibodies, followed by signal development and detection of the phosphorylated protein. A limitation of antibody-based targeted analyses is the limited availability of high quality, highly specific antibodies against many phosphorylation sites.

In cancer research, phosphoproteomic analyses contribute to precision medicine through the identification of phosphorylation sites and associated kinases/phosphatases that serve as biomarkers and therapeutic targets. The application of phosphoproteomic techniques has led to fundamental advances in the understanding of cancer signalling dynamics. Several studies have identified phosphorylation events as promising biomarkers of therapeutic response and prognosis (Carter *et al.* 2020; Parada *et al.* 2020). In addition, phosphorylation signatures associated with distinct cancer subtypes or mutational profiles can contribute to precision medicine (Mertins *et al.* 2016; Lin *et al.* 2019). In this study, a TMT-based LC-MS/MS analysis was performed on primary MM plasma cell lysates stratified based on their *ex vivo* drug response profiles to specific classes of FDA-approved and investigational therapeutics. The phosphoproteomic profiles associated with response to five drug classes, namely, proteasome inhibitor (PI), immunomodulatory drug (IMiD), heat shock protein 90 (HSP90) inhibitor, proline-

rich tyrosine kinase 2 (PYK2) and focal adhesion kinase (FAK) inhibitor, and a cyclin dependent kinase 9 (CDK9) inhibitor, were investigated to identify key phosphorylation sites, proteins and signalling pathways associated with drug sensitivity/resistance.

3.2 Experimental design and methods

Multiple myeloma remains an incurable malignancy as patients face repeated relapses mainly due to the development of drug resistance. The combination of *ex vivo* DSRT with 'omics' technologies is a promising approach to elucidate mechanisms of drug resistance and identify novel biomarkers of drug response. Furthermore, the field of functional precision medicine is emerging as an effective tool in clinical oncology, as highlighted by interim results of a prospective clinical trial demonstrating the ability of *ex vivo* venetoclax sensitivity testing to predict *in vivo* treatment response in acute myeloid leukemia (AML) (Kuusanmäki *et al.* 2022).

3.2.1 Patient samples and clinical information

Patient samples were collected after informed consent with ethical approval from the participating hospitals in compliance with the Declaration of Helsinki. Bone marrow aspirates were collected from 20 MM patients at various stages of disease. Patient characteristics are outlined in **Table 3.1**, along with treatment regimen information as outlined in **Table 3.2**. Cytogenetic information from each patient at the sampling date was recorded (**Figure 3.1**).

Table 3.1: Clinical characteristics of patient cohort. Table illustrating the patient ID, age at sample date, gender, heavy chain composition, and light chain composition of each patient.

Patient ID	Age at Sample Date	Gender	Heavy Chain	Light Chain
D_MM_7276	65	Female	Not detected	kappa
D_MM_7281	77	Female	IgA	kappa
D_MM_7396	50	Male	IgG	kappa
D_MM_7746	67	Female	IgG	lambda
D_MM_7983	63	Male	IgG	lambda
D_MM_8095	77	Male	IgA	kappa
D_MM_8597	53	Male	IgG	lambda
R_MM_1193	74	Male	IgA	lambda
R_MM_1878	69	Male	IgA	kappa
R_MM_1913	69	Female	IgG	kappa
R_MM_2662	62	Male	IgG	kappa
R_MM_3792	68	Male	IgG	kappa
R_MM_3823	71	Female	IgA	lambda
R_MM_4263	58	Female	IgG	kappa
R_MM_587	72	Female	IgG	kappa
R_MM_6211	64	Female	Not detected	kappa
R_MM_6261	53	Male	IgG	kappa
R_MM_6385	76	Male	IgA	lambda
R_MM_7171	70	Male	Unknown	Unknown
R_MM_8291	71	Male	Unknown	kappa

Table 3.2: Details of treatment course of each patient within the cohort. Table illustrating the disease stage at the time of sampling, the 1st next line of treatment, all lines of treatment, and the deepest response in next line of treatment. Bor, bortezomib; Dxm, dexamethasone; Cpm, cyclophosphamide; HD-Cyc, high-dose cyclophosphamide; AutoHSCT, autologous hematopoietic stem cell transplantation; HD-Mel, high-dose melphalan; Mel, melphalan; Pred, prednisone; Len, lenalidomide; Dara, daratumumab; VGPR, very good partial response; PR, partial response; PD, progressive disease; SD, stable disease.

Patient ID	Disease stage at sample date	Name of 1st next line treatment	Names of all next line treatments	Deepest response in next line treatment
D_MM_7276	Diagnosis	Bor/Dxm	Bor/Dxm Bor/Cpm/Dxm Mobilisation (HD-Cyc) Bor/Cpm/Dxm AutoHSCT (HD-Mel)	VGPR
D_MM_7281	Diagnosis	Bor/Mel/Pred	Bor/Mel/Pred	VGPR
D_MM_7396	Diagnosis	Bor/Cpm/Dxm	Bor/Cpm/Dxm Mobilisation (Cpm) AutoHSCT (HD-Mel) Bor/Dxm/Len Len	PR
D_MM_7746	Diagnosis	Ixazomib/Len/Dxm	Ixazomib/Len/Dxm	PR
D_MM_7983	Diagnosis	NA	NA	
D_MM_8095	Diagnosis	Bor/Dxm	Bor/Dxm Radiation therapy	VGPR
D_MM_8597	Diagnosis	Ixazomib/Len/Dxm	Ixazomib/Len/Dxm AutoHSCT (HD-Mel)	VGPR
R_MM_1193	Relapse	Carfilzomib/Dxm	Carfilzomib/Dxm	PD
R_MM_1878	Relapse	Carfilzomib/ Elotuzumab/Dxm	Carfilzomib/Elotuzumab /Dxm	VGPR
R_MM_1913	Relapse	Carfilzomib/ Elotuzumab/Dxm	Carfilzomib/Elotuzumab /Dxm	PR
R_MM_2662	Relapse	Carfilzomib/ Elotuzumab/Dxm	Carfilzomib/Elotuzumab /Dxm	VGPR
R_MM_3792	Relapse	NA	NA	NA
R_MM_3823	Relapse	NA	NA	NA
R_MM_4263	Relapse	Len/Dxm	Len/Dxm	NA
R_MM_587	Relapse	Treatment related to a study	Treatment related to a study	SD
R_MM_6211	Refractory	Bor/Dxm/Len	Bor/Dxm/Len	PD
R_MM_6261	Relapse	Dara/Bor/Dxm	Dara/Bor/Dxm	PD
R_MM_6385	Relapse	Treatment related to a study	Treatment related to a study	VGPR
R_MM_7171	Relapse	NA	NA	NA
R_MM_8291	Relapse	Carfilzomib/ Elotuzumab/Dxm	Carfilzomib/Elotuzumab /Dxm	VGPR

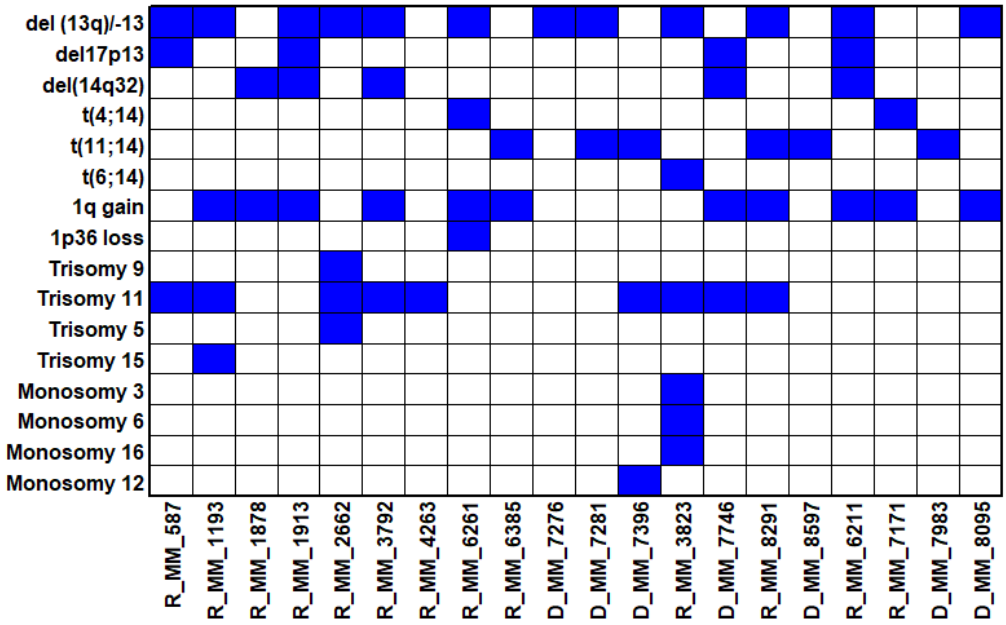

Figure 3.1: Cytogenetic data associated with the patient cohort. Cytogenetic analysis was performed on the sampling date.

3.2.2 Label-based mass spectrometry analysis of primary CD138$^+$ myeloma cells

The mononuclear cell fraction of bone marrow aspirates collected from 20 MM patients were subject to CD138$^+$ plasma cell enrichment using the EasySep Human CD138 Positive Selection kit (StemCell Technologies, Grenoble, France) at FIMM. Drug sensitivity scoring was performed at FIMM as described previously (Pemovska *et al.* 2013; Majumder *et al.* 2017; Tierney, Bazou, Majumder, *et al.* 2021). Briefly, the CD138$^+$ cells collected from the 20 myeloma patients were tested against a panel of compounds (>300 small molecule inhibitors) that were pre-plated on 384-well plates in 5 concentrations covering a 10,000-fold concentration range. CD138+ cells were added to the plates in conditioned medium prepared from the HS5 human bone marrow stromal cell line. The plates were incubated in a humidified environment at 37 °C and 5% CO2 for 72 hours, followed by measurement of cell viability using the CellTiter-Glo assay (Promega). Drug sensitivity data was calculated by comparing readouts between drug treated and negative control (DMSO only) treated cells. Drug sensitivity scores (DSS) were calculated as previously described (Yadav *et al.* 2014).

Isolated CD138$^+$ plasma cells were lysed in RIPA buffer (25mM Tris, pH 7–8; 150 mM NaCl; 0.1% SDS; 0.5% sodium deoxycholate and 1% NP-40). Protein quantitation was performed using the Pierce™ 660nm protein assay (Thermo Fisher

Scientific). FASP was applied for proteolytic digestion, as described in Chapter 2 (Wiśniewski *et al.* 2009). 30µg of protein from each sample was digested. For this mass spectrometry analysis, 50mM HEPES, pH 8.5 was used as the digestion buffer instead of 50mM ABC to ensure no interference with TMT reagents. Following buffer exchange, overnight trypsin digestion was performed at a 1:30 enzyme-to-protein ratio using Sequencing Grade Modified Trypsin (V5111, Promega), in 50mM HEPES, pH 8.5. Following overnight digestion, the filter units were transferred to new collection tubes and centrifuged at 14,000 x g for 10 minutes. 40µl of 50 mM HEPES, pH 8.5 was added to all samples, followed by centrifugation at 14,000 x g for 10 minutes to obtain ~80µl of peptide eluate.

TMT labelling was performed immediately after the FASP protocol, as described in Chapter 2. Two TMT10plex Isobaric Label Reagent Sets (Thermo Fisher Scientific Inc.) were used at a TMT label reagent to protein ratio of ~8:1. Following labelling, the pooled samples were partially dried, and acidified at a 1:7 ratio (1-part acidic sample buffer, 7 parts sample) using 2% TFA, 20% ACN. Sample clean-up to remove interfering contaminants was performed using Pierce C18 Spin Columns (Thermo Fisher Scientific Inc.), followed by sample drying using a speed vacuum. Dried labelled peptides were resuspended in 200µl of Binding/Wash Buffer for phosphopeptide enrichment using the High-Select™ Fe-NTA Phosphopeptide Enrichment Kit (Thermo Fisher Scientific Inc.). Phosphopeptide enrichment, as described in Chapter 2, resulted in a phosphorylated and unphosphorylated fraction for each TMTplex of 10 pooled samples. Mass spectrometry analysis was performed using the Thermo UltiMate 3000 nano system directly coupled in-line with the Thermo Orbitrap Fusion Tribrid mass spectrometer. The maximum loading amount, 6.4 µl, was loaded onto the system. The mass spectrometry analysis was performed as described previously (Chapter 2).

3.2.3 Data analysis and bioinformatic analysis of mass spectrometry results

To identify differentially abundant proteins and phosphorylation sites, statistical analysis was performed using ANOVA or two-sided t-test with permutation-based FDR statistics. Statistically significant differentially abundant (SSDA) proteins and phosphorylation sites between the chemosensitivity groups were identified based on an FDR threshold < 0.05 (s0 = 0.1) and fold change > 1.5. For the analysis of

individual drugs, SSDA proteins were identified based on an FDR threshold < 0.05 (s0 = 0.1) and fold change > 1.5, while phosphorylation sites were identified based on an FDR threshold < 0.1 (s0 = 0.1) and fold change > 1.5. To identify the biological functions of SSDA proteins and phosphoproteins, the SRPlot online platform (http://www.bioinformatics.com.cn/srplot) which is based on the "clusterProfiler" and "pathview" R packages, and g:Profiler gGOst (https://biit.cs.ut.ee/gprofiler/gost) were used. The SRPlot online tool was used to visualize the gene ontology results. Kinase-substrate enrichment analysis (KSEA) was performed using the KSEA App website (https://casecpb.shinyapps.io/ksea/) using PhosphoSitePlus and NetworKIN databases according to a NetworKIN cutoff of 1.5 and p-value cutoff of $p < 0.05$. Only kinases with a substrate count ≥ 3 are displayed on bar plots. To identify variant sequence motifs, the ±31 amino acid sequence windows of the significantly regulated phosphorylation sites were evaluated using the online software tool, MoMo (v5.5.3) (accessed November 2023) (Cheng *et al.* 2019). A 31-residue motif width, 15 occurrences, and a p-value of <0.000001 were set as the parameters for motif prediction.

3.2.4 Western blotting verification

Comparative immunoblot analyses were performed to verify the altered abundance of selected proteins and phosphorylation sites between chemosensitivity groups. Western blotting was performed as described in Chapter 2. 5µg of protein was loaded per lane. Primary antibodies were diluted in 5% BSA according to guidance from the manufacturer. Following overnight incubation with the primary antibody, nitrocellulose membranes were subject to a number of washing steps followed by incubation with the appropriate peroxidase-conjugated secondary antibodies. Immuno-decorated protein bands were visualized using the G:BOX Chemi XRQ or x-ray film. Densitometric analysis of each blot was performed using ImageJ software, followed by statistical analysis and graphical analysis in GraphPad Prism.

3.3 Results

3.3.1 Stratification of plasma samples based on *ex vivo* drug sensitivity resistance testing

Following *ex vivo* DSRT, $CD138^+$ myeloma cell samples were stratified into one of four groups: Group 1, very sensitive; Group 2, sensitive; Group 3, resistant; and Group 4, very resistant, as described previously (Majumder et al., 2017; Tierney et al., 2021). The groups are listed in **Table 3.3**.

Table 3.3: Sample groupings based on drug sensitivity/resistance. Samples were grouped based on *ex vivo* DSRT results, as described in (Majumder et al., 2017).

Group 1	Group 2	Group 3	Group 4
R_MM_6261	R_MM_1878	R_MM_3823	R_MM_1913
R_MM_7171	R_MM_6385	D_MM_7396	D_MM_7281
R_MM_3792	D_MM_7276	D_MM_7983	R_MM_1193
R_MM_2662	D_MM_7746	D_MM_8095	R_MM_587
R_MM_4263	R_MM_6211	D_MM_8597	R_MM_8291

3.3.2 Quantitative phosphoproteomics of $CD138^+$ myeloma cell lysates

Our quantitative phosphoproteomic mass spectrometry analysis identified a total of 1,473 proteins and 2,945 phosphorylation sites on 2,232 phosphopeptides from 690 phosphoproteins. A stringent phosphorylation site localization probability (>0.95) was used to ensure the inclusion of high confidence phosphorylation sites in downstream statistical analyses. The phosphopeptide and phosphosite residue distribution was similar to previous studies (Francavilla *et al.* 2013, 2017; Zhang *et al.* 2020) (**Figure 3.2**). As expected, the majority of phosphorylation sites identified involved serine residues (81.2%).

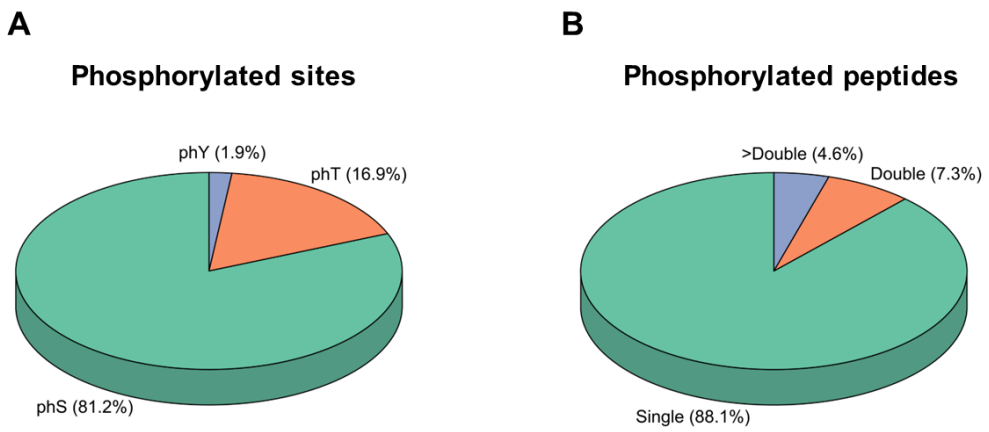

Figure 3.2: Visualization of phosphorylated peptides and sites distribution. (**A**) Distribution of serine (phS), threonine (phT), and tyrosine (phY) phosphorylation sites identified in this mass spectrometry analysis. (**B**) Distribution of phosphopeptides with one, two, or greater than two phosphorylation sites identified in this study.

3.3.2.1 Analysis of the proteome of CD138+ myeloma cell lysates stratified into four chemosensitivity groups

Firstly, the proteomic changes between the four chemosensitivity groups was analysed. Principal component analysis (PCA) of the intensity values of all 1,473 identified proteins revealed a clear cluster of Group 1 samples separate from the three other chemosensitivity groups. Groups 2 and 3 have some overlap, indicating a degree of similarity between the samples in these groups. Group 4 samples also form a separate cluster which also contains one sample from the 'resistant' Group 3 (**Figure 3.3A**). The second PCA of only Group 1 and Group 4 samples highlights the clear separation between the two chemosensitivity groups with a large total explained variance of 61.5% (**Figure 3.3B**). As expected, this suggests larger proteomic changes occur in myeloma cells considered 'very sensitive' and 'very resistant', whereas the proteomic changes occurring between Groups 2 and 3 are more ambiguous.

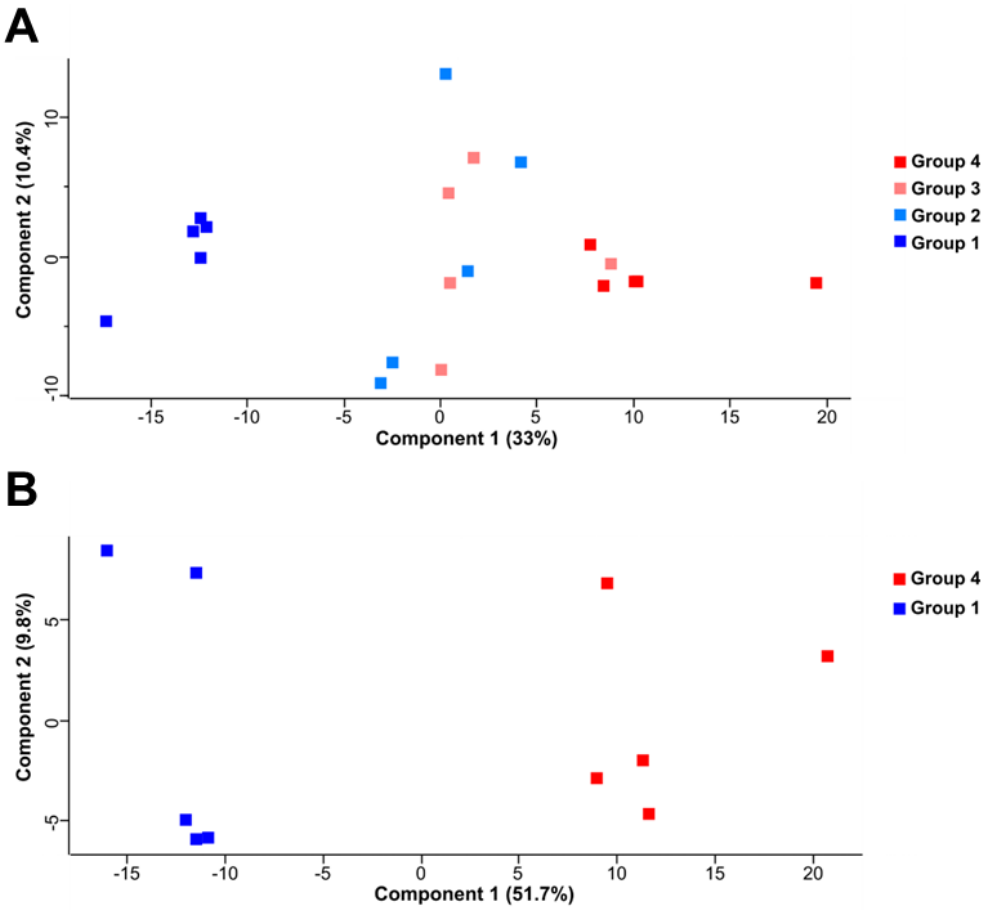

Figure 3.3: Principal component analysis (PCA) of reporter ion intensity values from proteins identified in the four chemosensitivity groups. (**A**) PCA of proteins identified in groups 1, 2, 3, and 4. The total explained variance for this PCA is 43.4%. (**B**) PCA of proteins identified in groups 1 and 4 highlighting the clear distinction between the very sensitive and very resistant groups. The total explained variance for this PCA is 61.5%.

To evaluate the proteomic changes in myeloma cells of the four chemosensitivity groups, we compared protein abundance across the four groups by ANOVA. Of the 1,473 proteins identified, 253 were found to be statistically significantly differentially abundant between the four chemosensitivity groups (ANOVA q-value < 0.05) (**Supp. File 3.1**). A Student's t-test was also performed to identify proteins associated with the 'very sensitive' and 'very resistant' phenotypes. A total of 320 SSDA proteins were identified (FDR q-value < 0.05, FC > 1.5) (**Supp. File 3.1**). Of the 320 SSDA proteins, 144 proteins were increased in abundance in Group 4 and 176 proteins were decreased in abundance in Group 4. Hierarchical clustering was performed on z-scored intensity values to illustrate the change in abundance of the SSDA proteins identified by ANOVA and Student's t-test (**Figure 3.4**).

Proteins found to be SSDA between the Group 1 and Group 4 were subject to gene ontology enrichment analysis. Proteins were separated into those increased in

abundance in Group 4 and those increased in abundance in Group 1. Group 4, which consisted of samples with a 'very resistant' chemosensitivity profile, had a high abundance of proteins associated with neutrophil activation, actin filament organization, and focal adhesions (**Figure 3.5**). Group 1, which consisted of samples with a 'very sensitive' chemosensitivity profile, had a high abundance of proteins associated with RNA binding, translation, and the proteasome complex (**Figure 3.6**) (**Supp. File 3.2**). The increased abundance of cytoskeletal-associated proteins in Group 4 may contribute to the development of CAM-DR, whereas the reduced abundance of proteasomal proteins in Group 4 may limit susceptibility to proteasome inhibitors.

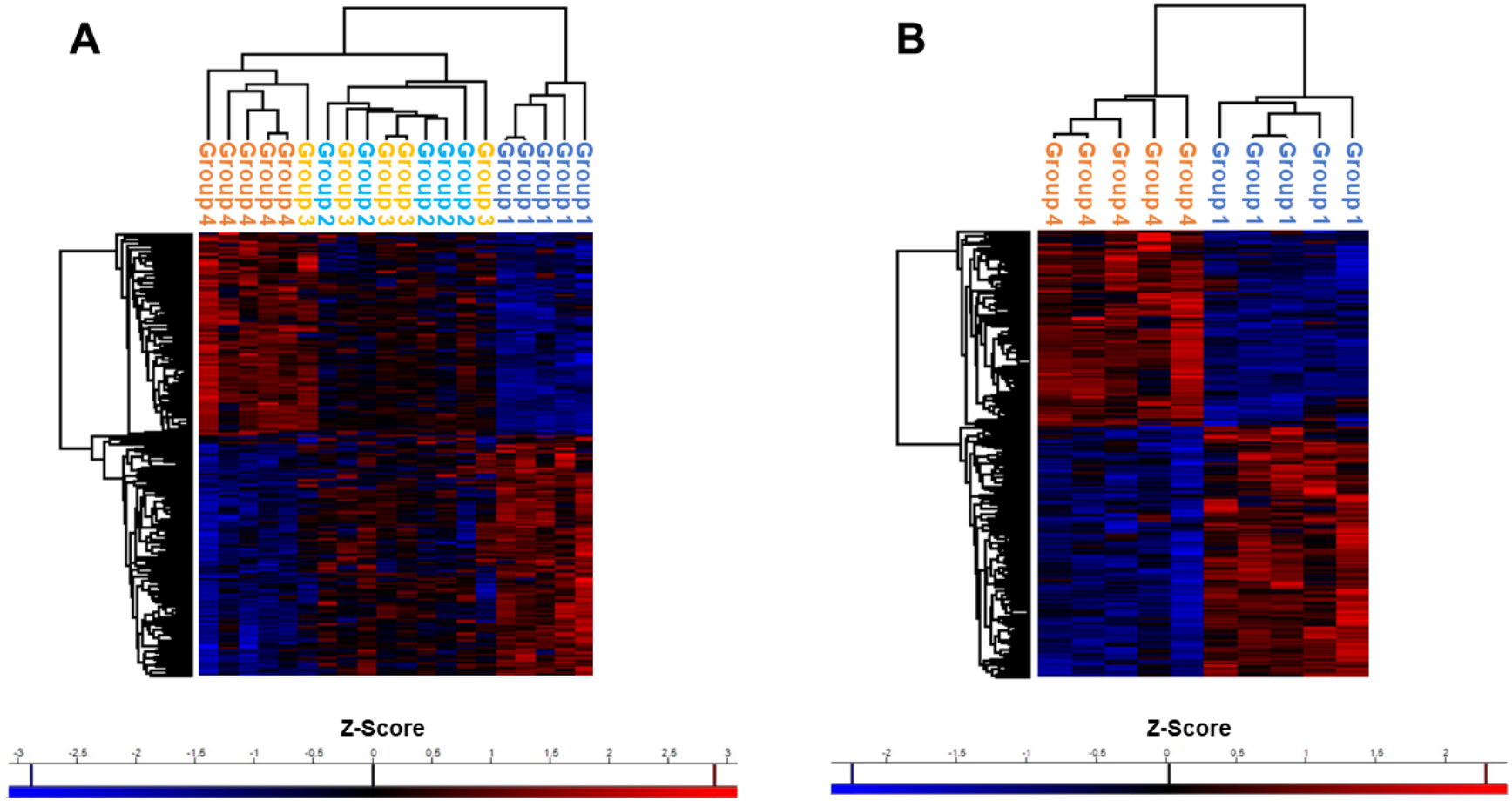

Figure 3.4: Hierarchical clustering analysis of statistically significant differentially abundant (SSDA) proteins. (**A**) Hierarchical clustering analysis of z-scored normalised intensity values of the 253 SSDA proteins across the four chemosensitivity groups. (**B**) Hierarchical clustering analysis of z-scored normalised intensity values of the 372 SSDA proteins identified from Student t-test analysis of Group 1 and 4.

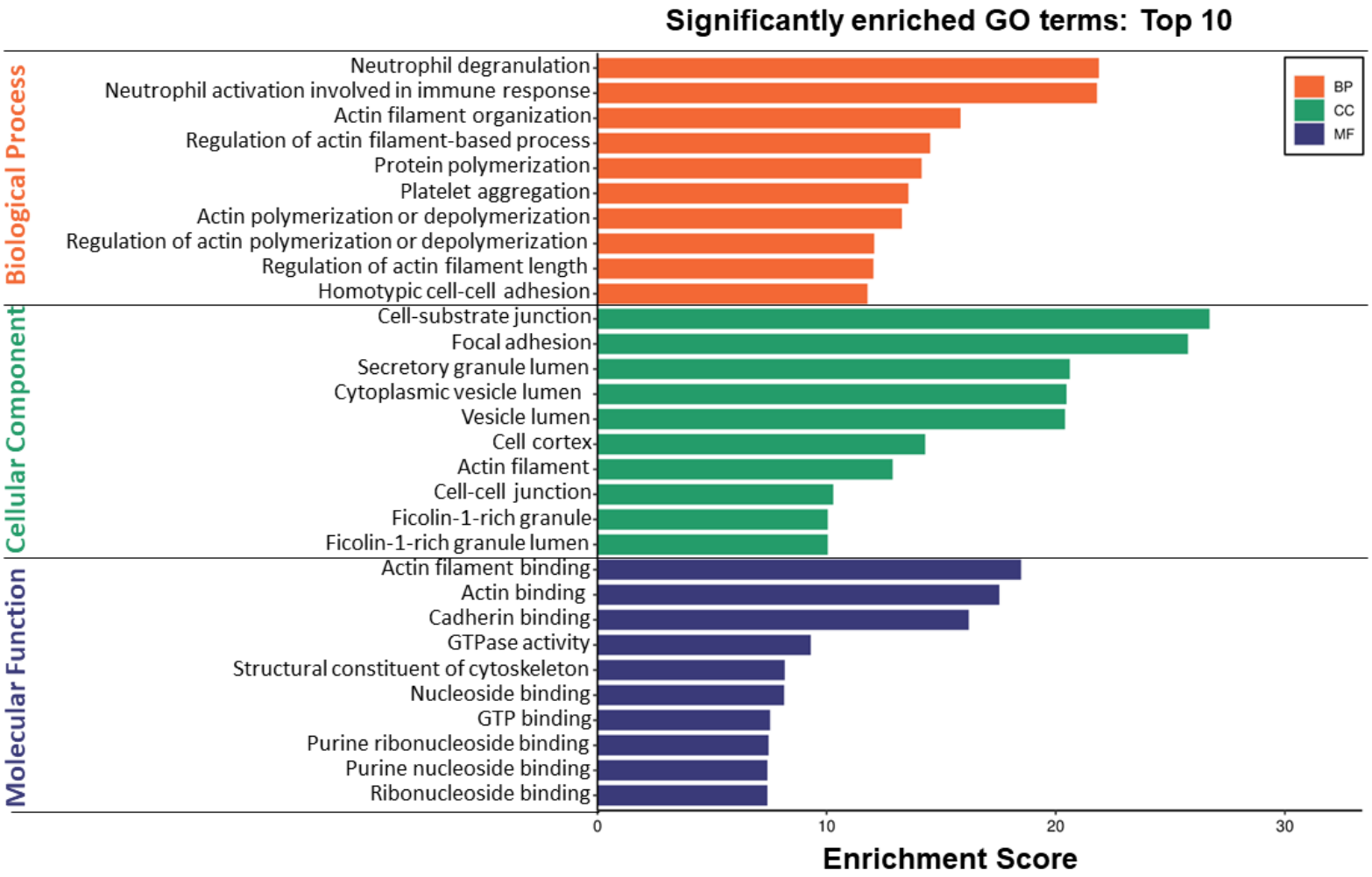

Figure 3.5: Gene ontology enrichment analysis of proteins found to be statistically significantly increased in Group 4. Graph highlights the top 10 most significantly enriched biological processes (orange), cellular components (green), and molecular functions (purple).

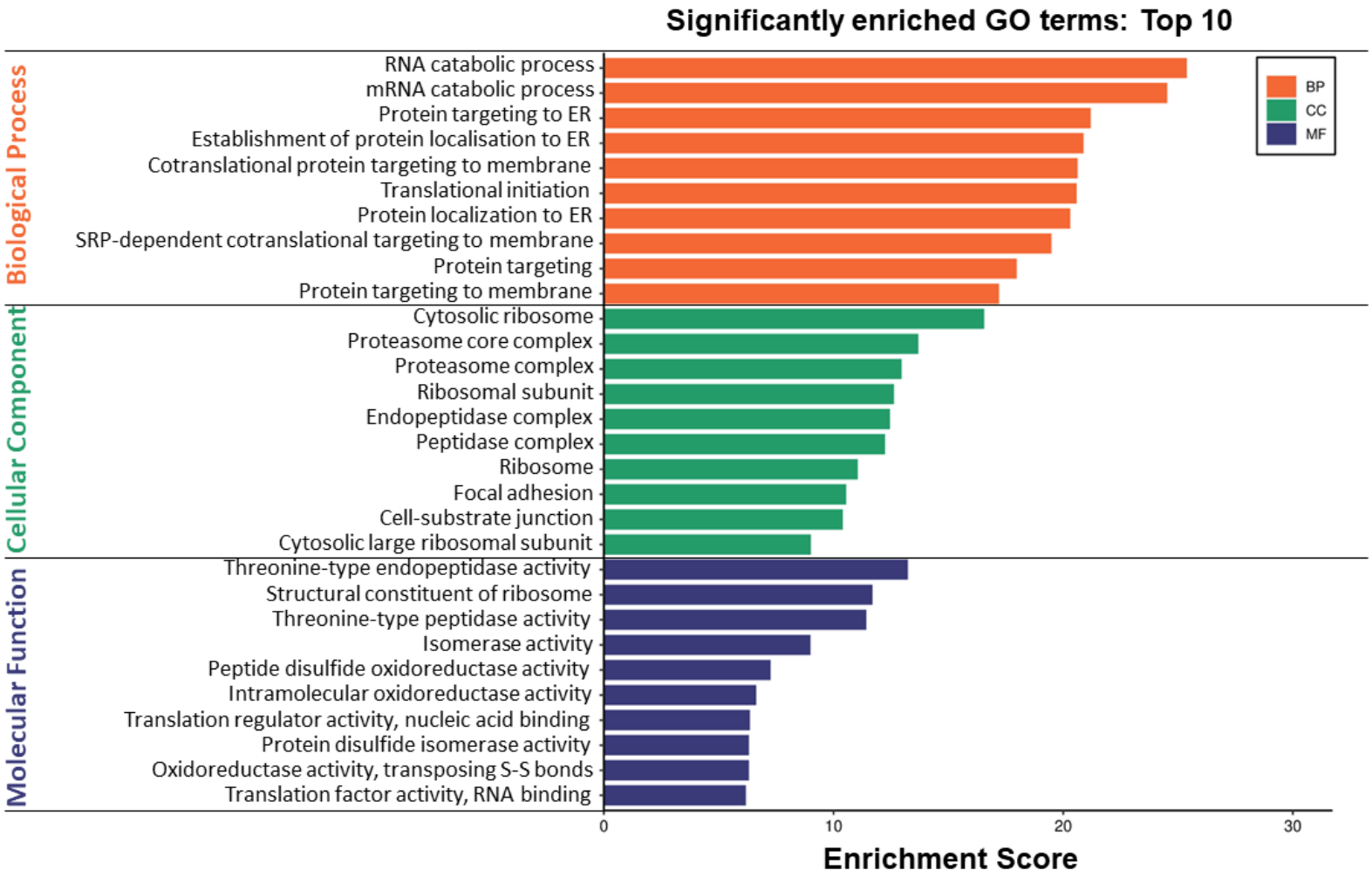

Figure 3.6: Gene ontology enrichment analysis of proteins found to be statistically significantly increased in Group 1. Graph highlights the top 10 most significantly enriched biological processes (orange), cellular components (green), and molecular functions (purple).

3.3.2.2 Analysis of the phosphoproteome of CD138+ myeloma cell lysates stratified into four chemosensitivity groups

PCA on the phosphopeptide intensity values revealed a clear separation between Group 1 and 4, highlighting a change in the phosphoproteome between these groups. Similarly to the proteomic PCA seen above, Groups 2 and 3 demonstrated some overlap, indicating a degree of similarity between the samples in these groups, whereas samples from Groups 1 and 4 have notably different phosphoproteomic profiles **(Figure 3.7**).

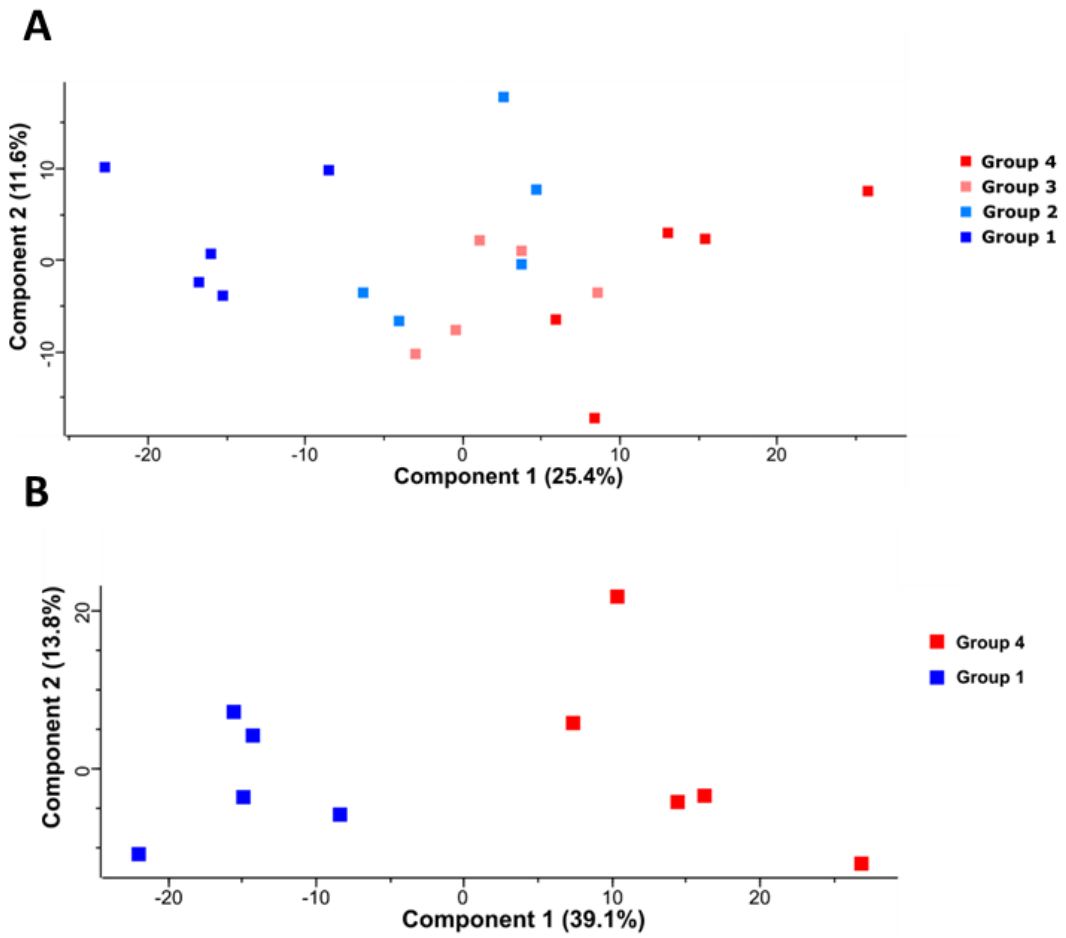

Figure 3.7: Principal component analysis (PCA) of reporter ion intensity values from phosphopeptides identified in the four chemosensitivity groups. (**A**) PCA of phosphopeptides identified in groups 1, 2, 3, and 4. (**B**) PCA of phosphopeptides identified in groups 1 and 4 highlighting the clear distinction between the very sensitive and very resistant groups.

To evaluate the phosphoproteomic changes in myeloma cells of the four chemosensitivity groups, we compared phosphopeptide abundance across the four groups by ANOVA. Of the 2,945 phosphorylation sites identified, 152

phosphorylation sites were SSDA between the four chemosensitivity groups (ANOVA q-value < 0.05) (**Supp. File 3.3**). A Student's t-test was also performed to identify phosphorylation sites associated with the 'very sensitive' and 'very resistant' phenotypes. A total of 212 SSDA phosphorylation sites were identified (FDR q-value < 0.05, FC > 1.5) (**Supp. File 3.3**). Hierarchical clustering was performed on z-scored intensity values to illustrate the change in abundance of the SSDA phosphopeptides identified by ANOVA and Student's t-test (**Figure 3.8**). Two distinct clusters representing phosphorylation sites increased in abundance in Group 1 and Group 4 are clearly visible. SSDA phosphoproteins were separated into those increased in abundance in Group 4 and those increased in abundance in Group 1 and subject to gene ontology enrichment analysis. As depicted in **Figure 3.9** and **Figure 3.10**, phosphoproteins increased in abundance in Group 4 and Group 1 show similar functional enrichments to the proteomic analysis above with phosphoproteins increased in abundance in Group 4 being associated with cytoskeletal organization whereas phosphoproteins increased in abundance in Group 1 are associated with RNA binding and translation (**Supp. File 3.4**). KSEA was used to predict potential kinase activity based on the phosphorylation levels of known substrates. This analysis showed significant enrichment of 11 kinases in drug resistant (Group 4) samples and significant enrichment of 4 kinases in drug sensitive (Group 1) samples (**Figure 3.11A**). Phosphorylation events are dependent on the action of protein kinases which recognise specific short (~5-15 amino acids) sequence motifs surrounding the serine, threonine or tyrosine residues which are subsequently phosphorylated. A motif analysis was performed using MoMo and the motif-x algorithm to better understand the upstream processes of the phosphopeptides identified in this study (**Figure 3.11B**). One motif, namely, S*P (* denotes phosphorylated residue), was significantly increased in both Group 4 and Group 1 phosphopeptides. The motif, RxxS*, was uniquely increased in phosphopeptides increased in abundance in Group 4 samples, while the motif, S*xxE, was uniquely increased in phosphopeptides increased in abundance in Group 1. The RxxS* motif is a phosphorylation site of protein kinase A (PKA) whose catalytic subunit (PRKACA) was significantly enriched in Group 4 samples from the KSEA (Pinna and Ruzzene 1996). Interestingly, the S*xxE motif is a consensus sequence motif of casein kinase 2 (CK2) whose catalytic subunit (CSNK2A1) was significantly enriched in Group 1 samples from the KSEA.

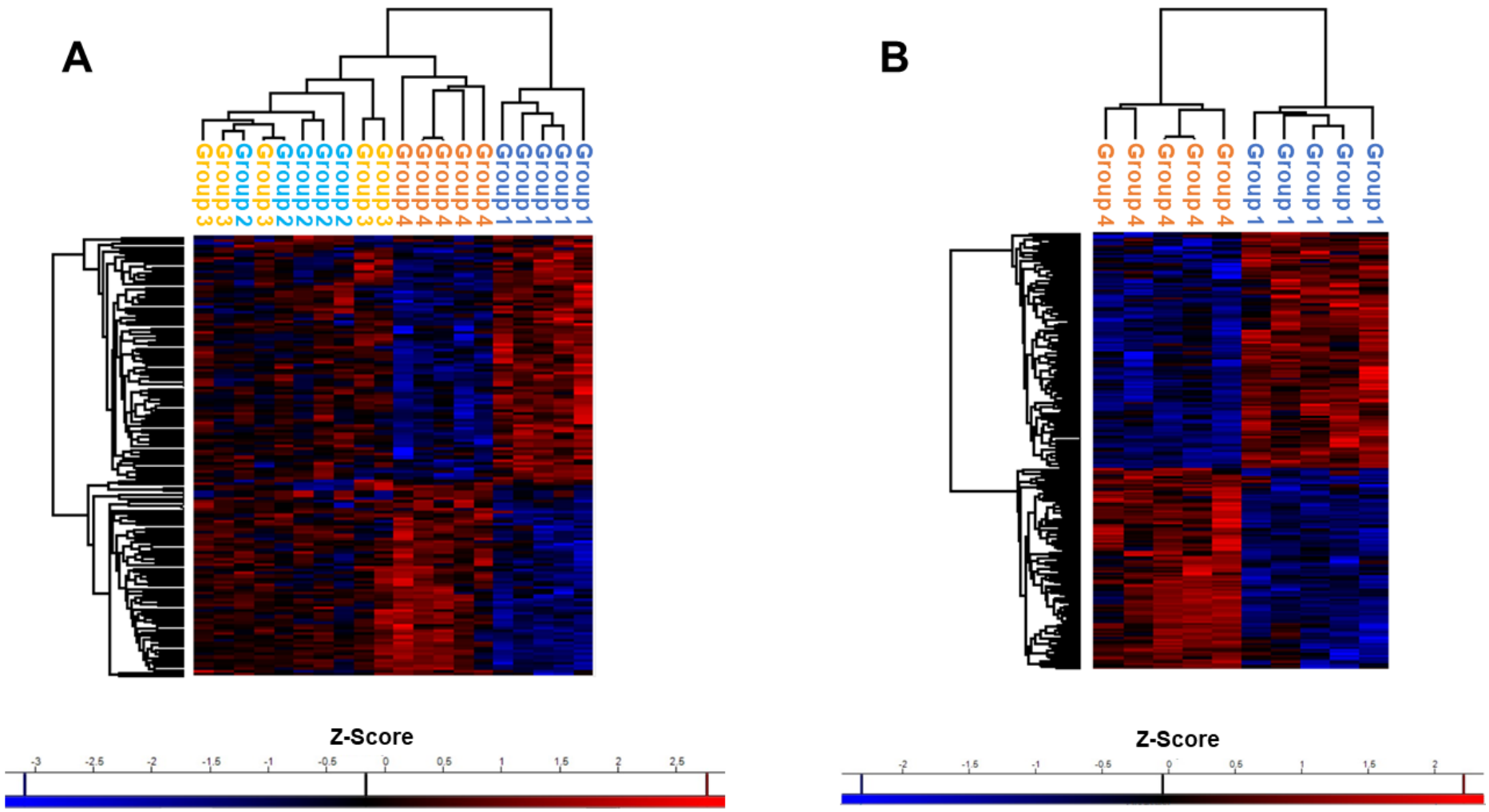

Figure 3.8: Hierarchical clustering analysis of statistically significantly differentially abundant (SSDA) phosphorylation sites. (**A**) Hierarchical clustering analysis of z-scored normalised intensity values of the 152 SSDA phosphosites across the four chemosensitivity groups. (**B**) Hierarchical clustering analysis of z-scored normalised intensity values of the 217 SSDA phosphosites.

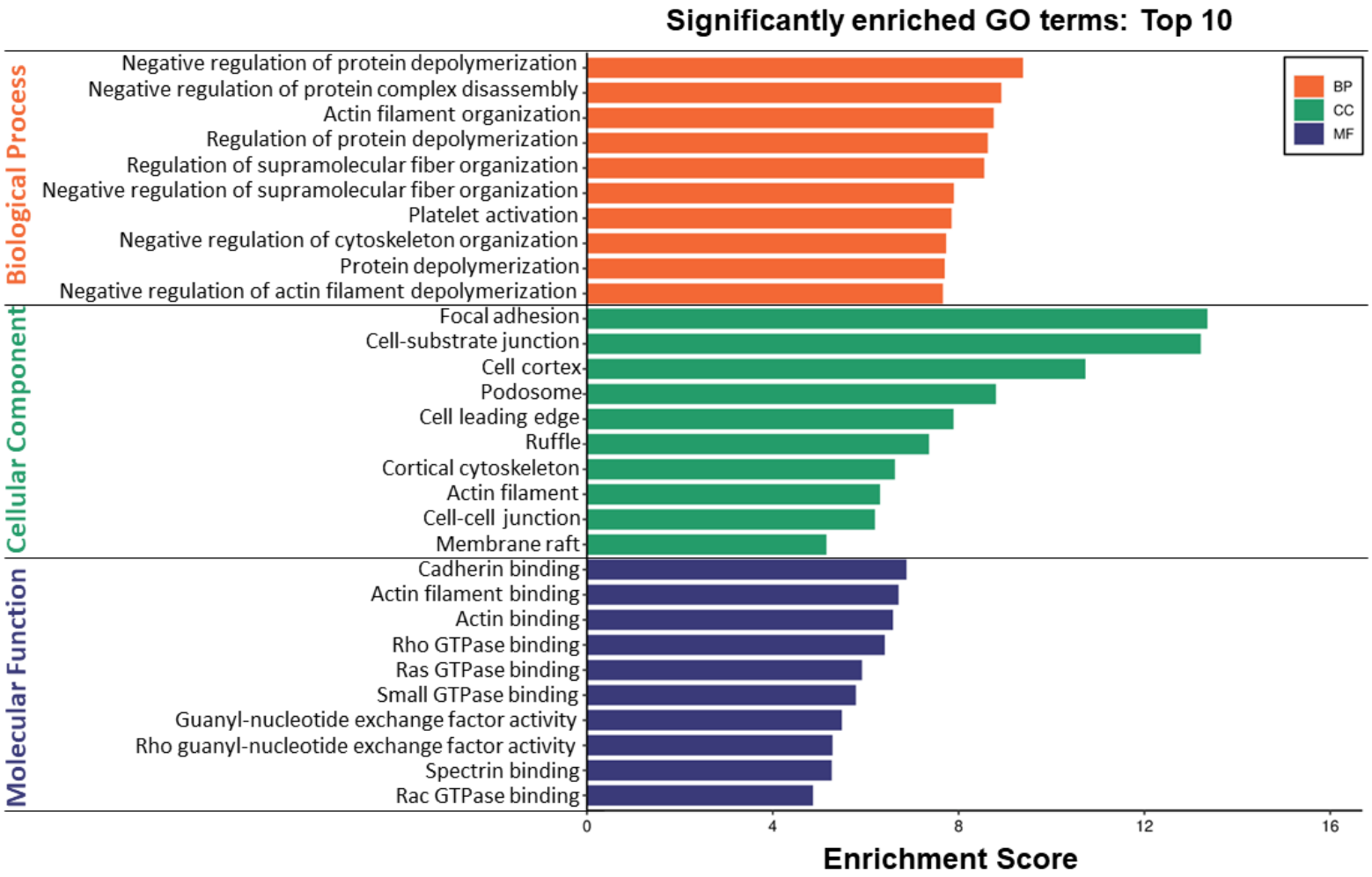

Figure 3.9: Gene ontology enrichment analysis of phosphoproteins found to be statistically significantly increased in Group 4. Graph highlights the top 10 most significantly enriched biological processes (orange), cellular components (green), and molecular functions (purple).

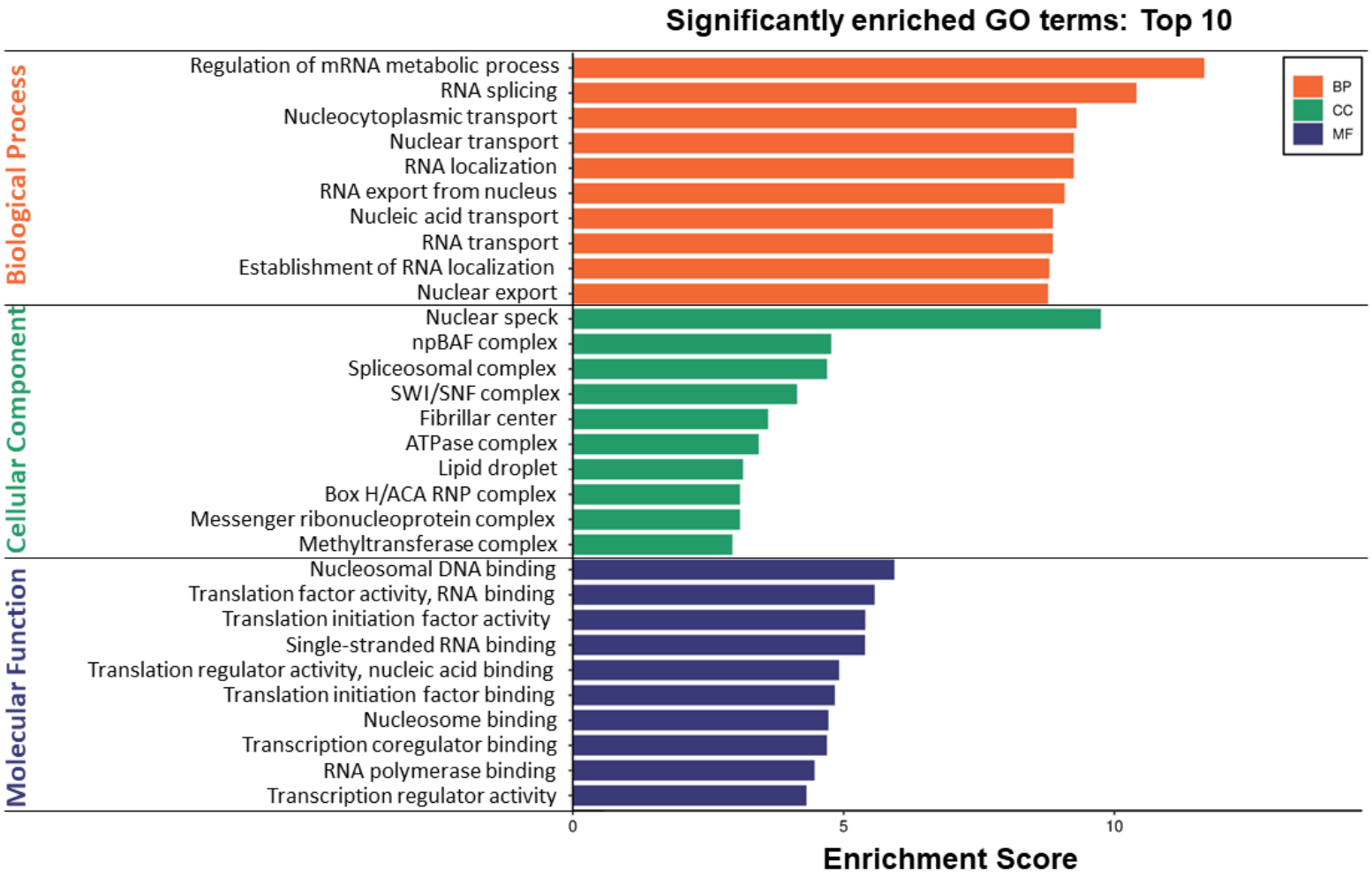

Figure 3.10: Gene ontology enrichment analysis of phosphoproteins found to be statistically significantly increased in Group 1. Graph highlights the top 10 most significantly enriched biological processes (orange), cellular components (green), and molecular functions (purple).

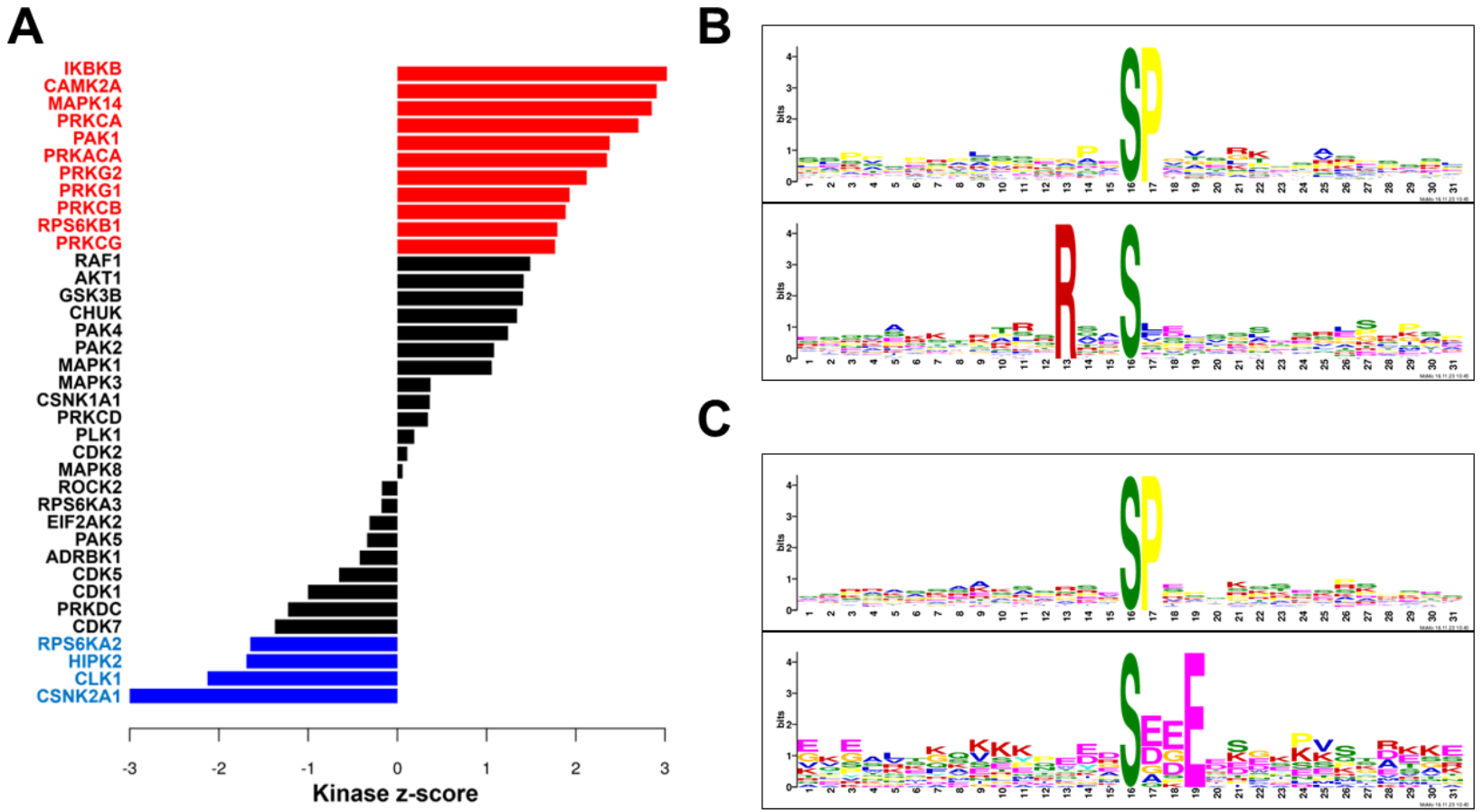

Figure 3.11: Bioinformatic analysis of phosphorylation motifs and upstream kinases. (**A**) Kinase-substrate enrichment analysis (KSEA) was performed to characterize kinase regulation based on drug resistance/sensitivity. Kinases with a p-value < 0.05 are highlighted as red and blue bars. Red bars indicate kinases predicted to be activated in drug resistant (Group 4) myeloma cells whereas blue bars indicate kinases predicted to be activated in drug sensitive (Group 1) myeloma cells. (**B**) Significantly enriched phosphorylation motifs from the phosphopeptides significantly increased in abundance in Group 4 samples. (**C**) Significantly enriched phosphorylation motifs from the phosphopeptides significantly increased in abundance in Group 1 samples.

3.3.3 Evaluation of MM patient response to individual drugs based on *ex vivo* drug sensitivity scores.

To identify phosphoproteomic events within myeloma cells that are associated with response to individual drugs, patient samples were stratified into "most sensitive" and "most resistant" groups based on the results of *ex vivo* DSRT. Patient samples with a low drug sensitivity score (DSS) are considered "most resistant" whereas those with high DSS are considered "most sensitive" to the individual drug being evaluated. The therapeutics evaluated in this study were selected to incorporate drugs from a variety of drug classes, including FDA-approved therapeutics and investigational targeted therapies. The individual drugs selected for this study are as follows: bortezomib (proteasome inhibitor), lenalidomide (immunomodulatory drug), luminespib (HSP90 inhibitor), PF 431396 (PYK2 and FAK inhibitor), and alvocidib (CDK9 inhibitor) (**Figure 3.12** and **Figure 3.13**).

Bortezomib	
Most Resistant	Most Sensitive
R_MM_8291	R_MM_7171
D_MM_7281	R_MM_3823
R_MM_1913	R_MM_3792
R_MM_587	D_MM_7746
	D_MM_7276

Lenalidomide	
Most Resistant	Most Sensitive
R_MM_6385	R_MM_7171
R_MM_3823	R_MM_6261
D_MM_8095	R_MM_2662
R_MM_6211	R_MM_3792
R_MM_1913	R_MM_4263
R_MM_1878	

Luminespib	
Most Resistant	Most Sensitive
D_MM_8597	R_MM_6261
R_MM_8291	D_MM_7276
R_MM_1913	R_MM_6211
D_MM_8095	R_MM_4263
D_MM_7281	R_MM_3792

PF 431396	
Most Resistant	Most Sensitive
D_MM_7746	R_MM_6261
D_MM_8597	R_MM_7171
R_MM_1913	R_MM_3792
D_MM_7281	D_MM_7396
R_MM_8291	D_MM_7983

Alvocidib	
Most Resistant	Most Sensitive
R_MM_1913	R_MM_6261
D_MM_7281	R_MM_3792
R_MM_587	D_MM_7276
R_MM_8291	R_MM_6211
	R_MM_1193

Figure 3.12: Sample stratification into "Most Resistant" and "Most Sensitive" groups for each of the five individual therapeutics analysed. Samples were stratified into "Most Resistant" and "Most Sensitive" groups based on DSS values. To investigate the samples considered most resistant or most sensitive, samples were separated into quartiles with those samples falling into the first quartile generally being considered "Most Resistant" and those in the fourth quartile generally being considered "Most Sensitive".

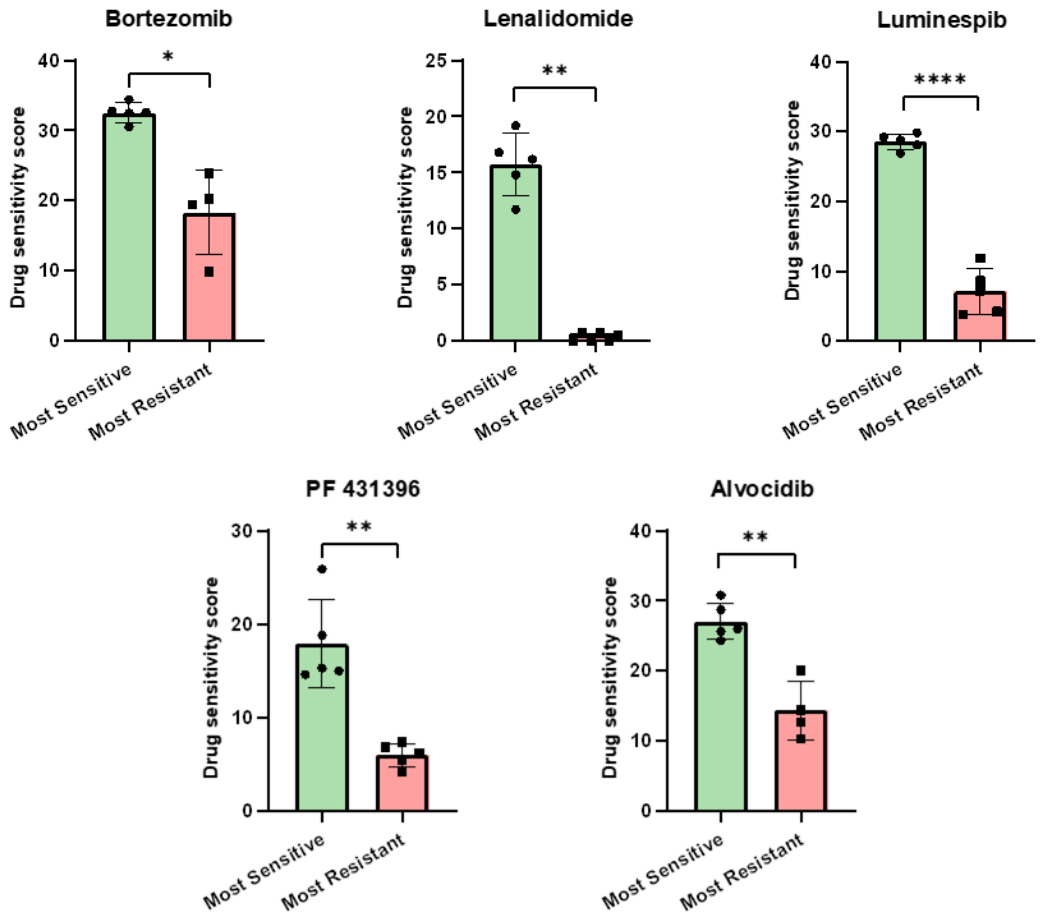

Figure 3.13: Comparison of drug sensitivity scores in "most sensitive" and "most resistant" groups associated with each individual drug. Normality was determined using the Shapiro-Wilk test. Statistical significance was evaluated by unpaired t-test with Welch correction. Significance is marked as follows: $P \leq 0.05$ '*', $P \leq 0.01$ '**', $P \leq 0.001$ '***', $P \leq 0.0001$ '****'.

3.3.3.1 Phosphoproteomic analysis of CD138+ myeloma cells based on sensitivity/resistance to proteasome inhibitors.

The proteomic and phosphoproteomic profiles of MM patient samples considered most sensitive and most resistant to bortezomib, were compared to identify proteins and phosphorylation sites associated with response to proteasome inhibitors (PIs). Volcano plot analysis identified 42 proteins increased in abundance in samples considered most resistant and 61 proteins increased in abundance in samples considered most sensitive to bortezomib (FDR q-value < 0.05, FC > 1.5) (**Figure 3.14A**)(**Supp. File 3.5**). 41 phosphorylation sites were increased in abundance in most resistant samples and 50 phosphorylation sites were increased in abundance in most sensitive samples (FDR q-value < 0.1, FC > 1.5) (**Figure 3.14B**)(**Supp. File 3.5**). To analyse the phosphoproteomic data set, the Cytoscape app, "Omics

Visualizer" was used to visualize site-specific information on a STRING network (**Figure 3.15A**). The minimum required interaction score was set to high confidence (0.7) and unconnected nodes were removed. Two clusters clearly separate the phosphoproteins associated bortezomib sensitivity, which are linked to RNA processing, and bortezomib resistance, which include proteins linked the cytoskeleton and integrin-mediated signalling. GO analysis of the combined protein and phosphoprotein results demonstrated an increase in adhesion and motility-linked biological processes in bortezomib resistant myeloma cells whereas protein translation and protein folding-associated biological processes were increased in bortezomib sensitive myeloma cells (**Figure 3.15B**)(**Supp. File 3.6**). KSEA was used to predict potential kinase activity based on the phosphorylation levels of known substrates. This analysis showed significant enrichment of 8 kinases in bortezomib resistant samples and 1 kinase in bortezomib sensitive samples (**Supp. Figure 3.1**). The NF-κβ signalling pathway associated kinases IKBKB and CHUK, which make up the catalytic subunits of the multimeric I kappa B kinase (IKK) complex, showed higher activity in bortezomib resistant samples, whereas the catalytic subunit of CK2, CSNK2A1, showed higher activity in bortezomib sensitive samples. Lists of the top 10 phosphorylation sites associated with bortezomib resistance and sensitivity are described in **Table 3.4** and **Table 3.5**, respectively.

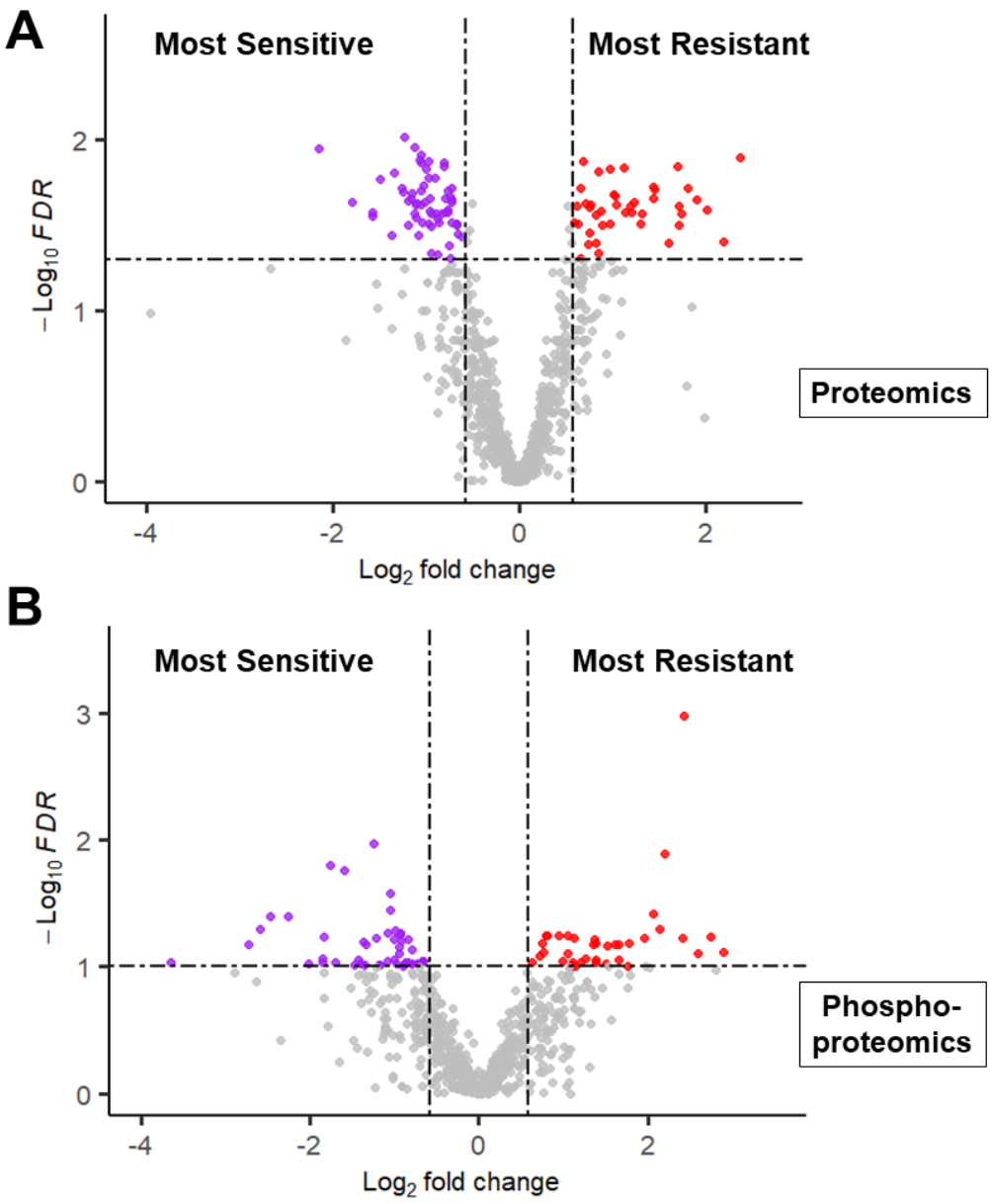

Figure 3.14: Volcano plots of CD138+ myeloma cells considered 'Most Sensitive' and 'Most Resistant' to bortezomib. (**A**) Volcano plot depicting SSDA proteins. (**B**) Volcano plot depicting SSDA phosphorylation sites. Purple points represent proteins/phosphosites increased in abundance in samples considered most sensitive to bortezomib. Red points represent proteins/phosphosites considered most resistant to bortezomib.

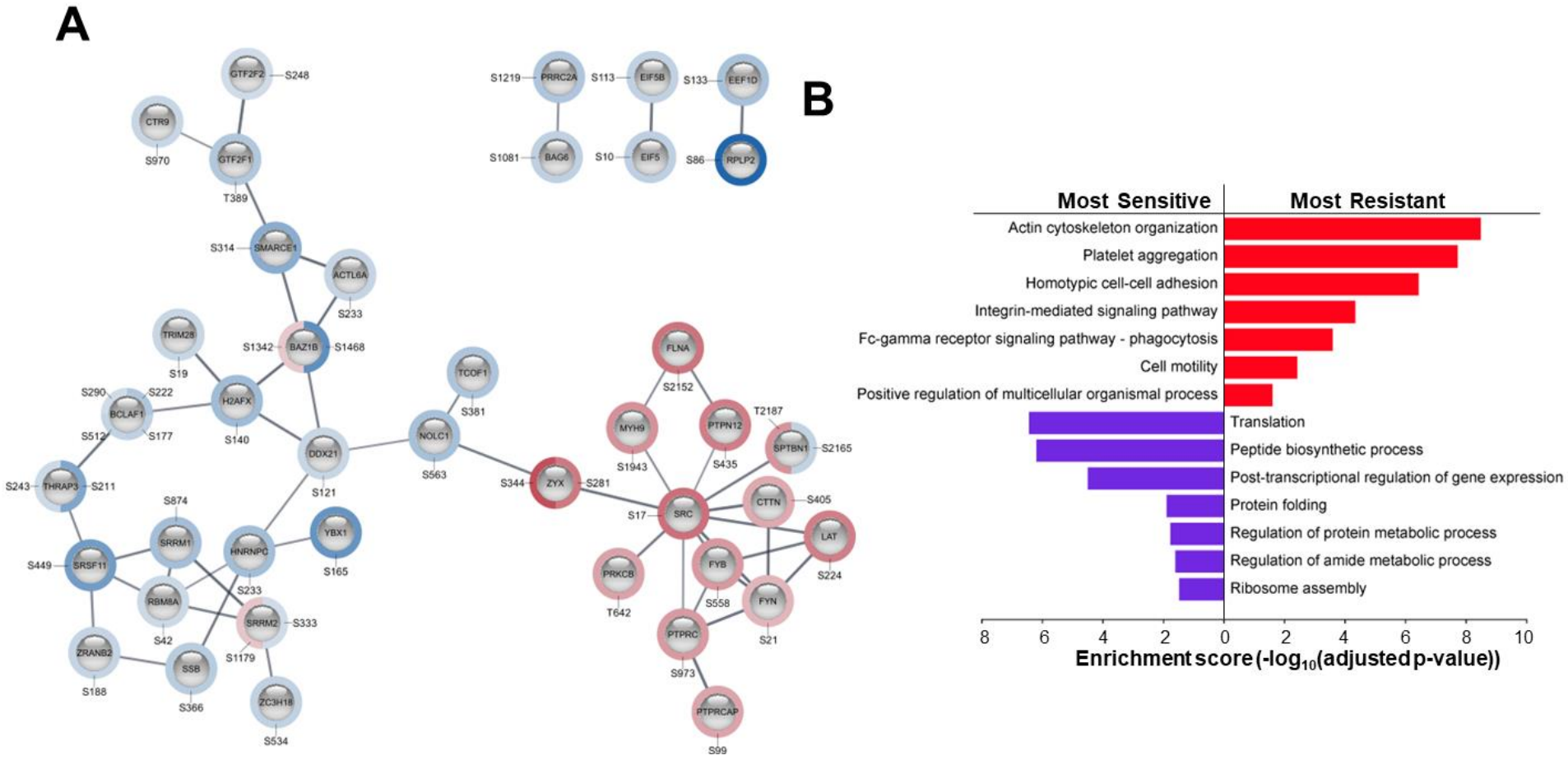

Figure 3.15: Bioinformatic analysis of phosphorylation sites associated with bortezomib sensitivity and resistance. (**A**) Protein-protein interaction (PPI) network of phosphorylation sites upregulated in MM samples considered most sensitive (blue) and most resistant (red) to bortezomib. (**B**) g:Profiler analysis of proteins and phosphoproteins upregulated in myeloma cells most resistant (red bars) and most sensitive (purple bars) to bortezomib. GO terms represent enriched biological processes highlighted as key terms in the g:Profiler analysis.

Table 3.4: Top 10 phosphorylation sites with significantly increased abundance in MM samples considered most resistant to bortezomib.

Protein Name	Gene Name	Biological Function	Phospho-Site	FDR q-value	FC
Heat shock protein beta-1	HSPB1	Molecular chaperone	S65	0	5.41
Proto-oncogene tyrosine-protein kinase Src	SRC	Cell adhesion	S17	0.013	4.60
Zyxin	ZYX	Cell adhesion	S281	0.038	4.19
Filamin-A	FLNA	Actin binding	S2152	0.051	4.42
Transmembrane protein 40	TMEM40	Membrane protein	S137	0.057	1.75
Tyrosine-protein kinase Fyn	FYN	Adaptive immunity	S21	0.057	2.08
Serine/arginine repetitive matrix protein 2	SRRM2	RNA binding	S1179	0.057	1.74
Zinc finger protein 609	ZNF609	Promoter-specific chromatin binding	S576	0.057	1.94
Zyxin	ZYX	Cell adhesion	S344	0.059	6.71
Sorting nexin-17	SNX17	Protein transport	S421	0.059	2.18

Table 3.5: Top 10 phosphorylation sites with significantly increased abundance in MM samples considered most sensitive to bortezomib.

Protein Name	Gene Name	Biological Function	Phospho-Site	FDR q-value	FC
Treacle protein	TCOF1	Regulation of translation	S381	0.011	2.38
Coiled-coil domain-containing protein 86	CCDC86	RNA binding	S18	0.016	3.40
Major vault protein	MVP	Protein transport	S445	0.018	3.02
Lupus La protein	SSB	RNA binding	S366	0.027	2.07
DNA fragmentation factor subunit alpha	DFFA	Deoxyribonuclease inhibitor activity	S315	0.036	2.08
Serine/arginine-rich splicing factor 11	SRSF11	RNA binding	S449	0.041	4.76
Nuclease-sensitive element-binding protein 1	YBX1	Nucleic acid binding	S165	0.041	5.53
Tyrosine-protein kinase BAZ1B	BAZ1B	Transcription regulation	S1468	0.051	6.04
Suppressor of SWI4 1 homolog	PPAN	RNA binding	S359	0.052	1.98
Cyclin-dependent kinase 12	CDK12	Serine/threonine protein kinase	S423	0.054	2.11

3.3.3.2 Phosphoproteomic analysis of CD138+ myeloma cells based on sensitivity/resistance to immunomodulatory drugs.

The proteomic and phosphoproteomic profiles of MM patient samples considered most sensitive and most resistant to lenalidomide were compared to identify proteins and phosphorylation sites associated with response to immunomodulatory drugs (IMiDs). Volcano plot analysis identified 42 proteins increased in abundance in samples considered most resistant and 23 proteins increased in abundance in samples considered most sensitive to lenalidomide (FDR q-value < 0.05, FC > 1.5) (**Figure 3.16A**)(**Supp. File 3.7**). 35 phosphorylation sites were increased in abundance in most resistant samples and 3 phosphorylation sites were increased in abundance in most sensitive samples (FDR q-value < 0.1, FC > 1.5) (**Figure 3.16B**)(**Supp. File 3.7**)). STRING network analysis using "Omics Visualizer" identified a single cluster of upregulated phosphosites in lenalidomide resistant myeloma cells associated with actin filament organization (**Figure 3.17A**). The minimum required interaction score was set to high confidence (0.7) and unconnected nodes were removed. KSEA analysis did not yield significant kinase enrichments. GO analysis of the combined protein and phosphoprotein results demonstrated an increase in adhesion and motility-linked biological processes in lenalidomide resistant myeloma cells whereas protein translation and metabolism-associated biological processes were increased in lenalidomide sensitive myeloma cells (**Figure 3.17B**)(**Supp. File 3.8**). We compiled a list of the phosphorylation sites most significantly increased in lenalidomide resistant and lenalidomide sensitive samples (**Table 3.6**, **Table 3.7**).

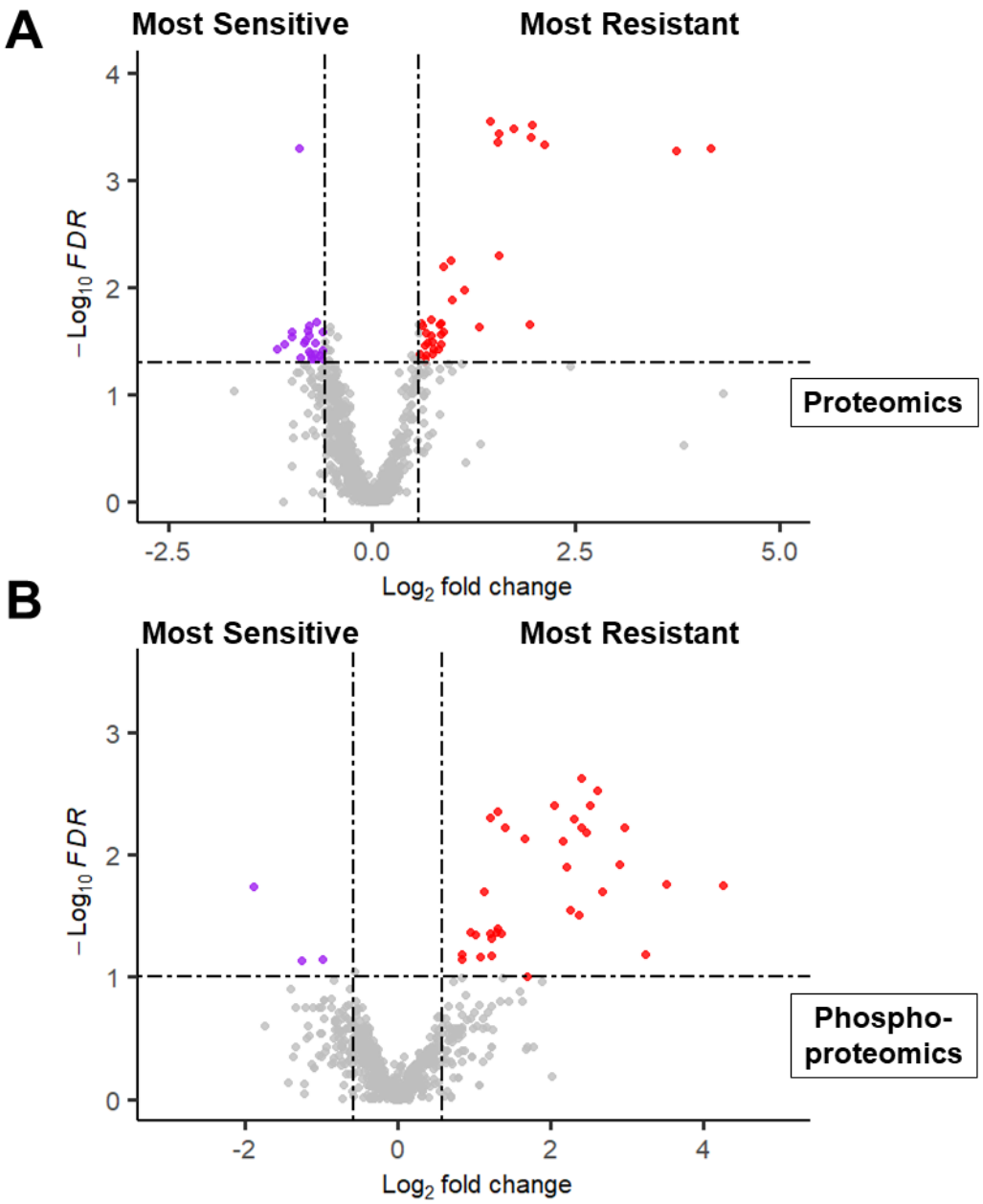

Figure 3.16: Volcano plots of CD138+ myeloma cells considered 'Most Sensitive' and 'Most Resistant' to lenalidomide. (**A**) Volcano plot depicting SSDA proteins. (**B**) Volcano plot depicting SSDA phosphorylation sites. Purple points represent proteins/phosphosites increased in abundance in samples considered most sensitive to lenalidomide. Red points represent proteins/phosphosites considered most resistant to lenalidomide.

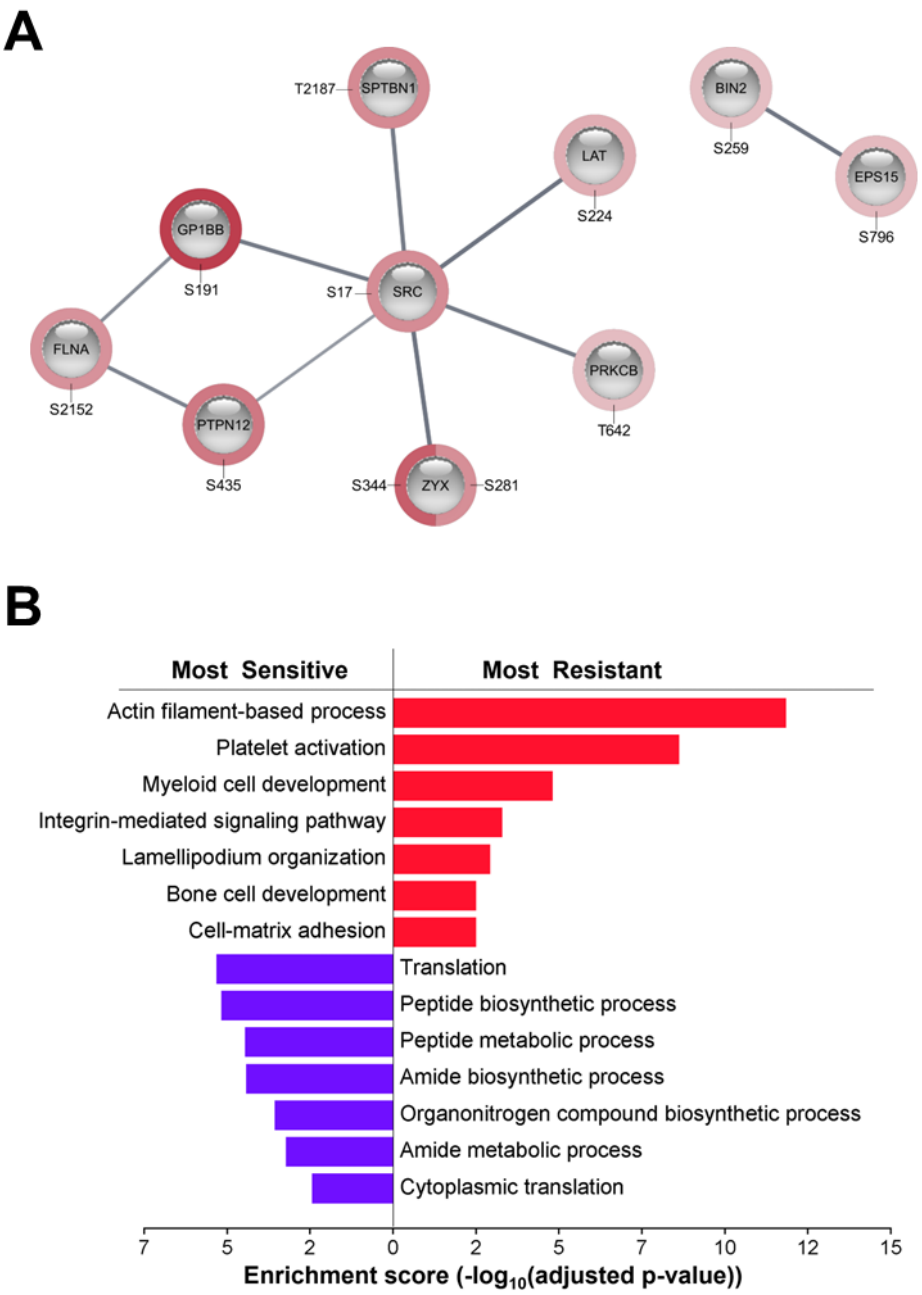

Figure 3.17: Bioinformatic analysis of phosphorylation sites associated with lenalidomide sensitivity and resistance. (**A**) Protein-protein interaction (PPI) network of phosphorylation sites upregulated in MM samples considered most resistant (red) to lenalidomide. Phosphorylation sites associated with lenalidomide sensitivity did not show connectivity. (**B**) g:Profiler analysis of proteins and phosphoproteins upregulated in myeloma cells most resistant (red bars) and most sensitive (purple bars) to lenalidomide. GO terms represent enriched biological processes highlighted as key terms in the g:Profiler analysis.

Table 3.6: Top 10 phosphorylation sites with significantly increased abundance in MM samples considered most resistant to lenalidomide.

Protein Name	Gene Name	Biological Function	Phospho-Site	FDR q-value	FC
Kalirin	KALRN	Guanine-nucleotide releasing factor	S1799	0.002	5.32
LIM domain and actin-binding protein 1	LIMA1	Actin binding	S490	0.003	6.15
Spectrin beta chain, non-erythrocytic 1	SPTBN1	Actin binding	T2187	0.004	5.72
Protein FAM63A	FAM63A	Cysteine-type deubiquitinase activity	S441	0.004	4.13
Bridging integrator 2	BIN2	Cell chemotaxis	S259	0.004	2.48
Neurobeachin-like protein 2	NBEAL2	Protein kinase binding	S2739	0.005	2.32
Filamin-A	FLNA	Actin binding	S2152	0.005	4.98
Serum deprivation-response protein	SDPR	Phosphatidylserine binding	S293	0.006	7.88
Zyxin	ZYX	Cell adhesion	S281	0.006	5.28
Epidermal growth factor receptor substrate 15	EPS15	Cadherin binding	S796	0.006	2.64

Table 3.7: Phosphorylation sites with significantly increased abundance in MM samples considered most sensitive to lenalidomide.

Protein Name	Gene Name	Biological Function	Phospho-Site	FDR q-value	FC
ADP-ribosylation factor-like protein 6-interacting protein 4	ARL6IP4	RNA binding	S332	0.018	3.71
Cytoskeleton-associated protein 4	CKAP4	RNA binding	S26	0.073	2.39
Nuclease-sensitive element-binding protein 1	YBX1	Nucleic acid binding	S165	0.071	1.98

3.3.3.3 Phosphoproteomic analysis of CD138+ myeloma cells based on sensitivity/resistance to a HSP90 inhibitor.

The proteomic and phosphoproteomic profiles of MM patient samples considered most sensitive and most resistant to the investigational HSP90 inhibitor, luminespib, were compared to identify proteins and phosphorylation sites associated with chemosensitivity. Volcano plot analysis identified 51 proteins increased in abundance in resistant myeloma cells and 57 proteins increased in abundance in samples considered most sensitive to lenalidomide (FDR q-value < 0.05, FC > 1.5) (**Figure 3.18A**)(**Supp. File 3.9**). 38 phosphorylation sites were increased in abundance in most resistant samples and 32 phosphorylation sites were increased in abundance in most sensitive samples (FDR q-value < 0.1, FC > 1.5) (**Figure**

3.18B)(**Supp. File 3.9)**. STRING network analysis using "Omics Visualizer" identified two distinct clusters. The minimum required interaction score was set to high confidence (0.7) and unconnected nodes were removed. One cluster largely consisting of phosphoproteins increased in abundance in luminespib resistant myeloma cells was associated with actin filament organization. A smaller cluster largely consisting of phosphoproteins increased in abundance in luminespib sensitive myeloma cells was associated with the regulation of translation initiation (**Figure 3.19**)(**Supp. File 3.10**). KSEA revealed a significant enrichment of 2 kinases, PRKACA and calcium/calmodulin-dependent protein kinase II alpha (CAMK2A), in myeloma cells most resistant to luminespib (**Supp. Figure 3.2**). The top ten phosphorylation sites significantly increased in myeloma cells most resistant and most sensitive to luminespib are listed in **Table 3.8** and **Table 3.9**, respectively.

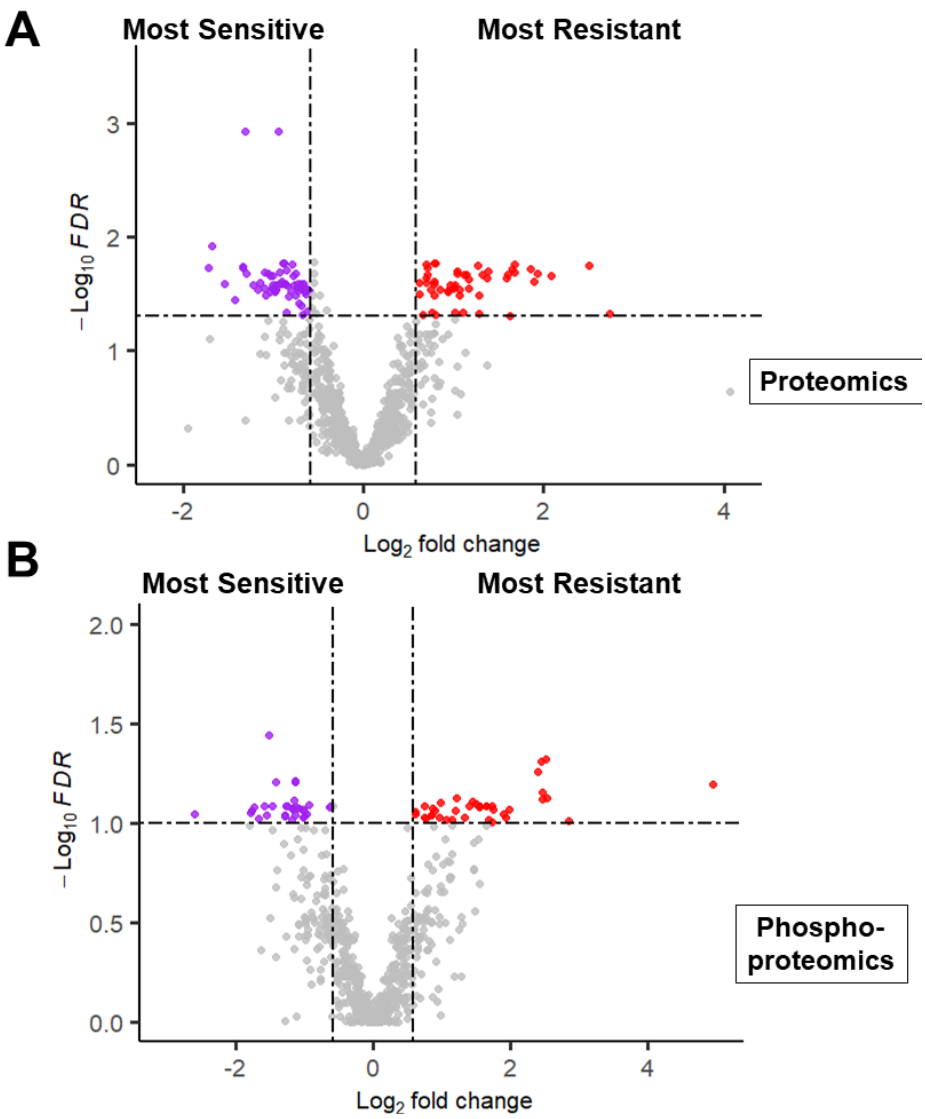

Figure 3.18: Volcano plots of CD138+ myeloma cells considered 'Most Sensitive' and 'Most Resistant' to luminespib. (**A**) Volcano plot depicting SSDA proteins. (**B**) Volcano plot depicting SSDA phosphorylation sites. Purple points represent proteins/phosphosites increased in abundance in samples considered most sensitive to luminespib. Red points represent proteins/phosphosites considered most resistant to luminespib.

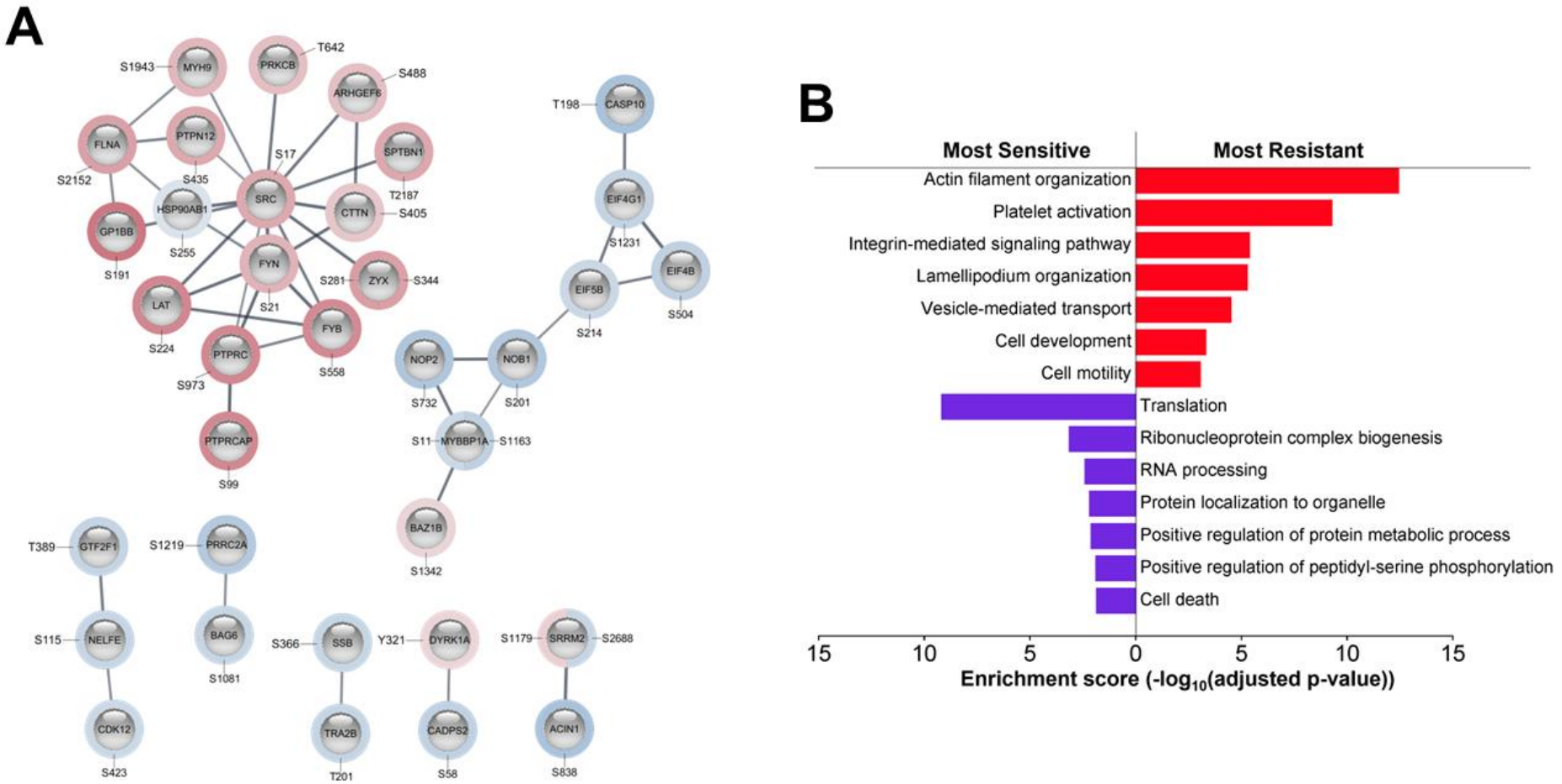

Figure 3.19: Bioinformatic analysis of phosphorylation sites associated with luminespib sensitivity and resistance. (**A**) Protein-protein interaction (PPI) network of phosphorylation sites upregulated in MM samples considered most resistant (red) and most sensitive (blue) to luminespib. (**B**) g:Profiler analysis of proteins and phosphoproteins upregulated in myeloma cells most resistant (red bars) and most sensitive (purple bars) to luminespib. GO terms represent enriched biological processes highlighted as key terms in the g:Profiler analysis.

Table 3.8: Top 10 phosphorylation sites with significantly increased abundance in MM samples considered most resistant to luminespib.

Protein Name	Gene Name	Biological Function	Phospho-Site	FDR q-value	FC
LIM domain and actin-binding protein 1	LIMA1	Actin binding	S490	0.048	5.75
Protein tyrosine phosphatase receptor type C-associated protein	PTPRCAP	Defence response	S99	0.049	5.47
FYN-binding protein	FYB	Immune response	S558	0.055	5.32
RAS guanyl-releasing protein 2	RASGRP2	Guanine-nucleotide releasing factor	S576	0.064	31.16
Receptor-type tyrosine-protein phosphatase C	PTPRC	B cell differentiation	S973	0.071	5.53
Serum deprivation-response protein	SDPR	Phosphatidylserine binding	S293	0.075	5.82
Protein kinase C beta type	PRKCB	Serine/threonine protein kinase	T642	0.075	2.34
Linker for activation of T-cells family member 1	LAT	Protein kinase binding	S224	0.076	5.57
Dematin	DMTN	Actin binding	S16	0.078	2.73
Histone-lysine N-methyltransferase SETD1A	SETD1A	DNA damage response	S1103	0.079	1.98

Table 3.9: Top 10 phosphorylation sites with significantly increased abundance in MM samples considered most sensitive to luminespib.

Protein Name	Gene Name	Biological Function	Phospho-Site	FDR q-value	FC
Protein PRRC2A	PRRC2A	RNA binding	S1219	0.036	2.86
Transformer-2 protein homolog beta	TRA2B	RNA binding	T201	0.061	2.20
Plasminogen activator inhibitor 1 RNA-binding protein	SERBP1	RNA binding	S234	0.062	2.68
Large proline-rich protein BAG6	BAG6	HSP70 protein binding	S1081	0.063	2.19
DNA fragmentation factor subunit alpha	DFFA	Deoxyribonuclease inhibitor activity	S315	0.077	2.20
Telomeric repeat-binding factor 2-interacting protein 1	TERF2IP	Telomeric DNA binding	S203	0.081	1.90
Uncharacterized protein C7orf50	C7orf50	RNA binding	S175	0.082	1.53
Nucleoprotein TPR	TPR	Chromatin binding	S2155	0.083	2.36
Calcium-dependent secretion activator 2	CADPS2	Protein transport	S58	0.083	2.41
RNA-binding protein NOB1	NOB1	RNA endonuclease activity	S201	0.083	3.01

3.3.3.4 Phosphoproteomic analysis of CD138+ myeloma cells based on sensitivity/resistance to a PYK2 and FAK inhibitor.

The proteomic and phosphoproteomic profiles of MM patient samples considered most sensitive and most resistant to the investigational PYK2 and FAK inhibitor, PF 431396, were compared to identify proteins and phosphorylation sites associated with chemosensitivity. Volcano plot analysis identified 38 proteins increased in abundance in resistant myeloma cells and 43 proteins increased in abundance in samples considered most sensitive to lenalidomide (FDR q-value < 0.05, FC > 1.5) (**Figure 3.20A**)(**Supp. File 3.11**). 20 phosphorylation sites were increased in abundance in most resistant samples and 12 phosphorylation sites were increased in abundance in most sensitive samples (FDR q-value < 0.1, FC > 1.5) (**Figure 3.20B**)(**Supp. File 3.11**). STRING network analysis using "Omics Visualizer" showed limited interactions between the significant phosphoproteins. The minimum required interaction score was set to high confidence (0.7) and unconnected nodes were removed. PTPN12, FLNA, and GP1BB, SERBP1 and RPLP2, and FYB and LAT showed connections with an interaction score > 0.7 (**Figure 3.21**)(**Supp. File 3.12**). KSEA analysis did not yield significant kinase enrichments. The top ten phosphorylation sites significantly increased in myeloma cells most resistant and most sensitive to PF 431396 are listed in **Table 3.10** and **Table 3.11**, respectively.

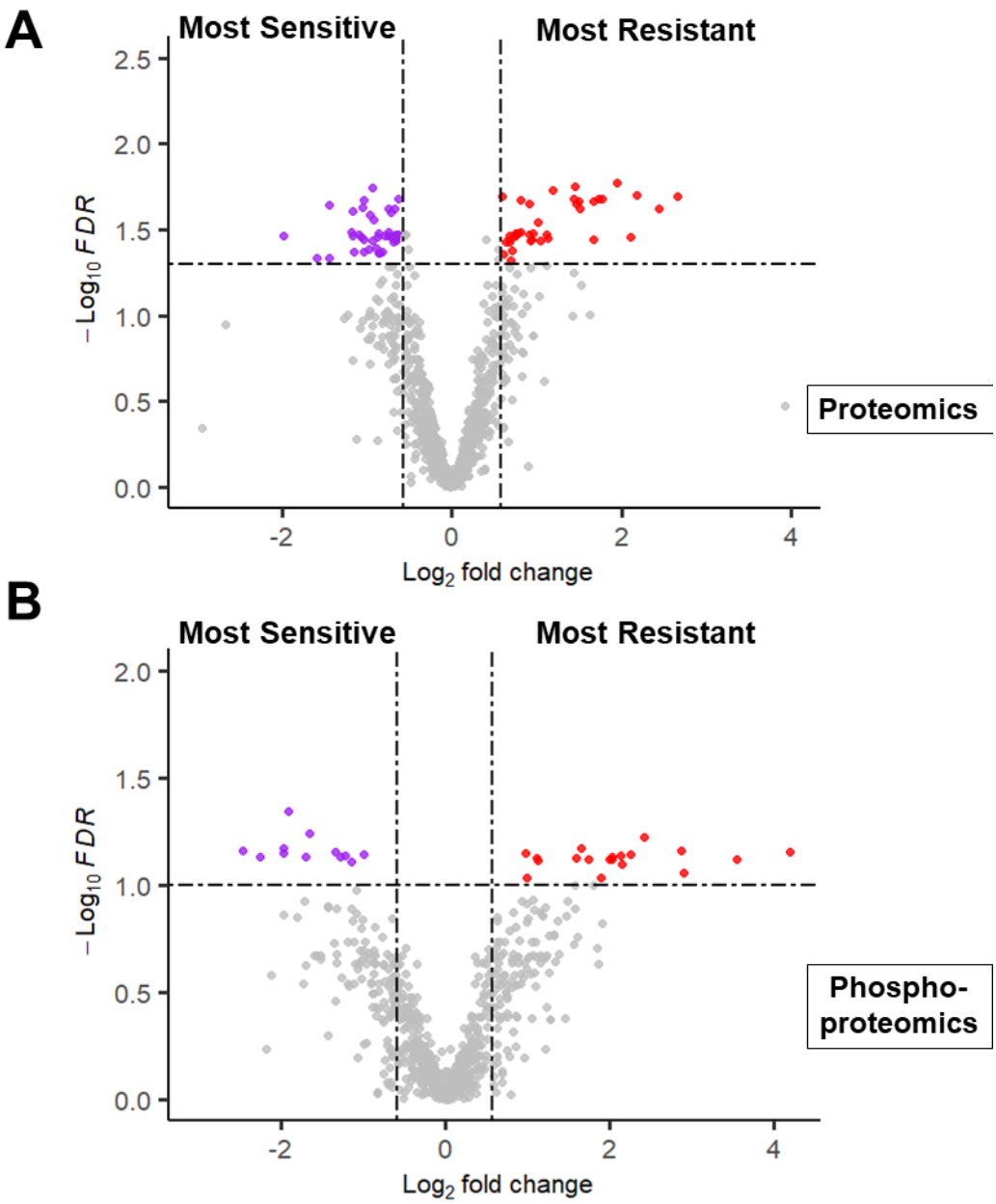

Figure 3.20: Volcano plots of CD138+ myeloma cells considered 'Most Sensitive' and 'Most Resistant' to PF 431396. (**A**) Volcano plot depicting SSDA proteins. (**B**) Volcano plot depicting SSDA phosphorylation sites. Purple points represent proteins/phosphosites increased in abundance in samples considered most sensitive to PF 431396. Red points represent proteins/phosphosites considered most resistant to PF 431396.

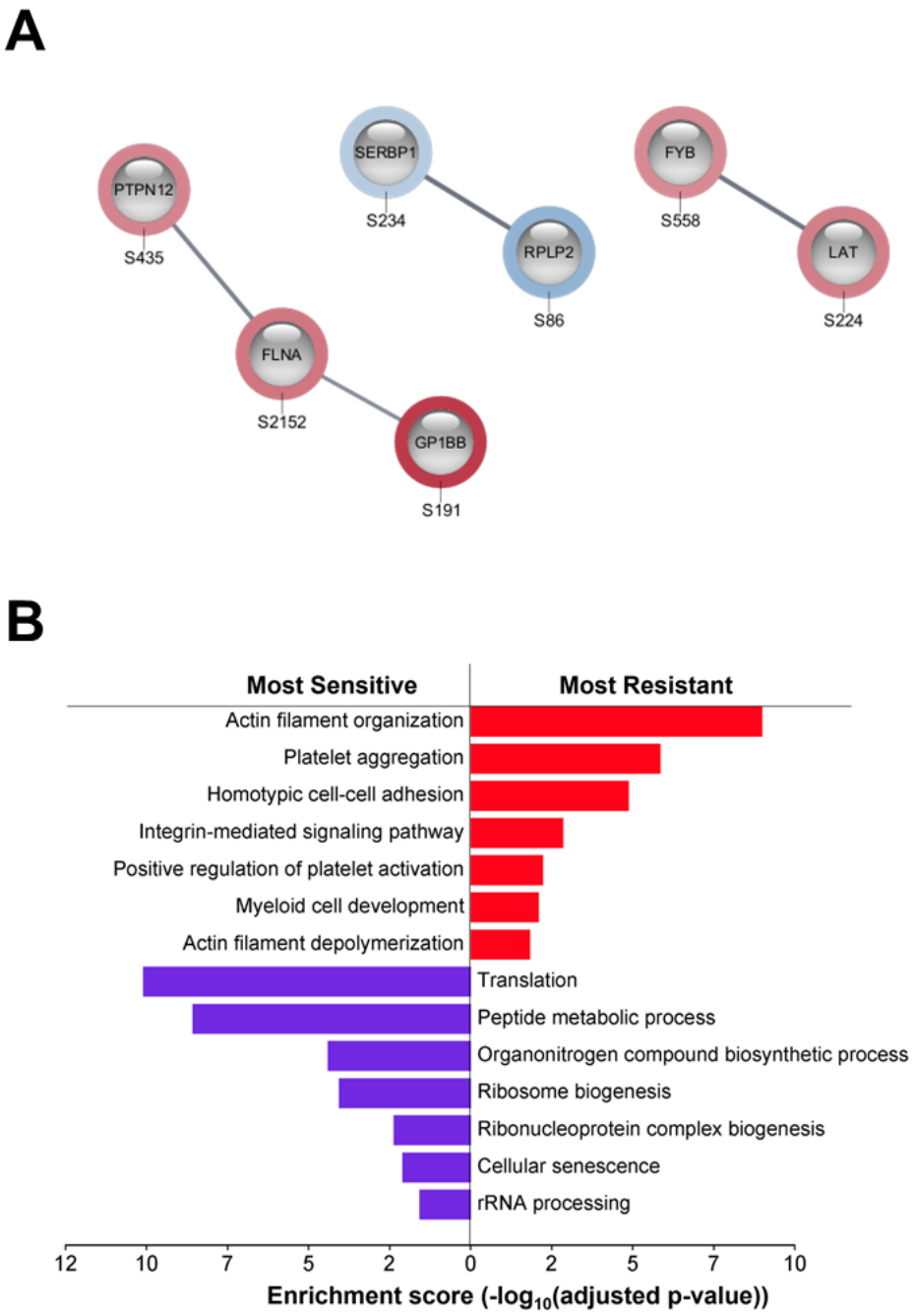

Figure 3.21: Bioinformatic analysis of phosphorylation sites associated with PF 431396 sensitivity and resistance. (**A**) Protein-protein interaction (PPI) network of phosphorylation sites upregulated in MM samples considered most resistant (red) and most sensitive (blue) to PF 431396. (**B**) g:Profiler analysis of proteins and phosphoproteins upregulated in myeloma cells most resistant (red bars) and most sensitive (purple bars) to PF 431396. GO terms represent enriched biological processes highlighted as key terms in the g:Profiler analysis.

Table 3.10: Top 10 phosphorylation sites with significantly increased abundance in MM samples considered most resistant to PF 431396.

Protein Name	Gene Name	Biological Function	Phospho-Site	FDR q-value	FC
Filamin-A	FLNA	Actin binding	S2152	0.060	5.36
Stromal interaction molecule 1	STIM1	Calcium transport	S575	0.067	3.13
Zyxin	ZYX	Cell adhesion	S344	0.069	7.31
RAS guanyl-releasing protein 2	RASGRP2	Guanine-nucleotide releasing factor	S576	0.070	18.26
Zinc finger protein 609	ZNF609	Promoter-specific chromatin binding	S576	0.071	1.96
Linker for activation of T-cells family member 1	LAT	Protein kinase binding	S224	0.072	4.75
LIM domain and actin-binding protein 1	LIMA1	Actin binding	S490	0.073	4.39
FYN-binding protein	FYB	Immune response	S558	0.074	4.10
Dematin	DMTN	Actin binding	S16	0.075	3.01
Polyhomeotic-like protein 3	PHC3	DNA binding	S263	0.075	2.16

Table 3.11: Top 10 phosphorylation sites with significantly increased abundance in MM samples considered most sensitive to PF 431396.

Protein Name	Gene Name	Biological Function	Phospho-Site	FDR q-value	FC
High mobility group protein HMG-I/HMG-Y	HMGA1	DNA binding	S44	0.045	3.73
Eukaryotic translation initiation factor 4 gamma 1	EIF4G1	RNA binding	S1231	0.058	3.14
60S acidic ribosomal protein P2	RPLP2	Ribosomal protein	S86	0.068	3.89
High mobility group protein HMG-I/HMG-Y	HMGA1	DNA binding	S9	0.069	5.48
Protein PRRC2A	PRRC2A	RNA binding	S1219	0.070	2.51
Thyroid hormone receptor-associated protein 3	THRAP3	mRNA processing	S211	0.071	3.89
Nucleoprotein TPR	TPR	Chromatin binding	S2155	0.072	1.98
Surfeit locus protein 6	SURF6	RNA binding	S138	0.073	2.32
Protein LYRIC	MTDH	RNA binding	S298	0.074	3.24
Plasminogen activator inhibitor 1 RNA-binding protein	SERBP1	RNA binding	S234	0.074	2.41

3.3.3.5 Phosphoproteomic analysis of CD138+ myeloma cells based on sensitivity/resistance to a CDK9 inhibitor.

The proteomic and phosphoproteomic profiles of MM patient samples considered most sensitive and most resistant to the investigational CDK9 inhibitor, alvocidib, were compared to identify proteins and phosphorylation sites associated with chemosensitivity. Volcano plot analysis identified 37 proteins increased in abundance in resistant myeloma cells and 49 proteins increased in abundance in samples considered most sensitive to alvocidib (FDR q-value < 0.05, FC > 1.5) (**Figure 3.22A**)(**Supp. File 3.13**). 30 phosphorylation sites were increased in abundance in most resistant samples and 15 phosphorylation sites were increased in abundance in most sensitive samples (FDR q-value < 0.1, FC > 1.5) (**Figure 3.22B**)(**Supp. File 3.13**). KSEA analysis did not yield significant kinase enrichments. STRING analysis revealed a single cluster of 7 phosphorylation sites upregulated in myeloma cells considered resistant to alvocidib (**Figure 3.23A**). GO biological processes (GOBPs) enriched in the most sensitive and most resistant groups showed a similar trend to those described above, with an increase in cytoskeletal organization and adhesion-linked biological processes in alvocidib resistant myeloma cells whereas protein translation-linked biological processes were increased in alvocidib sensitive myeloma cells (**Figure 3.23B**)(**Supp. File 3.14**). The phosphorylation sites most significantly upregulated in alvocidib resistant and alvocidib sensitive samples are outlined in **Table 3.12** and **Table 3.13**, respectively.

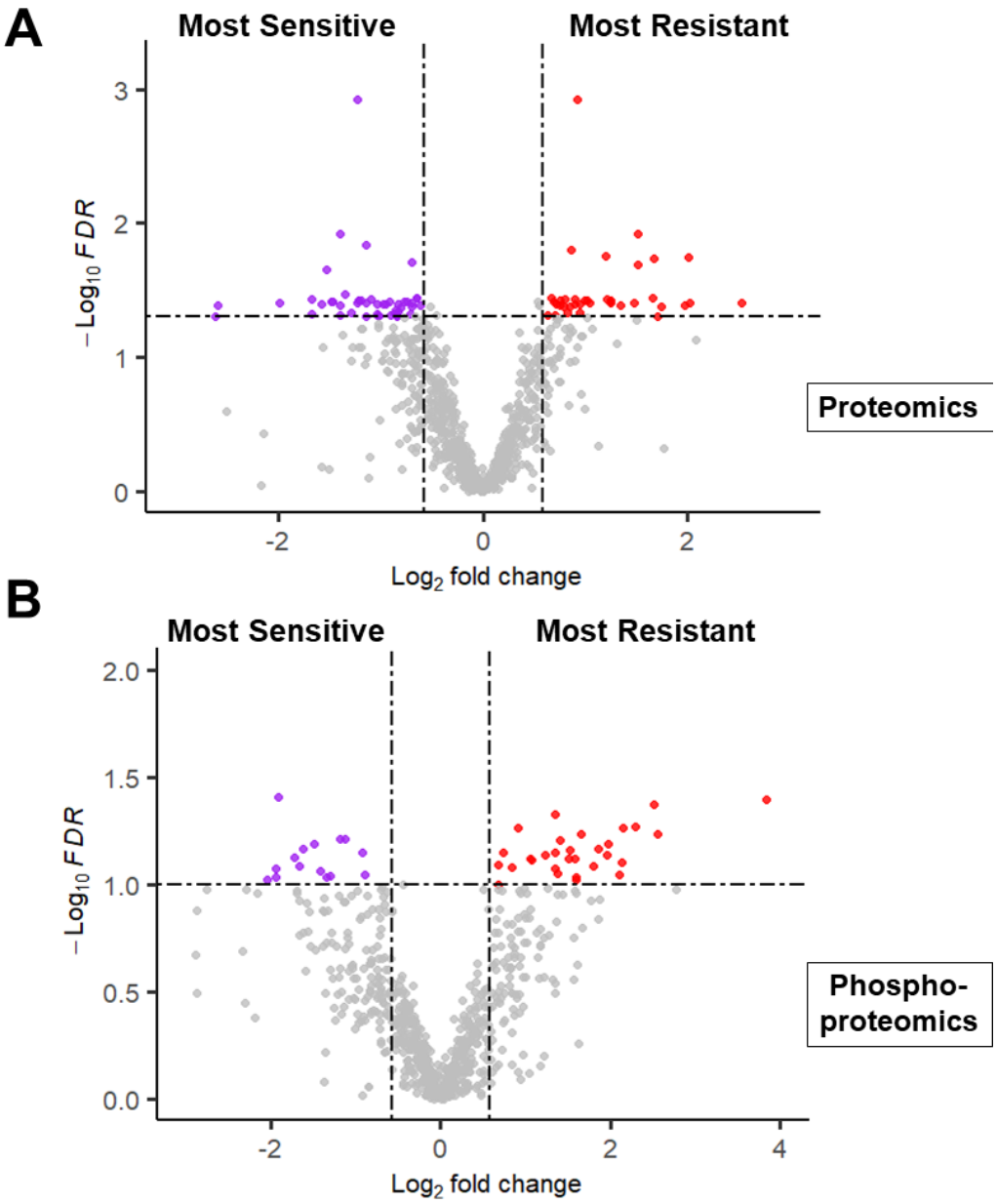

Figure 3.22: Volcano plots of CD138+ myeloma cells considered 'Most Sensitive' and 'Most Resistant' to alvocidib. (**A**) Volcano plot depicting SSDA proteins. (**B**) Volcano plot depicting SSDA phosphorylation sites. Purple points represent proteins/phosphosites increased in abundance in samples considered most sensitive to alvocidib. Red points represent proteins/phosphosites considered most resistant to PF alvocidib.

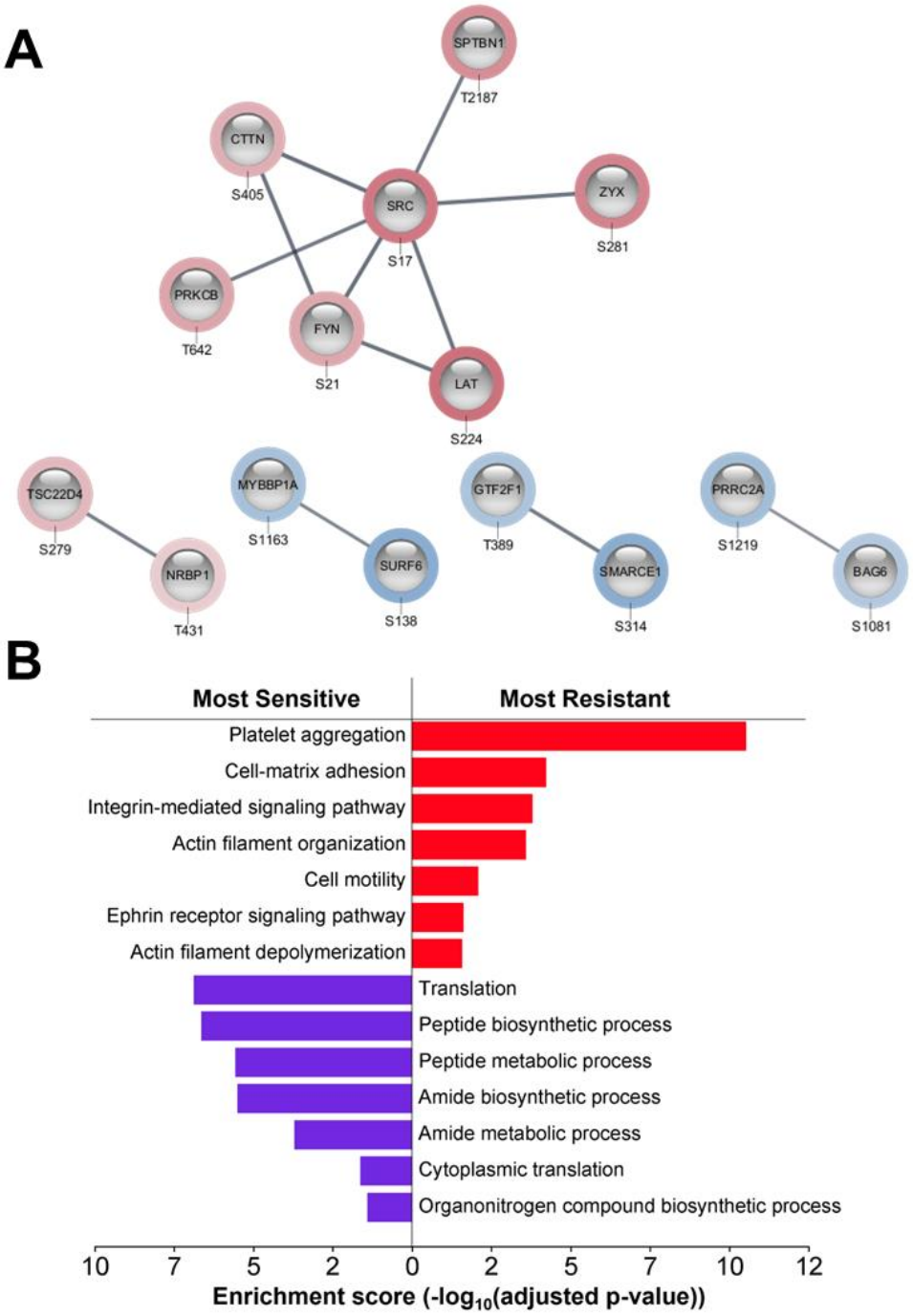

Figure 3.23: Bioinformatic analysis of phosphorylation sites associated with alvocidib sensitivity and resistance. (**A**) Protein-protein interaction (PPI) network of phosphorylation sites upregulated in MM samples considered most resistant (red) and most sensitive (blue) to alvocidib. (**B**) g:Profiler analysis of proteins and phosphoproteins upregulated in myeloma cells most resistant (red bars) and most sensitive (purple bars) to alvocidib. GO terms represent enriched biological processes highlighted as key terms in the g:Profiler analysis.

Table 3.12: Top 10 phosphorylation sites with significantly increased abundance in MM samples considered most resistant to alvocidib.

Protein Name	Gene Name	Biological Function	Phospho-Site	FDR q-value	FC
RAS guanyl-releasing protein 2	RASGRP2	Guanine-nucleotide releasing factor	S576	0.040	14.31
LIM domain and actin-binding protein 1	LIMA1	Actin binding	S490	0.043	5.72
N-acetyl-D-glucosamine kinase	NAGK	N-acetylglucosamine kinase activity	S76	0.047	2.56
Linker for activation of T-cells family member 1	LAT	Protein kinase binding	S224	0.054	4.92
Proto-oncogene tyrosine-protein kinase Src	SRC	Cell adhesion	S17	0.054	4.47
Serine/arginine repetitive matrix protein 2	SRRM2	RNA binding	S1179	0.055	1.88
Serum deprivation-response protein	SDPR	Phosphatidylserine binding	S293	0.058	5.92
Dematin	DMTN	Actin binding	S16	0.058	3.14
Protein kinase C beta type	PRKCB	Serine/threonine protein kinase	T642	0.063	2.65
Filamin-A	FLNA	Actin binding	S2152	0.065	3.93

Table 3.13: Top 10 phosphorylation sites with significantly increased abundance in MM samples considered most resistant to alvocidib.

Protein Name	Gene Name	Biological Function	Phospho-Site	FDR q-value	FC
Coiled-coil domain-containing protein 86	CCDC86	RNA binding	S18	0.039	3.79
Large proline-rich protein BAG6	BAG6	HSP70 protein binding	S1081	0.062	2.29
Cyclin-dependent kinase 12	CDK12	Serine/threonine protein kinase	S423	0.062	2.18
Protein PRRC2A	PRRC2A	RNA binding	S1219	0.065	2.83
Nuclear-interacting partner of ALK	ZC3HC1	Protein kinase binding	S62	0.069	3.08
Histone H1.5	HIST1H1B	DNA binding	S18	0.071	1.90
Chromatin complexes subunit BAP18	BAP18	DNA binding	S96	0.075	3.32
Ribosome-binding protein 1	RRBP1	RNA binding	S583	0.082	3.18
SWI/SNF-related matrix-associated actin-dependent regulator of chromatin subfamily E member 1	SMARCE1	Chromatin binding	S314	0.085	3.86
Myb-binding protein 1A	MYBBP1A	RNA binding	S1163	0.086	2.68

3.3.4 Western blotting verification of mass spectrometry results

Comparative immunoblotting was performed to verify the increased abundance of selected proteins and phosphorylation sites in myeloma cell lysates. The availability of high quality commercially available antibodies specific for the phosphorylation sites identified as potential markers of resistance was limited. Our MS proteomics results found the cytoskeletal protein, α-actinin, to be increased in abundance in Group 4 compared to Group 1 myeloma cells. This result was verified by western blotting, as depicted in **Figure 3.24**. Our MS phosphoproteomics analysis revealed an increased abundance of serine 2152 (S2152) phosphopeptide derived from filamin A (FLNA) in Group 4 compared to Group 1 myeloma cells. Intense bands corresponding to phosphorylated S2152 were seen in Group 4 samples while no bands were visible in Group 1 samples (**Figure 3.25**). Phosphorylated FLNA at S2152 was significantly increased in abundance in Group 4 samples (n=4) compared to Group 1 samples (n=4). Another blot measuring phosphorylated FLNA S2152 in Group 2 and 3 did not yield any detectable signal, indicating the presence of this phosphorylation event only in myeloma cells considered very drug resistant. Other phospho-specific antibodies were used in an attempt to verify additional phosphorylation sites; however, results were limited due to a lack of detectable signals. Furthermore, it is important to note that there are no loading controls for the western blots shown below. Despite attempting to use standard loading controls such as actin and GAPDH, the concentrations of these proteins varied likely due to the heterogeneity of the samples and role of the cytoskeleton in drug resistance in myeloma. This was further supported by altered concentrations of these proteins being detected in our mass spectrometry data. Although no loading controls were available, equal protein concentrations were visually confirmed using the Ponceau stain. However, as there are no loading controls to reflect this, the reliability of the results are affected. This may have been caused by dephosphorylation during freeze/thaw or sample processing, limited antibody quality, or simply a lack of the target within the samples being analysed. KSEA and motif analysis predicted a potential increase in the activity of PKA in Group 4 samples. Comparative immunoblotting found PRKACA levels to be increased in Group 4 samples compared to Group 1 samples, highlighting the potential of phosphoproteomics in

combination with *ex vivo* DSRT in identifying kinases involved in drug resistance/sensitivity (**Figure 3.26**).

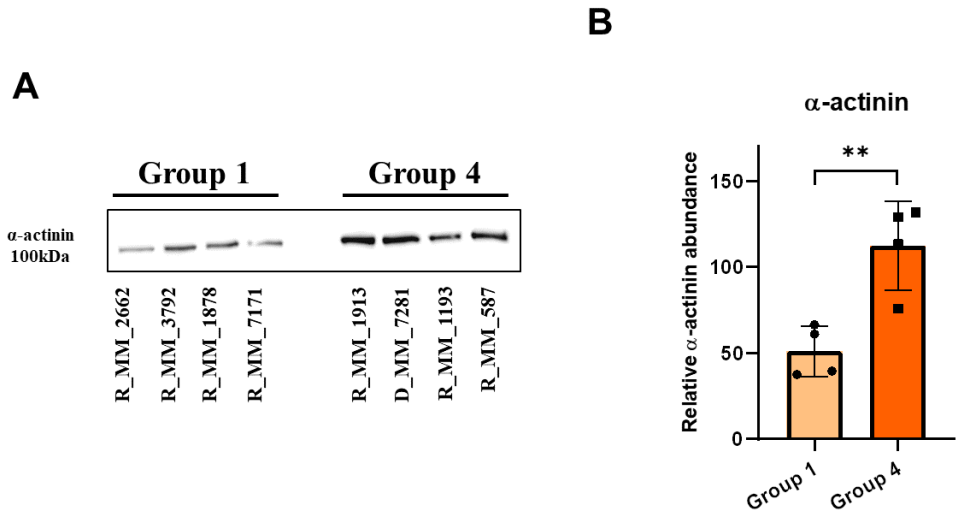

Figure 3.24: Comparative western blot analysis of α-actinin abundance in Group 4 and Group 1 myeloma cell lysates. (**A**) Representative immunoblot with bands labelled with antibodies to α-actinin clearly visible in Group 4 samples. (**B**) Densitometric analysis using ImageJ software followed by statistical analysis comparing band intensity between Group 1 and Group 4 samples. Significance was determined using a Student's t-test (** $p \leq 0.01$).

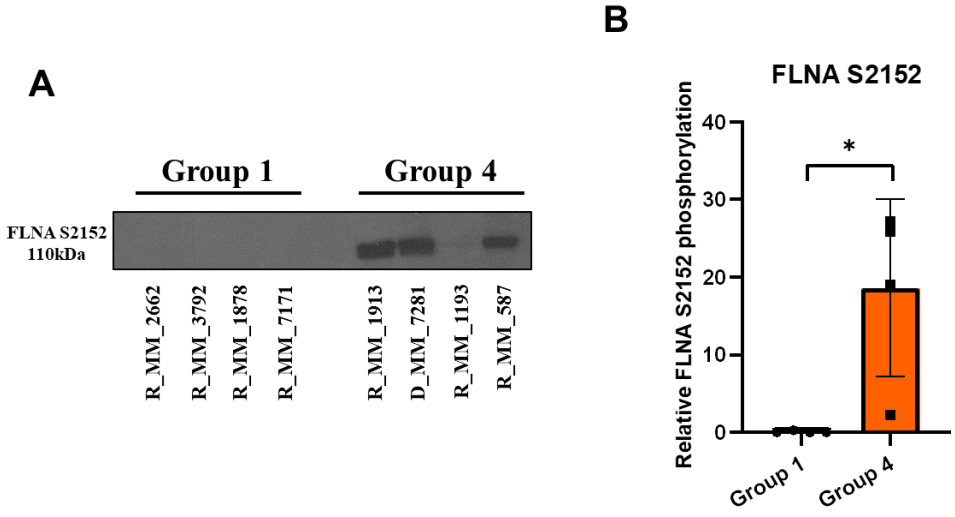

Figure 3.25: Comparative western blot analysis of FLNA S2152 abundance in Group 4 and Group 1 myeloma cell lysates. (**A**) Representative immunoblot with bands labelled with antibodies to FLNA S2152 phosphorylation clearly visible in Group 4 samples. (**B**) Densitometric analysis using ImageJ software followed by statistical analysis comparing band intensity between Group 1 and Group 4 samples. Significance was determined using a Mann-Whitney test (* $p \leq 0.05$).

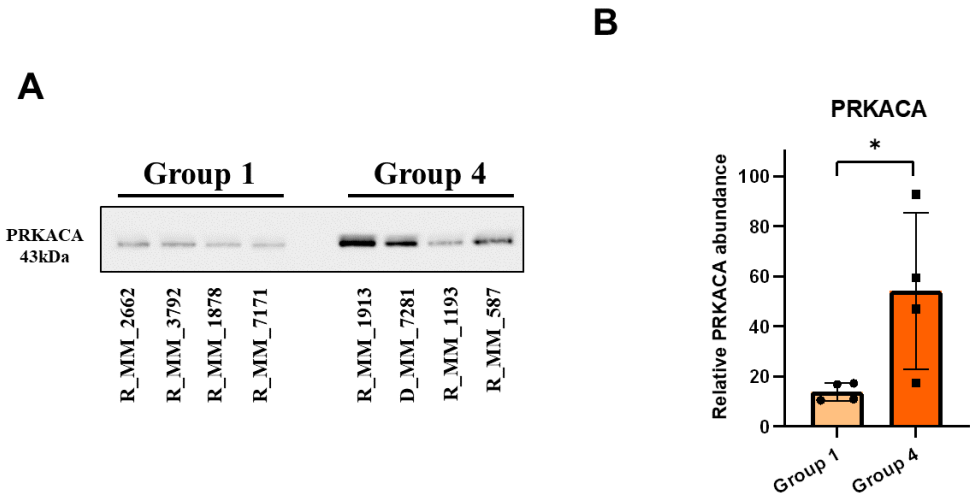

Figure 3.26: Comparative western blot analysis of PRKACA abundance in Group 4 and Group 1 myeloma cell lysates. (**A**) Representative immunoblot with bands labelled with antibodies to PRKACA clearly visible in Group 4 samples. (**B**) Densitometric analysis using ImageJ software followed by statistical analysis comparing band intensity between Group 1 and Group 4 samples. Significance was determined using a Student's t-test (* $p \leq 0.05$).

3.4 Discussion

Phosphoproteomics represents an important 'omics' approach to provide insight into the post-translational events involved in the pathogenesis of various diseases and cancers. As recent studies have demonstrated the clinical applicability of *ex vivo* DSRT, downstream molecular analyses investigating novel therapeutic targets and surrogate markers of drug sensitivity/resistance have clinical relevance (Kuusanmäki *et al.* 2022; Kropivsek *et al.* 2023). In this chapter, we have identified proteins and phosphorylation sites in myeloma cells that are associated with sensitivity/resistance to a selection of drugs based on *ex vivo* DSRT. This highlights the ability to combine 'omics' technologies with *ex vivo* DSRT to investigate mechanisms of drug resistance, identify predictive markers of drug response and identify potential targets to overcome drug resistance. Primary myeloma cells are also considered more biologically representative of MM than cell lines, thus enhancing the clinical relevance of results derived from *ex vivo* DSRT in combination with 'omics' approaches.

Our label-based mass spectrometry analysis identified a clear distinction in the proteomic and phosphoproteomic profiles of myeloma cells in the very sensitive and very resistant chemosensitivity groups. Functional enrichment analysis revealed an

increased abundance of proteins and phosphoproteins associated with cell adhesion and cytoskeletal organisation in drug resistant samples, re-emphasizing the link between cell adhesion molecules and drug resistance in MM (Lu *et al.* 2018; Bou Zerdan *et al.* 2022). The reduced levels of proteins involved in protein translation and the ribosome also indicate a slower cycling rate than drug sensitive myeloma cells, a process that reduces the susceptibility of these myeloma cells to chemotherapies such as bortezomib (Ge *et al.* 2021). These results corroborate with known mechanisms of drug resistance, namely, CAM-DR and the persistence of quiescent cancer cells (Huang *et al.* 2021; Lindell *et al.* 2023). Furthermore, western blot verification of selected MS results confirmed the differential abundance of α-actinin, a protein found to be increased in Group 4 samples, S2152 FLNA phosphorylation, a site found to hyperphosphorylated in Group 4 samples, and PRKACA, a protein kinase whose substrates were significantly enriched in Group 4 samples according to KSEA. Mass spectrometry analysis revealed an almost nine-fold increase in the abundance of the actin binding protein, α-actinin (ACTN1), in drug resistant myeloma cells. This result was verified by immunoblotting, highlighting the role of cytoskeletal organisation in drug resistance. Previous research found ACTN1 to be to be overexpressed in the PI-resistant cell line, KMS-20 (Tsubaki *et al.* 2021).

KSEA analysis revealed an enrichment of substrates of a number of kinases including PKA and protein kinase C beta (PRKCB). Although PKA was not detected in our mass spectrometry analysis, western blotting analysis revealed an increased abundance in PRKACA protein levels in chemoresistant myeloma cells. PKA is known to phosphorylate FLNA at S2152 and increased activity may contribute to resistance mechanisms in MM (Peverelli *et al.* 2018). Hyperphosphorylation at threonine 642 of PRKCB, a phosphorylation event that is essential for enzymatic activity, was identified in Group 4 samples, suggesting an association between increased PRKCB activity and chemoresistance in MM (Zhang *et al.* 1994). Interestingly, studies have reported synergistic activity between bortezomib and the protein kinase C inhibitor, enzastaurin, whose main target is PRKCB, in lymphoma cell lines (Cosenza *et al.* 2015). This, in combination with our findings, indicates that reduced PRKCB activity may enhance the chemosensitivity of myeloma cells. Determining the phosphoproteomic changes across chemosensitivity groups

highlights proteins, phosphorylation sites, and predicted kinases that may play roles in general drug resistance mechanisms. Furthermore, of the five classes of drugs evaluated in this work, phosphorylation sites commonly altered in abundance across these drugs can provide insight into the general mechanisms of resistance in myeloma cells.

While evaluating the proteomic and phosphoproteomic profiles of myeloma cells grouped based on their *ex vivo* sensitivity to hundreds of drugs provides important information on general or prominent resistant mechanisms, examining the molecular profiles of MM cells considered resistant/sensitive to individual drugs can identify resistance mechanisms and predictive biomarkers specific to the individual drugs being investigated. As described in Chapter 1, proteasome inhibitors (PIs) are a mainstay treatment of MM. The approval of bortezomib almost two decades ago dramatically improved patient outcomes, however, resistance remains a challenge. Our proteomic analysis identified seven 20S proteasome subunits as increased in abundance in bortezomib sensitive myeloma cells. Increased expression of the 20S proteasome has previously been proposed as a predictor of bortezomib sensitivity (Matondo *et al.* 2010; Walter *et al.* 2019). HSPB1 (also known as heat shock protein 27 (HSP27)), a small chaperone protein involved in preventing protein misfolding, was significantly increased in abundance in bortezomib resistant myeloma cells. In addition, phosphorylation events on serine 65 (S65) and serine 82 (S82) of HSP27 were increased in abundance in bortezomib resistant myeloma cells. HSP27 phosphorylation results in the formation of smaller oligomers with enhanced chaperone activity which prevents protein aggregation (Hayes *et al.* 2009). A recent study revealed a central role of HSP27 in the mechanism of action of bortezomib. MM patients who responded to a bortezomib-based treatment regimen had significantly lower expression of HSP27 compared to those who did not respond to bortezomib treatment. Furthermore, treatment of myeloma cell lines with the HSP27 inhibitor, OGX-427, resulted in similar apoptosis rates and expression patterns of HSP27, BCL-2 and Bax (Li, Zhang, *et al.* 2019). Blockade of HSP27 has been reported to restore sensitivity in bortezomib resistant cells, while ectopic expression of HSP27 rendered bortezomib sensitive cells resistant to bortezomib treatment (Chauhan *et al.* 2003). This highlights the ability of combining *ex vivo* DSRT with

phosphoproteomics to identify key proteins and phosphorylation sites associated with drug resistance.

Filamin A is an actin binding protein which acts as a scaffold for various protein partners including transmembrane proteins such as integrins. Phosphorylation of FLNA at S2152 is well-documented with several studies reporting that this phosphorylation event prevents cleavage of full length (280kDa) FLNA by calpains at the hinge region to the 110kDa fragment that is further cleaved into a 90kDa fragment (Chen and Stracher 1989; Bedolla *et al.* 2009). Western blotting analysis identified S2152 phosphorylation at ~110kDa indicating fragmentation of full length FLNA. As S2152 phosphorylation prevents FLNA cleavage, this result may be due to proteolysis during sample storage, however further investigations should be performed to confirm this. Full length FLNA is typically found in the cytoplasm whereas the 90kDa fragment is translocated into the nucleus, although some studies have reported the presence of full-length FLNA within the nucleolus (Deng *et al.* 2012). A study on prostate cancer reported differential pathological functions of cytoplasmic and nuclear FLNA, whereby cytoplasmic FLNA was linked to metastasis while nuclear FLNA prevented cell invasion, highlighting the role of FLNA cleavage and thus S2152 phosphorylation in cancer (Bedolla *et al.* 2009). Protein levels of FLNA were also increased in bortezomib resistant samples, however, the phosphorylation status of S2152 may provide more insight into the biological function and cellular location of FLNA in drug resistant myeloma. Interestingly, nuclear FLNA supresses the transcription of ribosomal RNA by preventing the recruitment of RNA polymerase I to the rDNA promoter. Ribosomal RNAs are required for ribosome biogenesis and protein production; thus, depletion of FLNA which results in increased rRNA levels was found to increase cell proliferation rates (Deng *et al.* 2012). The susceptibility of myeloma cells to proteasome inhibition is largely based on the high protein biosynthetic rate of myeloma cells which results in dependence on the proteasome to remove misfolded proteins. Therefore, one of the resistance mechanisms of bortezomib has been proposed to be a reduction in protein synthesis and proteasome workload (Bianchi *et al.* 2009; Cenci *et al.* 2012). Increased levels of FLNA may contribute to reducing the rate of protein synthesis in bortezomib-resistant cells, although more studies are required to confirm this hypothesis.

Interestingly, hypophosphorylation of serine 381 (S381) of TCOF1 was identified in bortezomib resistant myeloma cells while protein levels of TCOF1 were unchanged across the two groups. TCOF1 encodes the treacle phosphoprotein which is known to have roles in ribosome biogenesis and the DNA damage response (Lin and Yeh 2009; Larsen *et al.* 2014). Limited studies have investigated the effects of S381 on the function of TCOF1, however this site has been found to be hyperphosphorylated in various cancers including breast, colon, and ovarian (Deb *et al.* 2020). KSEA analysis revealed an enrichment of substrates of CK2 in Group 1 samples and those considered most sensitive to bortezomib. CK2 has diverse roles in carcinogenesis, and myeloma cells have been reported to rely on the activity of CK2 for survival (Piazza *et al.* 2006). CK2 stimulates the transcription of RNA polymerases which are required for rRNA synthesis and subsequent protein translation to support cell growth and proliferation (Hockman and Schultz 1996; Lin *et al.* 2006). Increased cell proliferation via CK2-based regulation of signalling pathways such as NF- κB and PI3K/AKT/mTOR, and increased protein synthesis stimulated by CK2, may increase the sensitivity of myeloma cells to various drugs due to the increased activity of drug targets. However, CK2 inhibition has demonstrated enhanced cytotoxicity in combination with bortezomib in MM (Manni *et al.* 2012, 2013; Xu, Ma, *et al.* 2019). Therefore, further investigation into the link between CK2 activity and drug response in MM is required.

KSEA analysis of bortezomib resistant myeloma revealed an enrichment of substrates of IKBKB and CHUK kinases, which constitute the two catalytic subunits of the IKK complex which acts as a central regulator for the activation of NF-κB signalling (Israël 2010). Activation of the IKK complex results in the phosphorylation of IκB, leading to its proteasomal degradation which releases NF-κB dimers, enabling their translocation to the nucleus where they stimulate the transcription of various genes involved in the inflammatory response, cell growth, and survival (Hinz and Scheidereit 2014). An important rationale for the use of PIs in the treatment of MM is to inhibit a key signalling pathway in MM pathogenesis, the NF-κB pathway. However, since the introduction of PIs, studies have found that bortezomib also induces the activation of the canonical NF-κB pathway via the downregulation of IκB. Signalling via IKBKB has been found to play a key role in bortezomib-induced NF-κB activation and the combination of bortezomib with an

IKBKB inhibitor has been reported to enhance bortezomib-induced cytotoxicity (Hideshima *et al.* 2009, 2014). Several studies have implicated NF-κB activity in bortezomib-resistance (Markovina *et al.* 2008b; Xie *et al.* 2020). Increased activity of IKBKB and CHUK kinases may contribute to bortezomib resistance and warrant further investigation as targets in bortezomib-resistant MM.

The activating phosphorylation site of tyrosine-protein kinase Fyn, S21, was hyperphosphorylated in Group 4 samples, and those considered most resistant to bortezomib, alvocidib, and luminespib, while phosphorylation of S558 on Fyn-binding protein was hyperphosphorylated in Group 4 samples, and those considered most resistant to luminespib and PF 431396. Fyn S21 is also a target of PKA (Yeo *et al.* 2011). Interestingly, CD45 has also been implicated in the activation of Fyn and other Src family kinases (SFKs) through the dephosphorylation of negative regulatory tyrosine phosphorylation sites. Hyperphosphorylation of CD45 and CD45-associated protein on serine 973 and serine 99, respectively, was identified in Group 4 samples compared to Group 1 samples. Previous studies have reported that IL-6 signalling leads to the activation of SFKs including Fyn in MM (Hallek *et al.* 1997). IL-6 has also been reported to induce CD45 expression which is required for the activation of Fyn in myeloma cell lines (Kawano *et al.* 2002). CD45 positive expression is typically associated with immature myeloma cells which have been linked to a more drug-resistant phenotype (Okikawa *et al.* 2004; Descamps *et al.* 2006; Iriyama *et al.* 2017; Ferguson *et al.* 2022). Fyn activation has been linked to drug resistance in a number of cancers including contributing to tamoxifen resistance in breast cancer and imatinib resistance in chronic myeloid leukemia (Elias *et al.* 2015; Irwin *et al.* 2015). Another member of the SFKs, Src, demonstrated hyperphosphorylation on serine 17 in drug resistant myeloma cells. Phosphorylation of Src at this site by PKA has been implicated in the activation of the small GTPase Rap1 which is involved in cell adhesion and extracellular signal-regulated kinases (ERKs) (Obara *et al.* 2004). The role of Rap1 in regulating integrin activation has resulted in studies suggesting the targeting of Rap1 to combat CAM-DR (Shain and Dalton 2001; de Bruyn *et al.* 2002; Emmons *et al.* 2011). Rap1 levels, which showed a greater than 4-fold increase in Group 4 samples compared to Group 1 samples, have also been linked to chemotherapy response in breast cancer whereby increased Rap1 levels predict a poor response (Khattar *et al.* 2019). Therefore, PKA-mediated

Src phosphorylation and subsequent activation of Rap1 may represent a mechanism of drug resistance in MM.

Certain phosphorylation sites were uniquely hypo- or hyper-phosphorylated based on response to individual drugs. For example, phosphorylation of S9 and S44 on HMGA1 was increased in samples considered most sensitive to the PYK2 and FAK inhibitor, PF-431396. One study reported a role of HMGA1 in regulating the urokinase plasminogen activator system in the secretome of breast cancer cells. Interestingly, silencing of HMGA1 resulted in a down-regulation of FAK, one of the main transducers of urokinase plasminogen activator system signalling (Resmini *et al.* 2017). Furthermore, a long non-coding RNA regulated by FAK, LINC01614, was found to promote colorectal cancer via the modulation of the miR-217-5p/HMGA1 axis and subsequently increased abundance of HMGA1 (Vishnubalaji *et al.* 2019; Jia *et al.* 2023). These findings suggest a link between HMGA1 abundance and FAK activation; therefore, increased abundance of phosphorylated HMGA1 may indicate increased FAK activity, and consequently increased susceptibility to FAK inhibitors such as PF 431396.

Of the phosphorylation sites found to be hypo- or hyper-phosphorylated in this study, the impact of many of these phosphorylation events on protein function is poorly understood. Our study identifies phosphorylation sites that warrant further investigation to determine their effect on protein function and their potential role in drug resistance or MM pathogenesis. For example, tyrosine protein kinase BAZ1B phosphorylation at S1468 was increased in bortezomib-sensitive myeloma cells. An RNA interference screen identified the BAZ1B gene as a bortezomib sensitizer in MM, however, the effect of S1468 phosphorylation on the function of BAZ1B is unknown (Zhu, Tiedemann, *et al.* 2011). Although phosphorylation events including dematin S16, large proline-rich protein BAG6 S1081, and kalirin S1799, are listed in the PhosphoSitePlus database, many have only been identified in large scale mass spectrometry phosphoproteomic analyses with limited information on their roles in protein function and biological processes.

This study used *ex vivo* drug sensitivity resistance testing to stratify patients based on their response to a panel or individual drugs. However, it is important to note that *ex vivo* chemosensitivity assays have limitations that must be considered when

interpreting results. Only plasma cells are incubated and assessed as part of this approach. Although the cells were incubated with stromal cell conditioned media, cell-to-cell contact and contact with the extracellular matrix could not be recreated which likely influence the *ex vivo* drug responses observed during the assay. Furthermore, in this assay, only drugs that act directly on the tumour cells can be evaluated and not those that target the microenvironment (Zhang, Ji, *et al.* 2022). Nevertheless, a comparison of *in vitro* data with clinical outcomes has shown a predictive accuracy of 50%-80% for drug sensitivity and over 90% for drug resistance (Volm and Efferth 2015). Furthermore, this assay facilitates the rapid assessment of the impact of hundreds of drugs at several concentrations on individual patient samples (Majumder *et al.* 2017).

Our discovery phosphoproteomics analysis to predict drug response in MM patients provides a dataset with valuable information for future predictive biomarker studies and mechanistic studies. As depicted in **Figure 3.11**, bioinformatic analysis of phosphoproteomic datasets can identify central kinases and motifs involved in drug response which represent valid therapeutic targets to restore drug sensitivity in MM patients. *Ex vivo* drug sensitivity platforms are not widely available and require additional resources, instrumentation, and adapted protocols to be established in new locations. As few clinical research groups have access to *ex vivo* drug screening platforms, the integration of molecular profiling strategies such as phosphoproteomics to establish predictive biomarker panels that act as surrogate markers of *ex vivo* drug sensitivity resistance testing is crucial to expand the application of this precision medicine approach. A limitation of the *ex vivo* drug screening approach used in this study is that monoclonal antibodies cannot be evaluated on this platform. As immunotherapies have become key players in MM treatment regimens, the investigation of sensitivity/resistance to immunotherapies would be beneficial. Furthermore, evaluation of molecular biomarkers associated with sensitivity/resistance to combination therapies such as bortezomib/lenalidomide/dexamethasone, which are commonly used in a clinical setting will help to identify the most clinically relevant biomarkers for future validation. To validate our findings, large scale studies with sufficient statistical power are required to translate these preclinical findings into clinically relevant predictive assays. A large-scale comprehensive study combining extensive clinical

data on outcomes and cytogenetics with DSRT and downstream omics technologies would undoubtedly aid in the translation on the results presented in this chapter to the clinical setting

3.5 Conclusion

In conclusion, this work confirms that the combination of phosphoproteomics and *ex vivo* DSRT can provide insight into the biological mechanisms associated with drug resistance/sensitivity. Several well-documented mechanisms of resistance were identified in this study, reaffirming our confidence in the use of this approach to detect novel resistance mechanisms and predictive biomarkers of drug response. Our results indicate an increase in cell-adhesion associated processes and a decrease in cell growth via decreased protein translation in multi-drug resistant myeloma cells based on *ex vivo* DSRT. Phosphorylation sites and kinases associated with drug resistance were identified and further studies should investigate the potential involvement of these kinases in the development of resistance to the individual drugs analysed in this study. Although information on the biological functions of many of the phosphorylation sites identified in this study are limited, it is hoped that future studies evaluating the impact of these phosphorylation events on biological processes will provide insight into the potential links between these phosphorylation patterns and drug resistance.

Chapter 4

Using untargeted and targeted plasma proteomics to identify plasma biomarkers of therapeutic response based on *ex vivo* drug sensitivity resistance testing

4.1 Introduction

Drug resistance remains one of the biggest challenges facing the effective treatment of multiple myeloma patients. Although some patients achieve a prolonged response following treatment, many patients successively relapse and become refractory to current myeloma therapeutics. Many MM patients receive 5 or more lines of therapy, and the length of remission is often reduced following each sequential relapse (Kumar *et al.* 2004; Rajkumar and Kumar 2020). This highlights the need for biomarkers of therapeutic response in MM to ensure patients receive a drug combination that they are most likely to respond to. Biofluids represent an ideal source of predictive markers of therapeutic response and markers to monitor drug response during treatment. Specifically, collecting serum and plasma is inexpensive and minimally invasive when compared to the collection tumour cells from the bone marrow of MM patients. In addition, monitoring plasma-derived biomarkers of drug sensitivity or resistance is easily implementable in clinical settings (Dunphy, O'Mahoney, *et al.* 2021).

With the current availability of over 20 FDA-approved MM therapies, it is crucial to be able to determine which drug or drug combination a patient will respond best to in order to prolong the duration of remission and improve patient outcomes. Functional precision medicine has garnered increasing attention in recent years as a method to guide clinical decision making in a personalized manner. Functional precision medicine in oncology often refers to the use of an *ex vivo* drug screening approach to evaluate the therapeutic efficacy of numerous drugs on live tumour cells (Letai 2022). The use of *ex vivo* DSRT has shown promise in a variety of hematological malignancies. A recent clinical trial investigating the usability of *ex vivo* drug sensitivity testing for selecting acute myeloid leukemia (AML) patients who are responsive to venetoclax therapy yielded excellent results with venetoclax sensitivity testing being successful in 38 of the 39 AML patients evaluated (Kuusanmäki *et al.* 2022). This highlights the clinical usability of this approach to guide personalized therapeutic decision-making.

Studies have used *ex vivo* drug screening to evaluate mechanisms of drug resistance and to identify biological markers of drug sensitivity/resistance using genomics, transcriptomics, and proteomics (Tierney, Bazou, Majumder, *et al.* 2021; Ntafoulis

et al. 2023). In MM, numerous molecular biology techniques have been combined with *ex vivo* drug screening approaches to investigate drug response. A recent study reported a single-cell image-based *ex vivo* drug testing approach as a clinically relevant strategy to improve treatment decision-making in MM. The data obtained from this approach, termed pharmacoscopy, can be used to detect novel biomarkers of drug response and facilitates patient stratification (Kropivsek *et al.* 2023). Another *ex vivo* drug sensitivity screening found that a gain(1q21) cytogenetic abnormality was associated with decreased sensitivity to the BCL-2 inhibitor, venetoclax, while the presence of a t(11;14) translocation was associated with increased sensitivity to venetoclax (Giliberto *et al.* 2022). Tierney and colleagues identified protein signatures associated with drug response to five drugs from different drug classes based on *ex vivo* DSRT (Tierney, Bazou, Majumder, *et al.* 2021). A high-throughput drug screening of 25 RRMM patients identified genetic mutations in 12 genes linked to ex vivo sensitivity or resistance to 21 drugs. Furthermore, differential expression of over 100 genes was correlated with the in vitro cytotoxicity of numerous drugs analysed as part of the high-throughput drug screen (Coffey *et al.* 2021). Using an ex vivo drug testing approach, increased expression of aminopeptidases in MM plasma cells has been linked to melflufen sensitivity (Miettinen *et al.* 2021). In addition to detecting markers of drug response, *ex vivo* DSRT has also proved to be a valuable method in the identification of synergistic drug combinations in MM (Sudalagunta *et al.* 2020; Giliberto *et al.* 2022).

Although meaningful efforts are being made to apply a functional precision medicine approach to clinical settings, there are many challenges that must first be addressed. Firstly, ex vivo DSRT assays require fresh, viable tumour biopsies which must be evaluated in a timely manner to ensure limited biological variation and cell death during storage and transportation. Thus, adequate sample handling protocols must be established in a clinical setting to facilitate ex vivo DSRT. A sufficient number of tumour cells must be obtained from patients to perform the assay. Furthermore, results of the ex vivo DSRT assay must be communicated to clinicians within an adequate time frame to ensure these results can contribute to the clinical decision-making process (Letai *et al.* 2022). The studies described above have focused on evaluating biopsied tumour tissues and isolated tumour cells to identify drug sensitivity/resistance mechanisms and biomarkers of drug response. As these studies

have successfully identified potential biomarkers, we hypothesized that blood plasma collected on the same date as tumour biopsies subjected to *ex vivo* DSRT could be analysed to identify potential circulating markers of drug sensitivity or resistance. As the limitations associated with *ex vivo* DSRT may affect widespread clinical application, the identification of surrogate markers in blood may constitute a method of predicting drug response that can be easily implemented in a clinical setting. Thus, in this pilot study, an untargeted mass spectrometry-based analysis and a targeted proximity extension assay-based analysis was performed to identify potential surrogate markers of *ex vivo* DSRT in MM plasma.

4.2 Experimental design and methods

The development of drug resistance remains the most prominent issue facing the successful treatment of MM patients. To improve risk classification and treatment decision-making, a precision medicine approach is required with robust and sensitive biomarkers to predict the likelihood of an individual patient responding to specific drugs or drug classes. As the process of obtaining bone marrow biopsies from patients is invasive and painful, identifying minimally invasive biomarkers in biological fluids is preferred (Aberuyi *et al.* 2020).

4.2.1 Patient samples

A total of 44 EDTA plasma samples were obtained from the FHRB in Finland. Samples were collected from MM patients (n=41) on the same date as bone marrow aspirates which were subject to *ex vivo* drug sensitivity resistance testing at FIMM. Therefore, corresponding *ex vivo* drug sensitivity data is available for all 44 samples. Longitudinal samples were collected from three patients. Sample collection, with informed consent, took place between 2013 and 2019. Patient characteristics are summarised in **Table 4.1**. The median age of the cohort is 65 and it includes 20 males and 21 females. No exclusion criteria were applied to the patients. Details surrounding the treatment course of the patient cohort are outlined in **Table 4.2**. Cytogenetics found on the sampling date are illustrated in **Figure 4.1**. No cytogenetics data was available for patients MM_6931, MM_7171_01, MM_7171_05, MM_6948, MM_4691, MM_7904, and MM_4774. One sample (sMM_6369) was collected at the time of diagnosis of smouldering MM.

Table 4.1: Clinical characteristics of patient cohort. Table illustrating patient ID, age at sample date, gender, heavy chain composition, and light chain composition of each patient.

Patient ID	Age at Sample Date	Gender	Heavy chain	Light chain
MM_1910	63	Female	IgG	Kappa
MM_6931	61	Male	IgA	Lambda
MM_7171_01	69	Male	Unknown	Unknown
MM_7171_05	70	Male	Unknown	Unknown
MM_1926	67	Female	IgG	Kappa
MM_3792	68	Male	IgG	Kappa
MM_1878_03	67	Male	IgA	Kappa
MM_1878_10	67	Male	IgA	Kappa
MM_6948	26	Female	Unknown	Kappa
MM_6261	51	Male	IgG	Kappa
MM_7276	64	Female	Unknown	Kappa
MM_7281	76	Female	IgA	Kappa
MM_7396	50	Male	IgG	Kappa
MM_7566	54	Male	IgG	Kappa
MM_4534	65	Female	Unknown	Lambda
MM_4691	70	Female	IgG	Kappa
MM_7904	53	Female	Unknown	Unknown
MM_8095	77	Male	IgA	Kappa
MM_7968	63	Male	IgG	Kappa
MM_7983	65	Male	IgG	Lambda
MM_6211	63	Female	Unknown	Kappa
MM_8694	75	Female	IgG	Kappa
MM_8728	73	Male	IgG	Lambda
MM_1152	54	Female	IgA	Lambda
MM_933	74	Male	IgA	Lambda
MM_5207	83	Female	IgA	Lambda
MM_4981	65	Female	Unknown	Kappa
MM_4865	66	Male	Unknown	Kappa
MM_4783	53	Male	Unknown	Kappa
MM_4774	78	Male	IgA	Kappa
MM_156	67	Female	IgA	Kappa
MM_921	64	Female	Unknown	Lambda
MM_3767	54	Female	IgA	Lambda
MM_917	63	Male	IgG	Kappa
MM_8825	69	Female	IgA	Lambda
MM_3717	53	Male	Unknown	Kappa
MM_3586	60	Male	Unknown	Kappa
MM_1994	68	Female	IgG	Lambda
MM_911_13	68	Female	IgA	Lambda
MM_911_14	69	Female	IgA	Lambda
MM_4312	65	Female	IgG	Lambda
sMM_6369	60	Female	IgA	Lambda
MM_6463	76	Male	IgA	Kappa
MM_3129	64	Male	IgG	Kappa

Table 4.2: Details of treatment course of each patient within the cohort. Table illustrating the disease status at the time of sampling, the 1st next line of treatment, all lines of treatment, and the deepest response in next line of treatment.

Patient ID	Disease status at sample date	Name of 1st next line treatment	Names of all next line treatments	Deepest response in next line treatment
MM_1910	PD	Drug study treatment	Pom/Dxm Pom/Cpm/Dxm	PR
MM_6931	PD	NA	NA	NA
MM_7171_01	PD	Radiotherapy	Drug study treatment	PD
MM_7171_05	PD			Exitus
MM_1926	PD	Drug study treatment	Drug study treatment Pom/Dxm Pom/Cpm/Dxm	Minimal response
MM_3792	PD	NA	NA	NA
MM_1878_03	PD	NA	NA	NA
MM_1878_10	PD	NA	NA	NA
MM_6948	PR	Bor/Cpm/Dxm	Bor/Cpm/Dxm Cpm Car/Dxm HD-Melphalan (ASCT) Bor/Cpm/Dxm Len Len/Dxm Len Len/Dxm	PR
MM_6261	PD	Dara/Dxm/Len /Bor	Dara/Dxm/Len/Bor Cis/Cpm/Dxm/Dox/Eto/Len Cis/Cpm/Dxm/Dox/Eto/Pom	VGPR
MM_7276	Dg	Bor/Dxm	Bor/Dxm Bor/Cpm/Dxm Mobilization (Cpm) HD-Melphalan (ASCT)	VGPR
MM_7281	Dg	Bor/Mel/Pred	Bor/Mel/Pred Len/Dxm Len Len/Dxm	PR
MM_7396	Dg	Bor/Cpm/Dxm	Bor/Cpm/Dxm Mobilization (Cpm) HD-Melphalan (ASCT) Bor/Dxm/Len Len	PR
MM_7566	Dg	Ixa/Len/Dxm	Ixa/Len/Dxm HD-Melphalan (ASCT) Ixa/Len/Dxm Len	PR
MM_4534	Clinical relapse	Bor/Dxm/Len	Bor/Dxm/Len Pomal/Cpm/Dxm Car/Dxm	VGPR
MM_4691	PD	Car/Len/Dxm	Car/Len/Dxm Len/Dxm Dxm	sCR

Patient ID	Disease status at sample date	Name of 1st next line treatment	Names of all next line treatments	Deepest response in next line treatment
			Dara/Dxm/Len	
MM_7904	Dg	NA	NA	NA
MM_8095	Dg	Bor/Dxm	Bor/Dxm Radiotherapy Len/Dxm Len	VGPR
MM_7968	Dg	Ixa/Len/Dxm	Ixa/Len/Dxm Mobilization (Cpm) HD-Melphalan (ASCT) Ixa/Len/Dxm Len Car/Len/Dxm Drug study treatment	VGPR
MM_7983	NA	NA	NA	NA
MM_6211	PD	Bor/Dxm/Len	Bor/Dxm/Len Dara/Dxm/Len HD-Melphalan (ASCT) Dara/Dxm/Len Dara Car/Dxm	PD
MM_8694	Dg	Bor/Dxm/Len	Bor/Dxm/Len Len/Dxm Len	VGPR
MM_8728	Dg	NA	NA	NA
MM_1152	Clinical relapse	Len/Dxm	Len/Dxm Radiotherapy Len/Dxm Len Len/Dxm Dxm Car/Dxm Pom/Cpm/Dxm	VGPR
MM_933	PD	Bor/Cpm/Dxm	Bor/Cpm/Dxm Bor/Dxm Venetoclax Benda/Pred Car/Dxm	SD
MM_5207	Dg	Bor/Dxm	Bor/Dxm Mel/Pred	PR
MM_4981	Dg	Bor/Dxm	Bor/Dxm Radiotherapy Bor/Cpm/Dxm Mobilization (Cpm) HD-Melphalan (ASCT) Dara/Dxm/Len Dara Dara/Bor/Dxm Pom/Cpm/Dxm Pom/Dxm Ixa/Dxm/Pom	PR

Patient ID	Disease status at sample date	Name of 1st next line treatment	Names of all next line treatments	Deepest response in next line treatment
			Radiotherapy Car/Dxm Radiotherapy	
MM_4865	Dg	Bor/Cpm/Dxm	Bor/Cpm/Dxm Mobilization (Cpm) Len/Dxm HD-Melphalan (ASCT)	VGPR
MM_4783	Dg	Bor/Cpm/Dxm	Bor/Cpm/Dxm Radiotherapy Cpm/Dxm Mobilization (Cpm) HD-Melphalan (ASCT) Len Dara/Dxm/Car Len/Dxm Dara/Dxm/Car Dara/Dxm Len/Dxm	VGPR
MM_4774	PD	Cis/Cpm/Dxm /Dox/Eto/Len	Cis/Cpm/Dxm/Dox/Eto/Len	PR
MM_156	PD	Radiotherapy	Radiotherapy Bor/Dxm/Len Len/Dxm Len/Dxm Len/Dxm Cpm/Pred Len/Dxm	PD
MM_921	PD	Len/Dxm	Len/Dxm Dxm DLI (x2) Len/Dxm Len Car/Len/Dxm Len/Dxm Dara	PR
MM_3767	Dg	Bor/Dxm/Len	Bor/Dxm/Len Mobilization (G-CSF) Bor/Cpm/Dxm HD-Melphalan (ASCT)	PR
MM_917	PD	Bor/Dxm	Bor/Dxm Bor/Dxm/Len	SD
MM_8825	Dg	Ixa/Len/Dxm	Ixa/Len/Dxm Mobilization (Cpm) HD-Melphalan (ASCT)	VGPR
MM_3717	Dg	Bor/Dxm	Bor/Dxm Mobilization (Cpm) Bor/Dxm/Len HD-Melphalan (ASCT) AlloHSCT(Flud/Treo)	VGPR
MM_3586	Dg	Bor/Dxm/Len	Bor/Dxm/Len	PR

Patient ID	Disease status at sample date	Name of 1st next line treatment	Names of all next line treatments	Deepest response in next line treatment
			Mobilization (G-CSF) HD-Melphalan (ASCT) Len Bor/Dxm Bor/Cpm/Dxm Bor/Dxm Benda/Pred Benda/Pred	
MM_1994	PD	Bor/Cpm/Dxm	Bor/Cpm/Dxm Bor/Dxm/Len Bor/Cpm/Dxm/Len Dxm	PD
MM_911_13	PD	Bor/Dxm	Bor/Dxm Bor/Dxm/Len Len/Dxm Bor/Dxm/Len Radiotherapy Cis/Cpm/Dxm/Dox/Eto/Len	PR
MM_911_14	PD	Bor/Dxm/Len	Bor/Dxm/Len Len/Dxm Bor/Dxm/Len Radiotherapy Cis/Cpm/Dxm/Dox/Eto/Len	VGPR
MM_4312	PD	Bor/Dxm/Len	Bor/Dxm/Len Ven Ven/Bor/Dxm Benda/Pred Radiotherapy	PR
sMM_6369	Dg	Ixa/Len/Dxm	Ixa/Len/Dxm Mobilization (Cpm) HD-Melphalan (ASCT) Ixa/Len/Dxm Len Bor/Cpm/Dxm Bor/Dxm Dara/Pom/Dxm	PR
MM_6463	Dg	Dxm	Dxm Radiotherapy Len/Dxm Bor/Dxm/Len Car/Len/Dxm Car/Pom/Dxm Car/Cpm/Pom/Dxm Benda/Pred Benda/Dxm/Len	PR
MM_3129	PD	Benda/Bor/Pred	Benda/Bor/Pred Bor/PegDoxo/Dxm Pom/Dxm	SD

Abbreviations: PD, progressive disease; Pom, pomalidomide; Dxm, dexamethasone; Cpm, cyclophosphamide; PR, partial response; Bor, bortezomib; Car, carfilzomib; HD-Melphalan, high-dose melphalan; ASCT, autologous stem cell transplantation; Len, lenalidomide; Dara, daratumumab; Cis, cisplatin; Dox, doxorubicin; Eto, etoposide; VGPR, very good partial response; Dg, diagnosis; Mel, melphalan; Pred, prednisone; Ixa, ixazomib; sCR, stringent complete response; Benda, bendamustine; SD, stable disease; G-CSF, granulocyte-colony stimulating factor; DLI, donor lymphocyte infusion; AlloHSCT, allogeneic hematopoietic stem cell transplantation; Flud, fludarabine; Treo, treosulfan; Ven, venetoclax; PegDoxo, pegylated liposomal doxorubicin.

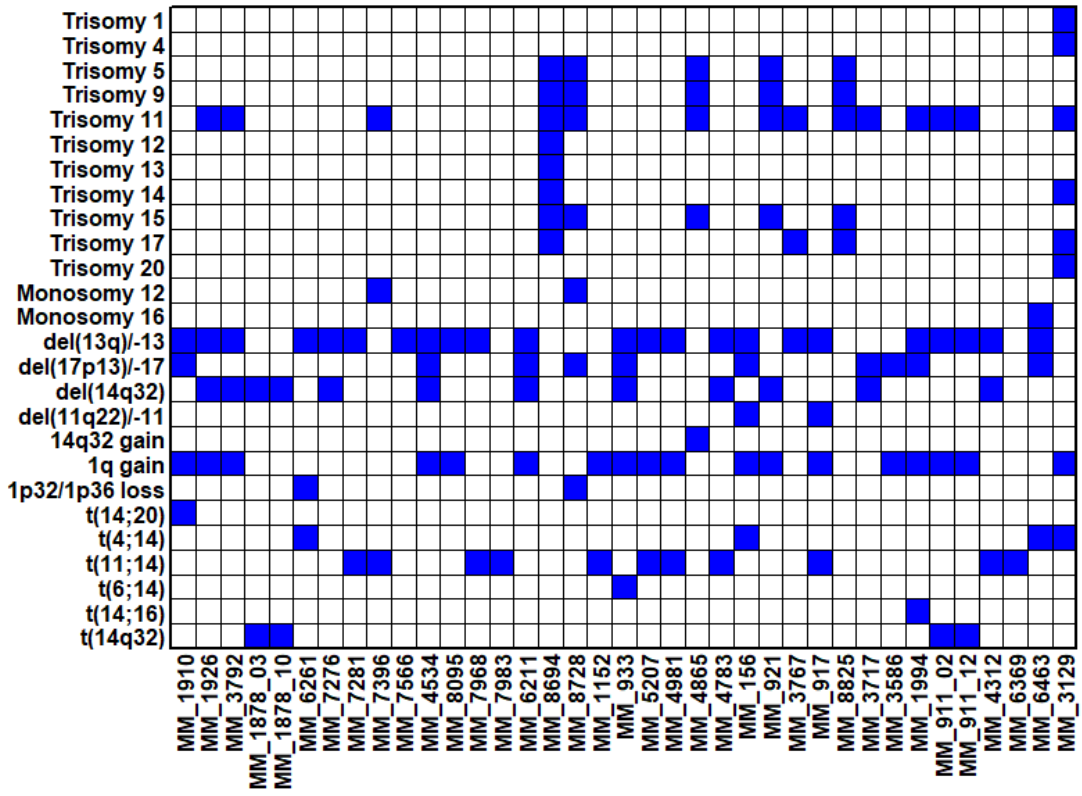

Figure 4.1: Cytogenetic data from sampling date of patient cohort. Cytogenetics data was available for 37/44 samples collected.

4.2.2 Label-free mass spectrometry analysis of MM plasma

To reduce ion suppression, high abundant plasma proteins were depleted prior to mass spectrometry analysis using the Proteome Purify 12 Human Serum Protein Immunodepletion Resin (R&D Systems, Minneapolis, MN, USA), as described in Chapter 2. Briefly, 10 µL of plasma was mixed with 1 mL of immunodepletion resin for 60 min on a rotary shaker. The mixture was transferred to Spin-X filter units and centrifuged. Protein concentration of the immunodepleted plasma was determined

using the Qubit protein assay. Protein digestion was performed using the FASP protocol, as described in Chapter 2. A total of 6µg of protein was digested at a 1:25 enzyme-to-protein ratio. The tryptic digest was acidified at a 1:8 ratio using 2% TFA, 20% ACN.

Mass spectrometry analysis was performed using the Thermo UltiMate 3000 nano system directly coupled in-line with the Thermo Orbitrap Fusion Tribrid mass spectrometer. The maximum loading amount, equivalent to ~400ng of protein was loaded onto the system. Peptides were resolved on an analytical column using a binary gradient. The mass spectrometry analysis was performed as described previously (Chapter 2).

4.2.3 Data analysis of mass spectrometry results

Raw files containing quantitative information from the mass spectrometry analysis were analysed using Progenesis QI for Proteomics (version 2.0). Proteome Discoverer 2.2 was employed for peptide and protein identification using a recently downloaded UniProtKB-SwissProt Homo Sapiens reference database. Search parameters for protein identification are described in Chapter 2. Contaminating keratins were removed from the analysis. Protein identifications were deemed to be of differential abundance based on an ANOVA p-value of ≤ 0.05 between experimental groups, fold change ≥ 1.3 between experimental groups, proteins with ≥ 2 unique peptides contributing to the identification, and quantification data in $\geq$ 70% of samples. Perseus v.1.5.6.0 was used for visualisation of heatmaps. To generate STRING protein-protein interaction networks, the accession numbers of significant proteins were inputted into the online STRING platform. The interaction score was set to high confidence (>0.7) and protein networks were exported to Cytoscape (version 3.10.0) for visualization and functional enrichment using the stringApp.

4.2.4 Targeted proteomic analysis using the Olink Target 48 panel

Plasma concentrations of 45 cytokines in MM (n=26) with varying drug response profiles based on *ex vivo* DSRT were evaluated using the Olink Target 48 panel, as described in Chapter 2. As the resulting data was not normally distributed, a Kruskal-Wallis test and two-sided Wilcoxon rank sum tests were performed using

the R package, Olink® Analyze. Graphs were generated using Graphpad Prism (8.0.2.263). Spearman rank correlation analysis was performed using MedCalc (version 20.118).

4.3 Results

4.3.1 Stratification of plasma samples based on *ex vivo* drug sensitivity resistance testing

Based on the results of *ex vivo* drug sensitivity resistance testing on matched $CD138^+$ myeloma cells, plasma samples were stratified into one of four groups: Group 1, very sensitive; Group 2, sensitive; Group 3, resistant; and Group 4, very resistant, as described previously (Majumder *et al.* 2017; Tierney, Bazou, Majumder, *et al.* 2021). The groups are listed in **Table 4.3**. To determine the relationship between the chemosensitivity groups and overall survival, a log-rank test was performed and demonstrated a significant change in overall survival (OS) between the groups (Log-rank = 9.511, p = 0.023) (**Figure 4.2**). Despite being associated with drug sensitivity, OS was shortest in Group 1 patients. This is in line with previous publications reporting decreased OS in Group 1 patients (Majumder *et al.* 2017; Tierney, Bazou, Majumder, *et al.* 2021). Previous work has shown that Group 1 patients displayed a higher mutational load with elevated expressions of genes involved in DNA replication and self-renewal. This indicated highly proliferative disease and may explain the decreased OS associated with Group 1 patients (Majumder, 2018).

Table 4.3: Sample groupings based on *ex vivo* drug sensitivity/resistance. Samples were grouped based on *ex vivo* DSRT results, as described in (Majumder *et al*. 2017).

Group 1	Group 2	Group 3	Group 4
MM_3792	MM_4783	MM_7904	MM_1152
MM_6931	MM_7171_01	sMM_6369	MM_1994
MM_911_13	MM_7276	MM_917	MM_3767
MM_4691	MM_4981	MM_156	MM_3717
MM_8095	MM_6211	MM_3586	MM_6948
MM_4534	MM_8825	MM_921	
MM_4312	MM_1926	MM_4865	
MM_7983	MM_7396	MM_7281	
MM_6261	MM_5207	MM_7566	
MM_7171_05	MM_911_14	MM_7968	
MM_4774		MM_6463	
		MM_933	
		MM_1910	
		MM_8694	
		MM_8728	
		MM_1878_03	
		MM_1878_10	
		MM_3129	

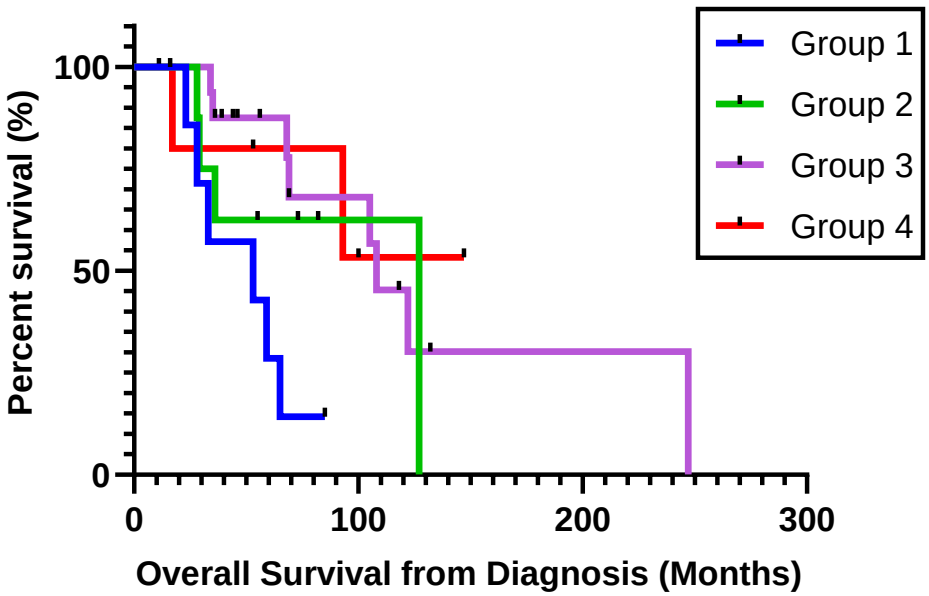

Figure 4.2: Clinical information on the overall survival of the four chemosensitivity groups. Survival graph illustrating the difference in overall survival between Group 1, Group 2, Group 3, and Group 4. The log-rank test was applied to compare the trend in overall survival between the four groups.

4.3.2 Plasma proteomic analysis using label-free LC-MS/MS

4.3.2.1 Statistical analysis reveals a change in the plasma proteome between the four chemosensitivity groups

To evaluate the plasma proteomic changes between the four chemosensitivity groups, we compared the abundance of plasma proteins identified by LC-MS/MS. A total of 45 plasma proteins were SSDA across the four groups (ANOVA p-value < 0.05, FC > 1.3) (**Table 4.4**). As Groups 1 and 2 are linked to drug sensitivity while Groups 3 and 4 are associated with drug resistance, we compared the proteomic profile of Groups 1 and 2 combined versus Group 3 and 4 combined to identify proteins with a clear trend of upwards or downwards abundance across the chemosensitivity groups (**Table 4.5**). A total of 16 SSDA proteins were identified between the sensitive group (1&2) and resistant group (3&4).

Table 4.4: Proteins of differential abundance between the four chemosensitivity groups. Statistically significantly differentially abundant proteins are defined by the criteria: ANOVA p-value < 0.05, FC > 1.3.

Protein name	Gene name	Protein ID	Highest mean condition	Lowest mean condition	Max fold change	P-value
Complement C5	C5	P01031	Group 1	Group 4	1.43	0.026
Fibrinogen beta chain	FGB	P02675	Group 1	Group 2	1.82	0.026
Fibrinogen gamma chain	FGG	P02679	Group 1	Group 2	1.75	0.018
von Willebrand factor	VWF	P04275	Group 1	Group 2	4.34	0.009
Alpha-1B-glycoprotein	A1BG	P04217	Group 1	Group 4	1.9	0.025
Serum amyloid A-2 protein	SAA2	P0DJI9	Group 1	Group 2	7.54	0.045
Plasminogen	PLG	P00747	Group 1	Group 4	1.95	0.048
Fibronectin	FN1	P02751	Group 1	Group 4	3.7	0.002
Beta-Ala-His dipeptidase	CNDP1	Q96KN2	Group 1	Group 4	4.31	0.016
Apolipoprotein B-100	APOB	P04114	Group 2	Group 1	1.38	0.043
Heparin cofactor 2	SERPIND1	P05546	Group 2	Group 1	1.34	0.013
Apolipoprotein A-IV	APOA4	P06727	Group 2	Group 4	1.76	0.041
Ficolin-3	FCN3	O75636	Group 2	Group 4	2.03	0.0002
Transthyretin	TTR	P02766	Group 3	Group 4	1.73	0.0005
Selenoprotein P	SELENOP	P49908	Group 3	Group 1	1.77	0.022
Vitamin D-binding protein	GC	P02774	Group 3	Group 4	2.08	0.018

Protein name	Gene name	Protein ID	Highest mean condition	Lowest mean condition	Max fold change	P-value
Complement C3	C3	P01024	Group 4	Group 3	1.57	0.028
Fibrinogen alpha chain	FGA	P02671	Group 4	Group 2	1.67	0.006
Ceruloplasmin	CP	P00450	Group 4	Group 1	2.06	0.0001
Apolipoprotein A-I	APOA1	P02647	Group 4	Group 1	1.61	0.008
Complement C4-A	C4A	P0C0L4	Group 4	Group 3	2.29	0.024
Gelsolin	GSN	P06396	Group 4	Group 1	1.45	0.004
Complement factor B	CFB	P00751	Group 4	Group 3	2.13	0.0009
Corticosteroid-binding globulin	SERPINA6	P08185	Group 4	Group 1	1.53	0.002
Albumin	ALB	P02768	Group 4	Group 1	2.78	0.018
Alpha-2-antiplasmin	SERPINF2	P08697	Group 4	Group 3	1.76	0.0002
Complement C1s subcomponent	C1S	P09871	Group 4	Group 2	1.94	0.0008
Thyroxine-binding globulin	SERPINA7	P05543	Group 4	Group 3	2.38	0.003
Plasma kallikrein	KLKB1	P03952	Group 4	Group 1	2.4	0.0005
Apolipoprotein L1	APOL1	O14791	Group 4	Group 1	2.08	0.001
Attractin	ATRN	O75882	Group 4	Group 1	2.16	0.001
C4b-binding protein alpha chain	C4BPA	P04003	Group 4	Group 3	1.34	0.024
Complement component C9	C9	P02748	Group 4	Group 2	1.97	0.003
Alpha-2-HS-glycoprotein	AHSG	P02765	Group 4	Group 1	2.02	0.002
Complement C2	C2	P06681	Group 4	Group 1	2.11	0.0003
Alpha-1-antichymotrypsin	SERPINA3	P01011	Group 4	Group 2	2.15	0.033
Complement component C8 alpha chain	C8A	P07357	Group 4	Group 1	2.23	0.005
Complement C1r subcomponent-like protein	C1RL	Q9NZP8	Group 4	Group 1	2.65	0.0007
Serotransferrin	TF	P02787	Group 4	Group 1	4.45	0.021
Pregnancy zone protein	PZP	P20742	Group 4	Group 3	4.75	0.040
Prothrombin	F2	P00734	Group 4	Group 3	1.5	0.016
Apolipoprotein A-II	APOA2	P02652	Group 4	Group 1	1.98	0.025
Carboxypeptidase N catalytic chain	CPN1	P15169	Group 4	Group 1	2.16	0.006
Lumican	LUM	P51884	Group 4	Group 1	2.55	0.012
Complement C1q subcomponent subunit C	C1QC	P02747	Group 4	Group 3	3.15	0.018

Table 4.5: Proteins of differential abundance between sensitive (Group 1&2) and resistant (Group 3&4) groups. Statistically significantly differentially abundant proteins are defined by the criteria: ANOVA p-value < 0.05, FC > 1.3.

Protein name	Gene name	Protein ID	Highest mean condition	Lowest mean condition	Fold Change	P-value
Gelsolin	GSN	P06396	Group 3&4	Group 1&2	1.32	0.001
Alpha-2-HS-glycoprotein	AHSG	P02765	Group 3&4	Group 1&2	1.37	0.001
Fibrinogen alpha chain	FGA	P02671	Group 3&4	Group 1&2	1.6	0.009
Alpha-2-macroglobulin	A2M	P01023	Group 3&4	Group 1&2	1.98	0.011
Attractin	ATRN	O75882	Group 3&4	Group 1&2	1.56	0.002
Antithrombin-III	SERPINC1	P01008	Group 3&4	Group 1&2	1.57	0.002
Kininogen-1	KNG1	P01042	Group 3&4	Group 1&2	1.42	0.006
Serotransferrin	TF	P02787	Group 3&4	Group 1&2	1.6	0.028
Apolipoprotein B-100	APOB	P04114	Group 1&2	Group 3&4	3.68	0.002
Haptoglobin	HP	P00738	Group 1&2	Group 3&4	4.25	0.018
Complement C4-A	C4A	P0C0L4	Group 1&2	Group 3&4	1.48	0.043
Fibrinogen beta chain	FGB	P02675	Group 1&2	Group 3&4	1.35	0.035
Apolipoprotein C-IV	APOC4	P55056	Group 1&2	Group 3&4	2.4	0.000
Apolipoprotein E	APOE	P02649	Group 1&2	Group 3&4	1.34	0.009
Mannan-binding lectin serine protease 2	MASP2	O00187	Group 1&2	Group 3&4	1.46	0.010
von Willebrand factor	VWF	P04275	Group 1&2	Group 3&4	1.93	0.032

4.3.2.2 Plasma samples can be stratified based on drug sensitivity scores related to individual drugs

To identify plasma proteomic changes associated with response to individual drugs, samples were stratified into “most sensitive” and “most resistant” groups based on *ex vivo* DSRT of $CD138^{+}$ myeloma cells collected on the same sampling date as the plasma samples in this study (**Figure 4.3**). Patient samples with low DSS are considered “most resistant” whereas those with high DSS are considered “most sensitive” to the individual drug being evaluated. The therapeutics evaluated in this study were selected based on the desire to incorporate drugs from a variety of drug classes. The individual drugs analysed were selected independently of Chapter 3 and include: bortezomib (proteasome inhibitor), lenalidomide (IMiD), dinaciclib (CDK inhibitor), PF-04691502 (PI3K and mTOR inhibitor), quisinostat (HDAC inhibitor), venetoclax (BCL2 inhibitor) and navitoclax (BCL2, BCLxL inhibitor) (**Figure 4.4**).

Bortezomib	
Most Resistant	Most Sensitive
MM_1152	MM_8694
MM_1994	MM_6261
MM_3767	MM_7171_05
MM_6948	MM_3129
MM_3717	MM_911_13
MM_4865	MM_156
MM_7968	MM_3792
MM_933	MM_4783
MM_7281	MM_8825
MM_7566	MM_4534
MM_921	MM_7276

Lenalidomide	
Most Resistant	Most Sensitive
MM_1994	MM_7171_01
MM_3767	MM_6931
MM_3717	MM_8825
MM_1152	MM_8694
MM_6369	MM_7171_05
MM_933	MM_1910
MM_6463	MM_6261
MM_4783	MM_3792
MM_1878_03	MM_4774
MM_917	MM_4312
MM_8095	MM_4691
MM_7904	

Dinaciclib	
Most Resistant	Most Sensitive
MM_1994	MM_7171_01
MM_3767	MM_7396
MM_6948	MM_8825
MM_3717	MM_6261
MM_1152	MM_4691
MM_4865	MM_4981
MM_8694	MM_3792
MM_7968	MM_7171_05
MM_921	MM_7983
MM_1910	MM_4534
MM_6369	MM_4312

PF-04691502	
Most Resistant	Most Sensitive
MM_6948	MM_911_13
MM_1994	MM_6931
MM_7566	MM_3129
MM_933	MM_6211
MM_3717	MM_7171_01
MM_3767	MM_7276
MM_4865	MM_4312
MM_3586	MM_6261
MM_7968	MM_7983
MM_6463	MM_4534
MM_1878_10	MM_3792

Quisinostat	
Most Resistant	Most Sensitive
MM_1994	MM_8825
MM_6948	MM_4534
MM_1152	MM_6931
MM_921	MM_4981
MM_3717	MM_911_13
MM_3767	MM_4774
MM_4865	MM_4312
MM_7904	MM_5207
MM_7968	MM_6211
MM_7566	MM_8825
MM_6463	MM_7983

Venetoclax	
Most Resistant	Most Sensitive
MM_6211	MM_8095
MM_3586	MM_6463
MM_156	MM_7904
MM_7171_05	MM_6931
MM_6261	MM_917
MM_4981	MM_4534
MM_1878_03	MM_7396
MM_921	MM_5207
MM_4783	MM_4312
MM_3767	MM_4691
MM_8694	MM_7983

Navitoclax	
Most Resistant	Most Sensitive
MM_1152	MM_917
MM_7171_05	MM_5207
MM_4783	MM_8095
MM_1878_03	MM_7281
MM_8825	MM_7968
MM_3586	MM_7904
MM_6261	MM_3717
MM_4981	MM_4865
MM_1910	MM_6948
MM_156	MM_1994
MM_1878_10	MM_7983

Figure 4.3: Sample stratification into "Most Resistant" and "Most Sensitive" groups for each of the seven individual therapeutics analysed. Samples were stratified into "Most Resistant" and "Most Sensitive" groups based on DSS values. To investigate the samples considered most resistant or most sensitive, samples were separated into quartiles with those samples falling into the first quartile being considered "Most Resistant" and those in the fourth quartile being considered "Most Sensitive".

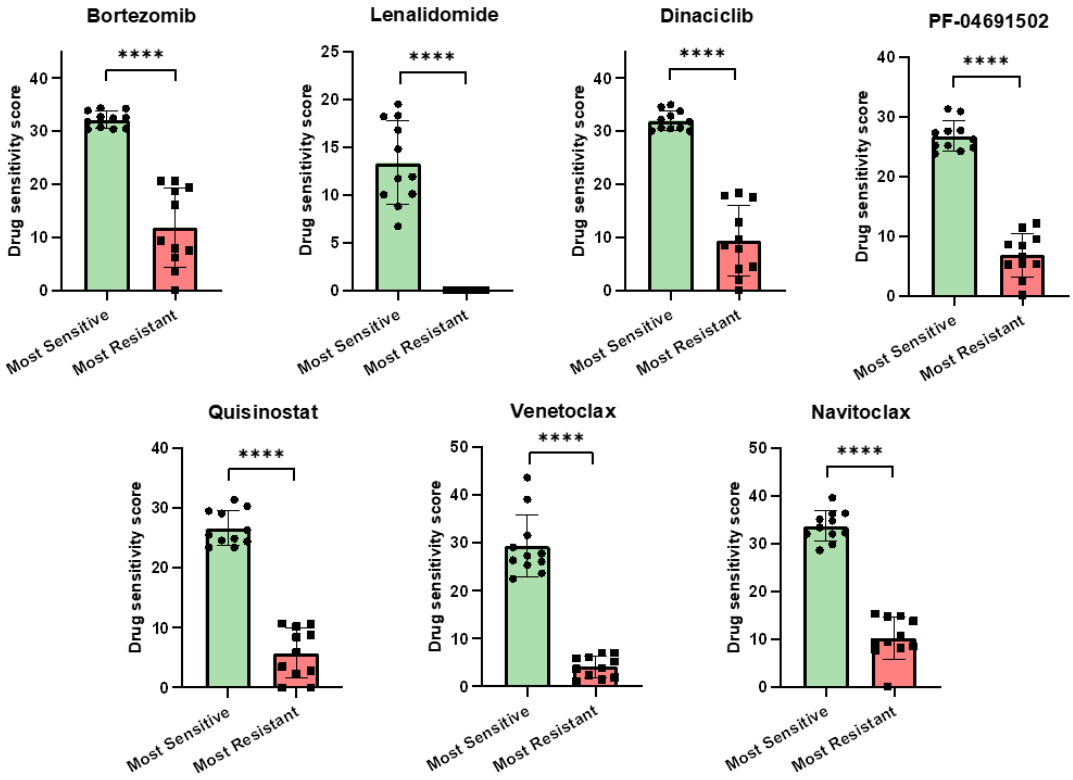

Figure 4.4: Comparison of drug sensitivity scores in "most sensitive" and "most resistant" groups associated with each individual drug. All statistical comparisons for each group yielded p-values < 0.0001. p ≤ 0.0001, '****'.

4.3.2.3 Proteomic analysis of plasma based on sensitivity/resistance to bortezomib

Proteomic analysis of plasma samples considered "most sensitive" and "most resistant" to bortezomib revealed 37 proteins of differential abundance between the two groups (ANOVA p-value < 0.05, FC > 1.3) (**Supp. File 4.1**). Of these proteins, 16 were increased in abundance and 21 proteins were decreased in abundance in plasma from patients highly resistant to bortezomib. Hierarchical clustering was performed on all identified SSDA proteins. LFQ intensity values were Z-score normalised followed by clustering of the proteins using Euclidean distance and average linkage (**Figure 4.5A**). Protein-protein interactions between the SSDA proteins were evaluated using STRING analysis. As depicted in **Figure 4.5B**, many of the SSDA proteins showed strong interactions with the identification of two protein clusters associated with complement activation and lipid metabolism. This indicates a potential change in the abundance of plasma proteins involved in complement activation and lipid metabolism in MM patients with varying responses to bortezomib.

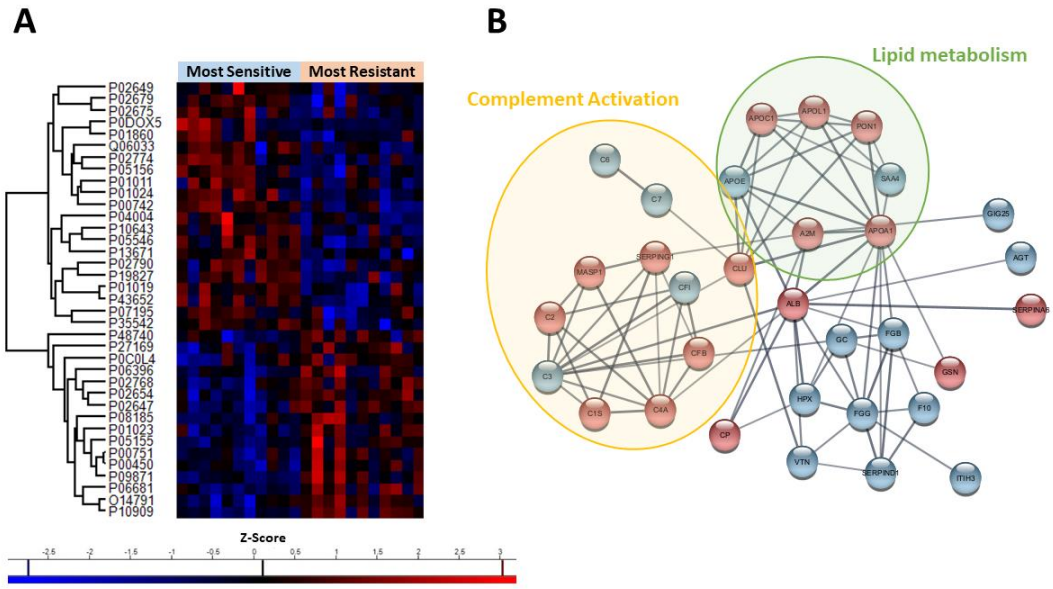

Figure 4.5: Label-free quantitative proteomic analysis of plasma samples "most sensitive" and "most resistant" to the proteasome inhibitor, bortezomib. (**A**) Hierarchical clustering of z-scored normalised LFQ intensity values for 37 SSDA proteins illustrating the alterations in plasma protein abundance. (**B**) String enrichment analysis on SSDAs identified via Student's t-test comparison of "most sensitive" and "most resistant" bortezomib groups. Red nodes represent proteins increased in abundance in the "most resistant" group, whereas blue nodes represent proteins decreased in abundance in the "most resistant" group. Nodes representing proteins associated with complement activation are circled in yellow. Nodes representing proteins associated with lipid metabolism are circled in green. Unconnected nodes were removed from the figure.

4.3.2.4 Proteomic analysis of plasma based on sensitivity/resistance to lenalidomide

Proteomic analysis of plasma samples considered "most sensitive" and "most resistant" to lenalidomide revealed 16 proteins of differential abundance between the two groups (ANOVA p-value < 0.05, FC > 1.3) (**Supp. File 4.2**). Of these proteins, 11 were increased in abundance and 5 were decreased in abundance in plasma from patients highly resistant to lenalidomide. Hierarchical clustering of SSDA proteins was performed as described above (**Figure 4.6A**). Of the 16 proteins of differential abundance between the two groups, 13 proteins are linked to vesicle-mediated transport (**Figure 4.6B**).

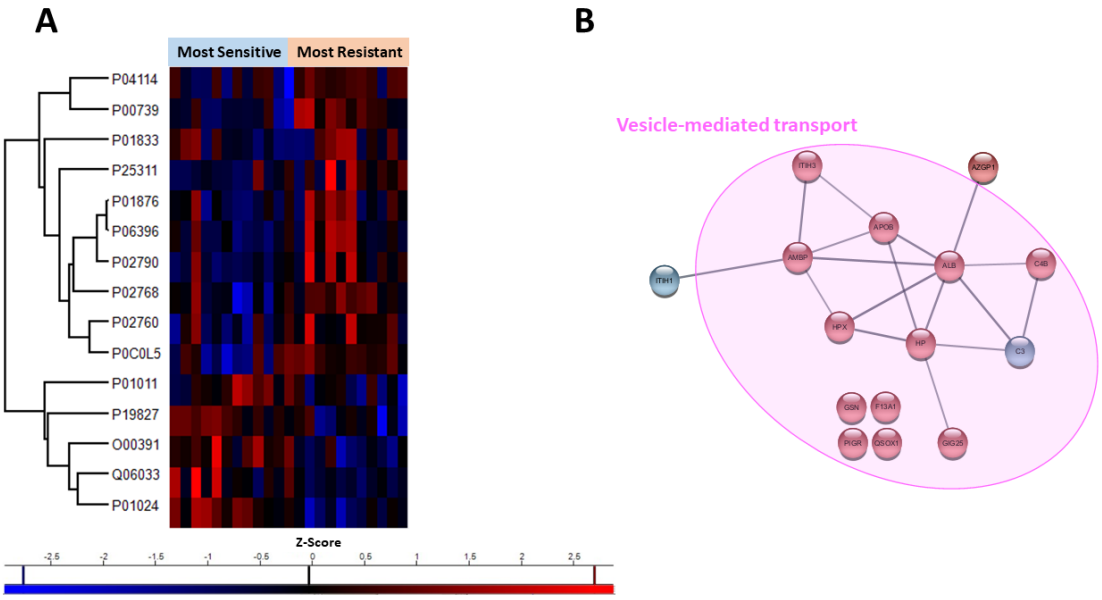

Figure 4.6: Label-free quantitative proteomic analysis of plasma samples "most sensitive" and "most resistant" to the immunomodulatory drug, lenalidomide. (**A**) Hierarchical clustering of z-scored normalised LFQ intensity values for 16 SSDA proteins illustrating the alterations in plasma protein abundance. (**B**) String enrichment analysis on SSDAs identified via Student's t-test comparison of "most sensitive" and "most resistant" lenalidomide groups. Red nodes represent proteins increased in abundance in the "most resistant" group, whereas blue nodes represent proteins decreased in abundance in the "most resistant" group. Nodes representing proteins associated with vesicle-mediated transport are circled in pink.

4.3.2.5 Proteomic analysis of plasma based on sensitivity/resistance to dinaciclib

Proteomic analysis of plasma samples considered "most sensitive" and "most resistant" to dinaciclib revealed 30 proteins of differential abundance between the two groups (ANOVA p-value < 0.05, FC > 1.3) (**Supp. File 4.3**). Of these proteins, 16 were increased in abundance and 14 were decreased in abundance in plasma from patients highly resistant to dinaciclib. As depicted in **Figure 4.7A**, there is a clear change in the abundance of the 30 significant plasma proteins across the two chemoresistance groups. STRING analysis found a highly connected protein network including proteins associated with phosphatidylcholine binding being increased in abundance in those most resistant to dinaciclib and proteins linked to extracellular matrix structural constituents being decreased in abundance in the plasma of those most sensitive to dinaciclib (**Figure 4.7B**).

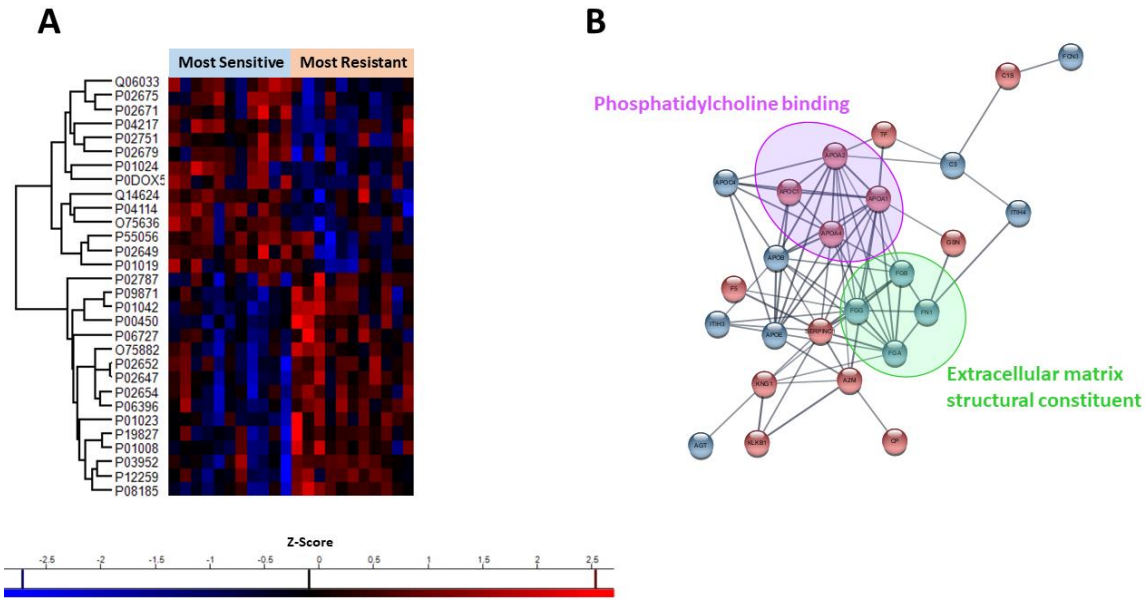

Figure 4.7: Label-free quantitative proteomic analysis of plasma samples "most sensitive" and "most resistant" to the cyclin dependent kinase (CDK) inhibitor, dinaciclib. (**A**) Hierarchical clustering of z-scored normalised LFQ intensity values for 30 SSDA proteins illustrating the alterations in plasma protein abundance. (**B**) String enrichment analysis on SSDAs identified via Student's t-test comparison of "most sensitive" and "most resistant" dinaciclib groups. Red nodes represent proteins increased in abundance in the "most resistant" group, whereas blue nodes represent proteins decreased in abundance in the "most resistant" group. Nodes representing proteins associated with phosphatidylcholine binding are circled in purple. Nodes representing proteins linked to extracellular matrix structural constituents are circled in green. Unconnected nodes were removed from the figure.

4.3.2.6 Proteomic analysis of plasma based on sensitivity/resistance to PF-04691502

Proteomic analysis of plasma samples considered "most sensitive" and "most resistant" to PF-04691502 revealed 24 proteins of differential abundance between the two groups (ANOVA p-value < 0.05, FC > 1.3) (**Supp. File 4.4**). Of these proteins, 14 were increased and 10 were decreased in abundance in the "most resistant" to PF-04691502 group. The change in abundance of these proteins is illustrated in **Figure 4.8A**. Protein-protein interaction analysis revealed a highly interconnected network across all SSDAs. Proteins associated with cell-substrate adhesion were decreased in abundance and those associated with cholesterol metabolism were increased in abundance in the "most resistant" chemosensitivity group (**Figure 4.8B**).

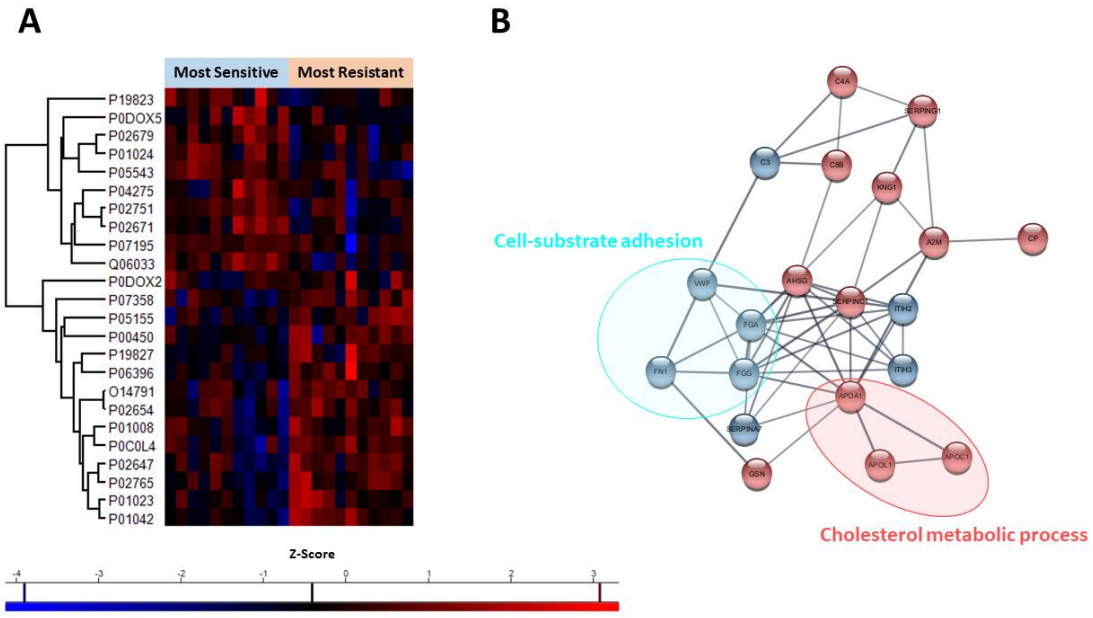

Figure 4.8: Label-free quantitative proteomic analysis of plasma samples "most sensitive" and "most resistant" to the PI3K and mTOR inhibitor, PF-04691502. (**A**) Hierarchical clustering of z-scored normalised LFQ intensity values for 24 SSDA proteins illustrating the alterations in plasma protein abundance. (**B**) String enrichment analysis on SSDAs identified via Student's t-test comparison of "most sensitive" and "most resistant" PF-04691502 groups. Red nodes represent proteins increased in abundance in the "most resistant" group, whereas blue nodes represent proteins decreased in abundance in the "most resistant" group. Nodes representing proteins associated with cell-substrate adhesion are circled in bright blue. Nodes representing proteins linked to cholesterol metabolism are circled in red. Unconnected nodes were removed from the figure.

4.3.2.7 Proteomic analysis of plasma based on sensitivity/resistance to quisinostat

Proteomic analysis of plasma samples considered "most sensitive" and "most resistant" to quisinostat revealed 15 proteins of differential abundance between the two groups (ANOVA p-value < 0.05, FC > 1.3) (**Supp. File 4.5**). Of these proteins, 11 were increased and 4 were decreased in abundance in the "most resistant" to quisinostat group. The change in abundance of these proteins is illustrated in **Figure 4.9A**. Protein-protein interaction analysis revealed a highly interconnected network across all SSDAs. Four unconnected nodes were removed from the figure. Proteins associated with cholesterol efflux were increased in abundance in the "most resistant" to quisinostat group (**Figure 4.9B**).

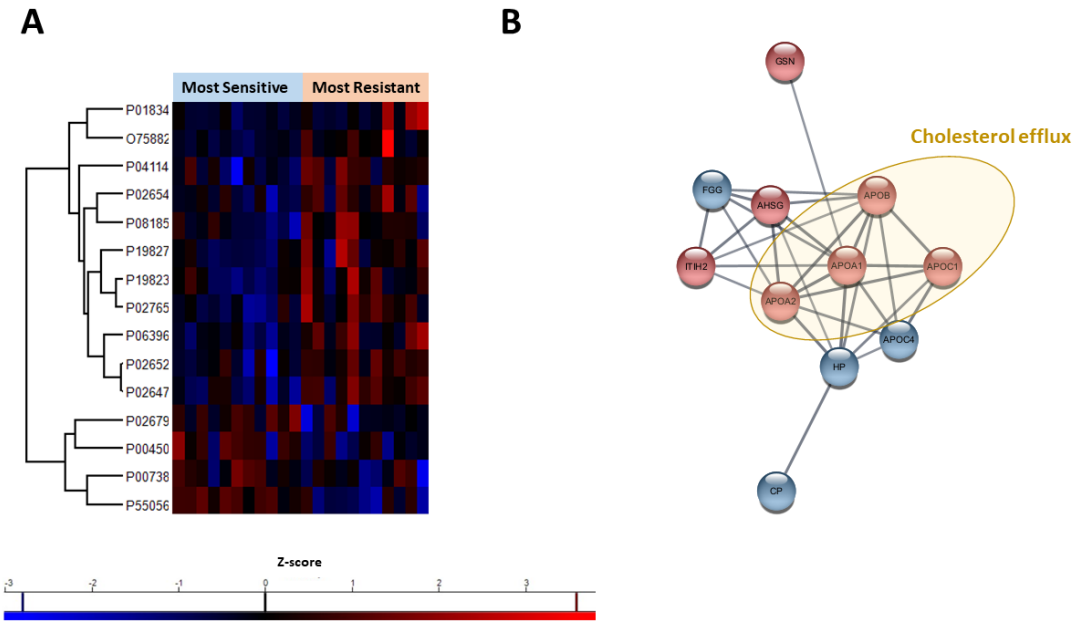

Figure 4.9: Label-free quantitative proteomic analysis of plasma samples "most sensitive" and "most resistant" to the pan-HDAC inhibitor, quisinostat. (**A**) Hierarchical clustering of z-scored normalised LFQ intensity values for 15 SSDA proteins illustrating the alterations in plasma protein abundance. (**B**) String enrichment analysis on SSDAs identified via Student's t-test comparison of "most sensitive" and "most resistant" quisinostat groups. Red nodes represent proteins increased in abundance in the "most resistant" group, whereas blue nodes represent proteins decreased in abundance in the "most resistant" group. Nodes representing proteins associated with cholesterol efflux are circled in yellow. Unconnected nodes were removed from the figure.

4.3.2.8 Proteomic analysis of plasma based on sensitivity/resistance to venetoclax

Proteomic analysis of plasma samples considered "most sensitive" and "most resistant" to venetoclax revealed 17 proteins of differential abundance between the two groups (ANOVA p-value < 0.05, FC > 1.3) (**Supp. File 4.6**). Of these proteins, 9 were increased and 8 were decreased in abundance in the "most resistant" to venetoclax group. The change in abundance of these proteins is illustrated in **Figure 4.10A**. Protein-protein interaction analysis revealed a highly interconnected network across all SSDAs. Three unconnected nodes were removed from the figure. Proteins associated with cell activation were decreased in abundance in the "most resistant" to venetoclax group group (**Figure 4.10B**).

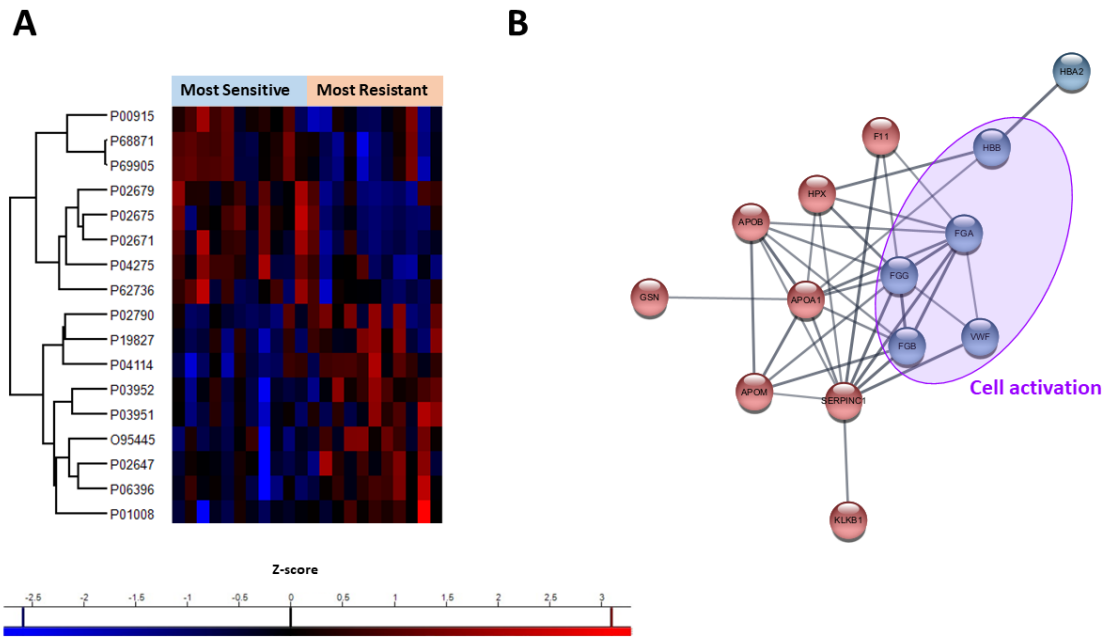

Figure 4.10: Label-free quantitative proteomic analysis of plasma samples "most sensitive" and "most resistant" to the BCL2 inhibitor, venetoclax. (**A**) Hierarchical clustering of z-scored normalised LFQ intensity values for 17 SSDA proteins illustrating the alterations in plasma protein abundance. (**B**) String enrichment analysis on SSDAs identified via Student's t-test comparison of "most sensitive" and "most resistant" venetoclax groups. Red nodes represent proteins increased in abundance in the "most resistant" group, whereas blue nodes represent proteins decreased in abundance in the "most resistant" group. Nodes representing proteins associated with cell activation are circled in purple. Unconnected nodes were removed from the figure.

4.3.2.9 Proteomic analysis of plasma based on sensitivity/resistance to navitoclax

Proteomic analysis of plasma samples considered "most sensitive" and "most resistant" to navitoclax revealed 9 proteins of differential abundance between the two groups (ANOVA p-value < 0.05, FC > 1.3) (**Supp. File 4.7**). Of these proteins, 4 were increased and 5 were decreased in abundance in the "most resistant" to navitoclax group. The change in abundance of these proteins is illustrated in **Figure 4.11A**. Protein-protein interaction analysis revealed a highly interconnected network across all SSDAs (**Figure 4.11B**).

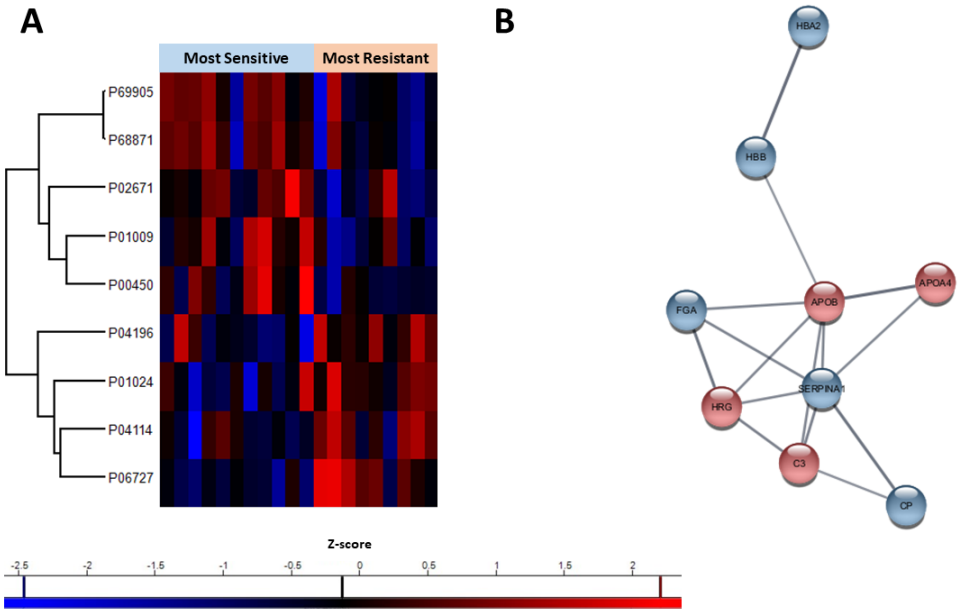

Figure 4.11: Label-free quantitative proteomic analysis of plasma samples "most sensitive" and "most resistant" to the BCL-2 and BCL-xL inhibitor, navitoclax. (**A**) Hierarchical clustering of z-scored normalised LFQ intensity values for 9 SSDA proteins illustrating the alterations in plasma protein abundance. (**B**) String enrichment analysis on SSDAs identified via Student's t-test comparison of "most sensitive" and "most resistant" navitoclax groups. Red nodes represent proteins increased in abundance in the "most resistant" group, whereas blue nodes represent proteins decreased in abundance in the "most resistant" group.

4.3.3 Plasma proteomic analysis using targeted proximity extension assay technology

Plasma proteomics by mass spectrometry is well-known to be complicated due to the high dynamic range of protein abundance whereby high abundance proteins make up over 90% of the plasma proteome. Despite the application of immunodepletion, immunoenrichment, and/or fractionation methods to remove high abundance proteins, it is extremely difficult to detect low abundance proteins such as cytokines in an MS-based plasma proteomic experiment. Therefore, we performed a targeted analysis to detect the plasma concentrations of 45 cytokines in MM plasma patients (n=26) stratified based on *ex vivo* drug responses. The same individual drugs analysed as part of our mass spectrometry analysis were evaluated. Statistical analysis of cytokine concentrations in MM patients considered most sensitive and most resistant to bortezomib did not yield any significant alterations (**Supp. File 4.1**).

4.3.3.1 Targeted analysis of cytokine concentrations across four chemosensitivity groups

Across the four chemosensitivity groups, five cytokines were found to be statistically significantly differentially abundant (Kruskal-Wallis p-value < 0.05) (**Table 4.6**) (**Supp. File 4.8**). Fms-related tyrosine kinase 3 ligand (FLT3LG), granulocyte-macrophage colony-stimulating factor (CSF2), lymphotoxin-alpha (LTA), interleukin-10 (IL-10), and interleukin-15 (IL-15) demonstrated increased concentrations in Group 1 MM patients when compared to the other chemosensitivity groups (**Figure 4.12**). As Group 1 MM patients typically have a reduced overall survival, we evaluated whether increased levels of these five cytokines are associated with reduced OS in this MM cohort. Patients were binarized into high and low expression of the five cytokines, however survival analysis did not yield significant changes in the OS of the high and low expression groups.

Table 4.6: List of significantly differentially abundant cytokines across the four MM chemosensitivity groups. Statistical analysis was performed using non-parametric Kruskal-Wallis tests followed by Wilcoxon post-hoc analysis with Benjamini-Hochberg p-value adjustment. Significance is marked as follows: P ≤ 0.05 '*', ns 'not significant'.

Protein name	Gene name	Kruskal-Wallis p-value	G1 v G2	G1 v G3	G1 v G4	G2 v G3	G2 v G4	G3 v G4
Fms-related tyrosine kinase 3 ligand	FLT3LG	**0.014**	*	*	*	ns	ns	ns
Granulocyte-macrophage colony-stimulating factor	CSF2	**0.025**	*	*	ns	ns	ns	ns
Lymphotoxin-alpha	LTA	**0.025**	*	*	*	ns	ns	ns
Interleukin 10	IL-10	**0.025**	0.054	*	ns	ns	ns	ns
Interleukin 15	IL-15	**0.029**	ns	0.075	0.053	ns	ns	ns

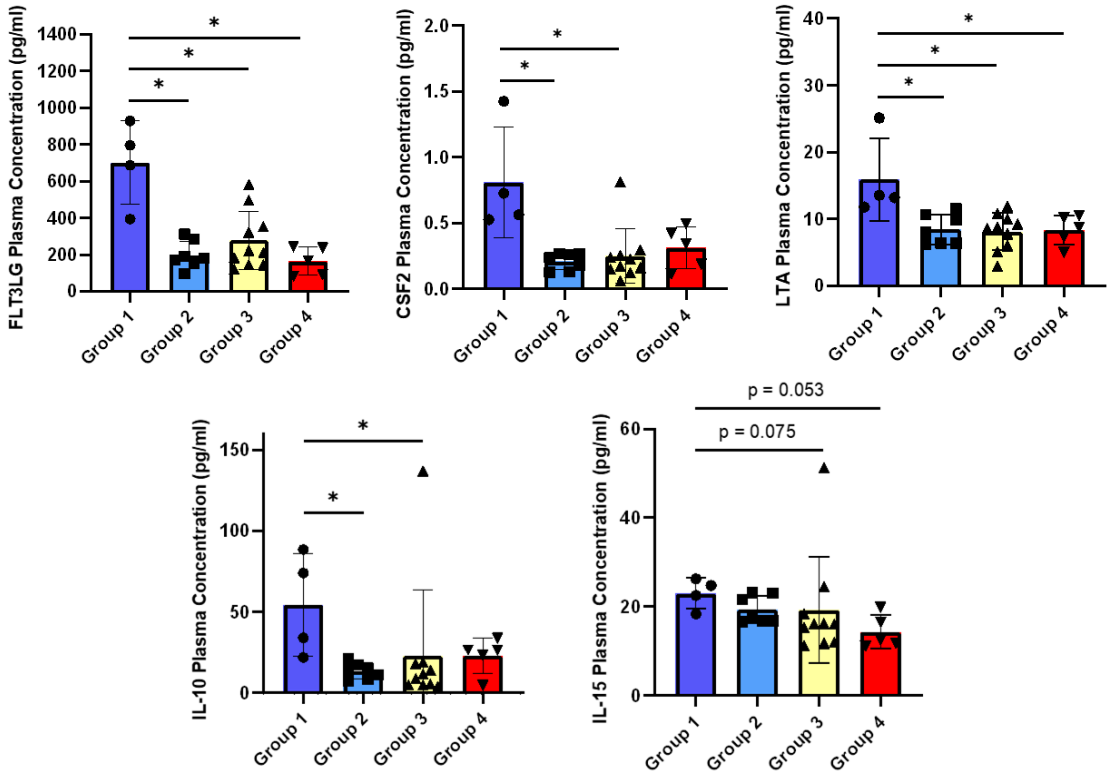

Figure 4.12: Plasma concentrations of differentially abundant cytokines across chemosensitivity groups. Kruskal-Wallis statistical analysis identified FLT3LG, CSF2, LTA, IL-10, and IL-15 as significantly differentially abundant (p-value < 0.05). Significance is based on Wilcoxon post-hoc analysis with Benjamini-Hochberg p-value adjustment. Significance is marked as follows: p-value ≤ 0.05 '*'.

4.3.3.2 Evaluation of cytokine concentrations in MM plasma stratified based on drug sensitivity/resistance to individual drugs

Targeted analysis of plasma samples considered "most sensitive" and "most resistant" to lenalidomide revealed five cytokines of differential abundance between the two groups (Wilcoxon p-value < 0.05) (**Figure 4.13**) (**Supp. File 4.2**). All five of the cytokines were significantly increased in patients considered most sensitive to lenalidomide. Regarding dinaciclib, two cytokines, namely LTA and IL-15, were identified as SSDA between the "most sensitive" and "most resistant" groups (**Figure 4.14**) (**Supp. File 4.3**). LTA and IL-15 were significantly increased in the plasma of patients considered most sensitive to dinaciclib. Targeted analysis of the investigational PI3K/mTOR dual inhibitor, PF-04691502, revealed CSF2, IL-15, and FLT3LG as differentially abundant in the plasma of MM patients considered "most sensitive" and "most resistant" to PF-04691502 (**Figure 4.15**) (**Supp. File 4.4**). All three cytokines were significantly increased in most sensitive MM patient plasma.

MM patients most sensitive to quisinostat were found to have increased plasma concentrations of IL-15 (p = 0.008) (**Supp. File 4.5**). Two BCL2 inhibitors, namely venetoclax and navitoclax were evaluated to identify plasma cytokines associated with drug response. Increased plasma concentrations of interleukin-1β (IL-1β) and matrix metalloproteinase 12 (MMP12) were associated with sensitivity to venetoclax (**Figure 4.16A**) (**Supp. File 4.6**). For the dual BCL-2 and BCL-xL inhibitor, navitoclax, increased levels of interleukin-6 and colony stimulating factor 1 (CSF1) were associated with sensitivity (**Figure 4.16B**) (**Supp. File 4.7**).

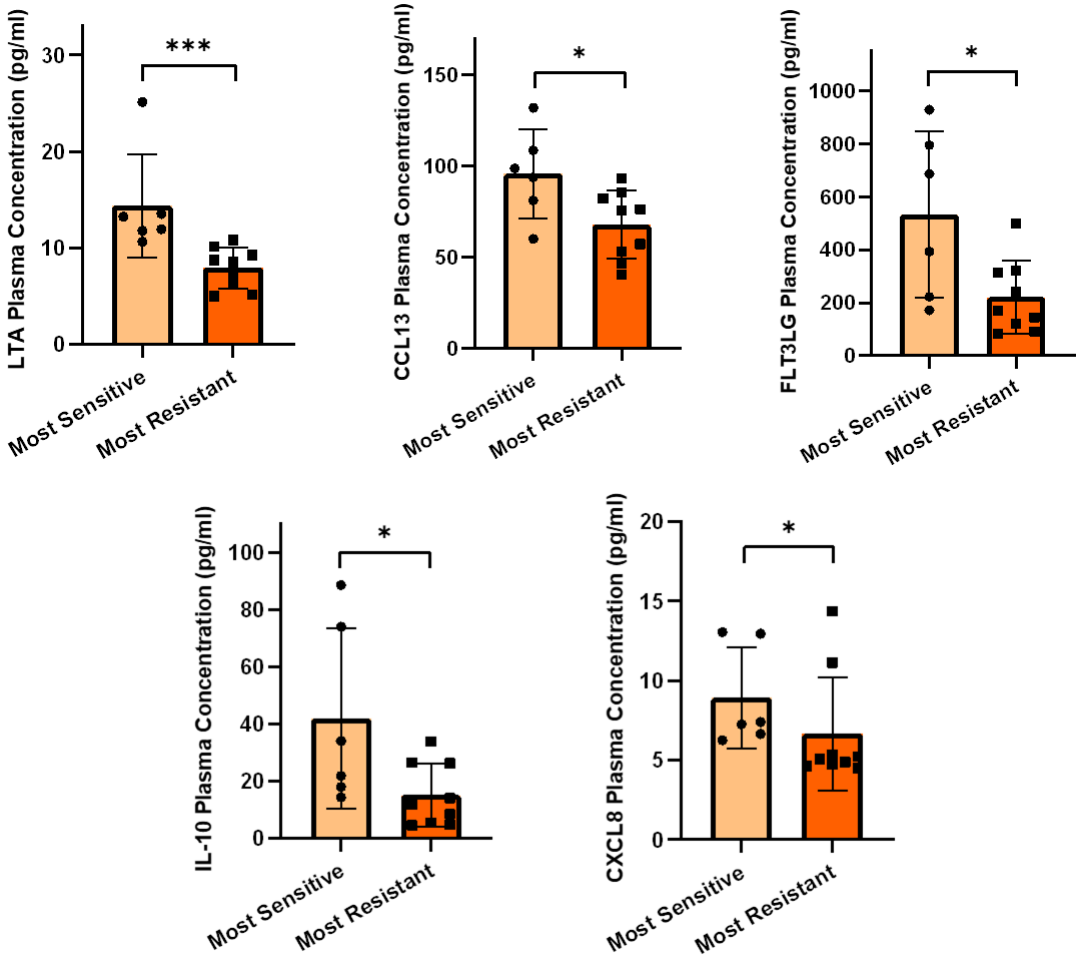

Figure 4.13: Plasma concentrations of cytokines identified as differentially abundant between groups considered 'most sensitive' and 'most resistant' to lenalidomide. Wilcoxon rank sum analysis identified LTA, CCL13, FLT3LG, IL-10, and CXCL8 as significantly differentially abundant (p-value < 0.05). Significance is marked as follows: p-value ≤ 0.05 '*', p-value ≤ 0.001 '***'.

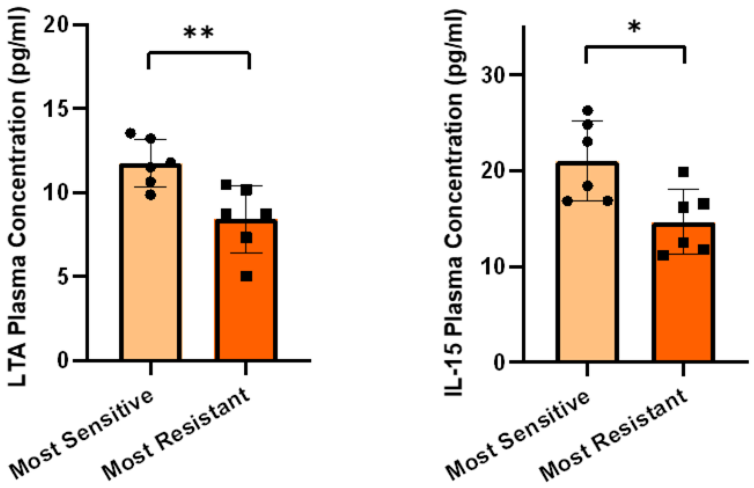

Figure 4.14: Plasma concentrations of cytokines identified as differentially abundant between groups considered 'most sensitive' and 'most resistant' to dinaciclib. Wilcoxon rank sum analysis identified LTA and IL-15 as significantly differentially abundant (p-value < 0.05). Significance is marked as follows: p-value ≤ 0.05 '*', p-value ≤ 0.01 '**'.

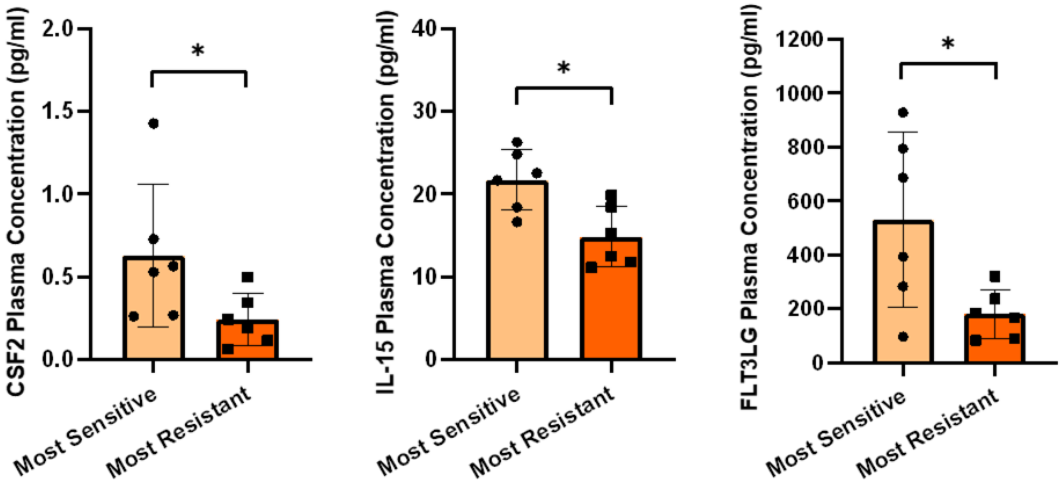

Figure 4.15: Plasma concentrations of cytokines identified as differentially abundant between groups considered 'most sensitive' and 'most resistant' to PF-04691502. Wilcoxon rank sum analysis identified LTA and IL-15 as significantly differentially abundant (p-value < 0.05). Significance is marked as follows: p-value ≤ 0.05 '*'.

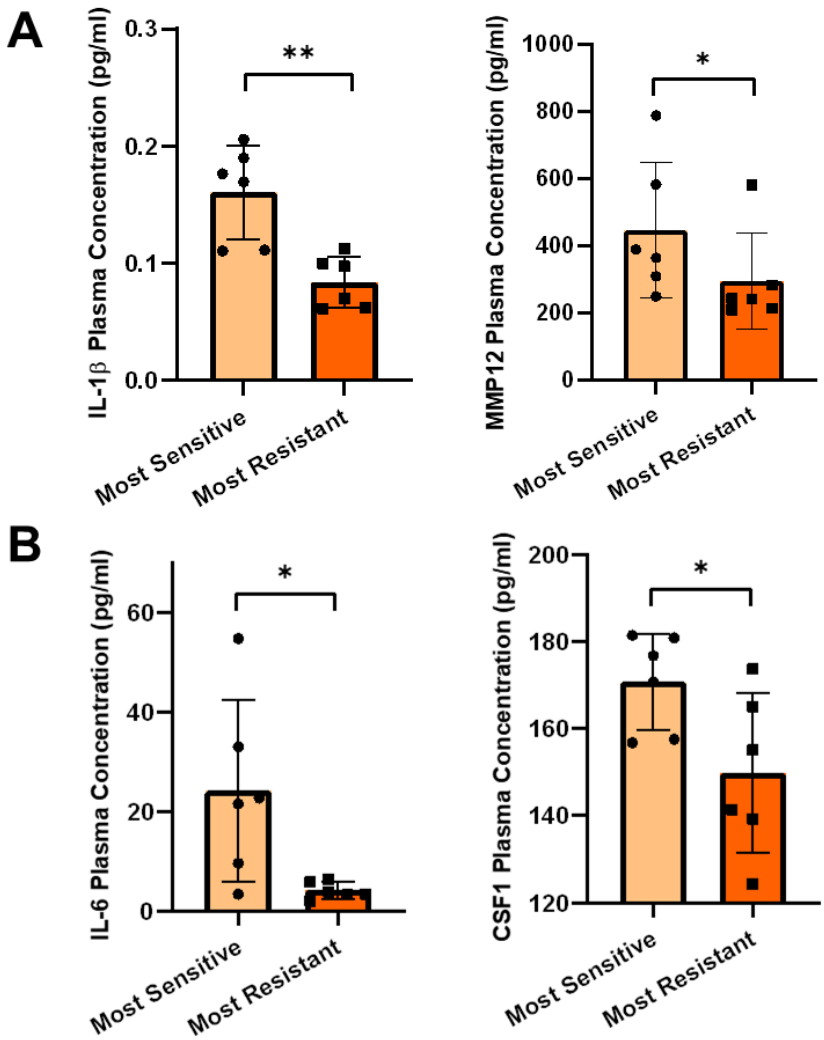

Figure 4.16: Plasma concentrations of cytokines identified as differentially abundant based on *ex vivo* drug response to venetoclax and navitoclax. (**A**) IL-1β and MMP12 were identified as differentially abundant between groups considered 'most sensitive' and 'most resistant' to venetoclax. (**B**) IL-6 and CSF1 showed differential abundance between groups considered 'most sensitive' and 'most resistant' to navitoclax. Significance is marked as follows: p-value ≤ 0.05 '*', p-value ≤ 0.01 '**'.

4.3.3.3 Increased plasma levels of interleukin-15 correlate with sensitivity to MEK inhibitors

As outlined above, IL-15 was found to be increased in the plasma of MM patients most sensitive to PF-04691502, quisinostat, and dinaciclib, which target PI3K/mTOR, HDACs, and CDKs, respectively. IL-15 is known to activate PI3K/mTOR and RAS/Raf/MEK/ERK pathways and modulate the expression of HDACs in immune cells (Mishra *et al.* 2016; Hawke *et al.* 2020). Therefore, we investigated whether increased plasma IL-15 levels were also associated with sensitivity to MEK inhibitors. Indeed, plasma IL-15 concentrations were significantly increased in MM patients considered most sensitive to the MEK

inhibitors, pimasertib, trametinib, selumetinib and refametinib (**Supp. Figure 4.1**). Incorporating the full cohort (n=26), we identified a positive correlation between IL-15 levels and sensitivity to PF-04691502, quisinostat, dinaciclib, pimasertib, refametinib, and trametinib (**Table 4.7**).

Table 4.7: Spearman rank correlation analysis between individual drug sensitivity scores and plasma concentrations of IL-15. Significant correlations are marked with an asterisk (*).

Drug	Mechanism/Target	Spearman's rho	95% Confidence Interval	*p*-value
PF-04691502	PI3K/mTOR inhibitor	0.44	0.0635 - 0.707	0.025*
Quisinostat	Pan-HDAC inhibitor	0.543	0.197 - 0.769	0.004*
Dinaciclib	Pan-CDK inhibitor	0.601	0.279 - 0.802	0.001*
Pimasertib	MEK 1/2 inhibitor	0.489	0.126 - 0.737	0.011*
Trametinib	MEK 1/2 inhibitor	0.496	0.134 - 0.741	0.01*
Selumetinib	MEK 1/2 inhibitor	0.345	0.0492 - 0.646	0.085
Refametinib	MEK 1/2 inhibitor	0.448	0.0736 - 0.712	0.022*

4.4 Discussion

As the number of approved treatment options for MM patients increases, there is a growing need for precision medicine approaches to ensure patients receive the most effective therapeutic regimen and avoid unnecessary toxicities from ineffective treatments. Many clinical trials evaluating targeted therapeutics show efficacy in a limited number of patients, highlighting the need to identify markers that predict which patients will respond to these therapies. Studies focusing on the identification of circulating predictive biomarkers in MM are limited. The measurement of circulating protein biomarkers of therapeutic response represents a rapid, inexpensive, and clinically implementable precision medicine approach. In this chapter, we have used targeted and untargeted proteomic approaches to identify plasma-derived proteins associated with drug response based on *ex vivo* DSRT of CD138+ cells from MM patients. The circulating proteins identified in this pilot study represent potential surrogate markers of *ex vivo* DSRT that are easily measurable in a clinical setting.

Our untargeted mass spectrometry analysis identified numerous high abundance plasma proteins that are differentially abundant across general chemosensitivity groups and individual drug sensitivity/resistance. Evaluating plasma proteomic

changes across chemosensitivity groups aids in the identification of plasma proteins associated with general resistance to a wide range of drugs and/or drug classes. Furthermore, defining patients into chemosensitive or chemoresistance groups based on *ex vivo* response to a selection of drugs holds relevance for assessing response to combination treatment regimens. However, evaluating plasma proteins linked to sensitivity/resistance to individual drugs can provide insight into drug-specific resistance mechanisms. Prior proteomic analysis of myeloma cells in combination with *ex vivo* DSRT, revealed similar protein signatures associated with drug response to bortezomib, quizinostat and PF-04691502, while a distinct protein signature was associated with response to navitoclax (Tierney, Bazou, Majumder, *et al.* 2021). Our study reveals a similar trend in plasma, with many statistically significant proteins commonly identified across sensitivity to bortezomib, quisinostat, PF-04691502, and dinaciclib. Lenalidomide and venetoclax show some common statistically significant proteins while of the few statistically significant proteins associated with response to navitoclax, only three proteins were commonly identified as significant in bortezomib, quisinostat, PF-04691502, and/or dinaciclib analyses.

Gelsolin is an actin-binding protein which can be found as an 80kDa cytosolic protein or can be secreted into circulation as an 83kDa isoform called plasma gelsolin (pGSN). GSN plays a multifunctional role in tumorigenesis and has been reported to function as a tumour suppressor in certain cancers such as lung cancer and leukemias, and as an oncogene in other cancers including oral cancer and osteosarcoma (Sagawa *et al.* 2003; Shirkoohi *et al.* 2012; Deng, Hao, *et al.* 2015; Ma *et al.* 2016; Hsieh and Wang 2022). Here, plasma GSN was significantly increased in Group 4 (very resistant) MM patients and in those considered most resistant to bortezomib, lenalidomide, PF-04691502, dinaciclib, quisinostat, and venetoclax. Interestingly, previous research from our group found GSN to be significantly increased in myeloma cells from MM patients considered most resistant to bortezomib, quisinostat, and PF-04691502 based on *ex vivo* DSRT (Tierney, Bazou, Majumder, *et al.* 2021). Limited published studies have explored the role of GSN in MM, however, various studies have reported a link between plasma GSN and chemoresistance. Increased pGSN has been associated with cisplatin resistance in head and neck cancer and ovarian cancer (Wang, Abedini, *et al.* 2014; Asare-Werehene *et al.* 2022). In contrast, circulating levels of pGSN were recently reported

to be reduced in chemoresistant ovarian cancer patients while small extracellular vesicle-derived pGSN was significantly increased in chemoresistant ovarian cancer patients (Gerber *et al.* 2023). More research is needed to determine the localized role of pGSN within the myeloma BME and the role of circulating pGSN in drug resistance in MM.

Alpha-2-Heremans Schmid-glycoprotein (AHSG), also known as fetuin-A, is a multifunctional glycoprotein known to play roles in calcium metabolism, endocytosis, and bone remodelling (Dabrowska *et al.* 2015). Circulating AHSG is an important chemoattractant in serum and has been reported to stimulate chemotaxis synergistically with CXCL12 in tumour cells (Nangami *et al.* 2013). Initial studies reported reduced levels of AHSG in the serum of MM patients compared to healthy controls, while a recent study reported an increase in serum AHSG levels in MM patients compared to controls (Bíró *et al.* 1998; Salman *et al.* 2020). In our study, AHSG was found to be increased in Group 4 MM patients as well as in those considered most resistant to PF-04691502 and quisinostat. Studies investigating the role of AHSG in cancer have reported a link between AHSG expression and chemoresistance. In hepatocellular carcinoma, AHSG has been reported as a potential predictive marker of drug resistance following a study reporting an upregulation of AHSG in multi-drug resistant (MDR) cell lines and enhanced sensitivity to several anticancer drugs in AHSG knockdown MDR cell lines (Xiang *et al.* 2015). AHSG was also identified as hub gene in sorafenib-resistant hepatocellular carcinoma, further highlighting a potential role of AHSG in drug resistance. Several studies have described the involvement of AHSG in regulating the TGF-β signalling pathway by sequestering TGF-β, thus preventing binding to its receptor, TGF-β II receptor. This has been reported to promote tumour progression by impeding the tumour suppressive TGF-β pathway (Demetriou *et al.* 1996; Guillory *et al.* 2010; Dong *et al.* 2022). The role of AHSG in regulating the TGF-β signalling pathway in MM has not yet been elucidated.

Several complement proteins were found to be of differential abundance across the chemosensitivity groups. Complement C3, a central component of the complement proteolytic cascade, was increased in the plasma of patients considered most sensitive to bortezomib, lenalidomide, PF-04691502 and dinaciclib. In contrast, C3

was increased in the plasma of patients considered most resistant to navitoclax. Following activation of the complement system, C3 is cleaved into two anaphylatoxins termed C3a and C3b, which induce inflammation and opsonization, respectively (Revel *et al.* 2020). In MM, serum complement C3 levels are increased compared to healthy controls, and positively correlate with myeloma bone disease (Li, Xia, *et al.* 2019). Renal injury due to excessive immunoglobulin in the bloodstream is a common symptom in MM. MM has also been linked to the deposition of complement C3 in glomeruli, known as C3 glomerulonephritis, due to dysregulated complement activation (Xu *et al.* 2021). Interestingly, increased C3 deposition negatively correlated with plasma levels of C3 in gastric cancer with high C3 deposition in tumour tissue and reduced plasma C3 levels associated with a poor prognosis (Yuan *et al.* 2020). Several studies have reported a link between high C3 expression levels and drug resistance (Zha *et al.* 2019). A pan-cancer analysis found high expression of C3 to be associated with drug resistance based on the Genomics of Drug Sensitivity in Cancer database (Lawal *et al.* 2021). Furthermore, C3 was significantly increased in the pre-treatment serum of MM patients who responded (VGPR or PR) to a bortezomib-based therapeutic regimen (Ting *et al.* 2017).

Two hemoglobin subunits, hemoglobin subunit beta (HBB) and hemoglobin alpha 2 (HBA2), were uniquely increased in plasma from MM patients considered most sensitive to BCL-2 inhibitors, venetoclax and navitoclax. Interestingly, a study correlating the expression of BCL-2, BCL-2 associated X (BAX), and P-glycoprotein with clinical factors in AML with normal karyotype patients, found patients with increased BCL-2 expression had higher hemoglobin levels (Pravdic *et al.* 2023). Treatment with venetoclax and navitoclax has also been linked to a reduction in plasma hemoglobin levels, further highlighting the association between BCL-2 levels and hemoglobulin levels (Scherr *et al.* 2020; Abdel-Samad and Sughayar 2021). BCL-xL is required for erythroid cell survival and plays a key role in erythroid maturation and heme synthesis (Motoyama *et al.* 1995; Hafid-Medheb *et al.* 2003). A more recent study found that the expression of *BCL2L1* (BCL-xL) regulates the expression of hemoglobin genes including *HBG*, *HBB* and *HBA*. Treatment with a BCL-xL inhibitor led to a significant reduction in *HBG* and *HBB* expression (Dai *et al.* 2019). Increased levels of hemoglobin subunits may indicate increased expression

of BCL-2 and/or BCL-xL, and consequently, increased sensitivity to BCL-2 inhibitors.

While several plasma proteins were commonly significantly differentially abundant across individual drug sensitivities, proteins uniquely differentially abundant to specific drug responses were also identified. For example, zinc alpha 2-glycoprotein (AZGP1 or ZAG) was uniquely increased in MM patients considered most resistant to lenalidomide. ZAG is a 41kDa secreted protein that plays roles in lipid mobilization, immunoregulation and cell adhesion (Araki *et al.* 1988; Russell *et al.* 2004; Liu, Han, *et al.* 2018). ZAG has been identified as a tumour suppressor in certain cancers and a tumour promoter in others such as colorectal cancer (Kong *et al.* 2010; Ji *et al.* 2019). Increased expression of ZAG has been implicated in cancer cachexia and has been suggested as a potential therapeutic target in individuals with cachexia (Mracek *et al.* 2011; Elattar *et al.* 2018). A single-cell transcriptomic analysis found ZAG to be significantly increased in triple-negative breast cancer patients who did not respond to neoadjuvant chemotherapy (Vishnubalaji and Alajez 2021). Furthermore, pre-treatment serum concentrations of ZAG were significantly increased in MM patients that did not respond to a thalidomide-based induction therapy, highlighting increased circulating ZAG levels as a potential biomarker of reduced response to immunomodulatory drugs (Rajpal *et al.* 2011). Two other proteins uniquely increased in abundance in MM patient plasma considered most resistant to lenalidomide, polymeric immunoglobulin receptor (PIGR) and alpha-1-microglobulin/bikunin precursor (Protein AMBP), have been implicated in chemoresistance in solid cancers (Huang, Han, *et al.* 2013; Ohkuma *et al.* 2020).

Investigating the plasma proteome is a difficult task that often requires the combination of analytical techniques to improve proteome coverage. Untargeted mass spectrometry approaches are limited by their diminished ability to identify and quantify low abundance proteins. Therefore, combining untargeted LC-MS/MS plasma proteomics with targeted proximity extension assays enables in-depth exploration of the plasma proteome (Petrera *et al.* 2021). With the understanding that many of the proteins identified in our untargeted mass spectrometry analysis were high abundant plasma proteins whose abundance may be influenced by biological and pathological conditions, we also performed a targeted proteomic analysis to

quantify low abundance cytokines in plasma. FLT3LG was significantly increased in the plasma of Group 1 MM patients and those considered most sensitive to lenalidomide and PF-04691502. FLT3LG is the ligand for the receptor tyrosine kinase, fms-like tyrosine kinase receptor 3 (FLT3), and upon binding, induces autophosphorylation and the initiation of multiple signalling pathways which mediate cell proliferation and survival in hematopoietic cells (Kazi and Rönnstrand 2019). Overexpression of FLT3 in a subgroup of MM patients has been associated with a shorter PFS in MM, corroborating with our results as Group 1 patients have a reduced overall survival when compared to other groups (Steiner *et al.* 2020). Plasma levels of FLT3LG have been linked to disease progression in MM, whereby plasma concentrations increase from MGUS to NDMM to RRMM (Steiner *et al.* 2017). FLT3LG plays a key role in hematopoiesis and the expansion of FLT3+ early hematopietic progenitors (Wodnar-Filipowicz 2003). Disruption of FLT3LG expression in mice resulted in a reduction in the number of myeloid and lymphoid progenitors in the bone marrow and natural killer cells and dendritic cells in secondary immune organs (McKenna *et al.* 2000). Due to its role in the generation of conventional and plasmacytoid dendritic cells, FLT3LG has been explored as a potential therapeutic to enhance T cell immunity in various cancers including colon cancer and breast cancer (Morse *et al.* 2000; Disis *et al.* 2002). A recent editorial proposed the measurement of serum FLT3LG as a potential biomarker of immune activation by immunogenic cell death-inducing chemotherapeutics (Pol *et al.* 2020). This followed on from several studies reporting that patients with increased FLT3LG levels after oxaliplatin-based neoadjuvant therapy had improved long-term outcomes in colorectal cancer patients with liver metastases and high-risk rectal cancer (Kalanxhi *et al.* 2018; Abrahamsson *et al.* 2020). Measurement of serum FLT3LG during induction therapy in AML has also been proposed to be predictive of response to therapy. Increased levels of FLT3LG were seen in patients who achieved morphological complete response, while patients who did not respond to chemotherapy had undetectable levels of FLTLG (Milne *et al.* 2019). Furthermore, FLT3LG has been shown to mediate the abscopal effect of ionizing radiation by triggering T-cell antitumour responses and FLT3LG release from NK cells improves response to radioimmunotherapy in a mouse model of head and neck squamous cell carcinoma (Demaria *et al.* 2004; Bickett *et al.* 2021). Altogether, increased levels of circulating FLT3LG can indicate a “beneficial” antitumour immune response that

may enhance the sensitivity of chemotherapeutics that invoke an immune response as part of their mechanism of action. The relationship between FLT3LG levels and response to immunomodulatory drugs has yet to be explored.

CSF2, or granulocyte-macrophage colony stimulating factor (GM-CSF), is a monomeric glycoprotein that acts as a growth factor by stimulating the activation, proliferation and survival of immune cells (Huang *et al.* 2020). In this work, plasma CSF2 was increased in Group 1 MM patients and in those considered most sensitive to PF-04691502. RNA sequencing and immunohistochemistry analysis found increased expression of CSF2 to be associated with drug resistance in small-cell lung cancer and colorectal cancer (Xu, Zhang, *et al.* 2019; Li, Zhong, *et al.* 2022). In MM, CSF2 has been investigated as a means to mobilize hematopoietic stem cells for collection prior to high-dose chemotherapy and ASCT, however, CSF3 showed similar efficacy with reduced toxicity and is commonly used for mobilization in MM (Demuynck *et al.* 1995; Luo *et al.* 2022). Similarly to FLT3LG, CSF2 has been investigated as an adjuvant to cancer vaccine studies to prime the immune system and enhance antigen presentation (Ji *et al.* 2005). A recent proof-of-principle clinical trial which treated 15 patients with an allogeneic multiple myeloma GM-CSF-secreting vaccine in combination with lenalidomide, reported prolonged clinical responses in MM patients in near complete remission (Biavati *et al.* 2021). Increased plasma levels of CSF2 may indicate immune response, however, the link between plasma CSF2 levels and drug resistance in MM has not been investigated. Lymphotoxin alpha (LTA) is a member of the TNF superfamily and exists as a soluble homotrimer or as a heterotrimeric form with membrane-bound lymphotoxin beta (Browning *et al.* 1995). Serum levels of LTA were reduced in late-stage pancreatic ductal adenocarcinoma (PDAC) compared to early-stage PDAC (Mellby *et al.* 2018). In MM, polymorphisms that enhance the production of LTA have been linked to an increased risk of developing MGUS and MM and LTA has growth-stimulating effects on myeloma cell lines (Hjorth-Hansen *et al.* 1999; Davies *et al.* 2000). Our study found plasma LTA levels to be significantly increased in Group 1 MM patients and those considered most resistant to lenalidomide and dinaciclib.

Two interleukins, IL-10 and IL-15 were increased in the plasma of Group 1 MM patients. IL-10 is a multifunctional cytokine reported to have both anti-inflammatory

and immune-stimulatory properties. Although IL-10 has strong immunosuppressive effects on monocytes, macrophages, and dendritic cells, it is a stimulator of B lymphocytes, NK cells, and mast cells (Carlini *et al.* 2023). A pan-cancer meta-analysis revealed that high serum IL-10 is associated with worse clinical outcome in the majority of cancers (Zhao *et al.* 2015). Indeed, increased levels of serum IL-10 are associated with a poor prognosis and advanced disease in MM (Wang, Wang, *et al.* 2016; Shekarriz *et al.* 2018). Increased IL-10 levels have also been identified in extramedullary MM patients, however the link between serum IL-10 and drug resistance in MM has yet to be elucidated. IL-15 is an essential cytokine involved in the activation of immune cells including T cells and NK cells. IL-15 has become a key factor in NK cell-mediated cancer immunotherapy as it is required for the persistence and proliferation of primary NK cells. Cord-blood NK cells genetically engineered to express CAR-CD19 and IL-15 rather than CAR-CD19 alone, showed enhanced proliferation, persistence and anti-tumour activity (Liu, Tong, *et al.* 2018). A first-in-class engineered T cell receptor natural killer cell therapy (NY-ESO-1 TCR/IL-15 NK) has recently been cleared by the FDA for a Phase I study in RRMM, which is expected to begin in late 2023. IL-15 agonists in combination with chemotherapy have also been explored to enhance anti-tumour activity (Robinson and Schluns 2017). Studies combining IL-15 with chemotherapies such as cyclophosphamide and 5-fluoracil have demonstrated that IL-15 potentiates their anti-tumour activity (Evans *et al.* 1997; Cao *et al.* 1998). IL-15 has also shown promise in combination with immunotherapies such as anti-PD-L1 (Waldmann *et al.* 2020; Shi *et al.* 2023). These studies highlight the ability of IL-15 to enhance the anti-tumour immune response. A study investigating lymphoma remission following CD19 CAR-T cell therapy also reported significantly higher IL-15 serum levels in patients who achieved remission than those who did not. Interestingly, increased serum IL-10 was also associated with lymphoma remission (Kochenderfer *et al.* 2017). In this study, we have reported an increase in plasma IL-15 levels in Group 1 MM patients and those considered most sensitive to dinaciclib, quisinostat, PF-04691502, and MEK inhibitors. The increased plasma levels of IL-15 in drug sensitive MM patients may indicate patients that can stimulate a stronger anti-tumour immune response following chemotherapy. On the other hand, the increased levels of circulating IL-15 may indicate an increased activation of PI3K/mTOR and RAS/Raf/MEK/ERK pathways in tumour cells, thus increasing the susceptibility of

the tumour cells to PI3K/mTOR, MEK, and CDK inhibitors. Monitoring IL-15 levels, or IL-15 levels in combination with other immunostimulatory cytokines identified in this study, may identify MM patients most likely to respond to specific chemotherapeutic drugs. As the intermittent IL-15 administration in non-human primates has been reported to be safe, patients exhibiting low levels of circulating IL-15 may benefit from treatments which increase endogenous IL-15 concentrations (Berger *et al.* 2009).

Cytokines significantly increased in abundance in the plasma of MM patients considered most sensitive to BCL-2 inhibitors were unique to venetoclax and navitoclax. IL-1β and MMP12 were significantly increased in the plasma of venetoclax-sensitive patients. IL-1β is not typically expressed by plasma cells but is abnormally expressed by myeloma cells (Lacy *et al.* 1999). Proinflammatory cytokines including IL-1β and TNF-α, stimulate the canonical NF-κB signalling pathway in MM which subsequently increases the expression of anti-apoptotic proteins including BCL-2 and BCL-xL (Yu *et al.* 2020). The implication of increased plasma IL-1β and MMP12 in sensitivity to venetoclax is unknown. Regarding navitoclax, increased plasma levels of IL-6 and CSF1 were associated with sensitivity. Like IL-1β, IL-6 is a key cytokine involved in activating NF-κB signalling in MM. Increased serum IL-6 levels have been linked to disease progression and a poor prognosis in MM (Ludwig *et al.* 1991; Nachbaur *et al.* 1991). Increased serum concentrations of CSF1 are also linked to reduced survival in MM patients (Kowalska *et al.* 2011). CSF1 has been reported to increase the expression of BCL-xL, the target of navitoclax, in osteoclasts, however this has not been further investigated in other cell types ((Woo *et al.* 2002). Further research is required to determine whether circulating IL-6 and CSF1 are associated with sensitivity to navitoclax.

The results presented in this study show huge potential and it is hoped that validation studies will yield promising predictive biomarkers with broad clinical usability. It is not feasible to repeatedly perform full clinical workups with bone marrow biopsy collection throughout the disease course of MM patients. Therefore, there is a need to identify easily measurable, minimally invasive biomarkers in the blood. Plasma proteins can be quantified using immunoassays that are already standard in clinical

laboratories which simplifies the translation of these results to clinical use. This chapter demonstrates that there are plasma-derived proteins that can aid in the prediction of sensitivity/resistance to various drugs that are active against MM. As MM is an extensively heterogeneous disease, it is unlikely a single biomarker will accurately predict patient response to individual drugs clinically approved for the treatment of MM. Therefore, I believe a panel of biomarkers has the best potential to have sufficient sensitivity and specificity to accurately predict patient response to individual drugs. Additional studies validating the most promising biomarkers identified in this study may aid in developing clinically meaningful predictive biomarker panels.

It is important to note that some of the MM patient cohort analysed in this study have been exposed to bortezomib and lenalidomide prior to this analysis which may impact plasma protein levels. Furthermore, changes in protein levels are often detected during the disease course from NDMM to RRMM. Therefore, future studies with a larger cohort of samples should evaluate protein levels at different stages of disease, incorporating factors such as the extent of bone disease to identify clinical factors that may influence protein concentrations and confound the predictive ability of the surrogate markers described in this study. As described in Chapter 3, the *ex vivo* DSRT approach has limitations that must be considered when interpreting the results of this study. Nonetheless, our study highlights the potential of identifying easily measurable plasma-derived surrogate markers of *ex vivo* DSRT using proteomics. Although the *ex vivo* DSRT approach used in this study is limited to small molecule inhibitors, the combination of untargeted and targeted plasma proteomics could be applied to identify protein markers of response to other therapeutic groups, such as immunotherapies.

4.5 Conclusion

This chapter demonstrates the potential of combining *ex vivo* DSRT with targeted and/or untargeted proteomics to identify circulating proteins which may serve as surrogate markers of *ex vivo* drug sensitivity/resistance. Although further research is needed to confirm the clinical application of *ex vivo* DSRT in MM, significant developments in other hematological malignancies, such as AML, highlight the capacity of this functional precision medicine approach to yield clinically relevant

results. Future clinical trials testing the clinical usability of *ex vivo* DSRT may benefit from collecting plasma/serum samples to evaluate the presence of circulating surrogate markers.

Chapter 5

Proteomic profiling of bone marrow mononuclear cells in extramedullary multiple myeloma

5.1 Introduction

Extramedullary multiple myeloma (EMM) is an aggressive sub entity of multiple myeloma. Despite being considered a rare manifestation, the incidence of EMM is thought to be increasing as the sensitivity of imaging technologies improve and MM patients exhibit prolonged survival due to the introduction of novel therapeutics (Bansal *et al.* 2021). The presence of extramedullary disease is associated with a poor prognosis with patients having a significantly shorter progression free survival and overall survival when compared with MM patients without EMD (Usmani *et al.* 2012). Little is known about the molecular pathogenesis of EMM and no bone marrow-derived or blood-derived markers have been identified for the diagnosis of EMM or to predict EMM transition.

Cytogenetic factors and dysregulation of adhesion molecules and pathways have been implicated in the pathogenesis of EMM (Billecke *et al.* 2013; Janjetovic *et al.* 2021). Neural cell adhesion molecule (NCAM or CD56) is a membrane glycoprotein well known to be expressed on natural killer (NK) cells but has also been detected on other immune cells such as dendritic cells and T cells (Roothans *et al.* 2013; Almehmadi *et al.* 2014; Van Acker *et al.* 2017). CD56 is not typically expressed on plasma cells but has been reported to be expressed on between 70-80% of malignant myeloma cells (Mateo *et al.* 2005). Several studies have linked a lack of CD56 expression on myeloma cells to a more plasmablastic phenotype, a poor prognosis, and extramedullary transformation (Dahl *et al.* 2002; Sahara *et al.* 2002; Koumpis *et al.* 2021). CD56 plays a key role in binding malignant plasma cells to each other and to other components of the bone marrow. The exact mechanism by which CD56 promotes extramedullary transformation is unknown, however the downregulation of CD56 could weaken myeloma cell interactions with the bone marrow microenvironment to stimulate intravasation (Zhang, Huang, *et al.* 2022). Furthermore, CD56 was previously found to attenuate the secretion of matrix metalloproteinase 9 (MMP9), which suggests a decrease in CD56 expression may stimulate MMP9 secretion and degradation of the extracellular matrix to facilitate migration (Edvardsen *et al.* 1993).

The adhesion molecule, CD44, is significantly increased on the surface of malignant plasma cells in EMM (Dahl *et al.* 2002; Ning *et al.* 2021). CD44 is a ubiquitously

expressed hyaluronan receptor, that has been implicated in a variety of tumorigenic processes including metastasis (Misra *et al.* 2015). Hyaluronan-mediated CD44 activation modulates various downstream cellular processes including cytoskeletal rearrangement, Rho signalling, and Ca^{2+} mobilization (Bourguignon 2008). Using a bone marrow metastatic model, one study found that CD44 binding to hyaluronan on bone marrow endothelial cells (BMECs) played a key role in migration and transendothelial invasion (Okada *et al.* 1999). Furthermore, a recent study implicated hyaluronan-induced homophilic myeloma cell interactions through CD44 variants as an initiating factor of EMM development (Kikuchi *et al.* 2022). Platelet/endothelial cell adhesion molecule-1 (PECAM1 or CD31) is an adhesion molecule whose gene expression has previously been reported to be increased in tumour cells derived from extramedullary plasmacytomas (Hedvat *et al.* 2003). Furthermore, through immunohistochemical staining, CD31 protein was detected on the membranes of malignant plasma cells and endothelial cells at extramedullary sites (Govender *et al.* 1997; Hedvat *et al.* 2003).

The heterodimer of integrin α4 and integrin β1, known as very late antigen 4 (VLA-4), plays a prominent role in MM cell adhesion, migration, and drug resistance (Hosen 2020). Cells of the bone marrow, including bone marrow stromal cells, express the primary ligands of VLA-4; vascular cell adhesion molecule 1 (VCAM1) and fibronectin (FN) (Sanz-Rodríguez *et al.* 1999). The binding of VLA-4 to its ligands on other cells in the BME promotes myeloma cell retention in the bone marrow, as well as the activation of various downstream signalling pathways (Damiano and Dalton 2000; Bou Zerdan *et al.* 2022). The knockdown of VLA-4 in myeloma cells revealed a reduced medullary tumour burden, while simultaneously stimulating the formation of extramedullary lesions (Hathi *et al.* 2022). Thus, the loss of VLA-4 has been widely reported to contribute to the evolution of EMM due to the loss of myeloma cell adhesion to the bone marrow stroma (Gupta *et al.* 2022).

Various cytogenetic, genomic and transcriptomic studies have provided insight into genetic events that occur during the progression of MM to EMM (Bhutani *et al.* 2020). As mentioned previously, MM is a highly heterogenous malignancy, whereby sequential genetic events contribute to MM pathogenesis and patient prognosis (Chng *et al.* 2007). Sites of EMD have been associated with complex cytogenetic

abnormalities, highlighting clonal evolution as a factor in EMM development. As expected, high-risk genetic abnormalities including del(17), t(4;14), and 1q gain have been linked to EMM transformation (Billecke *et al.* 2013; Qu *et al.* 2015; Besse *et al.* 2016). Furthermore, abnormalities in chromosome 1 in bone marrow myeloma cells have been linked to MM progression to EMM (Kriegova *et al.* 2021). NRAS and KRAS mutations which drive MAPK signalling and TP53 mutations have been implicated in EMM (de Haart *et al.* 2016; Long *et al.* 2020; Ryu *et al.* 2020). The precise influence of these genomic abnormalities on the pathogenesis of EMM remain unknown (McAvera *et al.* 2023).

Neutrophils are the most abundant immune cell and play a key role in the innate immune response. Initially discovered as an innate immune response mechanism, the web-like structures generated by neutrophils known as neutrophil extracellular traps (NETs), have been implicated in the progression of various diseases including cancer and autoimmune diseases (Brinkmann *et al.* 2004; Zhao and Jin 2022; Wigerblad and Kaplan 2023). NETs contribute to the innate immune response by immobilizing pathogens including bacteria, fungi, and viruses, to prevent dissemination and kill microbes. NETs are extracellular structures composed of decondensed chromatin decorated with histones, proteinases, and cytosolic proteins. The NET proteome varies in response to the stimulus but includes common proteins that are present irrespective of the stimulus. These common proteins include core histones, the granular proteins neutrophil elastase (ELA2), cathepsin G, and proteinase-3, myeloperoxidase (MPO), calprotectin and catalase (Urban *et al.* 2009). Following binding of a NET stimulant to its respective receptor, downstream signalling involving the Raf-MEK-ERK pathway, calcium mobilization, NADPH oxidase activation, and ROS generation contributes to the activation and translocation of PAD4, ELA2, and MPO into the nucleus (**Figure 5.1**) (Hakkim *et al.* 2011; Keshari *et al.* 2012). An association between NETs and metastasis has been reported in recent years (Yang and Liu 2021).

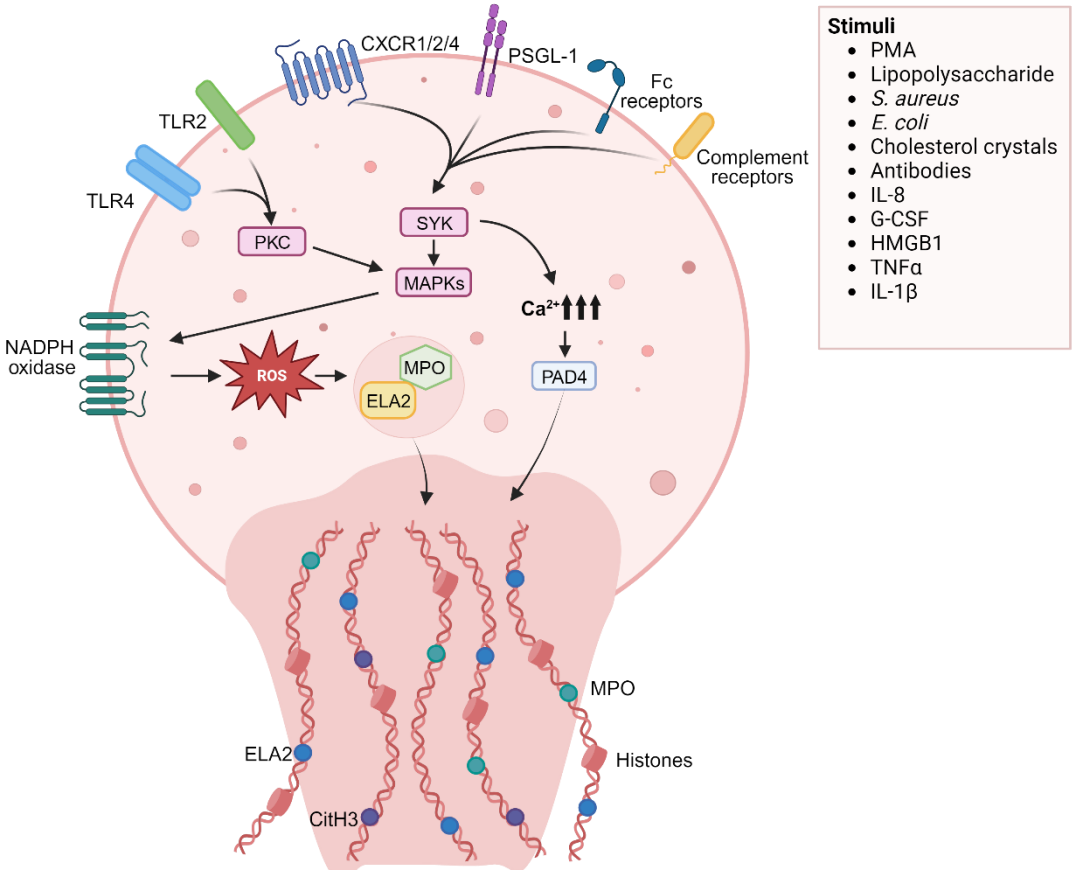

Figure 5.1: Overview of neutrophil extracellular trap (NET) formation. Neutrophils are triggered to release NETs by various stimuli including pathogenic organisms and cytokines released from surrounding cells. These factors bind to their respective receptors on the neutrophil surface, activating downstream signalling pathways which increase cytoplasmic calcium (Ca^{2+}) levels leading to the activation of protein-arginine deiminase type-4 (PAD4). The protein kinase C (PKC) and Raf-MEK-ERK signalling pathways also lead to the activation of nicotinamide adenine dinucleotide phosphate (NADPH) oxidase, resulting in the generation of reactive oxygen species (ROS) and subsequent release of neutrophil elastase (ELA2) and myeloperoxidase (MPO) from neutrophil granules. Following translocation to the nucleus, PAD4 catalyses the citrullination of histones which causes chromatin decondensation. ELA2 and MPO also translocate to the nucleus where they contribute to chromatin decondensation. Decondensed chromatin decorated with ELA2, MPO, and other neutrophilic proteins are subsequently released to for NETs. CitH3, Citrullinated histone 3; SYK, Tyrosine-protein kinase SYK; TLR, Toll-like receptor; CXCR, C-X-C motif chemokine receptor; PSGL-1, prostaglandin-1; PMA, phorbol 12-myristate 13-acetate; IL-8, interleukin-8; G-CSF, granulocyte-colony stimulating factor; HMGB1, high mobility group box 1; TNFα, tumour necrosis factor alpha; IL-1β, interleukin-1 beta.

Despite the identification of various proteins and genetic factors associated with migration and invasion in MM, the molecular phenotype of EMM has not been widely reported. As proteins are often used as biomarkers of disease and therapeutic targets, we hypothesized that a proteomic analysis of bone marrow mononuclear cells (BMNCs) from patients with EMM would reveal molecular characteristics associated with EMM pathogenesis. Thus, we performed a label-free mass

spectrometric analysis of BMNCs from MM patients with and without extramedullary spread. It is important to note that throughout this thesis, EMM refers to patients with soft tissue plasmacytomas outside of the bone marrow and not those with paraskeletal plasmacytomas (Weinstock and Ghobrial 2013).

5.2 Experimental design and methodology

Recent reports suggesting an increase in the incidence of EMM as the overall survival of MM patients improves highlights the need for further research on this aggressive subtype of MM (Bansal *et al.* 2021). The limited proteomics analyses focused on EMM in the literature meant it was of interest to investigate the potential proteomic changes between MM patients with and without extramedullary spread. Furthermore, identifying novel potential markers of EMM and potential cellular processes associated with extramedullary transition may help guide validation studies and novel drug development strategies.

5.2.1 Patient samples and clinical information

Bone marrow mononuclear cells (BMNCs) and EDTA blood plasma was obtained from the Finnish Hematology Registry and Clinical Biobank (FHRB) in Helsinki, Finland. The FHRB is authorised and approved by the Finnish National Supervisory Authority for Welfare and Health (Valvira) and Finnish National Medical Ethics Committee, respectively. BMNCs were collected from age- and gender-matched MM (n = 8) and EMM patients (n = 9, 1 serial sample). Sample collection, with informed consent, took place between 2013 and 2020 across several Finnish university hospitals and other hematology units. The median age was 65, and 2 females and 6 males were present in each group. Patient characteristics are summarised in **Table 5.1**. Samples were stored at −80 °C.

Table 5.1: Clinical and demographic characteristics of patient cohort. Characteristics include diagnosis, status at diagnosis, sex, age, and overall survival in months.

Sample ID	Diagnosis	Status	Sex	Age	OS (mo) from diagnosis
D_EMM_2689	Myeloma, extramedullary	Diagnostic	Male	65	80
D_EMM_3497	Myeloma, extramedullary	Diagnostic	Male	65	87 *
D_EMM_3674	Myeloma, extramedullary	Diagnostic	Male	58	8
D_EMM_4296	Myeloma, extramedullary	Diagnostic	Male	65	22
D_EMM_1994	Myeloma, extramedullary	Diagnostic	Female	67	16
D_EMM_40725	Myeloma, extramedullary	Diagnostic	Male	49	2
PD_EMM_874	Myeloma, extramedullary	Progressive disease	Male	72	31
PD_EMM_1994 †	Myeloma, extramedullary	Progressive disease	Female	68	16
PD_EMM_40795	Myeloma, extramedullary	Progressive disease	Female	69	7
D_MM_5215	Myeloma, no extramedullary	Diagnostic	Male	65	61 *
D_MM_4314	Myeloma, no extramedullary	Diagnostic	Male	65	53
D_MM_5187	Myeloma, no extramedullary	Diagnostic	Male	59	62 *
D_MM_4317	Myeloma, no extramedullary	Diagnostic	Male	65	65
D_MM_40141	Myeloma, no extramedullary	Diagnostic	Male	49	43 *
PD_MM_899	Myeloma, no extramedullary	Progressive disease	Male	72	124
PD_MM_1579	Myeloma, no extramedullary	Progressive disease	Female	68	83
PD_MM_40301	Myeloma, no extramedullary	Progressive disease	Female	70	129 *

* Patient was alive at last follow-up. † D_EMM_1994 and PD_EMM_1994 were collected from the same patient. PD_EMM_1994 sample was collected approximately 1 year after D_EMM_1994.

5.2.2 Label-free mass spectrometry analysis of BMNCs using Thermo Orbitrap Fusion Tribrid mass spectrometer.

Bone marrow mononuclear cells (BMNCs) were isolated and lysed as described previously. Protein quantitation was performed using the Pierce™ 660nm protein assay (Thermo Fisher Scientific). Filter aided sample preparation (FASP) was applied for proteolytic digestion (Wiśniewski *et al.* 2009). 15µg of protein from each sample was digested. Following buffer exchange, overnight trypsin digestion was

carried out using a 1:25 enzyme-to-protein ratio using trypsin gold in 50mM ammonium bicarbonate digestion buffer and 0.05% ProteaseMax. The tryptic digest was acidified at a 1:10 ratio using 2% TFA, 20% ACN. Mass spectrometry analysis was performed using the Thermo UltiMate 3000 nano system directly coupled in-line with the Thermo Orbitrap Fusion Tribrid mass spectrometer. The maximum loading amount, equivalent to ~800ng of protein was loaded onto the system. The mass spectrometry analysis was performed as described previously (Chapter 2).

5.2.3 Data analysis and bioinformatic analysis of mass spectrometry results

Peptide and protein identification was performed using Proteome Discoverer 2.2. Sequest HT (Thermo Fisher Scientific). A recently downloaded UniProtKB-SwissProt Homo Sapiens database (June, 2021) was used as the reference database. Progenesis QI for Proteomics (version 2.0; Nonlinear Dynamics, Waters, Newcastle upon Tyne, UK) was used for quantitative data analysis. Datasets were imported into Progenesis QI software. Protein identifications were deemed to be differentially expressed when specific criteria were met: ANOVA p-value of ≤ 0.05 between experimental groups, fold change ≥ 1.5 between experimental groups, proteins with ≥ 2 unique peptides contributing to the identification, and quantification data in > 60% of samples. Proteins significantly altered in abundance between MM patients with and without extramedullary spread were subject to pathway enrichment and GO enrichment analysis. Proteins significantly increased or decreased in EMM were analysed separately. GOBP and KEGG pathway analysis results were obtained by submitting unique protein IDs to the g:Profiler online bioinformatics tool (https://biit.cs.ut.ee/gprofiler/gost) with term size set to between 5 and 2000 (Raudvere *et al.* 2019). GOBP results were visualized using the EnrichmentMap package in Cytoscape (version 3.10.0) based on a published protocol (Reimand *et al.* 2019). KEGG pathways were visualized using the 'KEGG Mapper—Colour Pathway' tool. For GOMF and GOCC analysis, SRplot (http://www.bioinformatics.com.cn/srplot), an online platform for data analysis and visualization, was used to visualize the results on bubble plots.

5.2.4 Gene expression analysis using the MMRF CoMMpass dataset

The MMRF CoMMpass dataset – accessed through the UCSC Xena browser - was used to analyse RNA-seq data from primary MM patient samples (Settino *et al.* 2020). Specifically, mRNA expression data from the MMRF CoMMpass study was used to determine the association between specific gene expression and MM prognosis. Using the R packages "deseq2", "survival" and "RegParallel", survival curves were illustrated using the Kaplan Meier method. Proteins significantly changed between EMM BMNCs and MM BMNCs were analysed to identify the prognostic relevance of the gene expression of these proteins. Median expression values were used to binarise the genes. Gene expression results with log-rank p-values < 0.05 were considered significantly associated with MM survival.

5.2.5 Evaluation of neutrophil extracellular traps in EMM plasma

EDTA plasma samples collected on the same date as the BMNC samples analysed by mass spectrometry were evaluated for the presence of neutrophil extracellular traps (NETs). The concentrations of three proteins (neutrophil elastase (ELA2), myeloperoxidase (MPO), and calprotectin (S100A8/S100A9)) in blood plasma were measures by ELISA (DuoSet ELISA kits, R&D Systems), as described in Chapter 2. Circulating citrullinated histone 3 was measured using a modified ELISA protocol described in Chapter 2. Circulating nucleosomes were quantified using the commercially available Cell Death Detection ELISA^{PLUS} kit (Roche Diagnostics, Mannheim, Germany), as described in Chapter 2.

5.3 Results

5.3.1 Comparison of clinical information from MM patients with and without extramedullary spread

Clinical data from eight patients with MM and eight patients with EMM was obtained as part of this study. Cytogenetic information from each patient at the sampling date was recorded (**Figure 5.2A**). Overall survival (OS) was statistically significantly decreased in patients with EMM compared to MM patients without extramedullary spread (Log-rank = 3.977, p = 0.046) (**Figure 5.2B**). The median OS

of patients with EMM and those without extramedullary spread was 19 months and 83 months, respectively.

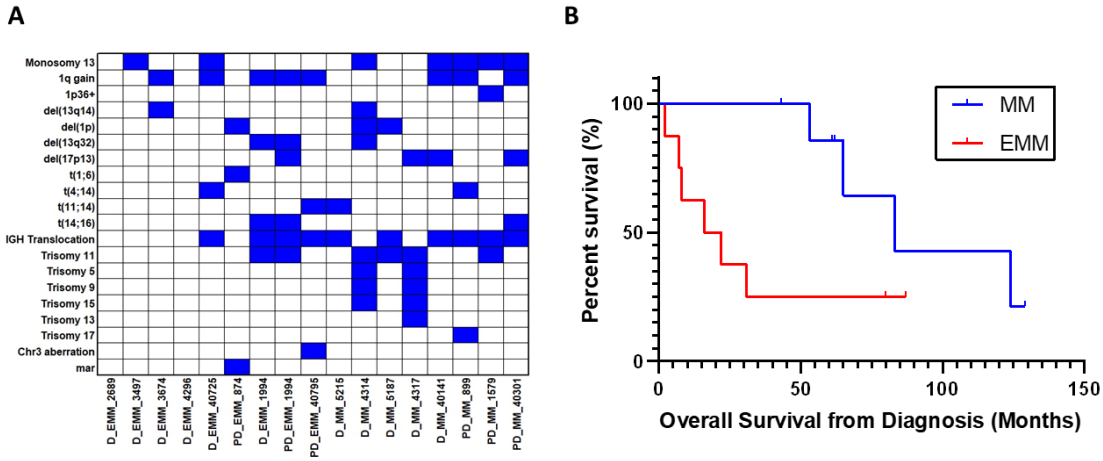

Figure 5.2: Clinical information of the patient cohort. (**A**) Cytogenetics of patient cohort at the time of sampling. (**B**) Survival graph illustrating the difference in overall survival between the EMM group (n=8) and medullary MM group (n=8).

5.3.2 Identification of differentially abundant proteins in the bone marrow of MM patients with and without extramedullary spread

To examine proteomic changes in the bone marrow of MM patients with and without EMM, BMNCs were isolated and proteolytically digested. 9 EMM samples – including one serial sample – and 8 MM without extramedullary spread samples were analysed by LC-MS/MS. A total of 4589 proteins were identified with 225 proteins found to be statistically significantly differentially abundant based on ANOVA p-value < 0.05 and fold change >1.5 (**Figure 5.3A**, **Supp. File 5.1**). Of these, 139 proteins were increased in abundance and 86 proteins were decreased in abundance in EMM BMNCs compared to MM BMNCs (**Table 5.2**, **Table 5.3**). Hierarchical clustering of protein abundance and PCA demonstrated a clear change in the proteomic profile of mononuclear cells from MM patients with extramedullary spread and those without (**Figure 5.3A**, **B**).

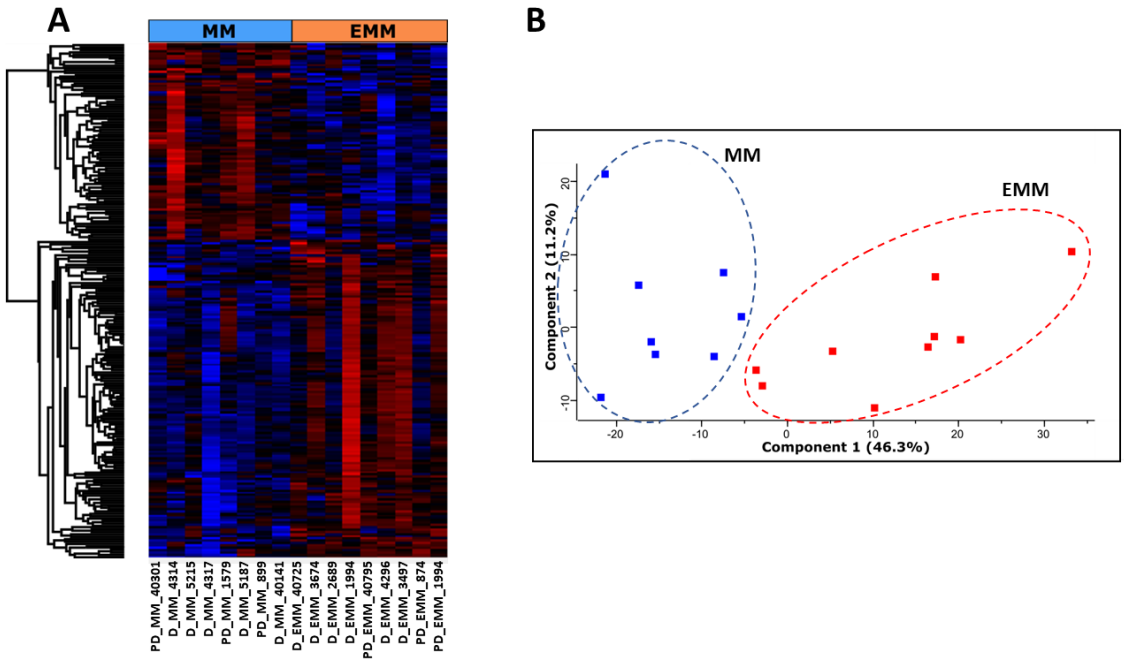

Figure 5.3: Proteomic profile of BMNCs from EMM patients and medullary MM patients. (**A**) Hierarchical clustering analysis of the statistically significant differentially abundant proteins between MM and EMM groups. The colours from blue to red represent the relative protein levels between the two groups. (**B**) Principal component analysis (PCA) illustrating a clear distinction between MM patients with EMM and those without. Each dot represents a patient sample with EMM samples highlighted in red and MM samples highlighted in blue.

Table 5.2: List of 25 proteins most significantly increased in abundance in EMM BMNCs compared to MM BMNCs. Proteins were selected based on the lowest p-values. A comprehensive list of significant proteins is provided in **Supp. File 5.1**.

Uniprot ID	Description	Gene Name	Fold Change	*p*-value
P00918	Carbonic anhydrase 2	CA2	4.42	0.0001
Q8NBJ5	Procollagen galactosyltransferase 1	COLGALT1	1.77	0.0003
P09382	Galectin-1	LGALS1	1.94	0.0005
Q5JRX3	Presequence protease, mitochondrial	PITRM1	3.05	0.0006
P37802	Transgelin-2	TAGLN2	4.65	0.0006
P17301	Integrin alpha-2	ITGA2	34.90	0.0009
Q86WV6	Stimulator of interferon genes protein	TMEM173	3.02	0.0009
Q32MZ4	Leucine-rich repeat flightless-interacting protein 1	LRRFIP1	2.13	0.0009
Q15833	Syntaxin-binding protein 2	STXBP2	2.26	0.0011
P62328	Thymosin beta-4	TMSB4X	8.64	0.0011
P08567	Pleckstrin	PLEK	5.45	0.0015
Q9UGT4	Sushi domain-containing protein 2	SUSD2	53.35	0.0017
O60610	Protein diaphanous homolog 1	DIAPH1	2.21	0.0018
P08758	Annexin A5	ANXA5	7.68	0.0018
P07951	Tropomyosin beta chain	TPM2	3.45	0.0019
Q7LDG7	RAS guanyl-releasing protein 2	RASGRP2	3.54	0.0019
Q14019	Coactosin-like protein	COTL1	2.38	0.0020
P18054	Polyunsaturated fatty acid lipoxygenase ALOX12	ALOX12	26.46	0.0020
Q9NYL9	Tropomodulin-3	TMOD3	2.90	0.0020
P63000	Ras-related C3 botulinum toxin substrate 1	RAC1	2.73	0.0025
P37840	Alpha-synuclein	SNCA	18.57	0.0025
Q9HBI1	Beta-parvin	PARVB	12.09	0.0026
P18206	Vinculin	VCL	5.78	0.0028
Q15942	Zyxin	ZYX	4.93	0.0029
P06753	Tropomyosin alpha-3 chain	TPM3	2.07	0.0030

Table 5.3: List of 25 proteins most significantly decreased in abundance in EMM BMNCs compared to MM BMNCs. Proteins were selected based on the lowest p-values. A comprehensive list of significant proteins is provided in **Supp. File 5.1**.

Uniprot ID	Description	Gene Name	Fold Change	*p*-value
P22087	rRNA 2′-O-methyltransferase fibrillarin	FBL	1.65	0.0003
P16402	Histone H1.3	HIST1H1D	2.89	0.0007
Q8NBS9	Thioredoxin domain-containing protein 5	TXNDC5	4.33	0.0008
Q99798	Aconitate hydratase, mitochondrial	ACO2	1.61	0.0012
Q9NSE4	Isoleucine--tRNA ligase, mitochondrial	IARS2	2.22	0.0014
Q9Y320	Thioredoxin-related transmembrane protein 2	TMX2	5.92	0.0014
Q13263	Transcription intermediary factor 1-beta	TRIM28	2.19	0.0015
P30837	Aldehyde dehydrogenase X, mitochondrial	ALDH1B1	8.19	0.0015
Q9BY50	Signal peptidase complex catalytic subunit SEC11C	SEC11C	5.19	0.0016
Q13813	Spectrin alpha chain, non-erythrocytic 1	SPTAN1	2.10	0.0023
Q3SY69	Mitochondrial 10-formyltetrahydrofolate dehydrogenase	ALDH1L2	7.33	0.0033
P08240	Signal recognition particle receptor subunit alpha	SRPR	2.48	0.0035
P30044	Peroxiredoxin-5, mitochondrial	PRDX5	1.77	0.0037
Q7KZF4	Staphylococcal nuclease domain-containing protein 1	SND1	2.91	0.0042
P49257	Protein ERGIC-53	LMAN1	2.44	0.0043
Q9Y4P3	Transducin beta-like protein 2	TBL2	4.53	0.0045
P09874	Poly [ADP-ribose] polymerase 1	PARP1	2.67	0.0047
Q01105	Protein SET	SET	3.29	0.0054
Q92506	Estradiol 17-beta-dehydrogenase 8	HSD17B8	3.37	0.0054
P12235	ADP/ATP translocase 1	SLC25A4	4.43	0.0055
Q13310	Polyadenylate-binding protein 4	PABPC4	4.47	0.0056
P53992	Protein transport protein Sec24C	SEC24C	38.68	0.0057
Q16706	Alpha-mannosidase 2	MAN2A1	6.43	0.0058
Q01082	Spectrin beta chain, non-erythrocytic 1	SPTBN1	1.96	0.0060
P54886	Delta-1-pyrroline-5-carboxylate synthase	ALDH18A1	10.26	0.0072

5.3.3 Evaluating the association of significantly increased proteins in EMM BMNCs with MM prognosis using MMRF CoMMpass study data

MM patients with extramedullary lesions have a poor prognosis compared to those without extramedullary spread. We, therefore, hypothesized that the expression of proteins significantly increased in abundance in EMM BMNCs may be linked to MM prognosis. To examine this, we performed a Kaplan–Meier gene expression analysis on the 25 proteins most significantly increased in abundance in EMM BMNCs using RNAseq data from the MMRF CoMMpass dataset. Expression data was binarized into “high expression” and “low expression” for each gene based on the median value. Increased expression of seven genes was associated with a significantly worse prognosis in MM (**Figure 5.4**). These included genes associated with focal adhesion and actin regulation, transgelin 2 (TAGLN2), integrin alpha 2 (ITGA2), the tropomyosin beta chain (TPM2) and the tropomyosin alpha-3 chain (TPM3), in addition to carbonic anhydrase 2 (CA2), galectin-1 (LGALS1) and tropomodulin-3 (TMOD3). To evaluate the association between the abundance of these proteins and prognosis in our cohort, we divided the samples into high and low abundance groups for each of the seven biomarkers based on the median intensity value. Survival analysis revealed a trend towards decreased overall survival in those with high expression of six (TAGLN2, CA2, ITGA2, LGALS1, TPM2, TMOD3) out of the seven proteins analysed. The high expression of TMOD3 was significantly associated with a poorer overall survival compared to those with a low expression of TMOD3 (**Figure 5.5**). Thus, the increased abundance of these proteins is associated with the aggressive EMM phenotype, as well as poorer overall survival in MM.

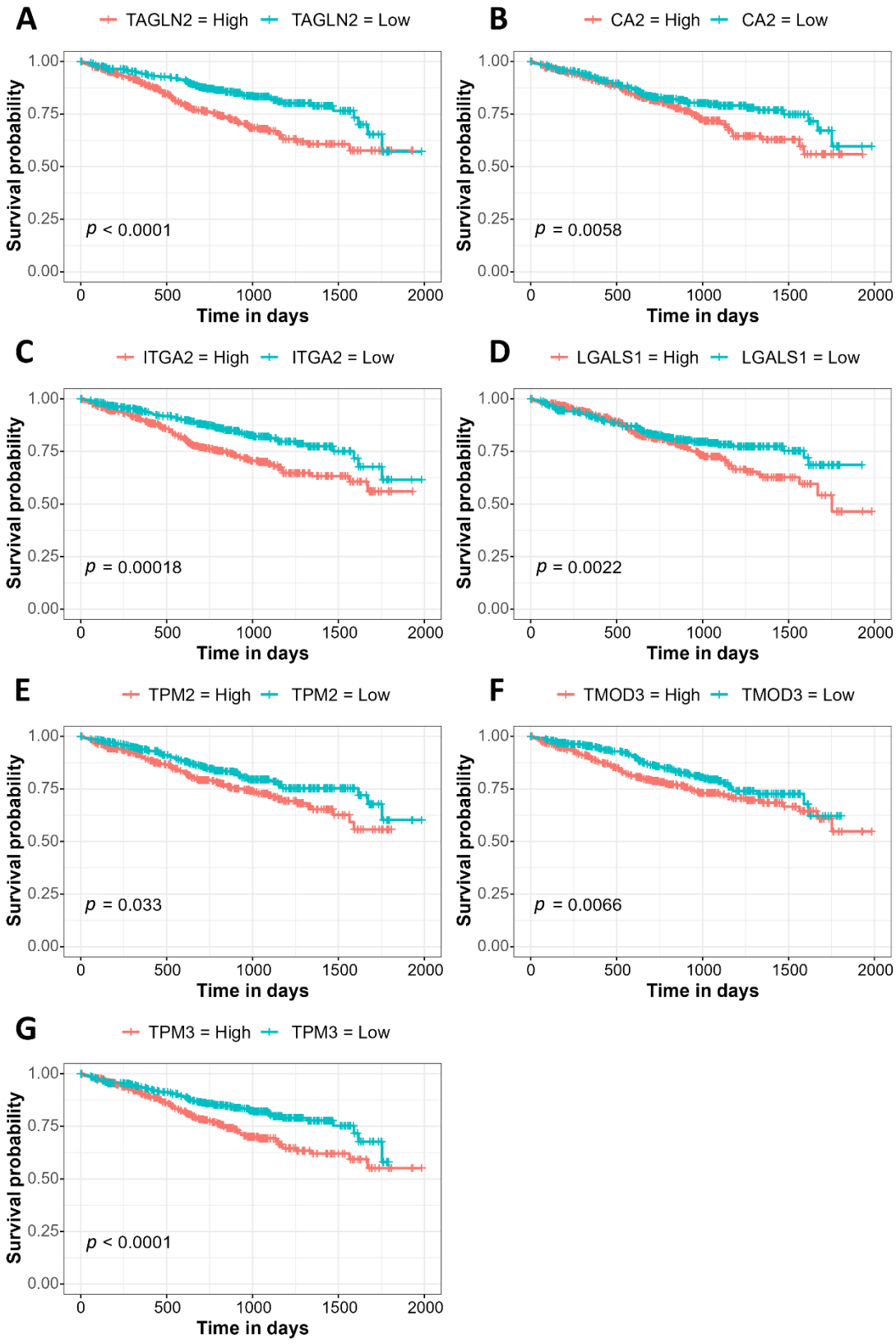

Figure 5.4: Kaplan–Meier curves illustrating genes whose expression (high/low) is significantly associated with survival in MM using the MMRF CoMMpass RNASeq dataset. (**A**) TAGLN2, (**B**) CA2, (**C**) ITGA2, (**D**) LGALS1, (**E**) TPM2, (**F**) TMOD3, (**G**) TPM3.

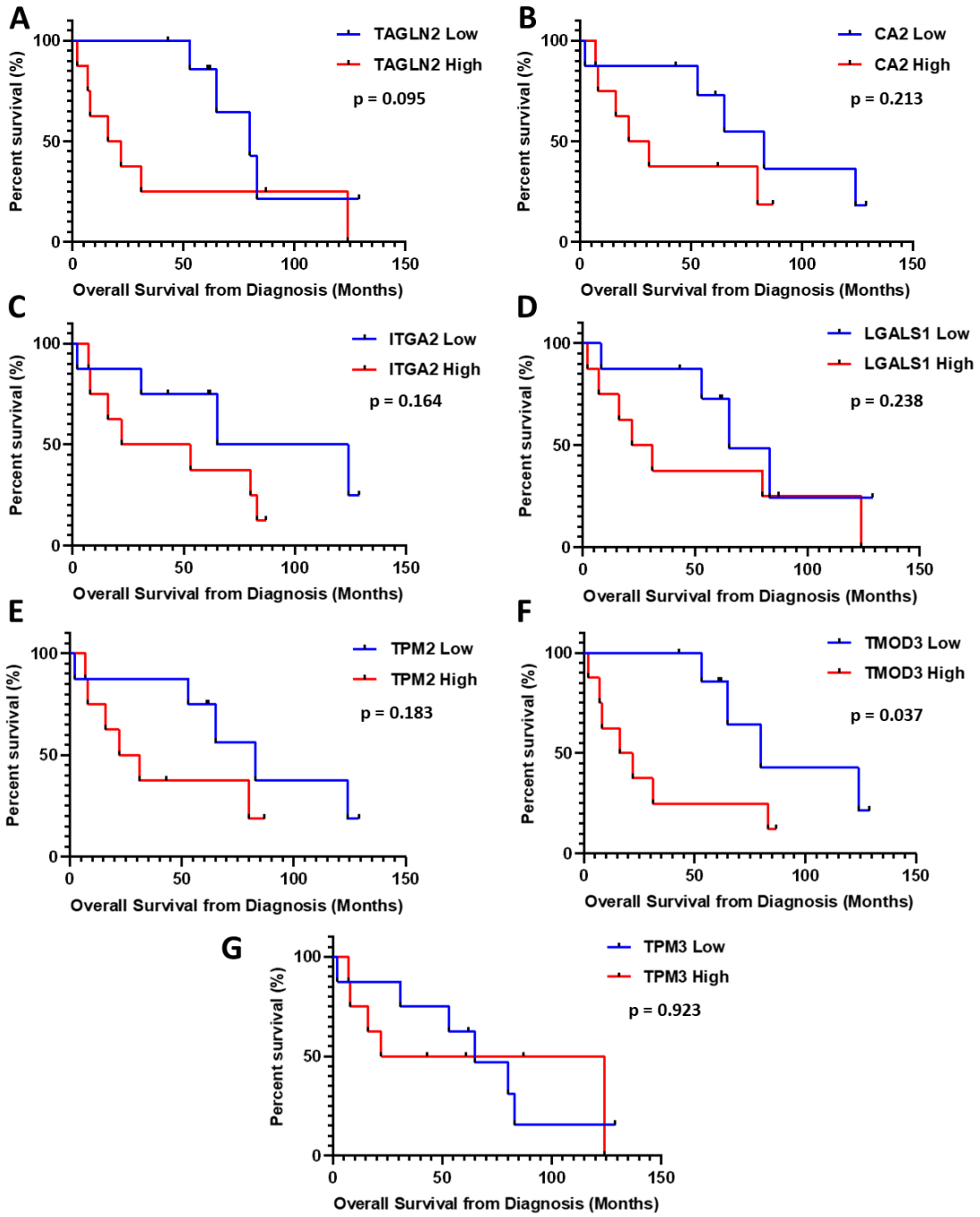

Figure 5.5: Survival graphs illustrating the difference in OS between patients with high expression and low expression of the seven proteins identified as potential prognostic biomarkers in the CoMMpass dataset. Samples were divided based on median expression levels. (**A**) TAGLN2 (**B**) CA2 (**C**) ITGA2 (**D**) LGALS1 (**E**) TPM2 (**F**) TMOD3 (**G**) TPM3.

5.3.4 Bioinformatics of differential proteins in EMM bone marrow mononuclear cells versus MM bone marrow mononuclear cells

To identify biological processes or pathways associated with the EMM phenotype in the bone marrow, proteins found to be increased or decreased in abundance in EMM were characterized based on GO enrichment and KEGG pathway enrichment using g:profiler. Enrichment analysis of the 139 proteins increased in abundance in EMM mononuclear cells based on gene ontology annotations for biological processes was performed. The resulting significant ($p < 0.05$) GO terms were imported to Cytoscape and visualized using the EnrichmentMap application. As the enrichment map clusters similar GO terms, the AutoAnnotate Cytoscape application was used to summarize each cluster based on the word frequency within the GO terms (Reimand *et al.* 2019). The summarized terms highlight the association of proteins increased in abundance in the EMM bone marrow with adhesion and migratory biological processes including "actin filament polymerization", "assembly substrate junction", "cell junction organization", and "integrin mediated signalling" (**Figure 5.6**). Enrichment analysis was also performed on the 86 proteins decreased in abundance in EMM mononuclear cells based on gene ontology annotations for biological processes, followed by visualization of significant ($p < 0.05$) GO terms using the EnrichmentMap application. The key biological processes linked to proteins decreased in abundance EMM bone marrow (blue nodes) were associated with metabolic process, namely "tricarboxylic acid cycle" and "oxoacid metabolic process" (**Figure 5.6**). Similar to the biological process analysis, proteins increased in abundance in EMM BMNCs are enriched in molecular functions associated with adhesion and motility including cadherin binding, integrin binding, and extracellular matrix binding (**Figure 5.7A**). Proteins significantly increased in MM BMNCs compared to EMM BMNCs are enhanced in small nucleolar RNA (snoRNA) binding and oxidoreductase activity, in relation to molecular functions (**Figure 5.7B**). In addition, in terms of the cellular component, many proteins increased in abundance in EMM BMNCs are derived from the cell-cell junction, cell-substrate junction, and focal adhesions (**Figure 5.8A**). In contrast, proteins decreased in abundance in EMM BMNCs are largely derived from secretory vesicles and the mitochondrial matrix (**Figure 5.8B**).

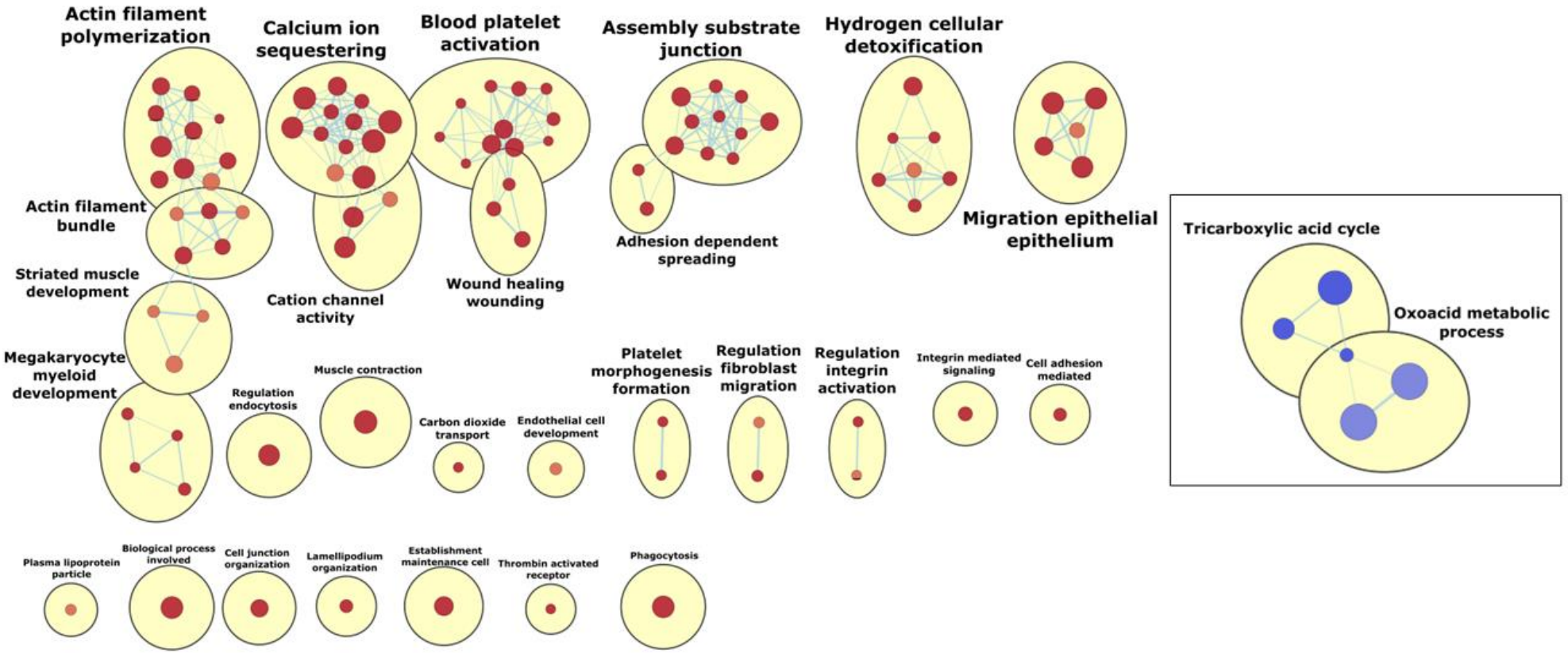

Figure 5.6: Enrichment map of proteins increased (red) and decreased (blue) in abundance in EMM highlights the functional clusters associated with EMM. Nodes represent GO biological process terms (Q-value < 0.01 (red) Q-value < 0.05 (blue)) and lines illustrate the connectivity between nodes. Clusters of similar GO terms are circled and named based on a summary of the nodes present in the cluster. Red nodes represent enriched GO biological process terms for the proteins increased in abundance in EMM BMNCs. Blue nodes represent enriched GO biological process terms for the proteins decreased in abundance in EMM BMNCs. Darker red or blue node colouring indicate lower q-values.

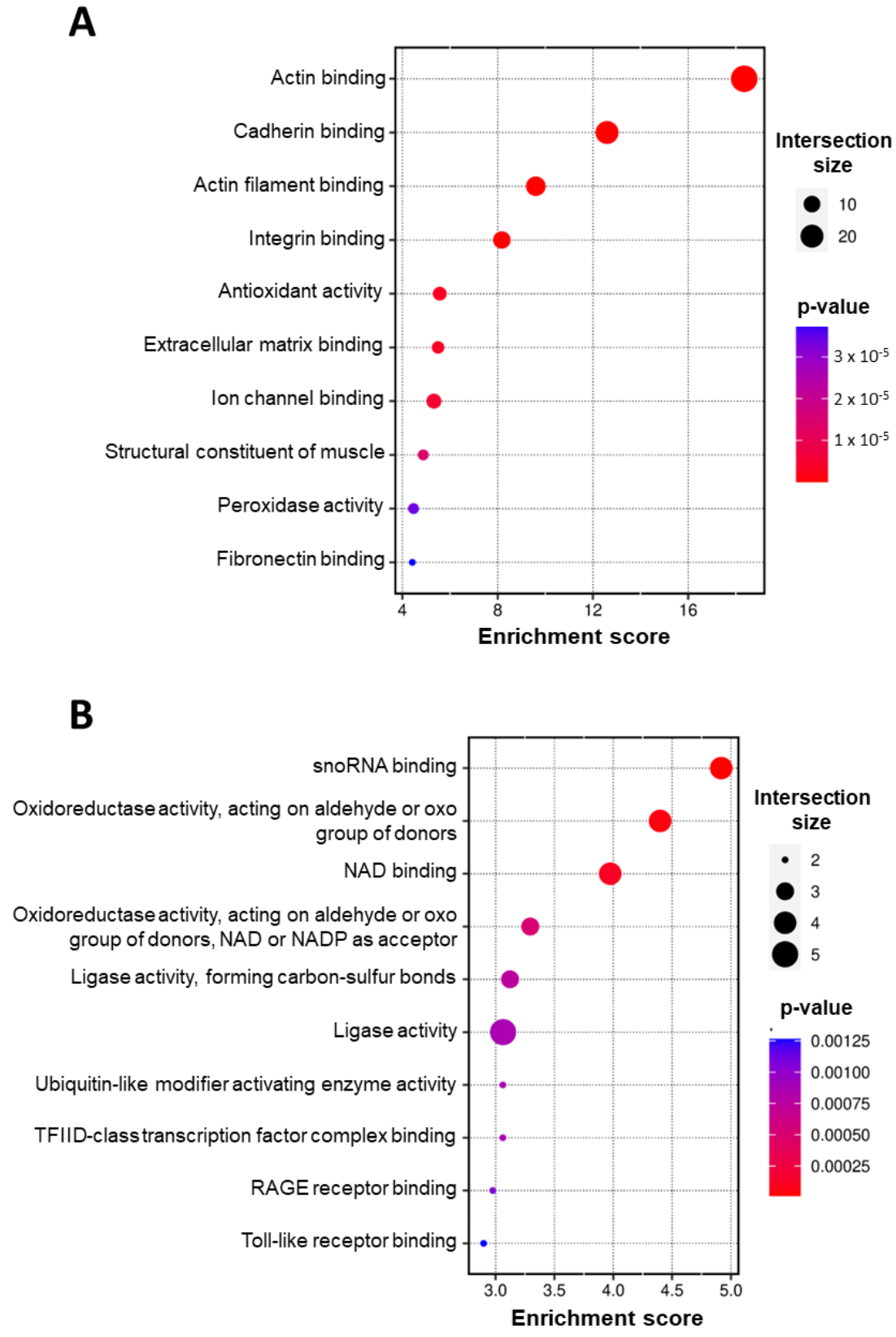

Figure 5.7: Bubble maps for GOMF analyses of differentially abundant proteins. (**A**) GOMF analysis on proteins increased in abundance in EMM BMNCs. (**B**) GOMF analysis on proteins decreased in abundance in EMM BMNCs.

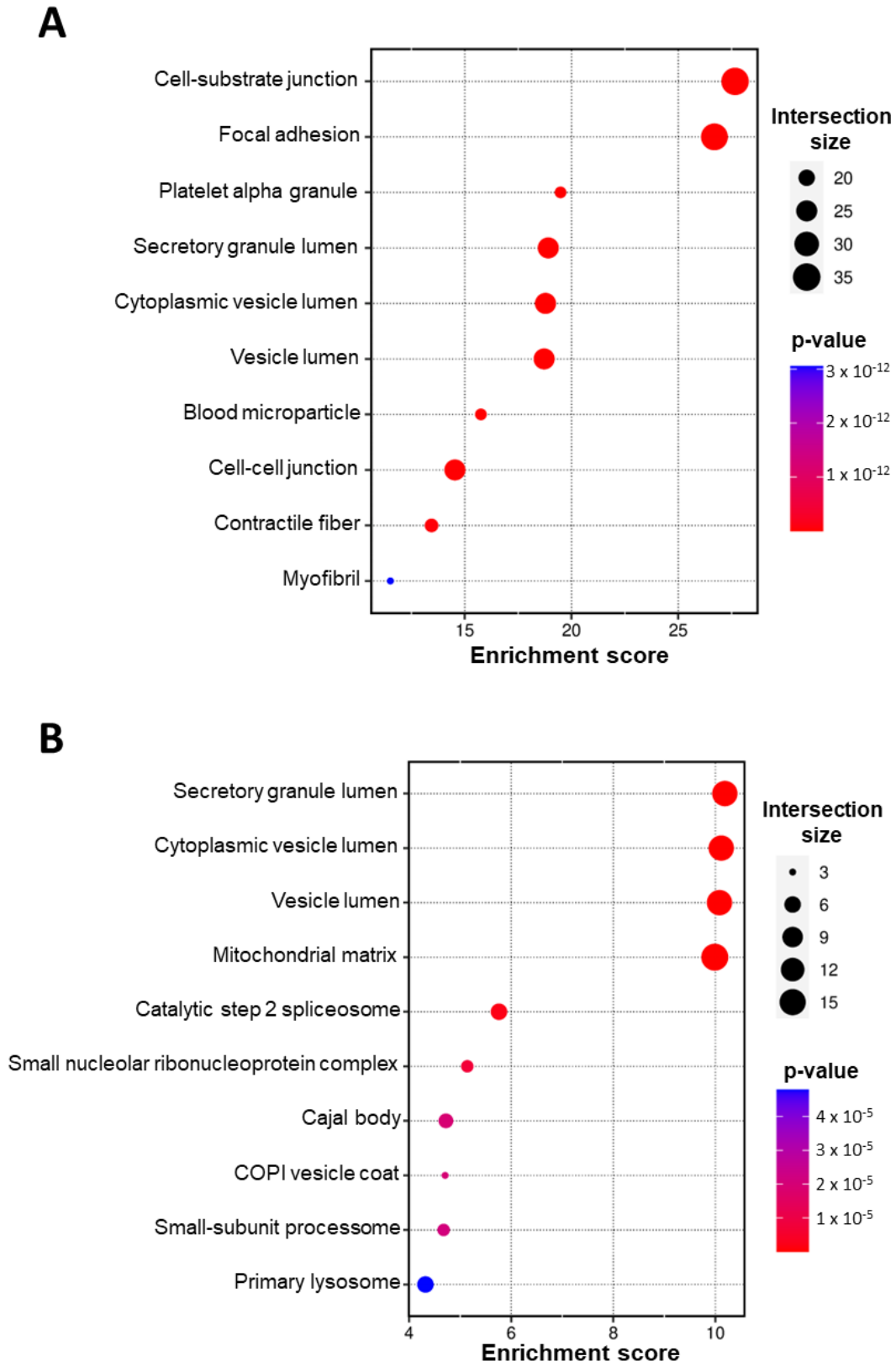

Figure 5.8: Bubble maps for GOCC analyses of differentially abundant proteins. (**A**) GOCC analysis on proteins increased in abundance in EMM BMNCs. (**B**) GOCC analysis on proteins decreased in abundance in MM BMNCs.

KEGG pathway enrichment analysis (adjusted p-value < 0.05) of 139 proteins increased in abundance in EMM identified 21 statistically significant pathways, whereas KEGG pathway enrichment analysis of the 86 proteins decreased in abundance in EMM identified 5 statistically significant pathways (**Table 5.4, Table 5.5)**. As seen in the gene ontology analysis, proteins increased in abundance in EMM mononuclear cells were associated with various migratory pathways, including focal adhesion, tight junction, Rap1 signalling pathway and leukocyte endothelial migration, whereas proteins decreased in abundance in EMM BMNCs were associated with metabolic pathways, including the tricarboxylic acid (TCA) cycle. As depicted in the KEGG map, eight proteins involved in leukocyte transendothelial migration were increased in abundance in EMM (PECAM1, ITGB1, ACTB, ACTN1, VASP, VCL, RAP1B, RAC1, ROCK2) and may indicate a potential mechanism by which specific MM clones exit the bone marrow niche during extramedullary transition (

Figure 5.**9**). Additional significantly enriched pathways linked to cancer cell migration, including the Rap1 signalling pathway, focal adhesion pathway, and neutrophil extracellular trap formation pathway are depicted in KEGG maps (**Figure 5.10**, **Figure 5.11**, **Figure 5.12**). The clear change in the functional clusters associated with EMM and MM highlights the phenotypic changes that occur within the bone marrow in EMM. GO and pathway enrichment analysis suggest an increase in proteins associated with adhesion and migration and a decrease in proteins associated with certain metabolic pathways including the TCA in the bone marrow of EMM patients.

Table 5.4: KEGG enrichment analysis of proteins significantly increased in abundance in EMM BMNCs. Table highlights the number of differentially abundant proteins identified in this study that are associated with each KEGG pathway, alongside an adjusted p-value.

KEGG Pathway	Number of genes in pathway	Number of differentially abundant proteins	Adjusted p-value
Platelet activation	124	18	2.76×10^{13}
Focal adhesion	202	19	1.40×10^{10}
Regulation of actin cytoskeleton	227	18	1.03×10^{8}
Rap1 signaling pathway	210	15	1.78×10^{6}
Hypertrophic cardiomyopathy	90	10	7.78×10^{6}
Dilated cardiomyopathy	95	10	1.31×10^{5}
ECM-receptor interaction	88	9	7.26×10^{5}
Tight junction	169	11	0.00039
Leukocyte transendothelial migration	114	9	0.00064
Phagosome	147	10	0.00074
Pathogenic Escherichia coli infection	196	11	0.0016
Malaria	49	6	0.0019
Proteoglycans in cancer	205	11	0.0025
Shigellosis	246	12	0.0027
Bacterial invasion of epithelial cells	77	7	0.0028
Hematopoietic cell lineage	95	7	0.011
Adherens junction	71	6	0.016
Fluid shear stress and atherosclerosis	138	8	0.019
Arrhythmogenic right ventricular cardiomyopathy	77	6	0.025
Cholesterol metabolism	51	5	0.028
Neutrophil extracellular trap formation	187	9	0.031

Table 5.5: KEGG enrichment analysis of proteins significantly decreased in abundance in EMM BMNCs. Table highlights the number of differentially abundant proteins identified in this study that are associated with each KEGG pathway, alongside an adjusted p-value.

KEGG Pathway	Number of genes in pathway	Number of differentially abundant proteins	Adjusted p-value
Citrate cycle (TCA cycle)	30	6	7.001×10^{6}
Protein processing in endoplasmic reticulum	168	10	4.28×10^{5}
Carbon metabolism	115	8	0.0002
Biosynthesis of amino acids	74	5	0.021
2-Oxocarboxylic acid metabolism	19	3	0.032

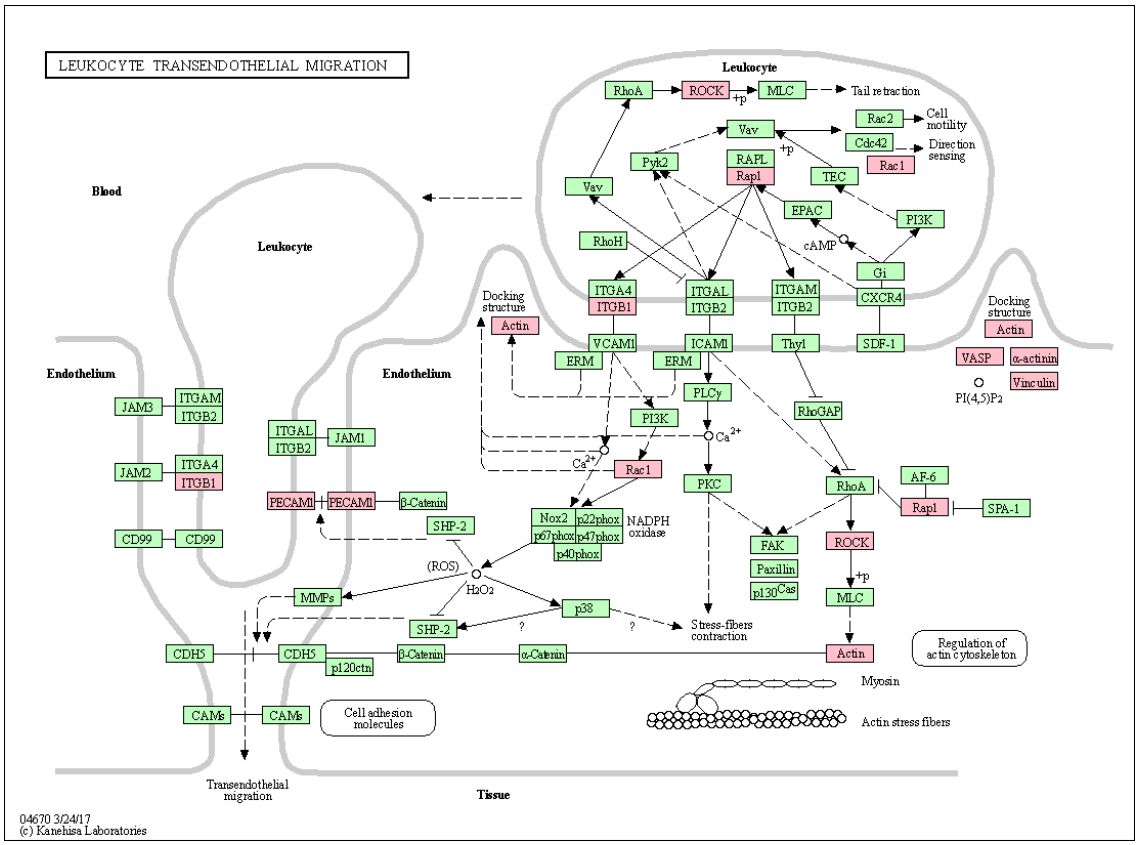

Figure 5.9: KEGG map highlighting proteins associated with leukocyte transendothelial migration. A number of proteins significantly increased in abundance in EMM BMNCs (red) are involved in the leukocyte transendothelial migration pathway.

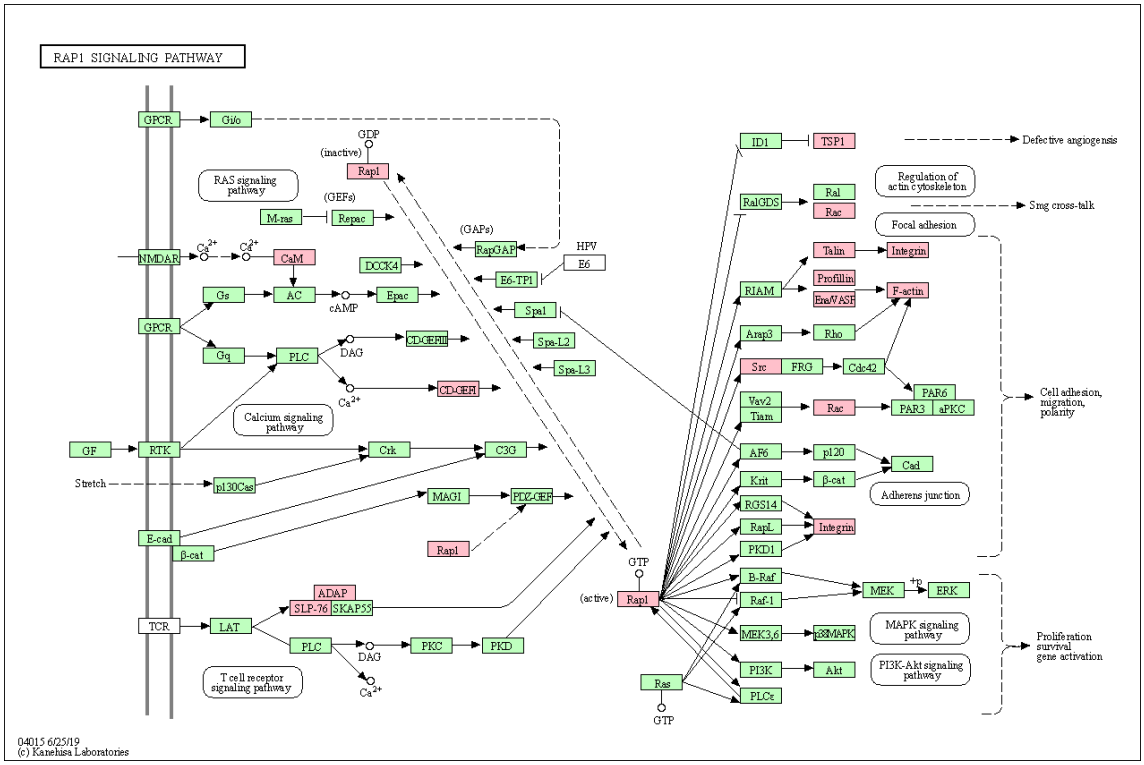

Figure 5.10: KEGG map highlighting proteins associated with the RAP1 signalling pathway. A number of proteins significantly increased in abundance in EMM BMNCs (red) are involved in the RAP1 signalling pathway.

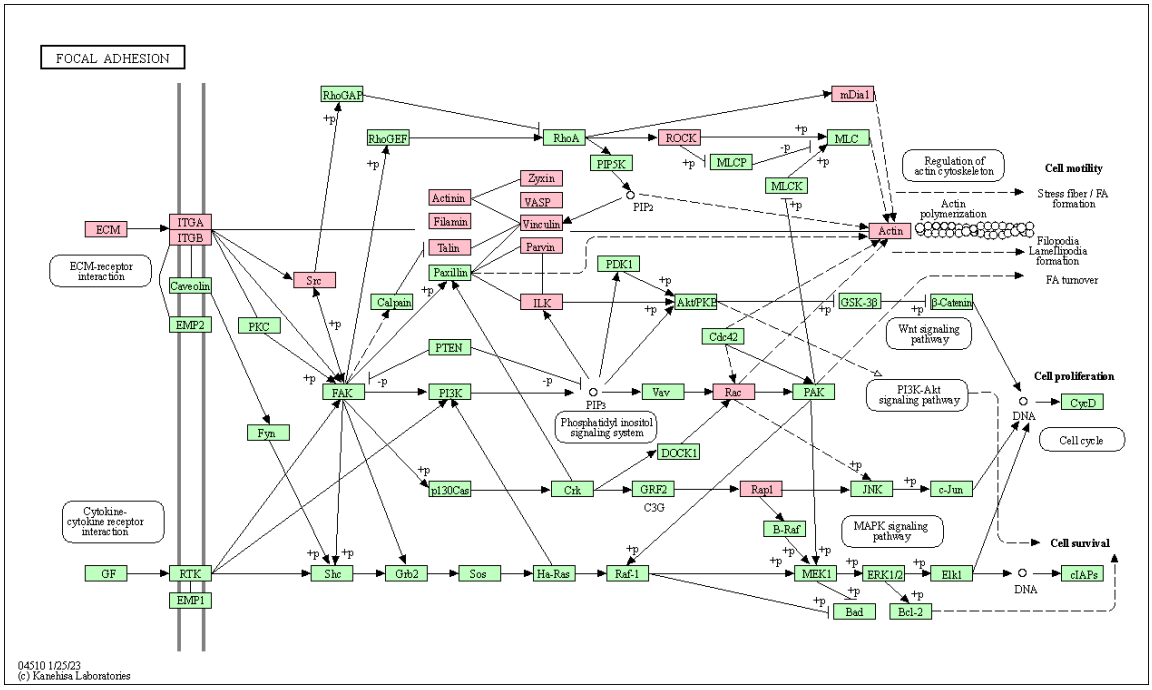

Figure 5.11: KEGG map highlighting proteins associated with the focal adhesion pathway. A number of proteins significantly increased in abundance in EMM BMNCs (red) are involved in focal adhesions.

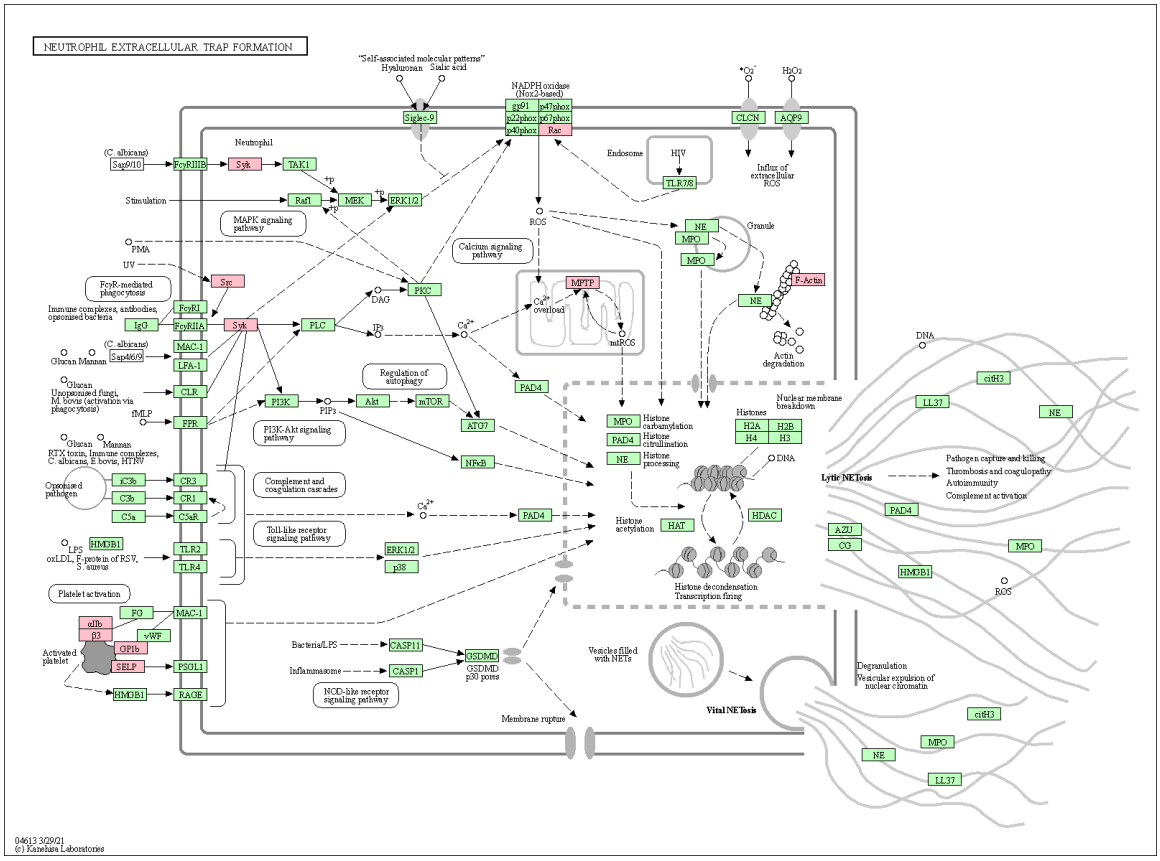

Figure 5.12: KEGG map highlighting proteins associated with neutrophil extracellular trap formation. A number of proteins significantly increased in abundance in EMM BMNCs (red) are associated with neutrophil extracellular traps.

5.3.5 Evaluating the heparanase/CD138 axis in EMM patients

The results of our mass spectrometry analysis identified a significant increase in heparanase (HPSE) levels in the bone marrow of EMM patients (**Figure 5.13A**). A recent study found that HPSE promotes an invasive phenotype in MM through the cleavage of CD138 from the surface of MM cells. Shed CD138 subsequently binds to vascular endothelial cell growth factor receptor-2 (VEGFR2) and VLA-4 which triggers the polarised migration of MM cells (Jung *et al.* 2016). Interestingly, CD138 levels were decreased in abundance in the bone marrow of EMM patients (**Figure 5.13B**). Due to the potential shedding of CD138 by HPSE in the EMM bone marrow, we hypothesized that plasma levels of shed CD138 may be increased. Indeed, the evaluation of CD138 levels in plasma showed a trend towards increased abundance in EMM plasma, highlighting a potential role of HPSE-induced CD138 shedding in the development of EMM (**Figure 5.13C,D**).

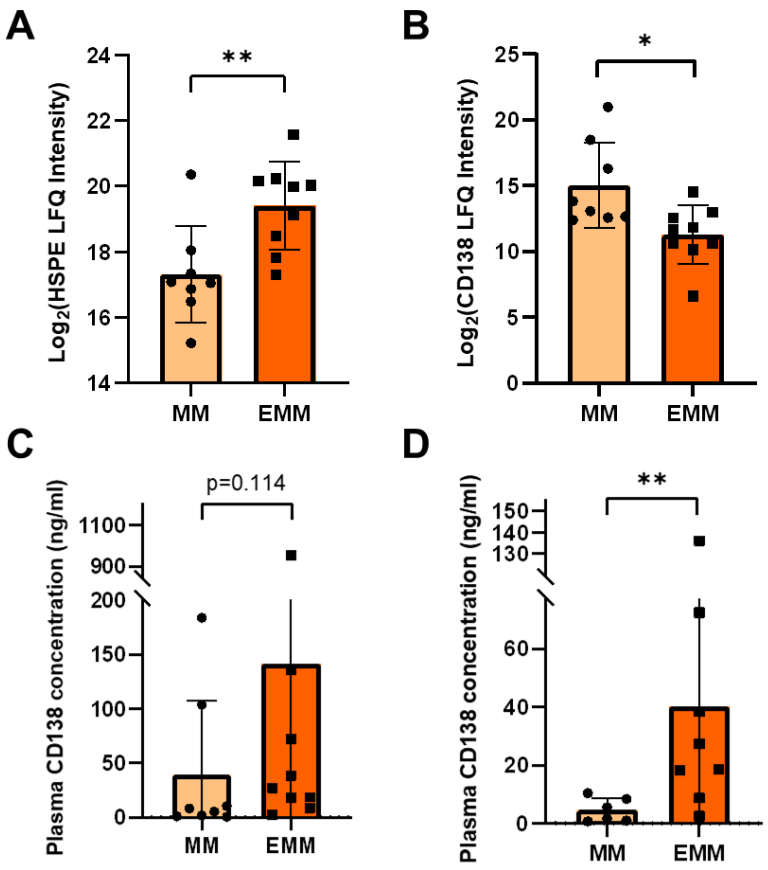

Figure 5.13: Alterations in heparanase, CD138, and circulating CD138 levels in bone marrow and plasma of EMM and MM patients. (**A**) Heparanase was significantly increased in abundance in EMM BMNCs, while (**B**) CD138 levels were significantly decreased in EMM BMNCs compared to MM BMNCs**.** (**C**) Circulating CD138 levels (no outlier removal) were increased in EMM plasma, although this did not reach significance. (**D**) CD138 levels with outlier removal (ROUT method, Q=1%) were significantly increased in EMM plasma compared to MM plasma.

5.3.6 Evaluation of "neutrophil extracellular trap formation" in EMM plasma.

The list of proteins statistically significantly increased in abundance in EMM BMNCs was enriched in proteins associated with neutrophil extracellular trap formation according to KEGG pathway analysis. Recent studies have highlighted the role of neutrophil extracellular traps (NETs) in promoting cancer metastasis (Kaltenmeier *et al.* 2021; Yang and Liu 2021). Blood and plasma-based markers of NETs are commonly quantified to evaluate NET formation in various diseases (Oklu *et al.* 2017; Thålin *et al.* 2017; Matta *et al.* 2022; Fedorov *et al.* 2023). As biofluid-derived biomarkers are more clinically useful, we evaluated NET formation in corresponding plasma samples collected on the same date as the BMNCs. To assess NET formation in EMM, markers of neutrophil formation including neutrophil

elastase (ELA2), myeloperoxidase (MPO), calprotectin (S100A8/A9 heterodimer), citrullinated histone H3 bound to cell-free DNA and circulating nucleosomes, were evaluated in EMM patient plasma compared to MM patient plasma. Plasma levels of ELA2 were significantly increased in EMM patient plasma compared to MM patient plasma, whereas MPO and calprotectin plasma levels showed a trend towards increased concentrations in EMM patient plasma, although this did not reach significance (p = 0.175 and p = 0.139, respectively) (**Figure 5.14**).

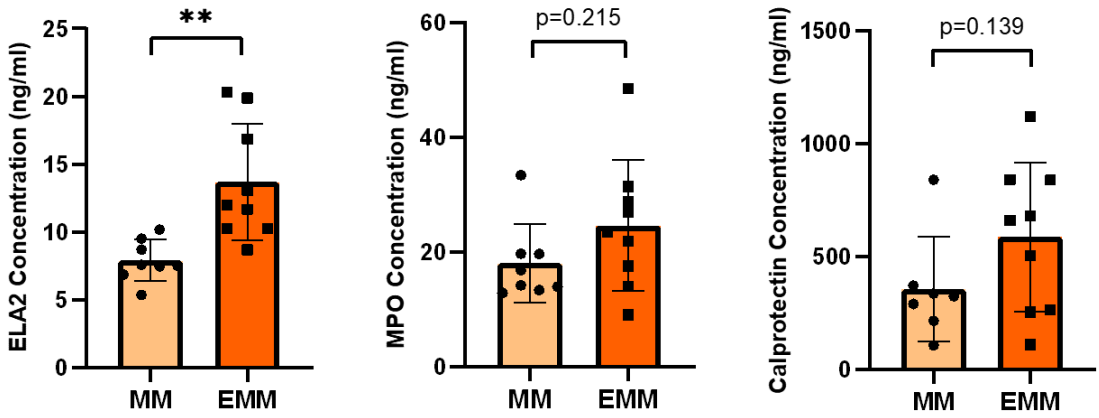

Figure 5.14: Plasma concentrations of neutrophil elastase (ELA2), myeloperoxidase (MPO), and calprotectin in MM patient plasma compared to EMM patient plasma using ELISA. Normality was determined using the D'Agostino and Pearson test. For non-normal distributions, values were log-transformed. Statistical significance was evaluated by unpaired students t-test. '**' represents p-value < 0.01.

Neutrophil extracellular traps are composed of decondensed chromatin decorated with proteins including histones, ELA2, and MPO. Citrullination of histone H3 by peptidyl arginine deaminase 4 (PAD4) occurs during the production of NETs – known as NETosis. Thus, citrullinated histone H3 bound to cell-free DNA (CitH3) is considered a hallmark of NETs. Cell-free nucleosomes have also been reported as a surrogate marker of NETs, however, it is important to note that levels of cell-free nucleosomes may also partially reflect other cell death mechanisms such as necrosis (Ebrahimi *et al.* 2018). Neither CitH3 nor circulating nucleosomes were significantly increased in EMM plasma, although CitH3 demonstrated a slight trend towards increased concentrations in EMM plasma (**Figure 5.15)**

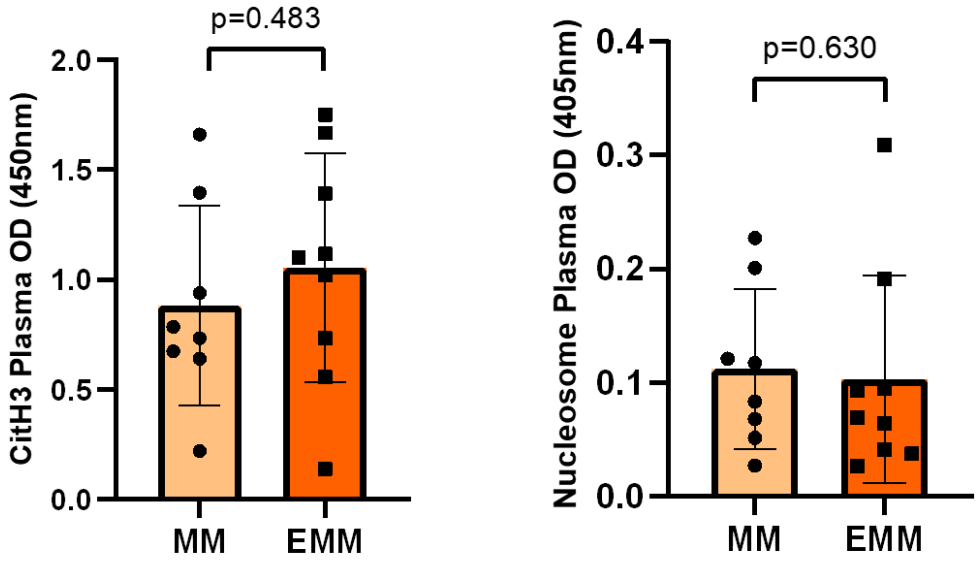

Figure 5.15: Plasma levels of citrullinated histone H3 and nucleosomes in MM patient plasma compared to EMM patient plasma. Normality was determined using the D'Agostino and Pearson test. For non-normal distributions, values were log-transformed. Statistical significance was evaluated by unpaired students t-test. OD, optical density.

5.4 Discussion

The molecular mechanisms driving EMM development remain unclear. Few studies have been conducted to elucidate the molecular pathogenesis of EMM, more than likely due to rarity of this MM manifestation. Case studies are often published which provide valuable information on the clinical course of patients with EMM but provide little information on the biological processes contributing to EMM pathogenesis. Recent genomic and transcriptomic analyses have provided some valuable insights into EMM; however, a quantitative proteomics analysis using mass spectrometry had not yet been applied for the study of EMM (Ryu *et al.* 2020; Kriegova *et al.* 2021). Examining changes at the protein level provides a comprehensive insight into the molecular events underlying disease pathogenesis. We used a label-free mass spectrometry approach to effectively quantify the proteomic differences in the bone marrow of MM patients with and without extramedullary involvement. In this work, we identified 225 statistically significantly differentially abundant proteins in BMNCs from EMM and MM patients. Bioinformatic analysis revealed biological processes and pathways significantly enriched in BMNCs from EMM patients compared to MM patients.

Furthermore, using the MMRF CoMMpass dataset, proteins linked to EMM and a poor overall survival in MM were identified.

Studies have implicated genetic factors, changes in the bone marrow microenvironment, the differential expression of adhesion molecules, and immune evasion in the pathogenesis of EMM (Ryu *et al.* 2020; Kriegova *et al.* 2021; Bou Zerdan *et al.* 2022; Gregorova *et al.* 2022). In this work, cell adhesion associated pathways were enriched in EMM BMNCs, while metabolism and protein processing associated pathways were enriched in MM BMNCs. The increased abundance of proteins linked to motility-associated pathways including the focal adhesion pathway, Rap1 signalling pathway, integrin-mediated signalling, and leukocyte transendothelial migration, suggests the presence of clones with a higher migratory capacity than in the bone marrow mononuclear fraction of MM patients without extramedullary involvement. Eight proteins involved in leukocyte transendothelial migration were increased in abundance in EMM (PECAM1, ITGB1, ACTB, ACTN1, VASP, VCL, RAP1B, RAC1, ROCK2) and may indicate a potential mechanism by which specific MM clones exit the bone marrow niche during extramedullary transition. Further research should be performed to evaluate the presence of these potentially pro-migratory MM sub-clones in the bone marrow. The dynamic regulation of adhesion proteins during the intravasation of MM cells from the bone marrow has not yet been fully elucidated, however, the increased presence of these motility-associated proteins in the bone marrow of EMM patients indicates their potential involvement in the intravasation of myeloma cells into the bloodstream. One study reported that the loss of VLA4 (integrin α4 and integrin β1) increases extramedullary disease burden, whereas a recent transcriptomic analysis found that integrin α4 and integrin β1 are co-expressed on EMM cells, highlighting the uncertainty surrounding the role of adhesion proteins in myeloma cell migration (Ryu *et al.* 2020; Hathi *et al.* 2022). Although ITGA4 was not detected in our analysis, ITGB1 was significantly increased in EMM BMNCs. PECAM1 (CD31) was also found to be significantly increased in abundance in EMM BMNCs, which corroborates with a previous study whereby PECAM1 was expressed at higher levels in extramedullary plasmacytomas compared to primary MM cells (Hedvat *et al.* 2003).

Focal adhesions (FAs) are dynamic protein structures that act as molecular bridges by connecting the cytoskeleton of a cell with the extracellular matrix. The association between FAs and cell migration is well-known, however, the complete mechanism by which FAs influence migration is not fully understood (Nagano *et al.* 2012; De Pascalis and Etienne-Manneville 2017). Gene expression of focal adhesion kinase (FAK), a nonreceptor tyrosine kinase that plays a central role in FA signalling, was previously found to be significantly increased in bone marrow-derived myeloma cells from patients with EMM compared to MM patients without extramedullary spread (Wang *et al.* 2012). KEGG enrichment analysis revealed an increase in proteins associated with FAs in EMM BMNCs. One important FA protein is integrin linked kinase (ILK), a multifunctional serine/threonine kinase with reported kinase-dependent and kinase-independent roles (Hannigan *et al.* 2011; Górska and Mazur 2022). In cancer, ILK has been found to contribute to cell proliferation, survival, migration, and angiogenesis (Attwell *et al.* 2000; Tan *et al.* 2004; Rhee *et al.* 2013; Qu *et al.* 2017). ILK can interact with LIM and senescent cell antigen-like-containing domain protein 1 (LIMS1/PINCH1) and Parvins, such as β-Parvin, to form the ILK-PINCH-Parvin (IPP) complex (Zhang *et al.* 2002; Górska and Mazur 2022). ILK and the IPP complex have been reported to contribute to metastasis by promoting a variety of cellular processes, including epithelial mesenchymal transition (EMT) and cell motility (Greco *et al.* 2021; Kilinc *et al.* 2021; McDonald and Dedhar 2022).

All three components of the IPP complex and another binding partner of PINCH1, Ras suppressor protein 1 (RSU1), were significantly increased in EMM BMNCs (**Supp.File 5.1**). A recent study reported that ILK promotes lung adenocarcinoma progression and metastasis through the regulation of KRAS, the IPP complex and RSU1. Interestingly, all components of the IPP complex and RSU1 were increased in KRAS-mutant compared to non-KRAS-mutant lung adenocarcinomas (Nikou *et al.* 2020). Although RSU1 was initially identified as a suppressor of Ras-dependent oncogenic transformation, current literature indicates a role of RSU1 in linking RAS activation with the IPP complex and cell migration (Cutler *et al.* 1992; Dougherty *et al.* 2008; Barbazán *et al.* 2012). Several studies have hypothesized that there is a link between RAS mutations and EMM development (Rasmussen *et al.* 2005; de Haart *et al.* 2016). This potential link between RAS activation and the IPP complex may

explain the mechanism by which RAS-mutated myeloma cells stimulate migration, however, further studies are required to elucidate the role of the IPP complex, RSU1, and RAS in extramedullary myeloma. Research focused on the role of ILK in MM is somewhat limited, potentially because ILK is considered dispensable for myeloma cell survival. A study investigating the silencing of ILK in MM cell lines and primary samples, found no effects on the viability of MM cells (Steinbrunn *et al.* 2012). However, a small molecule inhibitor of ILK has previously been shown to reduce the invasive capabilities of MM cell lines, suggesting a possible role in myeloma cell migration (Wang *et al.* 2011). The increased abundance of numerous components of the ILK signalling pathway in EMM BMNCs indicates a potential role of this signalling pathway in the migration of myeloma cells to extramedullary sites.

Proteins involved in the tricarboxylic acid (TCA) pathway were decreased in EMM BMNCs compared to MM BMNCs, indicating a potential metabolic change during extramedullary transition. In contrast, hydrogen peroxide and reactive oxygen species (ROS) metabolic processes were enriched based on GOBP analysis of proteins increased in abundance in EMM BMNCs, indicating a potential increase in ROS within the EMM bone marrow microenvironment. Interestingly, hypoxic conditions, which paradoxically increase ROS levels in MM, promote the dissemination of myeloma cells into peripheral blood via the stabilization of hypoxia-inducible factor 1-alpha (HIF1α) and subsequent activation of EMT-related proteins (Azab *et al.* 2012; Abe *et al.* 2023). In addition, a recent transcriptomic study described an upregulation of HIF1α in EMM (Ryu *et al.* 2020). HIF1α affects cell metabolism by suppressing the TCA cycle and enhancing the rate of glycolysis (Kim *et al.* 2006; Lum *et al.* 2007). Transcriptional downregulation of mitochondrial phosphoenolpyruvate carboxykinase (PCK2) by HIF1α has been reported to contribute to the attenuation of the TCA cycle and growth of breast cancer cells (Tang *et al.* 2019). An almost 5-fold decrease in PCK2 abundance in EMM BMNCs was identified in this study. Increased levels of HIF1α in EMM may explain the decreased levels TCA cycle-associated proteins and increased levels of ROS metabolism-associated proteins seen in EMM BMNCs.

Three glycolytic enzymes, namely phosphofructokinase (PFKP), aldolase, and pyruvate kinase (PKM2) were significantly increased in abundance in EMM BMNCs. Previous transcriptomic analysis reported the emergence of a metabolic cluster involving pyruvate kinase (PKM2) during extramedullary transition (Ryu *et al.* 2020). PKM2 has previously been linked to myeloma proliferation and adhesion, with one study showing that the silencing of PKM2 promoted cell adhesion in cell lines (He *et al.* 2015). Interestingly, PKM2 is a target gene of HIF1α, and participates in a positive feedback loop by acting as a co-activator of HIF1α under hypoxic conditions (Luo *et al.* 2011). Secreted forms of PKM2 have also been found to contribute to metastasis in certain cancers through interaction with integrin β1, which was also found to be increased in EMM BMNCs (Kim *et al.* 2020; Wang *et al.* 2020). The roles of glycolytic and mitochondrial metabolism in the progression of MM to EMM remains unclear. A recent study found that primary tumours and distant metastases have unique metabolic requirements, highlighting the potential metabolic change between MM cells and EMM cells (Bennett *et al.* 2022). Our results indicate a change in the metabolic phenotype within the bone marrow microenvironment during extramedullary transition. Further research on the metabolic pathways active within the bone marrow of MM patients and at extramedullary sites of EMM patients may identify specific metabolic targets for the treatment of EMM.

Various clinical and morphological characteristics have been linked to EMM. An immature or plasmablastic morphology is often associated with EMM (Touzeau and Moreau 2016; Dah *et al.* 2021). Interestingly, several of the cytoskeletal proteins increased in EMM BMNCs included proteins associated with a plasmablastic morphology (CNN2, PFN1, TMOD3, VASP, TLN1, TMSB4X, PLEK, ZYX) (Qi *et al.* 2007). Hypoxic conditions have also been found to promote an immature phenotype in MM through the decreased expression of terminal differentiation markers such as syndecan 1 (CD138), which was decreased in abundance in EMM BMNCs (Kawano *et al.* 2013; Muz *et al.* 2014). Myeloma cells expressing CD138 at low levels are more motile with a higher propensity for dissemination and egress from the bone marrow into blood vessels more often than those with high expression of CD138 (Akhmetzyanova *et al.* 2020). Heparanase is a promoter of myeloma stemness and a key metastatic enzyme that was significantly increased in EMM

BMNCs compared to MM BMNCs (Tripathi *et al.* 2020). As described, heparanase has been reported to promote an invasive phenotype in MM via CD138 cleavage from the MM cell surface (Jung *et al.* 2016). The increased abundance of heparanase in EMM bone marrow mononuclear cells supports previous research findings that heparanase is a key determinant of myeloma cell dissemination. Increased levels of circulating CD138 in EMM plasma support the hypothesis of increased HPSE-induced shedding in EMM bone marrow. Although it is not known if this increase in CD138 plasma levels is a direct result of HPSE activity, further research exploring the HPSE/CD138 axis may yield promising therapeutic targets for the treatment of EMM. An increase in heparanase levels may contribute to the creation of a pro-migratory niche within the bone marrow. Further investigations should be performed to elucidate the roles of these proteins associated with the more aggressive, plasmablastic phenotype in extramedullary transition.

As EMM is associated with a poor prognosis in MM, we hypothesized that certain proteins increased in abundance in EMM BMNCs may also be increased in MM patients with reduced overall survival. The MMRF CoMMpass dataset was used to evaluate the association between gene expression and overall survival of the 25 most significantly increased in abundance proteins in EMM. Increased gene expression of seven genes, namely TAGLN2, ITGA2, TPM2, TPM3, CA2, LGALS1, and TMOD3, were associated with a reduced overall survival in MM. Interestingly, TAGLN2, a protein involved in stabilizing the actin cytoskeleton, has been linked to high-risk MM and the development of plasma cell leukemia (Heuck *et al.* 2014; Schinke *et al.* 2020; Bruinink *et al.* 2022), This suggests a potential role for TAGLN2 in the migration of myeloma cells from the bone marrow into blood. Galectin-1 (LGALS1) is homodimeric β-galactoside binding protein, that is involved in a myriad of malignant cellular processes including survival, drug resistance, angiogenesis, and metastasis (Storti *et al.* 2017). In MM, galectin-1 is upregulated under hypoxic conditions and has been identified as a potential target of angiogenesis as galectin-1 inhibition led to the downregulation of pro-angiogenic genes, and upregulation of anti-angiogenic genes (Storti *et al.* 2016). Furthermore, LGALS1 is overexpressed in circulating tumour cells when compared to matched bone marrow-derived myeloma cells (Garcés *et al.* 2020). Although few studies have evaluated the role of ITGA2, TPM2, TPM3, CA2, and TMOD3 in multiple

myeloma, an association between these proteins and metastasis have been identified in other cancers (Annan *et al.* 2019; Ren *et al.* 2019; Zheng *et al.* 2019; Chen, Shen, *et al.* 2021; Mele *et al.* 2022).

More focus has been placed on the role of the tumour microenvironment in cancer progression and metastasis in recent years. Tumour-associated neutrophils (TANs) have been found to accelerate metastasis via the secretion of various cytokines and inflammatory factors (Li, Cong, *et al.* 2019; Yan *et al.* 2022). Furthermore, NETs have garnered increased attention as potential instigators of metastatic dissemination (Yang and Liu 2021). KEGG pathway analysis revealed an enrichment of proteins involved in neutrophil extracellular trap formation in EMM BMNCs. The enriched proteins included the tyrosine kinases, proto-oncogene tyrosine-protein kinase Src (SRC) and spleen tyrosine kinase (SYK), which showed a 3-fold and 4-fold increase in EMM BMNCs compared to MM BMNCs. Inhibition or deletion of SYK results in defects in NET formation in response to various stimuli, including β-glucans, lipopolysaccharides and plasma from patients hospitalized with coronavirus disease 2019, highlighting the key role SYK plays in NET formation (Nanì *et al.* 2014; Strich *et al.* 2020, 2023). Despite SYK being considered a less relevant target in MM compared to other hematological malignancies such as CLL, SYK inhibitors have been found to reduce viability and hinder migration in a selection of MM cell lines. Furthermore, while SYK is relatively lowly expressed in primary myeloma cells, an increased level of total and phosphorylated SYK has been identified in plasma cell leukemia patients, suggesting a potential link between SYK expression and myeloma cell migration from the bone marrow (Koerber *et al.* 2015; Lorenz *et al.* 2016).

To investigate NETs, we evaluated plasma concentrations of the main NET markers, ELA2, MPO, CitH3, and circulating nucleosomes in EMM. Significant elevations in the abundance of plasma ELA2 in EMM was identified. A non-significant increase in MPO, calprotectin, and citH3 plasma levels in EMM was identified, while no significant change in circulating nucleosome levels were identified. While ELA2 and MPO are major components of NETs suggesting a potential link between EMM and increased NET formation in EMM, the increased levels of ELA2 and MPO observed in EMM plasma may also be the result of a NET-independent cellular process associated with myeloma cell dissemination. Following neutrophil activation, MPO

catalyses the production of ROS which can directly or indirectly damage the extracellular matrix (ECM), thus facilitating cancer cell migration and invasion (Valadez-Cosmes *et al.* 2022). ELA2 also participates in the degradation of the ECM by digesting ECM proteins including elastin and laminin (Albrengues *et al.* 2018). A global deletion of ELA2 in a lung carcinoma mouse model reduced the number and size of metastatic lesions compared to those with wild-type ELA2, highlighting its role in the metastatic cascade, especially at pre-metastatic niches (Houghton *et al.* 2010). NET formation has been implicated in myeloma progression. Myeloma cells incubated with neutrophils were found to stimulate NET formation, while inhibition of PAD4 significantly prolonged survival and reduced tumour burden in MM-bearing mice (Li *et al.* 2020). NETs have also been suggested to contribute to hypercoagulability in MM (Ciepiela *et al.* 2021). Increased NET levels correlate with increased cell-free DNA (cfDNA) plasma concentrations (Henry *et al.* 2022). A recent study found MM patients with extramedullary multiple myeloma have significantly higher concentrations of plasma cfDNA when compared to MM patients without extramedullary spread (Long *et al.* 2020). Interestingly, the DNA sensing transmembrane receptor, CCDC25, has been found to sense NET-DNA and subsequently trigger the ILK-β-parvin pathway discussed above, to promote cancer metastasis (Yang *et al.* 2020). NET-DNA also acts as a chemotactic factor attracting tumour cells through CCDC25. It has been hypothesized that accumulating neutrophils can promote an inflammatory milieu which contributes to the formation of a pre-metastatic niche in distal organs (Jablonska *et al.* 2017). The chemotactic effects of NET-DNA at these sites may attract circulating tumour cells to these primed metastatic sites through CCDC25 (Liu *et al.* 2020). The enrichment of NET-associated proteins and ILK-β-parvin pathway proteins within the EMM bone marrow mononuclear fraction compared to the MM bone marrow mononuclear fraction indicates a potential involvement of these signalling pathways in the development of EMM. Furthermore, the trend towards increased levels of NET markers in EMM plasma compared to MM plasma confirms the need for further research on a larger cohort of samples to determine the involvement of NETs in EMM development.

It is important to note that this work contains a small sample size and lacks cellular proteomic verification which limits the generalization of these results across all

EMM patients. However, EMM is a rare manifestation of multiple myeloma which hinders our ability to collect samples from a large number of patients for initial analysis and subsequent validation. Studies including clinical samples from EMM patients are often published as case studies or have small sample sizes due to difficulties obtaining sufficient sample numbers (Vong *et al.* 2020; Kolagatla *et al.* 2022; Chen *et al.* 2023). Furthermore, EMM represents an under-researched area of multiple myeloma, with few studies focusing on the molecular mechanisms that distinguish EMM from MM without extramedullary involvement. Our analysis represents a pilot study which confirms that there is a unique proteomic profile associated with EMM that is clearly distinct from MM without extramedullary involvement. The use of the MMRF CoMMpass dataset to determine the prognostic value of the most significantly increased proteins in EMM BMNCs provides some insight into the association of these proteins with more aggressive disease; however, validation in an independent cohort of EMM patients is required to confirm the association of significant proteins identified in this study with EMM. Furthermore, BMNCs from EMM and MM patients were used for proteomic analysis, which means that proteomic changes seen between the two groups are not solely associated with myeloma cells and are instead associated with changes in the mononuclear fraction. We postulated that the presence of extramedullary lesions is derived from clonal changes in the bone marrow microenvironment, and we evaluated the change in the proteomic profile of the bone marrow in the context of EMM by analysing BMNCs. However, this is a limitation of the study as it is difficult to differentiate molecular signals deriving from myeloma cells and those originating from cells in the mononuclear fraction. Further research isolating $CD138^{+}$ myeloma cells from the mononuclear fraction would help decipher pro-migratory myeloma sub-clones in the bone marrow of EMM patients. Nonetheless, this study clearly identified a major change in the proteomic profile of bone marrow mononuclear cells in patients with and without extramedullary disease.

5.5 Conclusion

This chapter highlights the alterations in the proteomic profile within the bone marrow mononuclear fraction of EMM patients compared to MM patients without extramedullary spread. At the time of writing, our study represents the first LC-

MS/MS study evaluating proteomic changes in EMM and MM patients. As mentioned previously, EMM remains an understudied, aggressive manifestation of MM with no targeted treatment options or therapeutic regimens specifically aimed at the treatment of EMM. Molecular analyses identifying genetic, epigenetic, transcriptomic, and/or proteomic targets in EMM are crucial to inform future clinical trials and improve patient outcome in EMM. Our characterisation of the BMNC proteome in EMM compared to MM, identified specific proteins and pathways which may contribute to the dissemination of myeloma cells to distal sites. Future studies validating the differential abundance of these proteins in EMM samples may have clinical relevance, whereby bone marrow aspirates from MM patients may be screened for these markers of EMM, and subsequently prompt more detailed patient evaluations when differential abundance of these markers are detected. We hope our results will inform future experimental designs to validate protein targets and translate these findings into clinically relevant biomarkers and therapeutic targets in EMM.

Chapter 6

Proteomic profiling of blood plasma from multiple myeloma patients with and without extramedullary spread

6.1 Introduction

Extramedullary multiple myeloma (EMM) is an aggressive sub entity of multiple myeloma associated with a reduced overall survival. Currently, EMM is detected using imaging modalities including whole-body MRI and ^{18}F-FDG PET/CT. The introduction of these imaging techniques with improved sensitivity and specificity has improved EMM detection, as highlighted by the increase in the incidence of EMM in the post PET/CT era (Bladé *et al.* 2022b). The International Myeloma Working Group (IMWG) recently recommended incorporating ^{18}F-FDG PET/CT as part of diagnostic and prognostic investigations of patients with newly diagnosed multiple myeloma, as the availability of whole-body MRI remains limited. The use of ^{18}F-FDG PET/CT during myeloma investigations has many advantages including the ability to accurately evaluate disease burden, identify metabolically active lesions and detect medullary and extramedullary lesions with high sensitivity (**Figure 6.1**)(Cavo *et al.* 2017). Limitations associated with ^{18}F-FDG PET/CT include the high cost, limited availability, and lack of imaging standardization which hinders the reproducibility of result interpretations. Furthermore, an estimated 10-30% of MM patients present with non-FDG-avid multiple myeloma which can lead to false negative results (Bartel *et al.* 2009; Zamagni *et al.* 2011; Ulaner and Landgren 2020). A study comparing ^{18}F-FDG PET/CT and diffusion-weighted whole-body MRI (WB-DWI) for detecting intramedullary and extramedullary lesions in multiple myeloma found that of 113 extramedullary lesions, 12 were not detected by ^{18}F-FDG PET/CT and characterised as non-FDG-avid lesions. This highlights the need for additional clinical tests to detect EMM at an early stage.

Figure 6.1: Appearance of intra- and extra-medullary lesions in multiple myeloma by ^{18}F-FDG PET/CT. Left figure shows a sagittal image illustrating diffuse myelomatous infiltration in the spine and sternum. Right figure shows a coronal image illustrating metabolic activity at intra- and extra-medullary foci.

*Image adapted from (Hanrahan *et al.* 2010).

Biofluids, such as plasma and urine, remain the preferred sources of novel biomarkers due to the minimally invasive nature of sample collection. Proteomic analysis of biofluids is commonly used for biomarker discovery, with various studies identifying promising circulating markers of advanced disease stage in breast and ovarian cancer (Darlix *et al.* 2016; Tomás-Pérez *et al.* 2023). A major challenge in the analysis of biofluids, especially serum and plasma, is the large dynamic range between the proteins of highest and lowest abundance. A large proportion of the serum/plasma proteome (>90%) is made up of high abundance proteins (HAPs) such as albumin, immunoglobulins, fibrinogen, transferrin, and lipoproteins. During mass spectrometry analysis of serum or plasma, high abundance proteins can have a 'masking' effect, whereby peptides originating from HAPs are repeatedly selected for fragmentation, thus hindering the detection and quantitation of low abundance proteins (Borberg *et al.* 2021). To overcome this limitation, additional sample

preparation steps including the enrichment of low abundant proteins (e.g., ENRICH-iST kit), immunodepletion of HAPs (e.g., Proteome Purify™ Immunodepletion Kits, R&D Systems) and sequential fractionation, are often performed to reduce sample complexity and improve proteome coverage (Lee *et al.* 2019).

The ability to quantify highly sensitive circulating protein markers that are indicative of extramedullary lesions during routine check-ups would help inform clinicians on the need for follow-up imaging tests and may guide prognostication and therapeutic decision-making. At the time of writing, no published studies have evaluated proteomic changes in the plasma or serum of MM patients with and without extramedullary lesions. One study analysed the abundance of various cytokines in the bone marrow plasma of EMM and MM patients, identifying 8 cytokines as significantly differentially abundant (Gregorova *et al.* 2022). Namely, epidermal growth factor (EGF) and brain-derived neurotrophic factor (BDNF) were decreased in abundance whereas neutrophil activating peptide 2 (NAP-2), adiponectin (ADIPOQ), C-reactive protein (CRP), tumour necrosis factor ligand superfamily member 13B (BAFF), C-X-C motif chemokine 9 (CXCL9), and thrombospondin 1 (THBS1), were increased in abundance in EMM bone marrow plasma. In this chapter, an untargeted label-free mass spectrometry analysis was conducted on blood plasma from MM and EMM patients to identify circulating markers of extramedullary disease. Verification of selected SSDA proteins was performed using targeted ELISAs to identify promising plasma-derived markers of extramedullary multiple myeloma. A targeted PEA-based immunoassay was also performed to detect changes in plasma cytokine levels between MM and EMM patients.

6.2 Experimental design and methods

Oncology researchers are continuously searching for minimally invasive biomarkers that provide clinicians with reliable information to aid diagnosis, prognosis, and risk stratification. Plasma is an ideal source of molecular biomarkers which can be routinely tested during follow-up. Extramedullary multiple myeloma has been reported to occur due to the hematogenous spread of myeloma cells from the bone marrow, further highlighting plasma as a promising source of EMM biomarkers.

6.2.1 Patient samples and clinical information

A total of 17 EDTA plasma samples were obtained from the FHRB biobank. Plasma samples were collected from MM patients (n=8) and EMM patients (n=9, one serial sample). FHRB is authorized and approved by the Finnish National Supervisory Authority for Welfare and Health (Valvira) and Finnish National Medical Ethics Committee, respectively. Samples were stored at -80ºC. Full patient details are outlined in Chapter 5. Four EMM patients with two serial samples at different stages of disease were obtained from the FHRB for this analysis. A second independent cohort of MM plasma samples (n=44) with corresponding *ex vivo* drug sensitivity resistance testing data was analysed as part of this work. Full patient details for this cohort are outlined in Chapter 4.

6.2.2 Label-free mass spectrometry analysis of EMM and MM plasma samples using a Q-Exactive mass spectrometer.

Prior to mass spectrometry analysis, high abundant plasma proteins were depleted using the Proteome Purify 12 Human Serum Protein Immunodepletion Resin (R&D Systems, Minneapolis, MN, USA), as described in Chapter 2. Briefly, 10 µL of plasma was mixed with 1 mL of immunodepletion resin for 60 min on a rotary shaker. The mixture was transferred to Spin-X filter units and centrifuged. Protein digestion was performed using the FASP protocol, as described in Chapter 2. A total of 10 µg of protein was digested at a 1:25 enzyme-to-protein ratio. The tryptic digest was acidified at a 1:8 ratio using 2% TFA, 20% ACN.

LC-MS/MS was performed using the Ultimate 3000 NanoLC system (Dionex Corporation, Sunnyvale, CA, USA) coupled with a Q-Exactive mass spectrometer (Thermo Fisher Scientific). A total of 14 µL, containing ~1µg of digested protein was loaded. Samples were loaded onto a C18 trap column (C18 PepMap, 300 µm id × 5 mm, 5 µm particle size, 100 Å pore size; Thermo Fisher Scientific) and resolved on an analytical Biobasic C18 Picofrit column (C18 PepMap, 75 µm id × 50 cm, 2 µm particle size, 100 Å pore size; Dionex). Peptides generated were eluted over a 120 min 2-40% acetonitrile gradient. The Q-Exactive was operated in positive, data-dependent acquisition (DDA) mode and externally calibrated using HeLa digest (300ng), as described in Chapter 2.

6.2.3 Data analysis of mass spectrometry results

Raw files containing quantitative information from the mass spectrometry analysis were searched using the proteomics analysis software, Proteome Discoverer 2.5 (Thermo Fisher Scientific). Protein identification and label-free quantitation (LFQ) was performed. The resulting dataset was imported into Perseus (1.6.14.0). Proteins identified by ≥2 peptides and quantitative values in >70% samples were retained for downstream analysis. Missing values were replaced by imputation using a width of 0.3 and a down-shift of 1.8. Statistically significantly differentially abundant proteins were identified by performing a two-sample t-test with a FDR-adjusted p-value < 0.1 and fold change >1.5 between experimental groups.

6.2.4 Verification of results using enzyme-linked immunosorbent assays (ELISAs)

The concentrations of six proteins (vascular cell adhesion protein 1 (VCAM1), aminopeptidase N (CD13), butyrylcholinesterase (BCHE), hepatocyte growth factor activator (HGFA), alpha 2-macroglobulin (A2M) and pigment epithelium-derived factor (PEDF)) in blood plasma were measured by ELISA (DuoSet ELISA kits, R&D Systems). The following plasma dilutions were used: VCAM1 (1:1500), CD13 (1:75), BCHE (1:2000), HGFA (1:2000), A2M (1:100,000) and PEDF (1:8000). The plasma concentrations of VCAM1, PEDF and HGFA, at the same dilutions, were also analysed in the second MM patient cohort (n = 44).

6.2.5 Statistical analysis of ELISA results

The statistical analysis of ELISA results, receiver-operating characteristic (ROC) curve analysis and correlation analyses were performed using Graphpad Prism (8.0.2.263) and MedCalc (version 20.118). Parametric t-tests were used to evaluate statistical significance. Outliers were removed using the ROUT method (Q = 1%). ROC curve analysis was used to determine the discriminatory performance of the verified SSDA plasma proteins. The ROC curves evaluated the specificity (false positive fraction) and sensitivity (true positive fraction) of the potential protein biomarkers. Optimal cut-off points were selected using Youden's index. The area under the curve (AUC) was calculated to summarise the accuracy of the

classification. Logistic regression analysis was performed in MedCalc using the Enter method.

6.2.6 Targeted proteomic analysis using the Olink Target 48 panel

Plasma concentrations of 45 cytokines in EMM (n=8) and MM (n=25) were evaluated using the Olink Target 48 panel, as described in Chapter 2.

6.3 Results

6.3.1 Identification of significantly differentially abundant proteins in the plasma of EMM and MM patients

Blood plasma samples from MM (n = 8) and EMM (n = 9, 1 serial sample) patients were analysed using label-free LC-MS/MS to identify changes in the plasma proteome of patients with and without extramedullary lesions. A total of 524 proteins and 22 SSDA proteins were identified based on an FDR corrected p-value < 0.1 and fold change >1.5 (**Figure 6.2, Table 6.1**). All 22 significant proteins were increased in abundance in EMM plasma samples compared to MM patient plasma without extramedullary spread. STRING with functional enrichment analysis was used to visualize the plasma proteomic changes. The minimum required interaction score was set to medium confidence (0.4) and two unconnected nodes (OAF, APMAP) were removed. Proteins associated with complement activation were enriched in EMM plasma (**Figure 6.3**).

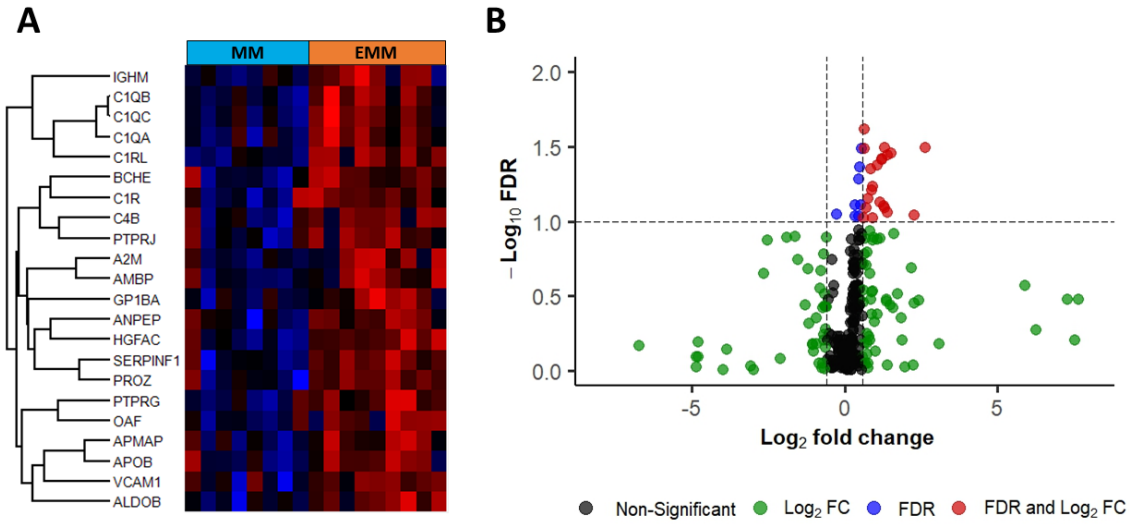

Figure 6.2: Differential abundance analysis of quantitative proteomics data from EMM and MM plasma. (**A**) Hierarchical clustering of z-scored normalised intensity values of SSDA proteins. The colours from blue to red represent the relative protein levels between the two groups. (**B**) Volcano plot illustrating the distribution of identified proteins based on false discovery rate (FDR) p-value and fold change. Red points represent proteins significantly increased in abundance in EMM plasma. Green points indicate proteins with a fold change >1.5 but FDR *p*-value > 0.1. Blue points indicate proteins with an FDR *p*-value < 0.1 but fold change <1.5. Black points indicate proteins with FDR p-values > 0.1 and fold change > 1.5.

Table 6.1: List of statistically significantly differentially abundant proteins in the plasma of EMM patients compared to MM patients without extramedullary spread.

Uniprot ID	Description	Gene Name	Fold Change	FDR-Adjusted *p*-value
Q9NZP8	Complement C1r subcomponent-like protein	C1RL	1.58	0.012
P02747	Complement C1q subcomponent subunit C	C1QC	2.45	0.030
P36955	Pigment epithelium-derived factor	PEDF	1.56	0.031
P23470	Receptor-type tyrosine-protein phosphatase gamma	PTPRG	2.87	0.035
P02745	Complement C1q subcomponent subunit A	C1QA	2.33	0.038
Q04756	Hepatocyte growth factor activator	HGFA	2.09	0.038
P05062	Fructose-bisphosphate aldolase B	ALDOB	2.31	0.039
P02746	Complement C1q subcomponent subunit B	C1QB	2.66	0.041
P22891	Vitamin K-dependent protein Z	PROZ	1.83	0.042
P06276	Cholinesterase	BCHE	1.88	0.056
Q9HDC9	Adipocyte plasma membrane-associated protein	APMAP	1.85	0.058
P02760	Protein AMBP	AMBP	1.69	0.062
P07359	Platelet glycoprotein Ib alpha chain	GP1BA	2.40	0.070
P19320	Vascular cell adhesion protein 1	VCAM1	2.23	0.078
P01023	Alpha-2-macroglobulin	A2M	2.50	0.079
P00736	Complement C1r subcomponent	C1R	1.63	0.079
P15144	Aminopeptidase N	ANPEP	2.65	0.081
P01871	Ig mu chain C region	IGHM	4.84	0.083
P04114	Apolipoprotein B-100	APOB	1.54	0.083
Q86UD1	Out at first protein homolog	OAF	2.24	0.085
P0C0L5	Complement C4-B	C4B	1.88	0.085
Q12913	Receptor-type tyrosine-protein phosphatase eta	PTPRJ	1.79	0.095

Functional enrichment (GOBP)	FDR value
Complement activation, classical pathway	6.13 x10^{-8}
Regulation of complement activation	1.43 x10^{-7}
Regulation of immune response	1.35 x10^{-5}

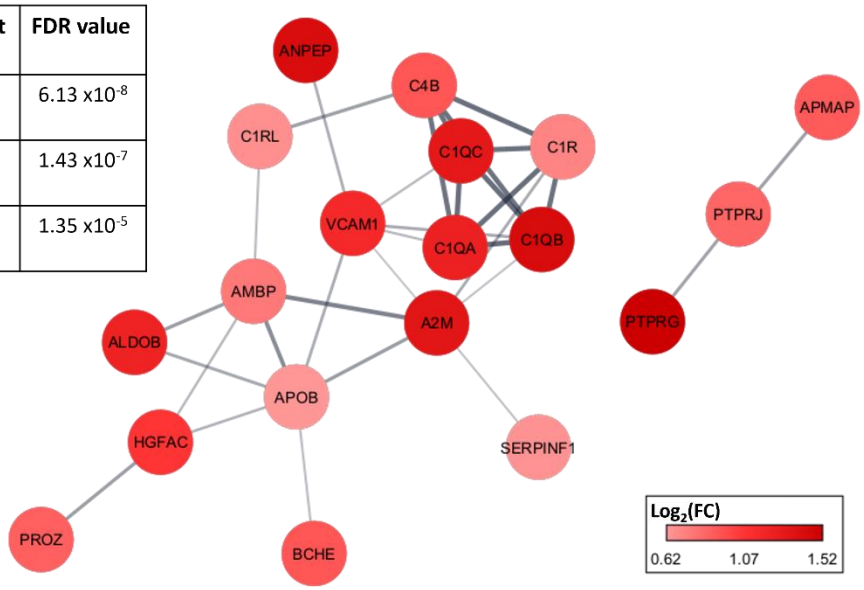

Figure 6.3: STRING analysis with functional enrichment of significantly differentially abundant proteins in EMM versus MM plasma. Information on protein-protein interactions were obtained from the STRING database (minimum interaction score > 0.4). Each node represents a protein, and each connecting line indicates an interaction. The thicker the connecting line, the higher the interaction score. FC, fold change.

6.3.2 ELISA verification analysis of differentially abundant plasma proteins in EMM plasma

ELISA analysis was used to verify a selection of the SSDA proteins identified by LC-MS/MS. Six proteins (ANPEP, VCAM1, BCHE, HGFA, PEDF, A2M) found to be increased in abundance in the blood plasma of EMM patients were verified via ELISA. Box and whisker plots were constructed to visualize the results of the ELISA assays, and include the range, median and quartiles for each protein analysed (**Figure 6.4**). Three of the six proteins analysed, namely VCAM1, HGFA, and PEDF, were verified as significantly increased in abundance in EMM plasma with p-values of 0.045, 0.014, and 0.0005, respectively. ANPEP, BCHE and A2M did not reach statistical significance, yielding p-values of 0.959, 0.488, and 0.112, respectively. Despite the large p-value regarding ANPEP, a trend towards increased abundance in EMM plasma can be observed as a single high ANPEP concentration value in the MM group largely contributes to the overall increase in the mean ANPEP concentration. Therefore, ANPEP and A2M warrant further investigation in a larger cohort of samples.

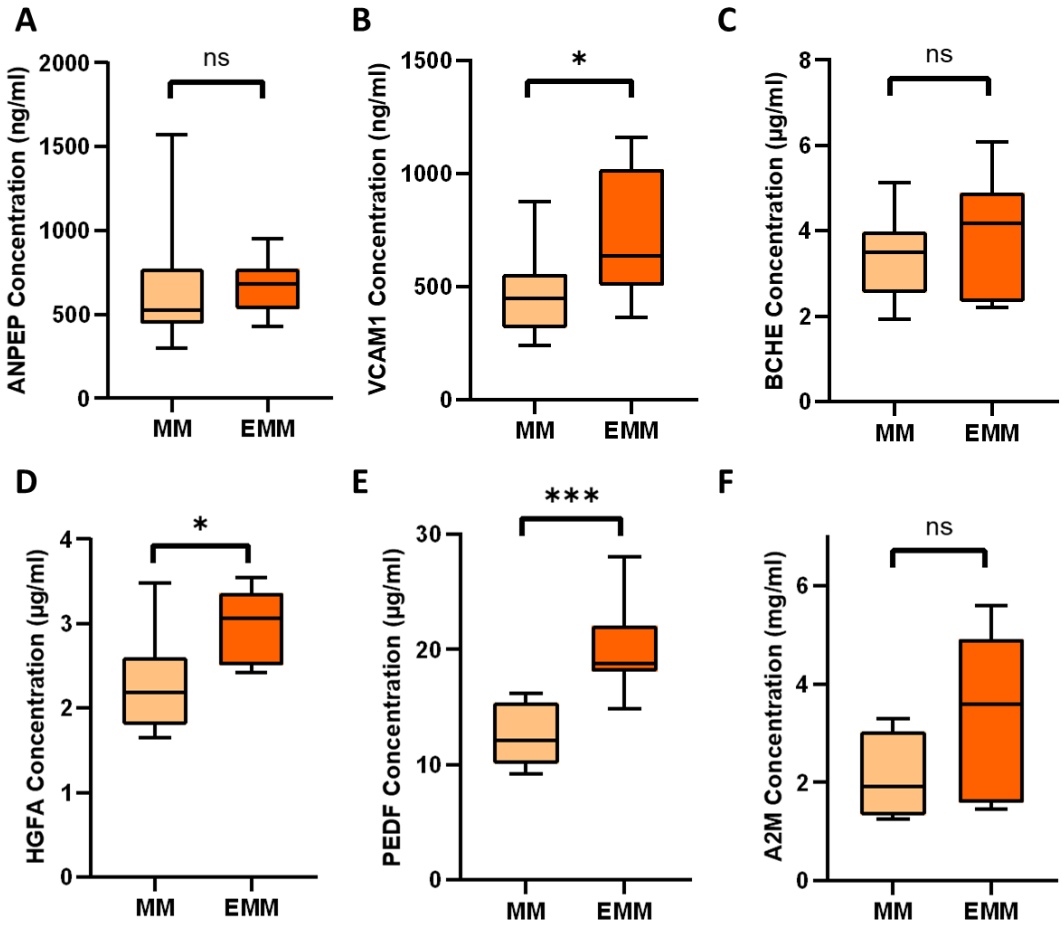

Figure 6.4: Plasma levels of statistically significantly differentially abundant proteins measured by ELISA. (**A**) ANPEP, (**B**) VCAM1, (**C**) BCHE, (**D**) HGFA, (**E**) PEDF and (**F**) A2M plasma levels in the EMM and medullary MM groups. Significance is marked as follows: not significant 'ns', $p \leq 0.05$ '*', $p \leq 0.001$ '***'.

To determine the capacity of VCAM1, HGFA, and PEDF to distinguish MM samples from EMM samples, we performed individual ROC curve analyses and a multivariate analysis. In chapter 5, as part of the evaluation of neutrophil extracellular trap formation, the plasma concentration of neutrophil elastase 2 (ELA2) was found to be significantly increased in EMM plasma compared to MM plasma. Here, we also evaluated the potential of ELA2 as a plasma-based biomarker of EMM using ROC curve analysis. ROC curves were constructed and the area under the curve (AUC) values were calculated (**Figure 6.5**). VCAM1 was found to have good predictive power showing a sensitivity of 66.67, specificity of 87.5, and AUC value of 0.806 ($p = 0.0057$). HGFA also displayed good predictive power with a sensitivity of 100, specificity of 75, and AUC value of 0.847 ($p = 0.0028$). PEDF showed a sensitivity of 87.5, specificity of 100, and AUC value of 0.969 ($p < 0.0001$), indicating excellent discriminatory power. ELA2 also showed excellent

predictive power with a sensitivity of 88.89, specificity of 100, and an AUC value of 0.965 ($p < 0.0001$).

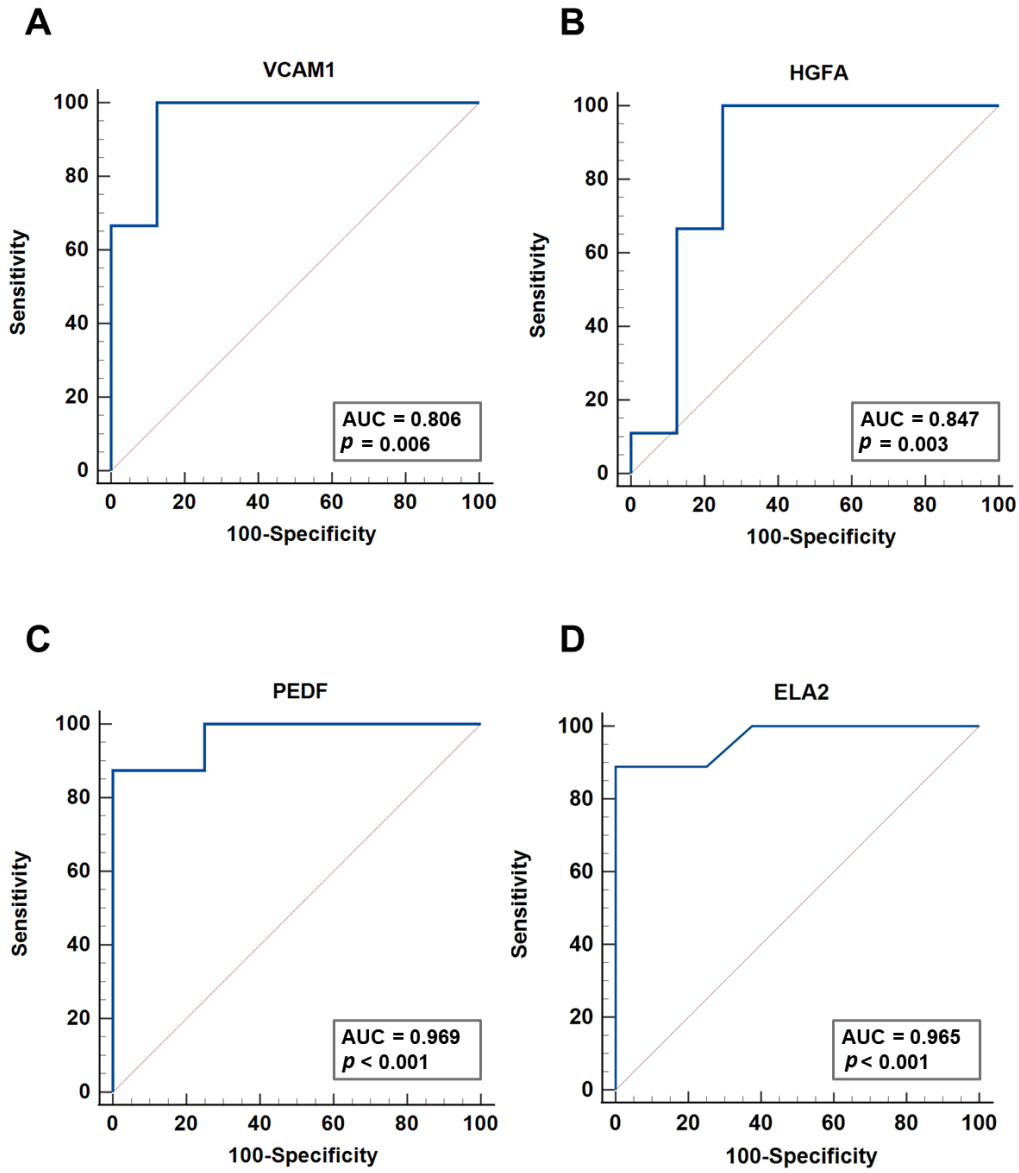

Figure 6.5: Receiver operating characteristic (ROC) curve analysis of four potential EMM biomarkers. (**A**) VCAM1, (**B**) HGFA (**C**) PEDF and (**D**) ELA2 ROC curves.

Clinical tests measuring multiple biomarkers typically outperform single biomarker tests. Therefore, logistic regression analysis was performed to determine the predictive power of the biomarkers combined. The combination of all four biomarkers resulted in a sensitivity of 100, specificity of 100, an AUC value of 1 and a 95% confidence interval of 0.794–1 (**Figure 6.6**). This highlights the promising potential of combining these plasma proteins into a biomarker panel to detect EMM.

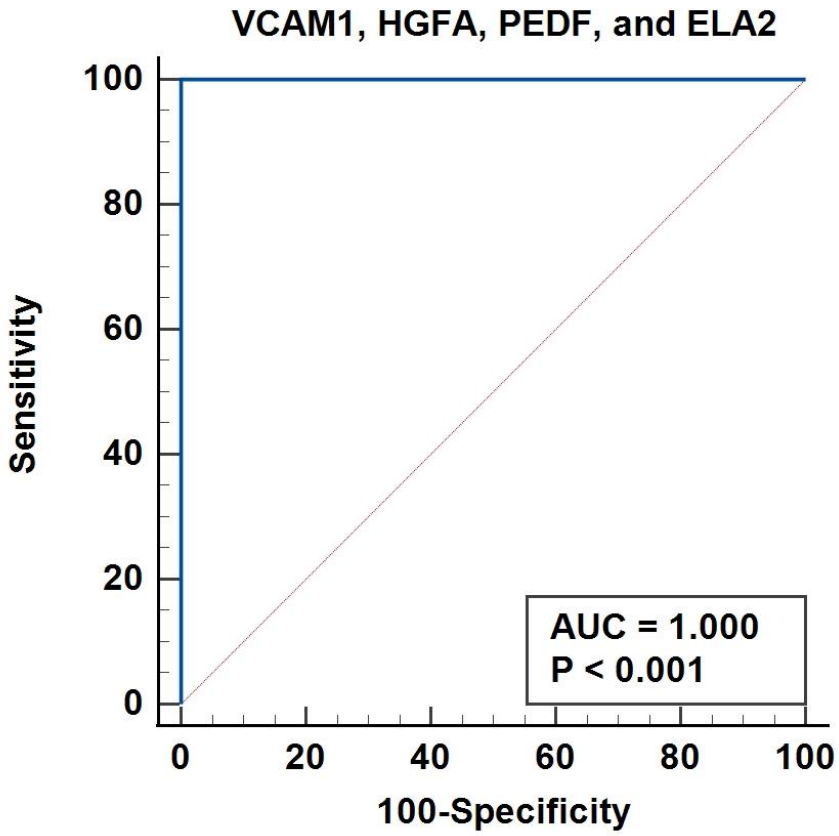

Figure 6.6: Logistic regression analysis evaluating four-biomarker panel performance. ROC curve based on illustrating the discriminatory power of combining VCAM1, HGFA, PEDF, and ELA2.

6.3.3 ELISA analysis of serial EMM plasma samples

Serial samples from four EMM patients at different disease stages were evaluated for plasma concentrations of VCAM1, HGFA, and PEDF to investigate whether plasma levels of these protein markers showed changes during the disease course (**Figure 6.7**). Serial samples from two EMM patients were collected at diagnosis and at the time of disease progression, samples from one patient were collected at diagnosis and near complete response to treatment and samples from the fourth patient were collected at diagnosis and at complete response to treatment. Due to the low number of serial samples available for analysis, no statistical analyses could be performed. Plasma levels of VCAM1 and PEDF showed slight increases in progressive disease samples compared to diagnostic samples, with the exception of Patient 1, which showed a dramatic increase in VCAM1 levels at progressive disease. In contrast, HGFA levels were slightly decreased in progressive disease samples compared to diagnostic samples. Plasma levels of HGFA were slightly increased during response

to treatment when compared to diagnostic samples, whereas VCAM1 and PEDF levels showed varying concentrations across the two serial samples. A clear trend in VCAM1, HGFA, or PEDF levels at different disease stages could not be determined from this analysis.

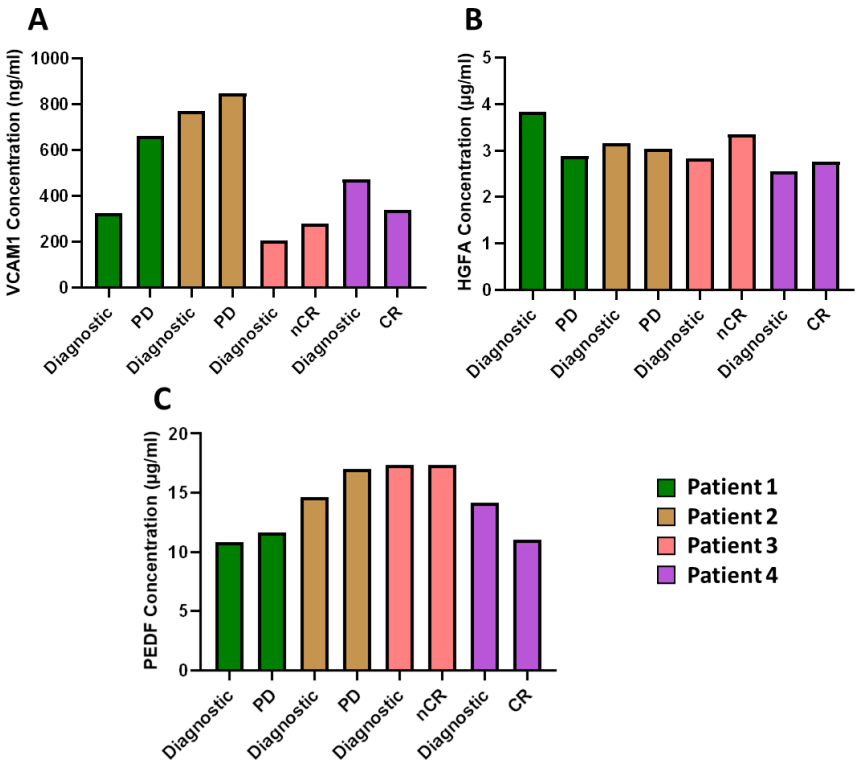

Figure 6.7: Bar charts illustrating ELISA analysis of four serial EMM samples. (**A**) VCAM1, (**B**) HGFA, and (**C**) PEDF plasma concentrations detected in the plasma of four EMM serial samples. PD, progressive disease; nCR, near complete response; CR, complete response.

6.3.4 Evaluation of VCAM1, HGFA, PEDF, and ELA2 plasma concentrations in an independent MM patient cohort

As EMM is often associated with drug resistance, we tested the plasma levels of VCAM1, HGFA, PEDF, and ELA2 in the MM patient cohort (n=44) with *ex vivo* DSRT data evaluated in Chapter 4. Firstly, VCAM1, HGFA, PEDF and ELA2 plasma concentrations in this independent set of MM samples (n = 43, excluding 1 EMM sample) were compared to EMM plasma concentrations. The plasma concentrations in this independent cohort showed a similar pattern to that observed in the MM group above. As described in **Table 6.2**, VCAM1, HGFA, and PEDF plasma concentrations were significantly increased in EMM plasma compared to this MM cohort. In addition, the median concentrations of VCAM1, HGFA and PEDF

observed in this MM sample set were considerably lower than the median concentrations observed in the EMM group above (VCAM1 = 634.7 ng/mL, HGFA = 3.068 µg/mL, PEDF = 18.77 µg/mL) supporting our findings that these three proteins are increased in abundance in EMM patient plasma. In addition, the single EMM plasma sample in this cohort showed the highest plasma concentration of VCAM1 and PEDF within the cohort.

Table 6.2: Statistical comparison of VCAM1, HGFA, and PEDF plasma concentrations in second MM patient cohort and EMM patient cohort. Values within parentheses indicate the minimum and maximum values detected in the sample set.

Protein	Mean plasma concentration – MM N=43	Mean plasma concentration – EMM N=9	*P*-value
VCAM1	301 ng/ml (150.9 - 488.2 ng/ml)	730.3 ng/ml (362.9 - 1159 ng/ml)	0.0016
HGFA	2.143 µg/ml (1.039 - 3.372 µg/ml)	2.967 µg/ml (2.418 - 3.542 µg/ml)	0.0002
PEDF	13.39 µg/ml (8.901 - 19.22 µg/ml	20.02 µg/ml (14.81 - 28.03 µg/ml)	0.0017
ELA2	15.54 ng/ml (5.1 – 32.98 ng/ml)	13.67 ng/ml (8.699 – 20.31 ng/ml)	0.4360

6.3.5 Association of VCAM1, HGFA, PEDF and ELA2 plasma concentrations with clinical parameters

Next, VCAM1, HGFA, PEDF, and ELA2 plasma concentrations were evaluated to determine whether there is an association with prognosis and/or high-risk disease. For our MM cohort (n=39, excluding samples without OS information and serial samples), samples were divided into high and low concentration groups based on the median value for each of the four biomarkers. Survival analysis revealed a clear trend towards decreased overall survival in those with a high plasma concentration of VCAM1 and ELA2, although this did not reach significance (**Figure 6.8**).

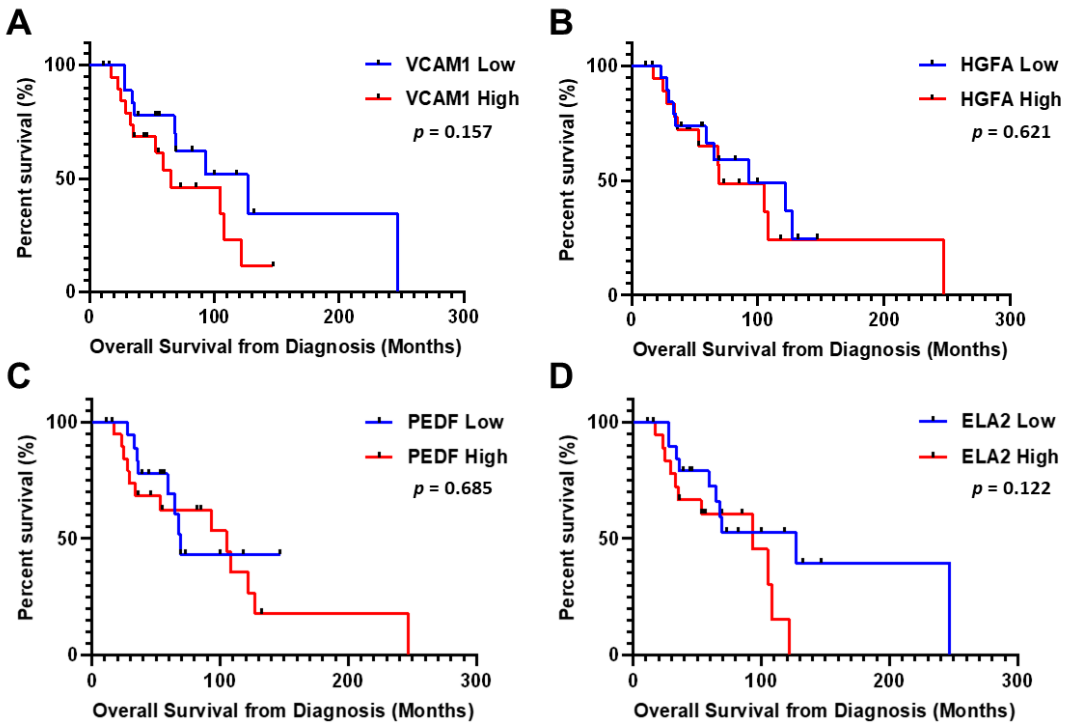

Figure 6.8: Survival analysis of MM patient samples to identify the prognostic potential of circulating plasma proteins. Kaplan–Meier curves illustrating the OS of MM patients with high/low plasma concentrations of (**A**) VCAM1, (**B**) HGFA, (**C**) PEDF, and (**D**) ELA2. Samples were divided based on median expression levels.

Cytogenetic abnormalities are commonly used for risk stratification of MM patients. The presence of high-risk cytogenetic abnormalities (HRCAs) which include t(4;14), t(14;16), t(14;20), 1q gain, and del(17p), are well-established predictors of a poor prognosis. To determine whether the plasma concentrations of the four potential biomarkers were linked to HRCAs, plasma concentrations in MM patients with none, one or two or more HRCAs was compared (**Figure 6.9**). No significant changes were seen between the three groups for any of the four proteins evaluated, however, plasma concentrations of HGFA showed an almost significant increase in patients with two or more HRCAs when compared to those with zero or one HRCA. The association of plasma protein concentrations with the presence of individual HRCAs was also analysed. Interestingly, the presence of the HRCA, del(17p) which often results in the loss of the *TP53* gene, was associated with a significant increase in VCAM1 and HGFA plasma levels, and an almost significant ($p = 0.072$) increase in PEDF plasma levels (**Figure 6.9**).

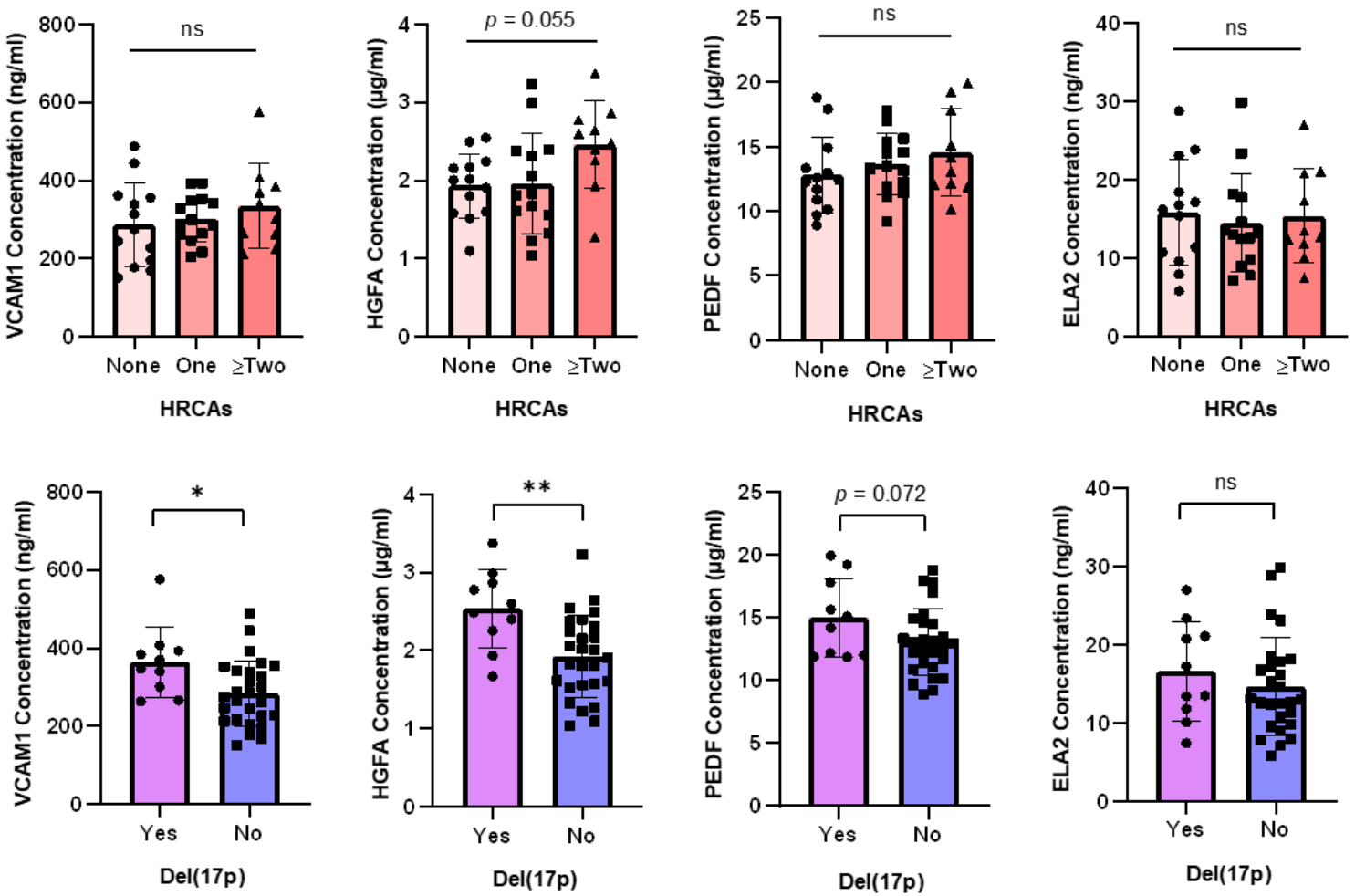

Figure 6.9: Association of VCAM1, HGFA, PEDF, and ELA2 plasma concentrations with high-risk cytogenetic abnormalities (HRCAs). The plasma levels of these four proteins were compared in MM patients with none, one, or two or more HRCAs. HRCAs include t(4;14), t(14;16), t(14;20), 1q gain, and del(17p). Significance is marked as follows: ns 'not significant', $p \leq 0.05$ '*', $p \leq 0.01$ '**'.

6.3.6 Association of VCAM1, HGFA, PEDF, and ELA2 plasma concentrations with drug response

Plasma levels of VCAM1, HGFA, and PEDF were evaluated in the MM patient cohort stratified into four groups based on *ex vivo* DSRT, Group 1 (most sensitive), Group 2 (sensitive), Group 3 (resistant), and Group 4 (very resistant). HGFA, PEDF and ELA2 plasma concentrations did not show a significant change between the four chemosensitivity groups. Results of the ANOVA test of VCAM1 concentrations across the four groups found a significant change ($p = 0.045$) in VCAM1 levels (**Figure 6.10**). The highest concentrations of VCAM1 were found in Group 1, a group considered to be very sensitive to drug treatment. Previous studies have reported that patients within Group 1 had a significantly lower OS when compared to Groups 2, 3, and 4 (Majumder *et al.* 2017; Tierney, Bazou, Majumder, *et al.* 2021). As increased plasma concentrations of VCAM1 correlate with advanced disease and poor survival, this may explain why we see the increase in VCAM1 plasma concentrations in Group 1 samples (Terpos *et al.* 2016).

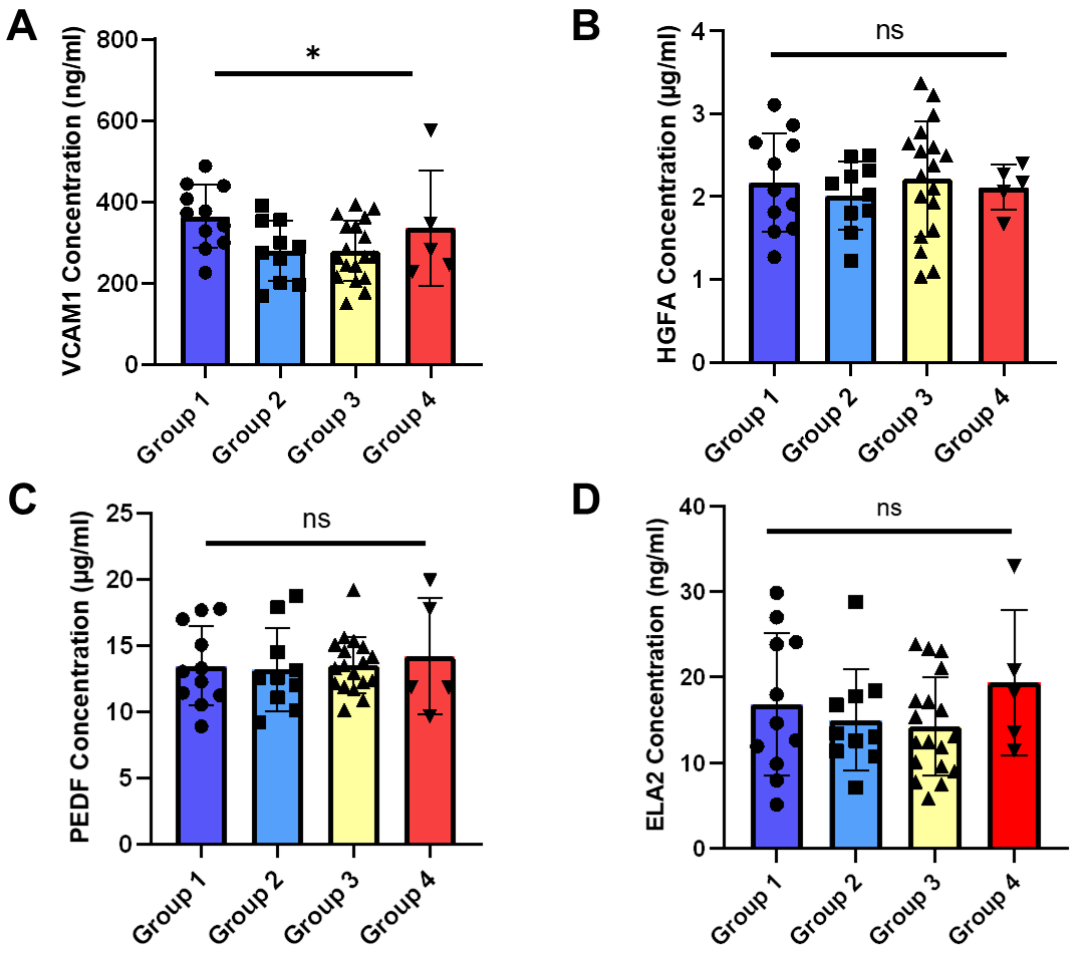

Figure 6.10: Plasma concentrations of VCAM1, HGFA, PEDF, and ELA2 in MM patients stratified based on *ex vivo* drug sensitivity resistance testing (DSRT). (**A**) VCAM1, (**B**) HGFA, and (**C**) PEDF plasma concentrations across four chemosensitivity groups. Significance is marked as follows: ns 'not significant', $p \leq 0.05$ '*'.

Pearson's correlation analysis was applied to evaluate whether plasma concentrations of VCAM1, HGFA, PEDF, and ELA2 correlated with patient sensitivity to individual drugs based on the individual DSS (**Supp. File 6.1**). Individual DSSs of 14 drugs significantly correlated with VCAM1 plasma concentrations, DSSs of 3 drugs significantly correlated with PEDF plasma concentrations and HGFA and ELA2 plasma concentrations did not show significant correlations with any individual DSSs (**Table 6.3**). Based on the DSSs of individual drugs found to significantly correlate with VCAM1 and PEDF plasma concentrations, samples were separated into quartiles with those samples falling into the first quartile being considered "Most Resistant" and those in the fourth quartile being considered "Most Sensitive". Unpaired t-test analyses revealed circulating VCAM1 to be increased in the plasma of MM patients considered most sensitive to fedratinib, NMS-873, navitoclax, and venetoclax, while circulating PEDF was

increased in the plasma of MM patients considered most resistant to fedratinib, SGC-CBP30, and TPCA-1 (**Figure 6.11**). Interestingly, increased plasma VCAM1 levels were associated with sensitivity to both BCL2 inhibitors, navitoclax and venetoclax. Higher levels of sVCAM1 weakly correlated with increased sensitivity to venetoclax and navitoclax (Pearson's correlation coefficient r = 0.38 (p = 0.0116) and r = 0.44 (p = 0.0026), respectively) (**Figure 6.12A&B**). Furthermore, one patient from this cohort had an EMM diagnosis at the time of sampling and therefore had corresponding DSS values available. As expected, this patient was found to be resistant to many of the drugs tested. Interestingly, this sample was highly sensitive to navitoclax and demonstrated some sensitivity to the other BCL-2 inhibitors tested, AT 101, venetoclax and obatoclax (**Figure 6.12C**).

Table 6.3: Summary of significant correlations between individual drug sensitivity scores and plasma concentrations of VCAM1, HGFA, PEDF, and ELA2. Correlation coefficients were determined using Pearson correlation analysis.

Drug	Mechanism/Target	Circulating protein	Correlation coefficient	*p*-value
APR-246	p53 activator	VCAM1	0.3142	0.0378
BX-912	PDK1 inhibitor	VCAM1	0.3544	0.0397
Fedratinib	JAK2 inhibitor	VCAM1	0.5436	0.0009
GSK-1838705A	IGF1R, INSR, ALK inhibitor	VCAM1	0.4099	0.016
Idasanutlin	p53-MDM2 inhibitor	VCAM1	0.3887	0.0231
Navitoclax	Bcl-2, Bcl-XL inhibitor	VCAM1	0.443	0.0026
NMS-873	p97/VCP inhibitor	VCAM1	0.3977	0.0198
Pimasertib	MEK1/2 inhibitor	VCAM1	0.3093	0.041
Refametinib	MEK1/2 inhibitor	VCAM1	0.3227	0.0327
Selumetinib	MEK1/2 inhibitor	VCAM1	0.3154	0.037
Trametinib	MEK1/2 inhibitor	VCAM1	0.3471	0.021
SGC-CBP30	CREBBP/EP300 bromodomain inhibitor	VCAM1	0.5019	0.0025
Topotecan	Topoisomerase I inhibitor	VCAM1	0.316	0.0366
Venetoclax	Bcl-2 inhibitor	VCAM1	0.3772	0.0116
Fedratinib	JAK2 inhibitor	PEDF	-0.4177	0.014
SGC-CBP30	CREBBP/EP300 bromodomain inhibitor	PEDF	-0.4203	0.0133
TPCA-1	IKK-2 inhibitor	PEDF	-0.4782	0.0042

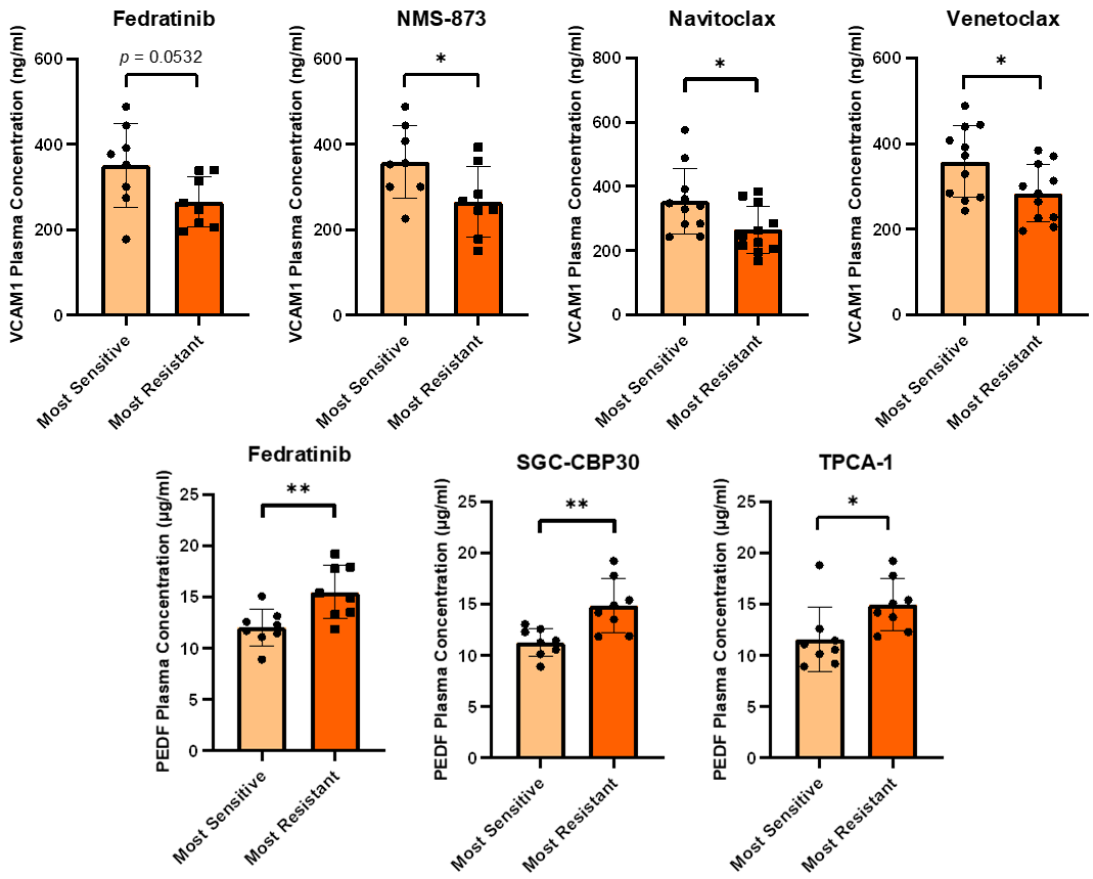

Figure 6.11: Association of plasma concentrations of VCAM1 and PEDF with drug response. Plasma concentrations of VCAM1 are increased in MM patients consider most sensitive to fedratinib, NMS-873, navitoclax and venetoclax based on *ex vivo* DSRT. Plasma concentrations of PEDF are increased in MM patients considered most resistant to fedratinib, SGC-CBP30 and TPCA-1 based on *ex vivo* DSRT. Significance is marked as follows: ns 'not significant', $p \leq 0.05$ '*', $p \leq 0.01$ '**'.

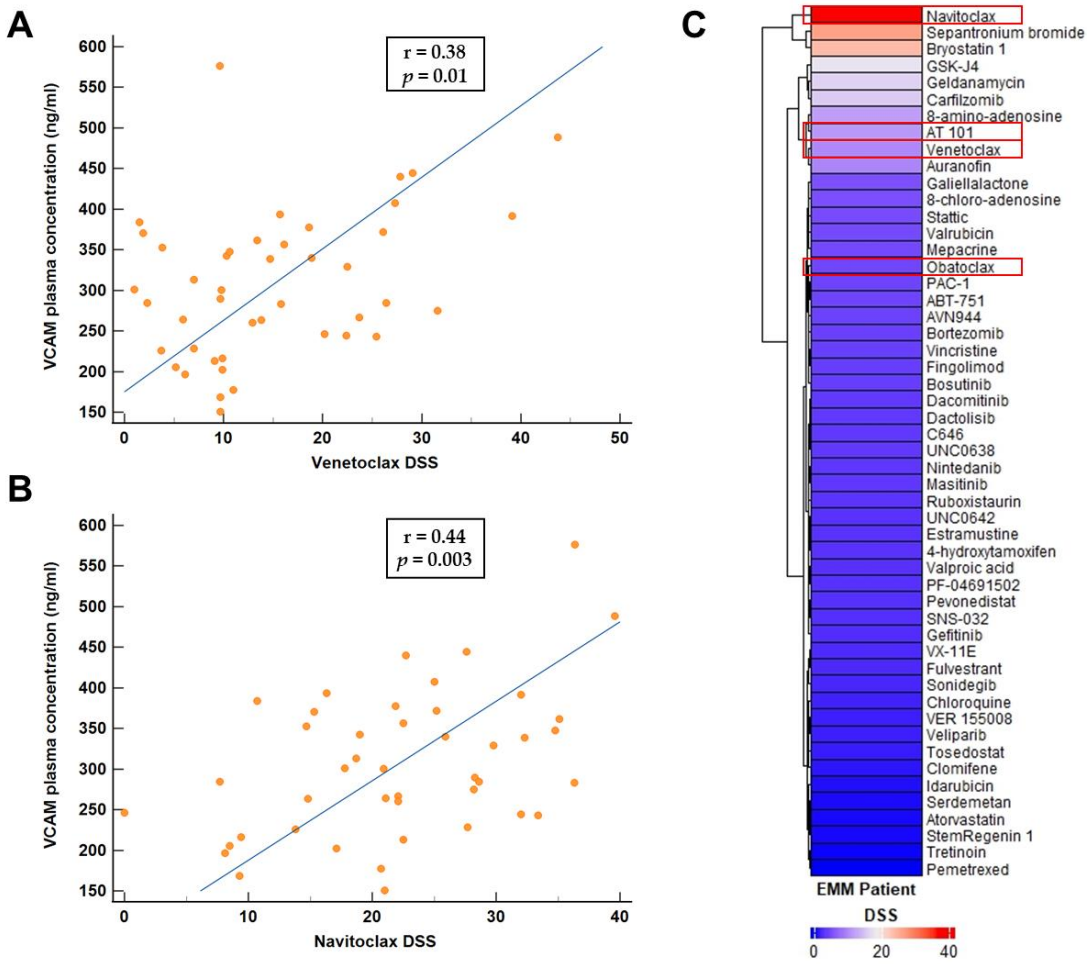

Figure 6.12: Correlation of VCAM1 plasma concentrations with BCL2 inhibitor sensitivity. (**A**) Correlation between VCAM1 plasma concentration and venetoclax DSSs. (**B**) Correlation between VCAM1 plasma concentration and navitoclax DSSs. (**C**) Heatmap illustrating the varying DSS scores of an EMM patient. Drugs with DSS = 0 were removed from this figure. Drugs from the BCL2 inhibitor drug family are highlighted by the red boxes.

6.3.7 Targeted proteomic analysis of EMM plasma using the PEA-based Olink Target 48 Cytokine panel

Finally, we investigated the concentrations of 45 cytokines in EMM (n=8) and MM (n=25) plasma. Statistical analysis identified three statistically significantly differentially abundant proteins between EMM and MM plasma samples (**Figure 6.13**)(**Supp. File 6.2**). Plasma levels of interleukin-10 (IL-10) and interleukin-6 (IL-6) were significantly increased in EMM compared to MM plasma. An almost 14-fold and almost 2-fold increase in IL-10 and IL-6 were quantified in EMM plasma, respectively. Interleukin-17C was significantly decreased in EMM plasma compared to MM plasma, showing an almost 4-fold decrease. ROC curve analysis of IL-10,

IL-6, and IL-17C was performed and found that these cytokines had the ability to discriminate between EMM and MM patients in this cohort (IL-10 AUC = 0.805, CI = 0.630-0.922; IL-6 AUC = 0.73; CI = 0.558-0.876; IL-17C AUC = 0.76, CI = 0.580-0.891). A combination of IL-10, IL-6, and IL-17C as a panel revealed an improved AUC value of 0.915 (**Supp. Figure 6.1**). This analysis shows quite large variations in the plasma cytokine concentration within the EMM samples, suggesting that while IL-10, IL-6, and IL-17C show promise as potential markers of EMM, certain EMM patients may present with cytokine concentrations similar to those seen in the MM cohort.

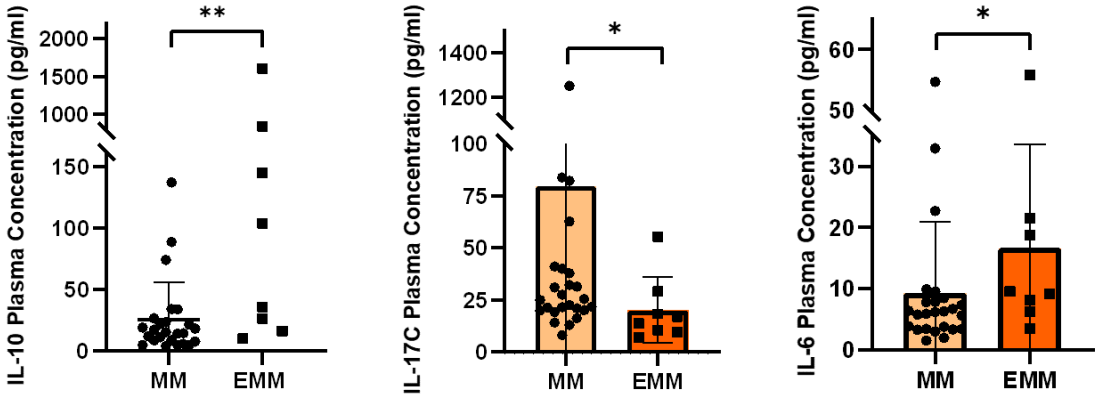

Figure 6.13: Plasma concentrations of statistically significantly differentially abundant cytokines as determined by proximity extension targeted proteomics assay. Levels of interleukin-10 (IL-10) and interleukin-6 (IL-6) were significantly increased in EMM plasma compared to MM plasma. Interleukin-17C (IL-17C) was significantly decreased in EMM plasma compared to MM plasma. Statistical analysis was performed using a Mann Whitney U test ($p < 0.05$).

6.4 Discussion

Blood-based biomarkers are of vital importance in the clinical evaluation of many diseases, including multiple myeloma. The levels of serum monoclonal protein, serum calcium, serum creatinine, and serum free light chains aid MM diagnosis. Furthermore, serum albumin, serum beta-2-microglobulin, and serum lactate dehydrogenase aid risk stratification of MM patients (Rajkumar 2022). Extramedullary lesions have been reported to develop via the hematogenous spread of MM cells to distal sites, highlighting the potential of serum/plasma as a source of EMM biomarkers (Bladé *et al.* 2011; Rosiñol *et al.* 2014). Enhanced sensitivities of imaging modalities have improved EMM diagnosis, resulting in an increased incidence of EMM in recent years. However, current imaging techniques have

several drawbacks including high cost, limited availability and lack of imaging standardization (Moreau *et al.* 2017; Filho *et al.* 2019). Novel blood-based protein markers for EMM that demonstrate high sensitivity and specificity are required to detect the emergence of EMM clones at an early stage. In this chapter, mass spectrometry analysis, immunoassays, and PEA-based assays have identified alterations in the plasma proteome of MM patients with and without extramedullary lesions, highlighting a phenotypic change occurring between these disease states. Particularly, VCAM1, HGFA, and PEDF were identified as promising markers of extramedullary multiple myeloma as they were found to be significantly elevated in abundance in EMM plasma by two orthogonal methods: LC-MS/MS and ELISA.

VCAM1 (also known as CD106) is a 90kDa glycoprotein and member of the IgG immunoglobulin family (Okugawa *et al.* 2010). VCAM1 is expressed primarily in endothelial cells but also in other cell types including bone marrow stromal cells, thymic epithelial cells, and certain populations of dendritic cells (Osborn *et al.* 1989; Rice and Bevilacqua 1989; Koopman *et al.* 1991; Salomon *et al.* 1997). VCAM1 is an inducible transmembrane protein that mediates leukocyte adhesion and migration, particularly during periods of high inflammation (Kong *et al.* 2018). Numerous studies have established VCAM1 as a contributor to inflammatory diseases, such as rheumatoid arthritis, and various cancers, including breast cancer, ovarian cancer, and multiple myeloma (Wilkinson *et al.* 1993; Michigami *et al.* 2000; Chen *et al.* 2011; Huang, Zhang, *et al.* 2013). The most studied VCAM1 binding partner is integrin α4β1 (also known as very late antigen-4, VLA4), although VCAM1 has shown some affinity for integrins α4β7, αMβ2, α9β1, and αDβ2 (Walsh *et al.* 1996; Grayson *et al.* 1998; Barthel *et al.* 2006; Kon *et al.* 2011). The interaction between VCAM1 and VLA4 has been widely implicated in cancer metastasis through the mediation of adhesion and vascular extravasation of tumour cells (Okahara *et al.* 1994; Sökeland and Schumacher 2019). In MM, the VCAM1-VLA4 interaction mediates the attachment of MM cells to bone marrow stromal cells within the BME, contributing to cell adhesion-mediated drug resistance in MM (Sanz-Rodríguez *et al.* 1999).

The extracellular domain of VCAM1 can be cleaved by certain members of the disintegrin and metalloproteinase protease family, including tumor necrosis factor-α-

converting enzyme (TACE, also known as ADAM17) (Garton *et al.* 2003). This cleavage process is regulated by tissue inhibitor of metalloproteinase (TIMP)-3 (Singh *et al.* 2005). The soluble form of VCAM1 (sVCAM1) can be detected in the serum or plasma and has been reported to be significantly increased in abundance in a number of malignancies (Banks *et al.* 1993). Furthermore, increased circulating VCAM1 levels have been proposed as promising prognostic markers in pancreatic cancer, prostate cancer, bladder cancer, ovarian cancer and multiple myeloma (Coskun *et al.* 2006; De Cicco *et al.* 2008; Takahashi *et al.* 2020; Song *et al.* 2023). Levels of sVCAM1 are increased in MM patients with advanced disease, with ISS-3 patients demonstrating higher levels of circulating VCAM1 when compared to ISS-1 and ISS-2 patients. Furthermore, increased sVCAM1 levels were associated with an inferior OS (Terpos *et al.* 2016). Our results also demonstrate the association of high circulating VCAM1 levels with an aggressive MM phenotype and show a trend ($p = 0.175$) towards a poorer overall survival in MM patients with high plasma VCAM1 concentrations.

C-X-C chemokine receptor type 4 (CXCR4) is a pleiotropic receptor widely reported to regulate extramedullary myeloma, albeit with contradicting results whereby certain studies have reported an increased expression of CXCR4 in EMD-prone myeloma cells which induces an EMT-like signature whereas others have reported a decreased expression of CXCR4 in EMD mouse models and in EMM patients which disrupts cell adhesion and homing in the bone marrow (Stessman *et al.* 2013; Roccaro *et al.* 2015; Weinstock *et al.* 2015; Marchica *et al.* 2017). Interestingly, CXCR4 was found to induce VCAM1 cleavage, thus increasing sVCAM1 levels, in non-small cell lung cancer via the regulation of the metalloproteinase, ADAM17 (Liao *et al.* 2018). The ablation of VLA4, the main binding partner of VCAM1, in MM cells has been reported to increase extramedullary disease burden, suggesting that a reduction in VLA4 or the VLA4-VCAM1 interaction may induce the egress of B cells into circulation (Hathi *et al.* 2022). Furthermore, an association between increased sVCAM1 levels and metastasis has been identified in numerous cancers (Silva *et al.* 2006; Okugawa *et al.* 2010; Tas *et al.* 2014). The mechanism by which circulating VCAM1 is linked to metastatic progression is unknown, however sVCAM1 has been identified as a chemotactic agent which induces the migration of several immune cells (Kitani *et al.* 1998; Tokuhira *et al.* 2000). In our study, the

origin of increased levels of circulating VCAM1 in EMM plasma is unknown and may derive from the shedding of VCAM1 from the surface of MM cells or from other cells known to express VCAM1, such as activated endothelial cells. Nonetheless, sVCAM1 represents a promising marker of EMM and warrants further investigation in a larger cohort of samples.

This work also found a link between plasma VCAM1 concentrations and response to selected drugs based on *ex vivo* DSRT. Increased sVCAM1 concentrations were associated with increased sensitivity to the JAK2 inhibitor, fedratinib, the valosin-containing protein (VCP) inhibitor, NMS-873, and the BCL2 inhibitors, navitoclax and venetoclax. IL-6/JAK/STAT signalling results in the downstream activation of the PI3K-AKT signalling pathway, the MAPK signalling pathway, and an upregulation of anti-apoptotic proteins in MM (Puthier *et al.* 1999; Harmer *et al.* 2019). Despite this, no JAK inhibitors have been approved for the treatment of MM. A study describing the biomarker profile of JAK2 inhibitors found that exposure to fedratinib resulted in a decrease in inflammation-linked proteins including VCAM1, eotaxin 3 and MIG (Singer *et al.* 2019). Combined with our results, this may indicate that tumour microenvironments with high expression of VCAM1 may be more susceptible to fedratinib treatment. Interestingly, increased levels of sVCAM1 correlated with increased sensitivity to two BCL-2 inhibitors, venetoclax and navitoclax, indicating a potential correlation with BCL-2 expression. VCAM1 and BCL2 are target genes of the NF-κB signalling pathway (Catz and Johnson 2001; Astarci *et al.* 2012). High NF-κB activity in MM may be stimulated by intrinsic and extrinsic processes. Activating mutations in the NF-κB pathway have been suggested to be late progression events which result in autonomous NF-κB pathway activation and reduced dependence on the bone marrow microenvironment (Demchenko *et al.* 2010; Cippitelli *et al.* 2023). Enhanced NF-κB activation may increase sVCAM1 and BCL2 levels, leading to increased susceptibility to BCL2 inhibitors, and making sVCAM1 a potential surrogate plasma-based biomarker of response to BCL-2 inhibitors. However, studies have reported an association between NF-κB pathway activation and venetoclax resistance in chronic lymphocytic leukemia (CLL) (Thijssen *et al.* 2022). Further studies in a larger cohort of patients are required to evaluate the link between sVCAM1 concentrations and response to BCL2 inhibitors.

Furthermore, the link between EMM and the constitutive activation of the NF-κB has yet to be evaluated.

Hepatocyte growth factor (HGF) is initially synthesized as an inactive precursor protein which is subsequently converted to its active form by proteolytic cleavage. Active HGF binds to its specific ligand receptor tyrosine kinase (MET), transducing pleiotropic signals that promote cell growth, survival, and migration in the target cell (Bottaro *et al.* 1991; Kataoka *et al.* 2018). HGF is a well-known tumour-promoting growth factor which contributes to tumorigenesis and disease progression by promoting proliferation, invasion, and the survival of tumour cells. Several proteases including HGFA, matriptase and hepsin have been identified as HGF activating proteases (Kataoka *et al.* 2003; Owen *et al.* 2010). HGFA is a trypsin-like serine endopeptidase, initially synthesized as an inactive zymogen which is subsequently catalysed to its active form via limited proteolysis (Shimomura *et al.* 1993). Increased serum/plasma levels of HGF and HGFA have been identified in various cancers including prostate cancer and multiple myeloma (Nagakawa *et al.* 2005; Wader *et al.* 2008; Sugie *et al.* 2016). Interestingly, breast cancer patients with lymph node involvement showed higher HGFA levels than those without lymph node involvement, indicating some link between HGFA expression and cancer metastasis (Parr *et al.* 2004).

Previous studies have found that serum and plasma HGF concentrations are elevated in MM patients compared to healthy controls, and are linked to an unfavourable prognosis in MM. (Seidel *et al.* 1998; Iwasaki *et al.* 2002; Rampa *et al.* 2014). Myeloma cell lines and primary MM cells have been reported to secrete HGFA which catalyses the activation of HGF secreted in an autocrine manner by MM cells or in a paracrine manner by stromal cells within the BME (Borset *et al.* 1996; Takai *et al.* 1997; Tjin *et al.* 2004). In contrast, a 2013 study found no expression of the HGFA gene in bone marrow biopsies from healthy volunteers, MGUS or MM patients. Interestingly, the MM cell line and primary MM cells analysed in the former study were derived from extramedullary lesions, suggesting a possible production of HGFA at extramedullary sites but not within the bone marrow microenvironment (Kristensen *et al.* 2013). This may explain the increase in

circulating HGFA levels in EMM patients compared to MM patients, although further studies are required to confirm this.

PEDF, or Serpin family F member 1 (SERPINF1), is a 50 kDa monomeric glycoprotein with neuroprotective, antiangiogenic, metabolic, and osteogenic biological properties (Apte *et al.* 2004; Rauch *et al.* 2012; Carnagarin *et al.* 2015; Bürger *et al.* 2020). Despite being a member of the serine protease inhibitor (serpin) superfamily, PEDF does not exhibit serine protease inhibitory activity. Various studies and reviews have described the antitumorigenic, antimetastatic, and antiangiogenic roles of PEDF in retinoblastoma, prostate cancer, pancreatic cancer, gastric cancers and others (Yang *et al.* 2009; Hirsch *et al.* 2011; Zhang *et al.* 2011; Ansari *et al.* 2019). PEDF binding to its putative receptors, adipose triglyceride lipase (ATGL) and laminin receptor (LR), has been reported to trigger antitumorigenic mechanisms including reduced angiogenesis via downregulation of VEGF, reduced proliferation, and the induction of apoptosis (Guan *et al.* 2007; Yang and Grossniklaus 2010; Tsuruhisa *et al.* 2021). Interestingly, the tumour-suppressive role of PEDF has stimulated studies evaluating PEDF as a cancer therapy (Hase *et al.* 2005; Honrubia-Gómez *et al.* 2019; Bao *et al.* 2020). However, several papers have reported PEDF as an oncogene and contributor to cancer progression, highlighting the complex and bidirectional functions of PEDF in different cancers (Hou *et al.* 2017; Tang *et al.* 2020; Ueno *et al.* 2022). Regarding circulating PEDF, low serum levels of PEDF were associated with various cancers, and found to correlate with a poor overall survival in colorectal cancer (Becerra and Notario 2013; Ji *et al.* 2013; Rivera-Pérez *et al.* 2018). However, increased circulating PEDF concentrations have been reported in hepatocellular cancer and gastric cancer when compared to healthy controls (Kawaguchi *et al.* 2010; Aksoy *et al.* 2019).

In MM, PEDF was found to inhibit VEGF-induced proliferation of U266 myeloma cell via the suppression of $p22^{phox}$, a membrane protein and component of the ROS-generating NADPH oxidase system. PEDF reduced ROS generation, prevented VEGF-reduced apoptosis and inhibited VEGF-induced proliferation of U266 myeloma cells (Seki *et al.* 2013). In this chapter, we found a significant increase in plasma PEDF levels in EMM patients compared to MM patients, indicating a potential association between PEDF levels and the migration of myeloma cells from

the bone marrow and colonization of distal sites. A recent review highlighted the contradictory reports on the role of PEDF in metastasis, suggesting a link between PEDF function and tissue type (Abooshahab *et al.* 2021). Two studies investigating hepatocellular carcinoma and oesophageal squamous cell carcinoma found that elevated levels of PEDF promoted metastasis and an EMT phenotype, as illustrated by the downregulation of E-cadherin and upregulation of N-cadherin, through the activation of MAPK/ERK signaling (Hou *et al.* 2017; Chen, Che, *et al.* 2021). In EMM, CXCR4 has been reported to regulate EMM through the transcriptional activation of an EMT-like signature including the downregulation of E-cadherin and upregulation of Snail, Slug, and Twist (Roccaro *et al.* 2015). PEDF may play a role in promoting an EMT-like signature in the context of EMM. Interestingly, a recent study found that overexpression of PEDF in osteosarcoma promoted mesenchymal-to-epithelial transition (MET) which can stimulate the development of metastatic lesions. Despite promoting MET, PEDF overexpression was also found to induce extravasation (Kuriyama *et al.* 2022). Given the complex and often contradictory functions of PEDF, an in-depth, focused investigation is required to determine the specific role of PEDF in the extramedullary transition of MM.

Although not identified in our mass spectrometry analysis of EMM plasma, ELA2 was evaluated in EMM plasma as a marker of NETs in Chapter 5. ELA2 was significantly increased in EMM plasma and ROC curve analysis found ELA2 had excellent discriminatory power (AUC =0.965) and represented a potential marker of EMM. In addition to its role in relation to NETs, ELA2 has independently been linked to tumorigenesis in a variety of cancers (Ho *et al.* 2014; Lerman and Hammes 2018; Ardi *et al.* 2020; Taya *et al.* 2020). As described previously, neutrophils play a role in carcinogenesis and metastasis. Studies focusing on ELA2, a neutrophil protease, have highlighted the role of ELA2 in promoting the metastatic potential of various cancers (Doi *et al.* 2002; Houghton *et al.* 2010). Interestingly, tumours supplemented with active ELA2 demonstrated increased angiogenesis, tumour cell intravasation and liver metastasis in a modified chorioallantoic membrane model. ELA2 enhanced chemotactic migration of tumour cells, in an enzymatic activity-dependent process and was required for the retention of vascular-arrested tumour cells in the lungs of mice (Deryugina *et al.* 2020). However, whether ELA2 participates in this early metastatic process in EMM remains unclear. The role of

ELA2 in NET-mediated metastasis has been described in Chapter 5. Interestingly, ELA2 has been shown to cleave VCAM1 from the surface of bone marrow stromal cells (BMSCs) during the mobilization of hematopoietic progenitor cells following G-CSF treatment, highlighting a potential link between ELA2 and VCAM1 shedding during metastasis (Lévesque *et al.* 2001).

Another interesting finding in this study was the association between increased plasma levels of VCAM1, HGFA, and PEDF and the high-risk cytogenetic abnormality, del(17p). The loss of the short arm of chromosome 17, detected by FISH, is found in approximately 10-15% of NDMM and RRMM patients (Liu *et al.* 2017). The well-known tumour suppressor, *TP53,* is located within this deleted region, leading to its monoallelic deletion (Flynt *et al.* 2020). A recent study found that biallelic inactivation of TP53 due to combined del(17p) and TP53 mutation exhibits an extremely poor prognosis, while isolated del(17p) also exhibits a poor prognosis in MM (Corre, Perrot, *et al.* 2021). P53 is a key tumour suppressing protein which promotes cell cycle arrest or apoptosis following DNA damage. Several studies have reported an association between the deletion of 17p and extramedullary involvement in MM (Chang *et al.* 2004; López-Anglada *et al.* 2010; Billecke *et al.* 2013; Besse *et al.* 2016). In addition, del(17p) is a common cytogenetic abnormality in plasma cell leukemia (PCL), occurring in up to 50% of primary PCL tumours and up to 75% of secondary PCL tumours (Tiedemann *et al.* 2008). Combined with our results, this suggests that myeloma subclones with del(17p) may have a higher propensity for dissemination from the bone marrow, increasing the likelihood of developing aggressive, advanced forms of MM (Zeissig *et al.* 2020). The association between increased plasma concentrations of VCAM1, HGFA, and PEDF, del(17p), and extramedullary multiple myeloma, is unknown and warrants further research.

The evaluation of the plasma cytokine profile of EMM patients compared to MM patients identified IL-10, IL-6, and IL-17C as being differentially abundant between the two groups. IL-10 is a pleiotropic, anti-inflammatory cytokine reported to have immunosuppressive effects within the tumour microenvironment (Musolino *et al.* 2017). IL-10 is a proliferation factor in MM and has been found to correlate with angiogenic and proliferation markers (Alexandrakis *et al.* 2015). High levels of

circulating IL-10 in NDMM patients have been associated to a worse PFS and overall OS (Wang, Wang, *et al.* 2016). Furthermore, a recent study evaluating the link between serum IL-10 levels and MM disease progression reported IL-10 levels to be significantly increased in EMM patients compared to MM patients without extramedullary involvement, supporting our results that IL-10 is increased in EMM plasma. Within the tumour microenvironment, IL-10 is known to induce M2 macrophages, specifically the M2c subset of M2 macrophages which have been implicated in process of tumour immunosuppression and tumour invasion in cancer (Mantovani *et al.* 2004; Yuan *et al.* 2015). Circulating IL-6 levels have also been reported to correlate with disease progression in MM (Bataille *et al.* 1989; Nachbaur *et al.* 1991). Despite these early studies highlighting the involvement of IL-6 in MM progression, the inhibition of IL-6 in advanced MM patients with EMM or PCL did not yield prolonged therapeutic efficacy (Bataille *et al.* 1995). Interestingly, IL-6 has been reported to induce M2 macrophage differentiation resulting in increased levels of IL-10 (Fu *et al.* 2017). IL-17C is a pro-inflammatory cytokine that has been implicated in carcinogenesis and tumour progression (Jungnickel *et al.* 2017; Brevi *et al.* 2020). Studies relating circulating IL-17C levels to cancer development and progression are limited. In addition, the role of IL-17C in MM is unknown highlighting the need for further research on IL-17C in the MM field.

The combination of HGFA, VCAM1, PEDF, and ELA2 as a four-marker panel demonstrated excellent ability to distinguish between EMM and MM patients. As biomarker panels tend to perform better in terms of specificity and sensitivity, this panel of EMM markers warrants validation as a method to detect EMM at an early stage. Furthermore, the identification of IL-10, IL-6, and IL-17C as differentially abundant cytokines in EMM plasma highlights a potential change in the plasma cytokine profile of EMM patients compared to those without extramedullary involvement. Despite the small sample size, the potential protein biomarkers identified in our study provides a basis for future studies with larger sample sizes to validate their clinical applicability. Many recent studies highlight the need for clinical trials specific for EMM, which presents a potential source of a large cohort of EMM patients for validation. In addition, future mechanistic studies involving these proteins will provide insight into the cellular processes that may contribute to

the differential levels of the proteins and cytokines identified in this study in EMM plasma.

6.5 Conclusion

To the best of my knowledge, this study using label-free mass spectrometry to identify novel markers of extramedullary multiple myeloma in blood plasma is the first of its kind. This body of work contributes to our understanding that EMM is a phenotypically distinct form of MM. Furthermore, evaluating the concentrations of the plasma proteins, VCAM1, HGFA, PEDF, and ELA2, may distinguish MM patients with and without extramedullary lesions. Monitoring these plasma-based biomarkers represents a low-cost, minimally invasive approach to quantify markers of extramedullary spread at follow-up appointments using minimal resources. Upon detection of high levels of EMM markers, patients may be further evaluated using imaging tests to confirm the presence of extramedullary lesions and treated accordingly. Incorporating the measurement of these blood plasma biomarkers in future EMM specific trials to monitor response to therapy may yield clinically relevant findings. As more EMM specific therapeutic regimes hopefully become available, the ability to switch between effective and ineffective treatments quickly based on monitoring biomarker profiles will be important.

Chapter 7

Targeted metabolomic analysis of blood plasma from multiple myeloma patients with and without extramedullary spread

7.1 Introduction

Metabolomics refers to the identification and quantitation of metabolites with a molecular weight <1500 Da in cells, tissues and/or biofluids. Almost a century ago, Otto Warburg first discovered the link between cancer and metabolism by describing the increased consumption of glucose by cancer cells to support sustained proliferation (Warburg *et al.* 1927). Since then, additional hallmarks of cancer cell metabolism have been identified including the deregulation of glucose and amino acid uptake, use of TCA cycle intermediates for the synthesis of macromolecules, and metabolic interactions with the tumour microenvironment (Hosios *et al.* 2016; Anderson *et al.* 2018; Dey *et al.* 2021; Pavlova *et al.* 2022). Metabolomics investigates the downstream products of the genome, transcriptome, and proteome, highlighting the key role of this "omic" technology in identifying phenotypic alterations. The complete set of metabolites in a biological sample is referred to as the metabolome. The presence/absence and concentration of these metabolites reflect the biochemical events occurring in an organism at a given time, thus providing a valuable source to analyse metabolic changes in various physiological or pathological conditions (Schmidt *et al.* 2021).

In recent years, metabolomics has garnered increasing attention as a promising technology in precision medicine (Clish 2015). Improvements in diagnostics, prognostics and treatment decision-making are possible through the identification of metabolic signatures or phenotypes associated with specific disease characteristics. Recent studies have highlighted the contribution of metabolomics to the goal of precision medicine by identifying metabolic signatures associated with various pathological conditions including coronary disease, breast cancer, type 2 diabetes, and coronavirus disease (Tam *et al.* 2017; Jiang *et al.* 2020; Julkunen *et al.* 2021; Xiao *et al.* 2022; Shah, Steffen, *et al.* 2023). As metabolites are frequently involved in or produced by disease pathways, they represent promising diagnostic, prognostic, and predictive biomarkers (Qiu *et al.* 2023). Biochemical assays are commonly employed for the measurement of specific proteins and metabolites in a clinical setting. Cholesterol and triglycerides are classic metabolite biomarkers evaluated to determine an individual's risk of adverse cardiovascular events (Kannel *et al.* 1971). Clinical metabolic testing has proved particularly useful in the detection of inborn

errors of metabolism (IEMs), a large group of inherited neurometabolic disorders. For example, diagnosis of the rare IEM, adenylosuccinate lyase deficiency, is based on the detection of succinylaminoimidazole carboxamide riboside and succinyladenosine in the plasma, urine, or cerebrospinal fluid of affected individuals (Donti *et al.* 2016).

Similar to proteomics, metabolomic technologies are unable to detect all metabolites in a given sample, a process hampered by the chemical similarities of metabolites in the form of isomeric and isobaric compounds (Tolstikov *et al.* 2020). Nevertheless, metabolomic techniques have been developed and improved in recent years into powerful, high-throughput methods capable of analysing a wide variety of biological sources including tissue, blood, and urine. Analytical techniques commonly used in metabolomic analyses include the spectroscopic technique, nuclear magnetic resonance (NMR), and mass spectrometry coupled with chromatographic techniques. These techniques can be broadly categorized into untargeted and targeted approaches. Untargeted metabolomics is an unbiased, comprehensive method that aims to measure all detectable analytes in a sample, however, this approach can be encumbered by the large number of unidentifiable peaks. Targeted metabolomics measures a defined set of metabolites, but has the disadvantage of potentially missing the detection of physiologically relevant metabolites (Roberts *et al.* 2012).

In addition to proteins, biofluids also represent an abundant source of metabolites. Furthermore, the collection of biofluids such as serum, plasma, saliva, and urine are minimally invasive, which increases the likelihood of analytical tests on biofluids being adopted in a clinical setting (Marchand et al. 2018). Plasma provides a global view of the systemic metabolic state of an individual, which can be dysregulated in pathological conditions such as cancer. Another reason blood-based biofluids represent valuable sources of biomarkers in the context of multiple myeloma and extramedullary multiple myeloma, is the close spatial association between the tumour cells and whole blood. Metabolic profiling has yielded promising results in blood cancer research. Recent studies have highlighted the value of metabolomic profiling using ^{1}H NMR as a diagnostic and predictive tool for a number of hematological malignancies including acute lymphoblastic leukemia (ALL), AML and follicular lymphoma (Banoei *et al.* 2022; Morad *et al.* 2022). A recent review

article has also provided guidance on potential applications of single-cell metabolomics as a method to improve our understanding of hematological malignancies (Zuo *et al.* 2022).

Changes in the plasma metabolite profile of MM patients at premalignant, newly diagnosed, and relapsed/refractory stages of disease have previously been reported (Steiner *et al.* 2018). However, at the time of writing, no metabolomics studies have been published investigating plasma metabolomic changes in extramedullary multiple myeloma compared to medullary multiple myeloma. EMM develops due to the hematogenous spread of myeloma cells to distant sites. These circulating myeloma cells and the impact of tumour development in soft-tissue or organs may contribute to changes in the plasma metabolome. The quantitation of metabolite levels in the plasma of EMM and MM patients could indicate metabolic changes derived from the tumour tissue itself, generating potential plasma-based markers of EMM.

In this chapter, metabolites were isolated from EMM patients (n=9, one serial sample) and MM patients (n=8) plasma and evaluated by mass spectrometry using a targeted metabolomic approach. The aim of this study was to identify metabolic changes in the plasma of MM patients with and without extramedullary spread and evaluate metabolites as potential markers of EMM.

7.2 Experimental design

As highlighted in previous chapters, we have identified proteomic alterations in the bone marrow and plasma of patients with EMM compared to MM patients with extramedullary spread. Our study and research from other groups indicate a change in metabolism in malignant plasma cells from EMM patients (Sun *et al.* 2023). Evaluating alterations in the abundance of plasma metabolites may provide insight into systemic metabolism changes in EMM. Furthermore, the plasma metabolome may yield potential markers of extramedullary spread in MM patients.

7.2.1 Patient samples

A total of 17 EDTA plasma samples were obtained from the FHRB biobank. Plasma samples were collected from MM patients (n=8) and EMM patients (n=9, one serial

sample), as described previously. Samples were stored at -80ºC. Full patient details are outlined in Chapter 5.

7.2.2 Targeted metabolomics analysis of MM and EMM patient plasma

Targeted metabolomic analysis of MM and EMM blood plasma samples was performed using the MxP® Quant 500 kit (Biocrates Life Sciences AG, Innsbruck, Austria) with a SCIEX QTRAP 6500plus mass spectrometer, as described in Chapter 2. The MxP® Quant 500 kit is capable of quantifying more than 600 metabolites from 26 compound classes. QC samples were employed to monitor the performance of the analysis with metabolite concentration in each sample normalised based on these QC samples. Isotopically labelled internal standards and seven-point calibration curves were used in the quantitation of amino acids and biogenic amines. Semi-quantitative analysis of other metabolites was performed using internal standards. Data quality was evaluated by checking the accuracy and reproducibility of QC samples. Metabolites were included only when the concentrations of the metabolites were above the LOD in >75% of plasma samples. Data was imported into MetaboAnalyst 5.0 for further analysis. Feature filtering was performed based on relative standard deviation and the resulting data was log-transformed. Supervised statistical approaches were used to interrogate the data. Metabolites of interest were identified based on p-value < 0.05 between experimental groups, variable importance in the projection (VIP) > 1, and FC >1.2 or < 0.833. Metabolite sums and ratios were evaluated using Graphpad prism. ROC curves were plotted using MedCalc (MedCalc® Statistical Software version 22.006, Ostend, Belgium) with sensitivity values (true positive fraction) on the y-axis and the equivalent specificity values (false positive fraction) on the x-axis. AUC values with corresponding 95% confidence intervals were calculated to evaluate overall classifier effectiveness. As a general consensus, AUC values ranging from 0.5 to 0.7 are classified as poor, 0.7 to 0.8 as average, 0.8 to 0.9 as good and >0.9 as outstanding.

7.3 Results

7.3.1 Data collection and cleaning

Using a targeted metabolomic/lipidomic technique, we compared the metabolic profile of age and gender-matched MM and EMM patient plasma. A total of 630 metabolites were measured using the MxP® Quant 500 kit. Initial filtering of metabolites was performed based on the LOD, whereby metabolites were included if concentrations were above the LOD in >75% of plasma samples. As a result, 509 metabolites remained for further analysis. The distribution of these metabolites across the chemical classes are displayed in **Figure 7.1**. To illustrate changes in the metabolomic profiles between EMM and MM plasma samples, Spearman correlation analysis was performed on the log-transformed metabolite concentrations to create correlation matrices, as depicted in **Figure 7.2**. Stronger metabolite-metabolite correlations are evident in MM plasma compared to EMM plasma. Specifically, there is strong clustering of triacylglycerols in MM plasma compared to EMM plasma.

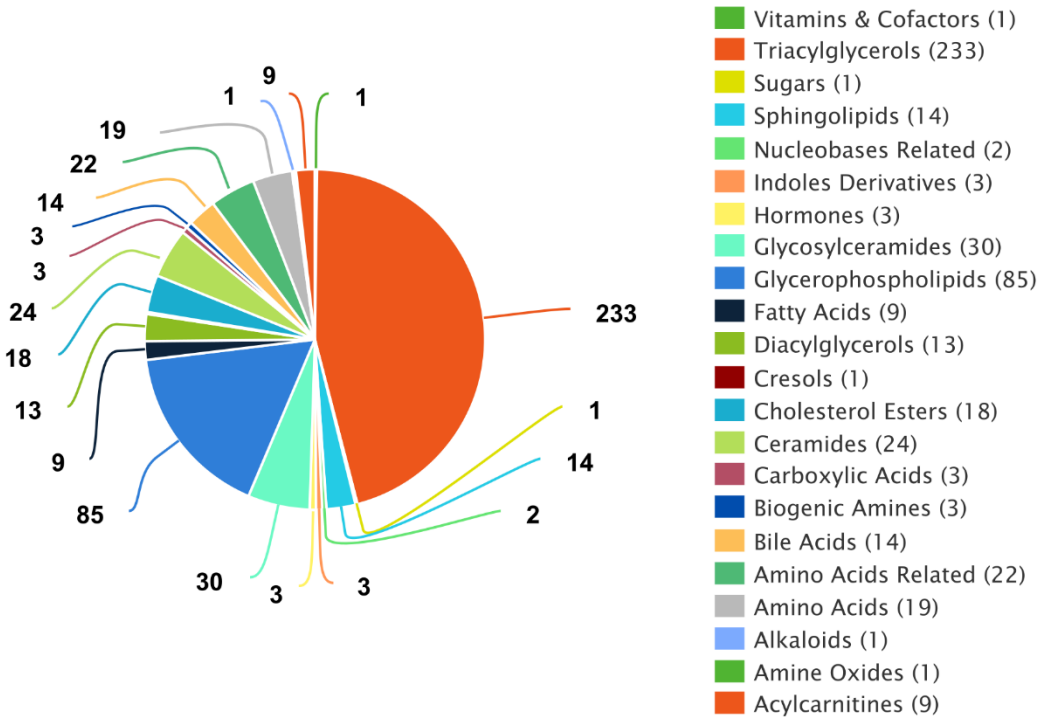

Figure 7.1: Metabolite coverage across chemical classes. Pie chart indicating the number of metabolites quantified across 22 chemical classes.

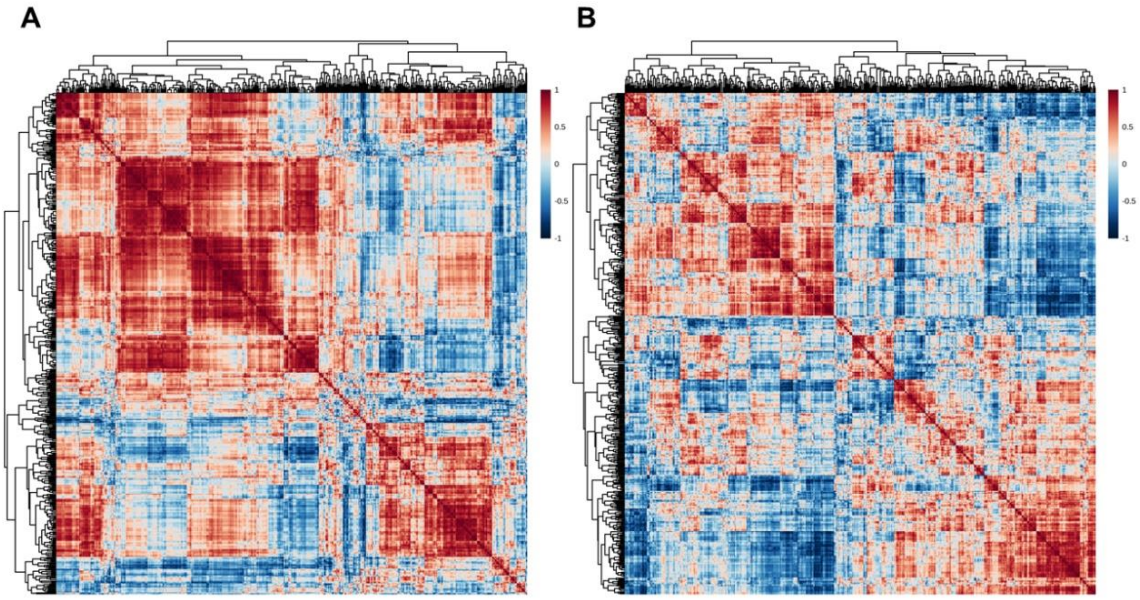

Figure 7.2: Metabolite-metabolite correlation analysis. (A) Correlation matrix of the 509 metabolites quantified in MM plasma. (**B**) Correlation matrix of the 509 metabolites quantified in EMM plasma. Positive correlations are shown in red. Negative correlations are shown in blue.

7.3.2 Comparison of metabolomic profiles identifies a trend towards increased lipid levels in EMM compared to MM plasma.

To obtain a broad overview of the distribution of metabolite and lipid classes in EMM and MM plasma, we evaluated the sum of quantified metabolites in individual chemical classes (**Figure 7.3**). A significant increase in the abundance of aromatic amino acids (phenylalanine, tryptophan, tyrosine, and histidine) was observed in EMM plasma. Although no significant changes were identified between the other compound classes illustrated in this figure, a clear trend towards an increase in lipids in EMM plasma can be seen. Total lipids, hexosylceramides, triacylglycerols, and monounsaturated fatty acids (MUFA) (phosphatidylcholine (PC)), are increased in abundance in EMM plasma (p-value < 0.1), however, this did not reach significance. The sum of the amino acid related class of metabolites showed a slight decrease in EMM plasma compared to MM plasma ($p = 0.068$).

7.3.3 Evaluation of biologically relevant metabolite ratios in EMM and MM plasma

Metabolite ratios have proven biologically relevant in various pathologies with several ratios currently being evaluated as part of clinical assessments in healthcare

settings (Fischer and Baldessarini 1971; Merritt and Chang 1993; Ishikawa 2012; Couce *et al.* 2013). Certain ratios can act as indicators of enzyme activity or inhibition as the metabolite ratio is directly altered as a result of enzyme action. This provides valuable insight into the enzymatic reactions occurring in pathological conditions or at the time of sampling (Badawy and Guillemin 2019). We compared a number of biological ratios with varying biological implications, as shown in **Table 7.1**. Only two of the ratios evaluated reached p-values below 0.1. Despite seeing no significant change in the sum of sphingolipids between MM and EMM plasma, the ratio of hydroxylated to non-hydroxylated sphingomyelins was significantly decreased in EMM plasma (p=0.024). In contrast, the ratio of L-Ornithine (Orn) to unmodified arginine, which acts as an indicator of arginase activity, was increased in EMM plasma compared to MM plasma (p=0.093).

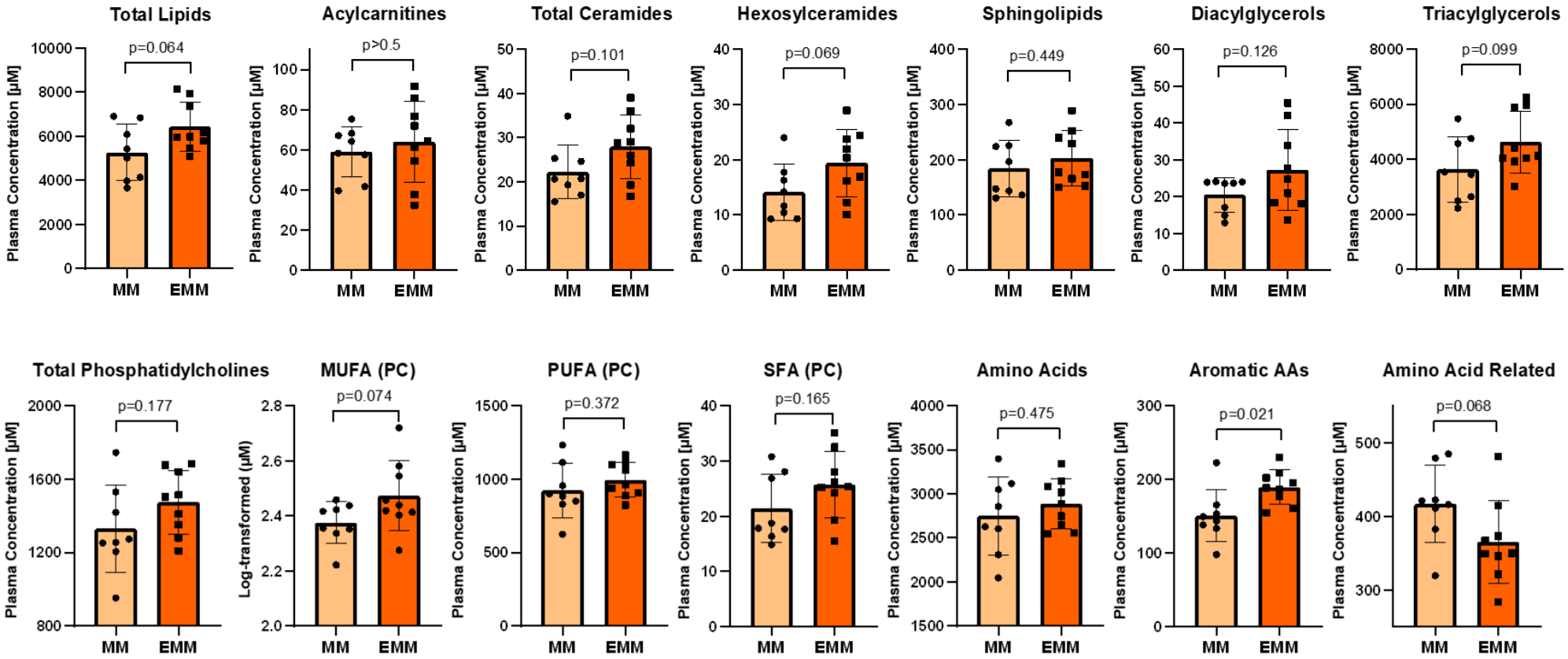

Figure 7.3: Comparison of plasma levels of various metabolite classes in EMM and MM patients. Plots indicate the sum of all metabolite concentrations within each chemical class. Normality was determined using the D'Agostino and Pearson test. Statistical significance was evaluated by unpaired t-test with Welch correction. Non-normally distributed datasets were log-transformed, tested for normality, and evaluated using the same method. P-values for each dataset are illustrated on the plots. MUFA, monounsaturated fatty acids; PC, phosphatidylcholine; PUFA, polyunsaturated fatty acids; SFA, saturated fatty acids; AA, amino acid.

Table 7.1: Statistical analysis of metabolite ratios in MM and EMM plasma. The D'Agostino and Pearson normality test and histograms revealed a non-normal dataset. Log transformation failed to yield a normally distributed dataset. Therefore, Mann-Whitney rank tests were applied to assess significance. Metabolite ratios with p-values < 0.1 are bolded and italicized. The biological significance of the metabolite ratios with p-values< 0.1 are listed.

Metabolite Ratio	Description	Fold Change (EMM/MM)	*P*-value
(C2+C3) / C0	Ratio of short chain acylcarnitines to free carnitine	0.97	0.481
ADMA / Arg	Fraction of asymmetrically dimethylated Arg of the unmodified Arg pool	1.896	0.114
C2 / C0	Ratio of acetylcarnitine to free carnitine	0.999	0.481
Cit / Arg	Ratio of Cit to Arg	1.514	0.167
Cit / Orn	Ratio of Cit to Orn	0.984	0.963
Kynurenine / Trp	Ratio of Kynurenine to Trp	1.648	0.606
MUFA (PC) / SFA (PC)	Ratio of mono-unsaturated to saturated glycerophosphocholines	1.018	0.481
Orn / Arg	Ratio of Orn to Arg	1.369	***0.093***
PUFA (PC) / MUFA (PC)	Ratio of poly-unsaturated to mono-unsaturated glycerophosphocholines	0.88	0.37
PUFA (PC) / SFA (PC)	Ratio of poly-unsaturated to saturated glycerophosphocholines	0.903	0.277
Putrescine / Orn	Ratio of putrescine to Orn	1.136	0.743
SDMA / Arg	Fraction of symmetrically dimethylated Arg of the unmodified Arg pool	1.382	0.963
Total AC / C0	Ratio of esterified to free carnitine	0.989	0.37
Total AC-DC / Total AC	Fraction of dicarboxyacylcarnitines of the total acylcarnitines	0.661	0.481
Total DMA / Arg	Fraction of dimethylated Arg of the unmodified Arg pool	1.593	0.321
Total lysoPC / Total PC	Ratio of lysoglycerophosphocholines to glycerophosphocholines	0.925	0.673
Total SM-OH / Total SM-non OH	Ratio of hydroxylated to non-hydroxylated sphingomyelins	0.831	***0.036***
Tyr / Phe	Ratio of Tyrosine to Phenylalanine	1.261	0.167

Significant Ratio	Description	Biological significance
Total SM-OH / Total SM-non OH	Ratio of hydroxylated to non-hydroxylated sphingomyelins	Indicator of sphingolipid hydroxylation
Orn / Arg	Ratio of Ornithine to Arginine	Indicator of arginase activity

7.3.4 Orthogonal projection to latent structure discriminant analysis (OPLS-DA) and identification of metabolites contributing to MM and EMM group distinction.

To remove metabolites that are unlikely to contribute to data modelling, feature filtering was performed based on the relative standard deviation. The remaining 381 metabolite concentrations were log-transformed and used for further analysis. Metabolites included for subsequent analysis comprised of 8 acylcarnitines, 1 alkaloid, 1 amine oxide, 5 amino acids, 18 amino acid-related metabolites, 14 bile acids, 1 biogenic amine, 1 carboxylic acid, 15 ceramides, 10 cholesterol esters, 1 cresol, 10 diacylglycerols, 9 fatty acids, 6 lysophosphatidylcholines, 37 phosphatidylcholines, 5 dihexosylceramides, 5 trihexosylceramides, 16 hexosylceramides, 3 hormones, 3 indole derivatives, 1 nucleobase-related, 5 sphingomyelins, and 206 triacylglycerols. PCA is a commonly used multivariate method of dimensionality reduction in metabolomic studies. However, clear separations between groups can only be visualized on PCA score plots if the intra-group variability is considerably lower than the inter-group variability. As plasma metabolic profiles can vary based on numerous environmental and dietary factors, supervised clustering approaches, such as partial least squares-discriminant analysis (PLS-DA) and orthogonal projection to latent structure discriminant analysis (OPLS-DA), which incorporate group classification are also used to optimize separation (Worley and Powers 2012; Ivanisevic and Want 2019). OPLS-DA is an upgraded version of PLS-DA which uses an orthogonal signal correction to separate the systematic variation in the X variable into components that are correlated to Y and those that are unique to X but uncorrelated to Y (Blasco *et al.* 2015). The ability of OPLS-DA to identify features that define experimental group separations, makes this approach popular for identifying biomarker candidates. Principal component analysis demonstrated no clear separation between the EMM patient group and the medullary MM patient group (**Figure 7.4A**), whereas OPLS-DA clustering identified a distinct separation between the two groups (**Figure 7.4B**). To validate the OPLS-DA model and ensure minimal overfitting of the data, a random permutation test was performed using 2000 permutations. In the OPLS-DA model, R2 refers to the explained variance between the components, whereas Q2 is calculated by full cross validation to indicate the goodness of prediction. R2 and Q2 values closer to 1 indicate a better

predictive model. Permutation analysis results (Q2 = 0.444, p = 0.048; R2Y = 0.99, p = 0.0365) demonstrated that the model was not overfitted (**Figure 7.4C**). In our analysis, the Q2 value of 0.444 indicated weak predictive power, however, due to the heterogeneity of human samples and the small sample size, a Q2 value > 0.4 is acceptable (Godzien *et al.* 2013; An *et al.* 2022). A scatter plot, known as an S-plot, which displays the modelled covariance versus the modelled correlation allows the visualization of important features within the OPLS-DA model (Gao *et al.* 2023). Metabolites with high p(corr) values as depicted in the upper right and lower left corners of the S-plot represent influential metabolites in the OPLS model classifications (**Figure 7.4D**).

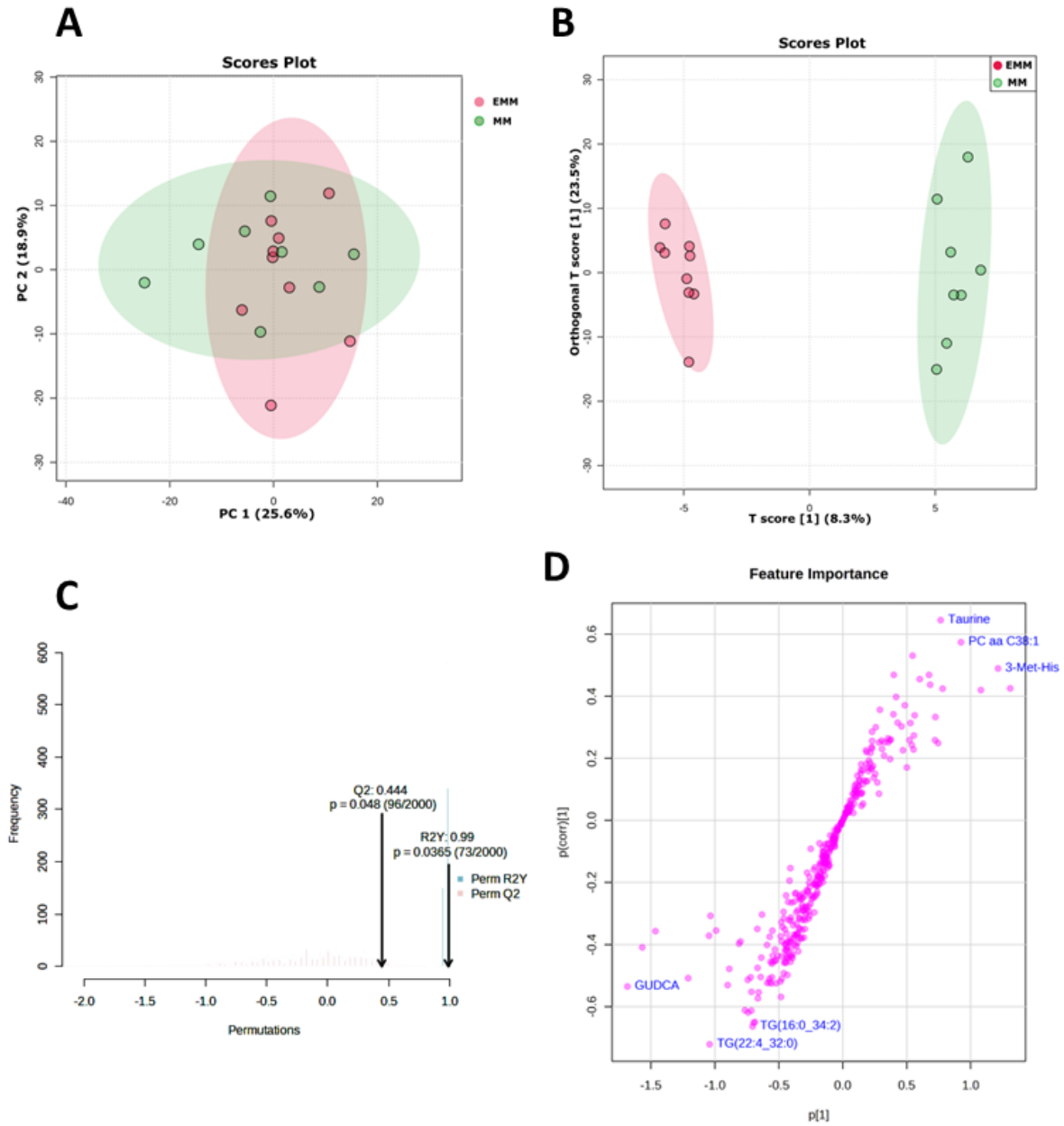

Figure 7.4: Metabolomics pattern recognition using multivariate approaches. **(A)** Principal component analysis (PCA) and **(B)** orthogonal projection to latent structure discriminant analysis (OPLS-DA) scores plots on plasma samples from EMM and MM patients. **(C)** Validation of the OPLS-DA model using a permutation test between one predictive (p1) and three orthogonal (o1, o2, and o3) components based on 2000 permutations. **(D)** S-plot with variables influencing the OPLS-DA separation labelled.

7.3.5 Identification of differentially abundant metabolites in MM and EMM plasma.

In addition to S-plot visualization, discriminatory variables responsible for group separation can be identified using the OPLS-DA VIP score. A total of 141 metabolites were identified as important discriminatory variables (VIP > 1). **Figure 7.5A** depicts the 20 metabolites with the highest VIP scores ranging from 1.8 to 2.5.

For univariate statistical analysis, volcano plot analysis was conducted to determine the distribution of metabolites from MM and EMM patient plasma. From this analysis, a total of 31 metabolites were SSDA with a fold change threshold set to > 1.3 (**Figure 7.5B**). Of the 31 SSDA metabolites, 28 were increased in abundance in EMM plasma whereas 3 were increased in abundance in MM plasma. The 28 metabolites increased in abundance in EMM included twenty triacylglycerols, two diacylglycerols, three hexosylceramides, one bile acid (GUDCA), one amino acid (Tyrosine), and one phosphatidylcholine (PC ae C44:4). The 3 metabolites increased in abundance in MM included two amino acid-related metabolites (Taurine, PheAlaBetaine) and one phosphatidylcholine (PC aa C38:1). Differentially abundant metabolites were identified based on the following criteria: VIP scores greater than 1, p-value ≤ 0.05, and FC > 1.3 or < 0.7 (**Figure 7.5C**). The full list of differentially abundant metabolites with corresponding fold changes, VIP scores, and p-values are listed in **Table 7.2**.

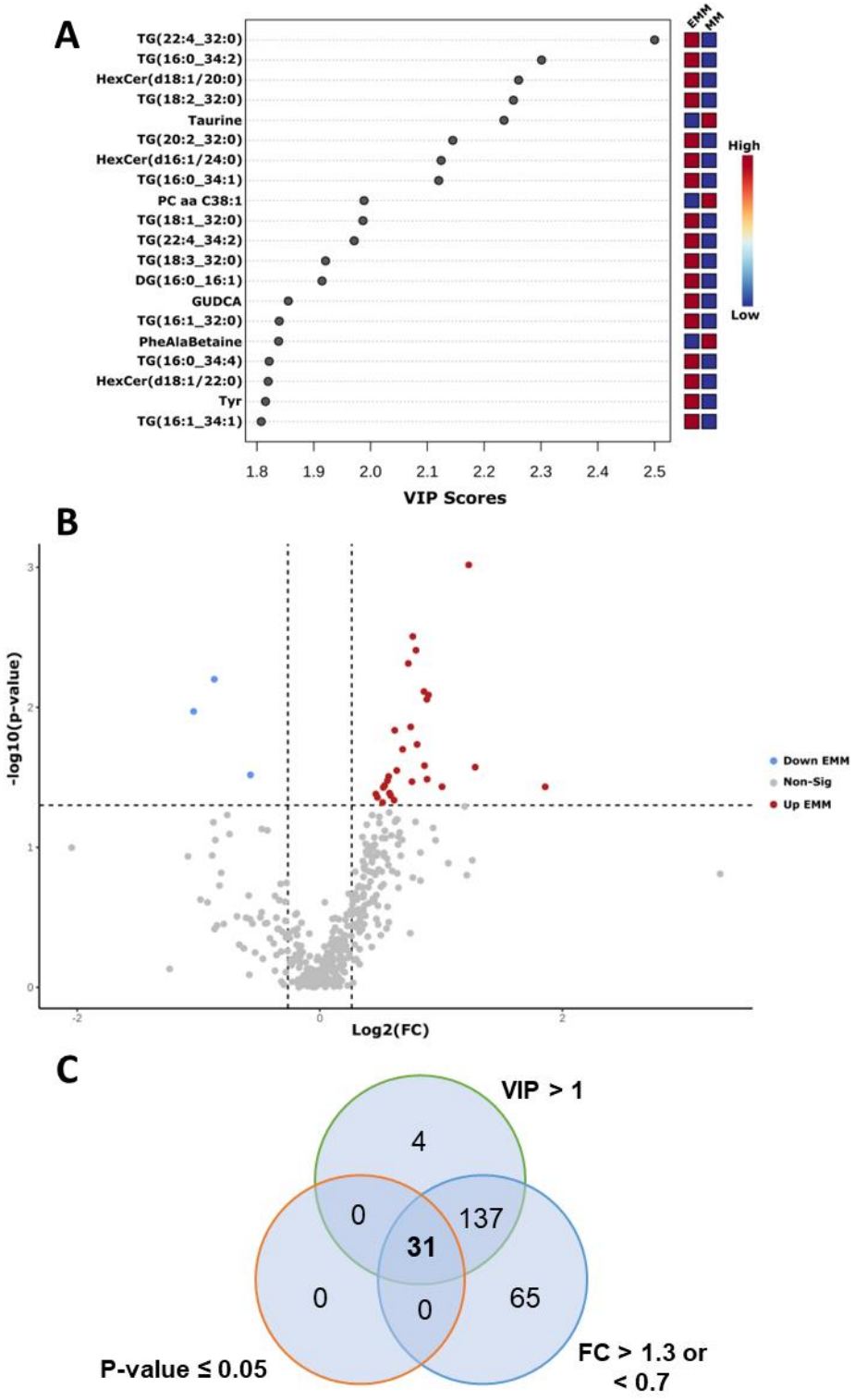

Figure 7.5: Identification of differentially abundant metabolites. (A) Top 20 important metabolites with highest variable importance in projection (VIP) scores obtained from OPLS-DA model. **(B)** Volcano plot showing statistically significantly differentially abundant (SSDA) metabolites between MM and EMM groups ($p \leq 0.05$, FC > 1.3). Each point represents a metabolite. Red points indicate metabolites increased in abundance in EMM plasma. Blue points indicate metabolites decreased in abundance in EMM. Grey points indicate non-significance. **(C)** Venn diagram illustrating the stepwise procedure of identifying 31 differentially abundant metabolites in EMM compared to MM patient plasma.

Table 7.2: Metabolites of differential abundance in the plasma of MM and EMM patients. Statistically significantly differentially abundant metabolites ($p \leq 0.05$, FC > 1.3 or < 0.7, VIP > 1).

Metabolite	Compound Class	Fold Change (EMM/MM)	VIP	*P*-value
TG(22:4_32:0)	Triacylglycerol	2.341	2.500	0.001
TG(16:0_34:2)	Triacylglycerol	1.701	2.301	0.003
HexCer(d18:1/20:0)	Hexosylceramide	1.732	2.261	0.004
TG(18:2_32:0)	Triacylglycerol	1.658	2.252	0.005
Taurine	Amino acid - related	0.547	2.235	0.006
TG(16:0_34:1)	Triacylglycerol	1.813	2.120	0.008
TG(20:2_32:0)	Triacylglycerol	1.860	2.145	0.008
HexCer(d16:1/24:0)	Hexosylceramide	1.843	2.124	0.009
PC aa C38:1	Phosphatidylcholine	0.486	1.989	0.011
TG(18:1_32:0)	Triacylglycerol	1.680	1.987	0.014
TG(22:4_34:2)	Triacylglycerol	1.534	1.971	0.015
DG(16:0_16:1)	Diacylglycerol	1.743	1.915	0.018
TG(18:3_32:0)	Triacylglycerol	1.605	1.921	0.020
TG(17:2_34:3)	Triacylglycerol	1.818	1.761	0.026
TG(16:1_32:0)	Triacylglycerol	2.429	1.839	0.027
TG(16:1_34:1)	Triacylglycerol	1.552	1.808	0.028
PheAlaBetaine	Amino acid - related	0.673	1.838	0.030
DG(16:0_18:1)	Diacylglycerol	1.481	1.800	0.031
TG(16:0_34:0)	Triacylglycerol	1.845	1.781	0.033
TG(16:0_34:4)	Triacylglycerol	1.472	1.822	0.033
TG(16:1_34:0)	Triacylglycerol	1.693	1.750	0.034
TG(18:0_34:2)	Triacylglycerol	1.448	1.752	0.036
TG(20:4_32:0)	Triacylglycerol	2.010	1.752	0.037
GUDCA	Bile acid	3.623	1.855	0.037
HexCer(d18:1/22:0)	Hexosylceramide	1.437	1.820	0.037
PC ae C44:4	Phosphatidylcholine	1.489	1.769	0.041
TG(16:0_35:2)	Triacylglycerol	1.377	1.726	0.042
TG(16:0_33:2)	Triacylglycerol	1.499	1.769	0.043
TG(20:2_32:1)	Triacylglycerol	1.389	1.706	0.044
TG(20:0_32:3)	Triacylglycerol	1.528	1.559	0.046
Tyr	Amino acid	1.432	1.815	0.048

7.3.6 Evaluation of differentially abundant metabolites/metabolite ratios as plasma-based markers of extramedullary myeloma.

To test the clinical utility of plasma-based metabolites in EMM diagnostics, we evaluated the discriminatory power of the significantly differentially abundant metabolites and metabolite sums/ratios in MM versus EMM plasma (**Table 7.3**). The Biocrates nomenclature for triglycerides (TGs) lists one fatty acid and the sum of the other two, meaning that more than one triglyceride fits the description. Therefore, specific TGs were not included in the following ROC curve analyses. Typically, biomarkers with an AUC value greater than 0.8 and p-value below 0.05 are considered to have good discriminatory power. From our analysis, 10 metabolites or metabolite sums/ratios (HexCer(d18:1/20:0), HexCer(d16:1/24:0), HexCer(d18:1/22:0), Tyr, Taurine, DG(16:0_16:1), PC aa C38:1, PC ae C44:4, sum of aromatic AAs, and Total SM-OH / Total SM-non-OH) have been identified as potential plasma-derived metabolite markers of EMM . Of the significant metabolites, HexCer(d18:1/20:0) and PC aa C38:1 had the highest AUC values of 0.875 (p-value < 0.0001), whereas HexCer(d18:1/22:0) and Tyr had the lowest AUC values of 0.806 (p-value = 0.0122) (**Figure 7.6**). In recent years, it has become widely accepted that identifying a single biomarker with adequate sensitivity and specificity for disease diagnosis or prediction is rare. As a result, combining multiple biomarkers into a diagnostic/predictive panel with statistical evaluation using a multivariate model has become increasingly popular. It is important to note that although adding many features to a metabolite panel can significantly improve prediction accuracy, the practicality and feasibility of analysing a larger number of features in a clinical setting must also be considered. Combining multiple promising biomarkers can improve discriminatory power and yield a higher AUC value. As illustrated in **Figure 7.7**, multivariate logistic regression analyses combining 2, 3, 4, and 5 metabolites were performed. Combining the two metabolites with the highest individual AUC values (PC aa C38:1 and HexCer(d18:1/20:0)) gave an improved AUC value of 0.972 (95% confidence interval = 0.759 – 1). Combining the three metabolites with the highest individual AUC values (PC aa C38:1, HexCer(d18:1/20:0), and Taurine) once again generated an improved AUC value of 1 (95% confidence interval = 0.805 – 1). Increasing the number of metabolites in the

model to four or five does not improve the discriminatory power of the models when compared to the three-metabolite combination.

Table 7.3: Receiver operating characteristic curve analysis of differentially abundant metabolites in MM and EMM plasma. Summary statistics for each metabolite in MM and EMM groups with the corresponding AUC value, p-value and 95% confidence interval.

	MM		EMM		MM vs EMM			
Metabolite	**Mean**	**SD**	**Mean**	**SD**	**AUC**	**p-value**	**95% Confidence Interval**	**↑/↓ EMM**
HexCer(d18:1/20:0)	0.203	0.07263	0.3516	0.0958	0.875	<0.0001	0.627 to 0.983	↑
HexCer(d16:1/24:0)	0.01538	0.004406	0.02833	0.012	0.833	0.0014	0.577 to 0.966	↑
HexCer(d18:1/22:0)	1.638	0.7273	2.3536	0.6853	0.806	0.0122	0.545 to 0.953	↑
GUDCA	0.03938	0.05216	0.1427	0.1823	0.792	0.013	0.530 to 0.946	↑
Tyr	51	21	72	18	0.806	0.0122	0.545 to 0.953	↑
Taurine	75	27	41	14	0.861	0.0001	0.610 to 0.978	↓
DG(16:0_16:1)	0.4228	0.1588	0.7368	0.267	0.875	0.0001	0.627 to 0.983	↑
DG(16:0_18:1)	3.6931	1.1841	5.4711	1.8212	0.778	0.0167	0.515 to 0.939	↑
PC aa C38:1	0.4503	0.2076	0.2189	0.1232	0.875	<0.0001	0.627 to 0.983	↓
PC ae C44:4	0.1694	0.04454	0.2521	0.08194	0.861	0.0013	0.610 to 0.978	↑
PheAlaBetaine	0.00925	0.003012	0.006222	0.002386	0.799	0.0081	0.538 to 0.950	↓
Sum of Aromatic AAs	151	35	190	23	0.861	0.0015	0.610 to 0.978	↑
Total SM-OH / Total SM-non-OH	0.1265	0.01507	0.1051	0.01972	0.806	0.0056	0.545 to 0.953	↓
Total TAG	3644	1184	4633	1124	0.722	0.1048	0.457 to 0.907	↑

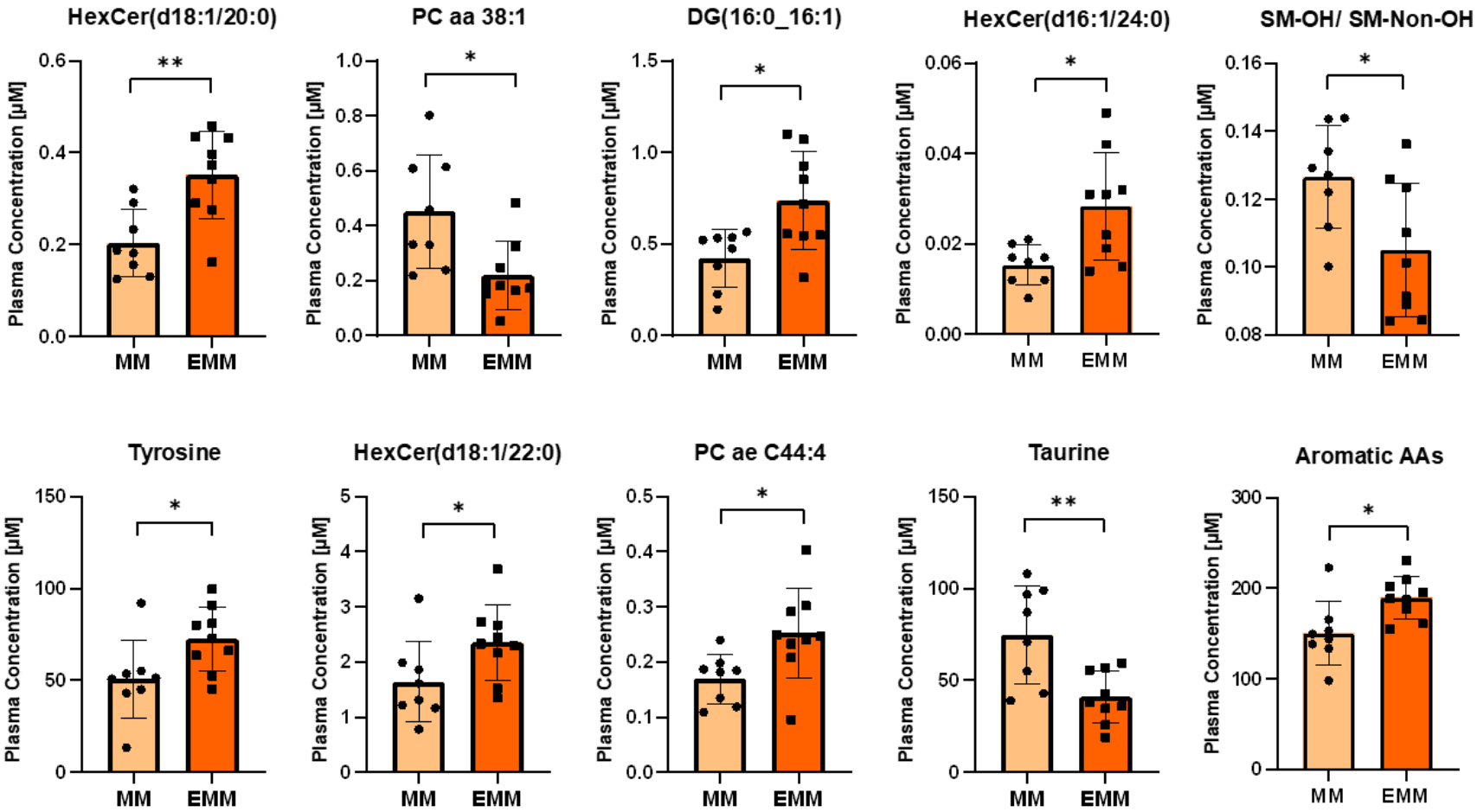

Figure 7.6: Plasma concentration [µM] of metabolites with AUC values > 0.8 plotted as boxplots. Significance is marked as follows: $P \leq 0.05$ '*', $P \leq 0.01$ '**'.

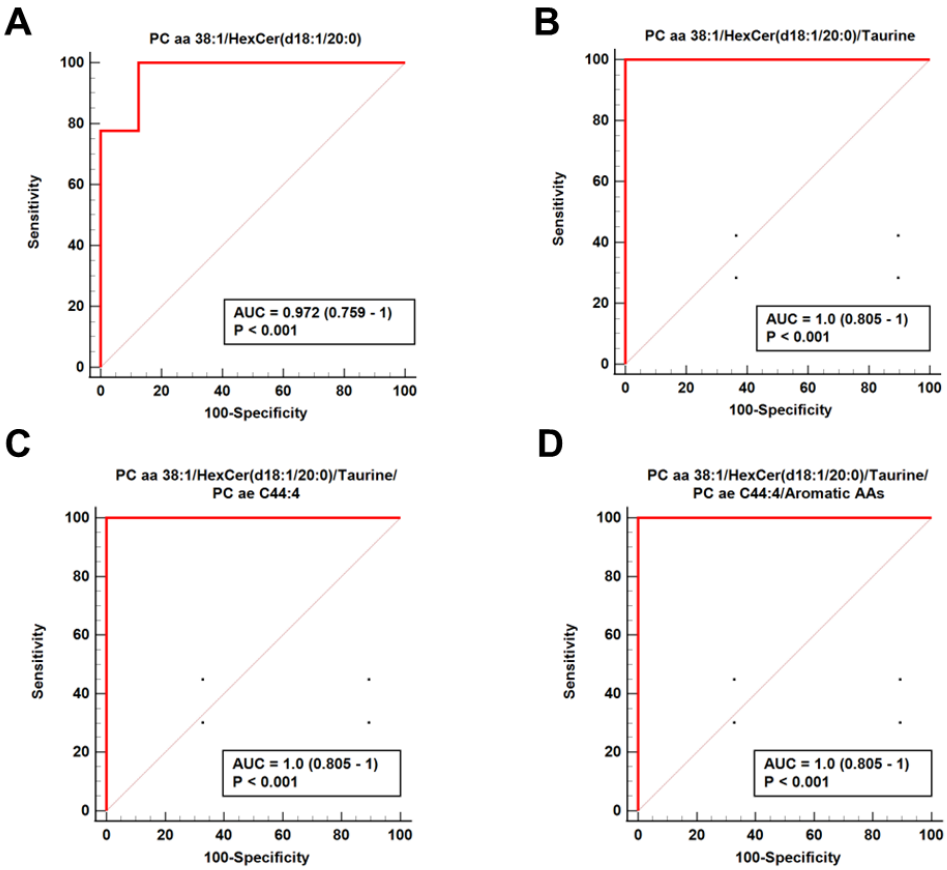

Figure 7.7: Multivariate receiver operating characteristic (ROC) curves indicating the discriminatory power of plasma metabolite combinations. (A) ROC curve computed based on the combination of PC aa 38:1 and HexCer(d18:1/20:0). **(B)** ROC curve computed based on the combination of PC aa 38:1, HexCer(d18:1/20:0), and Taurine. **(C)** ROC curve computed based on the combination of PC aa 38:1, HexCer(d18:1/20:0), Taurine, and PC ae C44:4. **(D)** ROC curve computed based on PC aa 38:1, HexCer(d18:1/20:0), Taurine, PC ae C44:4, and the sum of aromatic AAs. 95% confidence intervals are depicted in parentheses next to the AUC value.

7.3.7 Integration of plasma metabolomics and proteomics using correlation analysis

Multi-omics techniques can provide more comprehensive insights when compared to single-omics technologies. We integrated our mass spectrometry-based plasma proteomics analysis (Chapter 6) with this targeted metabolomics analysis by performing a correlation analysis of the metabolites/lipids and proteins identified in the plasma of EMM patients by Spearman's rank correlation (**Figure 7.8**). Taurine and phosphatidylcholine with diacyl residue sum C38:1 (PC aa C38:1) were negatively correlated with the proteins whereas all other metabolites identified were

positively correlated with the plasma proteins identified in our proteomics analysis. Integrating proteomic and metabolomic analyses can help to identify the most promising biomarkers for addition to a biomarker panel. Correlation analyses are valuable to investigate collinearity between potential biomarkers. Markers that have a strong correlation may indicate a dependency between these variables which can inflate standard errors in the model (Li *et al.* 2015). Feature selection methods, such as Least Absolute Shrinkage and Selection Operator (LASSO) regression, are often used to address collinearity issues (Huang, He, *et al.* 2022). A joint pathway analysis was performed using MetaboAnalyst 5.0, on the significant metabolites and proteins identified, however, no significant metabolic pathway changes were identified.

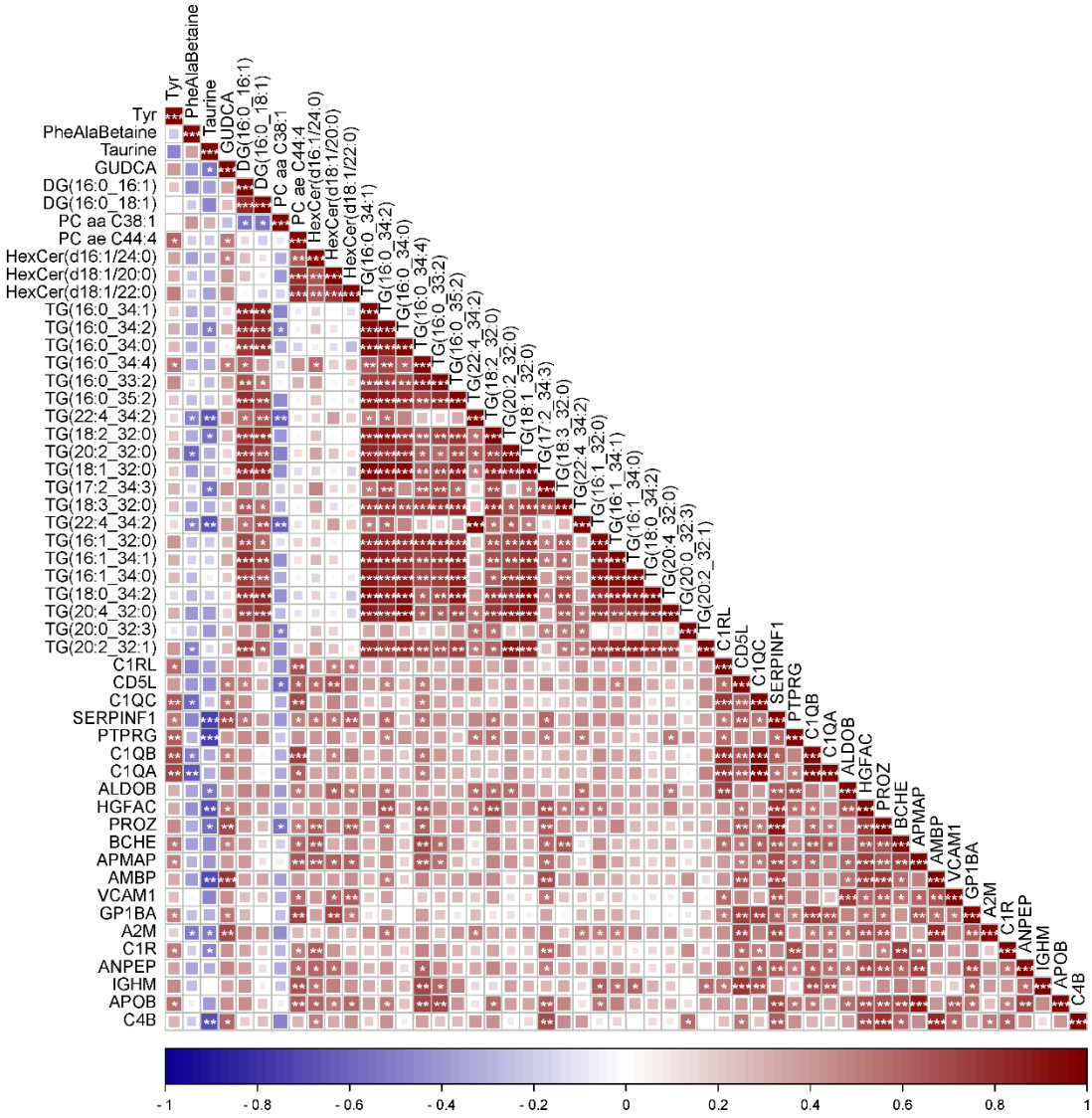

Figure 7.8: Spearman's correlation matrix between differential metabolites and proteins in EMM plasma. Blue colour indicates negative correlation; Red colour indicates positive correlation. Significant correlations regions were marked by stars (*P < 0.05, **P < 0.01, ***P < 0.001).

7.4 Discussion

The rewiring of cellular metabolism during carcinogenesis highlights the need for more research in cancer metabolomics. Recent studies focusing on breast cancer and gastric cancer have demonstrated the ability of metabolomic studies to enhance precision medicine by detecting disease subgroups with specific metabolic features (Wang *et al.* 2022; Xiao *et al.* 2022). Extramedullary lesions arise due to the hematogenous spread of myeloma cells combined with an unknown mechanism which facilitates myeloma cell intravasation and growth at soft-tissue sites. Therefore, we hypothesized that this may result in a change in the plasma metabolic profile of EMM patients compared to medullary MM patients.

Numerous studies have reported a metabolic change in the bone marrow and plasma of patients with multiple myeloma when compared to healthy controls. One of the earlier metabolomics studies on MM found that metabolite levels in the bone marrow and blood plasma quantified by ^{1}H-NMR spectroscopy and ultra-high performance LC-MS, respectively, could strongly differentiate between MM patients and healthy controls, whereas MGUS and MM patients had similar metabolic compositions that could only be weakly differentiated (Ludwig *et al.* 2020). Many of the differentially abundant compounds between MM plasma and healthy controls were classed as lipids suggesting a potential link between dysregulated lipid metabolism and myelomagenesis. A more recent study combining untargeted and targeted metabolomics/lipidomics of bone marrow plasma successfully differentiated patients with MGUS from those with active MM, reporting a decrease in BCAA levels and summed lipid species (phosphatidylethanolamines (PE), lactosylceramides (LCER) and phosphatidylinositols (PI)) in MM bone marrow plasma compared to MGUS bone marrow plasma (Gonsalves *et al.* 2020). Targeted metabolomics of peripheral blood plasma from healthy controls and patients with MGUS, NDMM, and RRMM supported previous studies by identifying a clear change in the plasma metabolic profile of healthy controls compared with those with plasma cell dyscrasias. Additionally, fewer significant changes were detected between MGUS, NDMM, and RRMM plasma (Steiner *et al.* 2018). Combined, this suggests a significant change occurs in the metabolome of the bone marrow niche and systemically at an early or

premalignant stage of MM, with smaller, less significant changes occurring during MGUS to MM transformation.

Studies deciphering the metabolic profiles related to drug resistant phenotypes and treatment response in MM have yielded promising results (Maekawa *et al.* 2019; Wei *et al.* 2022). The evaluation of serum metabolites in MM patients pre- and post-therapy identified abnormal levels of metabolites involved in the arginine, proline and glycerophospholipid pathways (Wei *et al.* 2022). Increased serine synthesis and enhanced activity of the pentose phosphate pathway was previously reported to sustain bortezomib resistance, with the increased expression of phosphoglycerate dehydrogenase facilitating increased serine synthesis (Zaal *et al.* 2017). Thus, there is a range of applications for metabolomics in deciphering the molecular mechanism associated with MM pathogenesis. Obesity has been defined as a risk factor for the progression of MGUS to active MM (Chang *et al.* 2017). However, the impact of obesity on survival outcomes and progression of MM is more controversial, with studies reporting conflicting results (Calle *et al.* 2003; Wallin and Larsson 2011; Marques-Mourlet *et al.* 2023). A recent study evaluating the link between obesity and survival outcomes in MM demonstrated that a lower overall survival was only associated with underweight and severely obese patients and not overweight or moderately obese patients, whereas a previous meta-analysis revealed increased body mass index as being associated with increased MM mortality (Wallin and Larsson 2011; Shah, Whiting, *et al.* 2023).

In this chapter, we demonstrated a trend towards increased lipid and triglyceride concentrations in the plasma of patients with EMM. Aberrant lipid metabolism has been linked to various cancers in recent years (Cheng *et al.* 2022). Interestingly, recent evidence found that individuals using statins for 48-72 months prior to diagnosis had a reduced a reduced risk of MM, and MM patients using statins had a 21% and 24% reduction in all-cause and MM-specific mortality, respectively (Sanfilippo *et al.* 2016; Epstein *et al.* 2017). In addition, statins have recently been reported to act as metastasis inhibitors in colorectal cancer via the inhibition metastasis associated in colon cancer 1 transcription (Juneja *et al.* 2017). Investigations into the preventative effects of statins in the progression of MM to advanced disease states such as EMM, may yield a new therapeutic approach to

prevent or slow MM disease progression. Increased abundance of the fatty acid binding protein (FABP), FABP5 has been linked to a poor prognosis and MM disease progression (Tierney, Bazou, Lê, *et al.* 2021; Farrell *et al.* 2023). Etomoxir and orlistat, which inhibit carnitine palmitoyl transferase I (CPT-1) and fatty acid synthase (FASN), respectively, reduce the proliferation of myeloma cells, highlighting the association between aberrant lipid metabolism and MM pathogenesis (Tirado-Vélez *et al.* 2012). Within the bone marrow microenvironment, bone marrow adipocytes (BMA) contribute to myeloma growth, survival, and migration (Caers *et al.* 2007; Liu *et al.* 2015, 2019). Furthermore, myeloma cells have been found to induce lipolysis in adipocytes resulting in the release of stored triglycerides and subsequent hydrolysis to yield free fatty acids and glycerol. These fatty acids can be taken up by myeloma cells through fatty acid transporter proteins and may be used to produce energy through fatty acid oxidation (Panaroni *et al.* 2022). Additionally, suppression of CD8+ T cell function within the MM BME has been linked to an increased uptake of long-chain fatty acids by CD8+ T cells. MM-induced lipolysis may contribute to creating an immunosuppressive environment within the bone marrow niche (Gudgeon *et al.* 2023).

Dyslipidemia is a component of metabolic syndrome, which has been reported to have a higher occurrence in MM compared to healthy controls (Markus *et al.* 2020). Reports of hyperlipidemic myeloma have been published since the 1960s, although the underlying incidence and mechanisms of this rare form of MM are unknown (Cohen *et al.* 1966; Aubert *et al.* 1967). Interestingly, several EMM case studies have reported hyperlipemia as part of the clinical presentation (Shimokihara *et al.* 2018; Ilyas *et al.* 2022). Furthermore, a review of cases of hyperlipidemic myeloma found that it occurs more predominantly in MM patients with IgA myeloma, which has also been linked to a higher risk of future EMM development (Misselwitz *et al.* 2010; Stork *et al.* 2022). Therefore, the increased lipid levels observed in EMM plasma may indicate a link between dysregulated lipid metabolism and EMM although further studies are required to confirm this.

The total sum of aromatic amino acids (phenylalanine, tryptophan, and tyrosine) was significantly increased in abundance in EMM plasma. Alterations in aromatic amino acid biosynthesis pathways have been reported in a number of cancers (Akbari *et al.*

2021; Di Cesare *et al.* 2023). Increased expression of aromatic amino acids in breast cancer tissue compared to healthy tissue has been identified as a potential diagnostic marker (Contorno *et al.* 2021). Serum levels of phenylalanine and tyrosine were found to be increased in MM patients compared to healthy controls (Puchades-Carrasco *et al.* 2013). Of the three aromatic amino acids, univariate analysis identified tyrosine as being significantly increased in EMM plasma, indicating that circulating levels of tyrosine may also be increased in MM patients with advanced disease. Dysregulation of tyrosine catabolism has been noted in several cancers, although limited research has been published in this area in MM (Kurup *et al.* 2003; More *et al.* 2017; Tong *et al.* 2021). Although evaluating the overall abundance of metabolite classes provides a broad overview of the plasma metabolome, examining the metabolome at the individual metabolite level provides in-depth information and may lead to the identification of strong disease-specific biomarkers. Combining powerful metabolite and protein indicators into a diagnostic, prognostic, or predictive biomarker panel can improve the overall specificity and sensitivity of the panel.

Metabolite ratios can act as indicators for molecular processes with biological and clinical relevance. For example, the kynurenine/tryptophan ratio which reflects the activity of indoleamine 2,3-dioxigenase 1 (IDO1), a rate-limiting enzyme involved in tryptophan catabolism, is a well-known metabolite ratio with relevance to various cancers (Badawy and Guillemin 2019). In this study, the ratio of hydroxylated to non-hydroxylated sphingomyelins was significantly decreased in EMM plasma, while a trend towards increased arginase activity (Orn/Arg) was observed in EMM plasma. Although no significant change in sphingolipid concentrations between MM and EMM plasma was identified, the decreased ratio of hydroxylated to non-hydroxylated sphingomyelins may indicate dysregulation in sphingolipid hydroxylation. As hydroxylation is an oxygen-dependent process, the extent of sphingomyelin hydroxylation may be affected by hypoxic conditions within the bone marrow. Arginase is an enzyme that catabolizes the production of ornithine from arginine. Ornithine can then be broken down into polyamines by ornithine decarboxylase (ODC) (Bednarz-Misa *et al.* 2020). Overexpression of arginase has been linked to a poor prognosis in various cancers including colorectal cancer and Hodgkin lymphoma (Romano *et al.* 2016; Ma, Lian, *et al.* 2019). In MM, inhibition of arginase was found to reduce tumour growth *in vivo* and has been suggested to

contribute to drug resistance (Romano *et al.* 2018; Ramji *et al.* 2022). The role of arginase in EMM has yet to be evaluated, however, our results indicate increased arginase activity in EMM compared to MM. Taurine, phenylalanine betaine and PC aa C38:1 were decreased in abundance in EMM plasma. Few studies have been published on the roles of these metabolites in cancer, however, several studies have suggested a strong anti-tumorigenic role of taurine; although this has not been thoroughly analysed in MM (Baliou *et al.* 2020; Ma *et al.* 2022). The integration of omics technologies is becoming an important aspect of precision medicine, whereby disease biomarkers and therapeutic targets are identified at different molecular levels providing a more comprehensive view of MM pathophysiology. Incorporating metabolite measurements into protein-based biomarker panels can enhance the sensitivity and specificity of the panel, as demonstrated previously in pancreatic cancer (Fahrmann *et al.* 2018). This approach is likely to be central to future biomarker research, where panels will be composed of proteins, metabolites, genetic features, and/or individual patient characteristics.

As outlined in previous chapters, a limitation of the study is the small sample size due to the rarity of EMM. Without validation of metabolite abundance in an independent cohort, it is difficult to conclusively state a role of the differentially abundant metabolites identified in EMM. Nevertheless, this pilot study does demonstrate a change in the plasma metabolome of EMM patients compared to medullary MM patients, highlighting the molecular alterations that distinguish EMM from MM. This study provides a starting point for future studies to assess the local and systemic metabolic changes in EMM to validate markers of disease identified in this study or reveal novel therapeutic targets. The impact of dysregulated lipid metabolism on EMM development warrants further investigation in a larger cohort of samples.

7.5 Conclusion

In conclusion, the findings reported in this chapter serve as a reference for future studies evaluating the metabolic signature that differentiates extramedullary multiple myeloma from medullary multiple myeloma. Increased levels of various lipid species in EMM plasma indicate a potential dysregulation of lipid metabolism that may contribute to the development of the more aggressive EMM phenotype. Specific

metabolites of differential abundance in EMM plasma compared to MM plasma were identified, however, validation of the results in a larger cohort of samples is required. This metabolomics analysis builds on the results reported in previous chapters by highlighting EMM as a phenotypically distinct condition when compared to medullary myeloma, and as such warrants a different therapeutic approach with novel drug targets and drug combinations to improve survival rates.

Chapter 8

General Discussion

8.1 Discussion

Multiple myeloma accounts for approximately 2% of all cancer diagnoses and cancer-related deaths (Padala *et al.* 2021). As with most cancers, early detection is associated with an improved prognosis (Li, Wang, *et al.* 2019). However, myeloma patients have some of the longest diagnostic intervals of all cancer patients, likely due to a lack of symptoms or vague symptoms such as fatigue, bone pain, and back pain, which can often be attributed to other diseases or conditions (Lyratzopoulos *et al.* 2012; Smith *et al.* 2022). Individuals diagnosed with the common myeloma precursor condition, MGUS, are monitored for myeloma biomarkers, but only approximately 1% progress to MM annually. Patients with sMM have an increased risk of progressing to active MM, and ongoing studies are aiming to determine the best time to begin treatment of sMM to improve long-term outcomes (Mateos *et al.* 2022; Vaxman and Gertz 2022). Delayed diagnosis of MM increases disease burden and many patients face repeated relapses and progression to more aggressive phenotypes including relapsed/refractory MM or extramedullary multiple myeloma (Carmichael *et al.* 2023). These aggressive MM phenotypes often progress quickly after treatment and novel therapeutic approaches are needed to improve outcomes of this patient cohort.

A number of analytical approaches including untargeted mass spectrometry, targeted proximity extension assays, and targeted immunoassays, were utilised throughout this thesis to identify protein, phosphorylation and metabolite signatures associated with drug-resistant MM and EMM. Protein abundance can reflect the dynamic downstream consequences of genomic and transcriptomic alterations, and examining changes in protein levels provides a comprehensive insight into the molecular events underlying MM pathogenesis (Boys *et al.* 2023). Investigating post translational modifications provides further insight into malignant phenotypes due to their influence on the spatial localization, structure, and biological functions of proteins. Finally, the evaluation of metabolite levels addresses another layer of complexity within the disease phenotype.

Discovery proteomics using mass spectrometry and a data-dependent acquisition (DDA) approach, are often used initially to quantify changes in protein abundance in biological samples. Limitations of DDA include precursor ion selection being biased

towards high abundant proteins and the stochastic nature of ion selection which hinders reproducibility (Barkovits *et al.* 2020). The data independent acquisition (DIA) approach for untargeted MS-based proteomics has garnered increased attention in recent years as it overcomes the under-sampling limitations of DDA. However, DDA remains the most widely used approach within the proteomics community, mainly due to its flexibility and ease of setup and data analysis (Hu *et al.* 2016). Following mass spectrometry analyses using DDA, targeted proteomic approaches are typically applied to narrow down potential biomarkers for further validation (Sobsey *et al.* 2020). Many proteomic studies have been conducted with the aim of identifying novel biomarkers or biomarker panels in MM (Dytfeld *et al.* 2016; Zhao *et al.* 2020; Setayesh *et al.* 2023). In fact, several well-established protein-based diagnostic and risk stratification biomarkers including B2M, LDH, and albumin, are currently used in the clinical work-up of MM patients (Rajkumar 2022). However, novel biomarkers are needed to unravel the clinical complexities of MM, especially regarding patient response to treatment. With the introduction of novel therapeutics with specific targets, detecting target expression in myeloma cells can help determine the likelihood of response to treatment. Many FDA-approved MM immunotherapies, including elranatamab, and investigational immunotherapies target BCMA on myeloma cells (Cho *et al.* 2020). Studies on BCMA CAR-T cells and bispecific T-cell engagers have identified soluble BCMA levels as a potential biomarker of response to BCMA-targeted treatment (Topp *et al.* 2020; Li, Xu, *et al.* 2023).

The work presented in this thesis sought to (1) identify phosphoproteomic changes in myeloma cells based on *ex vivo* drug response to a selection of drug classes, (2) identify plasma proteomic changes based on *ex vivo* drug response to a selection of drug classes, (3) compare the bone marrow proteome of MM patients with and without extramedullary spread, (4) identify and verify potential plasma-derived biomarkers of extramedullary multiple myeloma, and (5) assess metabolomic changes in the plasma of MM patients with and without extramedullary spread.

Few studies have used ‘omic’ approaches in combination with *ex vivo* DSRT to decipher resistance mechanisms and identify novel predictive biomarkers of therapeutic response in MM. Previous work from our research group utilised a label-

free quantitation (LFQ)-based MS approach in combination with *ex vivo* DSRT to identify proteomic changes that may inform therapeutic decision making in MM (Tierney, Bazou, Majumder, *et al.* 2021). The work presented in Chapter 3 aimed to expand on this work by utilising a label-based MS approach in combination with *ex vivo* DSRT to identify phosphoproteomic changes associated with drug response to a selection of FDA-approved and investigational therapeutics. Specifically, synchronous precursor selection (SPS)-MS^3-based quantitation of TMT-labelled peptides was performed. Label-based quantitation using TMT labels facilitates sample multiplicity and reduces the number of missing quantitation values when compared to LFQ. Furthermore, the use of SPS-MS^3 technology overcomes the issue of reporter ion interference, caused by co-isolated peptide ions, that is common in MS^2-based TMT experiments (Ting *et al.* 2011). Several large scale phosphoproteomic studies have used TMT-SPS-MS^3 methods and successfully measured global changes in protein phosphorylation (McAlister *et al.* 2014; Jiang *et al.* 2017; Babur *et al.* 2020).

Myeloma cells that demonstrated resistance to a large number of FDA-approved and investigational therapeutics had a distinct phosphoproteomic profile when compared to those that demonstrated sensitivity to the majority of drugs evaluated. Corroborating with previous research from our research group, proteins involved in cell adhesion and cytoskeletal organisation were associated with drug resistant myeloma cells, while proteins involved in protein synthesis and RNA processing were associated with drug sensitive myeloma cells. These findings translated to the phosphoproteome with functional enrichment analyses identifying an enrichment of similar biological processes in drug resistant and drug sensitive myeloma cells. The SSDA proteins and phosphorylation events identified between Group 1 and Group 4 samples likely promote resistance to a wide range of therapeutics through general resistance mechanisms including CAM-DR, slow cycling rates, and the avoidance of apoptosis. Increased abundance of α-actinin, phosphorylated FLNA (S2152), and PRKACA, were verified by immunoblot analysis, confirming the trends seen in our mass spectrometry analysis and subsequent KSEA. This highlights the proteins, phosphorylation sites and predicted kinases identified in this study as potential resistance markers for future investigation and validation.

Unique proteins and phosphorylation events identified as differentially abundant in myeloma cells with resistance/sensitivity to individual drugs may be linked to resistance mechanisms associated with a specific drug or drug class. The overlap of proteins and phosphorylation events found to be SSDA across the drug groups are visualized in **Figure 8.1**. Seven phosphorylation sites, namely, LAT S224, LIMA1 S490, ZYX S281, RASGRP2 S576, FLNA S2152, SDPR S293, DMTN S16, were commonly differentially abundant across the five individual drugs investigated. Phosphorylation sites and proteins demonstrating differential abundance unique to specific drugs represent interesting targets for more in-depth analyses into potential drug-specific resistance mechanisms. For example, increased levels of HMGA1 in PF-431396-sensitive myeloma cells, as described in Chapter 3, may be involved in enhancing the sensitivity of myeloma cells to this therapeutic.

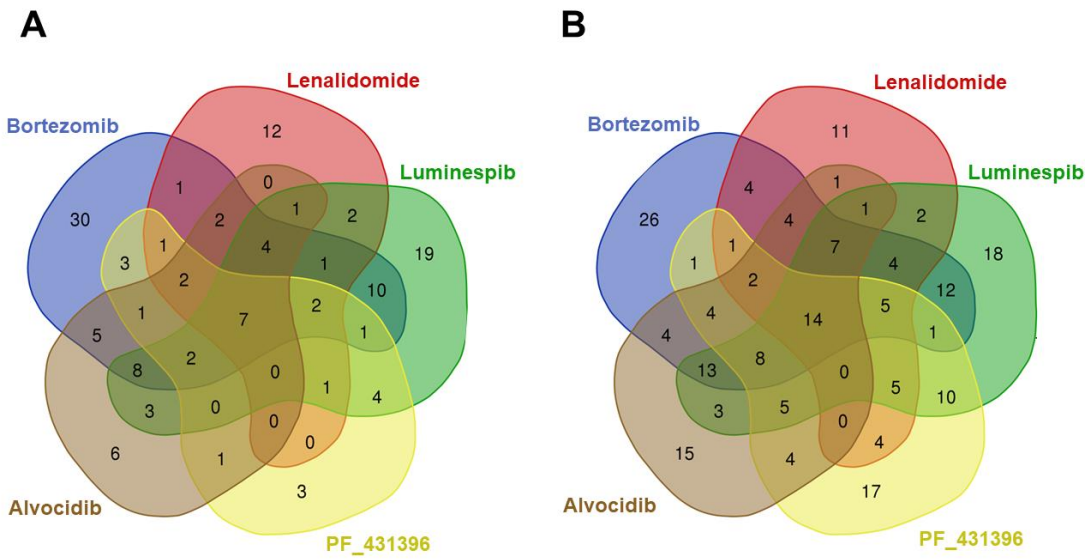

Figure 8.1: Cross-comparison of phosphoproteomics data across different drug sensitivities. (**A**) Venn diagram illustrating the common and unique phosphorylation sites found to be differentially abundant in Chapter 3. (**B**) Venn diagram illustrating the common and unique proteins found to be differentially abundant in Chapter 3. Venn diagrams were generated using an online tool from the Bioinformatics & Evolutionary Genomics website (https://bioinformatics.psb.ugent.be/webtools/Venn/).

This pilot study recommends the combination of phosphoproteomics with *ex vivo* DSRT to unravel signalling pathways associated with drug sensitivity/resistance. We have identified common and unique phosphorylation events associated with drug resistance to individual drugs that warrant further investigation. Future work focused on the validation of the results of this study will undoubtedly identify key proteins

and phosphorylation events associated with drug resistance in MM. This approach also has broad applications in other cancers that are suitable for *ex vivo* DSRT. Moreover, studies with a larger sample size and possibly a more in-depth phosphoproteomic analysis incorporating fractionation prior to MS analysis, hold potential to generate a large database specifying the differentially abundant proteins and phosphorylation events associated with sensitivity/resistance to a large number of FDA-approved and investigational drugs. This could provide valuable information to the broader cancer research community, especially as drug repurposing has emerged as a promising approach to identify novel therapeutics (K W To and Cho 2022).

In Chapter 4, a plasma proteomics analysis in combination with *ex vivo* DSRT was performed to identify potential circulating biomarkers of therapeutic response. Previous studies combining 'omics' approaches with *ex vivo* drug screening have focused on identifying molecular alterations within the malignant cells. To the best of my knowledge, this study is the first to evaluate changes in the plasma proteome based on *ex vivo* DSRT. Prior to LFQ-based MS, plasma samples were immunodepleted to remove high abundant proteins and improve the likelihood of detecting biologically relevant low abundant proteins. The detection of disease-specific biomarkers in MS-based plasma proteomic studies is more difficult than cellular proteomics due to the low number of proteins quantified when compared to the high protein composition of cells. Furthermore, despite significant improvements in the sensitivity and specificity of proteomic technologies, detecting and quantifying a protein produced by myeloma cells, secreted into the circulatory system in sufficient quantities and with an adequate half-life to facilitate detection, remains a significant challenge (Veenstra *et al.* 2005). However, establishing biomarker panels that are detectable in biofluids is crucial in the era of precision medicine. This is especially true in MM research as an invasive and painful lumbar puncture is required to collect tumour cells from the bone marrow of MM patients. Huge efforts have been made to characterise the plasma proteome to aid future biomarker discovery studies (Omenn 2004). In MM, circulating tumour cells (CTCs) are garnering increased attention as a source of minimally invasive, easily accessible biomarkers (Li, Zhang and Cai 2023). Evaluating the percentage of CTCs in the peripheral blood of myeloma patients has prognostic value, with greater than 0.01%

CTCs indicating an adverse prognosis (Garcés *et al.* 2022). Several studies have evaluated proteomic biomarkers in serum/plasma of MM patients versus healthy controls and in MM patients with differential response to treatment (Rajpal *et al.* 2011; Ma, Piao, *et al.* 2019; Chanukuppa *et al.* 2021).

Too many sets of drugs were analysed in Chapter 4 to visualize overlapping proteins from the mass spectrometry analysis on a Venn diagram, however, the full list is available in **Supp. File 8.1**. No protein was differentially abundant across all 7 drugs, however, two proteins, namely, Inter-alpha-trypsin inhibitor heavy chain H1 (ITIH1) and gelsolin (GSN), were SSDA across 6 of the 7 drugs analysed. Unique proteins linked to drug sensitivity/resistance were identified for each of the drugs: bortezomib (15), lenalidomide (8), dinaciclib (5), PF-04691502 (3), quisinostat (2), venetoclax (4), and navitoclax (2). As in Chapter 3, this highlights the potential of this approach to identify markers associated with general resistance mechanisms and drug-specific markers of response that may be incorporated into a biomarker panel for the prediction of drug resistance/sensitivity. Evaluating plasma cytokine levels in MM patients with differential *ex vivo* response to various drugs also yielded interesting results. A noteworthy finding was the correlation between increased IL-15 levels and increased sensitivity to a range of drugs including MEK inhibitors, PI3K/mTOR inhibitor, CDK inhibitors and HDAC inhibitors. This supports currents studies into the use of IL-15 agonists in combination with chemotherapies to enhance antitumour efficacy. Patients with higher circulating levels of IL-15 may exert a stronger anti-tumour immune response resulting in a higher susceptibility to certain therapeutics. In contrast, patients presenting with reduced plasma levels of IL-15 may benefit from IL-15 agonists to enhance the anti-tumour response and potentially overcome resistance to certain chemotherapies (Allegrezza *et al.* 2016; Shi *et al.* 2023). Furthermore, the link between increased plasma FLT3LG and drug response demonstrated in this work and other studies, highlights the positive implications of specific cytokine profiles on response to therapy. These findings may guide future research validating circulating cytokine profiles associated with drug response.

It is important to note that in Chapters 3 and 4, several drugs from different drug classes were selected for investigation. However, the *ex vivo* DSRT platform can evaluate the response of myeloma cells to hundreds of FDA-approved and

investigational drugs in a single experiment. Therefore, *ex vivo* DSRT in combination with 'omics' technologies can provide a huge amount of data on the molecular profiles of MM patients considered sensitive or resistant to hundreds of drugs. The small studies described in this thesis demonstrate the potential of larger studies with large sample sizes to define molecular drug response profiles to hundreds of drugs. This opens numerous avenues involving the use of this approach to discover novel mechanisms of resistance, especially against investigational therapeutics which may be in the early stages of clinical trials with limited data on the development of resistance in humans. Furthermore, as functional precision medicine approaches are now being evaluated in clinical trials, concomitant collection of additional myeloma cells and blood plasma for 'omic' analysis may identify predictive markers of drug response that can be easily measured in a clinical setting; for example, through the use of a multiplex ELISA panel that predicts response to specific therapeutics. These markers may also be valuable for monitoring drug response, however, longitudinal samples during treatment must be collected to evaluate this.

Although Chapters 3 and 4 focus on the discovery aspect of biomarker development, it is hoped that validation studies with large cohorts will identify the most sensitive and specific biomarkers for potential translation to a clinical setting. As mentioned, there is a growing need for biomarkers to predict drug response to cancer chemotherapeutics. This need is even more pronounced for MM patients who repeatedly relapse, often receiving greater than 5 lines of therapy. It is crucial that MM patients receive therapeutic regimens that will result in a prolonged duration of remission, as this is directly linked to overall survival (Migkou *et al.* 2011). To do this, a precision medicine approach is required and the use of multiplexed protein biomarker panels to predict drug response offers a straightforward, easily implementable means of bringing precision medicine to the clinic (**Figure 8.2**).

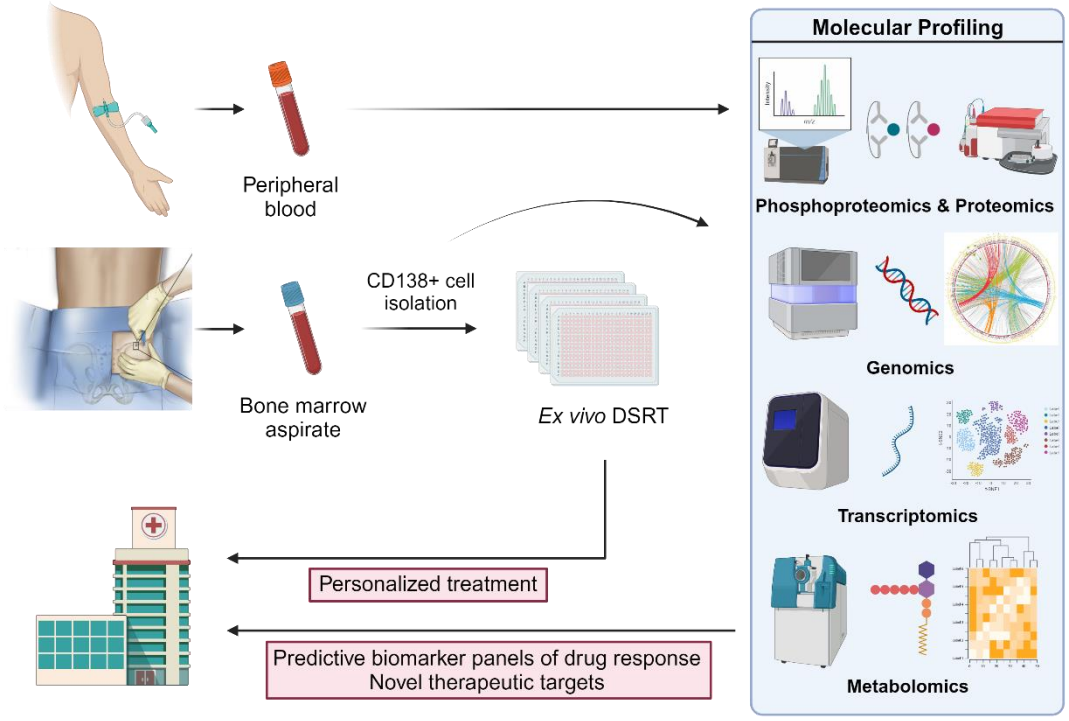

Figure 8.2: Framework for the clinical application of *ex vivo* drug screening in combination with molecular profiling. DSRT, drug sensitivity resistance testing.

Despite the fact that myeloma cells were collected from MM patients at diagnosis and relapse, a clear distinction can be seen between the very resistant and very sensitive chemosensitivity groups at both the proteomic and phosphoproteomic level. Although it will be necessary to adjust for these confounding factors in future validation phases, the distinct proteomic profiles identified in this study imply the presence of similar phosphoproteomic alterations linked to resistance both at diagnosis and relapse. The emergence of resistant myeloma subclones following treatment rather than intrinsic resistance is common in MM, and future studies with larger sample sizes should compare the phosphoproteomic changes in myeloma cells showing intrinsic resistance prior to treatment exposure, and those with acquired drug resistance following treatment exposure in a clinical setting. Furthermore, the analyses presented in Chapters 3 and 4 use *ex vivo* DSRT to stratify patients based on drug response. As outlined in Chapter 3, *ex vivo* DSRT has limitations including the inability to recreate the bone marrow microenvironment composition during the viability assay, which must be considered when evaluating the results of these chapters. Future studies combing large sample sizes, *ex vivo* DSRT, and downstream omics technologies should determine the accuracy of *ex vivo* drug responses by

comparing to patients' clinical outcomes. Although this requires extensive resources, collaboration with physicians, and time, this approach would strengthen the reliability of the results presented in this pilot study.

Chapters 5, 6, and 7 focus on deciphering the molecular phenotype of EMM. Our pilot studies using LFQ mass spectrometry to evaluate proteomic changes in the bone marrow and plasma of MM patients with and without extramedullary spread are the first of its kind. Chapter 7 builds on the results of Chapters 5 and 6 by identifying alterations in the plasma metabolome of MM patients with and without extramedullary spread. The combination of these chapters highlights the distinct molecular phenotype associated with EMM, while the individual chapters identify differentially abundant proteins and metabolites that warrant further validation as potential biomarkers of EMM. Proteomic analysis of bone marrow mononuclear cells from EMM and MM patients using LC-MS/MS had not previously been conducted. A clear shift in the proteome of the bone marrow mononuclear fraction in EMM compared to MM was identified. An enrichment of proteins linked to the focal adhesion pathway, ECM-receptor interactions, and leukocyte transendothelial migrations indicates cytoskeletal changes associated with alterations in cell adhesion and motility. Establishing protein signatures that are suggestive of cytoskeletal remodeling which favours cell motility may be informative for monitoring EMM development (Aseervatham 2020). An interesting pattern of increased abundance of proteins involved in the ILK signalling pathway was observed in EMM BMNCs, highlighting a potential role for this pathway in EMM development. Furthermore, a mechanism stimulating the emergence of subclones capable of extramedullary spread may involve the increased abundance of HPSE within the bone marrow which promotes dissemination via CD138 shedding. The results shown in Chapter 5 support this hypothesis. The main limitation of this study was the investigation of cells from the bone marrow and not myeloma cells from extramedullary sites. Unfortunately, samples from the site of extramedullary metastasis were unavailable for analysis. Therefore, it is important to remember the dynamic nature of protein expression, where decreased abundance of certain adhesion proteins in the bone marrow may facilitate intravasation, followed by re-expression of these proteins in circulation to facilitate tumour development at extramedullary sites. For example, there is evidence of dynamic surface expression of CD138 in myeloma cells where CD138-negative

cells promote dissemination while CD138-positive cells promote growth and survival. Evidence shows that CD138-negative cells can regain CD138 surface expression in circulation via unknown serum factors, which can promote extravasation to a new metastatic site (Akhmetzyanova *et al.* 2020). Furthermore, the evaluation of BMNCs instead of $CD138^+$ myeloma cells affects the interpretation of the results presented in Chapter 5. It is important to remember that the proteomic changes identified may originate from other cells in the mononuclear fraction.

Our plasma proteomics study (Chapter 6) identified plasma-derived markers of EMM that demonstrated excellent predictive power when used in combination. Although the mechanism that leads to increased levels of VCAM1, HGFA, and PEDF in EMM plasma is unknown, they represent promising biomarkers that can be easily quantified in patient plasma using immunoassays. Interestingly, VCAM1, HGFA, and PEDF levels were also increased in MM patients with del(17p), a cytogenetic abnormality linked to EMM development. It is hoped that future large-scale studies or clinical trials will evaluate the levels of these markers in the plasma of EMM patients to validate these findings and progress the development of these proteins as biomarkers for clinical use. Although proteins are more established as clinical biomarkers than individual metabolites and the initial focus should be placed on the validation of the significant proteins identified in Chapter 6, the metabolomic analysis seen in Chapter 7 highlights metabolic alterations in EMM compared to MM and supports further research investigating changes in the metabolism of EMM cells.

The limited efficacy of current MM therapeutics in the treatment of EMM is exemplified by the well-known poor prognosis of EMM patients (Lonial *et al.* 2021; Rosiñol *et al.* 2021). Despite the approval of novel MM therapeutics such as immunotherapies, preliminary studies have indicated that EMM patients do significantly worse in terms of the long-term efficacy of these treatments (Jelinek *et al.* 2022; Li, Liu, *et al.* 2022b). The research presented in this thesis illustrates a clear phenotypic change in the bone marrow niche and blood plasma of EMM patients compared to MM patients, suggesting a need for novel drug combinations or drug targets for the treatment of EMM to improve patient prognosis and treatment response (**Figure 8.3**). Several studies have reported the influence of the bone marrow microenvironment in myeloma cell dissemination (Forster and Radpour

2022; Gregorova *et al.* 2022). Targeting a pro-migratory BME may be a promising prophylactic approach to limit the emergence of myeloma subclones with capacity for extramedullary spread (Ho *et al.* 2022). Chapter 6 results show that sVCAM1 levels are increased in EMM patient plasma and correlate with sensitivity to the BCL-2 inhibitors, venetoclax and navitoclax, highlighting the potential of BCL-2 inhibitors for the treatment of EMM. Several proteins increased in abundance in EMM bone marrow mononuclear cells including LGALS1, HPSE, ROCK2, and ILK have specific inhibitors available that warrant investigation in the context of myeloma dissemination and EMM development. Monitoring heparanase levels within the BME to identify MM patients that may benefit from roneparstat treatment may represent a promising therapeutic option to prevent EMM progression. **Table 8.1** summarizes the protein targets that have been linked to EMM in the literature and in this thesis. This table also highlights specific inhibitors of these proteins that may represent promising therapeutics for the treatment of EMM. Crucially, large multi-centre studies are required to incorporate satisfactory sample sizes to evaluate the efficacy of novel drug combinations in EMM.

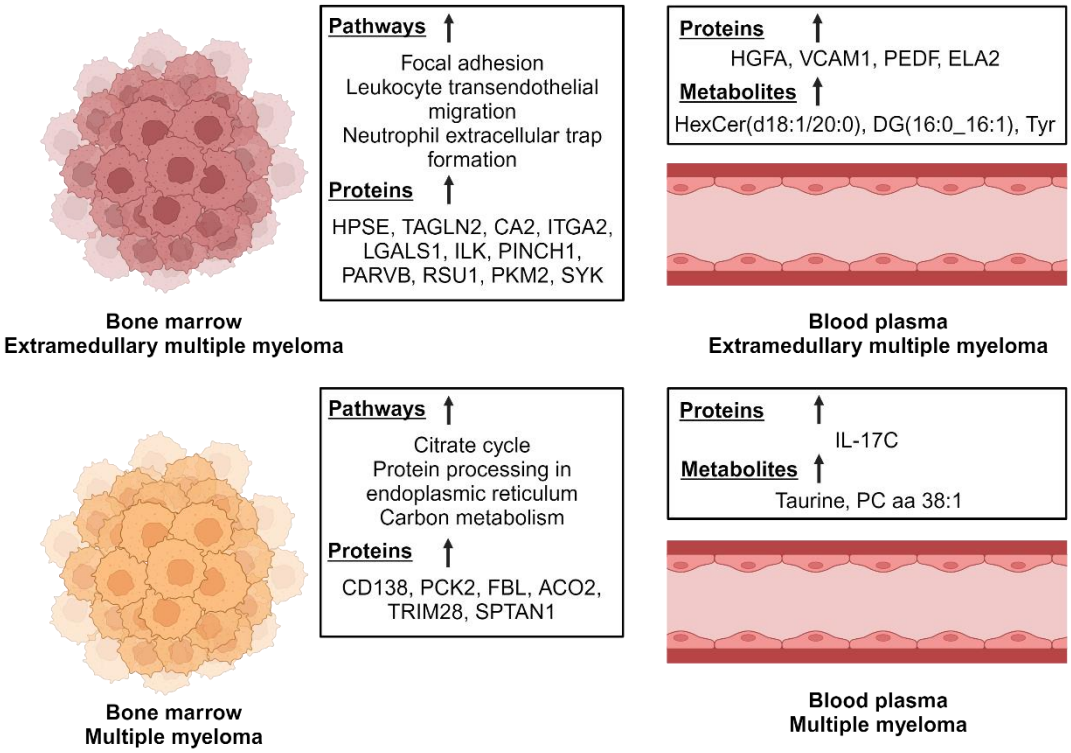

Figure 8.3: Summary of the proteomic alterations identified in this thesis when comparing extramedullary multiple myeloma and multiple myeloma without extramedullary spread. HPSE, heparanase; TAGLN2, transgelin-2; CA2, carbonic anhydrase 2; ITGA2, integrin alpha 2; LGALS1, galectin-1; ILK, integrin-linked kinase; PINCH1, particularly interesting new Cys-His protein; PARVB, β-parvin; RSU1, Ras suppressor protein 1; PKM2, pyruvate kinase M2; SYK, spleen tyrosine kinase; PCK2, phosphoenolpyruvate carboxykinase 2; FBL, rRNA 2'-O-methyltransferase fibrillarin; ACO2, aconitate hydratase; TRIM28, tripartite motif-containing 28; SPTAN1, spectrin alpha chain, non-erythrocytic; HGFA, hepatocyte growth factor activator; VCAM1, vascular cell adhesion molecule 1; PEDF, pigment epithelium derived factor; ELA2, elastase 2; HexCer, hexosylceramide; DG, diglyceride; IL-17C, interleukin-17C; PC, phosphatidylcholine.

Table 8.1: Potential targets/markers and associated therapeutics for the treatment of EMM patients based on the current literature.* This table provides a rationale for future studies focusing on the detection of drug targets in EMM.

Protein Target/Marker	Potential Therapeutic	Method of Target Detection	FDA Approval	Reference
Potential protein targets in extramedullary multiple myeloma (identified from the literature)				
BCL2	Venetoclax	Immunohistochemistry, qPCR, flow cytometry	Yes—Acute myeloid leukaemia, Chronic lymphocytic leukaemia	(Ludwig *et al.* 2019; Sidiqi *et al.* 2021)
BCL2, BCL-XL	Navitoclax	Immunohistochemistry, qPCR, flow cytometry	No	(Ackler *et al.* 2010; Ludwig *et al.* 2019)
XPO1	Selinexor	Immunohistochemistry	Yes—Multiple myeloma	(Bahlis *et al.* 2018; Yee *et al.* 2019)
Aminopeptidase expression	Melflufen	RNA sequencing	No	(Miettinen *et al.* 2021; Richardson *et al.* 2021)
MEK	Trametinib	Targeted sequencing for RAS mutations	Yes (in combination with dabrafenib)–Various metastatic solid tumours with BRAF V600 E mutation	(Touzeau and Moreau 2016; Sriskandarajah *et al.* 2020)
CD44v	4SCAR-CD44v6	Immunohistochemistry, flow cytometry	No	(Dahl *et al.* 2002; Gupta *et al.* 2022)
BRAF V600E	Vemurafenib, encorafenib, binimetinib	Allele-specific PCR	Yes–Metastatic melanoma with BRAF V600 E mutation	(Mey *et al.* 2017; Giesen *et al.* 2023)
Potential protein targets in extramedullary multiple myeloma (identified in this thesis)				
LGALS1	OTX008	Immunohistochemistry	No	(Storti *et al.* 2016, 2017; Mariño *et al.* 2023)
HPSE	Roneparstat	Immunohistochemistry	No	(Galli *et al.* 2018)
ROCK2	Belumosudil	qPCR, immunohistochemistry	Yes–Chronic graft-versus-host disease	(Cutler *et al.* 2021)
ILK	QLT0267, Compound 22	Immunohistochemistry	No	(Kalra *et al.* 2009; García-Marín *et al.* 2022)
Lipids	Statins	Unknown	Yes	(Brånvall *et al.* 2020; Gohlke *et al.* 2022)

*This table was adapted from (Dunphy *et al.* 2023).
Abbreviations: BCL2, B-cell lymphoma 2; qPCR, quantitative polymerase chain reaction; BCL-XL, B-cell lymphoma—extra large; XPO1, exportin 1; MEK, mitogen-activated protein kinase kinase; BRAF, B-Raf.

8.2 Future work

Despite decades of research on the pathogenesis of MM, it remains an incurable cancer with patients repeatedly relapsing over the course of the disease. Why is this? The treatment of chronic myeloid leukemia was revolutionized by the introduction of the tyrosine kinase inhibitor, imatinib (Hochhaus *et al.* 2017). Have we yet to identify the single molecular target that will facilitate curative treatment in MM? Maybe, however, as research methods have become more sophisticated and sensitive this possibility becomes unlikely. If this is the case, then how do we as scientists approach the study of a cancer as complex as MM to yield clinically relevant results that will directly improve the lives of MM patients? In my opinion, the stratification of MM patients based on risk or predictive drug response will need to include a combination of clinical data, genetic information, protein measurements, and potentially transcriptomic and/or metabolomic information to accurately predict the clinical course of MM patients and adapt therapeutic decision-making accordingly.

This project was exploratory in nature as we set out to identify novel molecular signatures of drug response and extramedullary myeloma. Therefore, several aspects of this project need rigorous follow-up investigation using large sample sizes to validate our findings and begin the next step of translating these results into a clinical setting. Our studies combining phosphoproteomics and plasma proteomics with *ex vivo* DSRT identified promising protein signatures associated with drug sensitivity/resistance to drugs from a variety of drug classes. Validation studies incorporating *ex vivo* DSRT, clinical data, and protein measurements are required to confirm the value of these biomarker signatures as predictors of drug response. The ability of *ex vivo* DSRT to examine response to hundreds of drugs is a powerful approach to precision medicine. I believe a large-scale study combining *ex vivo* DSRT with genomics, transcriptomics, proteomics, and metabolomics, would provide a wealth of information that would help construct clear sensitivity/resistance profiles that could be utilised to construct biomarker panels of drug sensitivity/resistance or identify proteins or pathways that can be targeted to overcome drug resistance. The use of this approach to construct predictive biomarker panels of drug response to individual therapeutics would aid therapeutic decision-

making and improve patient response to treatment, especially at late stages of disease as myeloma patients become refractory to a large number of therapeutics.

Regarding EMM, an international, collaborative initiative is required to decipher the mechanisms associated with EMM development, identify biomarkers with clinical usability and detect potential therapeutic targets. Currently, there are no EMM-specific treatment regimens and as response to current treatment options including immunotherapy remains poor, novel therapeutic targets must be identified to establish novel treatment regimens for EMM. In this work, we have identified a clear phenotypic change in the proteome of BMNCs and the plasma proteome and metabolome, highlighting EMM as a molecularly distinct form of MM. Thus, a novel therapeutic approach is required for the treatment of EMM. EMM can be diagnosed at diagnosis or relapse, and it is important to monitor the development of this aggressive sub-entity to inform clinical decision-making. In Chapter 6, we identified plasma-derived markers of EMM that warrant validation in a larger cohort of patients. These biomarkers can be longitudinally measured throughout the clinical course of MM patients, and if the levels of these markers are increased, advanced imaging tests can be performed to determine the presence of extramedullary lesions and adapt treatment accordingly. The use of these EMM markers will become increasingly important as EMM-specific clinical trials and standard treatment regimens become more common.

As mentioned, changes in the bone marrow microenvironment can influence myeloma cell dissemination into circulation. Therefore, I believe that the development of a prophylactic approach may hold relevance in EMM. In Chapter 5, we identified hundreds of proteins of differential abundance within the bone marrow of EMM patients compared to MM patients. Of particular interest was the increased abundance of proteins linked to leukocyte transendothelial migration, the ILK-PINCH-Parvin (IPP) complex, and the HPSE/CD138 axis. It is hoped that further validation of differential protein abundance will yield a protein signature that is indicative of a pro-migratory bone marrow microenvironment or EMM development. Subsequent longitudinal studies monitoring the abundance of these proteins throughout the disease course may identify a change to a pro-migratory phenotype within the bone marrow which promotes EMM development. Patients found to have

a pro-migratory bone marrow niche may benefit from treatment with therapeutics that target this niche to reduce myeloma cell dissemination and the establishment of lesions at extramedullary sites. Given the identification of HPSE as a key determinant of myeloma cell dissemination, the HPSE inhibitor, roneparstat, may benefit patients with increased likelihood of progression to EMM. As different clinical factors including the IgA immunoglobulin type, del(17p), and RAS mutations have been linked to EMM involvement, a risk prediction model incorporating these factors and the proteins identified in our study may accurately identify MM patients with increased risk of EMM progression. Although these statements represent my personal hypotheses on the future of EMM research, we believe that the research reported in Chapters 5, 6, and 7 provide a starting point for the future implementation of this approach in clinical settings. EMM-specific clinical trials are urgently needed to start the process of establishing standards for the clinical work-up and treatment of EMM patients.

As outlined in Chapters 3 and 4, the use of *ex vivo* DSRT holds promise as a precision medicine approach. An *ex vivo* drug screening of myeloma cells from extramedullary sites may help determine the susceptibility of these cells to a wide range of therapeutics. However, *ex vivo* drug screening approaches typically need a large number of fresh cells, which can be limited due to the rarity of EMM. Another aspect of EMM pathology that must be elucidated is the reason why circulating myeloma cells extravasate into specific soft tissues or organs such as the lungs, skin, or central nervous system. As mentioned in Chapter 5, neutrophils and NETs have been linked to the formation of a pre-metastatic niche at sites prior to the arrival of tumour cells (Chen and Yu 2023). Furthermore, from our results and the literature, hypoxia and the generation of ROS may play a role in stimulating the intravasation of myeloma cells into the peripheral blood in MM. Whether this is based on an intrinsic mechanism which increases the activity of HIF-1α or the location of the myeloma cells in an oxygen poor part of the bone marrow is unknown. Further research into the role of neutrophils and hypoxia in the process of EMM development are needed.

8.3 Conclusion

In conclusion, this thesis has used proteomic and metabolomic techniques to identify novel potential markers of the aggressive phenotypes of MM, drug-resistant MM and extramedullary multiple myeloma. This work has provided novel insight into the phosphoproteomic and proteomic alterations that are associated with drug response in myeloma cells and blood plasma, respectively. Furthermore, we have provided evidence of a distinct molecular phenotype associated with extramedullary multiple myeloma. The differentially abundant proteins and metabolites identified in Chapters 5, 6, and 7 contribute to our understanding of EMM pathophysiology. As biofluid-derived biomarkers are urgently required for rapid, non-invasive assessment of myeloma patients, proteomic profiling of blood plasma in drug-resistant MM and EMM identified promising protein biomarkers that warrant further validation in a large cohort of samples. Hepatocyte growth factor activator, vascular cell adhesion molecule 1 and pigment epithelium derived factor are significant biomarker candidates of interest for the detection of EMM. Throughout this work, overlapping biological processes, signalling pathways, and proteins were linked to drug-resistant MM and EMM, highlighting the need for novel therapeutic targets to combat these late-stage, aggressive phenotypes of MM. With further research expanding on the findings presented throughout this thesis, the molecular complexities associated with aggressive MM phenotypes can be elucidated and translated into clinical settings to improve patient outcomes.

Chapter 9

Bibliography

Abdallah, N., Rajkumar, S.V., Greipp, P., Kapoor, P., Gertz, M.A., Dispenzieri, A., Baughn, L.B., Lacy, M.Q., Hayman, S.R., Buadi, F.K., Dingli, D., Go, R.S., Hwa, Y.L., Fonder, A., Hobbs, M., Lin, Y., Leung, N., Kourelis, T., Warsame, R., Siddiqui, M., Lust, J., Kyle, R.A., Bergsagel, L., Ketterling, R., and Kumar, S.K. (2020) 'Cytogenetic abnormalities in multiple myeloma: association with disease characteristics and treatment response', *Blood Cancer Journal*, 10(8), 1–9, available: https://doi.org/10.1038/s41408-020-00348-5.

Abdel-Samad, N. and Sughayar, R. (2021) 'Can Treatment with Venetoclax for Chronic Lymphocytic Leukemia (CLL) Result In Autoimmune Hemolytic Anemia?', *The American Journal of Case Reports*, 22, e928514-1-e928514-3, available: https://doi.org/10.12659/AJCR.928514.

Abe, K., Ikeda, S., Nara, M., Kitadate, A., Tagawa, H., and Takahashi, N. (2023) 'Hypoxia-induced oxidative stress promotes therapy resistance via upregulation of heme oxygenase-1 in multiple myeloma', *Cancer Medicine*, 12(8), 9709–9722, available: https://doi.org/10.1002/cam4.5679.

Abe, M., Hiura, K., Wilde, J., Shioyasono, A., Moriyama, K., Hashimoto, T., Kido, S., Oshima, T., Shibata, H., Ozaki, S., Inoue, D., and Matsumoto, T. (2004) 'Osteoclasts enhance myeloma cell growth and survival via cell-cell contact: a vicious cycle between bone destruction and myeloma expansion', *Blood*, 104(8), 2484–2491, available: https://doi.org/10.1182/blood-2003-11-3839.

Abe, M., Kido, S., Hiasa, M., Nakano, A., Oda, A., Amou, H., and Matsumoto, T. (2006) 'BAFF and APRIL as osteoclast-derived survival factors for myeloma cells: a rationale for TACI-Fc treatment in patients with multiple myeloma', *Leukemia*, 20(7), 1313–1315, available: https://doi.org/10.1038/sj.leu.2404228.

Aberuyi, N., Rahgozar, S., Ghodousi, E.S., and Ghaedi, K. (2020) 'Drug Resistance Biomarkers and Their Clinical Applications in Childhood Acute Lymphoblastic Leukemia', *Frontiers in Oncology*, 9, available: https://www.frontiersin.org/articles/10.3389/fonc.2019.01496 [accessed 5 Jul 2023].

Abooshahab, R., Al-Salami, H., and Dass, C.R. (2021) 'The increasing role of pigment epithelium-derived factor in metastasis: from biological importance to a promising target', *Biochemical Pharmacology*, 193, 114787, available: https://doi.org/10.1016/j.bcp.2021.114787.

Abrahamsson, H., Jensen, B.V., Berven, L.L., Nielsen, D.L., Šaltytė Benth, J., Johansen, J.S., Larsen, F.O., Johansen, J.S., and Ree, A.H. (2020) 'Antitumour immunity invoked by hepatic arterial infusion of first-line oxaliplatin predicts durable colorectal cancer control after liver metastasis ablation: 8–12 years of follow-up', *International Journal of Cancer*, 146(7), 2019–2026, available: https://doi.org/10.1002/ijc.32847.

Ackler, S., Mitten, M.J., Foster, K., Oleksijew, A., Refici, M., Tahir, S.K., Xiao, Y., Tse, C., Frost, D.J., Fesik, S.W., Rosenberg, S.H., Elmore, S.W., and

Shoemaker, A.R. (2010) 'The Bcl-2 inhibitor ABT-263 enhances the response of multiple chemotherapeutic regimens in hematologic tumors in vivo', *Cancer Chemotherapy and Pharmacology*, 66(5), 869–880, available: https://doi.org/10.1007/s00280-009-1232-1.

Adam, K. and Hunter, T. (2018) 'Histidine kinases and the missing phosphoproteome from prokaryotes to eukaryotes', *Laboratory Investigation; a Journal of Technical Methods and Pathology*, 98(2), 233–247, available: https://doi.org/10.1038/labinvest.2017.118.

Akbari, Z., Dijojin, R.T., Zamani, Z., Hosseini, R.H., and Arjmand, M. (2021) 'Aromatic amino acids play a harmonizing role in prostate cancer: A metabolomics-based cross-sectional study', *International Journal of Reproductive Biomedicine*, 19(8), 741–750, available: https://doi.org/10.18502/ijrm.v19i8.9622.

Akhmetzyanova, I., McCarron, M.J., Parekh, S., Chesi, M., Bergsagel, P.L., and Fooksman, D.R. (2020) 'Dynamic CD138 surface expression regulates switch between myeloma growth and dissemination', *Leukemia*, 34(1), 245–256, available: https://doi.org/10.1038/s41375-019-0519-4.

Aksoy, E.K., Akpınar, M.Y., Doğan, Ö., Göktaş, Z., Sapmaz, F.P., Şimşek, G.G., Uzman, M., and Nazlıgül, Y. (2019) 'Clinical Significance of Serum Vascular Endothelial Growth Factor, Pigment Epithelium-Derived Factor, Tumor Necrosis Factor Alpha, and Progranulin Levels in Patients with Gastric Cancer and Gastric Precancerous Lesions', *Journal of Gastrointestinal Cancer*, 50(3), 537–542, available: https://doi.org/10.1007/s12029-019-00251-8.

Albrengues, J., Shields, M.A., Ng, D., Park, C.G., Ambrico, A., Poindexter, M.E., Upadhyay, P., Uyeminami, D.L., Pommier, A., Küttner, V., Bružas, E., Maiorino, L., Bautista, C., Carmona, E.M., Gimotty, P.A., Fearon, D.T., Chang, K., Lyons, S.K., Pinkerton, K.E., Trotman, L.C., Goldberg, M.S., Yeh, J.T.-H., and Egeblad, M. (2018) 'Neutrophil extracellular traps produced during inflammation awaken dormant cancer cells in mice', *Science (New York, N.Y.)*, 361(6409), eaao4227, available: https://doi.org/10.1126/science.aao4227.

Alexandrakis, M.G., Goulidaki, N., Pappa, C.A., Boula, A., Psarakis, F., Neonakis, I., and Tsirakis, G. (2015) 'Interleukin-10 Induces Both Plasma Cell Proliferation and Angiogenesis in Multiple Myeloma', *Pathology oncology research: POR*, 21(4), 929–934, available: https://doi.org/10.1007/s12253-015-9921-z.

Allegrezza, M.J., Rutkowski, M.R., Stephen, T.L., Svoronos, N., Tesone, A.J., Perales-Puchalt, A., Nguyen, J.M., Sarmin, F., Sheen, M.R., Jeng, E.K., Tchou, J., Wong, H.C., Fiering, S., and Conejo-Garcia, J.R. (2016) 'IL-15 AGONISTS OVERCOME THE IMMUNOSUPPRESSIVE EFFECTS OF MEK INHIBITORS', *Cancer research*, 76(9), 2561–2572, available: https://doi.org/10.1158/0008-5472.CAN-15-2808.

Almehmadi, M., Flanagan, B.F., Khan, N., Alomar, S., and Christmas, S.E. (2014) 'Increased numbers and functional activity of CD56+ T cells in healthy cytomegalovirus positive subjects', *Immunology*, 142(2), 258–268, available: https://doi.org/10.1111/imm.12250.

Alonso, R., Cedena, M.-T., Wong, S., Shah, N., Ríos-Tamayo, R., Moraleda, J.M., López-Jiménez, J., García, C., Bahri, N., Valeri, A., Sánchez, R., Collado-Yurrita, L., Martin, T., Wolf, J., Lahuerta, J.-J., and Martínez-López, J. (2020) 'Prolonged lenalidomide maintenance therapy improves the depth of response in multiple myeloma', *Blood Advances*, 4(10), 2163–2171, available: https://doi.org/10.1182/bloodadvances.2020001508.

An, R., Yu, H., Wang, Y., Lu, J., Gao, Y., Xie, X., and Zhang, J. (2022) 'Integrative analysis of plasma metabolomics and proteomics reveals the metabolic landscape of breast cancer', *Cancer & Metabolism*, 10(1), 13, available: https://doi.org/10.1186/s40170-022-00289-6.

Anand, S., Samuel, M., Ang, C.-S., Keerthikumar, S., and Mathivanan, S. (2017) 'Label-Based and Label-Free Strategies for Protein Quantitation', in Keerthikumar, S. and Mathivanan, S., eds., *Proteome Bioinformatics*, Methods in Molecular Biology, New York, NY: Springer, 31–43, available: https://doi.org/10.1007/978-1-4939-6740-7_4.

Anderson, N.M., Mucka, P., Kern, J.G., and Feng, H. (2018) 'The emerging role and targetability of the TCA cycle in cancer metabolism', *Protein & Cell*, 9(2), 216–237, available: https://doi.org/10.1007/s13238-017-0451-1.

Anderson, N.M. and Simon, M.C. (2020) 'The tumor microenvironment', *Current biology: CB*, 30(16), R921–R925, available: https://doi.org/10.1016/j.cub.2020.06.081.

Annan, D.A., Maishi, N., Soga, T., Dawood, R., Li, C., Kikuchi, H., Hojo, T., Morimoto, M., Kitamura, T., Alam, M.T., Minowa, K., Shinohara, N., Nam, J.-M., Hida, Y., and Hida, K. (2019) 'Carbonic anhydrase 2 (CAII) supports tumor blood endothelial cell survival under lactic acidosis in the tumor microenvironment', *Cell Communication and Signaling*, 17(1), 169, available: https://doi.org/10.1186/s12964-019-0478-4.

Ansari, D., Althini, C., Ohlsson, H., Bauden, M., and Andersson, R. (2019) 'The Role of PEDF in Pancreatic Cancer', *Anticancer Research*, 39(7), 3311–3315, available: https://doi.org/10.21873/anticanres.13473.

Apte, R.S., Barreiro, R.A., Duh, E., Volpert, O., and Ferguson, T.A. (2004) 'Stimulation of Neovascularization by the Anti-angiogenic Factor PEDF', *Investigative Ophthalmology & Visual Science*, 45(12), 4491–4497, available: https://doi.org/10.1167/iovs.04-0172.

Araki, T., Gejyo, F., Takagaki, K., Haupt, H., Schwick, H.G., Bürgi, W., Marti, T., Schaller, J., Rickli, E., and Brossmer, R. (1988) 'Complete amino acid sequence of human plasma Zn-alpha 2-glycoprotein and its homology to histocompatibility antigens', *Proceedings of the National Academy of*

Sciences of the United States of America, 85(3), 679–683, available: https://doi.org/10.1073/pnas.85.3.679.

Ardi, V.C., Deryugina, E.I., and Quigley, J.P. (2020) 'Neutrophil Elastase Facilitates Cancer Cell Motility via Induction of Akt Signaling Pathway', *The FASEB Journal*, 34(S1), 1–1, available: https://doi.org/10.1096/fasebj.2020.34.s1.04626.

Ardito, F., Giuliani, M., Perrone, D., Troiano, G., and Muzio, L.L. (2017) 'The crucial role of protein phosphorylation in cell signaling and its use as targeted therapy (Review)', *International Journal of Molecular Medicine*, 40(2), 271–280, available: https://doi.org/10.3892/ijmm.2017.3036.

Arendt, C.S. and Hochstrasser, M. (1997) 'Identification of the yeast 20S proteasome catalytic centers and subunit interactions required for active-site formation', *Proceedings of the National Academy of Sciences of the United States of America*, 94(14), 7156–7161.

Argyriou, A.A., Iconomou, G., and Kalofonos, H.P. (2008) 'Bortezomib-induced peripheral neuropathy in multiple myeloma: a comprehensive review of the literature', *Blood*, 112(5), 1593–1599, available: https://doi.org/10.1182/blood-2008-04-149385.

Asare-Werehene, M., Tsuyoshi, H., Zhang, H., Salehi, R., Chang, C.-Y., Carmona, E., Librach, C.L., Mes-Masson, A.-M., Chang, C.-C., Burger, D., Yoshida, Y., and Tsang, B.K. (2022) 'Plasma Gelsolin Confers Chemoresistance in Ovarian Cancer by Resetting the Relative Abundance and Function of Macrophage Subtypes', *Cancers*, 14(4), 1039, available: https://doi.org/10.3390/cancers14041039.

Aseervatham, J. (2020) 'Cytoskeletal Remodeling in Cancer', *Biology*, 9(11), 385, available: https://doi.org/10.3390/biology9110385.

Ashok, D., Polcik, L., Dannewitz Prosseda, S., and Hartmann, T.N. (2022) 'Insights Into Bone Marrow Niche Stability: An Adhesion and Metabolism Route', *Frontiers in Cell and Developmental Biology*, 9, available: https://www.frontiersin.org/articles/10.3389/fcell.2021.798604 [accessed 13 Apr 2023].

Astarci, E., Sade, A., Cimen, I., Savaş, B., and Banerjee, S. (2012) 'The NF-κB target genes ICAM-1 and VCAM-1 are differentially regulated during spontaneous differentiation of Caco-2 cells', *The FEBS journal*, 279(16), 2966–2986, available: https://doi.org/10.1111/j.1742-4658.2012.08677.x.

Attwell, S., Roskelley, C., and Dedhar, S. (2000) 'The integrin-linked kinase (ILK) suppresses anoikis', *Oncogene*, 19(33), 3811–3815, available: https://doi.org/10.1038/sj.onc.1203711.

Aubert, L., Arroyo, H., Detolle, P., Picard, D., and Cotte, G. (1967) '[Clinical and cytologic study of a 2nd case of xanthomatous IgA myeloma with circulating anti-lipoprotein antibodies]', *La Semaine Des Hopitaux: Organe Fonde Par*

l'Association D'enseignement Medical Des Hopitaux De Paris, 43(48), 3014–3021.

Ayhan, S., Nemutlu, E., Uçkan Çetinkaya, D., Kır, S., and Özgül, R.K. (2021) 'Characterization of human bone marrow niches with metabolome and transcriptome profiling', *Journal of Cell Science*, 134(6), jcs250720, available: https://doi.org/10.1242/jcs.250720.

Azab, A.K., Hu, J., Quang, P., Azab, F., Pitsillides, C., Awwad, R., Thompson, B., Maiso, P., Sun, J.D., Hart, C.P., Roccaro, A.M., Sacco, A., Ngo, H.T., Lin, C.P., Kung, A.L., Carrasco, R.D., Vanderkerken, K., and Ghobrial, I.M. (2012) 'Hypoxia promotes dissemination of multiple myeloma through acquisition of epithelial to mesenchymal transition-like features', *Blood*, 119(24), 5782–5794, available: https://doi.org/10.1182/blood-2011-09-380410.

Babur, Ö., Melrose, A.R., Cunliffe, J.M., Klimek, J., Pang, J., Sepp, A.-L.I., Zilberman-Rudenko, J., Tassi Yunga, S., Zheng, T., Parra-Izquierdo, I., Minnier, J., McCarty, O.J.T., Demir, E., Reddy, A.P., Wilmarth, P.A., David, L.L., and Aslan, J.E. (2020) 'Phosphoproteomic quantitation and causal analysis reveal pathways in GPVI/ITAM-mediated platelet activation programs', *Blood*, 136(20), 2346–2358, available: https://doi.org/10.1182/blood.2020005496.

Badawy, A.A.-B. and Guillemin, G. (2019) 'The Plasma [Kynurenine]/[Tryptophan] Ratio and Indoleamine 2,3-Dioxygenase: Time for Appraisal', *International Journal of Tryptophan Research : IJTR*, 12, 1178646919868978, available: https://doi.org/10.1177/1178646919868978.

Baghban, R., Roshangar, L., Jahanban-Esfahlan, R., Seidi, K., Ebrahimi-Kalan, A., Jaymand, M., Kolahian, S., Javaheri, T., and Zare, P. (2020) 'Tumor microenvironment complexity and therapeutic implications at a glance', *Cell Communication and Signaling*, 18(1), 59, available: https://doi.org/10.1186/s12964-020-0530-4.

Bahlis, N.J., Sutherland, H., White, D., Sebag, M., Lentzsch, S., Kotb, R., Venner, C.P., Gasparetto, C., Del Col, A., Neri, P., Reece, D., Kauffman, M., Shacham, S., Unger, T.J., Jeha, J., Saint-Martin, J.-R., Shah, J., and Chen, C. (2018) 'Selinexor plus low-dose bortezomib and dexamethasone for patients with relapsed or refractory multiple myeloma', *Blood*, 132(24), 2546–2554, available: https://doi.org/10.1182/blood-2018-06-858852.

Baliou, S., Kyriakopoulos, A.M., Spandidos, D.A., and Zoumpourlis, V. (2020) 'Role of taurine, its haloamines and its lncRNA TUG1 in both inflammation and cancer progression. On the road to therapeutics? (Review)', *International Journal of Oncology*, 57(3), 631–664, available: https://doi.org/10.3892/ijo.2020.5100.

Ball, L.E., Agana, B.A., Comte-Walters, S., Bethard, J.R., and Burnette, B.B. (2023) 'An Introduction to Mass Spectrometry-Based Proteomics', in Bradshaw, R.A., Hart, G.W. and Stahl, P.D., eds., *Encyclopedia of Cell Biology (Second*

Edition), Oxford: Academic Press, 132–140, available: https://doi.org/10.1016/B978-0-12-821618-7.00143-7.

Banks, R.E., Gearing, A.J., Hemingway, I.K., Norfolk, D.R., Perren, T.J., and Selby, P.J. (1993) 'Circulating intercellular adhesion molecule-1 (ICAM-1), E-selectin and vascular cell adhesion molecule-1 (VCAM-1) in human malignancies', *British Journal of Cancer*, 68(1), 122–124, available: https://doi.org/10.1038/bjc.1993.298.

Banoei, M.M., Mahé, E., Mansoor, A., Stewart, D., Winston, B.W., Habibi, H.R., and Shabani-Rad, M.-T. (2022) 'NMR-based metabolomic profiling can differentiate follicular lymphoma from benign lymph node tissues and may be predictive of outcome', *Scientific Reports*, 12(1), 8294, available: https://doi.org/10.1038/s41598-022-12445-5.

Bansal, R., Rakshit, S., and Kumar, S. (2021) 'Extramedullary disease in multiple myeloma', *Blood Cancer Journal*, 11(9), 161, available: https://doi.org/10.1038/s41408-021-00527-y.

Bantscheff,M., Lemeer, S., Savitski, M.M., and Kuster, B. (2012) 'Quantitative mass spectrometry in proteomics: critical review update from 2007 to the present', *Analytical and Bioanalytical Chemistry*, 404(4), 939–965, available: https://doi.org/10.1007/s00216-012-6203-4.

Bao, X., Zeng, J., Huang, H., Ma, C., Wang, L., Wang, F., Liao, X., and Song, X. (2020) 'Cancer-targeted PEDF-DNA therapy for metastatic colorectal cancer', *International Journal of Pharmaceutics*, 576, 118999, available: https://doi.org/10.1016/j.ijpharm.2019.118999.

Barbazán, J., Alonso-Alconada, L., Muinelo-Romay, L., Vieito, M., Abalo, A., Alonso-Nocelo, M., Candamio, S., Gallardo, E., Fernández, B., Abdulkader, I., de los Ángeles Casares, M., Gómez-Tato, A., López-López, R., and Abal, M. (2012) 'Molecular Characterization of Circulating Tumor Cells in Human Metastatic Colorectal Cancer', *PLoS ONE*, 7(7), e40476, available: https://doi.org/10.1371/journal.pone.0040476.

Bard, J.A.M., Goodall, E.A., Greene, E.R., Jonsson, E., Dong, K.C., and Martin, A. (2018) 'Structure and Function of the 26S Proteasome', *Annual review of biochemistry*, 87, 697–724, available: https://doi.org/10.1146/annurev-biochem-062917-011931.

Barkovits, K., Pacharra, S., Pfeiffer, K., Steinbach, S., Eisenacher, M., Marcus, K., and Uszkoreit, J. (2020) 'Reproducibility, Specificity and Accuracy of Relative Quantification Using Spectral Library-based Data-independent Acquisition', *Molecular & Cellular Proteomics : MCP*, 19(1), 181–197, available: https://doi.org/10.1074/mcp.RA119.001714.

Barlogie, B., Alexanian, R., Dicke, K.A., Zagars, G., Spitzer, G., Jagannath, S., and Horwitz, L. (1987) 'High-dose chemoradiotherapy and autologous bone marrow transplantation for resistant multiple myeloma', *Blood*, 70(3), 869–872.

Barrio, S., Stühmer, T., Da-Viá, M., Barrio-Garcia, C., Lehners, N., Besse, A., Cuenca, I., Garitano-Trojaola, A., Fink, S., Leich, E., Chatterjee, M., Driessen, C., Martinez-Lopez, J., Rosenwald, A., Beckmann, R., Bargou, R.C., Braggio, E., Stewart, A.K., Raab, M.S., Einsele, H., and Kortüm, K.M. (2019) 'Spectrum and functional validation of PSMB5 mutations in multiple myeloma', *Leukemia*, 33(2), 447–456, available: https://doi.org/10.1038/s41375-018-0216-8.

Bartel, T.B., Haessler, J., Brown, T.L.Y., Shaughnessy, J.D., van Rhee, F., Anaissie, E., Alpe, T., Angtuaco, E., Walker, R., Epstein, J., Crowley, J., and Barlogie, B. (2009) 'F18-fluorodeoxyglucose positron emission tomography in the context of other imaging techniques and prognostic factors in multiple myeloma', *Blood*, 114(10), 2068–2076, available: https://doi.org/10.1182/blood-2009-03-213280.

Barthel, S.R., Annis, D.S., Mosher, D.F., and Johansson, M.W. (2006) 'Differential engagement of modules 1 and 4 of vascular cell adhesion molecule-1 (CD106) by integrins alpha4beta1 (CD49d/29) and alphaMbeta2 (CD11b/18) of eosinophils', *The Journal of Biological Chemistry*, 281(43), 32175–32187, available: https://doi.org/10.1074/jbc.M600943200.

Bataille, R., Barlogie, B., Lu, Z.Y., Rossi, J.-F., Lavabre-Bertrand, T., Beck, T., Wijdenes, J., Brochier, J., and Klein, B. (1995) 'Biologic Effects of Anti-Interleukin-6 Murine Monoclonal Antibody in Advanced Multiple Myeloma', *Blood*, 86(2), 685–691, available: https://doi.org/10.1182/blood.V86.2.685.bloodjournal862685.

Bataille, R., Jourdan, M., Zhang, X.G., and Klein, B. (1989) 'Serum levels of interleukin 6, a potent myeloma cell growth factor, as a reflect of disease severity in plasma cell dyscrasias.', *The Journal of Clinical Investigation*, 84(6), 2008–2011, available: https://doi.org/10.1172/JCI114392.

Becerra, S.P. and Notario, V. (2013) 'The effects of PEDF on cancer biology: mechanisms of action and therapeutic potential', *Nature reviews. Cancer*, 13(4), 258–271, available: https://doi.org/10.1038/nrc3484.

Bednarz-Misa, I., Fortuna, P., Fleszar, M.G., Lewandowski, Ł., Diakowska, D., Rosińczuk, J., and Krzystek-Korpacka, M. (2020) 'Esophageal Squamous Cell Carcinoma Is Accompanied by Local and Systemic Changes in L-arginine/NO Pathway', *International Journal of Molecular Sciences*, 21(17), 6282, available: https://doi.org/10.3390/ijms21176282.

Bedolla, R.G., Wang, Y., Asuncion, A., Chamie, K., Siddiqui, S., Mudryj, M.M., Prihoda, T.J., Siddiqui, J., Chinnaiyan, A.M., Mehra, R., deVereWhite, R.W., and Ghosh, P.M. (2009) 'Nuclear vs Cytoplasmic localization of Filamin A in Prostate Cancer: Immunohistochemical Correlation with Metastases', *Clinical cancer research : an official journal of the American Association for Cancer Research*, 15(3), 788–796, available: https://doi.org/10.1158/1078-0432.CCR-08-1402.

Beksac, M., Seval, G.C., Kanellias, N., Coriu, D., Rosiñol, L., Ozet, G., Goranova-Marinova, V., Unal, A., Bila, J., Ozsan, H., Ivanaj, A., Balić, L.I., Kastritis, E., Bladé, J., and Dimopoulos, M.A. (2020) 'A real world multicenter retrospective study on extramedullary disease from Balkan Myeloma Study Group and Barcelona University: analysis of parameters that improve outcome', *Haematologica*, 105(1), 201–208, available: https://doi.org/10.3324/haematol.2019.219295.

Bennett, H.M., Stephenson, W., Rose, C.M., and Darmanis, S. (2023) 'Single-cell proteomics enabled by next-generation sequencing or mass spectrometry', *Nature Methods*, 20(3), 363–374, available: https://doi.org/10.1038/s41592-023-01791-5.

Bennett, N.K., Nakaoka, H.J., Laurent, D., Okimoto, R.A., Sei, Y., Horvai, A.E., Bivona, T.G., Hoeve, J. ten, Graeber, T.G., Nakamura, K., and Nakamura, J.L. (2022) 'Primary and metastatic tumors exhibit systems-level differences in dependence on mitochondrial respiratory function', *PLoS Biology*, 20(9), available: https://doi.org/10.1371/journal.pbio.3001753.

Berenson, J.R., Ma, H.M., and Vescio, R. (2001) 'The role of nuclear factor-κb in the biology and treatment of multiple myeloma', *Seminars in Oncology*, New Approaches to the Treatment of Multiple Myeloma, 28(6), 626–633, available: https://doi.org/10.1016/S0093-7754(01)90036-3.

Berger, C., Berger, M., Hackman, R.C., Gough, M., Elliott, C., Jensen, M.C., and Riddell, S.R. (2009) 'Safety and immunologic effects of IL-15 administration in nonhuman primates', *Blood*, 114(12), 2417–2426, available: https://doi.org/10.1182/blood-2008-12-189266.

Besse, A., Besse, L., Kraus, M., Mendez-Lopez, M., Bader, J., Xin, B.-T., Bruin, G. de, Maurits, E., Overkleeft, H.S., and Driessen, C. (2019) 'Proteasome Inhibition in Multiple Myeloma: Head-to-Head Comparison of Currently Available Proteasome Inhibitors', *Cell Chemical Biology*, 26(3), 340-351.e3, available: https://doi.org/10.1016/j.chembiol.2018.11.007.

Besse, A., Stolze, S.C., Rasche, L., Weinhold, N., Morgan, G.J., Kraus, M., Bader, J., Overkleeft, H.S., Besse, L., and Driessen, C. (2018) 'Carfilzomib resistance due to ABCB1/MDR1 overexpression is overcome by nelfinavir and lopinavir in multiple myeloma', *Leukemia*, 32(2), 391–401, available: https://doi.org/10.1038/leu.2017.212.

Besse, L., Sedlarikova, L., Greslikova, H., Kupska, R., Almasi, M., Penka, M., Jelinek, T., Pour, L., Adam, Z., Kuglik, P., Krejci, M., Hajek, R., and Sevcikova, S. (2016) 'Cytogenetics in multiple myeloma patients progressing into extramedullary disease', *European Journal of Haematology*, 97(1), 93–100, available: https://doi.org/10.1111/ejh.12688.

Bhutani, M., Foureau, D.M., Atrash, S., Voorhees, P.M., and Usmani, S.Z. (2020) 'Extramedullary multiple myeloma', *Leukemia*, 34(1), 1–20, available: https://doi.org/10.1038/s41375-019-0660-0.

Bianchi, G., Oliva, L., Cascio, P., Pengo, N., Fontana, F., Cerruti, F., Orsi, A., Pasqualetto, E., Mezghrani, A., Calbi, V., Palladini, G., Giuliani, N., Anderson, K.C., Sitia, R., and Cenci, S. (2009) 'The proteasome load versus capacity balance determines apoptotic sensitivity of multiple myeloma cells to proteasome inhibition', *Blood*, 113(13), 3040–3049, available: https://doi.org/10.1182/blood-2008-08-172734.

Biavati, L., Huff, C.A., Ferguson, A., Sidorski, A., Stevens, M.A., Rudraraju, L., Zucchinetti, C., Ali, S.A., Imus, P., Gocke, C.B., Gittelman, R.M., Johnson, S., Sanders, C., Vignali, M., Gandhi, A., Ye, X., Noonan, Kimberly.A., and Borrello, I. (2021) 'An allogeneic multiple myeloma GM-CSF-secreting vaccine with lenalidomide induces long-term immunity and durable clinical responses in patients in near complete remission', *Clinical cancer research : an official journal of the American Association for Cancer Research*, 27(24), 6696–6708, available: https://doi.org/10.1158/1078-0432.CCR-21-1916.

Bickett, T.E., Knitz, M., Darragh, L.B., Bhatia, S., Van Court, B., Gadwa, J., Bhuvane, S., Piper, M., Nguyen, D., Tu, H., Lenz, L., Clambey, E.T., Barry, K., and Karam, S.D. (2021) 'FLT3L Release by Natural Killer Cells Enhances Response to Radioimmunotherapy in Preclinical Models of HNSCC', *Clinical Cancer Research*, 27(22), 6235–6249, available: https://doi.org/10.1158/1078-0432.CCR-21-0971.

Billecke, L., Murga Penas, E.M., May, A.M., Engelhardt, M., Nagler, A., Leiba, M., Schiby, G., Kröger, N., Zustin, J., Marx, A., Matschke, J., Tiemann, M., Goekkurt, E., Heidtmann, H.-H., Vettorazzi, E., Dierlamm, J., Bokemeyer, C., and Schilling, G. (2013) 'Cytogenetics of extramedullary manifestations in multiple myeloma', *British Journal of Haematology*, 161(1), 87–94, available: https://doi.org/10.1111/bjh.12223.

Bíró, Domján, Falus, Jakab, Cseh, Kalabay, Tarkovács, Tresch, Malle, Kramer, Prohászka, Jákó, Füst, and Császár (1998) 'Cytokine regulation of the acute-phase protein levels in multiple myeloma', *European Journal of Clinical Investigation*, 28(8), 679–686, available: https://doi.org/10.1046/j.1365-2362.1998.00333.x.

Bladé, J., Beksac, M., Caers, J., Jurczyszyn, A., von Lilienfeld-Toal, M., Moreau, P., Rasche, L., Rosiñol, L., Usmani, S.Z., Zamagni, E., and Richardson, P. (2022a) 'Extramedullary disease in multiple myeloma: a systematic literature review', *Blood Cancer Journal*, 12(3), 45, available: https://doi.org/10.1038/s41408-022-00643-3.

Bladé, J., Beksac, M., Caers, J., Jurczyszyn, A., von Lilienfeld-Toal, M., Moreau, P., Rasche, L., Rosiñol, L., Usmani, S.Z., Zamagni, E., and Richardson, P. (2022b) 'Extramedullary disease in multiple myeloma: a systematic literature review', *Blood Cancer Journal*, 12(3), 45, available: https://doi.org/10.1038/s41408-022-00643-3.

Bladé, J., Fernández de Larrea, C., Rosiñol, L., Cibeira, M.T., Jiménez, R., and Powles, R. (2011) 'Soft-Tissue Plasmacytomas in Multiple Myeloma: Incidence, Mechanisms of Extramedullary Spread, and Treatment

Approach', *Journal of Clinical Oncology*, 29(28), 3805–3812, available: https://doi.org/10.1200/JCO.2011.34.9290.

Blasco, H., Błaszczyński, J., Billaut, J.C., Nadal-Desbarats, L., Pradat, P.F., Devos, D., Moreau, C., Andres, C.R., Emond, P., Corcia, P., and Słowiński, R. (2015) 'Comparative analysis of targeted metabolomics: Dominance-based rough set approach versus orthogonal partial least square-discriminant analysis', *Journal of Biomedical Informatics*, 53, 291–299, available: https://doi.org/10.1016/j.jbi.2014.12.001.

Bolli, N., Genuardi, E., Ziccheddu, B., Martello, M., Oliva, S., and Terragna, C. (2020) 'Next-Generation Sequencing for Clinical Management of Multiple Myeloma: Ready for Prime Time?', *Frontiers in Oncology*, 10, 189, available: https://doi.org/10.3389/fonc.2020.00189.

Borberg, E., Pashko, S., Koren, V., Burstein, L., and Patolsky, F. (2021) 'Depletion of Highly Abundant Protein Species from Biosamples by the Use of a Branched Silicon Nanopillar On-Chip Platform', *Analytical Chemistry*, 93(43), 14527–14536, available: https://doi.org/10.1021/acs.analchem.1c03506.

Borset, M., Lien, E., Espevik, T., Helseth, E., Waage, A., and Sundan, A. (1996) 'Concomitant expression of hepatocyte growth factor/scatter factor and the receptor c-MET in human myeloma cell lines', *The Journal of Biological Chemistry*, 271(40), 24655–24661, available: https://doi.org/10.1074/jbc.271.40.24655.

Bottaro, D.P., Rubin, J.S., Faletto, D.L., Chan, A.M.-L., Kmiecik, T.E., Vande Woude, G.F., and Aaronson, S.A. (1991) 'Identification of the hepatocyte growth factor receptor as the c-met proto-oncogene product', *Science (New York, N.Y.)*, 251(4995), available: https://doi.org/10.1126/science.1846706.

Bou Zerdan, M., Nasr, L., Kassab, J., Saba, L., Ghossein, M., Yaghi, M., Dominguez, B., and Chaulagain, C.P. (2022) 'Adhesion molecules in multiple myeloma oncogenesis and targeted therapy', *International Journal of Hematologic Oncology*, 11(2), IJH39, available: https://doi.org/10.2217/ijh-2021-0017.

Bourguignon, L.Y.W. (2008) 'Hyaluronan-mediated CD44 activation of RhoGTPase signaling and cytoskeleton function promotes tumor progression', *Seminars in cancer biology*, 18(4), 251–259, available: https://doi.org/10.1016/j.semcancer.2008.03.007.

Boys, E.L., Liu, J., Robinson, P.J., and Reddel, R.R. (2023) 'Clinical applications of mass spectrometry-based proteomics in cancer: Where are we?', *PROTEOMICS*, 23(7–8), 2200238, available: https://doi.org/10.1002/pmic.202200238.

Brånvall, E., Ekberg, S., Eloranta, S., Wästerlid, T., Birmann, B.M., and Smedby, K.E. (2020) 'Statin use is associated with improved survival in multiple myeloma: A Swedish population-based study of 4315 patients', *American*

Journal of Hematology, 95(6), 652–661, available: https://doi.org/10.1002/ajh.25778.

Brevi, A., Cogrossi, L.L., Grazia, G., Masciovecchio, D., Impellizzieri, D., Lacanfora, L., Grioni, M., and Bellone, M. (2020) 'Much More Than IL-17A: Cytokines of the IL-17 Family Between Microbiota and Cancer', *Frontiers in Immunology*, 11, 565470, available: https://doi.org/10.3389/fimmu.2020.565470.

Brinkmann, V., Reichard, U., Goosmann, C., Fauler, B., Uhlemann, Y., Weiss, D.S., Weinrauch, Y., and Zychlinsky, A. (2004) 'Neutrophil Extracellular Traps Kill Bacteria', *Science*, 303(5663), 1532–1535, available: https://doi.org/10.1126/science.1092385.

Brioli, A., Melchor, L., Cavo, M., and Morgan, G.J. (2014) 'The impact of intra-clonal heterogeneity on the treatment of multiple myeloma', *British Journal of Haematology*, 165(4), 441–454, available: https://doi.org/10.1111/bjh.12805.

Brosch, M., Yu, L., Hubbard, T., and Choudhary, J. (2009) 'Accurate and Sensitive Peptide Identification with Mascot Percolator', *Journal of proteome research*, 8(6), 3176–3181, available: https://doi.org/10.1021/pr800982s.

Browning, J.L., Dougas, I., Ngam-ek, A., Bourdon, P.R., Ehrenfels, B.N., Miatkowski, K., Zafari, M., Yampaglia, A.M., Lawton, P., and Meier, W. (1995) 'Characterization of surface lymphotoxin forms. Use of specific monoclonal antibodies and soluble receptors.', *The Journal of Immunology*, 154(1), 33–46, available: https://doi.org/10.4049/jimmunol.154.1.33.

Bruinink, D.H. op, Kuiper, R., Duin, M. van, Cupedo, T., Velden, V.H.J. van der, Hoogenboezem, R., Holt, B. van der, Beverloo, H.B., Valent, E.T., Vermeulen, M., Gay, F., Broijl, A., Avet-Loiseau, H., Munshi, N.C., Musto, P., Moreau, P., Zweegman, S., Donk, N.W.C.J. van de, and Sonneveld, P. (2022) 'Identification of High-Risk Multiple Myeloma With a Plasma Cell Leukemia-Like Transcriptomic Profile', *Journal of Clinical Oncology*, available: https://doi.org/10.1200/JCO.21.01217.

de Bruyn, K.M.T., Rangarajan, S., Reedquist, K.A., Figdor, C.G., and Bos, J.L. (2002) 'The small GTPase Rap1 is required for Mn(2+)- and antibody-induced LFA-1- and VLA-4-mediated cell adhesion', *The Journal of Biological Chemistry*, 277(33), 29468–29476, available: https://doi.org/10.1074/jbc.M204990200.

Bürger, S., Meng, J., Zwanzig, A., Beck, M., Pankonin, M., Wiedemann, P., Eichler, W., and Unterlauft, J.D. (2020) 'Pigment Epithelium-Derived Factor (PEDF) Receptors Are Involved in Survival of Retinal Neurons', *International Journal of Molecular Sciences*, 22(1), 369, available: https://doi.org/10.3390/ijms22010369.

Caers, J., Deleu, S., Belaid, Z., De Raeve, H., Van Valckenborgh, E., De Bruyne, E., Defresne, M.-P., Van Riet, I., Van Camp, B., and Vanderkerken, K. (2007)

‘Neighboring adipocytes participate in the bone marrow microenvironment of multiple myeloma cells’, *Leukemia*, 21(7), 1580–1584, available: https://doi.org/10.1038/sj.leu.2404658.

Calle, E.E., Rodriguez, C., Walker-Thurmond, K., and Thun, M.J. (2003) ‘Overweight, obesity, and mortality from cancer in a prospectively studied cohort of U.S. adults’, *The New England Journal of Medicine*, 348(17), 1625–1638, available: https://doi.org/10.1056/NEJMoa021423.

Cao, S., Troutt, A.B., and Rustum, Y.M. (1998) ‘Interleukin 15 protects against toxicity and potentiates antitumor activity of 5-fluorouracil alone and in combination with leucovorin in rats bearing colorectal cancer’, *Cancer Research*, 58(8), 1695–1699.

Cardona-Benavides, I.J., de Ramón, C., and Gutiérrez, N.C. (2021) ‘Genetic Abnormalities in Multiple Myeloma: Prognostic and Therapeutic Implications’, *Cells*, 10(2), 336, available: https://doi.org/10.3390/cells10020336.

Carlini, V., Noonan, D.M., Abdalalem, E., Goletti, D., Sansone, C., Calabrone, L., and Albini, A. (2023) ‘The multifaceted nature of IL-10: regulation, role in immunological homeostasis and its relevance to cancer, COVID-19 and post-COVID conditions’, *Frontiers in Immunology*, 14, available: https://www.frontiersin.org/articles/10.3389/fimmu.2023.1161067 [accessed 9 Nov 2023].

Carmichael, J., Seymour, F., McIlroy, G., Tayabali, S., Amerikanou, R., Feyler, S., Popat, R., Pratt, G., Parrish, C., Ashcroft, A.J., Jackson, G.H., and Cook, G. (2023) ‘Delayed diagnosis resulting in increased disease burden in multiple myeloma: the legacy of the COVID-19 pandemic’, *Blood Cancer Journal*, 13(1), available: https://doi.org/10.1038/s41408-023-00795-w.

Carnagarin, R., Dharmarajan, A.M., and Dass, C.R. (2015) ‘PEDF-induced alteration of metabolism leading to insulin resistance’, *Molecular and Cellular Endocrinology*, 401, 98–104, available: https://doi.org/10.1016/j.mce.2014.11.006.

Carter, A.M., Tan, C., Pozo, K., Telange, R., Molinaro, R., Guo, A., De Rosa, E., Martinez, J.O., Zhang, S., Kumar, N., Takahashi, M., Wiederhold, T., Ghayee, H.K., Oltmann, S.C., Pacak, K., Woltering, E.A., Hatanpaa, K.J., Nwariaku, F.E., Grubbs, E.G., Gill, A.J., Robinson, B., Gillardon, F., Reddy, S., Jaskula-Sztul, R., Mobley, J.A., Mukhtar, M.S., Tasciotti, E., Chen, H., and Bibb, J.A. (2020) ‘Phosphoprotein-based biomarkers as predictors for cancer therapy’, *Proceedings of the National Academy of Sciences*, 117(31), 18401–18411, available: https://doi.org/10.1073/pnas.2010103117.

Casneuf, T., Xu, X.S., Adams, H.C., Axel, A.E., Chiu, C., Khan, I., Ahmadi, T., Yan, X., Lonial, S., Plesner, T., Lokhorst, H.M., van de Donk, N.W.C.J., Clemens, P.L., and Sasser, A.K. (2017) ‘Effects of daratumumab on natural killer cells and impact on clinical outcomes in relapsed or refractory multiple myeloma’,

Blood Advances, 1(23), 2105–2114, available: https://doi.org/10.1182/bloodadvances.2017006866.

Cassese, G., Arce, S., Hauser, A.E., Lehnert, K., Moewes, B., Mostarac, M., Muehlinghaus, G., Szyska, M., Radbruch, A., and Manz, R.A. (2003) 'Plasma cell survival is mediated by synergistic effects of cytokines and adhesion-dependent signals', *Journal of Immunology (Baltimore, Md.: 1950)*, 171(4), 1684–1690, available: https://doi.org/10.4049/jimmunol.171.4.1684.

Castaneda, O. and Baz, R. (2019) 'Multiple Myeloma Genomics - A Concise Review', *Acta Medica Academica*, 48(1), 57–67, available: https://doi.org/10.5644/ama2006-124.242.

Catz, S.D. and Johnson, J.L. (2001) 'Transcriptional regulation of bcl-2 by nuclear factor kappa B and its significance in prostate cancer', *Oncogene*, 20(50), 7342–7351, available: https://doi.org/10.1038/sj.onc.1204926.

Cavo, M., Terpos, E., Nanni, C., Moreau, P., Lentzsch, S., Zweegman, S., Hillengass, J., Engelhardt, M., Usmani, S.Z., Vesole, D.H., San-Miguel, J., Kumar, S.K., Richardson, P.G., Mikhael, J.R., Costa, F.L. da, Dimopoulos, M.-A., Zingaretti, C., Abildgaard, N., Goldschmidt, H., Orlowski, R.Z., Chng, W.J., Einsele, H., Lonial, S., Barlogie, B., Anderson, K.C., Rajkumar, S.V., Durie, B.G.M., and Zamagni, E. (2017) 'Role of 18F-FDG PET/CT in the diagnosis and management of multiple myeloma and other plasma cell disorders: a consensus statement by the International Myeloma Working Group', *The Lancet Oncology*, 18(4), e206–e217, available: https://doi.org/10.1016/S1470-2045(17)30189-4.

Cenci, S., Oliva, L., Cerruti, F., Milan, E., Bianchi, G., Raule, M., Mezghrani, A., Pasqualetto, E., Sitia, R., and Cascio, P. (2012) 'Pivotal Advance: Protein synthesis modulates responsiveness of differentiating and malignant plasma cells to proteasome inhibitors', *Journal of Leukocyte Biology*, 92(5), 921–931, available: https://doi.org/10.1189/jlb.1011497.

Cetin, A.E., Stevens, M.M., Calistri, N.L., Fulciniti, M., Olcum, S., Kimmerling, R.J., Munshi, N.C., and Manalis, S.R. (2017) 'Determining therapeutic susceptibility in multiple myeloma by single-cell mass accumulation', *Nature Communications*, 8(1), 1613, available: https://doi.org/10.1038/s41467-017-01593-2.

Chang, H., Sloan, S., Li, D., and Keith Stewart, A. (2004) 'Multiple myeloma involving central nervous system: high frequency of chromosome 17p13.1 (p53) deletions', *British Journal of Haematology*, 127(3), 280–284, available: https://doi.org/10.1111/j.1365-2141.2004.05199.x.

Chang, S.-H., Luo, S., Thomas, T.S., O'Brian, K.K., Colditz, G.A., Carlsson, N.P., and Carson, K.R. (2017) 'Obesity and the Transformation of Monoclonal Gammopathy of Undetermined Significance to Multiple Myeloma: A Population-Based Cohort Study', *Journal of the National Cancer Institute*, 109(5), djw264, available: https://doi.org/10.1093/jnci/djw264.

Chanukuppa, V., Taware, R., Taunk, K., Chatterjee, T., Sharma, S., Somasundaram, V., Rashid, F., Malakar, D., Santra, M.K., and Rapole, S. (2021) 'Proteomic Alterations in Multiple Myeloma: A Comprehensive Study Using Bone Marrow Interstitial Fluid and Serum Samples', *Frontiers in Oncology*, 10, available: https://www.frontiersin.org/article/10.3389/fonc.2020.566804 [accessed 25 Apr 2022].

Chauhan, D., Li, G., Shringarpure, R., Podar, K., Ohtake, Y., Hideshima, T., and Anderson, K.C. (2003) 'Blockade of Hsp27 overcomes Bortezomib/proteasome inhibitor PS-341 resistance in lymphoma cells', *Cancer Research*, 63(19), 6174–6177.

Chauhan, D., Uchiyama, H., Akbarali, Y., Urashima, M., Yamamoto, K., Libermann, T.A., and Anderson, K.C. (1996) 'Multiple myeloma cell adhesion-induced interleukin-6 expression in bone marrow stromal cells involves activation of NF-kappa B', *Blood*, 87(3), 1104–1112.

Chen, E. and Yu, J. (2023) 'The role and metabolic adaptations of neutrophils in premetastatic niches', *Biomarker Research*, 11(1), 50, available: https://doi.org/10.1186/s40364-023-00493-6.

Chen, M. and Stracher, A. (1989) 'In situ Phosphorylation of Platelet Actin-binding Protein by cAMP-dependent Protein Kinase Stabilizes It against Proteolysis by Calpain', *Journal of Biological Chemistry*, 264(24), 14282–14289, available: https://doi.org/10.1016/S0021-9258(18)71675-X.

Chen, Q., Zhang, X.H.-F., and Massagué, J. (2011) 'Macrophage binding to receptor VCAM-1 transmits survival signals in breast cancer cells that invade the lungs', *Cancer Cell*, 20(4), 538–549, available: https://doi.org/10.1016/j.ccr.2011.08.025.

Chen, S., Shen, Z., Gao, L., Yu, S., Zhang, P., Han, Z., and Kang, M. (2021) 'TPM3 mediates epithelial-mesenchymal transition in esophageal cancer via MMP2/MMP9', *Annals of Translational Medicine*, 9(16), 1338, available: https://doi.org/10.21037/atm-21-4043.

Chen, T., Sun, Z., Cui, Y., Ji, J., Li, Y., and Qu, X. (2023) 'Identification of long noncoding RNA NEAT1 as a key gene involved in the extramedullary disease of multiple myeloma by bioinformatics analysis', *Hematology*, 28(1), 2164449, available: https://doi.org/10.1080/16078454.2022.2164449.

Chen, Z., Che, D., Gu, X., Lin, J., Deng, J., Jiang, P., Xu, K., Xu, B., and Zhang, T. (2021) 'Upregulation of PEDF Predicts a Poor Prognosis and Promotes Esophageal Squamous Cell Carcinoma Progression by Modulating the MAPK/ERK Signaling Pathway', *Frontiers in Oncology*, 11, 625612, available: https://doi.org/10.3389/fonc.2021.625612.

Cheng, A., Grant, C.E., Noble, W.S., and Bailey, T.L. (2019) 'MoMo: discovery of statistically significant post-translational modification motifs', *Bioinformatics*, 35(16), 2774–2782, available: https://doi.org/10.1093/bioinformatics/bty1058.

Cheng, H., Wang, M., Su, J., Li, Y., Long, J., Chu, J., Wan, X., Cao, Y., and Li, Q. (2022) 'Lipid Metabolism and Cancer', *Life*, 12(6), 784, available: https://doi.org/10.3390/life12060784.

Chesi, M. and Bergsagel, P.L. (2013) 'Molecular pathogenesis of multiple myeloma: basic and clinical updates', *International Journal of Hematology*, 97(3), 313–323, available: https://doi.org/10.1007/s12185-013-1291-2.

Child, J.A., Morgan, G.J., Davies, F.E., Owen, R.G., Bell, S.E., Hawkins, K., Brown, J., Drayson, M.T., and Selby, P.J. (2003) 'High-Dose Chemotherapy with Hematopoietic Stem-Cell Rescue for Multiple Myeloma', *New England Journal of Medicine*, 348(19), 1875–1883, available: https://doi.org/10.1056/NEJMoa022340.

Chng, W.J., Glebov, O., Bergsagel, P.L., and Kuehl, W.M. (2007) 'Genetic events in the pathogenesis of multiple myeloma', *Best practice & research. Clinical haematology*, 20(4), 571–596, available: https://doi.org/10.1016/j.beha.2007.08.004.

Cho, S.-F., Lin, L., Xing, L., Li, Y., Yu, T., Anderson, K.C., and Tai, Y.-T. (2020) 'BCMA-Targeting Therapy: Driving a New Era of Immunotherapy in Multiple Myeloma', *Cancers*, 12(6), 1473, available: https://doi.org/10.3390/cancers12061473.

Cho, S.-F., Yeh, T.-J., Anderson, K.C., and Tai, Y.-T. (2022) 'Bispecific antibodies in multiple myeloma treatment: A journey in progress', *Frontiers in Oncology*, 12, available: https://www.frontiersin.org/articles/10.3389/fonc.2022.1032775 [accessed 13 Apr 2023].

Chong, P.S.Y., Zhou, J., Lim, J.S.L., Hee, Y.T., Chooi, J.-Y., Chung, T.-H., Tan, Z.T., Zeng, Q., Waller, D.D., Sebag, M., and Chng, W.-J. (2019) 'IL6 Promotes a STAT3-PRL3 Feedforward Loop via SHP2 Repression in Multiple Myeloma', *Cancer Research*, 79(18), 4679–4688, available: https://doi.org/10.1158/0008-5472.CAN-19-0343.

Chretien, M.-L., Corre, J., Lauwers-Cances, V., Magrangeas, F., Cleynen, A., Yon, E., Hulin, C., Leleu, X., Orsini-Piocelle, F., Blade, J.-S., Sohn, C., Karlin, L., Delbrel, X., Hebraud, B., Roussel, M., Marit, G., Garderet, L., Mohty, M., Rodon, P., Voillat, L., Royer, B., Jaccard, A., Belhadj, K., Fontan, J., Caillot, D., Stoppa, A.-M., Attal, M., Facon, T., Moreau, P., Minvielle, S., and Avet-Loiseau, H. (2015) 'Understanding the role of hyperdiploidy in myeloma prognosis: which trisomies really matter?', *Blood*, 126(25), 2713–2719, available: https://doi.org/10.1182/blood-2015-06-650242.

Ciepiela, O., Małecka-Giełdowska, M., and Czyżewska, E. (2021) 'Neutrophil Extracellular Traps (NETs) and Hypercoagulability in Plasma Cell Dyscrasias—Is This Phenomenon Worthy of Exploration?', *Journal of Clinical Medicine*, 10(22), 5243, available: https://doi.org/10.3390/jcm10225243.

Cippitelli, M., Stabile, H., Kosta, A., Petillo, S., Lucantonio, L., Gismondi, A., Santoni, A., and Fionda, C. (2023) 'Role of NF-κB Signaling in the Interplay between Multiple Myeloma and Mesenchymal Stromal Cells', *International Journal of Molecular Sciences*, 24(3), 1823, available: https://doi.org/10.3390/ijms24031823.

Clarke, S.E., Fuller, K.A., and Erber, W.N. (2024) 'Chromosomal defects in multiple myeloma', *Blood Reviews*, 64, 101168, available: https://doi.org/10.1016/j.blre.2024.101168.

Clish, C.B. (2015) 'Metabolomics: an emerging but powerful tool for precision medicine', *Cold Spring Harbor Molecular Case Studies*, 1(1), available: https://doi.org/10.1101/mcs.a000588.

Coffey, D.G., Cowan, A.J., DeGraaff, B., Martins, T.J., Curley, N., Green, D.J., Libby, E.N., Silbermann, R., Chien, S., Dai, J., Morales, A., Gooley, T.A., Warren, E.H., and Becker, P.S. (2021) 'High-Throughput Drug Screening and Multi-Omic Analysis to Guide Individualized Treatment for Multiple Myeloma', *JCO Precision Oncology*, (5), 602–612, available: https://doi.org/10.1200/PO.20.00442.

Cohen, L., Blaisdell, R.K., Djordjevich, J., Ormiste, V., and Dobrilovic, L. (1966) 'Familial xanthomatosis and hyperlipidemia, and myelmatosis', *The American Journal of Medicine*, 40(2), 299–317, available: https://doi.org/10.1016/0002-9343(66)90111-2.

Collins, S.M., Bakan, C.E., Swartzel, G.D., Hofmeister, C.C., Efebera, Y.A., Kwon, H., Starling, G.C., Ciarlariello, D., Bhaskar, S., Briercheck, E.L., Hughes, T., Yu, J., Rice, A., and Benson, D.M. (2013) 'Elotuzumab directly enhances NK cell cytotoxicity against myeloma via CS1 ligation: evidence for augmented NK cell function complementing ADCC', *Cancer Immunology, Immunotherapy*, 62(12), 1841–1849, available: https://doi.org/10.1007/s00262-013-1493-8.

Contorno, S., Darienzo, R.E., and Tannenbaum, R. (2021) 'Evaluation of aromatic amino acids as potential biomarkers in breast cancer by Raman spectroscopy analysis', *Scientific Reports*, 11(1), 1698, available: https://doi.org/10.1038/s41598-021-81296-3.

Corre, J., Munshi, N.C., and Avet-Loiseau, H. (2021) 'Risk factors in multiple myeloma: is it time for a revision?', *Blood*, 137(1), 16–19, available: https://doi.org/10.1182/blood.2019004309.

Corre, J., Perrot, A., Caillot, D., Belhadj, K., Hulin, C., Leleu, X., Mohty, M., Facon, T., Buisson, L., Do Souto, L., Lannes, R., Dufrechou, S., Prade, N., Orsini-Piocelle, F., Voillat, L., Jaccard, A., Karlin, L., Macro, M., Brechignac, S., Dib, M., Sanhes, L., Fontan, J., Clement-Filliatre, L., Marolleau, J.-P., Minvielle, S., Moreau, P., and Avet-Loiseau, H. (2021) 'del(17p) without TP53 mutation confers a poor prognosis in intensively treated newly diagnosed patients with multiple myeloma', *Blood*, 137(9), 1192–1195, available: https://doi.org/10.1182/blood.2020008346.

Correa Rojo, A., Heylen, D., Aerts, J., Thas, O., Hooyberghs, J., Ertaylan, G., and Valkenborg, D. (2021) 'Towards Building a Quantitative Proteomics Toolbox in Precision Medicine: A Mini-Review', *Frontiers in Physiology*, 12, available: https://www.frontiersin.org/articles/10.3389/fphys.2021.723510 [accessed 26 Jul 2023].

Cosenza, M., Civallero, M., Pozzi, S., Marcheselli, L., Bari, A., and Sacchi, S. (2015) 'The combination of bortezomib with enzastaurin or lenalidomide enhances cytotoxicity in follicular and mantle cell lymphoma cell lines', *Hematological Oncology*, 33(4), 166–175, available: https://doi.org/10.1002/hon.2179.

Coskun, U., Sancak, B., Sen, I., Bukan, N., Tufan, M.A., Gülbahar, Ö., and Sozen, S. (2006) 'Serum P-selectin, soluble vascular cell adhesion molecule-I (s-VCAM-I) and soluble intercellular adhesion molecule-I (s-ICAM-I) levels in bladder carcinoma patients with different stages', *International Immunopharmacology*, Use of Immune Globulin Intravenous in Dermatology, 6(4), 672–677, available: https://doi.org/10.1016/j.intimp.2005.10.009.

Costa, F., Dalla Palma, B., and Giuliani, N. (2019) 'CD38 Expression by Myeloma Cells and Its Role in the Context of Bone Marrow Microenvironment: Modulation by Therapeutic Agents', *Cells*, 8(12), 1632, available: https://doi.org/10.3390/cells8121632.

Couce, M.L., Sánchez-Pintos, P., Diogo, L., Leão-Teles, E., Martins, E., Santos, H., Bueno, M.A., Delgado-Pecellín, C., Castiñeiras, D.E., Cocho, J.A., García-Villoria, J., Ribes, A., Fraga, J.M., and Rocha, H. (2013) 'Newborn screening for medium-chain acyl-CoA dehydrogenase deficiency: regional experience and high incidence of carnitine deficiency', *Orphanet Journal of Rare Diseases*, 8(1), 102, available: https://doi.org/10.1186/1750-1172-8-102.

Cruz-Munoz, M.-E., Dong, Z., Shi, X., Zhang, S., and Veillette, A. (2009) 'Influence of CRACC, a SLAM family receptor coupled to the adaptor EAT-2, on natural killer cell function', *Nature Immunology*, 10(3), 297–305, available: https://doi.org/10.1038/ni.1693.

Cutler, C., Lee, S.J., Arai, S., Rotta, M., Zoghi, B., Lazaryan, A., Ramakrishnan, A., DeFilipp, Z., Salhotra, A., Chai-Ho, W., Mehta, R., Wang, T., Arora, M., Pusic, I., Saad, A., Shah, N.N., Abhyankar, S., Bachier, C., Galvin, J., Im, A., Langston, A., Liesveld, J., Juckett, M., Logan, A., Schachter, L., Alavi, A., Howard, D., Waksal, H.W., Ryan, J., Eiznhamer, D., Aggarwal, S.K., Ieyoub, J., Schueller, O., Green, L., Yang, Z., Krenz, H., Jagasia, M., Blazar, B.R., and Pavletic, S. (2021) 'Belumosudil for chronic graft-versus-host disease after 2 or more prior lines of therapy: the ROCKstar Study', *Blood*, 138(22), 2278–2289, available: https://doi.org/10.1182/blood.2021012021.

Cutler, M.L., Bassin, R.H., Zanoni, L., and Talbot, N. (1992) 'Isolation of rsp-1, a novel cDNA capable of suppressing v-Ras transformation.', *Molecular and Cellular Biology*, 12(9), 3750–3756.

Dabrowska, A.M., Tarach, J.S., Wojtysiak-Duma, B., and Duma, D. (2015) 'Fetuin-A (AHSG) and its usefulness in clinical practice. Review of the literature', *Biomedical Papers of the Medical Faculty of the University Palacky, Olomouc, Czechoslovakia*, 159(3), 352–359, available: https://doi.org/10.5507/bp.2015.018.

D'Agostino, M., Cairns, D.A., Lahuerta, J.J., Wester, R., Bertsch, U., Waage, A., Zamagni, E., Mateos, M.-V., Dall'Olio, D., van de Donk, N.W.C.J., Jackson, G., Rocchi, S., Salwender, H., Bladé Creixenti, J., van der Holt, B., Castellani, G., Bonello, F., Capra, A., Mai, E.K., Dürig, J., Gay, F., Zweegman, S., Cavo, M., Kaiser, M.F., Goldschmidt, H., Hernández Rivas, J.M., Larocca, A., Cook, G., San-Miguel, J.F., Boccadoro, M., and Sonneveld, P. (2022) 'Second Revision of the International Staging System (R2-ISS) for Overall Survival in Multiple Myeloma: A European Myeloma Network (EMN) Report Within the HARMONY Project', *Journal of Clinical Oncology*, 40(29), 3406–3418, available: https://doi.org/10.1200/JCO.21.02614.

Dah, K., Lavezo, J.L., and Dihowm, F. (2021) 'Aggressive Plasmablastic Myeloma With Extramedullary Cord Compression and Hyperammonemic Encephalopathy: Case Report and Literature Review', *Anticancer Research*, 41(11), 5839–5845, available: https://doi.org/10.21873/anticanres.15403.

Dahl, I.M.S., Rasmussen, T., Kauric, G., and Husebekk, A. (2002) 'Differential expression of CD56 and CD44 in the evolution of extramedullary myeloma', *British Journal of Haematology*, 116(2), 273–277, available: https://doi.org/10.1046/j.1365-2141.2002.03258.x.

Dai, Y., Shaikho, E.M., Perez, J., Wilson, C.A., Liu, L.Y., White, M.R., Farrell, J.J., Chui, D.H.K., Sebastiani, P., and Steinberg, M.H. (2019) 'BCL2L1 is associated with γ-globin gene expression', *Blood Advances*, 3(20), 2995–3001, available: https://doi.org/10.1182/bloodadvances.2019032243.

Damiano, J.S. and Dalton, W.S. (2000) 'Integrin-Mediated Drug Resistance in Multiple Myeloma', *Leukemia & Lymphoma*, 38(1–2), 71–81, available: https://doi.org/10.3109/10428190009060320.

Darlix, A., Lamy, P.-J., Lopez-Crapez, E., Braccini, A.L., Firmin, N., Romieu, G., Thézenas, S., and Jacot, W. (2016) 'Serum NSE, MMP-9 and HER2 extracellular domain are associated with brain metastases in metastatic breast cancer patients: predictive biomarkers for brain metastases?', *International Journal of Cancer*, 139(10), 2299–2311, available: https://doi.org/10.1002/ijc.30290.

Davies, F.E., Raje, N., Hideshima, T., Lentzsch, S., Young, G., Tai, Y.-T., Lin, B., Podar, K., Gupta, D., Chauhan, D., Treon, S.P., Richardson, P.G., Schlossman, R.L., Morgan, G.J., Muller, G.W., Stirling, D.I., and Anderson, K.C. (2001) 'Thalidomide and immunomodulatory derivatives augment natural killer cell cytotoxicity in multiple myeloma', *Blood*, 98(1), 210–216, available: https://doi.org/10.1182/blood.V98.1.210.

Davies, F.E., Rollinson, S.J., Rawstron, A.C., Roman, E., Richards, S., Drayson, M., Child, J.A., and Morgan, G.J. (2000) 'High-producer haplotypes of tumor necrosis factor alpha and lymphotoxin alpha are associated with an increased risk of myeloma and have an improved progression-free survival after treatment', *Journal of Clinical Oncology: Official Journal of the American Society of Clinical Oncology*, 18(15), 2843–2851, available: https://doi.org/10.1200/JCO.2000.18.15.2843.

De Cicco, C., Ravasi, L., Zorzino, L., Sandri, M.T., Botteri, E., Verweij, F., Granchi, D., de Cobelli, O., and Paganelli, G. (2008) 'Circulating levels of VCAM and MMP-2 may help identify patients with more aggressive prostate cancer', *Current Cancer Drug Targets*, 8(3), 199–206, available: https://doi.org/10.2174/156800908784293613.

De Pascalis, C. and Etienne-Manneville, S. (2017) 'Single and collective cell migration: the mechanics of adhesions', *Molecular Biology of the Cell*, 28(14), 1833–1846, available: https://doi.org/10.1091/mbc.e17-03-0134.

Deb, B., Sengupta, P., Sambath, J., and Kumar, P. (2020) 'Bioinformatics Analysis of Global Proteomic and Phosphoproteomic Data Sets Revealed Activation of NEK2 and AURKA in Cancers', *Biomolecules*, 10(2), 237, available: https://doi.org/10.3390/biom10020237.

Demaria, S., Ng, B., Devitt, M.L., Babb, J.S., Kawashima, N., Liebes, L., and Formenti, S.C. (2004) 'Ionizing radiation inhibition of distant untreated tumors (abscopal effect) is immune mediated', *International Journal of Radiation Oncology, Biology, Physics*, 58(3), 862–870, available: https://doi.org/10.1016/j.ijrobp.2003.09.012.

Demchenko, Y.N., Glebov, O.K., Zingone, A., Keats, J.J., Bergsagel, P.L., and Kuehl, W.M. (2010) 'Classical and/or alternative NF-κB pathway activation in multiple myeloma', *Blood*, 115(17), 3541–3552, available: https://doi.org/10.1182/blood-2009-09-243535.

Demetriou, M., Binkert, C., Sukhu, B., Tenenbaum, H.C., and Dennis, J.W. (1996) 'Fetuin/alpha2-HS glycoprotein is a transforming growth factor-beta type II receptor mimic and cytokine antagonist', *The Journal of Biological Chemistry*, 271(22), 12755–12761, available: https://doi.org/10.1074/jbc.271.22.12755.

Demuynck, H., Delforge, M., Verhoef, G., Zachée, P., Vandenberghe, P., and Boogaerts, M. (1995) 'Comparative study of peripheral blood progenitor cell collection in patients with multiple myeloma after single-dose cyclophosphamide combined with rhGM-CSF or rhG-CSF', *British Journal of Haematology*, 90(2), 384–392, available: https://doi.org/10.1111/j.1365-2141.1995.tb05163.x.

Deng, R., Hao, J., Han, W., Ni, Y., Huang, X., and Hu, Q. (2015) 'Gelsolin regulates proliferation, apoptosis, migration and invasion in human oral carcinoma cells', *Oncology Letters*, 9(5), 2129–2134, available: https://doi.org/10.3892/ol.2015.3002.

Deng, S., Xu, Y., An, G., Sui, W., Zou, D., Zhao, Y., Qi, J., Li, F., Hao, M., and Qiu, L. (2015) 'Features of extramedullary disease of multiple myeloma: high frequency of p53 deletion and poor survival: a retrospective single-center study of 834 cases', *Clinical Lymphoma, Myeloma & Leukemia*, 15(5), 286–291, available: https://doi.org/10.1016/j.clml.2014.12.013.

Deng, W., Lopez-Camacho, C., Tang, J.-Y., Mendoza-Villanueva, D., Maya-Mendoza, A., Jackson, D.A., and Shore, P. (2012) 'Cytoskeletal protein filamin A is a nucleolar protein that suppresses ribosomal RNA gene transcription', *Proceedings of the National Academy of Sciences*, 109(5), 1524–1529, available: https://doi.org/10.1073/pnas.1107879109.

Deryugina, E., Carré, A., Ardi, V., Muramatsu, T., Schmidt, J., Pham, C., and Quigley, J.P. (2020) 'Neutrophil Elastase Facilitates Tumor Cell Intravasation and Early Metastatic Events', *iScience*, 23(12), 101799, available: https://doi.org/10.1016/j.isci.2020.101799.

Descamps, G., Wuillème-Toumi, S., Trichet, V., Venot, C., Debussche, L., Hercend, T., Collette, M., Robillard, N., Bataille, R., and Amiot, M. (2006) 'CD45neg but Not CD45pos Human Myeloma Cells Are Sensitive to the Inhibition of IGF-1 Signaling by a Murine Anti-IGF-1R Monoclonal Antibody, mAVE16421', *The Journal of Immunology*, 177(6), 4218–4223, available: https://doi.org/10.4049/jimmunol.177.6.4218.

Dey, P., Kimmelman, A.C., and DePinho, R.A. (2021) 'Metabolic Codependencies in the Tumor Microenvironment', *Cancer Discovery*, 11(5), 1067–1081, available: https://doi.org/10.1158/2159-8290.CD-20-1211.

Di Cesare, F., Vignoli, A., Luchinat, C., Tenori, L., and Saccenti, E. (2023) 'Exploration of Blood Metabolite Signatures of Colorectal Cancer and Polyposis through Integrated Statistical and Network Analysis', *Metabolites*, 13(2), 296, available: https://doi.org/10.3390/metabo13020296.

Disis, M.L., Rinn, K., Knutson, K.L., Davis, D., Caron, D., dela Rosa, C., and Schiffman, K. (2002) 'Flt3 ligand as a vaccine adjuvant in association with HER-2/neu peptide-based vaccines in patients with HER-2/neu–overexpressing cancers', *Blood*, 99(8), 2845–2850, available: https://doi.org/10.1182/blood.V99.8.2845.

Doi, K., Horiuchi, T., Uchinami, M., Tabo, T., Kimura, N., Yokomachi, J., Yoshida, M., and Tanaka, K. (2002) 'Neutrophil elastase inhibitor reduces hepatic metastases induced by ischaemia-reperfusion in rats', *The European Journal of Surgery = Acta Chirurgica*, 168(8–9), 507–510, available: https://doi.org/10.1080/110241502321116541.

Doll, S., Gnad, F., and Mann, M. (2019) 'The Case for Proteomics and Phospho-Proteomics in Personalized Cancer Medicine', *Proteomics. Clinical Applications*, 13(2), 1800113, available: https://doi.org/10.1002/prca.201800113.

Dong, Y., Ding, D., Gu, J., Chen, M., and Li, S. (2022) ‘Alpha-2 Heremans Schmid Glycoprotein (AHSG) promotes the proliferation of bladder cancer cells by regulating the TGF-β signalling pathway’, *Bioengineered*, 13(6), 14282–14298, available: https://doi.org/10.1080/21655979.2022.2081465.

van de Donk, N.W.C.J., Pawlyn, C., and Yong, K.L. (2021) ‘Multiple myeloma’, *The Lancet*, 397(10272), 410–427, available: https://doi.org/10.1016/S0140-6736(21)00135-5.

Donti, T.R., Cappuccio, G., Hubert, L., Neira, J., Atwal, P.S., Miller, M.J., Cardon, A.L., Sutton, V.R., Porter, B.E., Baumer, F.M., Wangler, M.F., Sun, Q., Emrick, L.T., and Elsea, S.H. (2016) ‘Diagnosis of adenylosuccinate lyase deficiency by metabolomic profiling in plasma reveals a phenotypic spectrum’, *Molecular Genetics and Metabolism Reports*, 8, 61–66, available: https://doi.org/10.1016/j.ymgmr.2016.07.007.

Dougherty, G.W., Jose, C., Gimona, M., and Cutler, M.L. (2008) ‘The Rsu-1-PINCH1-ILK complex is regulated by Ras activation in tumor cells’, *European journal of cell biology*, 87(8–9), 721–734, available: https://doi.org/10.1016/j.ejcb.2008.02.011.

Drabovich, A.P., Pavlou, M.P., Batruch, I., and Diamandis, E.P. (2013) ‘Chapter 2 - Proteomic and Mass Spectrometry Technologies for Biomarker Discovery’, in Issaq, H.J. and Veenstra, T.D., eds., *Proteomic and Metabolomic Approaches to Biomarker Discovery*, Boston: Academic Press, 17–37, available: https://doi.org/10.1016/B978-0-12-394446-7.00002-9.

D’Souza, L. and Bhattacharya, D. (2019) ‘Plasma cells: you are what you eat’, *Immunological reviews*, 288(1), 161–177, available: https://doi.org/10.1111/imr.12732.

Dunphy, K., Bazou, D., Henry, M., Meleady, P., Miettinen, J.J., Heckman, C.A., Dowling, P., and O’Gorman, P. (2023) ‘Proteomic and Metabolomic Analysis of Bone Marrow and Plasma from Patients with Extramedullary Multiple Myeloma Identifies Distinct Protein and Metabolite Signatures’, *Cancers*, 15(15), 3764, available: https://doi.org/10.3390/cancers15153764.

Dunphy, K., Dowling, P., Bazou, D., and O’Gorman, P. (2021) ‘Current Methods of Post-Translational Modification Analysis and Their Applications in Blood Cancers’, *Cancers*, 13(8), available: https://doi.org/10.3390/cancers13081930.

Dunphy, K., O’Mahoney, K., Dowling, P., O’Gorman, P., and Bazou, D. (2021) ‘Clinical Proteomics of Biofluids in Haematological Malignancies’, *International Journal of Molecular Sciences*, 22(15), 8021, available: https://doi.org/10.3390/ijms22158021.

Durie, B.G. and Salmon, S.E. (1975) ‘A clinical staging system for multiple myeloma. Correlation of measured myeloma cell mass with presenting clinical features, response to treatment, and survival’, *Cancer*, 36(3), 842–

854, available: https://doi.org/10.1002/1097-0142(197509)36:3<842::aid-cncr2820360303>3.0.co;2-u.

Dytfeld, D., Luczak, M., Wrobel, T., Usnarska-Zubkiewicz, L., Brzezniakiewicz, K., Jamroziak, K., Giannopoulos, K., Przybylowicz-Chalecka, A., Ratajczak, B., Czerwinska-Rybak, J., Nowicki, A., Joks, M., Czechowska, E., Zawartko, M., Szczepaniak, T., Grzasko, N., Morawska, M., Bochenek, M., Kubicki, T., Morawska, M., Tusznio, K., Jakubowiak, A., and Komarnicki, M. (2016) 'Comparative proteomic profiling of refractory/relapsed multiple myeloma reveals biomarkers involved in resistance to bortezomib-based therapy', *Oncotarget*, 7(35), 56726–56736, available: https://doi.org/10.18632/oncotarget.11059.

Ebrahimi, F., Giaglis, S., Hahn, S., Blum, C.A., Baumgartner, C., Kutz, A., Breda, S.V. van, Mueller, B., Schuetz, P., Christ-Crain, M., and Hasler, P. (2018) 'Markers of neutrophil extracellular traps predict adverse outcome in community-acquired pneumonia: secondary analysis of a randomised controlled trial', *European Respiratory Journal*, 51(4), available: https://doi.org/10.1183/13993003.01389-2017.

Edvardsen, K., Chen, W., Rucklidge, G., Walsh, F.S., Obrink, B., and Bock, E. (1993) 'Transmembrane neural cell-adhesion molecule (NCAM), but not glycosyl-phosphatidylinositol-anchored NCAM, down-regulates secretion of matrix metalloproteinases.', *Proceedings of the National Academy of Sciences of the United States of America*, 90(24), 11463–11467.

Elattar, S., Dimri, M., and Satyanarayana, A. (2018) 'The tumor secretory factor ZAG promotes white adipose tissue browning and energy wasting', *FASEB journal: official publication of the Federation of American Societies for Experimental Biology*, 32(9), 4727–4743, available: https://doi.org/10.1096/fj.201701465RR.

Elias, D., Vever, H., Lænkholm, A.-V., Gjerstorff, M.F., Yde, C.W., Lykkesfeldt, A.E., and Ditzel, H.J. (2015) 'Gene expression profiling identifies FYN as an important molecule in tamoxifen resistance and a predictor of early recurrence in patients treated with endocrine therapy', *Oncogene*, 34(15), 1919–1927, available: https://doi.org/10.1038/onc.2014.138.

Emmons, M.F., Gebhard, A.W., Nair, R.R., Baz, R., McLaughlin, M.L., Cress, A.E., and Hazlehurst, L.A. (2011) 'Acquisition of Resistance toward HYD1 Correlates with a Reduction in Cleaved α4 Integrin Expression and a Compromised CAM-DR Phenotype', *Molecular Cancer Therapeutics*, 10(12), 2257–2266, available: https://doi.org/10.1158/1535-7163.MCT-11-0149.

Epstein, M.M., Divine, G., Chao, C.R., Wells, K.E., Feigelson, H.S., Scholes, D., Roblin, D., Ulcickas Yood, M., Engel, L.S., Taylor, A., Fortuny, J., Habel, L.A., and Johnson, C.C. (2017) 'Statin use and risk of multiple myeloma: An analysis from the cancer research network', *International Journal of Cancer*, 141(3), 480–487, available: https://doi.org/10.1002/ijc.30745.

Evans, R., Fuller, J.A., Christianson, G., Krupke, D.M., and Troutt, A.B. (1997) 'IL-15 Mediates Anti-tumor Effects after Cyclophosphamide Injection of Tumor-Bearing Mice and Enhances Adoptive Immunotherapy: The Potential Role of NK Cell Subpopulations', *Cellular Immunology*, 179(1), 66–73, available: https://doi.org/10.1006/cimm.1997.1132.

Fahrmann, J.F., Bantis, L.E., Capello, M., Scelo, G., Dennison, J.B., Patel, N., Murage, E., Vykoukal, J., Kundnani, D.L., Foretova, L., Fabianova, E., Holcatova, I., Janout, V., Feng, Z., Yip-Schneider, M., Zhang, J., Brand, R., Taguchi, A., Maitra, A., Brennan, P., Max Schmidt, C., and Hanash, S. (2018) 'A Plasma-Derived Protein-Metabolite Multiplexed Panel for Early-Stage Pancreatic Cancer', *JNCI Journal of the National Cancer Institute*, 111(4), 372–379, available: https://doi.org/10.1093/jnci/djy126.

Farrell, M., Fairfield, H., Karam, M., D'Amico, A., Murphy, C.S., Falank, C., Pistofidi, R.S., Cao, A., Marinac, C.R., Dragon, J.A., McGuinness, L., Gartner, C.G., Iorio, R.D., Jachimowicz, E., DeMambro, V., Vary, C., and Reagan, M.R. (2023) 'Targeting the fatty acid binding proteins disrupts multiple myeloma cell cycle progression and MYC signaling', *eLife*, 12, e81184, available: https://doi.org/10.7554/eLife.81184.

Fedorov, K., Barouqa, M., Yin, D., Kushnir, M., Billett, H.H., and Reyes Gil, M. (2023) 'Identifying Neutrophil Extracellular Traps (NETs) in Blood Samples Using Peripheral Smear Autoanalyzers', *Life*, 13(3), 623, available: https://doi.org/10.3390/life13030623.

Ferguson, I.D., Patiño-Escobar, B., Tuomivaara, S.T., Lin, Y.-H.T., Nix, M.A., Leung, K.K., Kasap, C., Ramos, E., Nieves Vasquez, W., Talbot, A., Hale, M., Naik, A., Kishishita, A., Choudhry, P., Lopez-Girona, A., Miao, W., Wong, S.W., Wolf, J.L., Martin, T.G., Shah, N., Vandenberg, S., Prakash, S., Besse, L., Driessen, C., Posey, A.D., Mullins, R.D., Eyquem, J., Wells, J.A., and Wiita, A.P. (2022) 'The surfaceome of multiple myeloma cells suggests potential immunotherapeutic strategies and protein markers of drug resistance', *Nature Communications*, 13(1), 4121, available: https://doi.org/10.1038/s41467-022-31810-6.

Filho, A.G.O., Carneiro, B.C., Pastore, D., Silva, I.P., Yamashita, S.R., Consolo, F.D., Hungria, V.T.M., Sandes, A.F., Rizzatti, E.G., and Nico, M.A.C. (2019) 'Whole-Body Imaging of Multiple Myeloma: Diagnostic Criteria', *RadioGraphics*, available: https://doi.org/10.1148/rg.2019180096.

Fischer, J.E. and Baldessarini, R.J. (1971) 'False neurotransmitters and hepatic failure', *Lancet (London, England)*, 2(7715), 75–80, available: https://doi.org/10.1016/s0140-6736(71)92048-4.

Flynt, E., Bisht, K., Sridharan, V., Ortiz, M., Towfic, F., and Thakurta, A. (2020) 'Prognosis, Biology, and Targeting of TP53 Dysregulation in Multiple Myeloma', *Cells*, 9(2), 287, available: https://doi.org/10.3390/cells9020287.

Forster, S. and Radpour, R. (2022) 'Molecular Impact of the Tumor Microenvironment on Multiple Myeloma Dissemination and Extramedullary

Disease', *Frontiers in Oncology*, 12, available: https://www.frontiersin.org/articles/10.3389/fonc.2022.941437 [accessed 5 Oct 2022].

Francavilla, C., Lupia, M., Tsafou, K., Villa, A., Kowalczyk, K., Jersie-Christensen, R.R., Bertalot, G., Confalonieri, S., Brunak, S., Jensen, L.J., Cavallaro, U., and Olsen, J.V. (2017) 'Phosphoproteomics of Primary Cells Reveals Druggable Kinase Signatures in Ovarian Cancer', *Cell Reports*, 18(13), 3242–3256, available: https://doi.org/10.1016/j.celrep.2017.03.015.

Francavilla, C., Rigbolt, K.T.G., Emdal, K.B., Carraro, G., Vernet, E., Bekker-Jensen, D.B., Streicher, W., Wikström, M., Sundström, M., Bellusci, S., Cavallaro, U., Blagoev, B., and Olsen, J.V. (2013) 'Functional Proteomics Defines the Molecular Switch Underlying FGF Receptor Trafficking and Cellular Outputs', *Molecular Cell*, 51(6), 707–722, available: https://doi.org/10.1016/j.molcel.2013.08.002.

Fu, X.-L., Duan, W., Su, C.-Y., Mao, F.-Y., Lv, Y.-P., Teng, Y.-S., Yu, P.-W., Zhuang, Y., and Zhao, Y.-L. (2017) 'Interleukin 6 induces M2 macrophage differentiation by STAT3 activation that correlates with gastric cancer progression', *Cancer Immunology, Immunotherapy*, 66(12), 1597–1608, available: https://doi.org/10.1007/s00262-017-2052-5.

Gagelmann, N., Eikema, D.-J., Iacobelli, S., Koster, L., Nahi, H., Stoppa, A.-M., Masszi, T., Caillot, D., Lenhoff, S., Udvardy, M., Crawley, C., Arcese, W., Mariette, C., Hunter, A., Leleu, X., Schipperus, M., Delforge, M., Pioltelli, P., Snowden, J.A., Itälä-Remes, M., Musso, M., van Biezen, A., Garderet, L., and Kröger, N. (2018) 'Impact of extramedullary disease in patients with newly diagnosed multiple myeloma undergoing autologous stem cell transplantation: a study from the Chronic Malignancies Working Party of the EBMT', *Haematologica*, 103(5), 890–897, available: https://doi.org/10.3324/haematol.2017.178434.

Galli, M., Chatterjee, M., Grasso, M., Specchia, G., Magen, H., Einsele, H., Celeghini, I., Barbieri, P., Paoletti, D., Pace, S., Sanderson, R.D., Rambaldi, A., and Nagler, A. (2018) 'Phase I study of the heparanase inhibitor roneparstat: an innovative approach for ultiple myeloma therapy', *Haematologica*, 103(10), e469–e472, available: https://doi.org/10.3324/haematol.2017.182865.

Galustian, C., Meyer, B., Labarthe, M.-C., Dredge, K., Klaschka, D., Henry, J., Todryk, S., Chen, R., Muller, G., Stirling, D., Schafer, P., Bartlett, J.B., and Dalgleish, A.G. (2009) 'The anti-cancer agents lenalidomide and pomalidomide inhibit the proliferation and function of T regulatory cells', *Cancer immunology, immunotherapy: CII*, 58(7), 1033–1045, available: https://doi.org/10.1007/s00262-008-0620-4.

Gao, J., Zhao, M., Cheng, X., Yue, X., Hao, F., Wang, H., Duan, L., Han, C., and Zhu, L. (2023) 'Metabolomic analysis of human plasma sample after exposed to high altitude and return to sea level', *PLOS ONE*, 18(3), e0282301, available: https://doi.org/10.1371/journal.pone.0282301.

Garcés, J.-J., Cedena, M.-T., Puig, N., Burgos, L., Perez, J.J., Cordon, L., Flores-Montero, J., Sanoja-Flores, L., Calasanz, M.-J., Ortiol, A., Blanchard, M.-J., Rios, R., Martin, J., Martínez-Martinez, R., Bargay, J., Sureda, A., de la Rubia, J., Hernandez, M.-T., Rodriguez-Otero, P., de la Cruz, J., Orfao, A., Mateos, M.-V., Martinez-Lopez, J., Lahuerta, J.-J., Rosiñol, L., Blade, J., San-Miguel, J.F., and Paiva, B. (2022) 'Circulating Tumor Cells for the Staging of Patients With Newly Diagnosed Transplant-Eligible Multiple Myeloma', *Journal of Clinical Oncology*, 40(27), 3151–3161, available: https://doi.org/10.1200/JCO.21.01365.

Garcés, J.-J., Simicek, M., Vicari, M., Brozova, L., Burgos, L., Bezdekova, R., Alignani, D., Calasanz, M.-J., Growkova, K., Goicoechea, I., Agirre, X., Pour, L., Prosper, F., Rios, R., Martinez-Lopez, J., Millacoy, P., Palomera, L., Del Orbe, R., Perez-Montaña, A., Garate, S., Blanco, L., Lasa, M., Maiso, P., Flores-Montero, J., Sanoja-Flores, L., Chyra, Z., Vdovin, A., Sevcikova, T., Jelinek, T., Botta, C., El Omri, H., Keats, J., Orfao, A., Hajek, R., San-Miguel, J.F., and Paiva, B. (2020) 'Transcriptional profiling of circulating tumor cells in multiple myeloma: a new model to understand disease dissemination', *Leukemia*, 34(2), 589–603, available: https://doi.org/10.1038/s41375-019-0588-4.

García-Marín, J., Rodríguez-Puyol, D., and Vaquero, J.J. (2022) 'Insight into the mechanism of molecular recognition between human Integrin-Linked Kinase and Cpd22 and its implication at atomic level', *Journal of Computer-Aided Molecular Design*, 36(8), 575–589, available: https://doi.org/10.1007/s10822-022-00466-1.

García-Ortiz, A., Rodríguez-García, Y., Encinas, J., Maroto-Martín, E., Castellano, E., Teixidó, J., and Martínez-López, J. (2021) 'The Role of Tumor Microenvironment in Multiple Myeloma Development and Progression', *Cancers*, 13(2), 217, available: https://doi.org/10.3390/cancers13020217.

Garrett, I.R., Durie, B.G., Nedwin, G.E., Gillespie, A., Bringman, T., Sabatini, M., Bertolini, D.R., and Mundy, G.R. (1987) 'Production of lymphotoxin, a bone-resorbing cytokine, by cultured human myeloma cells', *The New England Journal of Medicine*, 317(9), 526–532, available: https://doi.org/10.1056/NEJM198708273170902.

Garton, K.J., Gough, P.J., Philalay, J., Wille, P.T., Blobel, C.P., Whitehead, R.H., Dempsey, P.J., and Raines, E.W. (2003) 'Stimulated Shedding of Vascular Cell Adhesion Molecule 1 (VCAM-1) Is Mediated by Tumor Necrosis Factor-α-converting Enzyme (ADAM 17) *', *Journal of Biological Chemistry*, 278(39), 37459–37464, available: https://doi.org/10.1074/jbc.M305877200.

Ge, M., Qiao, Z., Kong, Y., Liang, H., Sun, Y., Lu, H., Xu, Z., and Liu, H. (2021) 'Modulating proteasome inhibitor tolerance in multiple myeloma: an alternative strategy to reverse inevitable resistance', *British Journal of Cancer*, 124(4), 770–776, available: https://doi.org/10.1038/s41416-020-01191-y.

Gerber, E., Asare-Werehene, M., Reunov, A., Burger, D., Le, T., Carmona, E., Mes-Masson, A.-M., and Tsang, B.K. (2023) 'Predicting chemoresponsiveness in epithelial ovarian cancer patients using circulating small extracellular vesicle-derived plasma gelsolin', *Journal of Ovarian Research*, 16(1), 14, available: https://doi.org/10.1186/s13048-022-01086-x.

Giannakoulas, N., Ntanasis-Stathopoulos, I., and Terpos, E. (2021) 'The Role of Marrow Microenvironment in the Growth and Development of Malignant Plasma Cells in Multiple Myeloma', *International Journal of Molecular Sciences*, 22(9), 4462, available: https://doi.org/10.3390/ijms22094462.

Giesen, N., Chatterjee, M., Scheid, C., Poos, A.M., Besemer, B., Miah, K., Benner, A., Becker, N., Moehler, T., Metzler, I., Khandanpour, C., Seidel-Glaetzer, A., Trautmann-Grill, K., Kortüm, K.M., Müller-Tidow, C., Mechtersheimer, G., Goeppert, B., Stenzinger, A., Weinhold, N., Goldschmidt, H., Weisel, K., and Raab, M.S. (2023) 'A phase 2 clinical trial of combined BRAF/MEK inhibition for BRAFV600E-mutated multiple myeloma', *Blood*, 141(14), 1685–1690, available: https://doi.org/10.1182/blood.2022017789.

Giliberto, M., Thimiri Govinda Raj, D.B., Cremaschi, A., Skånland, S.S., Gade, A., Tjønnfjord, G.E., Schjesvold, F., Munthe, L.A., and Taskén, K. (2022) 'Ex vivo drug sensitivity screening in multiple myeloma identifies drug combinations that act synergistically', *Molecular Oncology*, 16(6), 1241–1258, available: https://doi.org/10.1002/1878-0261.13191.

Giuliani, N., Bataille, R., Mancini, C., Lazzaretti, M., and Barillé, S. (2001) 'Myeloma cells induce imbalance in the osteoprotegerin/osteoprotegerin ligand system in the human bone marrow environment', *Blood*, 98(13), 3527–3533, available: https://doi.org/10.1182/blood.v98.13.3527.

Godzien, J., Ciborowski, M., Angulo, S., and Barbas, C. (2013) 'From numbers to a biological sense: How the strategy chosen for metabolomics data treatment may affect final results. A practical example based on urine fingerprints obtained by LC-MS', *ELECTROPHORESIS*, 34(19), 2812–2826, available: https://doi.org/10.1002/elps.201300053.

Gohlke, B., Zincke, F., Eckert, A., Kobelt, D., Preissner, S., Liebeskind, J.M., Gunkel, N., Putzker, K., Lewis, J., Preissner, S., Kortüm, B., Walther, W., Mura, C., Bourne, P.E., Stein, U., and Preissner, R. (2022) 'Real-world evidence for preventive effects of statins on cancer incidence: A trans-Atlantic analysis', *Clinical and Translational Medicine*, 12(2), e726, available: https://doi.org/10.1002/ctm2.726.

Goldman, M.J., Craft, B., Hastie, M., Repečka, K., McDade, F., Kamath, A., Banerjee, A., Luo, Y., Rogers, D., Brooks, A.N., Zhu, J., and Haussler, D. (2020) 'Visualizing and interpreting cancer genomics data via the Xena platform', *Nature Biotechnology*, 38(6), 675–678, available: https://doi.org/10.1038/s41587-020-0546-8.

Goldman-Mazur, S., Vesole, D.H., and Jurczyszyn, A. (2021) 'Clinical implications of cytogenetic and molecular aberrations in multiple myeloma', *Acta*

Haematologica Polonica, 52(1), 18–28, available: https://doi.org/10.5603/AHP.2021.0004.

Gonsalves, W.I., Broniowska, K., Jessen, E., Petterson, X.-M., Bush, A.G., Gransee, J., Lacy, M.Q., Hitosugi, T., and Kumar, S.K. (2020) 'Metabolomic and Lipidomic Profiling of Bone Marrow Plasma Differentiates Patients with Monoclonal Gammopathy of Undetermined Significance from Multiple Myeloma', *Scientific Reports*, 10(1), 10250, available: https://doi.org/10.1038/s41598-020-67105-3.

Gooding, S., Ansari-Pour, N., Towfic, F., Ortiz Estévez, M., Chamberlain, P.P., Tsai, K.-T., Flynt, E., Hirst, M., Rozelle, D., Dhiman, P., Neri, P., Ramasamy, K., Bahlis, N., Vyas, P., and Thakurta, A. (2021) 'Multiple cereblon genetic changes are associated with acquired resistance to lenalidomide or pomalidomide in multiple myeloma', *Blood*, 137(2), 232–237, available: https://doi.org/10.1182/blood.2020007081.

Gormley, N.J., Ko, C.-W., Deisseroth, A., Nie, L., Kaminskas, E., Kormanik, N., Goldberg, K.B., Farrell, A.T., and Pazdur, R. (2017) 'FDA Drug Approval: Elotuzumab in Combination with Lenalidomide and Dexamethasone for the Treatment of Relapsed or Refractory Multiple Myeloma', *Clinical Cancer Research: An Official Journal of the American Association for Cancer Research*, 23(22), 6759–6763, available: https://doi.org/10.1158/1078-0432.CCR-16-2870.

Górska, A. and Mazur, A.J. (2022) 'Integrin-linked kinase (ILK): the known vs. the unknown and perspectives', *Cellular and Molecular Life Sciences*, 79(2), 100, available: https://doi.org/10.1007/s00018-021-04104-1.

Gottesman, M.M. and Pastan, I.H. (2015) 'The Role of Multidrug Resistance Efflux Pumps in Cancer: Revisiting a JNCI Publication Exploring Expression of the MDR1 (P-glycoprotein) Gene', *JNCI: Journal of the National Cancer Institute*, 107(9), djv222, available: https://doi.org/10.1093/jnci/djv222.

Govender, D., Harilal, P., Dada, M., and Chetty, R. (1997) 'CD31 (JC70) expression in plasma cells: an immunohistochemical analysis of reactive and neoplastic plasma cells.', *Journal of Clinical Pathology*, 50(6), 490–493.

Granger, K., Gaffney, K.J., and Davis, J.A. (2023) 'Newly approved and forthcoming T-cell-redirecting bispecific antibodies for the treatment of relapsed/refractory multiple myeloma', *Journal of Oncology Pharmacy Practice*, 29(3), 722–726, available: https://doi.org/10.1177/10781552231154809.

Grassl, N., Kulak, N.A., Pichler, G., Geyer, P.E., Jung, J., Schubert, S., Sinitcyn, P., Cox, J., and Mann, M. (2016) 'Ultra-deep and quantitative saliva proteome reveals dynamics of the oral microbiome', *Genome Medicine*, 8, 44, available: https://doi.org/10.1186/s13073-016-0293-0.

Grayson, M.H., Van der Vieren, M., Sterbinsky, S.A., Michael Gallatin, W., Hoffman, P.A., Staunton, D.E., and Bochner, B.S. (1998) 'alphadbeta2

integrin is expressed on human eosinophils and functions as an alternative ligand for vascular cell adhesion molecule 1 (VCAM-1)', *The Journal of Experimental Medicine*, 188(11), 2187–2191, available: https://doi.org/10.1084/jem.188.11.2187.

Greco, M.R., Moro, L., Forciniti, S., Alfarouk, K., Cannone, S., Cardone, R.A., and Reshkin, S.J. (2021) 'Integrin-Linked Kinase Links Integrin Activation to Invadopodia Function and Invasion via the p(T567)-Ezrin/NHERF1/NHE1 Pathway', *International Journal of Molecular Sciences*, 22(4), 2162, available: https://doi.org/10.3390/ijms22042162.

Gregorova, J., Vychytilova-Faltejskova, P., Kramarova, T., Knechtova, Z., Almasi, M., Stork, M., Pour, L., Kohoutek, J., and Sevcikova, S. (2022) 'Proteomic analysis of the bone marrow microenvironment in extramedullary multiple myeloma patients', *Neoplasma*, 69(02), 412–424, available: https://doi.org/10.4149/neo_2021_210527N715.

Greipp, P.R., San Miguel, J., Durie, B.G.M., Crowley, J.J., Barlogie, B., Bladé, J., Boccadoro, M., Child, J.A., Avet-Loiseau, H., Kyle, R.A., Lahuerta, J.J., Ludwig, H., Morgan, G., Powles, R., Shimizu, K., Shustik, C., Sonneveld, P., Tosi, P., Turesson, I., and Westin, J. (2005) 'International staging system for multiple myeloma', *Journal of Clinical Oncology: Official Journal of the American Society of Clinical Oncology*, 23(15), 3412–3420, available: https://doi.org/10.1200/JCO.2005.04.242.

Grogan, T., Spier, C., Salmon, S., Matzner, M., Rybski, J., Weinstein, R., Scheper, R., and Dalton, W. (1993) 'P-glycoprotein expression in human plasma cell myeloma: correlation with prior chemotherapy', *Blood*, 81(2), 490–495, available: https://doi.org/10.1182/blood.V81.2.490.490.

Guan, M., Jiang, H., Xu, C., Xu, R., Chen, Z., and Lu, Y. (2007) 'Adenovirus-mediated PEDF expression inhibits prostate cancer cell growth and results in augmented expression of PAI-2', *Cancer Biology & Therapy*, 6(3), 419–425, available: https://doi.org/10.4161/cbt.6.3.3757.

Gudgeon, N., Giles, H., Bishop, E.L., Fulton-Ward, T., Escribano-Gonzalez, C., Munford, H., James-Bott, A., Foster, K., Karim, F., Jayawardana, D., Mahmood, A., Cribbs, A.P., Tennant, D.A., Basu, S., Pratt, G., and Dimeloe, S. (2023) 'Uptake of long-chain fatty acids from the bone marrow suppresses CD8+ T-cell metabolism and function in multiple myeloma', *Blood Advances*, 7(20), 6035–6047, available: https://doi.org/10.1182/bloodadvances.2023009890.

Guillory, B., Sakwe, A.M., Saria, M., Thompson, P., Adhiambo, C., Koumangoye, R., Ballard, B., Binhazim, A., Cone, C., Jahanen-Dechent, W., and Ochieng, J. (2010) 'Lack of Fetuin-A (α2-HS-Glycoprotein) Reduces Mammary Tumor Incidence and Prolongs Tumor Latency via the Transforming Growth Factor-β Signaling Pathway in a Mouse Model of Breast Cancer', *The American Journal of Pathology*, 177(5), 2635–2644, available: https://doi.org/10.2353/ajpath.2010.100177.

Gupta, S., Master, S., and Graham, C. (2022) ‘Extramedullary Multiple Myeloma: A Patient-Focused Review of the Pathogenesis of Bone Marrow Escape’, *World Journal of Oncology*, 13(5), 311–319, available: https://doi.org/10.4021/wjon.v13i5.1521.

de Haart, S.J., Willems, S.M., Mutis, T., Koudijs, M.J., van Blokland, M.T., Lokhorst, H.M., de Weger, R.A., and Minnema, M.C. (2016) ‘Comparison of intramedullary myeloma and corresponding extramedullary soft tissue plasmacytomas using genetic mutational panel analyses’, *Blood Cancer Journal*, 6(5), e426–e426, available: https://doi.org/10.1038/bcj.2016.35.

Hafid-Medheb, K., Augery-Bourget, Y., Minatchy, M.-N., Hanania, N., and Robert-Lézénès, J. (2003) ‘Bcl-XL is required for heme synthesis during the chemical induction of erythroid differentiation of murine erythroleukemia cells independently of its antiapoptotic function’, *Blood*, 101(7), 2575–2583, available: https://doi.org/10.1182/blood-2002-02-0478.

Hagen, P., Zhang, J., and Barton, K. (2022) ‘High-risk disease in newly diagnosed multiple myeloma: beyond the R-ISS and IMWG definitions’, *Blood Cancer Journal*, 12(5), 83, available: https://doi.org/10.1038/s41408-022-00679-5.

Hakkim, A., Fuchs, T.A., Martinez, N.E., Hess, S., Prinz, H., Zychlinsky, A., and Waldmann, H. (2011) ‘Activation of the Raf-MEK-ERK pathway is required for neutrophil extracellular trap formation’, *Nature Chemical Biology*, 7(2), 75–77, available: https://doi.org/10.1038/nchembio.496.

Halasi, M., Pandit, B., and Gartel, A.L. (2014) ‘Proteasome inhibitors suppress the protein expression of mutant p53’, *Cell Cycle*, 13(20), 3202–3206, available: https://doi.org/10.4161/15384101.2014.950132.

Hallek, M., Neumann, C., Schäffer, M., Danhauser-Riedl, S., von Bubnoff, N., de Vos, G., Druker, B.J., Yasukawa, K., Griffin, J.D., and Emmerich, B. (1997) ‘Signal transduction of interleukin-6 involves tyrosine phosphorylation of multiple cytosolic proteins and activation of Src-family kinases Fyn, Hck, and Lyn in multiple myeloma cell lines’, *Experimental Hematology*, 25(13), 1367–1377.

Hanamura, I. (2021) ‘Gain/Amplification of Chromosome Arm 1q21 in Multiple Myeloma’, *Cancers*, 13(2), 256, available: https://doi.org/10.3390/cancers13020256.

Hanamura, I. (2022) ‘Multiple myeloma with high-risk cytogenetics and its treatment approach’, *International Journal of Hematology*, 115(6), 762–777, available: https://doi.org/10.1007/s12185-022-03353-5.

Hannigan, G.E., McDonald, P.C., Walsh, M.P., and Dedhar, S. (2011) ‘Integrin-linked kinase: Not so “pseudo” after all’, *Oncogene*, 30(43), 4375–4385, available: https://doi.org/10.1038/onc.2011.177.

Hanrahan, C.J., Christensen, C.R., and Crim, J.R. (2010) ‘Current Concepts in the Evaluation of Multiple Myeloma with MR Imaging and FDG PET/CT’,

RadioGraphics, 30(1), 127–142, available: https://doi.org/10.1148/rg.301095066.

Harmer, D., Falank, C., and Reagan, M.R. (2019) 'Interleukin-6 Interweaves the Bone Marrow Microenvironment, Bone Loss, and Multiple Myeloma', *Frontiers in Endocrinology*, 9, available: https://www.frontiersin.org/articles/10.3389/fendo.2018.00788 [accessed 20 Sep 2023].

Hartley-Brown, M. and Richardson, P. (2022) 'Antibody-drug conjugate therapies in multiple myeloma—what's next on the horizon?', *Exploration of Targeted Anti-tumor Therapy*, 3(1), 1–10, available: https://doi.org/10.37349/etat.2022.00067.

Hase, R., Miyamoto, M., Uehara, H., Kadoya, M., Ebihara, Y., Murakami, Y., Takahashi, R., Mega, S., Li, L., Shichinohe, T., Kawarada, Y., and Kondo, S. (2005) 'Pigment Epithelium–Derived Factor Gene Therapy Inhibits Human Pancreatic Cancer in Mice', *Clinical Cancer Research*, 11(24), 8737–8744, available: https://doi.org/10.1158/1078-0432.CCR-05-1323.

Hathi, D., Chanswangphuwana, C., Cho, N., Fontana, F., Maji, D., Ritchey, J., O'Neal, J., Ghai, A., Duncan, K., Akers, W.J., Fiala, M., Vij, R., DiPersio, J.F., Rettig, M., and Shokeen, M. (2022) 'Ablation of VLA4 in multiple myeloma cells redirects tumor spread and prolongs survival', *Scientific Reports*, 12(1), 30, available: https://doi.org/10.1038/s41598-021-03748-0.

Hawke, L.G., Mitchell, B.Z., and Ormiston, M.L. (2020) 'TGF-β and IL-15 Synergize through MAPK Pathways to Drive the Conversion of Human NK Cells to an Innate Lymphoid Cell 1–like Phenotype', *The Journal of Immunology*, 204(12), 3171–3181, available: https://doi.org/10.4049/jimmunol.1900866.

Hayes, D., Napoli, V., Mazurkie, A., Stafford, W.F., and Graceffa, P. (2009) 'Phosphorylation Dependence of Hsp27 Multimeric Size and Molecular Chaperone Function *', *Journal of Biological Chemistry*, 284(28), 18801–18807, available: https://doi.org/10.1074/jbc.M109.011353.

He, Y., Wang, Y., Liu, H., Xu, X., He, S., Tang, J., Huang, Y., Miao, X., Wu, Y., Wang, Q., and Cheng, C. (2015) 'Pyruvate kinase isoform M2 (PKM2) participates in multiple myeloma cell proliferation, adhesion and chemoresistance', *Leukemia Research*, 39(12), 1428–1436, available: https://doi.org/10.1016/j.leukres.2015.09.019.

Hecht, M., von Metzler, I., Sack, K., Kaiser, M., and Sezer, O. (2008) 'Interactions of myeloma cells with osteoclasts promote tumour expansion and bone degradation through activation of a complex signalling network and upregulation of cathepsin K, matrix metalloproteinases (MMPs) and urokinase plasminogen activator (uPA)', *Experimental Cell Research*, 314(5), 1082–1093, available: https://doi.org/10.1016/j.yexcr.2007.10.021.

Hedvat, C.V., Comenzo, R.L., Teruya-Feldstein, J., Olshen, A.B., Ely, S.A., Osman, K., Zhang, Y., Kalakonda, N., and Nimer, S.D. (2003) 'Insights into extramedullary tumour cell growth revealed by expression profiling of human plasmacytomas and multiple myeloma', *British Journal of Haematology*, 122(5), 728–744, available: https://doi.org/10.1046/j.1365-2141.2003.04481.x.

Heinemann, T., Kornauth, C., Severin, Y., Vladimer, G.I., Pemovska, T., Hadzijusufovic, E., Agis, H., Krauth, M.-T., Sperr, W.R., Valent, P., Jäger, U., Simonitsch-Klupp, I., Superti-Furga, G., Staber, P.B., and Snijder, B. (2022) 'Deep Morphology Learning Enhances Ex Vivo Drug Profiling-Based Precision Medicine', *Blood Cancer Discovery*, 3(6), 502–515, available: https://doi.org/10.1158/2643-3230.BCD-21-0219.

Heinemeyer, W., Fischer, M., Krimmer, T., Stachon, U., and Wolf, D.H. (1997) 'The Active Sites of the Eukaryotic 20 S Proteasome and Their Involvement in Subunit Precursor Processing *', *Journal of Biological Chemistry*, 272(40), 25200–25209, available: https://doi.org/10.1074/jbc.272.40.25200.

Henry, B.M., de Oliveira, M.H.S., Cheruiyot, I., Benoit, J., Rose, J., Favaloro, E.J., Lippi, G., Benoit, S., and Pode Shakked, N. (2022) 'Cell-Free DNA, Neutrophil extracellular traps (NETs), and Endothelial Injury in Coronavirus Disease 2019– (COVID-19–) Associated Acute Kidney Injury', *Mediators of Inflammation*, 2022, 9339411, available: https://doi.org/10.1155/2022/9339411.

Heuck, C.J., Qu, P., van Rhee, F., Waheed, S., Usmani, S.Z., Epstein, J., Zhang, Q., Edmondson, R., Hoering, A., Crowley, J., and Barlogie, B. (2014) 'Five gene probes carry most of the discriminatory power of the 70-gene risk model in multiple myeloma', *Leukemia*, 28(12), 2410–2413, available: https://doi.org/10.1038/leu.2014.232.

Hideshima, H., Yoshida, Y., Ikeda, H., Hide, M., Iwasaki, A., Anderson, K.C., and Hideshima, T. (2014) 'IKKβ inhibitor in combination with bortezomib induces cytotoxicity in breast cancer cells', *International Journal of Oncology*, 44(4), 1171–1176, available: https://doi.org/10.3892/ijo.2014.2273.

Hideshima, T., Ikeda, H., Chauhan, D., Okawa, Y., Raje, N., Podar, K., Mitsiades, C., Munshi, N.C., Richardson, P.G., Carrasco, R.D., and Anderson, K.C. (2009) 'Bortezomib induces canonical nuclear factor-κB activation in multiple myeloma cells', *Blood*, 114(5), 1046–1052, available: https://doi.org/10.1182/blood-2009-01-199604.

Hideshima, T., Mitsiades, C., Tonon, G., Richardson, P.G., and Anderson, K.C. (2007) 'Understanding multiple myeloma pathogenesis in the bone marrow to identify new therapeutic targets', *Nature Reviews Cancer*, 7(8), 585–598, available: https://doi.org/10.1038/nrc2189.

Hideshima, T., Qi, J., Paranal, R.M., Tang, W., Greenberg, E., West, N., Colling, M.E., Estiu, G., Mazitschek, R., Perry, J.A., Ohguchi, H., Cottini, F.,

Mimura, N., Görgün, G., Tai, Y.-T., Richardson, P.G., Carrasco, R.D., Wiest, O., Schreiber, S.L., Anderson, K.C., and Bradner, J.E. (2016) 'Discovery of selective small-molecule HDAC6 inhibitor for overcoming proteasome inhibitor resistance in multiple myeloma', *Proceedings of the National Academy of Sciences of the United States of America*, 113(46), 13162–13167, available: https://doi.org/10.1073/pnas.1608067113.

Hinz, M. and Scheidereit, C. (2014) 'The IκB kinase complex in NF-κB regulation and beyond', *EMBO Reports*, 15(1), 46–61, available: https://doi.org/10.1002/embr.201337983.

Hirsch, J., Johnson, C.L., Nelius, T., Kennedy, R., Riese, W. de, and Filleur, S. (2011) 'PEDF inhibits IL8 production in prostate cancer cells through PEDF receptor/phospholipase A2 and regulation of NFκB and PPARγ', *Cytokine*, 55(2), 202–210, available: https://doi.org/10.1016/j.cyto.2011.04.010.

Hjorth-Hansen, H., Waage, A., and Börset, M. (1999) 'Interleukin-15 blocks apoptosis and induces proliferation of the human myeloma cell line OH-2 and freshly isolated myeloma cells', *British Journal of Haematology*, 106(1), 28–34, available: https://doi.org/10.1046/j.1365-2141.1999.01510.x.

Ho, A.-S., Chen, C.-H., Cheng, C.-C., Wang, C.-C., Lin, H.-C., Luo, T.-Y., Lien, G.-S., and Chang, J. (2014) 'Neutrophil elastase as a diagnostic marker and therapeutic target in colorectal cancers', *Oncotarget*, 5(2), 473–480, available: https://doi.org/10.18632/oncotarget.1631.

Ho, M., Xiao, A., Yi, D., Zanwar, S., and Bianchi, G. (2022) 'Treating Multiple Myeloma in the Context of the Bone Marrow Microenvironment', *Current Oncology*, 29(11), 8975–9005, available: https://doi.org/10.3390/curroncol29110705.

Hochhaus, A., Larson, R.A., Guilhot, F., Radich, J.P., Branford, S., Hughes, T.P., Baccarani, M., Deininger, M.W., Cervantes, F., Fujihara, S., Ortmann, C.-E., Menssen, H.D., Kantarjian, H., O'Brien, S.G., and Druker, B.J. (2017) 'Long-Term Outcomes of Imatinib Treatment for Chronic Myeloid Leukemia', *The New England journal of medicine*, 376(10), 917–927, available: https://doi.org/10.1056/NEJMoa1609324.

Hockman, D.J. and Schultz, M.C. (1996) 'Casein Kinase II Is Required for Efficient Transcription by RNA Polymerase III', *Molecular and Cellular Biology*, available: https://doi.org/10.1128/MCB.16.3.892.

Holstein, S.A., Jung, S.-H., Richardson, P.G., Hofmeister, C.C., Hurd, D.D., Hassoun, H., Giralt, S., Stadtmauer, E.A., Weisdorf, D.J., Vij, R., Moreb, J.S., Callander, N.S., van Besien, K., Gentile, T.G., Isola, L., Maziarz, R.T., Bashey, A., Landau, H., Martin, T., Qazilbash, M.H., Rodriguez, C., McClune, B., Schlossman, R.L., Smith, S.E., Hars, V., Owzar, K., Jiang, C., Boyd, M., Schultz, C., Wilson, M., Hari, P., Pasquini, M.C., Horowitz, M.M., Shea, T.C., Devine, S.M., Linker, C., Anderson, K.C., and McCarthy, P.L. (2017) 'Updated analysis of CALGB 100104 (Alliance): a randomised phase III study evaluating lenalidomide vs placebo maintenance after single

autologous stem cell transplant for multiple myeloma', *The Lancet. Haematology*, 4(9), e431–e442, available: https://doi.org/10.1016/S2352-3026(17)30140-0.

Honrubia-Gómez, P., López-Garrido, M.-P., Gil-Gas, C., Sánchez-Sánchez, J., Alvarez-Simon, C., Cuenca-Escalona, J., Perez, A.F., Arias, E., Moreno, R., Sánchez-Sánchez, F., and Ramirez-Castillejo, C. (2019) 'Pedf derived peptides affect colorectal cancer cell lines resistance and tumour re-growth capacity', *Oncotarget*, 10(31), 2973–2986, available: https://doi.org/10.18632/oncotarget.26085.

Hoogstraten, B., Sheehe, P.R., Cuttner, J., Cooper, T., Kyle, R.A., Oberfield, R.A., Townsend, S.R., Harley, J.B., Hayes, D.M., Costa, G., and Holland, J.F. (1967) 'Melphalan in multiple myeloma', *Blood*, 30(1), 74–83.

Hosen, N. (2020) 'Integrins in multiple myeloma', *Inflammation and Regeneration*, 40(1), 4, available: https://doi.org/10.1186/s41232-020-00113-y.

Hosios, A.M., Hecht, V.C., Danai, L.V., Johnson, M.O., Rathmell, J.C., Steinhauser, M.L., Manalis, S.R., and Vander Heiden, M.G. (2016) 'Amino Acids Rather than Glucose Account for the Majority of Cell Mass in Proliferating Mammalian Cells', *Developmental Cell*, 36(5), 540–549, available: https://doi.org/10.1016/j.devcel.2016.02.012.

Hou, J., Ge, C., Cui, M., Liu, T., Liu, X., Tian, H., Zhao, F., Chen, T., Cui, Y., Yao, M., Li, J., and Li, H. (2017) 'Pigment epithelium-derived factor promotes tumor metastasis through an interaction with laminin receptor in hepatocellular carcinomas', *Cell Death & Disease*, 8(8), e2969–e2969, available: https://doi.org/10.1038/cddis.2017.359.

Hou, J., Wei, R., Qian, J., Wang, R., Fan, Z., Gu, C., and Yang, Y. (2019) 'The impact of the bone marrow microenvironment on multiple myeloma (Review)', *Oncology Reports*, 42(4), 1272–1282, available: https://doi.org/10.3892/or.2019.7261.

Houghton, A.M., Rzymkiewicz, D.M., Ji, H., Gregory, A.D., Egea, E.E., Metz, H.E., Stolz, D.B., Land, S.R., Marconcini, L.A., Kliment, C.R., Jenkins, K.M., Beaulieu, K.A., Mouded, M., Frank, S.J., Wong, K.K., and Shapiro, S.D. (2010) 'Neutrophil elastase-mediated degradation of IRS-1 accelerates lung tumor growth', *Nature Medicine*, 16(2), 219–223, available: https://doi.org/10.1038/nm.2084.

Howlader, N., Noone, A., Krapcho, M., Miller, D., Brest, A., Yu, M., Ruhl, J., Tatalovich, Z., Mariotto, A., Lewis, D., Chen, H., Feuer, E., and Cronin, K. (eds) (2019) SEER Cancer Statistics Review, 1975-2016 [online], *National Cancer Institute*, available: https://seer.cancer.gov/csr/1975_2016/ [accessed 22 Mar 2023].

Hsieh, C.-H. and Wang, Y.-C. (2022) 'Emerging roles of plasma gelsolin in tumorigenesis and modulating the tumor microenvironment', *The Kaohsiung*

Journal of Medical Sciences, 38(9), 819–825, available: https://doi.org/10.1002/kjm2.12578.

Hu, A., Noble, W.S., and Wolf-Yadlin, A. (2016) 'Technical advances in proteomics: new developments in data-independent acquisition', *F1000Research*, 5, F1000 Faculty Rev-419, available: https://doi.org/10.12688/f1000research.7042.1.

Hu, C., Yang, J., Qi, Z., Wu, H., Wang, B., Zou, F., Mei, H., Liu, J., Wang, W., and Liu, Q. (2022) 'Heat shock proteins: Biological functions, pathological roles, and therapeutic opportunities', *MedComm*, 3(3), e161, available: https://doi.org/10.1002/mco2.161.

Hu, Y., Li, J., Ni, F., Yang, Z., Gui, X., Bao, Z., Zhao, H., Wei, G., Wang, Y., Zhang, M., Hong, R., Wang, L., Wu, W., Mohty, M., Nagler, A., Chang, A.H., van den Brink, M.R.M., Li, M.D., and Huang, H. (2022) 'CAR-T cell therapy-related cytokine release syndrome and therapeutic response is modulated by the gut microbiome in hematologic malignancies', *Nature Communications*, 13(1), 5313, available: https://doi.org/10.1038/s41467-022-32960-3.

Huang, H., Han, Y., Gao, J., Feng, J., Zhu, L., Qu, L., Shen, L., and Shou, C. (2013) 'High level of serum AMBP is associated with poor response to paclitaxel–capecitabine chemotherapy in advanced gastric cancer patients', *Medical Oncology*, 30(4), 748, available: https://doi.org/10.1007/s12032-013-0748-8.

Huang, J., Chan, S.C., Lok, V., Zhang, L., Lucero-Prisno, D.E., Xu, W., Zheng, Z.-J., Elcarte, E., Withers, M., and Wong, M.C.S. (2022) 'The epidemiological landscape of multiple myeloma: a global cancer registry estimate of disease burden, risk factors, and temporal trends', *The Lancet Haematology*, 9(9), e670–e677, available: https://doi.org/10.1016/S2352-3026(22)00165-X.

Huang, J., Huang, X., and Huang, J. (2022) 'CAR-T cell therapy for hematological malignancies: Limitations and optimization strategies', *Frontiers in Immunology*, 13, available: https://www.frontiersin.org/articles/10.3389/fimmu.2022.1019115 [accessed 13 Apr 2023].

Huang, J., Zhang, J., Li, H., Lu, Z., Shan, W., Mercado-Uribe, I., and Liu, J. (2013) 'VCAM1 expression correlated with tumorigenesis and poor prognosis in high grade serous ovarian cancer', *American Journal of Translational Research*, 5(3), 336–346.

Huang, S.-Y., Lin, C.-W., Lin, H.-H., Yao, M., Tang, J.-L., Wu, S.-J., Chen, Y.-C., Lu, H.-Y., Hou, H.-A., Chen, C.-Y., Chou, W.-C., Tsay, W., Chou, S.-J., and Tien, H.-F. (2014) 'Expression of cereblon protein assessed by immunohistochemicalstaining in myeloma cells is associated with superior response of thalidomide- and lenalidomide-based treatment, but not bortezomib-based treatment, in patients with multiple myeloma', *Annals of Hematology*, 93(8), 1371–1380, available: https://doi.org/10.1007/s00277-014-2063-7.

Huang, T., He, W., Xie, Y., Lv, W., Li, Y., Li, H., Huang, J., Huang, J., Chen, Y., Guo, Q., and Wang, J. (2022) 'A LASSO-derived clinical score to predict severe acute kidney injury in the cardiac surgery recovery unit: a large retrospective cohort study using the MIMIC database', *BMJ open*, 12(6), e060258, available: https://doi.org/10.1136/bmjopen-2021-060258.

Huang, X., Hu, P., and Zhang, J. (2020) 'Genomic analysis of the prognostic value of colony-stimulating factors (CSFs) and colony-stimulating factor receptors (CSFRs) across 24 solid cancer types', *Annals of Translational Medicine*, 8(16), 994–994, available: https://doi.org/10.21037/atm-20-5363.

Huang, Y., Wang, Y., Tang, J., Qin, S., Shen, X., He, S., and Ju, S. (2021) 'CAM-DR: Mechanisms, Roles and Clinical Application in Tumors', *Frontiers in Cell and Developmental Biology*, 9, 698047, available: https://doi.org/10.3389/fcell.2021.698047.

Ilyas, U., Umar, Z., Pansuriya, A.M., Mahmood, A., and Lopez, R. (2022) 'Multiple Myeloma With Retroperitoneal Extramedullary Plasmacytoma Causing Renal Failure and Obstructive Shock From Inferior Vena Cava Compression: A Case Report', *Cureus*, 14(11), e31056, available: https://doi.org/10.7759/cureus.31056.

Iriyama, N., Miura, K., Hatta, Y., Kobayashi, S., Uchino, Y., Kurita, D., Sakagami, H., Takahashi, H., Sakagami, M., Kobayashi, Y., Nakagawa, M., Ohtake, S., Iizuka, Y., and Takei, M. (2017) 'Clinical effect of immunophenotyping on the prognosis of multiple myeloma patients treated with bortezomib', *Oncology Letters*, 13(5), 3803–3808, available: https://doi.org/10.3892/ol.2017.5920.

Irwin, M.E., Johnson, B.P., Manshouri, R., Amin, H.M., and Chandra, J. (2015) 'A NOX2/Egr-1/Fyn pathway delineates new targets for TKI-resistant malignancies', *Oncotarget*, 6(27), 23631–23646.

Ishida, T., Ito, S., Tanaka, J., Uchiyama, M., Kawano, Y., Moreau, P., Martin, T., Risse, M.-L., Tada, K., Suzuki, K., and Ishizawa, K. (2022) 'Isatuximab plus carfilzomib and dexamethasone in Japanese patients with relapsed multiple myeloma: subgroup analysis of the randomized, open label, phase 3 IKEMA study', *Japanese Journal of Clinical Oncology*, 52(12), 1446–1449, available: https://doi.org/10.1093/jjco/hyac137.

Ishikawa, T. (2012) 'Branched-chain amino acids to tyrosine ratio value as a potential prognostic factor for hepatocellular carcinoma', *World Journal of Gastroenterology : WJG*, 18(17), 2005–2008, available: https://doi.org/10.3748/wjg.v18.i17.2005.

Israël, A. (2010) 'The IKK Complex, a Central Regulator of NF-κB Activation', *Cold Spring Harbor Perspectives in Biology*, 2(3), a000158, available: https://doi.org/10.1101/cshperspect.a000158.

Ito, T., Ando, H., Suzuki, T., Ogura, T., Hotta, K., Imamura, Y., Yamaguchi, Y., and Handa, H. (2010) 'Identification of a Primary Target of Thalidomide

Teratogenicity', *Science*, 327(5971), 1345–1350, available: https://doi.org/10.1126/science.1177319.

Ivanisevic, J. and Want, E.J. (2019) 'From Samples to Insights into Metabolism: Uncovering Biologically Relevant Information in LC-HRMS Metabolomics Data', *Metabolites*, 9(12), 308, available: https://doi.org/10.3390/metabo9120308.

Iwasaki, T., Hamano, T., Ogata, A., Hashimoto, N., Kitano, M., and Kakishita, E. (2002) 'Clinical significance of vascular endothelial growth factor and hepatocyte growth factor in multiple myeloma', *British Journal of Haematology*, 116(4), 796–802, available: https://doi.org/10.1046/j.0007-1048.2002.03364.x.

Jablonska, J., Lang, S., Sionov, R.V., and Granot, Z. (2017) 'The regulation of pre-metastatic niche formation by neutrophils', *Oncotarget*, 8(67), 112132–112144, available: https://doi.org/10.18632/oncotarget.22792.

Jagosky, M.H. and Usmani, S.Z. (2020) 'Extramedullary Disease in Multiple Myeloma', *Current Hematologic Malignancy Reports*, 15(2), 62–71, available: https://doi.org/10.1007/s11899-020-00568-3.

Janjetovic, S., Lohneis, P., Nogai, A., Balci, D., Rasche, L., Jähne, D., Bokemeyer, C., Schilling, G., Blau, I.W., and Schmidt-Hieber, M. (2021) 'Clinical and Biological Characteristics of Medullary and Extramedullary Plasma Cell Dyscrasias', *Biology*, 10(7), 629, available: https://doi.org/10.3390/biology10070629.

Jelinek, T., Sevcikova, T., Zihala, D., Popkova, T., Kapustova, V., Broskevicova, L., Capkova, L., Rihova, L., Bezdekova, R., Sevcikova, S., Zidlik, V., Havel, M., Plonkova, H., Jungova, A., Minarik, J., Stork, M., Pour, L., Pavlicek, P., Spicka, I., Maisnar, V., Radocha, J., Simicek, M., and Hajek, R. (2022) 'Limited efficacy of daratumumab in multiple myeloma with extramedullary disease', *Leukemia*, 36(1), 288–291, available: https://doi.org/10.1038/s41375-021-01343-w.

Ji, D., Li, M., Zhan, T., Yao, Y., Shen, J., Tian, H., Zhang, Z., and Gu, J. (2013) 'Prognostic role of serum AZGP1, PEDF and PRDX2 in colorectal cancer patients', *Carcinogenesis*, 34(6), 1265–1272, available: https://doi.org/10.1093/carcin/bgt056.

Ji, M., Li, W., He, G., Zhu, D., Lv, S., Tang, W., Jian, M., Zheng, P., Yang, L., Qi, Z., Mao, Y., Ren, L., Zhong, Y., Tu, Y., Wei, Y., and Xu, J. (2019) 'Zinc-α2-glycoprotein 1 promotes EMT in colorectal cancer by filamin A mediated focal adhesion pathway', *Journal of Cancer*, 10(22), 5557–5566, available: https://doi.org/10.7150/jca.35380.

Ji, Q., Gondek, D., and Hurwitz, A.A. (2005) 'Provision of granulocyte-macrophage colony-stimulating factor converts an autoimmune response to a self-antigen into an antitumor response', *Journal of Immunology (Baltimore, Md.: 1950)*, 175(3), 1456–1463, available: https://doi.org/10.4049/jimmunol.175.3.1456.

Jia, J., Guo, P., Zhang, L., Kong, W., and Wang, F. (2023) 'LINC01614 Promotes Colorectal Cancer Cell Growth and Migration by Regulating miR-217-5p/HMGA1 Axis', *Analytical Cellular Pathology*, 2023, e6833987, available: https://doi.org/10.1155/2023/6833987.

Jiang, H., Jiang, H., Zhang, J., Chen, W., Luo, C., Li, H., Hau, W., Chen, B., and Wang, S. (2020) 'The Serum Metabolic Biomarkers in Early Diagnosis and Risk Stratification of Acute Coronary Syndrome', *Frontiers in Physiology*, 11, available: https://www.frontiersin.org/articles/10.3389/fphys.2020.00776 [accessed 16 May 2023].

Jiang, X., Bomgarden, R., Brown, J., Drew, D.L., Robitaille, A.M., Viner, R., and Huhmer, A.R. (2017) 'Sensitive and Accurate Quantitation of Phosphopeptides Using TMT Isobaric Labeling Technique', *Journal of Proteome Research*, 16(11), 4244–4252, available: https://doi.org/10.1021/acs.jproteome.7b00610.

Jiménez-Segura, R., Rosiñol, L., Cibeira, M.T., Fernández de Larrea, C., Tovar, N., Rodríguez-Lobato, L.G., Bladé, E., Moreno, D.F., Oliver-Caldés, A., and Bladé, J. (2022) 'Paraskeletal and extramedullary plasmacytomas in multiple myeloma at diagnosis and at first relapse: 50-years of experience from an academic institution', *Blood Cancer Journal*, 12(9), 1–8, available: https://doi.org/10.1038/s41408-022-00730-5.

Julkunen, H., Cichońska, A., Slagboom, P.E., Würtz, P., and Nightingale Health UK Biobank Initiative (2021) 'Metabolic biomarker profiling for identification of susceptibility to severe pneumonia and COVID-19 in the general population', *eLife*, 10, e63033, available: https://doi.org/10.7554/eLife.63033.

Juneja, M., Kobelt, D., Walther, W., Voss, C., Smith, J., Specker, E., Neuenschwander, M., Gohlke, B.-O., Dahlmann, M., Radetzki, S., Preissner, R., von Kries, J.P., Schlag, P.M., and Stein, U. (2017) 'Statin and rottlerin small-molecule inhibitors restrict colon cancer progression and metastasis via MACC1', *PLoS biology*, 15(6), e2000784, available: https://doi.org/10.1371/journal.pbio.2000784.

Jung, O., Trapp-Stamborski, V., Purushothaman, A., Jin, H., Wang, H., Sanderson, R.D., and Rapraeger, A.C. (2016) 'Heparanase-induced shedding of syndecan-1/CD138 in myeloma and endothelial cells activates VEGFR2 and an invasive phenotype: prevention by novel synstatins', *Oncogenesis*, 5(2), e202–e202, available: https://doi.org/10.1038/oncsis.2016.5.

Jungnickel, C., Schmidt, L.H., Bittigkoffer, L., Wolf, L., Wolf, A., Ritzmann, F., Kamyschnikow, A., Herr, C., Menger, M.D., Spieker, T., Wiewrodt, R., Bals, R., and Beisswenger, C. (2017) 'IL-17C mediates the recruitment of tumor-associated neutrophils and lung tumor growth', *Oncogene*, 36(29), 4182–4190, available: https://doi.org/10.1038/onc.2017.28.

Jurczyszyn, A., Charliński, G., Suska, A., and Vesole, D.H. (2021) 'The importance of cytogenetic and molecular aberrations in multiple myeloma', *Acta*

Haematologica Polonica, 52(4), 361–370, available: https://doi.org/10.5603/AHP.2021.0069.

K W To, K. and Cho, W.C.S. (2022) 'Drug Repurposing for Cancer Therapy in the Era of Precision Medicine', *Current Molecular Pharmacology*, 15(7), 895–903, available: https://doi.org/10.2174/1874467215666220214104530.

Kalanxhi, E., Meltzer, S., Schou, J.V., Larsen, F.O., Dueland, S., Flatmark, K., Jensen, B.V., Hole, K.H., Seierstad, T., Redalen, K.R., Nielsen, D.L., and Ree, A.H. (2018) 'Systemic immune response induced by oxaliplatin-based neoadjuvant therapy favours survival without metastatic progression in high-risk rectal cancer', *British Journal of Cancer*, 118(10), 1322–1328, available: https://doi.org/10.1038/s41416-018-0085-y.

Kalra, J., Warburton, C., Fang, K., Edwards, L., Daynard, T., Waterhouse, D., Dragowska, W., Sutherland, B.W., Dedhar, S., Gelmon, K., and Bally, M. (2009) 'QLT0267, a small molecule inhibitor targeting integrin-linked kinase (ILK), and docetaxel can combine to produce synergistic interactions linked to enhanced cytotoxicity, reductions in P-AKT levels, altered F-actin architecture and improved treatment outcomes in an orthotopic breast cancer model', *Breast cancer research: BCR*, 11(3), R25, available: https://doi.org/10.1186/bcr2252.

Kaltenmeier, C., Simmons, R.L., Tohme, S., and Yazdani, H.O. (2021) 'Neutrophil Extracellular Traps (NETs) in Cancer Metastasis', *Cancers*, 13(23), 6131, available: https://doi.org/10.3390/cancers13236131.

Kannel, W.B., Castelli, W.P., Gordon, T., and McNamara, P.M. (1971) 'Serum cholesterol, lipoproteins, and the risk of coronary heart disease. The Framingham study', *Annals of Internal Medicine*, 74(1), 1–12, available: https://doi.org/10.7326/0003-4819-74-1-1.

Kataoka, H., Kawaguchi, M., Fukushima, T., and Shimomura, T. (2018) 'Hepatocyte growth factor activator inhibitors (HAI-1 and HAI-2): Emerging key players in epithelial integrity and cancer', *Pathology International*, 68(3), 145–158, available: https://doi.org/10.1111/pin.12647.

Kataoka, H., Miyata, S., Uchinokura, S., and Itoh, H. (2003) 'Roles of hepatocyte growth factor (HGF) activator and HGF activator inhibitor in the pericellular activation of HGF/scatter factor', *Cancer Metastasis Reviews*, 22(2–3), 223–236, available: https://doi.org/10.1023/a:1023051500010.

Kawaguchi, T., Yamagishi, S., Itou, M., Okuda, K., Sumie, S., Kuromatsu, R., Sakata, M., Abe, M., Taniguchi, E., Koga, H., Harada, M., Ueno, T., and Sata, M. (2010) 'Pigment Epithelium-Derived Factor Inhibits Lysosomal Degradation of Bcl-xL and Apoptosis in HepG2 cells', *The American Journal of Pathology*, 176(1), 168–176, available: https://doi.org/10.2353/ajpath.2010.090242.

Kawaguchi, Y., Kovacs, J.J., McLaurin, A., Vance, J.M., Ito, A., and Yao, T.-P. (2003) 'The Deacetylase HDAC6 Regulates Aggresome Formation and Cell

Viability in Response to Misfolded Protein Stress', *Cell*, 115(6), 727–738, available: https://doi.org/10.1016/S0092-8674(03)00939-5.

Kawano, M., Hirano, T., Matsuda, T., Taga, T., Horii, Y., Iwato, K., Asaoku, H., Tang, B., Tanabe, O., and Tanaka, H. (1988) 'Autocrine generation and requirement of BSF-2/IL-6 for human multiple myelomas', *Nature*, 332(6159), 83–85, available: https://doi.org/10.1038/332083a0.

Kawano, M.M., Ishikawa, H., Tsuyama, N., Abroun, S., Liu, S., Li, F.-J., Otsuyama, K., and Zheng, X. (2002) 'Growth mechanism of human myeloma cells by interleukin-6', *International Journal of Hematology*, 76(1), 329–333, available: https://doi.org/10.1007/BF03165278.

Kawano, Y., Kikukawa, Y., Fujiwara, S., Wada, N., Okuno, Y., Mitsuya, H., and Hata, H. (2013) 'Hypoxia reduces CD138 expression and induces an immature and stem cell-like transcriptional program in myeloma cells', *International Journal of Oncology*, 43(6), 1809–1816, available: https://doi.org/10.3892/ijo.2013.2134.

Kazandjian, D. (2016) 'Multiple myeloma epidemiology and survival, a unique malignancy', *Seminars in oncology*, 43(6), 676–681, available: https://doi.org/10.1053/j.seminoncol.2016.11.004.

Kazi, J.U. and Rönnstrand, L. (2019) 'FMS-like Tyrosine Kinase 3/FLT3: From Basic Science to Clinical Implications', *Physiological Reviews*, 99(3), 1433–1466, available: https://doi.org/10.1152/physrev.00029.2018.

Kearney, P., Boniface, J.J., Price, N.D., and Hood, L. (2018) 'The building blocks of successful translation of proteomics to the clinic', *Current Opinion in Biotechnology*, Systems biology • Nanobiotechnology, 51, 123–129, available: https://doi.org/10.1016/j.copbio.2017.12.011.

Keshari, R.S., Jyoti, A., Dubey, M., Kothari, N., Kohli, M., Bogra, J., Barthwal, M.K., and Dikshit, M. (2012) 'Cytokines Induced Neutrophil Extracellular Traps Formation: Implication for the Inflammatory Disease Condition', *PLOS ONE*, 7(10), e48111, available: https://doi.org/10.1371/journal.pone.0048111.

Khattar, E., Maung, K.Z.Y., Chew, C.L., Ghosh, A., Mok, M.M.H., Lee, P., Zhang, J., Chor, W.H.J., Cildir, G., Wang, C.Q., Mohd-Ismail, N.K., Chin, D.W.L., Lee, S.C., Yang, H., Shin, Y.-J., Nam, D.-H., Chen, L., Kumar, A.P., Deng, L.W., Ikawa, M., Gunaratne, J., Osato, M., and Tergaonkar, V. (2019) 'Rap1 regulates hematopoietic stem cell survival and affects oncogenesis and response to chemotherapy', *Nature Communications*, 10, 5349, available: https://doi.org/10.1038/s41467-019-13082-9.

Kikuchi, J., Kodama, N., Takeshita, M., Ikeda, S., Kobayashi, T., Kuroda, Y., Uchiyama, M., Osada, N., Bogen, B., Yasui, H., Takahashi, N., Miwa, A., and Furukawa, Y. (2022) 'EMD originates from hyaluronan-induced homophilic interactions of CD44 variant-expressing MM cells under shear

stress', *Blood Advances*, bloodadvances.2022007291, available: https://doi.org/10.1182/bloodadvances.2022007291.

Kilinc, A.N., Han, S., Barrett, L.A., Anandasivam, N., and Nelson, C.M. (2021) 'Integrin-linked kinase tunes cell–cell and cell-matrix adhesions to regulate the switch between apoptosis and EMT downstream of TGFβ1', *Molecular Biology of the Cell*, 32(5), 402–412, available: https://doi.org/10.1091/mbc.E20-02-0092.

Kim, G.Y., Gabrea, A., Demchenko, Y.N., Bergsagel, L., Roschke, A.V., and Kuehl, W.M. (2014) 'Complex IGH Rearrangements in Multiple Myeloma: Frequent Detection Discrepancies Among Three Different Probe Sets', *Genes, chromosomes & cancer*, 53(6), 467–474, available: https://doi.org/10.1002/gcc.22158.

Kim, H., Kim, S.H., Hwang, D., An, J., Chung, H.S., Yang, E.G., and Kim, S.Y. (2020) 'Extracellular pyruvate kinase M2 facilitates cell migration by upregulating claudin-1 expression in colon cancer cells', *Biochemistry and Cell Biology*, 98(2), 219–226, available: https://doi.org/10.1139/bcb-2019-0139.

Kim, J., Tchernyshyov, I., Semenza, G.L., and Dang, C.V. (2006) 'HIF-1-mediated expression of pyruvate dehydrogenase kinase: A metabolic switch required for cellular adaptation to hypoxia', *Cell Metabolism*, 3(3), 177–185, available: https://doi.org/10.1016/j.cmet.2006.02.002.

Kimmerling, R.J., Prakadan, S.M., Gupta, A.J., Calistri, N.L., Stevens, M.M., Olcum, S., Cermak, N., Drake, R.S., Pelton, K., De Smet, F., Ligon, K.L., Shalek, A.K., and Manalis, S.R. (2018) 'Linking single-cell measurements of mass, growth rate, and gene expression', *Genome Biology*, 19(1), 207, available: https://doi.org/10.1186/s13059-018-1576-0.

Kitani, A., Nakashima, N., Izumihara, T., Inagaki, M., Baoui, X., Yu, S., Matsuda, T., and Matsuyama, T. (1998) 'Soluble VCAM-1 induces chemotaxis of Jurkat and synovial fluid T cells bearing high affinity very late antigen-4', *Journal of Immunology (Baltimore, Md.: 1950)*, 161(9), 4931–4938.

Klein, B., Zhang, X.G., Jourdan, M., Content, J., Houssiau, F., Aarden, L., Piechaczyk, M., and Bataille, R. (1989) 'Paracrine rather than autocrine regulation of myeloma-cell growth and differentiation by interleukin-6', *Blood*, 73(2), 517–526.

Kochenderfer, J.N., Somerville, R.P.T., Lu, T., Shi, V., Bot, A., Rossi, J., Xue, A., Goff, S.L., Yang, J.C., Sherry, R.M., Klebanoff, C.A., Kammula, U.S., Sherman, M., Perez, A., Yuan, C.M., Feldman, T., Friedberg, J.W., Roschewski, M.J., Feldman, S.A., McIntyre, L., Toomey, M.A., and Rosenberg, S.A. (2017) 'Lymphoma Remissions Caused by Anti-CD19 Chimeric Antigen Receptor T Cells Are Associated With High Serum Interleukin-15 Levels', *Journal of Clinical Oncology*, 35(16), 1803, available: https://doi.org/10.1200/JCO.2016.71.3024.

Koerber, R.-M., Held, S.A.E., Heine, A., Kotthoff, P., Daecke, S.N., Bringmann, A., and Brossart, P. (2015) 'Analysis of the anti-proliferative and the pro-apoptotic efficacy of Syk inhibition in multiple myeloma', *Experimental Hematology & Oncology*, 4, 21, available: https://doi.org/10.1186/s40164-015-0016-z.

Kolagatla, S., Jenkins, J.K., Strunk, H., Smith, F., Ganti, S.S., and Moka, N. (2022) 'Secondary Extramedullary Myeloma of the Gallbladder: A Case Report', *Journal of Investigative Medicine High Impact Case Reports*, 10, 23247096221117809, available: https://doi.org/10.1177/23247096221117809.

Kon, S., Atakilit, A., and Sheppard, D. (2011) 'Short form of α9 promotes α9β1 integrin-dependent cell adhesion by modulating the function of the full-length α9 subunit', *Experimental Cell Research*, 317(12), 1774–1784, available: https://doi.org/10.1016/j.yexcr.2011.04.005.

Kong, B., Michalski, C.W., Hong, X., Valkovskaya, N., Rieder, S., Abiatari, I., Streit, S., Erkan, M., Esposito, I., Friess, H., and Kleeff, J. (2010) 'AZGP1 is a tumor suppressor in pancreatic cancer inducing mesenchymal-to-epithelial transdifferentiation by inhibiting TGF-β-mediated ERK signaling', *Oncogene*, 29(37), 5146–5158, available: https://doi.org/10.1038/onc.2010.258.

Kong, D.-H., Kim, Y.K., Kim, M.R., Jang, J.H., and Lee, S. (2018) 'Emerging Roles of Vascular Cell Adhesion Molecule-1 (VCAM-1) in Immunological Disorders and Cancer', *International Journal of Molecular Sciences*, 19(4), 1057, available: https://doi.org/10.3390/ijms19041057.

Koopman, G., Parmentier, H.K., Schuurman, H.J., Newman, W., Meijer, C.J., and Pals, S.T. (1991) 'Adhesion of human B cells to follicular dendritic cells involves both the lymphocyte function-associated antigen 1/intercellular adhesion molecule 1 and very late antigen 4/vascular cell adhesion molecule 1 pathways', *The Journal of Experimental Medicine*, 173(6), 1297–1304, available: https://doi.org/10.1084/jem.173.6.1297.

Kortüm, K.M., Mai, E.K., Hanafiah, N.H., Shi, C.-X., Zhu, Y.-X., Bruins, L., Barrio, S., Jedlowski, P., Merz, M., Xu, J., Stewart, R.A., Andrulis, M., Jauch, A., Hillengass, J., Goldschmidt, H., Bergsagel, P.L., Braggio, E., Stewart, A.K., and Raab, M.S. (2016) 'Targeted sequencing of refractory myeloma reveals a high incidence of mutations in CRBN and Ras pathway genes', *Blood*, 128(9), 1226–1233, available: https://doi.org/10.1182/blood-2016-02-698092.

Koumpis, E., Tassi, I., Malea, T., Papathanasiou, K., Papakonstantinou, I., Serpanou, A., Tsolas, E., Kapsali, E., Vassilakopoulos, T.P., Papoudou-Bai, A., and Hatzimichael, E. (2021) 'CD56 expression in multiple myeloma: Correlation with poor prognostic markers but no effect on outcome', *Pathology - Research and Practice*, 225, 153567, available: https://doi.org/10.1016/j.prp.2021.153567.

Kowalska, M., Kaminska, J., Fuksiewicz, M., Kotowicz, B., Chechlinska, M., Druzd-Sitek, A., and Walewski, J. (2011) 'A survey of prognostic value of serum factors in multiple myeloma patients before treatment: macrophage-colony stimulating factor (M-CSF) is a powerful predictor of survival', *Medical Oncology*, 28(1), 194–198, available: https://doi.org/10.1007/s12032-009-9403-9.

Kraeber-Bodéré, F., Zweegman, S., Perrot, A., Hulin, C., Caillot, D., Facon, T., Leleu, X., Belhadj, K., Itti, E., Karlin, L., Bailly, C., Levin, M.-D., Minnema, M.C., Jamet, B., Bodet-Milin, C., de Keizer, B., Béné, M.C., Avet-Loiseau, H., Sonneveld, P., Pei, L., Rigat, F., de Boer, C., Vermeulen, J., Kampfenkel, T., Lambert, J., and Moreau, P. (2022) 'Prognostic value of positron emission tomography/computed tomography in transplant-eligible newly diagnosed multiple myeloma patients from CASSIOPEIA: the CASSIOPET study', *Haematologica*, 108(2), 621–626, available: https://doi.org/10.3324/haematol.2021.280051.

Kraus, M., Bader, J., Geurink, P.P., Weyburne, E.S., Mirabella, A.C., Silzle, T., Shabaneh, T.B., van der Linden, W.A., de Bruin, G., Haile, S.R., van Rooden, E., Appenzeller, C., Li, N., Kisselev, A.F., Overkleeft, H., and Driessen, C. (2015) 'The novel β2-selective proteasome inhibitor LU-102 synergizes with bortezomib and carfilzomib to overcome proteasome inhibitor resistance of myeloma cells', *Haematologica*, 100(10), 1350–1360, available: https://doi.org/10.3324/haematol.2014.109421.

Krejcik, J., Frerichs, K.A., Nijhof, I.S., van Kessel, B., van Velzen, J.F., Bloem, A.C., Broekmans, M.E.C., Zweegman, S., van Meerloo, J., Musters, R.J.P., Poddighe, P.J., Groen, R.W.J., Chiu, C., Plesner, T., Lokhorst, H.M., Sasser, A.K., Mutis, T., and van de Donk, N.W.C.J. (2017) 'Monocytes and granulocytes reduce CD38 expression levels on myeloma cells in patients treated with daratumumab', *Clinical cancer research : an official journal of the American Association for Cancer Research*, 23(24), 7498–7511, available: https://doi.org/10.1158/1078-0432.CCR-17-2027.

Kriegova, E., Fillerova, R., Minarik, J., Savara, J., Manakova, J., Petrackova, A., Dihel, M., Balcarkova, J., Krhovska, P., Pika, T., Gajdos, P., Behalek, M., Vasinek, M., and Papajik, T. (2021) 'Whole-genome optical mapping of bone-marrow myeloma cells reveals association of extramedullary multiple myeloma with chromosome 1 abnormalities', *Scientific Reports*, 11(1), 14671, available: https://doi.org/10.1038/s41598-021-93835-z.

Kristensen, I.B., Christensen, J.H., Lyng, M.B., Møller, M.B., Pedersen, L., Rasmussen, L.M., Ditzel, H.J., and Abildgaard, N. (2013) 'Hepatocyte growth factor pathway upregulation in the bone marrow microenvironment in multiple myeloma is associated with lytic bone disease', *British Journal of Haematology*, 161(3), 373–382, available: https://doi.org/10.1111/bjh.12270.

Krönke, J., Udeshi, N.D., Narla, A., Grauman, P., Hurst, S.N., McConkey, M., Svinkina, T., Heckl, D., Comer, E., Li, X., Ciarlo, C., Hartman, E., Munshi, N., Schenone, M., Schreiber, S.L., Carr, S.A., and Ebert, B.L. (2014) 'Lenalidomide causes selective degradation of IKZF1 and IKZF3 in multiple

myeloma cells', *Science (New York, N.Y.)*, 343(6168), 301–305, available: https://doi.org/10.1126/science.1244851.

Kropivsek, K., Kachel, P., Goetze, S., Wegmann, R., Festl, Y., Severin, Y., Hale, B.D., Mena, J., van Drogen, A., Dietliker, N., Tchinda, J., Wollscheid, B., Manz, M.G., and Snijder, B. (2023) 'Ex vivo drug response heterogeneity reveals personalized therapeutic strategies for patients with multiple myeloma', *Nature Cancer*, 4(5), 734–753, available: https://doi.org/10.1038/s43018-023-00544-9.

Kumar, S. and Rajkumar, S.V. (2008) 'Many facets of bortezomib resistance/susceptibility', *Blood*, 112(6), 2177–2178, available: https://doi.org/10.1182/blood-2008-07-167767.

Kumar, S.K., Therneau, T.M., Gertz, M.A., Lacy, M.Q., Dispenzieri, A., Rajkumar, S.V., Fonseca, R., Witzig, T.E., Lust, J.A., Larson, D.R., Kyle, R.A., and Greipp, P.R. (2004) 'Clinical course of patients with relapsed multiple myeloma', *Mayo Clinic Proceedings*, 79(7), 867–874, available: https://doi.org/10.4065/79.7.867.

Kuriyama, S., Tanaka, G., Takagane, K., Itoh, G., and Tanaka, M. (2022) 'Pigment Epithelium Derived Factor Is Involved in the Late Phase of Osteosarcoma Metastasis by Increasing Extravasation and Cell-Cell Adhesion', *Frontiers in Oncology*, 12, available: https://www.frontiersin.org/articles/10.3389/fonc.2022.818182 [accessed 29 Nov 2022].

Kurup, R. kumar, Nair, R.A., and Kurup, P.A. (2003) 'Isoprenoid pathway related cascade in multiple myeloma', *Pathology oncology research: POR*, 9(2), 107–114, available: https://doi.org/10.1007/BF03033754.

Kuusanmäki, H., Kytölä, S., Vänttinen, I., Ruokoranta, T., Ranta, A., Huuhtanen, J., Suvela, M., Parsons, A., Holopainen, A., Partanen, A., Kuusisto, M.E.L., Koskela, S., Räty, R., Itälä-Remes, M., Västrik, I., Dufva, O., Siitonen, S., Porkka, K., Wennerberg, K., Heckman, C.A., Ettala, P., Pyörälä, M., Rimpiläinen, J., Siitonen, T., and Kontro, M. (2022) 'Ex vivo venetoclax sensitivity testing predicts treatment response in acute myeloid leukemia', *Haematologica*, 108(7), 1768–1781, available: https://doi.org/10.3324/haematol.2022.281692.

Kwon, Y.W., Jo, H.-S., Bae, S., Seo, Y., Song, P., Song, M., and Yoon, J.H. (2021) 'Application of Proteomics in Cancer: Recent Trends and Approaches for Biomarkers Discovery', *Frontiers in Medicine*, 8, available: https://www.frontiersin.org/articles/10.3389/fmed.2021.747333 [accessed 26 Jul 2023].

Kyle, R.A., Gertz, M.A., Witzig, T.E., Lust, J.A., Lacy, M.Q., Dispenzieri, A., Fonseca, R., Rajkumar, S.V., Offord, J.R., Larson, D.R., Plevak, M.E., Therneau, T.M., and Greipp, P.R. (2003) 'Review of 1027 Patients With Newly Diagnosed Multiple Myeloma', *Mayo Clinic Proceedings*, 78(1), 21–33, available: https://doi.org/10.4065/78.1.21.

Kyle, R.A. and Rajkumar, S.V. (2008) ‘Multiple myeloma’, *Blood*, 111(6), 2962–2972, available: https://doi.org/10.1182/blood-2007-10-078022.

Lacy, M.Q., Donovan, K.A., Heimbach, J.K., Ahmann, G.J., and Lust, J.A. (1999) ‘Comparison of interleukin-1 beta expression by in situ hybridization in monoclonal gammopathy of undetermined significance and multiple myeloma’, *Blood*, 93(1), 300–305.

Lancet, T. (2021) ‘20 years of precision medicine in oncology’, *The Lancet*, 397(10287), 1781, available: https://doi.org/10.1016/S0140-6736(21)01099-0.

Landgren, O. and Weiss, B.M. (2009) ‘Patterns of monoclonal gammopathy of undetermined significance and multiple myeloma in various ethnic/racial groups: support for genetic factors in pathogenesis’, *Leukemia*, 23(10), 1691–1697, available: https://doi.org/10.1038/leu.2009.134.

Larsen, D.H., Hari, F., Clapperton, J.A., Gwerder, M., Gutsche, K., Altmeyer, M., Jungmichel, S., Toledo, L.I., Fink, D., Rask, M.-B., Grøfte, M., Lukas, C., Nielsen, M.L., Smerdon, S.J., Lukas, J., and Stucki, M. (2014) ‘The NBS1-Treacle complex controls ribosomal RNA transcription in response to DNA damage’, *Nature cell biology*, 16(8), 792–803, available: https://doi.org/10.1038/ncb3007.

Lavallée-Adam, M., Park, S.K.R., Martínez-Bartolomé, S., He, L., and Yates, J.R. (2015) ‘From Raw Data to Biological Discoveries: A Computational Analysis Pipeline for Mass Spectrometry-Based Proteomics’, *Journal of The American Society for Mass Spectrometry*, 26(11), 1820–1826, available: https://doi.org/10.1007/s13361-015-1161-7.

Lawal, B., Tseng, S.-H., Olugbodi, J.O., Iamsaard, S., Ilesanmi, O.B., Mahmoud, M.H., Ahmed, S.H., Batiha, G.E.-S., and Wu, A.T.H. (2021) ‘Pan-Cancer Analysis of Immune Complement Signature C3/C5/C3AR1/C5AR1 in Association with Tumor Immune Evasion and Therapy Resistance’, *Cancers*, 13(16), 4124, available: https://doi.org/10.3390/cancers13164124.

LeBlanc, R., Hideshima, T., Catley, L.P., Shringarpure, R., Burger, R., Mitsiades, N., Mitsiades, C., Cheema, P., Chauhan, D., Richardson, P.G., Anderson, K.C., and Munshi, N.C. (2004) ‘Immunomodulatory drug costimulates T cells via the B7-CD28 pathway’, *Blood*, 103(5), 1787–1790, available: https://doi.org/10.1182/blood-2003-02-0361.

Lee, J.W., Chung, H.Y., Ehrlich, L.A., Jelinek, D.F., Callander, N.S., Roodman, G.D., and Choi, S.J. (2004) ‘IL-3 expression by myeloma cells increases both osteoclast formation and growth of myeloma cells’, *Blood*, 103(6), 2308–2315, available: https://doi.org/10.1182/blood-2003-06-1992.

Lee, P.Y., Osman, J., Low, T.Y., and Jamal, R. (2019) ‘Plasma/serum proteomics: depletion strategies for reducing high-abundance proteins for biomarker discovery’, *Bioanalysis*, 11(19), 1799–1812, available: https://doi.org/10.4155/bio-2019-0145.

Lerman, I. and Hammes, S.R. (2018) 'Neutrophil elastase in the tumor microenvironment', *Steroids*, FASEB SRC – Steroid Signaling in Health and Disease, 133, 96–101, available: https://doi.org/10.1016/j.steroids.2017.11.006.

Letai, A. (2022) 'Functional Precision Medicine: Putting drugs on patient cancer cells and seeing what happens', *Cancer discovery*, 12(2), 290–292, available: https://doi.org/10.1158/2159-8290.CD-21-1498.

Letai, A., Bhola, P., and Welm, A.L. (2022) 'Functional precision oncology: testing tumors with drugs to identify vulnerabilities and novel combinations', *Cancer cell*, 40(1), 26–35, available: https://doi.org/10.1016/j.ccell.2021.12.004.

Lévesque, J.-P., Takamatsu, Y., Nilsson, S.K., Haylock, D.N., and Simmons, P.J. (2001) 'Vascular cell adhesion molecule-1 (CD106) is cleaved by neutrophil proteases in the bone marrow following hematopoietic progenitor cell mobilization by granulocyte colony-stimulating factor', *Blood*, 98(5), 1289–1297, available: https://doi.org/10.1182/blood.V98.5.1289.

Li, C., Xu, J., Luo, W., Liao, D., Xie, W., Wei, Q., Zhang, Y., Wang, X., Wu, Z., Kang, Y., Zheng, J., Xiong, W., Deng, J., Hu, Y., and Mei, H. (2023) 'Bispecific CS1-BCMA CAR-T cells are clinically active in relapsed or refractory multiple myeloma', *Leukemia*, 1–11, available: https://doi.org/10.1038/s41375-023-02065-x.

Li, C.-J., Xia, H.-L., Wu, Y.-M., Ding, G., and Xu, D.-D. (2019) '[Significance of Detecting Serum Complement C3 and C4 in Patients with Multiple Myeloma]', *Zhongguo shi yan xue ye xue za zhi*, 27(2), 472–476, available: https://doi.org/10.19746/j.cnki.issn.1009-2137.2019.02.026.

Li, H., Zhong, R., He, C., Tang, C., Cui, H., Li, R., Liu, Y., Lan, S., and Cheng, Y. (2022) 'Colony-stimulating factor CSF2 mediates the phenotypic plasticity of small-cell lung cancer by regulating the p-STAT3/MYC pathway', *Oncology Reports*, 48(1), 122, available: https://doi.org/10.3892/or.2022.8333.

Li, J., Wang, Y., and Liu, P. (2019) 'The impact on early diagnosis and survival outcome of M-protein screening-driven diagnostic approach to multiple myeloma in China: a cohort study', *Journal of Cancer*, 10(20), 4807–4813, available: https://doi.org/10.7150/jca.32103.

Li, J., Zhang, X., Shen, J., Guo, J., Wang, X., and Liu, J. (2019) 'Bortezomib promotes apoptosis of multiple myeloma cells by regulating HSP27', *Molecular Medicine Reports*, 20(3), 2410–2418, available: https://doi.org/10.3892/mmr.2019.10467.

Li, M., Lin, C., Deng, H., Strnad, J., Bernabei, L., Vogl, D.T., Burke, J., and Nefedova, Y. (2020) 'A novel peptidylarginine deiminase 4 (PAD4) inhibitor BMS-P5 blocks formation of neutrophil extracellular traps and delays progression of multiple myeloma', *Molecular cancer therapeutics*, 19(7), 1530–1538, available: https://doi.org/10.1158/1535-7163.MCT-19-1020.

Li, S., Cong, X., Gao, H., Lan, X., Li, Z., Wang, W., Song, S., Wang, Y., Li, C., Zhang, H., Zhao, Y., and Xue, Y. (2019) 'Tumor-associated neutrophils induce EMT by IL-17a to promote migration and invasion in gastric cancer cells', *Journal of experimental & clinical cancer research: CR*, 38(1), 6, available: https://doi.org/10.1186/s13046-018-1003-0.

Li, S., Zhang, E., and Cai, Z. (2023) 'Liquid biopsy by analysis of circulating myeloma cells and cell-free nucleic acids: a novel noninvasive approach of disease evaluation in multiple myeloma', *Biomarker Research*, 11(1), 27, available: https://doi.org/10.1186/s40364-023-00469-6.

Li, W., Liu, M., Yuan, T., Yan, L., Cui, R., and Deng, Q. (2022a) 'Efficacy and follow-up of humanized anti-BCMA CAR-T cell therapy in relapsed/refractory multiple myeloma patients with extramedullary-extraosseous, extramedullary-bone related, and without extramedullary disease', *Hematological Oncology*, 40(2), 223–232, available: https://doi.org/10.1002/hon.2958.

Li, W., Liu, M., Yuan, T., Yan, L., Cui, R., and Deng, Q. (2022b) 'Efficacy and follow-up of humanized anti-BCMA CAR-T cell therapy in relapsed/refractory multiple myeloma patients with extramedullary-extraosseous, extramedullary-bone related, and without extramedullary disease', *Hematological Oncology*, 40(2), 223–232, available: https://doi.org/10.1002/hon.2958.

Li, W., Zhang, B., Cao, W., Zhang, W., Li, T., Liu, L., Xu, L., Gao, F., Wang, Y., Wang, F., Xing, H., Jiang, Z., Shi, J., Bian, Z., and Song, Y. (2023) 'Identification of potential resistance mechanisms and therapeutic targets for the relapse of BCMA CAR-T therapy in relapsed/refractory multiple myeloma through single-cell sequencing', *Experimental Hematology & Oncology*, 12(1), 44, available: https://doi.org/10.1186/s40164-023-00402-5.

Li, Y., Ji, J., Lu, H., Li, J., and Qu, X. (2022) 'Pomalidomide-based therapy for extramedullary multiple myeloma', *Hematology*, 27(1), 88–94, available: https://doi.org/10.1080/16078454.2021.2019364.

Li, Y., Sun, Z., and Qu, X. (2022) 'Advances in the treatment of extramedullary disease in multiple myeloma', *Translational Oncology*, 22, 101465, available: https://doi.org/10.1016/j.tranon.2022.101465.

Li, Y., Yolken, R., Cowan, D., Boivin, M., Liu, T., and Niebuhr, D. (2015) 'Biomarker identification and effect estimation on schizophrenia –a high dimensional data analysis', *Frontiers in Public Health*, 3, available: https://www.frontiersin.org/articles/10.3389/fpubh.2015.00075 [accessed 23 Nov 2023].

Li, Z., Adams, R.M., Chourey, K., Hurst, G.B., Hettich, R.L., and Pan, C. (2012) 'Systematic comparison of label-free, metabolic labeling, and isobaric chemical labeling for quantitative proteomics on LTQ Orbitrap Velos', *Journal of Proteome Research*, 11(3), 1582–1590, available: https://doi.org/10.1021/pr200748h.

Liao, T., Chen, W., Sun, J., Zhang, Y., Hu, X., Yang, S., Qiu, H., Li, S., and Chu, T. (2018) 'CXCR4 Accelerates Osteoclastogenesis Induced by Non-Small Cell Lung Carcinoma Cells Through Self-Potentiation and VCAM1 Secretion', *Cellular Physiology and Biochemistry*, 50(3), 1084–1099, available: https://doi.org/10.1159/000494533.

Lin, C.-I. and Yeh, N.-H. (2009) 'Treacle recruits RNA polymerase I complex to the nucleolus that is independent of UBF', *Biochemical and Biophysical Research Communications*, 386(2), 396–401, available: https://doi.org/10.1016/j.bbrc.2009.06.050.

Lin, C.-Y., Navarro, S., Reddy, S., and Comai, L. (2006) 'CK2-mediated stimulation of Pol I transcription by stabilization of UBF–SL1 interaction', *Nucleic Acids Research*, 34(17), 4752–4766, available: https://doi.org/10.1093/nar/gkl581.

Lin, Y.-H.T., Way, G.P., Barwick, B.G., Mariano, M.C., Marcoulis, M., Ferguson, I.D., Driessen, C., Boise, L.H., Greene, C.S., and Wiita, A.P. (2019) 'Integrated phosphoproteomics and transcriptional classifiers reveal hidden RAS signaling dynamics in multiple myeloma', *Blood Advances*, 3(21), 3214–3227, available: https://doi.org/10.1182/bloodadvances.2019000303.

Lindell, E., Zhong, L., and Zhang, X. (2023) 'Quiescent Cancer Cells—A Potential Therapeutic Target to Overcome Tumor Resistance and Relapse', *International Journal of Molecular Sciences*, 24(4), 3762, available: https://doi.org/10.3390/ijms24043762.

Lionetti, M., Da Vià, M.C., Albano, F., Neri, A., Bolli, N., and Musto, P. (2021) 'Genomics of Smoldering Multiple Myeloma: Time for Clinical Translation of Findings?', *Cancers*, 13(13), 3319, available: https://doi.org/10.3390/cancers13133319.

Liu, E., Tong, Y., Dotti, G., Shaim, H., Savoldo, B., Mukherjee, M., Orange, J., Wan, X., Lu, X., Reynolds, A., Gagea, M., Banerjee, P., Cai, R., Bdaiwi, M.H., Basar, R., Muftuoglu, M., Li, L., Marin, D., Wierda, W., Keating, M., Champlin, R., Shpall, E., and Rezvani, K. (2018) 'Cord blood NK cells engineered to express IL-15 and a CD19-targeted CAR show long-term persistence and potent antitumor activity', *Leukemia*, 32(2), 520–531, available: https://doi.org/10.1038/leu.2017.226.

Liu, H., He, J., Koh, S.P., Zhong, Y., Liu, Z., Wang, Z., Zhang, Y., Li, Z., Tam, B.T., Lin, P., Xiao, M., Young, K.H., Amini, B., Starbuck, M.W., Lee, H.C., Navone, N.M., Davis, R.E., Tong, Q., Bergsagel, P.L., Hou, J., Yi, Q., Orlowski, R.Z., Gagel, R.F., and Yang, J. (2019) 'Reprogrammed marrow adipocytes contribute to myeloma-induced bone disease', *Science translational medicine*, 11(494), eaau9087, available: https://doi.org/10.1126/scitranslmed.aau9087.

Liu, J., Han, H., Fan, Z., El Beaino, M., Fang, Z., Li, S., and Ji, J. (2018) 'AZGP1 inhibits soft tissue sarcoma cells invasion and migration', *BMC Cancer*, 18(1), 89, available: https://doi.org/10.1186/s12885-017-3962-5.

Liu, J., Yang, H., Liang, X., Wang, Y., Hou, J., Liu, Y., Wang, J., and Zhou, F. (2017) 'Meta-analysis of the efficacy of treatments for newly diagnosed and relapsed/refractory multiple myeloma with del(17p)', *Oncotarget*, 8(37), 62435–62444, available: https://doi.org/10.18632/oncotarget.18722.

Liu, R., Zhao, E., Wang, F., and Cui, H. (2020) 'CCDC25: precise navigator for neutrophil extracellular traps on the prometastatic road', *Signal Transduction and Targeted Therapy*, 5(1), 1–2, available: https://doi.org/10.1038/s41392-020-00285-6.

Liu, Z., Xu, J., He, J., Liu, H., Lin, P., Wan, X., Navone, N.M., Tong, Q., Kwak, L.W., Orlowski, R.Z., and Yang, J. (2015) 'Mature adipocytes in bone marrow protect myeloma cells against chemotherapy through autophagy activation', *Oncotarget*, 6(33), 34329–34341, available: https://doi.org/10.18632/oncotarget.6020.

Long, X., Xu, Q., Lou, Y., Li, C., Gu, J., Cai, H., Wang, D., Xu, J., Li, T., Zhou, X., Xiao, M., Wang, Y., Mao, X., Zhou, J., and Chen, L. (2020) 'The utility of non-invasive liquid biopsy for mutational analysis and minimal residual disease assessment in extramedullary multiple myeloma', *British Journal of Haematology*, 189(2), e45–e48, available: https://doi.org/10.1111/bjh.16440.

Lonial, S., Jacobus, S., Fonseca, R., Weiss, M., Kumar, S., Orlowski, R.Z., Kaufman, J.L., Yacoub, A.M., Buadi, F.K., O'Brien, T., Matous, J.V., Anderson, D.M., Emmons, R.V., Mahindra, A., Wagner, L.I., Dhodapkar, M.V., and Rajkumar, S.V. (2020) 'Randomized Trial of Lenalidomide Versus Observation in Smoldering Multiple Myeloma', *Journal of Clinical Oncology*, 38(11), 1126–1137, available: https://doi.org/10.1200/JCO.19.01740.

Lonial, S., Lee, H.C., Badros, A., Trudel, S., Nooka, A.K., Chari, A., Abdallah, A., Callander, N., Sborov, D., Suvannasankha, A., Weisel, K., Voorhees, P.M., Womersley, L., Baron, J., Piontek, T., Lewis, E., Opalinska, J., Gupta, I., and Cohen, A.D. (2021) 'Longer term outcomes with single-agent belantamab mafodotin in patients with relapsed or refractory multiple myeloma: 13-month follow-up from the pivotal DREAMM-2 study', *Cancer*, 127(22), 4198–4212, available: https://doi.org/10.1002/cncr.33809.

Lonial, S., Lee, H.C., Badros, A., Trudel, S., Nooka, A.K., Chari, A., Abdallah, A.-O., Callander, N., Lendvai, N., Sborov, D., Suvannasankha, A., Weisel, K., Karlin, L., Libby, E., Arnulf, B., Facon, T., Hulin, C., Kortüm, K.M., Rodríguez-Otero, P., Usmani, S.Z., Hari, P., Baz, R., Quach, H., Moreau, P., Voorhees, P.M., Gupta, I., Hoos, A., Zhi, E., Baron, J., Piontek, T., Lewis, E., Jewell, R.C., Dettman, E.J., Popat, R., Esposti, S.D., Opalinska, J., Richardson, P., and Cohen, A.D. (2020) 'Belantamab mafodotin for relapsed or refractory multiple myeloma (DREAMM-2): a two-arm, randomised, open-label, phase 2 study', *The Lancet. Oncology*, 21(2), 207–221, available: https://doi.org/10.1016/S1470-2045(19)30788-0.

Lonial, S., Rajkumar, S.V., and Mateos, M.V. (2022) 'Risk stratified management approaches for smouldering multiple myeloma: clinical research becomes

clinical practice', *The Lancet. Haematology*, 9(2), e162–e165, available: https://doi.org/10.1016/S2352-3026(21)00335-5.

López-Anglada, L., Gutiérrez, N.C., García, J.L., Mateos, M.V., Flores, T., and San Miguel, J.F. (2010) 'P53 deletion may drive the clinical evolution and treatment response in multiple myeloma', *European Journal of Haematology*, 84(4), 359–361, available: https://doi.org/10.1111/j.1600-0609.2009.01399.x.

Lorenz, J., Waldschmidt, J., Wider, D., Follo, M., Ihorst, G., Chatterjee, M., May, A.M., Duyster, J., Rosenwald, A., Wäsch, R., Zirlik, K., and Engelhardt, M. (2016) 'From CLL to Multiple Myeloma - Spleen Tyrosine Kinase (SYK) influences multiple myeloma cell survival and migration', *British Journal of Haematology*, 174(6), 985–989, available: https://doi.org/10.1111/bjh.13825.

Lu, Y., Wang, Y., Xu, H., Shi, C., Jin, F., and Li, W. (2018) 'Profilin 1 induces drug resistance through Beclin1 complex-mediated autophagy in multiple myeloma', *Cancer Science*, 109(9), 2706–2716, available: https://doi.org/10.1111/cas.13711.

Lucas, F., Pennell, M., Huang, Y., Benson, D.M., Efebera, Y.A., Chaudhry, M., Hughes, T., Woyach, J.A., Byrd, J.C., Zhang, S., Jones, D., Guan, X., Burd, C.E., and Rosko, A.E. (2020) 'T Cell Transcriptional Profiling and Immunophenotyping Uncover LAG3 as a Potential Significant Target of Immune Modulation in Multiple Myeloma', *Biology of Blood and Marrow Transplantation*, 26(1), 7–15, available: https://doi.org/10.1016/j.bbmt.2019.08.009.

Ludwig, H., Nachbaur, D.M., Fritz, E., Krainer, M., and Huber, H. (1991) 'Interleukin-6 is a prognostic factor in multiple myeloma', *Blood*, 77(12), 2794–2795.

Ludwig, H., Novis Durie, S., Meckl, A., Hinke, A., and Durie, B. (2020) 'Multiple Myeloma Incidence and Mortality Around the Globe; Interrelations Between Health Access and Quality, Economic Resources, and Patient Empowerment', *The Oncologist*, 25(9), e1406–e1413, available: https://doi.org/10.1634/theoncologist.2020-0141.

Ludwig, L.M., Maxcy, K.L., and LaBelle, J.L. (2019) 'Flow Cytometry-Based Detection and Analysis of BCL-2 Family Proteins and Mitochondrial Outer Membrane Permeabilization (MOMP)', *Methods in molecular biology (Clifton, N.J.)*, 1877, 77–91, available: https://doi.org/10.1007/978-1-4939-8861-7_5.

Lum, J.J., Bui, T., Gruber, M., Gordan, J.D., DeBerardinis, R.J., Covello, K.L., Simon, M.C., and Thompson, C.B. (2007) 'The transcription factor HIF-1α plays a critical role in the growth factor-dependent regulation of both aerobic and anaerobic glycolysis', *Genes & Development*, 21(9), 1037–1049, available: https://doi.org/10.1101/gad.1529107.

Luo, C., Wu, G., Huang, X., Zhang, Y., Ma, Y., Huang, Y., Huang, Z., Li, H., Hou, Y., Chen, J., Li, X., and Xu, S. (2022) 'Efficacy of hematopoietic stem cell

mobilization regimens in patients with hematological malignancies: a systematic review and network meta-analysis of randomized controlled trials', *Stem Cell Research & Therapy*, 13(1), 123, available: https://doi.org/10.1186/s13287-022-02802-6.

Luo, W., Hu, H., Chang, R., Zhong, J., Knabel, M., O'Meally, R., Cole, R.N., Pandey, A., and Semenza, G.L. (2011) 'Pyruvate Kinase M2 Is a PHD3-Stimulated Coactivator for Hypoxia-Inducible Factor 1', *Cell*, 145(5), 732–744, available: https://doi.org/10.1016/j.cell.2011.03.054.

Lyratzopoulos, G., Neal, R.D., Barbiere, J.M., Rubin, G.P., and Abel, G.A. (2012) 'Variation in number of general practitioner consultations before hospital referral for cancer: findings from the 2010 National Cancer Patient Experience Survey in England', *The Lancet. Oncology*, 13(4), 353–365, available: https://doi.org/10.1016/S1470-2045(12)70041-4.

Lyu, X., Zhao, Q., Hui, J., Wang, T., Lin, M., Wang, K., Zhang, J., Shentu, J., Dalby, P.A., Zhang, H., and Liu, B. (2022) 'The global landscape of approved antibody therapies', *Antibody Therapeutics*, 5(4), 233, available: https://doi.org/10.1093/abt/tbac021.

Ma, J., Mo, Y., Tang, M., Shen, J., Qi, Y., Zhao, W., Huang, Y., Xu, Y., and Qian, C. (2021) 'Bispecific Antibodies: From Research to Clinical Application', *Frontiers in Immunology*, 12, available: https://www.frontiersin.org/articles/10.3389/fimmu.2021.626616 [accessed 13 Apr 2023].

Ma, N., He, F., Kawanokuchi, J., Wang, G., and Yamashita, T. (2022) 'Taurine and Its Anticancer Functions: In Vivo and In Vitro Study', *Advances in Experimental Medicine and Biology*, 1370, 121–128, available: https://doi.org/10.1007/978-3-030-93337-1_11.

Ma, T.-Z., Piao, Z., Jin, S.-Y., and Kwak, Y.-G. (2019) 'Differential expression of serum proteins in multiple myeloma', *Experimental and Therapeutic Medicine*, 17(1), 649–656, available: https://doi.org/10.3892/etm.2018.7010.

Ma, X., Sun, W., Shen, J., Hua, Y., Yin, F., Sun, M., and Cai, Z. (2016) 'Gelsolin promotes cell growth and invasion through the upregulation of p-AKT and p-P38 pathway in osteosarcoma', *Tumour Biology: The Journal of the International Society for Oncodevelopmental Biology and Medicine*, 37(6), 7165–7174, available: https://doi.org/10.1007/s13277-015-4565-x.

Ma, Z., Lian, J., Yang, M., Wuyang, J., Zhao, C., Chen, W., Liu, C., Zhao, Q., Lou, C., Han, J., and Zhang, Y. (2019) 'Overexpression of Arginase-1 is an indicator of poor prognosis in patients with colorectal cancer', *Pathology - Research and Practice*, 215(6), 152383, available: https://doi.org/10.1016/j.prp.2019.03.012.

Maekawa, K., Ri, M., Nakajima, M., Sekine, A., Ueda, R., Tohkin, M., Miyata, N., Saito, Y., and Iida, S. (2019) 'Serum lipidomics for exploring biomarkers of

bortezomib therapy in patients with multiple myeloma', *Cancer Science*, 110(10), 3267–3274, available: https://doi.org/10.1111/cas.14178.

Majumder, M.M. 2018. Improving Precision in Therapies for Hematological Malignancies. Doctoral Dissertation, University of Helsinki, Helsinki, Finland

Majumder, M.M., Silvennoinen, R., Anttila, P., Tamborero, D., Eldfors, S., Yadav, B., Karjalainen, R., Kuusanmäki, H., Lievonen, J., Parsons, A., Suvela, M., Jantunen, E., Porkka, K., and Heckman, C.A. (2017) 'Identification of precision treatment strategies for relapsed/refractory multiple myeloma by functional drug sensitivity testing', *Oncotarget*, 8(34), 56338–56350, available: https://doi.org/10.18632/oncotarget.17630.

Malek, M.A.Y.A., Jagannathan, S., Malek, E., Sayed, D.M., Elgammal, S.A., El-Azeem, H.G.A., Thabet, N.M., and Driscoll, J.J. (2014) 'Molecular chaperone GRP78 enhances aggresome delivery to autophagosomes to promote drug resistance in multiple myeloma', *Oncotarget*, 6(5), 3098–3110, available: https://doi.org/10.18632/oncotarget.3075.

Manasanch, E.E., Korde, N., Zingone, A., Tageja, N., Fernandez de Larrea, C., Bhutani, M., Wu, P., Roschewski, M., and Landgren, O. (2014) 'The proteasome: mechanisms of biology and markers of activity and response to treatment in multiple myeloma', *Leukemia & Lymphoma*, 55(8), 1707–1714, available: https://doi.org/10.3109/10428194.2013.828351.

Manier, S., Salem, K.Z., Park, J., Landau, D.A., Getz, G., and Ghobrial, I.M. (2017) 'Genomic complexity of multiple myeloma and its clinical implications', *Nature Reviews Clinical Oncology*, 14(2), 100–113, available: https://doi.org/10.1038/nrclinonc.2016.122.

Manni, S., Brancalion, A., Mandato, E., Tubi, L.Q., Colpo, A., Pizzi, M., Cappellesso, R., Zaffino, F., Di Maggio, S.A., Cabrelle, A., Marino, F., Zambello, R., Trentin, L., Adami, F., Gurrieri, C., Semenzato, G., and Piazza, F. (2013) 'Protein kinase CK2 inhibition down modulates the NF-κB and STAT3 survival pathways, enhances the cellular proteotoxic stress and synergistically boosts the cytotoxic effect of bortezomib on multiple myeloma and mantle cell lymphoma cells', *PloS One*, 8(9), e75280, available: https://doi.org/10.1371/journal.pone.0075280.

Manni, S., Brancalion, A., Tubi, L.Q., Colpo, A., Pavan, L., Cabrelle, A., Ave, E., Zaffino, F., Di Maira, G., Ruzzene, M., Adami, F., Zambello, R., Pitari, M.R., Tassone, P., Pinna, L.A., Gurrieri, C., Semenzato, G., and Piazza, F. (2012) 'Protein Kinase CK2 Protects Multiple Myeloma Cells from ER Stress–Induced Apoptosis and from the Cytotoxic Effect of HSP90 Inhibition through Regulation of the Unfolded Protein Response', *Clinical Cancer Research*, 18(7), 1888–1900, available: https://doi.org/10.1158/1078-0432.CCR-11-1789.

Mantovani, A., Sica, A., Sozzani, S., Allavena, P., Vecchi, A., and Locati, M. (2004) 'The chemokine system in diverse forms of macrophage activation and

polarization', *Trends in Immunology*, 25(12), 677–686, available: https://doi.org/10.1016/j.it.2004.09.015.

Marchica, V., Accardi, F., Storti, P., Mancini, C., Martella, E., Dalla Palma, B., Bolzoni, M., Todoerti, K., Marcatti, M., Schifano, C., Bonomini, S., Sammarelli, G., Neri, A., Ponzoni, M., Aversa, F., and Giuliani, N. (2017) 'Cutaneous localization in multiple myeloma in the context of bortezomib-based treatment: how do myeloma cells escape from the bone marrow to the skin?', *International Journal of Hematology*, 105(1), 104–108, available: https://doi.org/10.1007/s12185-016-2104-1.

Mariño, K.V., Cagnoni, A.J., Croci, D.O., and Rabinovich, G.A. (2023) 'Targeting galectin-driven regulatory circuits in cancer and fibrosis', *Nature Reviews Drug Discovery*, 22(4), 295–316, available: https://doi.org/10.1038/s41573-023-00636-2.

Markovic, U., Calafiore, V., Martino, E., Giubbolini, R., Parisi, M.S., Romano, A., Del Fabro, V., Di Raimondo, F., and Conticello, C. (2019) 'A rare case of multiple myeloma with intracranial extramedullary relapse: One or more myeloma clones?', *Clinical Case Reports*, 7(9), 1629–1636, available: https://doi.org/10.1002/ccr3.2292.

Markovina, S., Callander, N.S., O'Connor, S.L., Kim, J., Werndli, J.E., Raschko, M., Leith, C.P., Kahl, B.S., Kim, K., and Miyamoto, S. (2008a) 'Bortezomib-Resistant NF-κB Activity in Multiple Myeloma Cells', *Molecular cancer research : MCR*, 6(8), 1356–1364, available: https://doi.org/10.1158/1541-7786.MCR-08-0108.

Markovina, S., Callander, N.S., O'Connor, S.L., Kim, J., Werndli, J.E., Raschko, M., Leith, C.P., Kahl, B.S., Kim, K., and Miyamoto, S. (2008b) 'Bortezomib-Resistant Nuclear Factor-κB Activity in Multiple Myeloma Cells', *Molecular Cancer Research*, 6(8), 1356–1364, available: https://doi.org/10.1158/1541-7786.MCR-08-0108.

Markus, E., Trestman, S., Cohen, Y., Angel, Y., Sofer, Y., Mittelman, M., Avivi, I., Stern, N., and Izkhakov, E. (2020) 'Components of metabolic syndrome in patients with multiple myeloma and smoldering multiple myeloma', *BMC Cancer*, 20, 489, available: https://doi.org/10.1186/s12885-020-06976-1.

Marques-Mourlet, C., Di Iorio, R., Fairfield, H., and Reagan, M.R. (2023) 'Obesity and myeloma: Clinical and mechanistic contributions to disease progression', *Frontiers in Endocrinology*, 14, 1118691, available: https://doi.org/10.3389/fendo.2023.1118691.

Marrugo-Ramírez, J., Mir, M., and Samitier, J. (2018) 'Blood-Based Cancer Biomarkers in Liquid Biopsy: A Promising Non-Invasive Alternative to Tissue Biopsy', *International Journal of Molecular Sciences*, 19(10), 2877, available: https://doi.org/10.3390/ijms19102877.

Martin, T., Usmani, S.Z., Berdeja, J.G., Agha, M., Cohen, A.D., Hari, P., Avigan, D., Deol, A., Htut, M., Lesokhin, A., Munshi, N.C., O'Donnell, E., Stewart,

A.K., Schecter, J.M., Goldberg, J.D., Jackson, C.C., Yeh, T.-M., Banerjee, A., Allred, A., Zudaire, E., Deraedt, W., Olyslager, Y., Zhou, C., Pacaud, L., Madduri, D., Jakubowiak, A., Lin, Y., and Jagannath, S. (2023) 'Ciltacabtagene Autoleucel, an Anti-B-cell Maturation Antigen Chimeric Antigen Receptor T-Cell Therapy, for Relapsed/Refractory Multiple Myeloma: CARTITUDE-1 2-Year Follow-Up', *Journal of Clinical Oncology: Official Journal of the American Society of Clinical Oncology*, 41(6), 1265–1274, available: https://doi.org/10.1200/JCO.22.00842.

Mass, R.E. (1962) 'A comparison of the effect of prednisone and a placebo in the treatment of multiple myeloma', *Cancer Chemotherapy Reports*, 16, 257–259.

Mateo, G., Castellanos, M., Rasillo, A., Gutiérrez, N.C., Montalbán, Ma.A., Martín, Ma.L., Hernández, J.Ma., López-Berges, Ma.C., Montejano, L., Bladé, J., Mateos, Ma.V., Sureda, A., de la Rubia, J., Díaz-Mediavilla, J., Pandiella, A., Lahuerta, J.J., Orfao, A., and San Miguel, J.F. (2005) 'Genetic Abnormalities and Patterns of Antigenic Expression in Multiple Myeloma', *Clinical Cancer Research*, 11(10), 3661–3667, available: https://doi.org/10.1158/1078-0432.CCR-04-1489.

Mateos, M.-V., Hernández, M.-T., Giraldo, P., de la Rubia, J., de Arriba, F., Corral, L.L., Rosiñol, L., Paiva, B., Palomera, L., Bargay, J., Oriol, A., Prosper, F., López, J., Arguiñano, J.-M., Quintana, N., García, J.-L., Bladé, J., Lahuerta, J.-J., and Miguel, J.-F.S. (2016) 'Lenalidomide plus dexamethasone versus observation in patients with high-risk smouldering multiple myeloma (QuiRedex): long-term follow-up of a randomised, controlled, phase 3 trial', *The Lancet. Oncology*, 17(8), 1127–1136, available: https://doi.org/10.1016/S1470-2045(16)30124-3.

Mateos, M.-V., Rodriguez Otero, P., Koh, Y., Martinez-Lopez, J., Parmar, G., Prince, H.M., Quach, H., Ribas, P., Hermansen, E., Hungria, V.T.M., Besisik, S.K., Kim, J.S., Leleu, X., Pečeliūnas, V., Schjesvold, F., Sevindik, O.G., Lavrova, T., Dubin, F., Devisme, C., Lepine, L., Macé, S., Morisse, M., and Ghobrial, I. (2022) 'Isatuximab in Combination with Lenalidomide and Dexamethasone in Patients with High-Risk Smoldering Multiple Myeloma: Updated Safety Run-in Results from the Randomized Phase 3 Ithaca Study', *Blood*, 140(Supplement 1), 7317–7319, available: https://doi.org/10.1182/blood-2022-157302.

Matondo, M., Bousquet-Dubouch, M.-P., Gallay, N., Uttenweiler-Joseph, S., Recher, C., Payrastre, B., Manenti, S., Monsarrat, B., and Burlet-Schiltz, O. (2010) 'Proteasome inhibitor-induced apoptosis in acute myeloid leukemia: a correlation with the proteasome status', *Leukemia Research*, 34(4), 498–506, available: https://doi.org/10.1016/j.leukres.2009.09.020.

Matta, B., Battaglia, J., and Barnes, B.J. (2022) 'Detection of neutrophil extracellular traps in patient plasma: method development and validation in systemic lupus erythematosus and healthy donors that carry IRF5 genetic risk', *Frontiers in Immunology*, 13, available:

https://www.frontiersin.org/articles/10.3389/fimmu.2022.951254 [accessed 23 Nov 2023].

McAlister, G.C., Nusinow, D.P., Jedrychowski, M.P., Wühr, M., Huttlin, E.L., Erickson, B.K., Rad, R., Haas, W., and Gygi, S.P. (2014) 'MultiNotch MS3 Enables Accurate, Sensitive, and Multiplexed Detection of Differential Expression across Cancer Cell Line Proteomes', *Analytical Chemistry*, 86(14), 7150–7158, available: https://doi.org/10.1021/ac502040v.

McAvera, R., Quinn, J., Murphy, P., and Glavey, S. (2023) 'Genetic Abnormalities in Extramedullary Multiple Myeloma', *International Journal of Molecular Sciences*, 24(14), 11259, available: https://doi.org/10.3390/ijms241411259.

McCarthy, P.L., Holstein, S.A., Petrucci, M.T., Richardson, P.G., Hulin, C., Tosi, P., Bringhen, S., Musto, P., Anderson, K.C., Caillot, D., Gay, F., Moreau, P., Marit, G., Jung, S.-H., Yu, Z., Winograd, B., Knight, R.D., Palumbo, A., and Attal, M. (2017) 'Lenalidomide Maintenance After Autologous Stem-Cell Transplantation in Newly Diagnosed Multiple Myeloma: A Meta-Analysis', *Journal of Clinical Oncology*, 35(29), 3279–3289, available: https://doi.org/10.1200/JCO.2017.72.6679.

McDonald, P.C. and Dedhar, S. (2022) 'New Perspectives on the Role of Integrin-Linked Kinase (ILK) Signaling in Cancer Metastasis', *Cancers*, 14(13), 3209, available: https://doi.org/10.3390/cancers14133209.

McKenna, H.J., Stocking, K.L., Miller, R.E., Brasel, K., De Smedt, T., Maraskovsky, E., Maliszewski, C.R., Lynch, D.H., Smith, J., Pulendran, B., Roux, E.R., Teepe, M., Lyman, S.D., and Peschon, J.J. (2000) 'Mice lacking flt3 ligand have deficient hematopoiesis affecting hematopoietic progenitor cells, dendritic cells, and natural killer cells', *Blood*, 95(11), 3489–3497, available: https://doi.org/10.1182/blood.V95.11.3489.

Meads, M.B., Gatenby, R.A., and Dalton, W.S. (2009) 'Environment-mediated drug resistance: a major contributor to minimal residual disease', *Nature Reviews. Cancer*, 9(9), 665–674, available: https://doi.org/10.1038/nrc2714.

Megger, D.A., Pott, L.L., Ahrens, M., Padden, J., Bracht, T., Kuhlmann, K., Eisenacher, M., Meyer, H.E., and Sitek, B. (2014) 'Comparison of label-free and label-based strategies for proteome analysis of hepatoma cell lines', *Biochimica Et Biophysica Acta*, 1844(5), 967–976, available: https://doi.org/10.1016/j.bbapap.2013.07.017.

Mehta, J., Cavo, M., and Singhal, S. (2010) 'How I treat elderly patients with myeloma', *Blood*, 116(13), 2215–2223, available: https://doi.org/10.1182/blood-2009-10-163329.

Mele, V., Basso, C., Governa, V., Glaus Garzon, J.F., Muraro, M.G., Däster, S., Nebiker, C.A., Mechera, R., Bolli, M., Schmidt, A., Geiger, R., Spagnoli, G.C., Christoforidis, D., Majno, P.E., Borsig, L., and Iezzi, G. (2022) 'Identification of TPM2 and CNN1 as Novel Prognostic Markers in

Functionally Characterized Human Colon Cancer-Associated Stromal Cells', *Cancers*, 14(8), 2024, available: https://doi.org/10.3390/cancers14082024.

Mellby, L.D., Nyberg, A.P., Johansen, J.S., Wingren, C., Nordestgaard, B.G., Bojesen, S.E., Mitchell, B.L., Sheppard, B.C., Sears, R.C., and Borrebaeck, C.A.K. (2018) 'Serum Biomarker Signature-Based Liquid Biopsy for Diagnosis of Early-Stage Pancreatic Cancer', *Journal of Clinical Oncology*, 36(28), 2887–2894, available: https://doi.org/10.1200/JCO.2017.77.6658.

Merritt, J.L. and Chang, I.J. (1993) 'Medium-Chain Acyl-Coenzyme A Dehydrogenase Deficiency', in Adam, M.P., Mirzaa, G.M., Pagon, R.A., Wallace, S.E., Bean, L.J., Gripp, K.W. and Amemiya, A., eds., *GeneReviews*®, Seattle (WA): University of Washington, Seattle, available: http://www.ncbi.nlm.nih.gov/books/NBK1424/ [accessed 7 Jun 2023].

Mertins, P., Mani, D.R., Ruggles, K.V., Gillette, M.A., Clauser, K.R., Wang, P., Wang, X., Qiao, J.W., Cao, S., Petralia, F., Kawaler, E., Mundt, F., Krug, K., Tu, Z., Lei, J.T., Gatza, M.L., Wilkerson, M., Perou, C.M., Yellapantula, V., Huang, K., Lin, C., McLellan, M.D., Yan, P., Davies, S.R., Townsend, R.R., Skates, S.J., Wang, J., Zhang, B., Kinsinger, C.R., Mesri, M., Rodriguez, H., Ding, L., Paulovich, A.G., Fenyo, D., Ellis, M.J., and Carr, S.A. (2016) 'Proteogenomics connects somatic mutations to signaling in breast cancer', *Nature*, 534(7605), 55–62, available: https://doi.org/10.1038/nature18003.

Mesguich, C., Hulin, C., Latrabe, V., Lascaux, A., Bordenave, L., and Hindié, E. (2022) '18F-FDG PET/CT and MRI in the Management of Multiple Myeloma: A Comparative Review', *Frontiers in Nuclear Medicine*, 1, available: https://www.frontiersin.org/articles/10.3389/fnume.2021.808627 [accessed 30 Jun 2023].

Mey, U.J.M., Renner, C., and von Moos, R. (2017) 'Vemurafenib in combination with cobimetinib in relapsed and refractory extramedullary multiple myeloma harboring the BRAF V600E mutation', *Hematological Oncology*, 35(4), 890–893, available: https://doi.org/10.1002/hon.2353.

Michigami, T., Shimizu, N., Williams, P.J., Niewolna, M., Dallas, S.L., Mundy, G.R., and Yoneda, T. (2000) 'Cell–cell contact between marrow stromal cells and myeloma cells via VCAM-1 and α4β1-integrin enhances production of osteoclast-stimulating activity', *Blood*, 96(5), 1953–1960, available: https://doi.org/10.1182/blood.V96.5.1953.

Miettinen, J.J., Kumari, R., Traustadottir, G.A., Huppunen, M.-E., Sergeev, P., Majumder, M.M., Schepsky, A., Gudjonsson, T., Lievonen, J., Bazou, D., Dowling, P., O`Gorman, P., Slipicevic, A., Anttila, P., Silvennoinen, R., Nupponen, N.N., Lehmann, F., and Heckman, C.A. (2021) 'Aminopeptidase Expression in Multiple Myeloma Associates with Disease Progression and Sensitivity to Melflufen', *Cancers*, 13(7), 1527, available: https://doi.org/10.3390/cancers13071527.

Migkou, M., Kastritis, E., Roussou, M., Gkotzamanidou, M., Gavriatopoulou, M., Nikitas, N., Mparmparoussi, D., Matsouka, C., Gika, D., Terpos, E., and

Dimopoulos, M.A. (2011) ‘Short progression-free survival predicts for poor overall survival in older patients with multiple myeloma treated upfront with novel agent-based therapy’, *European Journal of Haematology*, 87(4), 323–329, available: https://doi.org/10.1111/j.1600-0609.2011.01659.x.

Mikhael, J. (2020) ‘Treatment Options for Triple-class Refractory Multiple Myeloma’, *Clinical Lymphoma Myeloma and Leukemia*, 20(1), 1–7, available: https://doi.org/10.1016/j.clml.2019.09.621.

Milne, P., Wilhelm-Benartzi, C., Grunwald, M.R., Bigley, V., Dillon, R., Freeman, S.D., Gallagher, K., Publicover, A., Pagan, S., Marr, H., Jones, G.L., Dickinson, A.M., Grech, A., Burnett, A.K., Russell, N.H., Levis, M., Knapper, S., and Collin, M. (2019) ‘Serum Flt3 ligand is a biomarker of progenitor cell mass and prognosis in acute myeloid leukemia’, *Blood Advances*, 3(20), 3052–3061, available: https://doi.org/10.1182/bloodadvances.2019000197.

Minnie, S.A. and Hill, G.R. (2021) ‘Autologous Stem Cell Transplantation for Myeloma: Cytoreduction or an Immunotherapy?’, *Frontiers in Immunology*, 12, available: https://doi.org/10.3389/fimmu.2021.651288.

Mishra, A., Perle, K.L., Kwiatkowski, S., Sullivan, L.A., Sams, G.H., Johns, J., Curphey, D.P., Wen, J., McConnell, K., Qi, J., Wong, H., Russo, G., Zhang, J., Marcucci, G., Bradner, J.E., Porcu, P., and Caligiuri, M.A. (2016) ‘Mechanism, consequences and therapeutic targeting of abnormal IL-15 signaling in cutaneous T-cell lymphoma’, *Cancer discovery*, 6(9), 986, available: https://doi.org/10.1158/2159-8290.CD-15-1297.

Misra, S., Hascall, V.C., Markwald, R.R., and Ghatak, S. (2015) ‘Interactions between Hyaluronan and Its Receptors (CD44, RHAMM) Regulate the Activities of Inflammation and Cancer’, *Frontiers in Immunology*, 6, available: https://www.frontiersin.org/articles/10.3389/fimmu.2015.00201 [accessed 6 Feb 2023].

Misselwitz, B., Goede, J.S., Pestalozzi, B.C., Schanz, U., and Seebach, J.D. (2010) ‘Hyperlipidemic myeloma: review of 53 cases’, *Annals of Hematology*, 89(6), 569–577, available: https://doi.org/10.1007/s00277-009-0849-9.

Mitsiades, N., Mitsiades, C.S., Poulaki, V., Chauhan, D., Fanourakis, G., Gu, X., Bailey, C., Joseph, M., Libermann, T.A., Treon, S.P., Munshi, N.C., Richardson, P.G., Hideshima, T., and Anderson, K.C. (2002) ‘Molecular sequelae of proteasome inhibition in human multiple myeloma cells’, *Proceedings of the National Academy of Sciences of the United States of America*, 99(22), 14374–14379, available: https://doi.org/10.1073/pnas.202445099.

Morad, H.M., Abou-Elzahab, M.M., Aref, S., and EL-Sokkary, A.M.A. (2022) ‘Diagnostic Value of 1H NMR-Based Metabolomics in Acute Lymphoblastic Leukemia, Acute Myeloid Leukemia, and Breast Cancer’, *ACS Omega*, 7(9), 8128–8140, available: https://doi.org/10.1021/acsomega.2c00083.

More, T.H., RoyChoudhury, S., Christie, J., Taunk, K., Mane, A., Santra, M.K., Chaudhury, K., and Rapole, S. (2017) 'Metabolomic alterations in invasive ductal carcinoma of breast: A comprehensive metabolomic study using tissue and serum samples', *Oncotarget*, 9(2), 2678–2696, available: https://doi.org/10.18632/oncotarget.23626.

Moreau, P., Attal, M., Caillot, D., Macro, M., Karlin, L., Garderet, L., Facon, T., Benboubker, L., Escoffre-Barbe, M., Stoppa, A.-M., Laribi, K., Hulin, C., Perrot, A., Marit, G., Eveillard, J.-R., Caillon, F., Bodet-Milin, C., Pegourie, B., Dorvaux, V., Chaleteix, C., Anderson, K., Richardson, P., Munshi, N.C., Avet-Loiseau, H., Gaultier, A., Nguyen, J.-M., Dupas, B., Frampas, E., and Kraeber-Bodere, F. (2017) 'Prospective Evaluation of Magnetic Resonance Imaging and [18F]Fluorodeoxyglucose Positron Emission Tomography-Computed Tomography at Diagnosis and Before Maintenance Therapy in Symptomatic Patients With Multiple Myeloma Included in the IFM/DFCI 2009 Trial: Results of the IMAJEM Study', *Journal of Clinical Oncology*, 35(25), 2911–2918, available: https://doi.org/10.1200/JCO.2017.72.2975.

Moreau, P., Attal, M., Hulin, C., Arnulf, B., Belhadj, K., Benboubker, L., Béné, M.C., Broijl, A., Caillon, H., Caillot, D., Corre, J., Delforge, M., Dejoie, T., Doyen, C., Facon, T., Sonntag, C., Fontan, J., Garderet, L., Jie, K.-S., Karlin, L., Kuhnowski, F., Lambert, J., Leleu, X., Lenain, P., Macro, M., Mathiot, C., Orsini-Piocelle, F., Perrot, A., Stoppa, A.-M., Donk, N.W. van de, Wuilleme, S., Zweegman, S., Kolb, B., Touzeau, C., Roussel, M., Tiab, M., Marolleau, J.-P., Meuleman, N., Vekemans, M.-C., Westerman, M., Klein, S.K., Levin, M.-D., Fermand, J.P., Escoffre-Barbe, M., Eveillard, J.-R., Garidi, R., Ahmadi, T., Zhuang, S., Chiu, C., Pei, L., Boer, C. de, Smith, E., Deraedt, W., Kampfenkel, T., Schecter, J., Vermeulen, J., Avet-Loiseau, H., and Sonneveld, P. (2019) 'Bortezomib, thalidomide, and dexamethasone with or without daratumumab before and after autologous stem-cell transplantation for newly diagnosed multiple myeloma (CASSIOPEIA): a randomised, open-label, phase 3 study', *The Lancet*, 394(10192), 29–38, available: https://doi.org/10.1016/S0140-6736(19)31240-1.

Moreau, P., Garfall, A.L., van de Donk, N.W.C.J., Nahi, H., San-Miguel, J.F., Oriol, A., Nooka, A.K., Martin, T., Rosinol, L., Chari, A., Karlin, L., Benboubker, L., Mateos, M.-V., Bahlis, N., Popat, R., Besemer, B., Martínez-López, J., Sidana, S., Delforge, M., Pei, L., Trancucci, D., Verona, R., Girgis, S., Lin, S.X.W., Olyslager, Y., Jaffe, M., Uhlar, C., Stephenson, T., Van Rampelbergh, R., Banerjee, A., Goldberg, J.D., Kobos, R., Krishnan, A., and Usmani, S.Z. (2022) 'Teclistamab in Relapsed or Refractory Multiple Myeloma', *New England Journal of Medicine*, 387(6), 495–505, available: https://doi.org/10.1056/NEJMoa2203478.

Moreaux, J., Legouffe, E., Jourdan, E., Quittet, P., Rème, T., Lugagne, C., Moine, P., Rossi, J.-F., Klein, B., and Tarte, K. (2004) 'BAFF and APRIL protect myeloma cells from apoptosis induced by interleukin 6 deprivation and dexamethasone', *Blood*, 103(8), 3148–3157, available: https://doi.org/10.1182/blood-2003-06-1984.

Morgan, G.J., Walker, B.A., and Davies, F.E. (2012) 'The genetic architecture of multiple myeloma', *Nature Reviews Cancer*, 12(5), 335–348, available: https://doi.org/10.1038/nrc3257.

Morse, M.A., Nair, S., Fernandez-Casal, M., Deng, Y., St Peter, M., Williams, R., Hobeika, A., Mosca, P., Clay, T., Cumming, R.I., Fisher, E., Clavien, P., Proia, A.D., Niedzwiecki, D., Caron, D., and Lyerly, H.K. (2000) 'Preoperative mobilization of circulating dendritic cells by Flt3 ligand administration to patients with metastatic colon cancer', *Journal of Clinical Oncology: Official Journal of the American Society of Clinical Oncology*, 18(23), 3883–3893, available: https://doi.org/10.1200/JCO.2000.18.23.3883.

Motoyama, N., Wang, F., Roth, K.A., Sawa, H., Nakayama, K., Nakayama, K., Negishi, I., Senju, S., Zhang, Q., and Fujii, S. (1995) 'Massive cell death of immature hematopoietic cells and neurons in Bcl-x-deficient mice', *Science (New York, N.Y.)*, 267(5203), 1506–1510, available: https://doi.org/10.1126/science.7878471.

Mracek, T., Stephens, N.A., Gao, D., Bao, Y., Ross, J.A., Rydén, M., Arner, P., Trayhurn, P., Fearon, K.C.H., and Bing, C. (2011) 'Enhanced ZAG production by subcutaneous adipose tissue is linked to weight loss in gastrointestinal cancer patients', *British Journal of Cancer*, 104(3), 441–447, available: https://doi.org/10.1038/sj.bjc.6606083.

Muller, G.W., Corral, L.G., Shire, M.G., Wang, H., Moreira, A., Kaplan, G., and Stirling, D.I. (1996) 'Structural modifications of thalidomide produce analogs with enhanced tumor necrosis factor inhibitory activity', *Journal of Medicinal Chemistry*, 39(17), 3238–3240, available: https://doi.org/10.1021/jm9603328.

Multiple Myeloma [online] (2020) *Irish Cancer Society*, available: https://www.cancer.ie/cancer-information-and-support/cancer-types/multiple-myeloma [accessed 22 Mar 2023].

Munshi, N.C., Anderson, L.D., Shah, N., Madduri, D., Berdeja, J., Lonial, S., Raje, N., Lin, Y., Siegel, D., Oriol, A., Moreau, P., Yakoub-Agha, I., Delforge, M., Cavo, M., Einsele, H., Goldschmidt, H., Weisel, K., Rambaldi, A., Reece, D., Petrocca, F., Massaro, M., Connarn, J.N., Kaiser, S., Patel, P., Huang, L., Campbell, T.B., Hege, K., and San-Miguel, J. (2021) 'Idecabtagene Vicleucel in Relapsed and Refractory Multiple Myeloma', *New England Journal of Medicine*, 384(8), 705–716, available: https://doi.org/10.1056/NEJMoa2024850.

Musolino, C., Allegra, A., Innao, V., Allegra, A.G., Pioggia, G., and Gangemi, S. (2017) 'Inflammatory and Anti-Inflammatory Equilibrium, Proliferative and Antiproliferative Balance: The Role of Cytokines in Multiple Myeloma', *Mediators of Inflammation*, 2017, 1852517, available: https://doi.org/10.1155/2017/1852517.

Muz, B., Kusdono, H.D., Azab, F., de la Puente, P., Federico, C., Fiala, M., Vij, R., Salama, N.N., and Azab, A.K. (2017) 'Tariquidar sensitizes multiple

myeloma cells to proteasome inhibitors via reduction of hypoxia-induced P-gp-mediated drug resistance', *Leukemia & Lymphoma*, 58(12), 2916–2925, available: https://doi.org/10.1080/10428194.2017.1319052.

Muz, B., de la Puente, P., Azab, F., Luderer, M., and Azab, A.K. (2014) 'Hypoxia promotes stem cell-like phenotype in multiple myeloma cells', *Blood Cancer Journal*, 4(12), e262–e262, available: https://doi.org/10.1038/bcj.2014.82.

Mynott, R.L. and Wallington-Beddoe, C.T. (2021) 'Inhibition of P-Glycoprotein Does Not Increase the Efficacy of Proteasome Inhibitors in Multiple Myeloma Cells', *ACS Pharmacology & Translational Science*, 4(2), 713–729, available: https://doi.org/10.1021/acsptsci.0c00200.

Nachbaur, D.M., Herold, M., Maneschg, A., and Huber, H. (1991) 'Serum levels of interleukin-6 in multiple myeloma and other hematological disorders: correlation with disease activity and other prognostic parameters', *Annals of Hematology*, 62(2–3), 54–58, available: https://doi.org/10.1007/BF01714900.

Nagakawa, O., Yamagishi, T., Fujiuchi, Y., Junicho, A., Akashi, T., Nagaike, K., and Fuse, H. (2005) 'Serum Hepatocyte Growth Factor Activator (HGFA) in Benign Prostatic Hyperplasia and Prostate Cancer', *European Urology*, 48(4), 686–690, available: https://doi.org/10.1016/j.eururo.2005.05.020.

Nagano, M., Hoshino, D., Koshikawa, N., Akizawa, T., and Seiki, M. (2012) 'Turnover of Focal Adhesions and Cancer Cell Migration', *International Journal of Cell Biology*, 2012, e310616, available: https://doi.org/10.1155/2012/310616.

Nangami, G.N., Watson, K., Parker-Johnson, K., Okereke, K.O., Sakwe, A., Thompson, P., Frimpong, N., and Ochieng, J. (2013) 'Fetuin-A (α2HS-glycoprotein) is a serum chemo-attractant that also promotes invasion of tumor cells through Matrigel', *Biochemical and Biophysical Research Communications*, 438(4), 660–665, available: https://doi.org/10.1016/j.bbrc.2013.07.125.

Nanì, S., Fumagalli, L., Sinha, U., Kamen, L., Scapini, P., and Berton, G. (2014) 'Src Family Kinases and Syk Are Required for Neutrophil Extracellular Trap Formation in Response to β-Glucan Particles', *Journal of Innate Immunity*, 7(1), 59–73, available: https://doi.org/10.1159/000365249.

Natoli, C., Perrucci, B., Perrotti, F., Falchi, L., Iacobelli, S., and Consorzio Interuniversitario Nazionale per Bio-Oncologia (CINBO) (2010) 'Tyrosine kinase inhibitors', *Current Cancer Drug Targets*, 10(5), 462–483, available: https://doi.org/10.2174/156800910791517208.

Nefedova, Y., Landowski, T.H., and Dalton, W.S. (2003) 'Bone marrow stromal-derived soluble factors and direct cell contact contribute to de novo drug resistance of myeloma cells by distinct mechanisms', *Leukemia*, 17(6), 1175–1182, available: https://doi.org/10.1038/sj.leu.2402924.

Neri, P., Maity, R., Tagoug, I., McCulloch, S., Duggan, P., Jimenez-Zepeda, V., Tay, J., Thakurta, A., and Bahlis, N. (2018) 'Immunome Single Cell Profiling

Reveals T Cell Exhaustion with Upregulation of Checkpoint Inhibitors LAG3 and Tigit on Marrow Infiltrating T Lymphocytes in Daratumumab and IMiDs Resistant Patients', *Blood*, 132(Supplement 1), 242, available: https://doi.org/10.1182/blood-2018-99-117531.

Ng, Y.L.D., Ramberger, E., Bohl, S.R., Dolnik, A., Steinebach, C., Conrad, T., Müller, S., Popp, O., Kull, M., Haji, M., Gütschow, M., Döhner, H., Walther, W., Keller, U., Bullinger, L., Mertins, P., and Krönke, J. (2022) 'Proteomic profiling reveals CDK6 upregulation as a targetable resistance mechanism for lenalidomide in multiple myeloma', *Nature Communications*, 13, 1009, available: https://doi.org/10.1038/s41467-022-28515-1.

van Nieuwenhuijzen, N., Spaan, I., Raymakers, R., and Peperzak, V. (2018) 'From MGUS to Multiple Myeloma, a Paradigm for Clonal Evolution of Premalignant Cells', *Cancer Research*, 78(10), 2449–2456, available: https://doi.org/10.1158/0008-5472.CAN-17-3115.

Nijhof, I.S., Casneuf, T., van Velzen, J., van Kessel, B., Axel, A.E., Syed, K., Groen, R.W.J., van Duin, M., Sonneveld, P., Minnema, M.C., Zweegman, S., Chiu, C., Bloem, A.C., Mutis, T., Lokhorst, H.M., Sasser, A.K., and van de Donk, N.W.C.J. (2016) 'CD38 expression and complement inhibitors affect response and resistance to daratumumab therapy in myeloma', *Blood*, 128(7), 959–970, available: https://doi.org/10.1182/blood-2016-03-703439.

Nikou, S., Arbi, M., Dimitrakopoulos, F.-I.D., Sirinian, C., Chadla, P., Pappa, I., Ntaliarda, G., Stathopoulos, G.T., Papadaki, H., Zolota, V., Lygerou, Z., Kalofonos, H.P., and Bravou, V. (2020) 'Integrin-linked kinase (ILK) regulates KRAS, IPP complex and Ras suppressor-1 (RSU1) promoting lung adenocarcinoma progression and poor survival', *Journal of Molecular Histology*, 51(4), 385–400, available: https://doi.org/10.1007/s10735-020-09888-3.

Ning, X., Wei, X., Chen, B., Li, Z., Zheng, Z., Yi, Z., Feng, R., Wei, Y., and Liu, Q. (2021) 'CD44 Expression in Different Plasma Cell Diseases', *Blood*, 138, 4754, available: https://doi.org/10.1182/blood-2021-146780.

Ntafoulis, I., Kleijn, A., Ju, J., Jimenez-Cowell, K., Fabro, F., Klein, M., Chi Yen, R.T., Balvers, R.K., Li, Y., Stubbs, A.P., Kers, T.V., Kros, J.M., Lawler, S.E., Beerepoot, L.V., Kremer, A., Idbaih, A., Verreault, M., Byrne, A.T., O'Farrell, A.C., Connor, K., Biswas, A., Salvucci, M., Prehn, J.H.M., Lambrechts, D., Dilcan, G., Lodi, F., Arijs, I., van den Bent, M.J., Dirven, C.M.F., Leenstra, S., and Lamfers, M.L.M. (2023) 'Ex vivo drug sensitivity screening predicts response to temozolomide in glioblastoma patients and identifies candidate biomarkers', *British Journal of Cancer*, 129(8), 1327–1338, available: https://doi.org/10.1038/s41416-023-02402-y.

Obara, Y., Labudda, K., Dillon, T.J., and Stork, P.J.S. (2004) 'PKA phosphorylation of Src mediates Rap1 activation in NGF and cAMP signaling in PC12 cells', *Journal of Cell Science*, 117(25), 6085–6094, available: https://doi.org/10.1242/jcs.01527.

Oben, B., Froyen, G., Maclachlan, K.H., Leongamornlert, D., Abascal, F., Zheng-Lin, B., Yellapantula, V., Derkach, A., Geerdens, E., Diamond, B.T., Arijs, I., Maes, B., Vanhees, K., Hultcrantz, M., Manasanch, E.E., Kazandjian, D., Lesokhin, A., Dogan, A., Zhang, Y., Mikulasova, A., Walker, B., Morgan, G., Campbell, P.J., Landgren, O., Rummens, J.-L., Bolli, N., and Maura, F. (2021) 'Whole-genome sequencing reveals progressive versus stable myeloma precursor conditions as two distinct entities', *Nature Communications*, 12, 1861, available: https://doi.org/10.1038/s41467-021-22140-0.

Obeng, E.A., Carlson, L.M., Gutman, D.M., Harrington, W.J., Lee, K.P., and Boise, L.H. (2006) 'Proteasome inhibitors induce a terminal unfolded protein response in multiple myeloma cells', *Blood*, 107(12), 4907–4916, available: https://doi.org/10.1182/blood-2005-08-3531.

Oerlemans, R., Franke, N.E., Assaraf, Y.G., Cloos, J., van Zantwijk, I., Berkers, C.R., Scheffer, G.L., Debipersad, K., Vojtekova, K., Lemos, C., van der Heijden, J.W., Ylstra, B., Peters, G.J., Kaspers, G.L., Dijkmans, B.A.C., Scheper, R.J., and Jansen, G. (2008) 'Molecular basis of bortezomib resistance: proteasome subunit β5 (PSMB5) gene mutation and overexpression of PSMB5 protein', *Blood*, 112(6), 2489–2499, available: https://doi.org/10.1182/blood-2007-08-104950.

Ohkuma, R., Yada, E., Ishikawa, S., Komura, D., Kubota, Y., Hamada, K., Horiike, A., Ishiguro, T., Hirasawa, Y., Ariizumi, H., Shida, M., Watanabe, M., Onoue, R., Ando, K., Tsurutani, J., Yoshimura, K., Sasada, T., Aoki, T., Murakami, M., Norose, T., Ohike, N., Takimoto, M., Kobayashi, S., Tsunoda, T., and Wada, S. (2020) 'High expression levels of polymeric immunoglobulin receptor are correlated with chemoresistance and poor prognosis in pancreatic cancer', *Oncology Reports*, 44(1), 252–262, available: https://doi.org/10.3892/or.2020.7610.

Okada, T., Hawley, R.G., Kodaka, M., and Okuno, H. (1999) 'Significance of VLA-4–VCAM-1 interaction and CD44 for transendothelial invasion in a bone marrow metastatic myeloma model', *Clinical & Experimental Metastasis*, 17(7), 623–629, available: https://doi.org/10.1023/A:1006715504719.

Okahara, H., Yagita, H., Miyake, K., and Okumura, K. (1994) 'Involvement of very late activation antigen 4 (VLA-4) and vascular cell adhesion molecule 1 (VCAM-1) in tumor necrosis factor alpha enhancement of experimental metastasis', *Cancer Research*, 54(12), 3233–3236.

Okikawa, Y., Sakai, A., Takimoto, Y., Noda, M., Imagawa, J., Katayama, Y., Kuroda, Y., Okita, H., Fujimura, K., and Kimuraa, A. (2004) 'Progressive Myeloma after Thalidomide Therapy in a Patient with Immature Phenotype of Myeloma (Plasma) Cells', *International Journal of Hematology*, 79(4), 364–368, available: https://doi.org/10.1532/IJH97.04005.

Oklu, R., Sheth, R.A., Wong, K.H.K., Jahromi, A.H., and Albadawi, H. (2017) 'Neutrophil extracellular traps are increased in cancer patients but does not associate with venous thrombosis', *Cardiovascular Diagnosis and Therapy*,

7(Suppl 3), S140-S14S149, available: https://doi.org/10.21037/cdt.2017.08.01.

Okugawa, Y., Miki, C., Toiyama, Y., Koike, Y., Yokoe, T., Saigusa, S., Tanaka, K., Inoue, Y., and Kusunoki, M. (2010) 'Soluble VCAM-1 and its relation to disease progression in colorectal carcinoma', *Experimental and Therapeutic Medicine*, 1(3), 463–469, available: https://doi.org/10.3892/etm_00000072.

Omenn, G.S. (2004) 'Advancement of biomarker discovery and validation through the HUPO plasma proteome project', *Disease Markers*, 20(3), 131–134, available: https://doi.org/10.1155/2004/579363.

Ong, S.-E. and Mann, M. (2006) 'A practical recipe for stable isotope labeling by amino acids in cell culture (SILAC)', *Nature Protocols*, 1(6), 2650–2660, available: https://doi.org/10.1038/nprot.2006.427.

Osborn, L., Hession, C., Tizard, R., Vassallo, C., Luhowskyj, S., Chi-Rosso, G., and Lobb, R. (1989) 'Direct expression cloning of vascular cell adhesion molecule 1, a cytokine-induced endothelial protein that binds to lymphocytes', *Cell*, 59(6), 1203–1211, available: https://doi.org/10.1016/0092-8674(89)90775-7.

Ou, F.-S., Michiels, S., Shyr, Y., Adjei, A.A., and Oberg, A.L. (2021) 'Biomarker Discovery and Validation: Statistical Considerations', *Journal of Thoracic Oncology*, 16(4), 537–545, available: https://doi.org/10.1016/j.jtho.2021.01.1616.

Owen, K.A., Qiu, D., Alves, J., Schumacher, A.M., Kilpatrick, L.M., Li, J., Harris, J.L., and Ellis, V. (2010) 'Pericellular activation of hepatocyte growth factor by the transmembrane serine proteases matriptase and hepsin, but not by the membrane-associated protease uPA', *The Biochemical Journal*, 426(2), 219–228, available: https://doi.org/10.1042/BJ20091448.

Padala, S.A., Barsouk, A., Barsouk, A., Rawla, P., Vakiti, A., Kolhe, R., Kota, V., and Ajebo, G.H. (2021) 'Epidemiology, Staging, and Management of Multiple Myeloma', *Medical Sciences*, 9(1), 3, available: https://doi.org/10.3390/medsci9010003.

Palomba, A., Abbondio, M., Fiorito, G., Uzzau, S., Pagnozzi, D., and Tanca, A. (2021) 'Comparative Evaluation of MaxQuant and Proteome Discoverer MS1-Based Protein Quantification Tools', *Journal of Proteome Research*, 20(7), 3497–3507, available: https://doi.org/10.1021/acs.jproteome.1c00143.

Palstrøm, N.B., Matthiesen, R., Rasmussen, L.M., and Beck, H.C. (2022) 'Recent Developments in Clinical Plasma Proteomics—Applied to Cardiovascular Research', *Biomedicines*, 10(1), 162, available: https://doi.org/10.3390/biomedicines10010162.

Palumbo, A., Avet-Loiseau, H., Oliva, S., Lokhorst, H.M., Goldschmidt, H., Rosinol, L., Richardson, P., Caltagirone, S., Lahuerta, J.J., Facon, T., Bringhen, S., Gay, F., Attal, M., Passera, R., Spencer, A., Offidani, M., Kumar, S., Musto, P., Lonial, S., Petrucci, M.T., Orlowski, R.Z., Zamagni, E., Morgan, G.,

Dimopoulos, M.A., Durie, B.G.M., Anderson, K.C., Sonneveld, P., San Miguel, J., Cavo, M., Rajkumar, S.V., and Moreau, P. (2015) 'Revised International Staging System for Multiple Myeloma: A Report From International Myeloma Working Group', *Journal of Clinical Oncology: Official Journal of the American Society of Clinical Oncology*, 33(26), 2863–2869, available: https://doi.org/10.1200/JCO.2015.61.2267.

Pan, D. and Richter, J. (2022) 'Where We Stand With Precision Therapeutics in Myeloma: Prosperity, Promises, and Pipedreams', *Frontiers in Oncology*, 11, 819127, available: https://doi.org/10.3389/fonc.2021.819127.

Panaroni, C., Fulzele, K., Mori, T., Siu, K.T., Onyewadume, C., Maebius, A., and Raje, N. (2022) 'Multiple myeloma cells induce lipolysis in adipocytes and uptake fatty acids through fatty acid transporter proteins', *Blood*, 139(6), 876–888, available: https://doi.org/10.1182/blood.2021013832.

Parada, C.A., Osbun, J.W., Busald, T., Karasozen, Y., Kaur, S., Shi, M., Barber, J., Adidharma, W., Cimino, P.J., Pan, C., Gonzalez-Cuyar, L.F., Rostomily, R., Born, D.E., Zhang, J., and Ferreira, M., Jr (2020) 'Phosphoproteomic and Kinomic Signature of Clinically Aggressive Grade I (1.5) Meningiomas Reveals RB1 Signaling as a Novel Mediator and Biomarker', *Clinical Cancer Research*, 26(1), 193–205, available: https://doi.org/10.1158/1078-0432.CCR-18-0641.

Parr, C., Watkins, G., Mansel, R.E., and Jiang, W.G. (2004) 'The Hepatocyte Growth Factor Regulatory Factors in Human Breast Cancer', *Clinical Cancer Research*, 10(1), 202–211, available: https://doi.org/10.1158/1078-0432.CCR-0553-3.

Parrondo, R.D., Ailawadhi, S., Sher, T., Chanan-Khan, A.A., and Roy, V. (2020) 'Autologous Stem-Cell Transplantation for Multiple Myeloma in the Era of Novel Therapies', *JCO Oncology Practice*, 16(2), 56–66, available: https://doi.org/10.1200/JOP.19.00335.

Pavlova, N.N., Zhu, J., and Thompson, C.B. (2022) 'The hallmarks of cancer metabolism: Still emerging', *Cell Metabolism*, 34(3), 355–377, available: https://doi.org/10.1016/j.cmet.2022.01.007.

Pawlyn, C., Melchor, L., Murison, A., Wardell, C.P., Brioli, A., Boyle, E.M., Kaiser, M.F., Walker, B.A., Begum, D.B., Dahir, N.B., Proszek, P., Gregory, W.M., Drayson, M.T., Jackson, G.H., Ross, F.M., Davies, F.E., and Morgan, G.J. (2015) 'Coexistent hyperdiploidy does not abrogate poor prognosis in myeloma with adverse cytogenetics and may precede IGH translocations', *Blood*, 125(5), 831–840, available: https://doi.org/10.1182/blood-2014-07-584268.

Pearse, R.N., Sordillo, E.M., Yaccoby, S., Wong, B.R., Liau, D.F., Colman, N., Michaeli, J., Epstein, J., and Choi, Y. (2001) 'Multiple myeloma disrupts the TRANCE/ osteoprotegerin cytokine axis to trigger bone destruction and promote tumor progression', *Proceedings of the National Academy of*

Sciences of the United States of America, 98(20), 11581–11586, available: https://doi.org/10.1073/pnas.201394498.

Pemovska, T., Kontro, M., Yadav, B., Edgren, H., Eldfors, S., Szwajda, A., Almusa, H., Bespalov, M.M., Ellonen, P., Elonen, E., Gjertsen, B.T., Karjalainen, R., Kulesskiy, E., Lagström, S., Lehto, A., Lepistö, M., Lundán, T., Majumder, M.M., Marti, J.M.L., Mattila, P., Murumägi, A., Mustjoki, S., Palva, A., Parsons, A., Pirttinen, T., Rämet, M.E., Suvela, M., Turunen, L., Västrik, I., Wolf, M., Knowles, J., Aittokallio, T., Heckman, C.A., Porkka, K., Kallioniemi, O., and Wennerberg, K. (2013) 'Individualized systems medicine strategy to tailor treatments for patients with chemorefractory acute myeloid leukemia', *Cancer Discovery*, 3(12), 1416–1429, available: https://doi.org/10.1158/2159-8290.CD-13-0350.

Petrera, A., von Toerne, C., Behler, J., Huth, C., Thorand, B., Hilgendorff, A., and Hauck, S.M. (2021) 'Multiplatform Approach for Plasma Proteomics: Complementarity of Olink Proximity Extension Assay Technology to Mass Spectrometry-Based Protein Profiling', *Journal of Proteome Research*, 20(1), 751–762, available: https://doi.org/10.1021/acs.jproteome.0c00641.

Peverelli, E., Giardino, E., Mangili, F., Treppiedi, D., Catalano, R., Ferrante, E., Sala, E., Locatelli, M., Lania, A.G., Arosio, M., Spada, A., and Mantovani, G. (2018) 'cAMP/PKA-induced filamin A (FLNA) phosphorylation inhibits SST2 signal transduction in GH-secreting pituitary tumor cells', *Cancer Letters*, 435, 101–109, available: https://doi.org/10.1016/j.canlet.2018.08.002.

Piazza, F.A., Ruzzene, M., Gurrieri, C., Montini, B., Bonanni, L., Chioetto, G., Di Maira, G., Barbon, F., Cabrelle, A., Zambello, R., Adami, F., Trentin, L., Pinna, L.A., and Semenzato, G. (2006) 'Multiple myeloma cell survival relies on high activity of protein kinase CK2', *Blood*, 108(5), 1698–1707, available: https://doi.org/10.1182/blood-2005-11-013672.

Pinna, L.A. and Ruzzene, M. (1996) 'How do protein kinases recognize their substrates?', *Biochimica et Biophysica Acta (BBA) - Molecular Cell Research*, 1314(3), 191–225, available: https://doi.org/10.1016/S0167-4889(96)00083-3.

Pinto, V., Bergantim, R., Caires, H.R., Seca, H., Guimarães, J.E., and Vasconcelos, M.H. (2020) 'Multiple Myeloma: Available Therapies and Causes of Drug Resistance', *Cancers*, 12(2), 407, available: https://doi.org/10.3390/cancers12020407.

Plubell, D.L., Wilmarth, P.A., Zhao, Y., Fenton, A.M., Minnier, J., Reddy, A.P., Klimek, J., Yang, X., David, L.L., and Pamir, N. (2017) 'Extended Multiplexing of Tandem Mass Tags (TMT) Labeling Reveals Age and High Fat Diet Specific Proteome Changes in Mouse Epididymal Adipose Tissue *', *Molecular & Cellular Proteomics*, 16(5), 873–890, available: https://doi.org/10.1074/mcp.M116.065524.

Pol, J.G., Le Naour, J., and Kroemer, G. (2020) 'FLT3LG - a biomarker reflecting clinical responses to the immunogenic cell death inducer oxaliplatin', *Oncoimmunology*, 9(1), 1755214, available: https://doi.org/10.1080/2162402X.2020.1755214.

Pour, L., Sevcikova, S., Greslikova, H., Kupska, R., Majkova, P., Zahradova, L., Sandecka, V., Adam, Z., Krejci, M., Kuglik, P., and Hajek, R. (2014) 'Soft-tissue extramedullary multiple myeloma prognosis is significantly worse in comparison to bone-related extramedullary relapse', *Haematologica*, 99(2), 360–364, available: https://doi.org/10.3324/haematol.2013.094409.

Pravdic, Z., Vukovic, N.S., Gasic, V., Marjanovic, I., Karan-Djurasevic, T., Pavlovic, S., and Tosic, N. (2023) 'The influence of BCL2, BAX, and ABCB1 gene expression on prognosis of adult de novo acute myeloid leukemia with normal karyotype patients', *Radiology and Oncology*, 57(2), 239–248, available: https://doi.org/10.2478/raon-2023-0017.

Puchades-Carrasco, L., Lecumberri, R., Martínez-López, J., Lahuerta, J.-J., Mateos, M.-V., Prósper, F., San-Miguel, J.F., and Pineda-Lucena, A. (2013) 'Multiple Myeloma Patients Have a Specific Serum Metabolomic Profile That Changes after Achieving Complete Remission', *Clinical Cancer Research*, 19(17), 4770–4779, available: https://doi.org/10.1158/1078-0432.CCR-12-2917.

Puthier, D., Bataille, R., and Amiot, M. (1999) 'IL-6 up-regulates mcl-1 in human myeloma cells through JAK / STAT rather than ras / MAP kinase pathway', *European Journal of Immunology*, 29(12), 3945–3950, available: https://doi.org/10.1002/(SICI)1521-4141(199912)29:12<3945::AID-IMMU3945>3.0.CO;2-O.

Qazilbash, M.H., Saliba, R.M., Ahmed, B., Parikh, G., Mendoza, F., Ashraf, N., Hosing, C., Flosser, T., Weber, D.M., Wang, M., Couriel, D.R., Popat, U., Kebriaei, P., Alousi, A.M., Anderlini, P., Naeem, R.C., Champlin, R.E., and Giralt, S.A. (2007) 'Deletion of the Short Arm of Chromosome 1 (del 1p) is a Strong Predictor of Poor Outcome in Myeloma Patients Undergoing an Autotransplant', *Biology of Blood and Marrow Transplantation*, 13(9), 1066–1072, available: https://doi.org/10.1016/j.bbmt.2007.05.014.

Qi, C.-F., Zhou, J.X., Lee, C.H., Naghashfar, Z., Xiang, S., Kovalchuk, A.L., Fredrickson, T.N., Hartley, J.W., Roopenian, D.C., Davidson, W.F., Janz, S., and Morse, H.C. (2007) 'Anaplastic, Plasmablastic, and Plasmacytic Plasmacytomas of Mice: Relationships to Human Plasma Cell Neoplasms and Late-Stage Differentiation of Normal B Cells', *Cancer Research*, 67(6), 2439–2447, available: https://doi.org/10.1158/0008-5472.CAN-06-1561.

Qiu, S., Cai, Y., Yao, H., Lin, C., Xie, Y., Tang, S., and Zhang, A. (2023) 'Small molecule metabolites: discovery of biomarkers and therapeutic targets', *Signal Transduction and Targeted Therapy*, 8(1), 1–37, available: https://doi.org/10.1038/s41392-023-01399-3.

Qu, X., Chen, L., Qiu, H., Lu, H., Wu, H., Qiu, H., Liu, P., Guo, R., and Li, J. (2015) 'Extramedullary Manifestation in Multiple Myeloma Bears High Incidence of

Poor Cytogenetic Aberration and Novel Agents Resistance', *BioMed Research International*, 2015, e787809, available: https://doi.org/10.1155/2015/787809.

Qu, Y., Hao, C., Xu, J., Cheng, Z., Wang, W., and Liu, H. (2017) 'ILK promotes cell proliferation in breast cancer cells by activating the PI3K/Akt pathway', *Molecular Medicine Reports*, 16(4), 5036–5042, available: https://doi.org/10.3892/mmr.2017.7180.

Rahman, S. and Mansour, M.R. (2019) 'The role of noncoding mutations in blood cancers', *Disease Models & Mechanisms*, 12(11), dmm041988, available: https://doi.org/10.1242/dmm.041988.

Rajkumar, S.V. (2018) 'Multiple myeloma: 2018 update on diagnosis, risk-stratification, and management', *American Journal of Hematology*, 93(8), 1091–1110, available: https://doi.org/10.1002/ajh.25117.

Rajkumar, S.V. (2020) 'Multiple myeloma: 2020 update on diagnosis, risk-stratification and management', *American Journal of Hematology*, 95(5), 548–567, available: https://doi.org/10.1002/ajh.25791.

Rajkumar, S.V. (2022) 'Multiple Myeloma: 2022 update on Diagnosis, Risk-stratification and Management', *American journal of hematology*, 97(8), 1086–1107, available: https://doi.org/10.1002/ajh.26590.

Rajkumar, S.V. and Kumar, S. (2020) 'Multiple myeloma current treatment algorithms', *Blood Cancer Journal*, 10(9), 1–10, available: https://doi.org/10.1038/s41408-020-00359-2.

Rajpal, R., Dowling, P., Meiller, J., Clarke, C., Murphy, W.G., O'Connor, R., Kell, M., Mitsiades, C., Richardson, P., Anderson, K.C., Clynes, M., and O'Gorman, P. (2011) 'A novel panel of protein biomarkers for predicting response to thalidomide-based therapy in newly diagnosed multiple myeloma patients', *PROTEOMICS*, 11(8), 1391–1402, available: https://doi.org/10.1002/pmic.201000471.

Ramji, K., Grzywa, T.M., Sosnowska, A., Paterek, A., Okninska, M., Pilch, Z., Barankiewicz, J., Garbicz, F., Borg, K., Bany-Laszewicz, U., Zerrouqi, A., Pyrzynska, B., Rodziewicz-Lurzynska, A., Papiernik, D., Sklepkiewicz, P., Kedzierska, H., Staruch, A., Sadowski, R., Ciepiela, O., Lech-Maranda, E., Juszczynski, P., Mackiewicz, U., Maczewski, M., Nowis, D., and Golab, J. (2022) 'Targeting arginase-1 exerts antitumor effects in multiple myeloma and mitigates bortezomib-induced cardiotoxicity', *Scientific Reports*, 12(1), 19660, available: https://doi.org/10.1038/s41598-022-24137-1.

Rampa, C., Tian, E., Våtsveen, T.K., Buene, G., Slørdahl, T.S., Børset, M., Waage, A., and Sundan, A. (2014) 'Identification of the source of elevated hepatocyte growth factor levels in multiple myeloma patients', *Biomarker Research*, 2(1), 8, available: https://doi.org/10.1186/2050-7771-2-8.

Ramsenthaler, C., Osborne, T.R., Gao, W., Siegert, R.J., Edmonds, P.M., Schey, S.A., and Higginson, I.J. (2016) 'The impact of disease-related symptoms and

palliative care concerns on health-related quality of life in multiple myeloma: a multi-centre study', *BMC Cancer*, 16(1), 427, available: https://doi.org/10.1186/s12885-016-2410-2.

Rasmussen, T., Kuehl, M., Lodahl, M., Johnsen, H.E., and Dahl, I.M.S. (2005) 'Possible roles for activating RAS mutations in the MGUS to MM transition and in the intramedullary to extramedullary transition in some plasma cell tumors', *Blood*, 105(1), 317–323, available: https://doi.org/10.1182/blood-2004-03-0833.

Rauch, F., Husseini, A., Roughley, P., Glorieux, F.H., and Moffatt, P. (2012) 'Lack of Circulating Pigment Epithelium-Derived Factor Is a Marker of Osteogenesis Imperfecta Type VI', *The Journal of Clinical Endocrinology & Metabolism*, 97(8), E1550–E1556, available: https://doi.org/10.1210/jc.2012-1827.

Raudvere, U., Kolberg, L., Kuzmin, I., Arak, T., Adler, P., Peterson, H., and Vilo, J. (2019) 'g:Profiler: a web server for functional enrichment analysis and conversions of gene lists (2019 update)', *Nucleic Acids Research*, 47(W1), W191–W198, available: https://doi.org/10.1093/nar/gkz369.

Reimand, J., Isserlin, R., Voisin, V., Kucera, M., Tannus-Lopes, C., Rostamianfar, A., Wadi, L., Meyer, M., Wong, J., Xu, C., Merico, D., and Bader, G.D. (2019) 'Pathway enrichment analysis and visualization of omics data using g:Profiler, GSEA, Cytoscape and EnrichmentMap', *Nature Protocols*, 14(2), 482–517, available: https://doi.org/10.1038/s41596-018-0103-9.

Ren, D., Zhao, J., Sun, Y., Li, D., Meng, Z., Wang, B., Fan, P., Liu, Z., Jin, X., and Wu, H. (2019) 'Overexpressed ITGA2 promotes malignant tumor aggression by up-regulating PD-L1 expression through the activation of the STAT3 signaling pathway', *Journal of Experimental & Clinical Cancer Research*, 38(1), 485, available: https://doi.org/10.1186/s13046-019-1496-1.

Resmini, G., Rizzo, S., Franchin, C., Zanin, R., Penzo, C., Pegoraro, S., Ciani, Y., Piazza, S., Arrigoni, G., Sgarra, R., and Manfioletti, G. (2017) 'HMGA1 regulates the Plasminogen activation system in the secretome of breast cancer cells', *Scientific Reports*, 7, 11768, available: https://doi.org/10.1038/s41598-017-11409-4.

Revel, M., Daugan, M.V., Sautés-Fridman, C., Fridman, W.H., and Roumenina, L.T. (2020) 'Complement System: Promoter or Suppressor of Cancer Progression?', *Antibodies*, 9(4), 57, available: https://doi.org/10.3390/antib9040057.

Rhee, S.H., Han, I., Lee, M.R., Cho, H.S., Oh, J.H., and Kim, H.-S. (2013) 'Role of integrin-linked kinase in osteosarcoma progression', *Journal of Orthopaedic Research: Official Publication of the Orthopaedic Research Society*, 31(10), 1668–1675, available: https://doi.org/10.1002/jor.22409.

Rice, G.E. and Bevilacqua, M.P. (1989) 'An inducible endothelial cell surface glycoprotein mediates melanoma adhesion', *Science (New York, N.Y.)*, 246(4935), 1303–1306, available: https://doi.org/10.1126/science.2588007.

Richardson, P.G., Hideshima, T., and Anderson, K.C. (2003) 'Bortezomib (PS-341): A Novel, First-in-Class Proteasome Inhibitor for the Treatment of Multiple Myeloma and Other Cancers', *Cancer Control*, 10(5), 361–369, available: https://doi.org/10.1177/107327480301000502.

Richardson, P.G., Oriol, A., Larocca, A., Bladé, J., Cavo, M., Rodriguez-Otero, P., Leleu, X., Nadeem, O., Hiemenz, J.W., Hassoun, H., Touzeau, C., Alegre, A., Paner, A., Maisel, C., Mazumder, A., Raptis, A., Moreb, J.S., Anderson, K.C., Laubach, J.P., Thuresson, S., Thuresson, M., Byrne, C., Harmenberg, J., Bakker, N.A., and Mateos, M.-V. (2021) 'Melflufen and Dexamethasone in Heavily Pretreated Relapsed and Refractory Multiple Myeloma', *Journal of Clinical Oncology*, 39(7), 757–767, available: https://doi.org/10.1200/JCO.20.02259.

Rimsza, L.M., Campbell, K., Dalton, W.S., Salmon, S., Willcox, G., and Grogan, T.M. (1999) 'The major vault protein (MVP), a new multidrug resistance associated protein, is frequently expressed in multiple myeloma', *Leukemia & Lymphoma*, 34(3–4), 315–324, available: https://doi.org/10.3109/10428199909050956.

Rivera-Pérez, J., Monter-Vera, M. del R., Barrientos-Alvarado, C., Toscano-Garibay, J.D., Cuesta-Mejías, T., and Flores-Estrada, J. (2018) 'Evaluation of VEGF and PEDF in prostate cancer: A preliminary study in serum and biopsies', *Oncology Letters*, 15(1), 1072–1078, available: https://doi.org/10.3892/ol.2017.7374.

Roberts, L.D., Souza, A.L., Gerszten, R.E., and Clish, C.B. (2012) 'Targeted Metabolomics', *Current Protocols in Molecular Biology*, CHAPTER, Unit30.2, available: https://doi.org/10.1002/0471142727.mb3002s98.

Robinson, T.O. and Schluns, K.S. (2017) 'The potential and promise of IL-15 in immuno-oncogenic therapies', *Immunology letters*, 190, 159–168, available: https://doi.org/10.1016/j.imlet.2017.08.010.

Roccaro, A.M., Mishima, Y., Sacco, A., Moschetta, M., Tai, Y.-T., Shi, J., Zhang, Y., Reagan, M.R., Huynh, D., Kawano, Y., Sahin, I., Chiarini, M., Manier, S., Cea, M., Aljawai, Y., Glavey, S., Morgan, E., Pan, C., Michor, F., Cardarelli, P., Kuhne, M., and Ghobrial, I.M. (2015) 'CXCR4 Regulates Extra-Medullary Myeloma through Epithelial-Mesenchymal-Transition-like Transcriptional Activation', *Cell Reports*, 12(4), 622–635, available: https://doi.org/10.1016/j.celrep.2015.06.059.

Romano, A., Parrinello, N.L., La Cava, P., Tibullo, D., Giallongo, C., Camiolo, G., Puglisi, F., Parisi, M., Pirosa, M.C., Martino, E., Conticello, C., Palumbo, G.A., and Di Raimondo, F. (2018) 'PMN-MDSC and arginase are increased in myeloma and may contribute to resistance to therapy', *Expert Review of*

Molecular Diagnostics, 18(7), 675–683, available: https://doi.org/10.1080/14737159.2018.1470929.

Romano, A., Parrinello, N.L., Vetro, C., Tibullo, D., Giallongo, C., La Cava, P., Chiarenza, A., Motta, G., Caruso, A.L., Villari, L., Tripodo, C., Cosentino, S., Ippolito, M., Consoli, U., Gallamini, A., Pileri, S., and Di Raimondo, F. (2016) 'The prognostic value of the myeloid-mediated immunosuppression marker Arginase-1 in classic Hodgkin lymphoma', *Oncotarget*, 7(41), 67333–67346, available: https://doi.org/10.18632/oncotarget.12024.

Roodman, G.D. (2009) 'Pathogenesis of myeloma bone disease', *Leukemia*, 23(3), 435–441, available: https://doi.org/10.1038/leu.2008.336.

Roothans, D., Smits, E., Lion, E., Tel, J., and Anguille, S. (2013) 'CD56 marks human dendritic cell subsets with cytotoxic potential', *Oncoimmunology*, 2(2), e23037, available: https://doi.org/10.4161/onci.23037.

Rosenquist, R., Bernard, E., Erkers, T., Scott, D.W., Itzykson, R., Rousselot, P., Soulier, J., Hutchings, M., Östling, P., Cavelier, L., Fioretos, T., and Smedby, K.E. (2023) 'Novel precision medicine approaches and treatment strategies in hematological malignancies', *Journal of Internal Medicine*, 294(4), 413–436, available: https://doi.org/10.1111/joim.13697.

Rosiñol, L., Beksac, M., Zamagni, E., Van de Donk, N.W.C.J., Anderson, K.C., Badros, A., Caers, J., Cavo, M., Dimopoulos, M.-A., Dispenzieri, A., Einsele, H., Engelhardt, M., Fernández de Larrea, C., Gahrton, G., Gay, F., Hájek, R., Hungria, V., Jurczyszyn, A., Kröger, N., Kyle, R.A., Leal da Costa, F., Leleu, X., Lentzsch, S., Mateos, M.V., Merlini, G., Mohty, M., Moreau, P., Rasche, L., Reece, D., Sezer, O., Sonneveld, P., Usmani, S.Z., Vanderkerken, K., Vesole, D.H., Waage, A., Zweegman, S., Richardson, P.G., and Bladé, J. (2021) 'Expert review on soft-tissue plasmacytomas in multiple myeloma: definition, disease assessment and treatment considerations', *British Journal of Haematology*, 194(3), 496–507, available: https://doi.org/10.1111/bjh.17338.

Rosiñol, L., Fernández de Larrea, C., and Bladé, J. (2014) 'Extramedullary Myeloma Spread Triggered by Surgical Procedures: An Emerging Entity?', *Acta Haematologica*, 132(1), 36–38, available: https://doi.org/10.1159/000354833.

Roth, K., Oehme, L., Zehentmeier, S., Zhang, Y., Niesner, R., and Hauser, A.E. (2014) 'Tracking plasma cell differentiation and survival', *Cytometry Part A*, 85(1), 15–24, available: https://doi.org/10.1002/cyto.a.22355.

Russell, S.T., Zimmerman, T.P., Domin, B.A., and Tisdale, M.J. (2004) 'Induction of lipolysis in vitro and loss of body fat in vivo by zinc-alpha2-glycoprotein', *Biochimica Et Biophysica Acta*, 1636(1), 59–68, available: https://doi.org/10.1016/j.bbalip.2003.12.004.

Ryu, D., Kim, S.J., Hong, Y., Jo, A., Kim, N., Kim, H.-J., Lee, H.-O., Kim, K., and Park, W.-Y. (2020) 'Alterations in the Transcriptional Programs of Myeloma Cells and the Microenvironment during Extramedullary Progression Affect

Proliferation and Immune Evasion', *Clinical Cancer Research: An Official Journal of the American Association for Cancer Research*, 26(4), 935–944, available: https://doi.org/10.1158/1078-0432.CCR-19-0694.

Sagawa, N., Fujita, H., Banno, Y., Nozawa, Y., Katoh, H., and Kuzumaki, N. (2003) 'Gelsolin suppresses tumorigenicity through inhibiting PKC activation in a human lung cancer cell line, PC10', *British Journal of Cancer*, 88(4), 606–612, available: https://doi.org/10.1038/sj.bjc.6600739.

Sahara, N., Takeshita, A., Shigeno, K., Fujisawa, S., Takeshita, K., Naito, K., Ihara, M., Ono, T., Tamashima, S., Nara, K., Ohnishi, K., and Ohno, R. (2002) 'Clinicopathological and prognostic characteristics of CD56-negative multiple myeloma', *British Journal of Haematology*, 117(4), 882–885, available: https://doi.org/10.1046/j.1365-2141.2002.03513.x.

Salman, A.S., S.Saleh, E., and S.Abass, M. (2020) 'Estimation of Beta Two Microglobulins, Fetuin-A, Resistin Serum Level in Iraqi Multiple Myeloma Patients', *Iraqi Journal of Pharmaceutical Sciences(P-ISSN 1683 - 3597 E-ISSN 2521 - 3512)*, 29(2), 80–87, available: https://doi.org/10.31351/vol29iss2pp80-87.

Salomon, D.R., Crisa, L., Mojcik, C.F., Ishii, J.K., Klier, G., and Shevach, E.M. (1997) 'Vascular Cell Adhesion Molecule-1 Is Expressed by Cortical Thymic Epithelial Cells and Mediates Thymocyte Adhesion. Implications for the Function of α4β1 (VLA4) Integrin in T-Cell Development', *Blood*, 89(7), 2461–2471, available: https://doi.org/10.1182/blood.V89.7.2461.

Salomon-Perzyński, A., Jamroziak, K., and Głodkowska-Mrówka, E. (2021) 'Clonal Evolution of Multiple Myeloma—Clinical and Diagnostic Implications', *Diagnostics*, 11(9), 1534, available: https://doi.org/10.3390/diagnostics11091534.

Saltarella, I., Desantis, V., Melaccio, A., Solimando, A.G., Lamanuzzi, A., Ria, R., Storlazzi, C.T., Mariggiò, M.A., Vacca, A., and Frassanito, M.A. (2020) 'Mechanisms of Resistance to Anti-CD38 Daratumumab in Multiple Myeloma', *Cells*, 9(1), 167, available: https://doi.org/10.3390/cells9010167.

Sánchez-Lanzas, R., Kalampalika, F., and Ganuza, M. (2022) 'Diversity in the bone marrow niche: Classic and novel strategies to uncover niche composition', *British Journal of Haematology*, 199(5), 647–664, available: https://doi.org/10.1111/bjh.18355.

Sanfilippo, K.M., Keller, J., Gage, B.F., Luo, S., Wang, T.-F., Moskowitz, G., Gumbel, J., Blue, B., O'Brian, K., and Carson, K.R. (2016) 'Statins Are Associated With Reduced Mortality in Multiple Myeloma', *Journal of Clinical Oncology*, 34(33), 4008–4014, available: https://doi.org/10.1200/JCO.2016.68.3482.

San-Miguel, J.F., Hungria, V.T.M., Yoon, S.-S., Beksac, M., Dimopoulos, M.A., Elghandour, A., Jedrzejczak, W.W., Günther, A., Nakorn, T.N., Siritanaratkul, N., Schlossman, R.L., Hou, J., Moreau, P., Lonial, S., Lee,

J.H., Einsele, H., Sopala, M., Bengoudifa, B.-R., Binlich, F., and Richardson, P.G. (2016) ‘Overall survival of patients with relapsed multiple myeloma treated with panobinostat or placebo plus bortezomib and dexamethasone (the PANORAMA 1 trial): a randomised, placebo-controlled, phase 3 trial’, *The Lancet Haematology*, 3(11), e506–e515, available: https://doi.org/10.1016/S2352-3026(16)30147-8.

Sanz-Rodríguez, F., Ruiz-Velasco, N., Pascual-Salcedo, D., and Teixidó, J. (1999) ‘Characterization of VLA-4-dependent myeloma cell adhesion to fibronectin and VCAM-1’, *British journal of haematology*, 107(4), 825–834, available: https://doi.org/10.1046/j.1365-2141.1999.01762.x.

Scherr, A.-L., Mock, A., Gdynia, G., Schmitt, N., Heilig, C.E., Korell, F., Rhadakrishnan, P., Hoffmeister, P., Metzeler, K.H., Schulze-Osthoff, K., Illert, A.L., Boerries, M., Trojan, J., Waidmann, O., Falkenhorst, J., Siveke, J., Jost, P.J., Bitzer, M., Malek, N.P., Vecchione, L., Jelas, I., Brors, B., Glimm, H., Stenzinger, A., Grekova, S.P., Gehrig, T., Schulze-Bergkamen, H., Jäger, D., Schirmacher, P., Heikenwalder, M., Goeppert, B., Schneider, M., Fröhling, S., and Köhler, B.C. (2020) ‘Identification of BCL-XL as highly active survival factor and promising therapeutic target in colorectal cancer’, *Cell Death & Disease*, 11(10), 875, available: https://doi.org/10.1038/s41419-020-03092-7.

Schinke, C., Boyle, E.M., Ashby, C., Wang, Y., Lyzogubov, V., Wardell, C., Qu, P., Hoering, A., Deshpande, S., Ryan, K., Thanendrarajan, S., Mohan, M., Yarlagadda, N., Khan, M., Choudhury, S.R., Zangari, M., van Rhee, F., Davies, F., Barlogie, B., Morgan, G., and Walker, B.A. (2020) ‘Genomic analysis of primary plasma cell leukemia reveals complex structural alterations and high-risk mutational patterns’, *Blood Cancer Journal*, 10(6), 1–9, available: https://doi.org/10.1038/s41408-020-0336-z.

Schmidt, D.R., Patel, R., Kirsch, D.G., Lewis, C.A., Vander Heiden, M.G., and Locasale, J.W. (2021) ‘Metabolomics in cancer research and emerging applications in clinical oncology’, *CA: A Cancer Journal for Clinicians*, 71(4), 333–358, available: https://doi.org/10.3322/caac.21670.

Seidel, C., Børset, M., Turesson, I., Abildgaard, N., Sundan, A., and e Nordic Myeloma Study Group, A.W. for th (1998) ‘Elevated Serum Concentrations of Hepatocyte Growth Factor in Patients With Multiple Myeloma’, *Blood*, 91(3), 806–812, available: https://doi.org/10.1182/blood.V91.3.806.

Seki, R., Yamagishi, S., Matsui, T., Yoshida, T., Torimura, T., Ueno, T., Sata, M., and Okamura, T. (2013) ‘Pigment epithelium-derived factor (PEDF) inhibits survival and proliferation of VEGF-exposed multiple myeloma cells through its anti-oxidative properties’, *Biochemical and Biophysical Research Communications*, 431(4), 693–697, available: https://doi.org/10.1016/j.bbrc.2013.01.057.

Setayesh, S.M., Ndacayisaba, L.J., Rappard, K.E., Hennes, V., Rueda, L.Y.M., Tang, G., Lin, P., Orlowski, R.Z., Symer, D.E., Manasanch, E.E., Shishido, S.N., and Kuhn, P. (2023) ‘Targeted single-cell proteomic analysis identifies new

liquid biopsy biomarkers associated with multiple myeloma', *npj Precision Oncology*, 7(1), 1–10, available: https://doi.org/10.1038/s41698-023-00446-0.

Settino, M., Arbitrio, M., Scionti, F., Caracciolo, D., Di Martino, M.T., Tagliaferri, P., Tassone, P., and Cannataro, M. (2020) 'MMRF-CoMMpass Data Integration and Analysis for Identifying Prognostic Markers', *Computational Science – ICCS 2020*, 12139, 564–571, available: https://doi.org/10.1007/978-3-030-50420-5_42.

Sezer, O., Heider, U., Zavrski, I., Kühne, C.A., and Hofbauer, L.C. (2003) 'RANK ligand and osteoprotegerin in myeloma bone disease', *Blood*, 101(6), 2094–2098, available: https://doi.org/10.1182/blood-2002-09-2684.

Shah, R.V., Steffen, L.M., Nayor, M., Reis, J.P., Jacobs, D.R., Allen, N.B., Lloyd-Jones, D., Meyer, K., Cole, J., Piaggi, P., Vasan, R.S., Clish, C.B., and Murthy, V.L. (2023) 'Dietary metabolic signatures and cardiometabolic risk', *European Heart Journal*, 44(7), 557–569, available: https://doi.org/10.1093/eurheartj/ehac446.

Shah, U.A., Whiting, K., Devlin, S., Ershler, R., Kanapuru, B., Lee, D.J., Tahri, S., Gwise, T., Rustad, E.H., Mailankody, S., Lesokhin, A.M., Kazandjian, D., Maura, F., Auclair, D., Birmann, B.M., Usmani, S.Z., Gormley, N., Marinac, C.R., and Landgren, O. (2023) 'Extreme body mass index and survival in newly diagnosed multiple myeloma patients', *Blood Cancer Journal*, 13(1), 1–5, available: https://doi.org/10.1038/s41408-022-00782-7.

Shain, K.H. and Dalton, W.S. (2001) 'Cell Adhesion Is a Key Determinant in de Novo Multidrug Resistance (MDR): New Targets for the Prevention of Acquired MDR', *Molecular Cancer Therapeutics*, 1(1), 69–78.

Shami-Shah, A., Norman, M., and Walt, D.R. (2023) 'Ultrasensitive Protein Detection Technologies for Extracellular Vesicle Measurements', *Molecular & Cellular Proteomics*, 22(6), 100557, available: https://doi.org/10.1016/j.mcpro.2023.100557.

Sharma, M., Zhang, M.-J., Zhong, X., Abidi, M.H., Akpek, G., Bacher, U., Callander, N.S., Dispenzieri, A., Freytes, C.O., Fung, H.C., Gale, R.P., Gasparetto, C., Gibson, J., Holmberg, L.A., Kindwall-Keller, T.L., Klumpp, T.R., Krishnan, A.Y., Landau, H.J., Lazarus, H.M., Lonial, S., Maiolino, A., Marks, D.I., Mehta, P., Med, J.R.M., Nishihori, T., Olsson, R., Ramanathan, M., Roy, V., Savani, B.N., Schouten, H.C., Scott, E., Tay, J., To, L.B., Vesole, D.H., Vogl, D.T., and Hari, P. (2014) 'Older Patients with Myeloma Derive Similar Benefit from Autologous Transplantation', *Biology of blood and marrow transplantation : journal of the American Society for Blood and Marrow Transplantation*, 20(11), 1796–1803, available: https://doi.org/10.1016/j.bbmt.2014.07.013.

Shekarriz, R., Janbabaei, G., and Kenari, S.A. (2018) 'Prognostic Value of IL-10 and Its Relationship with Disease Stage in Iranian Patients with Multiple

Myeloma', *Asian Pacific Journal of Cancer Prevention : APJCP*, 19(1), 27–32, available: https://doi.org/10.22034/APJCP.2018.19.1.27.

Shi, W., Lv, L., Liu, N., Wang, H., Wang, Y., Zhu, W., Liu, Z., Zhu, J., and Lu, H. (2023) 'A novel anti-PD-L1/IL-15 immunocytokine overcomes resistance to PD-L1 blockade and elicits potent antitumor immunity', *Molecular Therapy: The Journal of the American Society of Gene Therapy*, 31(1), 66–77, available: https://doi.org/10.1016/j.ymthe.2022.08.016.

Shimokihara, K., Kawahara, T., Chiba, S., Takamoto, D., Yao, M., and Uemura, H. (2018) 'Extramedullary plasmacytoma of the testis: A case report', *Urology Case Reports*, 16, 101–103, available: https://doi.org/10.1016/j.eucr.2017.11.007.

Shimomura, T., Kondo, J., Ochiai, M., Naka, D., Miyazawa, K., Morimoto, Y., and Kitamura, N. (1993) 'Activation of the zymogen of hepatocyte growth factor activator by thrombin', *The Journal of Biological Chemistry*, 268(30), 22927–22932.

Shirkoohi, R., Fujita, H., Darmanin, S., and Takimoto, M. (2012) 'Gelsolin induces promonocytic leukemia differentiation accompanied by upregulation of p21CIP1', *Asian Pacific journal of cancer prevention: APJCP*, 13(9), 4827–4834, available: https://doi.org/10.7314/apjcp.2012.13.9.4827.

Short, K.D., Rajkumar, S.V., Larson, D., Buadi, F., Hayman, S., Dispenzieri, A., Gertz, M., Kumar, S., Mikhael, J., Roy, V., Kyle, R.A., and Lacy, M.Q. (2011) 'Incidence of extramedullary disease in patients with multiple myeloma in the era of novel therapy, and the activity of pomalidomide on extramedullary myeloma', *Leukemia*, 25(6), 906–908, available: https://doi.org/10.1038/leu.2011.29.

Sidiqi, M.H., Al Saleh, A.S., Kumar, S.K., Leung, N., Jevremovic, D., Muchtar, E., Gonsalves, W.I., Kourelis, T.V., Warsame, R., Buadi, F.K., Lacy, M.Q., Kyle, R.A., Go, R., Hobbs, M., Dispenzieri, A., Dingli, D., Hayman, S.R., Gertz, M.A., Rajkumar, S.V., and Kapoor, P. (2021) 'Venetoclax for the treatment of multiple myeloma: Outcomes outside of clinical trials', *American Journal of Hematology*, 96(9), 1131–1136, available: https://doi.org/10.1002/ajh.26269.

Siegel, R.L., Miller, K.D., and Jemal, A. (2019) 'Cancer statistics, 2019', *CA: A Cancer Journal for Clinicians*, 69(1), 7–34, available: https://doi.org/10.3322/caac.21551.

Silva, H.C., Garcao, F., Coutinho, E.C., De Oliveira, C.F., and Regateiro, F.J. (2006) 'Soluble VCAM-1 and E-selectin in breast cancer: relationship with staging and with the detection of circulating cancer cells', *Neoplasma*, 53(6), 538–543.

Singer, J.W., Al-Fayoumi, S., Taylor, J., Velichko, S., and O'Mahony, A. (2019) 'Comparative phenotypic profiling of the JAK2 inhibitors ruxolitinib, fedratinib, momelotinib, and pacritinib reveals distinct mechanistic

signatures', *PLOS ONE*, 14(9), e0222944, available: https://doi.org/10.1371/journal.pone.0222944.

Singh, R.J.R., Mason, J.C., Lidington, E.A., Edwards, D.R., Nuttall, R.K., Khokha, R., Knauper, V., Murphy, G., and Gavrilovic, J. (2005) 'Cytokine stimulated vascular cell adhesion molecule-1 (VCAM-1) ectodomain release is regulated by TIMP-3', *Cardiovascular Research*, 67(1), 39–49, available: https://doi.org/10.1016/j.cardiores.2005.02.020.

Singhal, S., Mehta, J., Desikan, R., Ayers, D., Roberson, P., Eddlemon, P., Munshi, N., Anaissie, E., Wilson, C., Dhodapkar, M., Zeldis, J., Siegel, D., Crowley, J., and Barlogie, B. (1999) 'Antitumor Activity of Thalidomide in Refractory Multiple Myeloma', *New England Journal of Medicine*, 341(21), 1565–1571, available: https://doi.org/10.1056/NEJM199911183412102.

Sinha, A. and Mann, M. (2020) 'A beginner's guide to mass spectrometry–based proteomics', *The Biochemist*, 42(5), 64–69, available: https://doi.org/10.1042/BIO20200057.

Sinitcyn, P., Rudolph, J.D., and Cox, J. (2018) 'Computational Methods for Understanding Mass Spectrometry–Based Shotgun Proteomics Data', *Annual Review of Biomedical Data Science*, 1(1), 207–234, available: https://doi.org/10.1146/annurev-biodatasci-080917-013516.

Smith, J.G. and Gerszten, R.E. (2017) 'Emerging Affinity-Based Proteomic Technologies for Large-Scale Plasma Profiling in Cardiovascular Disease', *Circulation*, 135(17), 1651–1664, available: https://doi.org/10.1161/CIRCULATIONAHA.116.025446.

Smith, L., Carmichael, J., Cook, G., Shinkins, B., and Neal, R.D. (2022) 'Diagnosing myeloma in general practice: how might earlier diagnosis be achieved?', *The British Journal of General Practice*, 72(723), 462–463, available: https://doi.org/10.3399/bjgp22X720737.

Sobsey, C.A., Ibrahim, S., Richard, V.R., Gaspar, V., Mitsa, G., Lacasse, V., Zahedi, R.P., Batist, G., and Borchers, C.H. (2020) 'Targeted and Untargeted Proteomics Approaches in Biomarker Development', *PROTEOMICS*, 20(9), 1900029, available: https://doi.org/10.1002/pmic.201900029.

Sökeland, G. and Schumacher, U. (2019) 'The functional role of integrins during intra- and extravasation within the metastatic cascade', *Molecular Cancer*, 18(1), 12, available: https://doi.org/10.1186/s12943-018-0937-3.

Solimando, A.G., Malerba, E., Leone, P., Prete, M., Terragna, C., Cavo, M., and Racanelli, V. (2022) 'Drug resistance in multiple myeloma: Soldiers and weapons in the bone marrow niche', *Frontiers in Oncology*, 12, available: https://www.frontiersin.org/articles/10.3389/fonc.2022.973836 [accessed 17 Jun 2023].

Song, J., Sokoll, L.J., Zhang, Z., and Chan, D.W. (2023) 'VCAM-1 complements CA-125 in detecting recurrent ovarian cancer', *Clinical Proteomics*, 20(1), 25, available: https://doi.org/10.1186/s12014-023-09414-z.

Spinner, M.A., Aleshin, A., Santaguida, M.T., Schaffert, S.A., Zehnder, J.L., Patterson, A.S., Gekas, C., Heiser, D., and Greenberg, P.L. (2020) 'Ex vivo drug screening defines novel drug sensitivity patterns for informing personalized therapy in myeloid neoplasms', *Blood Advances*, 4(12), 2768–2778, available: https://doi.org/10.1182/bloodadvances.2020001934.

Sriskandarajah, P., De Haven Brandon, A., MacLeod, K., Carragher, N.O., Kirkin, V., Kaiser, M., and Whittaker, S.R. (2020) 'Combined targeting of MEK and the glucocorticoid receptor for the treatment of RAS-mutant multiple myeloma', *BMC Cancer*, 20(1), 269, available: https://doi.org/10.1186/s12885-020-06735-2.

Standal, T., Seidel, C., Hjertner, Ø., Plesner, T., Sanderson, R.D., Waage, A., Borset, M., and Sundan, A. (2002) 'Osteoprotegerin is bound, internalized, and degraded by multiple myeloma cells', *Blood*, 100(8), 3002–3007, available: https://doi.org/10.1182/blood-2002-04-1190.

Steen, H., Jebanathirajah, J.A., Rush, J., Morrice, N., and Kirschner, M.W. (2006) 'Phosphorylation Analysis by Mass Spectrometry: Myths, Facts, and the Consequences for Qualitative and Quantitative Measurements*', *Molecular & Cellular Proteomics*, 5(1), 172–181, available: https://doi.org/10.1074/mcp.M500135-MCP200.

Steinbrunn, T., Siegmund, D., Andrulis, M., Grella, E., Kortüm, M., Einsele, H., Wajant, H., Bargou, R.C., and Stühmer, T. (2012) 'Integrin-linked kinase is dispensable for multiple myeloma cell survival', *Leukemia Research*, 36(9), 1165–1171, available: https://doi.org/10.1016/j.leukres.2012.05.005.

Steiner, N., Hajek, R., Sevcikova, S., Borjan, B., Jöhrer, K., Göbel, G., Untergasser, G., and Gunsilius, E. (2017) 'High levels of FLT3-ligand in bone marrow and peripheral blood of patients with advanced multiple myeloma', *PLoS ONE*, 12(7), e0181487, available: https://doi.org/10.1371/journal.pone.0181487.

Steiner, N., Jöhrer, K., Plewan, S., Brunner-Véber, A., Göbel, G., Nachbaur, D., Wolf, D., Gunsilius, E., and Untergasser, G. (2020) 'The FMS like Tyrosine Kinase 3 (FLT3) Is Overexpressed in a Subgroup of Multiple Myeloma Patients with Inferior Prognosis', *Cancers*, 12(9), available: https://doi.org/10.3390/cancers12092341.

Steiner, N., Müller, U., Hajek, R., Sevcikova, S., Borjan, B., Jöhrer, K., Göbel, G., Pircher, A., and Gunsilius, E. (2018) 'The metabolomic plasma profile of myeloma patients is considerably different from healthy subjects and reveals potential new therapeutic targets', *PLoS ONE*, 13(8), e0202045, available: https://doi.org/10.1371/journal.pone.0202045.

Stessman, H. a. F., Mansoor, A., Zhan, F., Janz, S., Linden, M.A., Baughn, L.B., and Van Ness, B. (2013) 'Reduced CXCR4 expression is associated with extramedullary disease in a mouse model of myeloma and predicts poor survival in multiple myeloma patients treated with bortezomib', *Leukemia*, 27(10), 2075–2077, available: https://doi.org/10.1038/leu.2013.148.

Stork, M., Sevcikova, S., Minarik, J., Krhovska, P., Radocha, J., Pospisilova, L., Brozova, L., Jarkovsky, J., Spicka, I., Straub, J., Pavlicek, P., Jungova, A., Jelinek, T., Sandecka, V., Maisnar, V., Hajek, R., and Pour, L. (2022) 'Identification of patients at high risk of secondary extramedullary multiple myeloma development', *British Journal of Haematology*, 196(4), 954–962, available: https://doi.org/10.1111/bjh.17925.

Storti, P., Marchica, V., Airoldi, I., Donofrio, G., Fiorini, E., Ferri, V., Guasco, D., Todoerti, K., Silbermann, R., Anderson, J.L., Zhao, W., Agnelli, L., Bolzoni, M., Martella, E., Mancini, C., Campanini, N., Noonan, D.M., Petronini, P.G., Neri, A., Aversa, F., Roodman, G.D., and Giuliani, N. (2016) 'Galectin-1 suppression delineates a new strategy to inhibit myeloma-induced angiogenesis and tumoral growth in vivo', *Leukemia*, 30(12), 2351–2363, available: https://doi.org/10.1038/leu.2016.137.

Storti, P., Marchica, V., and Giuliani, N. (2017) 'Role of Galectins in Multiple Myeloma', *International Journal of Molecular Sciences*, 18(12), 2740, available: https://doi.org/10.3390/ijms18122740.

Strachan, D.C., Gu, C.J., Kita, R., Anderson, E.K., Richardson, M.A., Yam, G., Pimm, G., Roselli, J., Schweickert, A., Terrell, M., Rashid, R., Gonzalez, A.K., Oviedo, H.H., Alozie, M.C., Ilangovan, T., Marcogliese, A.N., Tada, H., Santaguida, M.T., and Stevens, A.M. (2022) 'Ex Vivo Drug Sensitivity Correlates with Clinical Response and Supports Personalized Therapy in Pediatric AML', *Cancers*, 14(24), 6240, available: https://doi.org/10.3390/cancers14246240.

Strich, J., Chertow, D., Ramos-Benitez, M., and Warner, S. (2023) '1129: SYK INHIBITION ABROGATES NEUTROPHIL HYPERACTIVATION IN RESPONSE TO LIPOPOLYSACCHARIDES', *Critical Care Medicine*, 51(1), 562, available: https://doi.org/10.1097/01.ccm.0000910252.25085.7b.

Strich, J.R., Ramos-Benitez, M.J., Randazzo, D., Stein, S.R., Babyak, A., Davey, R.T., Suffredini, A.F., Childs, R.W., and Chertow, D.S. (2020) 'Fostamatinib Inhibits Neutrophils Extracellular Traps Induced by COVID-19 Patient Plasma: A Potential Therapeutic', *The Journal of Infectious Diseases*, 223(6), 981–984, available: https://doi.org/10.1093/infdis/jiaa789.

Sudalagunta, P., Silva, M.C., Canevarolo, R.R., Alugubelli, R.R., DeAvila, G., Tungesvik, A., Perez, L., Gatenby, R., Gillies, R., Baz, R., Meads, M.B., Shain, K.H., and Silva, A.S. (2020) 'A pharmacodynamic model of clinical synergy in multiple myeloma', *EBioMedicine*, 54, 102716, available: https://doi.org/10.1016/j.ebiom.2020.102716.

Sugie, S., Mukai, S., Yamasaki, K., Kamibeppu, T., Tsukino, H., and Kamoto, T. (2016) 'Plasma macrophage-stimulating protein and hepatocyte growth factor levels are associated with prostate cancer progression', *Human Cell*, 29(1), 22–29, available: https://doi.org/10.1007/s13577-015-0123-5.

Sun, Z., Ji, J., Li, Y., Cui, Y., Fan, L., Li, J., and Qu, X. (2023) 'Identification of evolutionary mechanisms of myelomatous effusion by single-cell RNA

sequencing', *Blood Advances*, 7(15), 4148–4159, available: https://doi.org/10.1182/bloodadvances.2022009477.

Tai, Y.-T., Cho, S.-F., and Anderson, K.C. (2018) 'Osteoclast Immunosuppressive Effects in Multiple Myeloma: Role of Programmed Cell Death Ligand 1', *Frontiers in Immunology*, 9, 1822, available: https://doi.org/10.3389/fimmu.2018.01822.

Tai, Y.-T., Dillon, M., Song, W., Leiba, M., Li, X.-F., Burger, P., Lee, A.I., Podar, K., Hideshima, T., Rice, A.G., van Abbema, A., Jesaitis, L., Caras, I., Law, D., Weller, E., Xie, W., Richardson, P., Munshi, N.C., Mathiot, C., Avet-Loiseau, H., Afar, D.E.H., and Anderson, K.C. (2008) 'Anti-CS1 humanized monoclonal antibody HuLuc63 inhibits myeloma cell adhesion and induces antibody-dependent cellular cytotoxicity in the bone marrow milieu', *Blood*, 112(4), 1329–1337, available: https://doi.org/10.1182/blood-2007-08-107292.

Takahashi, R., Ijichi, H., Sano, M., Miyabayashi, K., Mohri, D., Kim, J., Kimura, G., Nakatsuka, T., Fujiwara, H., Yamamoto, K., Kudo, Y., Tanaka, Y., Tateishi, K., Nakai, Y., Morishita, Y., Soma, K., Takeda, N., Moses, H.L., Isayama, H., and Koike, K. (2020) 'Soluble VCAM-1 promotes gemcitabine resistance via macrophage infiltration and predicts therapeutic response in pancreatic cancer', *Scientific Reports*, 10(1), 21194, available: https://doi.org/10.1038/s41598-020-78320-3.

Takai, K., Hara, J., Matsumoto, K., Hosoi, G., Osugi, Y., Tawa, A., Okada, S., and Nakamura, T. (1997) 'Hepatocyte growth factor is constitutively produced by human bone marrow stromal cells and indirectly promotes hematopoiesis', *Blood*, 89(5), 1560–1565.

Tam, Z.Y., Ng, S.P., Tan, L.Q., Lin, C.-H., Rothenbacher, D., Klenk, J., and Boehm, B.O. (2017) 'Metabolite profiling in identifying metabolic biomarkers in older people with late-onset type 2 diabetes mellitus', *Scientific Reports*, 7, 4392, available: https://doi.org/10.1038/s41598-017-01735-y.

Tan, C., Cruet-Hennequart, S., Troussard, A., Fazli, L., Costello, P., Sutton, K., Wheeler, J., Gleave, M., Sanghera, J., and Dedhar, S. (2004) 'Regulation of tumor angiogenesis by integrin-linked kinase (ILK)', *Cancer Cell*, 5(1), 79–90, available: https://doi.org/10.1016/s1535-6108(03)00281-2.

Tang, D.-R., Li, C.-L., Xu, K.-P., Wu, Q.-Q., Chen, Q.-Y., Lv, J.-J., Ji, J., Zang, B., Chen, C., Gu, B., and Zhao, J.-Q. (2020) 'Pigment Epithelium-Derived Factor Promotes the Growth and Migration of Human Esophageal Squamous Cell Carcinoma', *Frontiers in Oncology*, 9, 1520, available: https://doi.org/10.3389/fonc.2019.01520.

Tang, K., Yu, Y., Zhu, L., Xu, P., Chen, J., Ma, J., Zhang, H., Fang, H., Sun, W., Zhou, L., Wei, K., Li, F., Lv, J., Xie, J., Liu, Y., and Huang, B. (2019) 'Hypoxia-reprogrammed tricarboxylic acid cycle promotes the growth of human breast tumorigenic cells', *Oncogene*, 38(44), 6970–6984, available: https://doi.org/10.1038/s41388-019-0932-1.

Tas, F., Karabulut, S., Serilmez, M., Ciftci, R., and Duranyildiz, D. (2014) 'Clinical significance of serum epithelial cell adhesion molecule (EPCAM) and vascular cell adhesion molecule-1 (VCAM-1) levels in patients with epithelial ovarian cancer', *Tumour Biology: The Journal of the International Society for Oncodevelopmental Biology and Medicine*, 35(4), 3095–3102, available: https://doi.org/10.1007/s13277-013-1401-z.

Taya, M., Garcia-Hernandez, M. de la L., Rangel-Moreno, J., Minor, B., Gibbons, E., and Hammes, S.R. (2020) 'Neutrophil elastase from myeloid cells promotes TSC2-null tumor growth', *Endocrine-Related Cancer*, 27(4), 261–274, available: https://doi.org/10.1530/ERC-19-0431.

Terpos, E., Migkou, M., Christoulas, D., Gavriatopoulou, M., Eleutherakis-Papaiakovou, E., Kanellias, N., Iakovaki, M., Panagiotidis, I., Ziogas, D.C., Fotiou, D., Kastritis, E., and Dimopoulos, M.A. (2016) 'Increased circulating VCAM-1 correlates with advanced disease and poor survival in patients with multiple myeloma: reduction by post-bortezomib and lenalidomide treatment', *Blood Cancer Journal*, 6(5), e428, available: https://doi.org/10.1038/bcj.2016.37.

Thålin, C., Aguilera, K., Hall, N.W., Marunde, M.R., Burg, J.M., Rosell, A., Daleskog, M., Månsson, M., Hisada, Y., Meiners, M.J., Sun, Z.-W., Whelihan, M.F., Cheek, M.A., Howard, S.A., Saxena-Beem, S., Noubouossie, D.F., Key, N.S., Sheikh, S.Z., Keogh, M.-C., Cowles, M.W., Lundström, S., Mackman, N., Wallén, H., and Johnstone, A.L. (2020) 'Quantification of citrullinated histones: Development of an improved assay to reliably quantify nucleosomal H3Cit in human plasma', *Journal of Thrombosis and Haemostasis*, 18(10), 2732–2743, available: https://doi.org/10.1111/jth.15003.

Thålin, C., Daleskog, M., Göransson, S.P., Schatzberg, D., Lasselin, J., Laska, A.-C., Kallner, A., Helleday, T., Wallén, H., and Demers, M. (2017) 'Validation of an enzyme-linked immunosorbent assay for the quantification of citrullinated histone H3 as a marker for neutrophil extracellular traps in human plasma', *Immunologic Research*, 65(3), 706–712, available: https://doi.org/10.1007/s12026-017-8905-3.

Thijssen, R., Tian, L., Anderson, M.A., Flensburg, C., Jarratt, A., Garnham, A.L., Jabbari, J.S., Peng, H., Lew, T.E., Teh, C.E., Gouil, Q., Georgiou, A., Tan, T., Djajawi, T.M., Tam, C.S., Seymour, J.F., Blombery, P., Gray, D.H.D., Majewski, I.J., Ritchie, M.E., Roberts, A.W., and Huang, D.C.S. (2022) 'Single-cell multiomics reveal the scale of multilayered adaptations enabling CLL relapse during venetoclax therapy', *Blood*, 140(20), 2127–2141, available: https://doi.org/10.1182/blood.2022016040.

Tiedemann, R.E., Gonzalez-Paz, N., Kyle, R.A., Santana-Davila, R., Price-Troska, T., Van Wier, S.A., Chng, W.J., Ketterling, R.P., Gertz, M.A., Henderson, K., Greipp, P.R., Dispenzieri, A., Lacy, M.Q., Rajkumar, S.V., Bergsagel, P.L., Stewart, A.K., and Fonseca, R. (2008) 'Genetic aberrations and survival in plasma cell leukemia', *Leukemia*, 22(5), 1044–1052, available: https://doi.org/10.1038/leu.2008.4.

Tierney, C., Bazou, D., Lê, G., Dowling, P., and O'Gorman, P. (2021) 'Saliva-omics in plasma cell disorders- Proof of concept and potential as a non-invasive tool for monitoring disease burden', *Journal of Proteomics*, 231, 104015, available: https://doi.org/10.1016/j.jprot.2020.104015.

Tierney, C., Bazou, D., Majumder, M.M., Anttila, P., Silvennoinen, R., Heckman, C.A., Dowling, P., and O'Gorman, P. (2021) 'Next generation proteomics with drug sensitivity screening identifies sub-clones informing therapeutic and drug development strategies for multiple myeloma patients', *Scientific Reports*, 11(1), 12866, available: https://doi.org/10.1038/s41598-021-90149-y.

Ting, K.R., Henry, M., Meiller, J., Larkin, A., Clynes, M., Meleady, P., Bazou, D., Dowling, P., and O'Gorman, P. (2017) 'Novel panel of protein biomarkers to predict response to bortezomib-containing induction regimens in multiple myeloma patients', *BBA Clinical*, 8, 28–34, available: https://doi.org/10.1016/j.bbacli.2017.05.003.

Ting, L., Rad, R., Gygi, S.P., and Haas, W. (2011) 'MS3 eliminates ratio distortion in isobaric labeling-based multiplexed quantitative proteomics', *Nature methods*, 8(11), 937–940, available: https://doi.org/10.1038/nmeth.1714.

Tirado-Vélez, J.M., Joumady, I., Sáez-Benito, A., Cózar-Castellano, I., and Perdomo, G. (2012) 'Inhibition of Fatty Acid Metabolism Reduces Human Myeloma Cells Proliferation', *PLoS ONE*, 7(9), e46484, available: https://doi.org/10.1371/journal.pone.0046484.

Tjin, E.P.M., Derksen, P.W.B., Kataoka, H., Spaargaren, M., and Pals, S.T. (2004) 'Multiple myeloma cells catalyze hepatocyte growth factor (HGF) activation by secreting the serine protease HGF-activator', *Blood*, 104(7), 2172–2175, available: https://doi.org/10.1182/blood-2003-12-4386.

Tokuhira, M., Hosaka, S., Volin, M.V., Haines III, G.K., Katschke Jr., K.J., Kim, S., and Koch, A.E. (2000) 'Soluble vascular cell adhesion molecule 1 mediation of monocyte chemotaxis in rheumatoid arthritis', *Arthritis & Rheumatism*, 43(5), 1122–1133, available: https://doi.org/10.1002/1529-0131(200005)43:5<1122::AID-ANR23>3.0.CO;2-7.

Tolstikov, V., Moser, A.J., Sarangarajan, R., Narain, N.R., and Kiebish, M.A. (2020) 'Current Status of Metabolomic Biomarker Discovery: Impact of Study Design and Demographic Characteristics', *Metabolites*, 10(6), 224, available: https://doi.org/10.3390/metabo10060224.

Tomás-Pérez, S., Oto, J., Aghababyan, C., Herranz, R., Cuadros-Lozano, A., González-Cantó, E., Mc Cormack, B., Arrés, J., Castaño, M., Cana, F., Martínez-Fernández, L., Santonja, N., Ramírez, R., Herreros-Pomares, A., Cañete-Mota, S., Llueca, A., Marí-Alexandre, J., Medina, P., and Gilabert-Estellés, J. (2023) 'Increased levels of NETosis biomarkers in high-grade serous ovarian cancer patients' biofluids: Potential role in disease diagnosis and management', *Frontiers in Immunology*, 14, available:

https://www.frontiersin.org/articles/10.3389/fimmu.2023.1111344 [accessed 6 Sep 2023].

Tong, M., Wong, T.-L., Zhao, H., Zheng, Y., Xie, Y.-N., Li, C.-H., Zhou, L., Che, N., Yun, J.-P., Man, K., Lee, T.K.-W., Cai, Z., and Ma, S. (2021) 'Loss of tyrosine catabolic enzyme HPD promotes glutamine anaplerosis through mTOR signaling in liver cancer', *Cell Reports*, 36(8), 109617, available: https://doi.org/10.1016/j.celrep.2021.109617.

Topp, M.S., Duell, J., Zugmaier, G., Attal, M., Moreau, P., Langer, C., Krönke, J., Facon, T., Salnikov, A.V., Lesley, R., Beutner, K., Kalabus, J., Rasmussen, E., Riemann, K., Minella, A.C., Munzert, G., and Einsele, H. (2020) 'Anti–B-Cell Maturation Antigen BiTE Molecule AMG 420 Induces Responses in Multiple Myeloma', *Journal of Clinical Oncology*, 38(8), 775–783, available: https://doi.org/10.1200/JCO.19.02657.

Touzeau, C. and Moreau, P. (2016) 'How I treat extramedullary myeloma', *Blood*, 127(8), 971–976, available: https://doi.org/10.1182/blood-2015-07-635383.

Towbin, H., Staehelin, T., and Gordon, J. (1979) 'Electrophoretic transfer of proteins from polyacrylamide gels to nitrocellulose sheets: procedure and some applications', *Proceedings of the National Academy of Sciences of the United States of America*, 76(9), 4350–4354, available: https://doi.org/10.1073/pnas.76.9.4350.

Tripathi, K., Ramani, V.C., Bandari, S.K., Amin, R., Brown, E.E., Ritchie, J.P., Stewart, M.D., and Sanderson, R.D. (2020) 'Heparanase promotes myeloma stemness and in vivo tumorigenesis', *Matrix Biology*, 88, 53–68, available: https://doi.org/10.1016/j.matbio.2019.11.004.

Trudel, S., Lendvai, N., Popat, R., Voorhees, P.M., Reeves, B., Libby, E.N., Richardson, P.G., Anderson, L.D., Sutherland, H.J., Yong, K., Hoos, A., Gorczyca, M.M., Lahiri, S., He, Z., Austin, D.J., Opalinska, J.B., and Cohen, A.D. (2018) 'Targeting B-cell maturation antigen with GSK2857916 antibody-drug conjugate in relapsed or refractory multiple myeloma (BMA117159): a dose escalation and expansion phase 1 trial', *The Lancet. Oncology*, 19(12), 1641–1653, available: https://doi.org/10.1016/S1470-2045(18)30576-X.

Tsai, D.-Y., Hung, K.-H., Chang, C.-W., and Lin, K.-I. (2019) 'Regulatory mechanisms of B cell responses and the implication in B cell-related diseases', *Journal of Biomedical Science*, 26(1), 64, available: https://doi.org/10.1186/s12929-019-0558-1.

Tsubaki, M., Takeda, T., Matsuda, T., Seki, S., Tomonari, Y., Koizumi, S., Nagatakiya, M., Katsuyama, M., Yamamoto, Y., Tsurushima, K., Ishizaka, T., and Nishida, S. (2021) 'Activation of Serum/Glucocorticoid Regulated Kinase 1/Nuclear Factor-κB Pathway Are Correlated with Low Sensitivity to Bortezomib and Ixazomib in Resistant Multiple Myeloma Cells', *Biomedicines*, 9(1), 33, available: https://doi.org/10.3390/biomedicines9010033.

Tsuruhisa, S., Matsui, T., Koga, Y., Sotokawauchi, A., Yagi, M., and Yamagishi, S.-I. (2021) 'Pigment epithelium-derived factor inhibits advanced glycation end product-induced proliferation, VEGF and MMP-9 expression in breast cancer cells via interaction with laminin receptor', *Oncology Letters*, 22(2), 1–9, available: https://doi.org/10.3892/ol.2021.12890.

Turner, J.G., Gump, J.L., Zhang, C., Cook, J.M., Marchion, D., Hazlehurst, L., Munster, P., Schell, M.J., Dalton, W.S., and Sullivan, D.M. (2006) 'ABCG2 expression, function, and promoter methylation in human multiple myeloma', *Blood*, 108(12), 3881–3889, available: https://doi.org/10.1182/blood-2005-10-009084.

Tyanova, S. and Cox, J. (2018) 'Perseus: A Bioinformatics Platform for Integrative Analysis of Proteomics Data in Cancer Research', in von Stechow, L., ed., *Cancer Systems Biology: Methods and Protocols*, Methods in Molecular Biology, New York, NY: Springer, 133–148, available: https://doi.org/10.1007/978-1-4939-7493-1_7.

Tyczyńska, A., Turski, M., Zarzycka, E., and Zaucha, J.M. (2023) 'Isolated Progression of Multiple Myeloma into the Extramedullary Plasmacytoma of Dura Mater: A Case Report and Review of the Literature', *Biomedicines*, 11(4), 1225, available: https://doi.org/10.3390/biomedicines11041225.

Uchiyama, H., Barut, B.A., Chauhan, D., Cannistra, S.A., and Anderson, K.C. (1992) 'Characterization of Adhesion Molecules on Human Myeloma Cell Lines', *Blood*, 80(9), 2306–2314, available: https://doi.org/10.1182/blood.V80.9.2306.2306.

Uchiyama, H., Barut, B.A., Mohrbacher, A.F., Chauhan, D., and Anderson, K.C. (1993) 'Adhesion of human myeloma-derived cell lines to bone marrow stromal cells stimulates interleukin-6 secretion', *Blood*, 82(12), 3712–3720.

Ueno, S., Sudo, T., Saya, H., and Sugihara, E. (2022) 'Pigment epithelium-derived factor promotes peritoneal dissemination of ovarian cancer through induction of immunosuppressive macrophages', *Communications Biology*, 5, 904, available: https://doi.org/10.1038/s42003-022-03837-4.

Ulaner, G.A. and Landgren, C.O. (2020) 'Current and Potential Applications of Positron Emission Tomography for Multiple Myeloma and Plasma Cell Disorders', *Best practice & research. Clinical haematology*, 33(1), 101148, available: https://doi.org/10.1016/j.beha.2020.101148.

Urban, C.F., Ermert, D., Schmid, M., Abu-Abed, U., Goosmann, C., Nacken, W., Brinkmann, V., Jungblut, P.R., and Zychlinsky, A. (2009) 'Neutrophil Extracellular Traps Contain Calprotectin, a Cytosolic Protein Complex Involved in Host Defense against Candida albicans', *PLoS Pathogens*, 5(10), e1000639, available: https://doi.org/10.1371/journal.ppat.1000639.

Usmani, S.Z., Alonso Alonso, A., Quach, H., Koh, Y., Guenther, A., Min, C.-K., Zhou, X.L., Kaisermann, M., Mis, L.M., Williams, D., Yeakey, A., Ferron-Brady, G., Figueroa, D.J., Kremer, B.E., Gupta, I., and Janowski, W. (2021)

‘DREAMM-9: Phase I Study of Belantamab Mafodotin Plus Standard of Care in Patients with Transplant-Ineligible Newly Diagnosed Multiple Myeloma’, *Blood*, 138(Supplement 1), 2738, available: https://doi.org/10.1182/blood-2021-153315.

Usmani, S.Z., Heuck, C., Mitchell, A., Szymonifka, J., Nair, B., Hoering, A., Alsayed, Y., Waheed, S., Haider, S., Restrepo, A., Rhee, F.V., Crowley, J., and Barlogie, B. (2012) ‘Extramedullary disease portends poor prognosis in multiple myeloma and is over-represented in high-risk disease even in the era of novel agents’, *Haematologica*, 97(11), 1761–1767, available: https://doi.org/10.3324/haematol.2012.065698.

Vacca, A., Ribatti, D., Presta, M., Minischetti, M., Iurlaro, M., Ria, R., Albini, A., Bussolino, F., and Dammacco, F. (1999) ‘Bone marrow neovascularization, plasma cell angiogenic potential, and matrix metalloproteinase-2 secretion parallel progression of human multiple myeloma’, *Blood*, 93(9), 3064–3073.

Valadez-Cosmes, P., Raftopoulou, S., Mihalic, Z.N., Marsche, G., and Kargl, J. (2022) ‘Myeloperoxidase: Growing importance in cancer pathogenesis and potential drug target’, *Pharmacology & Therapeutics*, 236, 108052, available: https://doi.org/10.1016/j.pharmthera.2021.108052.

Van Acker, H.H., Capsomidis, A., Smits, E.L., and Van Tendeloo, V.F. (2017) ‘CD56 in the Immune System: More Than a Marker for Cytotoxicity?’, *Frontiers in Immunology*, 8, available: https://www.frontiersin.org/articles/10.3389/fimmu.2017.00892 [accessed 6 Feb 2023].

VanValkenburg, M.E., Pruitt, G.I., Brill, I.K., Costa, L., Ehtsham, M., Justement, I.T., Innis-Shelton, R.D., Salzman, D., Reddy, E.S.P., Godby, K.N., Mikhail, F.M., Carroll, A.J., Reddy, V.B., Sanderson, R.D., Justement, L.B., Sanders, P.W., and Brown, E.E. (2016) ‘Family history of hematologic malignancies and risk of multiple myeloma: differences by race and clinical features’, *Cancer Causes & Control*, 27(1), 81–91, available: https://doi.org/10.1007/s10552-015-0685-2.

Varettoni, M., Corso, A., Pica, G., Mangiacavalli, S., Pascutto, C., and Lazzarino, M. (2010) ‘Incidence, presenting features and outcome of extramedullary disease in multiple myeloma: a longitudinal study on 1003 consecutive patients’, *Annals of Oncology*, 21(2), 325–330, available: https://doi.org/10.1093/annonc/mdp329.

Varga, C., Xie, W., Laubach, J., Ghobrial, I.M., O’Donnell, E.K., Weinstock, M., Paba-Prada, C., Warren, D., Maglio, M.E., Schlossman, R., Munshi, N.C., Raje, N., Weller, E., Anderson, K.C., Mitsiades, C.S., and Richardson, P.G. (2015) ‘Development of extramedullary myeloma in the era of novel agents: no evidence of increased risk with lenalidomide–bortezomib combinations’, *British Journal of Haematology*, 169(6), 843–850, available: https://doi.org/10.1111/bjh.13382.

Vaxman, I. and Gertz, M.A. (2022) ‘How I approach smoldering multiple myeloma’, *Blood*, 140(8), 828–838, available: https://doi.org/10.1182/blood.2021011670.

Veenstra, T.D., Conrads, T.P., Hood, B.L., Avellino, A.M., Ellenbogen, R.G., and Morrison, R.S. (2005) ‘Biomarkers: mining the biofluid proteome’, *Molecular & cellular proteomics: MCP*, 4(4), 409–418, available: https://doi.org/10.1074/mcp.M500006-MCP200.

Verkleij, C.P.M., Frerichs, K.A., Broekmans, M.E.C., Duetz, C., O’Neill, C.A., Bruins, W.S.C., Homan-Weert, P.M., Minnema, M.C., Levin, M.-D., Broijl, A., Bos, G.M.J., Kersten, M.J., Klein, S.K., Shikhagaie, M.M., Casneuf, T., Abraham, Y., Smets, T., Vanhoof, G., Cortes-Selva, D., van Steenbergen, L., Ramos, E., Verona, R.I., Krevvata, M., Sonneveld, P., Zweegman, S., Mutis, T., and van de Donk, N.W.C.J. (2023) ‘NK Cell Phenotype Is Associated With Response and Resistance to Daratumumab in Relapsed/Refractory Multiple Myeloma’, *HemaSphere*, 7(5), e881, available: https://doi.org/10.1097/HS9.0000000000000881.

Vishnubalaji, R. and Alajez, N.M. (2021) ‘Transcriptional landscape associated with TNBC resistance to neoadjuvant chemotherapy revealed by single-cell RNA-seq’, *Molecular Therapy - Oncolytics*, 23, 151–162, available: https://doi.org/10.1016/j.omto.2021.09.002.

Vishnubalaji, R., Shaath, H., Elkord, E., and Alajez, N.M. (2019) ‘Long non-coding RNA (lncRNA) transcriptional landscape in breast cancer identifies LINC01614 as non-favorable prognostic biomarker regulated by TGFβ and focal adhesion kinase (FAK) signaling’, *Cell Death Discovery*, 5(1), 1–15, available: https://doi.org/10.1038/s41420-019-0190-6.

Vogl, D.T., Raje, N., Jagannath, S., Richardson, P., Hari, P., Orlowski, R., Supko, J.G., Tamang, D., Yang, M., Jones, S.S., Wheeler, C., Markelewicz, R.J., and Lonial, S. (2017) ‘Ricolinostat, the first selective histone deacetylase 6 inhibitor, in combination with bortezomib and dexamethasone for relapsed or refractory multiple myeloma’, *Clinical cancer research : an official journal of the American Association for Cancer Research*, 23(13), 3307–3315, available: https://doi.org/10.1158/1078-0432.CCR-16-2526.

Volm, M. and Efferth, T. (2015) ‘Prediction of Cancer Drug Resistance and Implications for Personalized Medicine’, *Frontiers in Oncology*, 5, 282, available: https://doi.org/10.3389/fonc.2015.00282.

Vong, S., Navarro, S.M., Darrow, M., and Aminololama-Shakeri, S. (2020) ‘Extramedullary Plasmacytoma of the breast in a patient with Multiple Myeloma’, *Journal of Radiology Case Reports*, 14(12), 14–23, available: https://doi.org/10.3941/jrcr.v14i12.4110.

Wader, K.F., Fagerli, U.M., Holt, R.U., Stordal, B., Børset, M., Sundan, A., and Waage, A. (2008) ‘Elevated serum concentrations of activated hepatocyte growth factor activator in patients with multiple myeloma’, *European*

Journal of Haematology, 81(5), 380–383, available: https://doi.org/10.1111/j.1600-0609.2008.01130.x.

Waldmann, T.A., Dubois, S., Miljkovic, M.D., and Conlon, K.C. (2020) 'IL-15 in the Combination Immunotherapy of Cancer', *Frontiers in Immunology*, 11, available: https://www.frontiersin.org/articles/10.3389/fimmu.2020.00868 [accessed 10 Nov 2023].

Wallin, A. and Larsson, S.C. (2011) 'Body mass index and risk of multiple myeloma: a meta-analysis of prospective studies', *European Journal of Cancer (Oxford, England: 1990)*, 47(11), 1606–1615, available: https://doi.org/10.1016/j.ejca.2011.01.020.

Walsh, G.M., Symon, F.A., Lazarovils, A.L., and Wardlaw, A.J. (1996) 'Integrin alpha 4 beta 7 mediates human eosinophil interaction with MAdCAM-1, VCAM-1 and fibronectin', *Immunology*, 89(1), 112–119, available: https://doi.org/10.1046/j.1365-2567.1996.d01-713.x.

Walter, R.F.H., Sydow, S.R., Berg, E., Kollmeier, J., Christoph, D.C., Christoph, S., Eberhardt, W.E.E., Mairinger, T., Wohlschlaeger, J., Schmid, K.W., and Mairinger, F.D. (2019) 'Bortezomib sensitivity is tissue dependent and high expression of the 20S proteasome precludes good response in malignant pleural mesothelioma', *Cancer Management and Research*, 11, 8711–8720, available: https://doi.org/10.2147/CMAR.S194337.

Wang, C., Zhang, S., Liu, J., Tian, Y., Ma, B., Xu, S., Fu, Y., and Luo, Y. (2020) 'Secreted Pyruvate Kinase M2 Promotes Lung Cancer Metastasis through Activating the Integrin Beta1/FAK Signaling Pathway', *Cell Reports*, 30(6), 1780-1797.e6, available: https://doi.org/10.1016/j.celrep.2020.01.037.

Wang, H., Wang, L., Chi, P., Wang, W., Chen, X., Geng, Q., Xia, Z., and Lu, Y. (2016) 'High level of interleukin-10 in serum predicts poor prognosis in multiple myeloma', *British Journal of Cancer*, 114(4), 463–468, available: https://doi.org/10.1038/bjc.2016.11.

Wang, J., Hendrix, A., Hernot, S., Lemaire, M., De Bruyne, E., Van Valckenborgh, E., Lahoutte, T., De Wever, O., Vanderkerken, K., and Menu, E. (2014) 'Bone marrow stromal cell-derived exosomes as communicators in drug resistance in multiple myeloma cells', *Blood*, 124(4), 555–566, available: https://doi.org/10.1182/blood-2014-03-562439.

Wang, J., Kunzke, T., Prade, V.M., Shen, J., Buck, A., Feuchtinger, A., Haffner, I., Luber, B., Liu, D.H.W., Langer, R., Lordick, F., Sun, N., and Walch, A. (2022) 'Spatial Metabolomics Identifies Distinct Tumor-Specific Subtypes in Gastric Cancer Patients', *Clinical Cancer Research*, 28(13), 2865–2877, available: https://doi.org/10.1158/1078-0432.CCR-21-4383.

Wang, P.-W., Abedini, M.R., Yang, L.-X., Ding, A.-A., Figeys, D., Chang, J.-Y., Tsang, B.K., and Shieh, D.-B. (2014) 'Gelsolin regulates cisplatin sensitivity in human head-and-neck cancer', *International Journal of Cancer*, 135(12), 2760–2769, available: https://doi.org/10.1002/ijc.28928.

Wang, S.-Y., Hao, H.-L., Deng, K., Li, Y., Cheng, Z.-Y., Lv, C., Liu, Z.-M., Yang, J., and Pan, L. (2012) 'Expression levels of phosphatase and tensin homolog deleted on chromosome 10 (PTEN) and focal adhesion kinase in patients with multiple myeloma and their relationship to clinical stage and extramedullary infiltration', *Leukemia & Lymphoma*, 53(6), 1162–1168, available: https://doi.org/10.3109/10428194.2011.647311.

Wang, X., Zhang, Z., and Yao, C. (2011) 'Targeting integrin-linked kinase increases apoptosis and decreases invasion of myeloma cell lines and inhibits IL-6 and VEGF secretion from BMSCs', *Medical Oncology*, 28(4), 1596–1600, available: https://doi.org/10.1007/s12032-010-9616-y.

Wang, Y., Sanchez, L., Siegel, D.S., and Wang, M.L. (2016) 'Elotuzumab for the treatment of multiple myeloma', *Journal of Hematology & Oncology*, 9(1), 55, available: https://doi.org/10.1186/s13045-016-0284-z.

Warburg, O., Wind, F., and Negelein, E. (1927) 'THE METABOLISM OF TUMORS IN THE BODY', *The Journal of General Physiology*, 8(6), 519–530.

Wei, Y., Wang, J., Chen, F., Li, X., Zhang, J., Shen, M., Tang, R., and Huang, Z. (2022) 'Serum Abnormal Metabolites for Evaluating Therapeutic Response and Prognosis of Patients With Multiple Myeloma', *Frontiers in Oncology*, 12, 808290, available: https://doi.org/10.3389/fonc.2022.808290.

Weinstock, M., Aljawai, Y., Morgan, E.A., Laubach, J., Gannon, M., Roccaro, A.M., Varga, C., Mitsiades, C.S., Paba-Prada, C., Schlossman, R., Munshi, N., Anderson, K.C., Richardson, P.P., Weller, E., and Ghobrial, I.M. (2015) 'Incidence and clinical features of extramedullary multiple myeloma in patients who underwent stem cell transplantation', *British Journal of Haematology*, 169(6), 851–858, available: https://doi.org/10.1111/bjh.13383.

Weinstock, M. and Ghobrial, I.M. (2013) 'Extramedullary multiple myeloma', *Leukemia & Lymphoma*, 54(6), 1135–1141, available: https://doi.org/10.3109/10428194.2012.740562.

Wigerblad, G. and Kaplan, M.J. (2023) 'Neutrophil extracellular traps in systemic autoimmune and autoinflammatory diseases', *Nature Reviews Immunology*, 23(5), 274–288, available: https://doi.org/10.1038/s41577-022-00787-0.

Wilkinson, L.S., Edwards, J.C., Poston, R.N., and Haskard, D.O. (1993) 'Expression of vascular cell adhesion molecule-1 in normal and inflamed synovium', *Laboratory Investigation; a Journal of Technical Methods and Pathology*, 68(1), 82–88.

Wiśniewski, J.R., Zougman, A., Nagaraj, N., and Mann, M. (2009) 'Universal sample preparation method for proteome analysis', *Nature Methods*, 6(5), 359–362, available: https://doi.org/10.1038/nmeth.1322.

Wodnar-Filipowicz, A. (2003) 'Flt3 Ligand: Role in Control of Hematopoietic and Immune Functions of the Bone Marrow', *Physiology*, 18(6), 247–251, available: https://doi.org/10.1152/nips.01452.2003.

Woo, J. and Zhang, Q. (2023) ‘A Streamlined High-Throughput Plasma Proteomics Platform for Clinical Proteomics with Improved Proteome Coverage, Reproducibility, and Robustness’, *Journal of the American Society for Mass Spectrometry*, 34(4), 754–762, available: https://doi.org/10.1021/jasms.3c00022.

Woo, K.M., Kim, H.-M., and Ko, J.S. (2002) ‘Macrophage colony-stimulating factor promotes the survival of osteoclast precursors by up-regulating Bcl-X(L)’, *Experimental & Molecular Medicine*, 34(5), 340–346, available: https://doi.org/10.1038/emm.2002.48.

Worley, B. and Powers, R. (2012) ‘Multivariate Analysis in Metabolomics’, *Current Metabolomics*, 1(1), 92–107, available: https://doi.org/10.2174/2213235X11301010092.

Wu, P., Davies, F.E., Boyd, K., Thomas, K., Dines, S., Saso, R.M., Potter, M.N., Ethell, M.E., Shaw, B.E., and Morgan, G.J. (2009) ‘The impact of extramedullary disease at presentation on the outcome of myeloma’, *Leukemia & Lymphoma*, 50(2), 230–235, available: https://doi.org/10.1080/10428190802657751.

Xiang, Y., Liu, Y., Yang, Y., Hu, H., Hu, P., Ren, H., and Zhang, D. (2015) ‘A secretomic study on human hepatocellular carcinoma multiple drug-resistant cell lines’, *Oncology Reports*, 34(3), 1249–1260, available: https://doi.org/10.3892/or.2015.4106.

Xiao, Y., Ma, D., Yang, Y.-S., Yang, F., Ding, J.-H., Gong, Y., Jiang, L., Ge, L.-P., Wu, S.-Y., Yu, Q., Zhang, Q., Bertucci, F., Sun, Q., Hu, X., Li, D.-Q., Shao, Z.-M., and Jiang, Y.-Z. (2022) ‘Comprehensive metabolomics expands precision medicine for triple-negative breast cancer’, *Cell Research*, 32(5), 477–490, available: https://doi.org/10.1038/s41422-022-00614-0.

Xie, H., Gu, Y., Wang, W., Wang, X., Ye, X., Xin, C., Lu, M., Reddy, B.A., and Shu, P. (2020) ‘Silencing of SENP2 in Multiple Myeloma Induces Bortezomib Resistance by Activating NF-κB Through the Modulation of IκBα Sumoylation’, *Scientific Reports*, 10(1), 766, available: https://doi.org/10.1038/s41598-020-57698-0.

Xie, X., Wu, W., Zhu, Y., Liu, D., Dong, W., Li, H., Li, Q., and Gu, W. (2015) ‘Successful treatment with lenalidomide of secondary multiple myeloma with extramedullary liver plasmacytoma in a renal transplant recipient: A case report and review of the literature’, *Oncology Letters*, 10(5), 2931–2936, available: https://doi.org/10.3892/ol.2015.3729.

Xu, J., Yu, X., Wang, S., Yan, M., Wang, M., Ou, J., Wang, L., Liu, H., and Cen, X. (2021) ‘C3 glomerulonephritis along with light chain proximal tubulopathy without crystal deposits in multiple myeloma: a case report’, *World Journal of Surgical Oncology*, 19(1), 24, available: https://doi.org/10.1186/s12957-021-02135-3.

Xu, S., De Veirman, K., De Becker, A., Vanderkerken, K., and Van Riet, I. (2018) 'Mesenchymal stem cells in multiple myeloma: a therapeutical tool or target?', *Leukemia*, 32(7), 1500–1514, available: https://doi.org/10.1038/s41375-018-0061-9.

Xu, W.-F., Ma, Y.-C., Ma, H.-S., Shi, L., Mu, H., Ou, W.-B., Peng, J., Li, T.-T., Qin, T., Zhou, H.-M., Fu, X.-Q., and Li, X.-H. (2019) 'Co-targeting CK2α and YBX1 suppresses tumor progression by coordinated inhibition of the PI3K/AKT signaling pathway', *Cell Cycle*, 18(24), 3472–3490, available: https://doi.org/10.1080/15384101.2019.1689474.

Xu, Z., Zhang, Y., Xu, M., Zheng, X., Lin, M., Pan, J., Ye, C., Deng, Y., Jiang, C., Lin, Y., Lu, X., and Chi, P. (2019) 'Demethylation and Overexpression of CSF2 are Involved in Immune Response, Chemotherapy Resistance, and Poor Prognosis in Colorectal Cancer', *OncoTargets and Therapy*, 12, 11255–11269, available: https://doi.org/10.2147/OTT.S216829.

Yadav, B., Pemovska, T., Szwajda, A., Kulesskiy, E., Kontro, M., Karjalainen, R., Majumder, M.M., Malani, D., Murumägi, A., Knowles, J., Porkka, K., Heckman, C., Kallioniemi, O., Wennerberg, K., and Aittokallio, T. (2014) 'Quantitative scoring of differential drug sensitivity for individually optimized anticancer therapies', *Scientific Reports*, 4, 5193, available: https://doi.org/10.1038/srep05193.

Yakubu, R.R., Nieves, E., and Weiss, L.M. (2019) 'The Methods employed in Mass Spectrometric Analysis of Posttranslational Modifications (PTMs) and Protein–Protein Interactions (PPIs)', *Advances in experimental medicine and biology*, 1140, 169–198, available: https://doi.org/10.1007/978-3-030-15950-4_10.

Yan, M., Zheng, M., Niu, R., Yang, X., Tian, S., Fan, L., Li, Y., and Zhang, S. (2022) 'Roles of tumor-associated neutrophils in tumor metastasis and its clinical applications', *Frontiers in Cell and Developmental Biology*, 10, 938289, available: https://doi.org/10.3389/fcell.2022.938289.

Yang, D. and Liu, J. (2021) 'Neutrophil Extracellular Traps: A New Player in Cancer Metastasis and Therapeutic Target', *Journal of Experimental & Clinical Cancer Research*, 40(1), 233, available: https://doi.org/10.1186/s13046-021-02013-6.

Yang, H., Cheng, R., Liu, G., Zhong, Q., Li, C., Cai, W., Yang, Z., Ma, J., Yang, X., and Gao, G. (2009) 'PEDF inhibits growth of retinoblastoma by anti-angiogenic activity', *Cancer Science*, 100(12), 2419–2425, available: https://doi.org/10.1111/j.1349-7006.2009.01332.x.

Yang, H. and Grossniklaus, H.E. (2010) 'Constitutive overexpression of pigment epithelium-derived factor inhibition of ocular melanoma growth and metastasis', *Investigative Ophthalmology & Visual Science*, 51(1), 28–34, available: https://doi.org/10.1167/iovs.09-4138.

Yang, L., Liu, Q., Zhang, X., Liu, X., Zhou, B., Chen, J., Huang, D., Li, J., Li, H., Chen, F., Liu, J., Xing, Y., Chen, X., Su, S., and Song, E. (2020) 'DNA of neutrophil extracellular traps promotes cancer metastasis via CCDC25', *Nature*, 583(7814), 133–138, available: https://doi.org/10.1038/s41586-020-2394-6.

Yee, A.J., Huff, C.A., Chari, A., Vogl, D.T., Gavriatopoulou, M., Nooka, A.K., Moreau, P., Dingli, D., Cole, C.E., Lonial, S., Dimopoulos, M.A., Richter, J.R., Vij, R., Tuchman, S.A., Hoffman, J.E., Costa, L.J., Parker, T.L., Vlummens, P., Doyen, C., Biran, N., Siegel, D.S., Shah, J., Picklesimer, C., Saint-Martin, J.-R., Li, L., Kauffman, M.G., Shacham, S., Richardson, P.G., and Jagannath, S. (2019) 'Response to Therapy and the Effectiveness of Treatment with Selinexor and Dexamethasone in Patients with Penta-Exposed Triple-Class Refractory Myeloma Who Had Plasmacytomas', *Blood*, 134, 3140, available: https://doi.org/10.1182/blood-2019-129038.

Yeo, M.G., Oh, H.J., Cho, H.-S., Chun, J.S., Marcantonio, E.E., and Song, W.K. (2011) 'Phosphorylation of Ser 21 in Fyn regulates its kinase activity, focal adhesion targeting, and is required for cell migration', *Journal of Cellular Physiology*, 226(1), 236–247, available: https://doi.org/10.1002/jcp.22335.

Yip, H.Y.K. and Papa, A. (2021) 'Signaling Pathways in Cancer: Therapeutic Targets, Combinatorial Treatments, and New Developments', *Cells*, 10(3), 659, available: https://doi.org/10.3390/cells10030659.

Yu, H., Lin, L., Zhang, Z., Zhang, H., and Hu, H. (2020) 'Targeting NF-κB pathway for the therapy of diseases: mechanism and clinical study', *Signal Transduction and Targeted Therapy*, 5(1), 1–23, available: https://doi.org/10.1038/s41392-020-00312-6.

Yuan, A., Hsiao, Y.-J., Chen, H.-Y., Chen, H.-W., Ho, C.-C., Chen, Y.-Y., Liu, Y.-C., Hong, T.-H., Yu, S.-L., Chen, J.J.W., and Yang, P.-C. (2015) 'Opposite Effects of M1 and M2 Macrophage Subtypes on Lung Cancer Progression', *Scientific Reports*, 5(1), 14273, available: https://doi.org/10.1038/srep14273.

Yuan, K., Ye, J., Liu, Z., Ren, Y., He, W., Xu, J., He, Y., and Yuan, Y. (2020) 'Complement C3 overexpression activates JAK2/STAT3 pathway and correlates with gastric cancer progression', *Journal of Experimental & Clinical Cancer Research*, 39(1), 9, available: https://doi.org/10.1186/s13046-019-1514-3.

Zaal, E.A., Wu, W., Jansen, G., Zweegman, S., Cloos, J., and Berkers, C.R. (2017) 'Bortezomib resistance in multiple myeloma is associated with increased serine synthesis', *Cancer & Metabolism*, 5, 7, available: https://doi.org/10.1186/s40170-017-0169-9.

Zahavi, D. and Weiner, L. (2020) 'Monoclonal Antibodies in Cancer Therapy', *Antibodies*, 9(3), 34, available: https://doi.org/10.3390/antib9030034.

Zamagni, E., Patriarca, F., Nanni, C., Zannetti, B., Englaro, E., Pezzi, A., Tacchetti, P., Buttignol, S., Perrone, G., Brioli, A., Pantani, L., Terragna, C.,

Carobolante, F., Baccarani, M., Fanin, R., Fanti, S., and Cavo, M. (2011) 'Prognostic relevance of 18-F FDG PET/CT in newly diagnosed multiple myeloma patients treated with up-front autologous transplantation', *Blood*, 118(23), 5989–5995, available: https://doi.org/10.1182/blood-2011-06-361386.

Zeissig, M.N., Zannettino, A.C.W., and Vandyke, K. (2020) 'Tumour Dissemination in Multiple Myeloma Disease Progression and Relapse: A Potential Therapeutic Target in High-Risk Myeloma', *Cancers*, 12(12), 3643, available: https://doi.org/10.3390/cancers12123643.

Zha, H., Wang, X., Zhu, Y., Chen, D., Han, X., Yang, F., Gao, J., Hu, C., Shu, C., Feng, Y., Tan, Y., Zhang, J., Li, Y., Wan, Y.Y., Guo, B., and Zhu, B. (2019) 'Intracellular Activation of Complement C3 Leads to PD-L1 Antibody Treatment Resistance by Modulating Tumor-Associated Macrophages', *Cancer Immunology Research*, 7(2), 193–207, available: https://doi.org/10.1158/2326-6066.CIR-18-0272.

Zhang, J., Wang, L., Schwartz, J., Bond, R.W., and Bishop, W.R. (1994) 'Phosphorylation of Thr642 is an early event in the processing of newly synthesized protein kinase C beta 1 and is essential for its activation', *The Journal of Biological Chemistry*, 269(30), 19578–19584.

Zhang, L., Huang, Y., Lin, Y., Zhang, A., Zou, R., Xu, H., and Wang, S. (2022) 'Prognostic significance of CD56 expression in patients with multiple myeloma: a meta-analysis', *Hematology*, 27(1), 122–131, available: https://doi.org/10.1080/16078454.2021.2019365.

Zhang, Y., Chen, K., Tu, Y., Velyvis, A., Yang, Y., Qin, J., and Wu, C. (2002) 'Assembly of the PINCH-ILK-CH-ILKBP complex precedes and is essential for localization of each component to cell-matrix adhesion sites', *Journal of Cell Science*, 115(Pt 24), 4777–4786, available: https://doi.org/10.1242/jcs.00166.

Zhang, Y., Han, J., Yang, X., Shao, C., Xu, Z., Cheng, R., Cai, W., Ma, J., Yang, Z., and Gao, G. (2011) 'Pigment epithelium-derived factor inhibits angiogenesis and growth of gastric carcinoma by down-regulation of VEGF', *Oncology Reports*, 26(3), 681–686, available: https://doi.org/10.3892/or.2011.1318.

Zhang, Y., Ji, M., Zhao, J.-Y., Wang, H.-F., Wang, C.-W., Li, W., Ye, J.-J., Lu, F., Lin, L.-H., Gao, Y.-T., Jin, J., Li, L., Ji, C.-Y., Ballesteros, J., and Zhu, H.-H. (2022) 'Ex Vivo Chemosensitivity Profiling of Acute Myeloid Leukemia and Its Correlation With Clinical Response and Outcome to Chemotherapy', *Frontiers in Oncology*, 11, 793773, available: https://doi.org/10.3389/fonc.2021.793773.

Zhang, Y., Yao, W., Wang, F., Su, Y., Zhang, D., Hu, S., and Zhang, X. (2020) 'AGC protein kinase AGC1-4 mediates seed size in Arabidopsis', *Plant Cell Reports*, 39(6), 825–837, available: https://doi.org/10.1007/s00299-020-02533-z.

Zhao, J. and Jin, J. (2022) ‘Neutrophil extracellular traps: New players in cancer research’, *Frontiers in Immunology*, 13, available: https://www.frontiersin.org/articles/10.3389/fimmu.2022.937565 [accessed 22 Oct 2023].

Zhao, J., Wang, M., He, P., Chen, Y., Wang, X., and Zhang, M. (2020) ‘Identification of glutathione S-transferase π 1 as a prognostic proteomic biomarker for multiple myeloma using proteomic profiling’, *Oncology Letters*, 19(3), 2153–2162, available: https://doi.org/10.3892/ol.2020.11321.

Zhao, S., Wu, D., Wu, P., Wang, Z., and Huang, J. (2015) ‘Serum IL-10 Predicts Worse Outcome in Cancer Patients: A Meta-Analysis’, *PLoS ONE*, 10(10), e0139598, available: https://doi.org/10.1371/journal.pone.0139598.

Zheng, H., Yang, Y., Hong, Y.-G., Wang, M.-C., Yuan, S.-X., Wang, Z.-G., Bi, F.-R., Hao, L.-Q., Yan, H.-L., and Zhou, W.-P. (2019) ‘Tropomodulin 3 modulates EGFR-PI3K-AKT signaling to drive hepatocellular carcinoma metastasis’, *Molecular Carcinogenesis*, 58(10), 1897–1907, available: https://doi.org/10.1002/mc.23083.

Zhou, N., Gutierrez-Uzquiza, A., Zheng, X.Y., Chang, R., Vogl, D.T., Garfall, A.L., Bernabei, L., Saraf, A., Florens, L., Washburn, M.P., Illendula, A., Bushweller, J.H., and Busino, L. (2019) ‘RUNX proteins desensitize multiple myeloma to lenalidomide via protecting IKZFs from degradation’, *Leukemia*, 33(8), 2006–2021, available: https://doi.org/10.1038/s41375-019-0403-2.

Zhou, X., Flüchter, P., Nickel, K., Meckel, K., Messerschmidt, J., Böckle, D., Knorz, S., Steinhardt, M.J., Krummenast, F., Danhof, S., Einsele, H., Kortüm, K.M., and Rasche, L. (2020) ‘Carfilzomib Based Treatment Strategies in the Management of Relapsed/Refractory Multiple Myeloma with Extramedullary Disease’, *Cancers*, 12(4), 1035, available: https://doi.org/10.3390/cancers12041035.

Zhu, Y.X., Braggio, E., Shi, C.-X., Bruins, L.A., Schmidt, J.E., Van Wier, S., Chang, X.-B., Bjorklund, C.C., Fonseca, R., Bergsagel, P.L., Orlowski, R.Z., and Stewart, A.K. (2011) ‘Cereblon expression is required for the antimyeloma activity of lenalidomide and pomalidomide’, *Blood*, 118(18), 4771–4779, available: https://doi.org/10.1182/blood-2011-05-356063.

Zhu, Y.X., Shi, C.-X., Bruins, L.A., Wang, X., Riggs, D.L., Porter, B., Ahmann, J.M., de Campos, C.B., Braggio, E., Bergsagel, P.L., and Stewart, A.K. (2019) ‘Identification of lenalidomide resistance pathways in myeloma and targeted resensitization using cereblon replacement, inhibition of STAT3 or targeting of IRF4’, *Blood Cancer Journal*, 9(2), 19, available: https://doi.org/10.1038/s41408-019-0173-0.

Zhu, Y.X., Tiedemann, R., Shi, C.-X., Yin, H., Schmidt, J.E., Bruins, L.A., Keats, J.J., Braggio, E., Sereduk, C., Mousses, S., and Stewart, A.K. (2011) ‘RNAi screen of the druggable genome identifies modulators of proteasome inhibitor sensitivity in myeloma including CDK5’, *Blood*, 117(14), 3847–3857, available: https://doi.org/10.1182/blood-2010-08-304022.

Zuo, F., Yu, J., and He, X. (2022) ‘Single-Cell Metabolomics in Hematopoiesis and Hematological Malignancies’, *Frontiers in Oncology*, 12, 931393, available: https://doi.org/10.3389/fonc.2022.931393.

Chapter 10

Appendix

Supplementary files can be accessed with the link provided: Thesis - Supplementary Files

Chapter 2

Supp. File 2.1: List of metabolites analysed in the MxP® Quant 500 assay.

Chapter 3

Supp. File 3.1: Statistically significantly differentially abundant proteins between chemosensitivity groups

Supp. File 3.2: Gene ontology analysis of statistically significantly differentially abundant proteins between chemosensitivity groups

Supp. File 3.3: Statistically significantly differentially abundant phosphopeptides between chemosensitivity groups

Supp. File 3.4: Gene ontology analysis of statistically significantly differentially abundant phosphopeptides between chemosensitivity groups

Supp. File 3.5: Statistically significantly differentially abundant proteins and phosphopeptides based on drug response to bortezomib.

Supp. File 3.6: Gene ontology analysis of statistically significantly differentially abundant proteins and phosphoproteins between bortezomib-sensitive and bortezomib-resistant myeloma cells

Supp. File 3.7: Statistically significantly differentially abundant proteins and phosphopeptids based on drug response to lenalidomide.

Supp. File 3.8: Gene ontology analysis of statistically significantly differentially abundant proteins and phosphoproteins between lenalidomide-sensitive and lenalidomide-resistant myeloma cells

Supp. File 3.9: Statistically significantly differentially abundant proteins and phosphopeptids based on drug response to luminespib.

Supp. File 3.10: Gene ontology analysis of statistically significantly differentially abundant proteins and phosphoproteins between luminespib-sensitive and luminespib-resistant myeloma cells

Supp. File 3.11: Statistically significantly differentially abundant proteins and phosphopeptids based on drug response to PF 431396.

Supp. File 3.12: Gene ontology analysis of statistically significantly differentially abundant proteins and phosphoproteins between PF 431396-sensitive and PF 431396-resistant myeloma cells

Supp. File 3.13: Statistically significantly differentially abundant proteins and phosphopeptids based on drug response to alvocidib.

Supp. File 3.14: Gene ontology analysis of statistically significantly differentially abundant proteins and phosphoproteins between alvocidib-sensitive and alvocidib-resistant myeloma cells.

Chapter 4

Supp. File 4.1: Statistical analysis of proteomic changes in the plasma of myeloma patients considered most sensitive or most resistant to bortezomib.

Supp. File 4.2: Statistical analysis of proteomic changes in the plasma of myeloma patients considered most sensitive or most resistant to lenalidomide.

Supp. File 4.3: Statistical analysis of proteomic changes in the plasma of myeloma patients considered most sensitive or most resistant to dinaciclib.

Supp. File 4.4: Statistical analysis of proteomic changes in the plasma of myeloma patients considered most sensitive or most resistant to PF-04691502.

Supp. File 4.5: Statistical analysis of proteomic changes in the plasma of myeloma patients considered most sensitive or most resistant to quisinostat.

Supp. File 4.6: Statistical analysis of proteomic changes in the plasma of myeloma patients considered most sensitive or most resistant to venetoclax.

Supp. File 4.7: Statistical analysis of proteomic changes in the plasma of myeloma patients considered most sensitive or most resistant to navitoclax.

Supp. File 4.8: Statistical analysis of plasma cytokine levels between the four chemosensitivity groups.

Chapter 5

Supp. File 5.1: Statistically significantly differentially abundant proteins identified in bone marrow mononuclear cells from multiple myeloma patients with and without extramedullary spread.

Chapter 6

Supp. File 6.1: Pearson's correlation analysis of VCAM1, HGFA, PEDF, and ELA2 concentrations against individual drug sensitivity scores.

Supp. File 6.2: Statistical analysis of differential cytokine abundance in EMM plasma compared to MM plasma.

Chapter 8

Supp. File 8.1: Venn analysis of SSDA plasma proteins identified in Chapter 4.

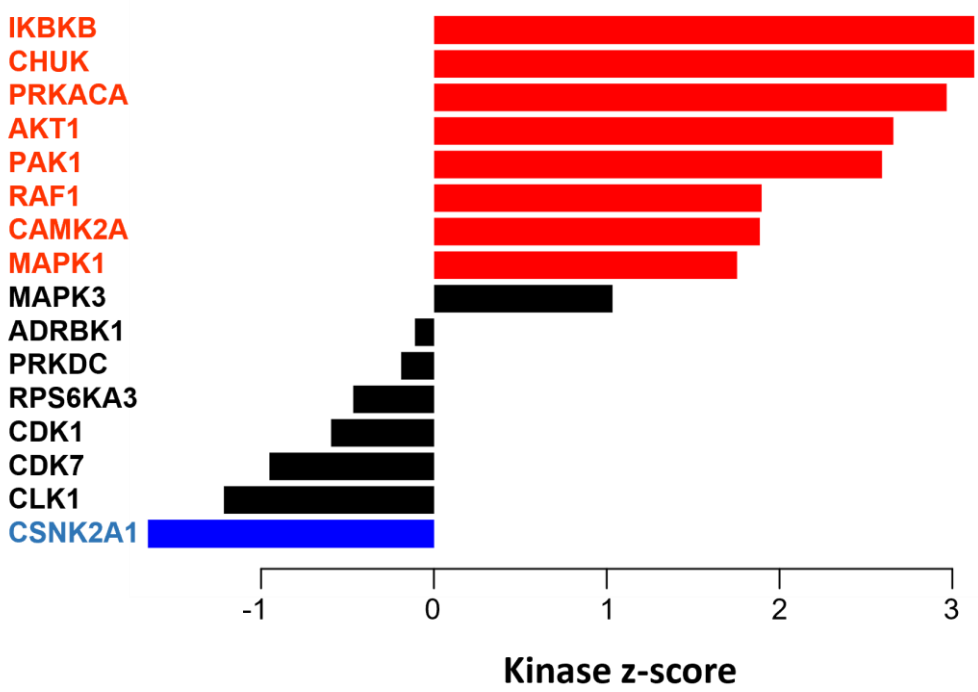

Supp. Figure 3.1: Kinase substrate enrichment analysis (KSEA) based on response to bortezomib. KSEA was performed to characterize kinase regulation based on drug resistance/sensitivity to bortezomib. Kinases with a p-value < 0.05 are highlighted as red and blue bars. Red bars indicate kinases predicted to be activated in myeloma cells most resistant to bortezomib whereas blue bars indicate kinases predicted to be activated in myeloma cells most sensitive to bortezomib.

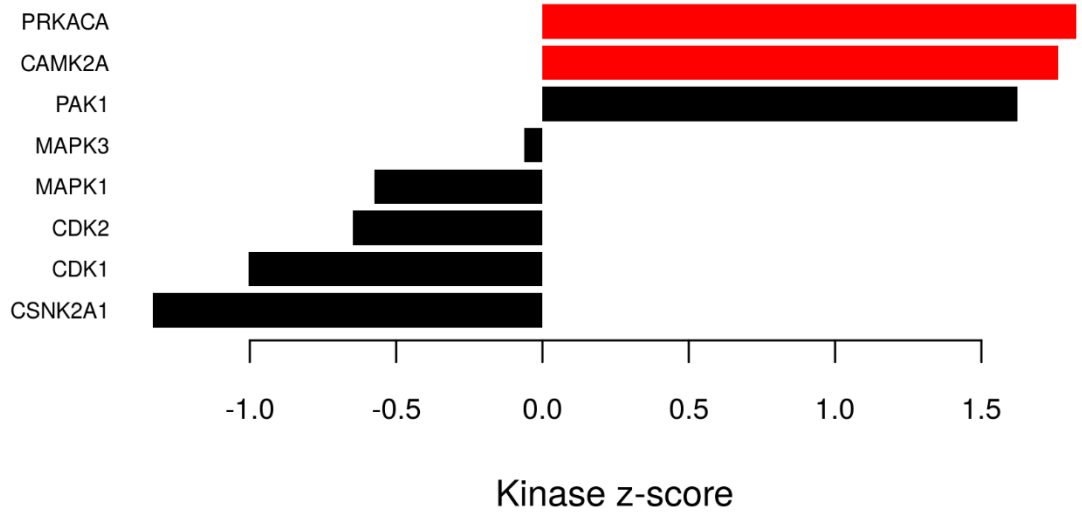

Supp. Figure 3.2: Kinase substrate enrichment analysis (KSEA) based on response to luminespib. KSEA was performed to characterize kinase regulation based on drug resistance/sensitivity to luminespib**.** Red bars indicate kinases predicted to be activated in myeloma cells most resistant to luminespib.

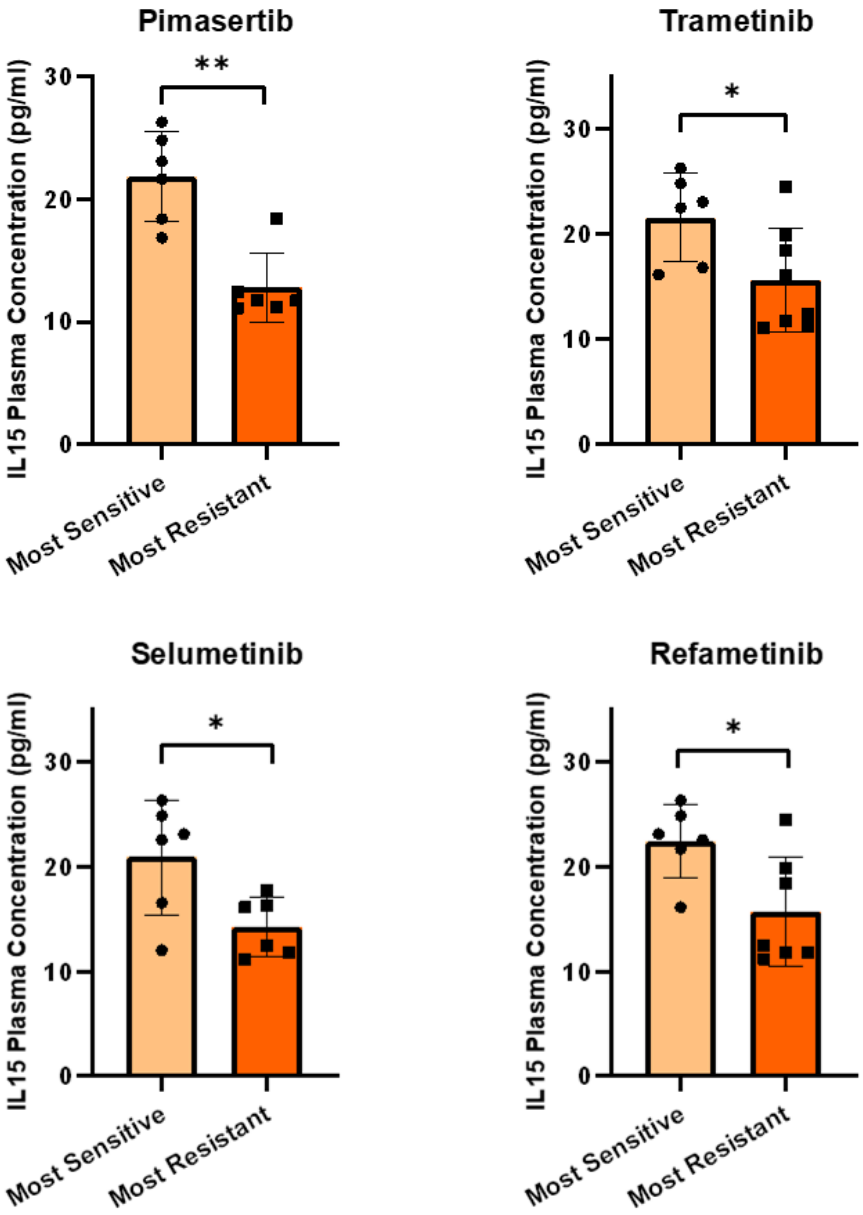

Supp. Figure 4.1: Association between plasma concentrations of interleukin-15 and sensitivity to MEK inhibitors. Plasma levels of IL-15 were significantly increased in patients considered most sensitive to MEK inhibitors based on *ex vivo* drug sensitivity resistance testing.

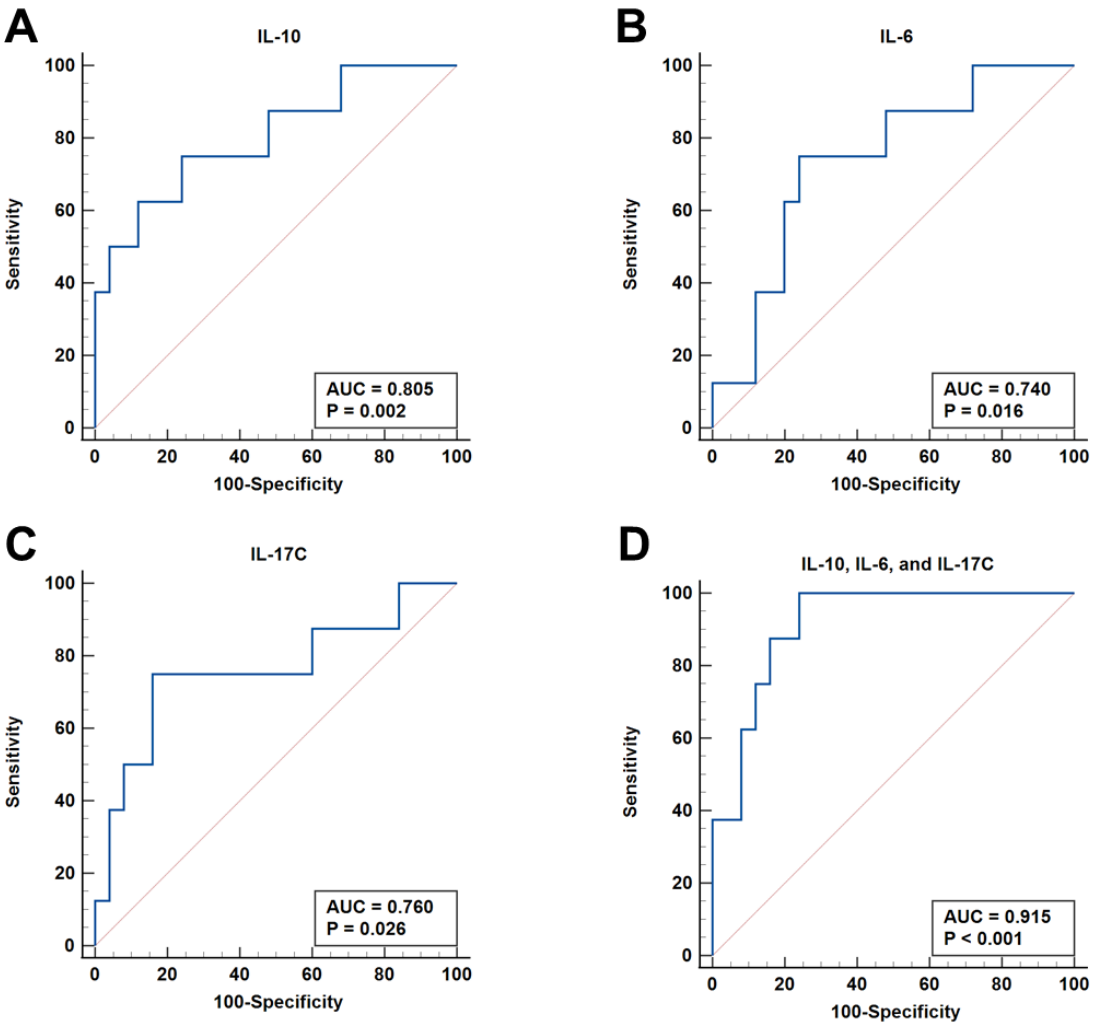

Supp. Figure 6.1: Receiver operating characteristic (ROC) curve analysis of statistically significant differentially abundant cytokines in EMM plasma. (**A**) Interleukin-10 (IL-10) (**B**) Interleukin-6 (IL-6) (**C**) Interleukin-17C (IL-17C) (**D**) Combined ROC curve evaluating the ability of IL-10, IL-6, and IL-17C combined as discriminatory markers of EMM.